



New meta-Terphenyl-Derived Primary Amines in Asymmetric Catalysis

The Harvard community has made this article openly available. [Please share](#) how this access benefits you. Your story matters

Citation	Witten, Michael R. 2015. New meta-Terphenyl-Derived Primary Amines in Asymmetric Catalysis. Doctoral dissertation, Harvard University, Graduate School of Arts & Sciences.
Citable link	http://nrs.harvard.edu/urn-3:HUL.InstRepos:17467173
Terms of Use	This article was downloaded from Harvard University's DASH repository, and is made available under the terms and conditions applicable to Other Posted Material, as set forth at http://nrs.harvard.edu/urn-3:HUL.InstRepos:dash.current.terms-of-use#LAA

New *meta*-Terphenyl-Derived Primary Amines in Asymmetric Catalysis

A dissertation presented

by

Michael R. Witten

to

The Department of Chemistry and Chemical Biology

in partial fulfillment of the requirements

for the degree of

Doctor of Philosophy

in the subject of

Chemistry

Harvard University

Cambridge, Massachusetts

January 2015

© 2015 – Michael R. Witten

All rights reserved.

New *meta*-Terphenyl-Derived Primary Amines in Asymmetric Catalysis

Abstract

In this dissertation, two distinct asymmetric reaction types are described: [5 + 2] pyrylium cycloadditions and aldehyde α -functionalizations. Both reactions are mediated by simple, organic primary amine catalysts bearing bulky *meta*-terphenyl moieties. The main text of this thesis is divided into five chapters outlining the relevant background and the original research.

Chapter 1 provides a thorough historical overview of [5 + 2] oxidopyrylium cycloadditions and related asymmetric [3 + 2] cycloadditions. Early discoveries of intermolecular and intramolecular processes, asymmetric precedents, and pertinent frontier molecular orbital considerations are examined. The application of these transformations to the synthesis of natural products and bioactive compounds is also discussed.

In Chapter 2, a new method for effecting catalytic enantioselective intramolecular [5 + 2] cycloadditions based on oxidopyrylium intermediates is presented. The development and employment of a dual catalyst system—consisting of a chiral *m*-terphenyl-containing primary aminothiourea and a second achiral thiourea—are described. Experimental evidence points to a new type of cooperative catalysis with each species being necessary to generate a reactive pyrylium ion pair that undergoes subsequent cycloaddition with high enantioselectivity.

Chapter 3 details the successful expansion of the enantioselective [5 + 2] methodology to intermolecular reactions. Highly enantioselective intermolecular [5 + 2] cycloadditions of

pyrylium ion intermediates with electron-rich alkenes are promoted by the same dual catalyst system as in Chapter 2. The observed enantioselectivity is highly dependent on the substitution pattern of the 5π component, and the basis for this effect is analyzed in detail using experimental and computational evidence. The resultant 8-oxabicyclo[3.2.1]octane derivatives possess a scaffold common in natural products and medicinally active compounds and are also versatile chiral building blocks for further manipulations. Several stereoselective complexity-generating transformations of the 8-oxabicyclooctane products are described.

In Chapter 4, we transition into a literature survey of catalytic asymmetric α -functionalizations of α -branched aldehydes. First, the challenges associated with the efficient functionalization of such substrates, relative to their unbranched counterparts, are detailed. This introduction is followed by a comprehensive overview of catalytic, enantioselective α -heterofunctionalizations: aminations, oxygenations, sulfenylations, and fluorinations. Advantages and drawbacks to previously described methods are analyzed in detail.

Chapter 5 recounts our own contributions to this area. A new chiral *m*-terphenyl-containing primary amine catalyst for the asymmetric α -hydroxylation and α -fluorination of α -branched aldehydes is reported. The products of the title transformations are isolated in high yields and exceptional enantioselectivities within short reaction times. Both processes can be performed at high concentrations and on gram scale. The remarkable similarity between the procedures, combined with computational evidence, implies a possible general catalytic mechanism for α -functionalizations. Promising initial results for α -amination and α -chlorination support this hypothesis.

Table of Contents

Abstract	iii
Table of Contents	v
Acknowledgments	ix
List of Abbreviations and Symbols	xv
Chapter 1. An Overview of [5 + 2] Cycloadditions of Oxidopyrylium Dipoles and Related Ylides	1
1.1 Introduction	1
1.2 Oxidopyrylium Generation from Acetoxypyranones	2
1.2.1 Intermolecular Oxidopyrylium Cycloadditions from Acetoxypyranones	3
1.2.2 Intramolecular Oxidopyrylium Cycloadditions from Acetoxypyranones	7
1.3 Oxidopyrylium Generation from Alternate Starting Materials	8
1.3.1 Epoxyindanones as Oxidopyrylium Precursors	8
1.3.2 β -Hydroxy- γ -pyrones as Oxidopyrylium Precursors	11
1.4 Asymmetric Access to the 8-Oxabicyclo[3.2.1]octane Core	15
1.4.1 Diastereoselective [5 + 2] Oxidopyrylium Cycloadditions	16
1.4.2 Catalytic Enantioselective [3 + 2] Carbonyl Ylide Cycloadditions	19
1.4.3 Catalytic Enantioselective [5 + 2] Benzopyrylium Cycloadditions	24
1.5 [5 + 2] Oxidopyrylium Cycloadditions in Total Syntheses	25
1.6 Outlook	33
Chapter 2. Hydrogen-Bonding and Primary Amine Catalysis in Enantioselective [5 + 2] Pyrylium Cycloadditions	34
2.1 Introduction	34
2.2 Reaction Development	38

2.3 Substrate Scope	40
2.4 Mechanistic Studies	43
2.4.1 Catalyst Structure–Activity Study	43
2.4.2 An FMO Analysis to Support an Aminopyrylium Intermediate	46
2.4.3 Rationalization of Stereoselectivity by DFT Calculations	49
2.5 Conclusions and Outlook	51
2.6 Experimental Details	52
2.6.1 General Information	52
2.6.2 Synthesis and Characterization of Catalysts	53
2.6.3 Synthesis and Characterization of Substrates	55
2.6.4 Procedures for Cycloadditions and Characterization of Products	79
2.6.5 Computational Procedures and Results	87
2.6.6 Frontier Molecular Orbital Methods	95
2.6.7 Additional Optimization Studies	96
2.6.8 Results with Sub-Optimal and Unreactive Substrates	97
2.6.9 Crystallographic Information	99
Chapter 3. Expansion of Catalytic Asymmetric [5 + 2] Cycloadditions to Intermolecular Reactions	105
3.1 Introduction	105
3.1.1 The Catalytic Asymmetric [5 + 2] Pyrylium Cycloaddition	107
3.1.2 Asymmetric Intermolecular [5 + 2] Pyrylium Cycloadditions	108
3.2 Reaction Development	111
3.3 Substrate Scope	116
3.4 An Asymmetric Total Synthesis of (–)-Descurainin	118

3.5 Mechanistic Studies	119
3.6 Derivatization of Cycloadducts	122
3.7 Conclusions and Outlook	125
3.8 Experimental Details	125
3.8.1 General Information	125
3.8.2 Synthesis and Characterization of Substrates	126
3.8.3 Procedures for Cycloadditions and Characterization of Products	140
3.8.4 Synthesis and Characterization of Product Derivatives	148
3.8.5 Computational Procedures and Results	159
3.8.6 Additional Optimization Studies	168
3.8.7 Results with Sub-Optimal and Unreactive Substrates	171
3.8.8 Crystallographic Information	172
Chapter 4. An Overview of Amine-Catalyzed α-Functionalizations of Branched Aldehydes	175
4.1 Introduction	175
4.2 α -Amination Reactions	180
4.3 α -Oxygenation Reactions	186
4.4 α -Sulfonylation Reactions	190
4.5 α -Fluorination Reactions	191
4.6 Outlook	195
Chapter 5. A New Primary Amine Catalyst for Efficient Asymmetric α-Functionalizations of Branched Aldehydes	197
5.1 Introduction	197
5.1.1 α -Oxygenation Reactions	199

5.1.2 α -Fluorination Reactions	201
5.1.3 α -Functionalization Reactions from the Jacobsen Lab	202
5.2 Reaction Development	203
5.2.1 An <i>N</i> -Sulfonyloxaziridine Hydroxylating Reagent	203
5.2.2 Condition Optimization	205
5.3 Regarding Benzamide Catalysts	208
5.4 Substrate Scope	212
5.5 Mechanistic Studies	217
5.5.1 A DFT Model for Enantioinduction	217
5.5.2 Investigation of Other α -Functionalizations	219
5.6 Conclusions and Outlook	223
5.7 Experimental Details	223
5.7.1 General Information	223
5.7.2 Synthesis and Characterization of Catalyst 38	224
5.7.3 Synthesis and Characterization of Substrates	227
5.7.4 Procedures for α -Functionalizations and Characterization of Products	239
5.7.5 Computational Procedures and Results	270
5.7.6 Additional Optimization Studies	277
5.7.7 Results with Additional Substrates	288
5.7.8 Crystallographic Information	289

Acknowledgments

There are several people without whom this thesis (and by extension my own career) would not have been possible. Foremost among them is my advisor. Eric Jacobsen has managed to cultivate a group that shares his own enthusiasm for science and zeal for diligent research. His intellectual curiosity has served as an inspiration and his attitude towards advising has afforded me the freedom to develop as an independent researcher. Although we have not always seen eye-to-eye (usually due to my own dimwittedness), I cannot imagine having had a more enjoyable graduate school experience and consider myself truly fortunate to join his chemical family tree—even if I am the figurative beech bark disease.

I must also express my gratitude towards Professors Andrew Myers and Tobias Ritter who have served on my graduate advising committee for the entirety of my five years in the Jacobsen group. Their advice and encouragement during committee meetings, especially in response to my independent research proposal, have been invaluable. Their feedback has been instrumental in my development as both a scientist and a public speaker. I must also give recognition to Professor Dan Kahne for providing additional feedback on my research proposal.

Throughout the entire ordeal of navigating graduate school, Nicole Minotti has kept the ship on course. Although graduate students typically have a reputation for working ridiculously long hours (hey, at least the pay is awful!), Nicole has often worked even longer and harder at making sure the Jacobsen group remains afloat. Remarkably, she always does so with a smile on her face. The minutes before entering Eric's office prior to committee meetings could have been some of the most grueling in all of graduate school, but Nicole's jokes and words of encouragement always kept me levelheaded prior to jumping into the shark tank.

Before I even fully grasped what chemistry was, I had the dual influences of two excellent

high school teachers, Mrs. Ronee Krashes and Mr. Matthew Corcoran. Let's face it, high school chemistry can be a real drag, but these two made the coursework more about scientific inquiry and less about rote memorization. Without them, I would not be writing this work today, nor would you be reading it. Honorable mention goes to my high school physics teacher and all around fascinating fellow Dr. Dan Seeley.

When I arrived at New York University, I was still undecided with respect to what I wanted to study, but had a pretty good idea that it would be chemistry or physics. My freshman general chemistry classes with Professors Phil Lukeman and Paul Gans settled that question. In sophomore year I took Professor Paramjit "Bobby" Arora's organic chemistry class and my love for organic reactions was born. In some ways unwittingly, Bobby has had the most profound impact on both my professional and personal (more on that later) lives. I was ecstatic to begin research in his group as I came into the homestretch of my sophomore year.

As I've seen other research groups and other universities over the years since college, I've come to realize that undergraduates are often treated as second-class citizens. This was never the case in the Arora lab. I was given my own project from the beginning, and always felt like an independent researcher and a real contributor. In addition to Bobby, much of this sense of community derived from the incredible group of students and postdocs with whom I shared my time there, specifically Irina Bergenfeld, Petra Tošovská, and Anupam Patgiri. In particular Stephen Miller remains a good friend. Mention must also be made of the other great professors who helped to push me in the right direction back in those days. Professors Jim Canary, Neville Kallenbach, Burt Goldberg, and J. David Warren prepared me extremely well for my time at Harvard.

Over the years, I have had a lot of great coworkers in the Jacobsen lab. Specifically, I must

single out two excellent postdocs who have served as sources of advice and enthusiasm. Rob Knowles (now a professor at Princeton) was my first mentor when I rotated in the group, and continued to put up with my questions amiably after I joined. Having this fount of wisdom directly behind my desk for the first year and a half of my time in the lab was incredibly valuable. Noah Burns (now a professor at Stanford, natch) allowed me to ride shotgun on his project for my first year and a half in the lab, and, even more remarkably, let me take the wheel as he was wrapping up. I am immensely lucky to have had him as a mentor and owe nearly all of my technical knowledge and chemical intuition to his guidance.

Some of the most talented postdocs in the world have come through our group during my time here. I must also thank Ellie Beck, Alan Hyde, Cheyenne Brindle, Katrien Brak, Dave Stewart, Corinna Schindler, Dan Lehnherr, Roland Appel, Sean Kedrowski, Mike Ardolino, Kaid Harper, Jon Medley, Charles Yeung, Eugene Kwan, Nadine Kuhl, Libby Hennessy, David Hardee, Eric Woerly, and Pam Tadross for their advice and their friendship.

Joining a lab and starting fresh with a group of senior graduate students who seem (and in fact are) much more competent and intelligent than oneself can be a terrifying process. Thankfully, through it all, Amanda Turek has been my classmate, labmate, and friend. We came into Harvard together, worked on homework together, and griped about the challenges of getting out together. I look forward to many more years of friendship, as well as her own successes in the future.

Fortunately, joining the lab was made easy by the very group of intelligent but welcoming graduate students already mentioned. Bekka Klausen and Chris Uyeda set a terrific example of how to be successful scientists and also how to be well-balanced people. Their professionalism and cordiality helped facilitate my transition into graduate school. Adam Brown, Naomi Rajapaksa, Dave Ford, Jim Birrell, Song Lin, and Andy Rötheli were also excellent colleagues,

providing lively discussion in meetings and advice in lab. Whether doing chemistry in M202, sharing drinks at the Cellar, or “dancing” on the umpteenth floor of Hong Kong, they provided a lively atmosphere.

I leave behind a group of talented graduate students to keep fighting the good fight in my absence. In the year below me, YP “Don’t call me Yongho” Park and Gary “Call me Hu (Tiger)” Zhang have already been responsible for some exciting chemistry and I look forward to their continued work in the future. It has been a pleasure to watch Steven Banik, Rose Kennedy, and Ania Levina grow as scientists and also to join them in a conversation or two of little chemical consequence. They all have promising careers ahead of them. Towards the end of my time here, I had the good fortune to take on a talented rotator, Andrew Bendel Smith. I’ll keep my eyes peeled for new developments from him and his classmates, Andrew Mayfield and Chris Kim.

Portions of this thesis have been graciously proofread by Jon Medley, Amanda Turek, Mike Ardolino, Eric Woerly, and Charles Yeung. So what if I mentioned them already? This is my thesis after all. And they deserve the extra kudos.

Finally, I would like to thank all of my family and friends for their support, not only over the past six years, but also over the preceding twenty-two. My parents have been my biggest supporters and my greatest sources of encouragement. With nearly infinite patience, they have seen me through all the twists and turns that have brought me to this writing. Having them so close during graduate school could be annoying sometimes, but come laundry day, it was also be a huge advantage.

Chemistry has opened a lot of doors for me, and hopefully will open many more as my career progresses. The greatest discovery I ever made in a chemistry lab happened during my time at NYU, when I noticed Rebecca Wissner joining the Arora group. Since then, she has been a

constant companion, despite the physical distance that has separated us. Rebecca has been my most important source of inspiration, and also, when asked, my best critic. Every step through graduate school, we have taken together. I am a better scientist and a better person for having her to take this journey with.

to my parents

Mark and Meryl Witten

List of Abbreviations and Symbols

Å	angstrom
Ac	acetyl
acac	acetylacetonate
AcOH	acetic acid
APCI	atmospheric-pressure chemical ionization
aq.	aqueous
Ar	aryl
α	Hückel Coulomb integral
$[\alpha]_D^X$	specific rotation at X °C and 589 nm
B3LYP	Becke-3-Lee-Yang-Parr
BHT	butylated hydroxytoluene
Bn	benzyl
Boc	<i>tert</i> -butoxycarbonyl
BPTV	<i>N</i> -benzene-fused phthaloyl-valine
Bz	benzoyl
BzOH	benzoic acid
β	Hückel resonance integral
<i>c</i>	concentration
°C	degrees Celsius
calcd.	calculated
cat.	catalyst
Cbz	carboxybenzyl

<i>cis</i>	on the same side
cm	centimeters
conc.	concentration
CPME	cyclopentyl methyl ether
D	dextrorotatory
D	deuterium
DBU	1,8-diazabicycloundec-8-ene
DCA	dichloroacetic acid
DDBNP	6,6'-didodecyl-1,1'-binaphthyl-2,2'-phosphate
<i>de</i>	diastereomeric excess
DFT	density functional theory
DIAD	diisopropyl azodicarboxylate
diast.	diastereomer
DMAP	4-dimethylaminopyridine
DMF	<i>N,N</i> -dimethylformamide
DMSO	dimethyl sulfoxide
DOSP	<i>N</i> -[(4-dodecylphenyl) sulphonyl]proline
<i>dr</i>	diastereomeric ratio
δ	chemical shift in parts per million
Δ	heat
ΔG	difference in energy
<i>E</i>	entgegen (German)
E	energy

EDC	<i>N</i> -(3-dimethylaminopropyl)- <i>N'</i> -ethylcarbodiimide hydrochloride
<i>ee</i>	enantiomeric excess
<i>ent</i>	enantiomeric
eq.	equation
equiv	equivalents
ESI	electrospray ionization
Et	ethyl
Et ₂ O	diethyl ether
EtOAc	ethyl acetate
EtOH	ethanol
eV	electronvolts
FMO	frontier molecular orbital
FT	Fourier transform
g	grams
G	Gibbs free energy
GC	gas chromatography
h	hours
HFIP	1,1,1,3,3,3-hexafluoroisopropanol
hν	light
HOMO	highest occupied molecular orbital
HPLC	high-performance liquid chromatography
Hz	hertz
<i>i</i> Bu	<i>iso</i> -butyl

imid.	imidazole
<i>i</i> Pr	<i>iso</i> -propyl
<i>i</i> Pr ₂ NEt	<i>N,N</i> -diisopropylethylamine
<i>i</i> PrOH	isopropanol
IR	infrared
<i>J</i>	coupling constant
K	kelvin
<i>k</i> ₂	second-order rate constant
kcal	kilocalories
<i>K</i> _{eq}	equilibrium constant
L	levorotatory
L	liters
L*	chiral ligand
LC	liquid chromatography
LUMO	lowest unoccupied molecular orbital
λ	wavelength
<i>m</i>	<i>meta</i>
m	milli-
M	molar; mass of compound
MCA	monochloroacetic acid
<i>m</i> CPBA	<i>meta</i> -chloroperoxybenzoic acid
Me	methyl
MeCN	acetonitrile

MeOH	methanol
MHz	megahertz
MIA	monoiodoacetic acid
min	minutes
mol	mole(s)
mol%	mole percent
MOM	methoxymethyl
Ms	mesyl
MS	mass spectrometry
MsOH	methanesulfonic acid
μ	micro-
μW	microwave
<i>N</i>	nucleophilicity parameter
N	normal
NBSA	nitrobenzenesulfonic acid
<i>n</i> BuLi	<i>n</i> -butyllithium
n.d.	not determined
NEt ₃	triethylamine
NFSI	<i>N</i> -fluorobenzenesulfonimide
nm	nanometers
NMO	<i>N</i> -methylmorpholine- <i>N</i> -oxide
NMR	nuclear magnetic resonance
<i>n</i> Pr	<i>n</i> -propyl

v	frequency
<i>o</i>	<i>ortho</i>
OTf	trifluoromethanesulfonate
oxone	potassium peroxydisulfate
<i>p</i>	<i>para</i>
PDC	pyridinium dichromate
Ph	phenyl
PhCF ₃	α,α,α -trifluorotoluene
PMB	<i>para</i> -methoxybenzyl
ppm	parts per million
PPTS	pyridinium <i>para</i> -toluenesulfonate
psi	pounds per square inch
<i>p</i> Tol	<i>para</i> -methylphenyl
PTTL	<i>N</i> -phthaloyl- <i>tert</i> -leucinate
pyr.	pyridine
<i>R</i>	rectus (Latin)
<i>rac</i>	racemic
ref.	reference
R _f	retention factor
<i>rr</i>	regioisomeric ratio
s	seconds
<i>S</i>	sinister (Latin)
sat.	saturated

SFC	supercritical fluid chromatography
S _N 1	unimolecular nucleophilic substitution
<i>syn</i>	same side
σ_{para}	substituent parameter in <i>para</i> -position
TBAF	tetrabutylammonium fluoride
TBDPS	<i>tert</i> -butyldiphenylsilyl
<i>t</i> BME	<i>tert</i> -butyl methyl ether
TBS	<i>tert</i> -butyldimethylsilyl
<i>t</i> Bu	<i>tert</i> -butyl
TCA	trichloroacetic acid
TD-DFT	time-dependent density functional theory
TEMPO	2,2,6,6-tetramethyl-1-piperidinyloxy free radical
TFA	trifluoroacetic acid
THF	tetrahydrofuran
THP	tetrahydropyran
TIPS	triisopropylsilyl
TLC	thin-layer chromatography
TMP	2,2,6,6-tetramethylpiperidine
TMS	trimethylsilyl
TOF	time-of-flight
Trp	trispyrazolylborate
<i>t_R</i>	retention time
<i>trans</i>	on opposite sides

TRIP	3,3'-bis(2,4,6-triisopropylphenyl)-1,1'-binaphthyl-2,2'-diyl hydrogenphosphate
Ts	tosyl
wt%	weight percent
Z	zusammen (German)

“Who sent this new serpent to our ruinous garden, already too fouled, too crowded to qualify as any locus of innocence—unless innocence be our age’s neutral, our silent passing into the machineries of indifference—something that Kekulé’s Serpent had come to—not to destroy, but to define to us the loss of . . . we had been given certain molecules, certain combinations and not others . . . we used what we found in Nature, unquestioning, shamefully perhaps—but the Serpent whispered, ‘*They can be changed*, and new molecules assembled from the debris of the given. . . .’ Can anyone tell me what else he whispered to us? Come—who knows?”

Thomas Pynchon, *Gravity’s Rainbow*

“What, me worry?”

Alfred E. Neuman, *Mad Magazine*

An Overview of [5 + 2] Cycloadditions of Oxidopyrylium Dipoles and Related Ylides

1.1 Introduction

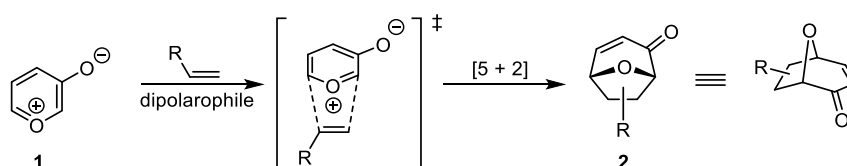
Owing to their ability to rapidly generate molecular complexity by simultaneously forming two carbon–carbon bonds, cycloaddition reactions occupy a central role in organic chemistry. Oxidopyrylium ylides (i.e., **1**, Scheme 1.1) constitute a class of zwitterionic heterocycles which proficiently undergo [5 + 2] cycloaddition reactions with two-carbon dipolarophiles to construct chiral 8-oxabicyclo[3.2.1]oct-3-en-2-one architectures **2**.¹ In addition to their structural relationship to numerous natural products (Figure 1.1)² and biologically active compounds,³ such

¹ For recent reviews, see: (a) Singh, V.; Krishna, U. M.; Vikrant; Trivedi, G. K. *Tetrahedron* **2008**, *64*, 3405–3428. (b) Pellissier, H. *Adv. Synth. Catal.* **2011**, *353*, 189–218. (c) Ylijoki, K. E. O.; Stryker, J. M. *Chem. Rev.* **2013**, *113*, 2244–2266.

² For example, Englerin A: (a) Ratnayake, R.; Covell, D.; Ransom, T. T.; Gustafson, K. R.; Beutler, J. A. *Org. Lett.* **2009**, *11*, 57–60. Phorbol: (b) Hecker, E.; Schmidt, R. *Fortschr. Chem. Org. Naturst.* **1974**, *31*, 377–467. Secodolastanes: (c) Teixeira, V. L.; Tomassini, T.; Fleury, B. G.; Kelecom, A. *J. Nat. Prod.* **1986**, *49*, 570–575. Cortistatin A: (d) Aoki, S.; Watanabe, Y.; Sanagawa, M.; Setiawan, A.; Kotoku, N.; Kobayashi, M. *J. Am. Chem. Soc.* **2006**, *128*, 3148–3149. Anthecularin: (e) Karioti, A.; Skaltsa, H.; Linden, A.; Perozzo, R.; Brun, R.; Tasdemir, D. *J. Org. Chem.* **2007**, *72*, 8103–8106. Intricarene: (f) Marrero, J.; Rodríguez, A. D.; Barnes, C. L. *Org. Lett.* **2005**, *7*, 1877–1880. Komaroviquinone: (g) Uchiyama, N.; Kiuchi, F.; Ito, M.; Honda, G.; Takeda, Y.; Khodzhimatov, O. K.; Ashurmetov, O. A. *J. Nat. Prod.* **2003**, *66*, 128–131. Descurainin: (h) Sun, K.; Li, X.; Li, W.; Wang, J.; Liu, J.; Sha, Y. *Chem. Pharm. Bull.* **2004**, *52*, 1483–1486. Cartorimine: (i) Yin, H.-B.; He, Z.-S.; Ye, Y. *J. Nat. Prod.* **2000**, *63*, 1164–1165.

³ Compounds containing the chiral 8-oxabicyclo[3.2.1]octane core have been identified recently as psychoactive analogues of the tropane alkaloids with promising therapeutic potential: (a) Meltzer, P. C.; Liang, A. Y.; Blundell, P.; Gonzalez, M. D.; Chen, Z.; George, C.; Madras, B. K. *J. Med. Chem.* **1997**, *40*, 2661–2673. (b) Meltzer, P. C.; Liu,

cycloadducts have proven to be highly valuable intermediates in the synthesis of functionalized seven-membered carbocycles and tetrahydrofuran derivatives.⁴ In this chapter, we will concisely review the history of oxidopyrylium-based [5 + 2] cycloadditions as well as other notable approaches to the 8-oxabicyclo[3.2.1]octane scaffold.



Scheme 1.1. The [5 + 2] oxidopyrylium cycloaddition.

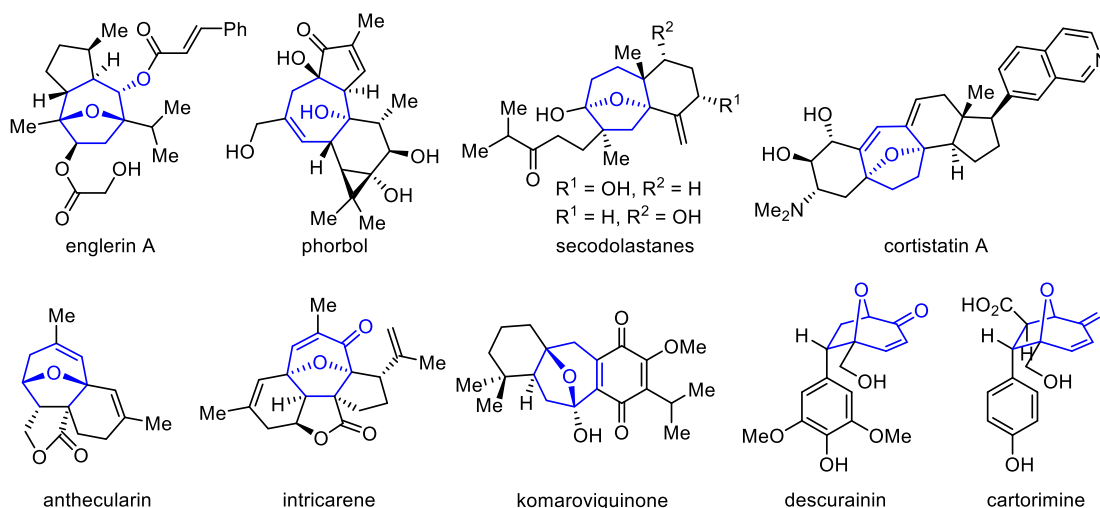


Figure 1.1. The 8-oxabicyclo[3.2.1]octane core in selected natural products.

1.2 Oxidopyrylium Generation from Acetoxypyranones

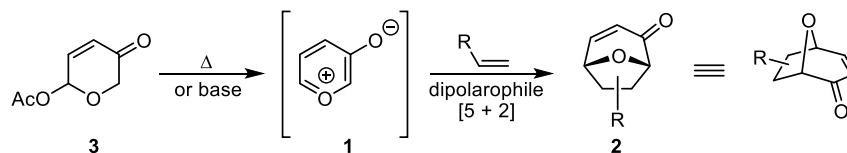
Of the three reported methods for oxidopyrylium ylide formation, elimination from acetoxypyranones is the most commonly represented in the literature and the one that pertains most significantly to the original research described in Chapters 2 and 3. In this section, intermolecular and intramolecular examples of acetoxypyranone cycloadditions will be treated separately.

S.; Blanchette, H. S.; Blundell, P.; Madras, B. K. *Bioorg. Med. Chem.* **2002**, *10*, 3583–3591. (c) Meltzer, P. C.; Kryatova, O.; Pham-Huu, D.-P.; Donovan, P.; Janowsky, A. *Bioorg. Med. Chem.* **2008**, *16*, 1832–1841.

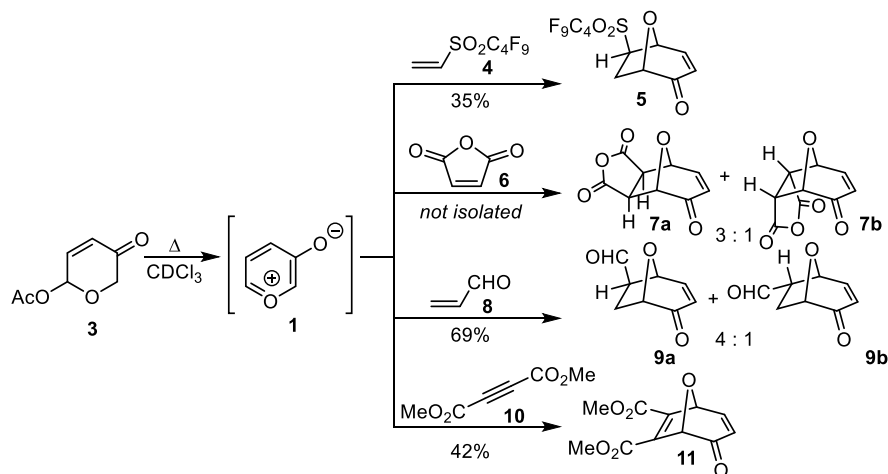
⁴ For details, see Section 1.5.

1.2.1 Intermolecular Oxidopyrylium Cycloadditions from Acetoxypyranones

In 1980, Hendrickson and Farina reported a new [5 + 2] dipolar cycloaddition, in which the reactive 5 π 3-oxidopyrylium component **1** was generated from an acetoxypyranone starting material (**3**, Scheme 1.2) upon heating or treatment with base.⁵ In this preliminary publication, the authors observed successful reactions but variable stereoselectivities with electron-deficient 2 π dipolarophiles (Scheme 1.3). For example, reaction with fluorinated sulfone **4** afforded exclusively *exo*-adduct **5**. However, use of maleic anhydride **6** resulted in the formation of products *exo*-**7a** and *endo*-**7b** in a 3:1 ratio. Acrolein **8** reacted with oxidopyrylium **1** with increased efficiency but likewise afforded a 4:1 mixture of *exo*-**9a** and *endo*-**9b**. Alkyne **10** could also participate as a 2 π component, generating cycloadduct **11** in 42% yield.



Scheme 1.2. Oxidopyrylium generation from an acetoxypyranone and subsequent cycloaddition.

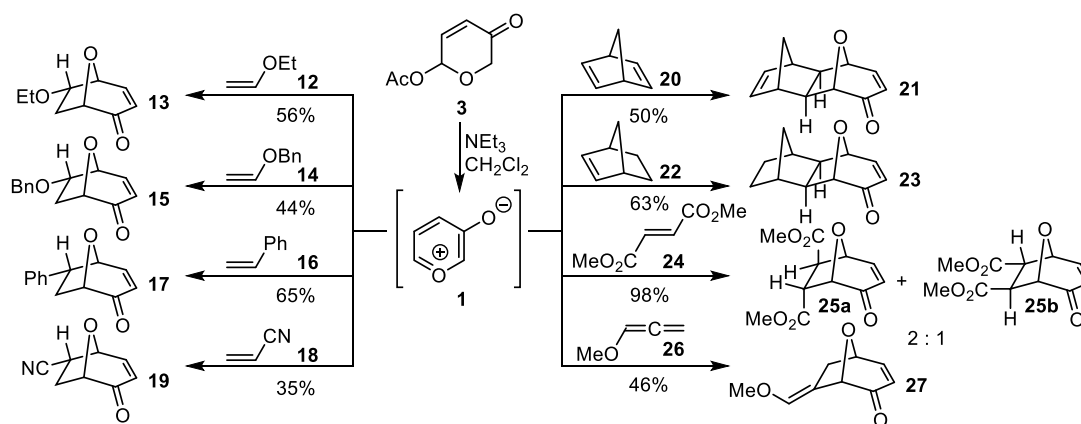


Scheme 1.3. Initially reported [5 + 2] dipolarophile scope.

Following the pioneering work of Hendrickson and Farina, Sammes and Street continued

⁵ Hendrickson, J. B.; Farina, J. S. *J. Org. Chem.* **1980**, *45*, 3359–3361.

to investigate the scope of these novel transformations, including electron-rich and strained dipolarophiles in their examination (Scheme 1.4).⁶ In contrast to the dipolarophiles that had been studied previously, ethyl vinyl ether **12**,^{6a} benzyl vinyl ether **14**,^{6b} styrene **16**,^{6a} and acrylonitrile **18**^{6c} exhibited only *endo*-selectivity in products **13**, **15**, **17**, and **19** respectively. Norbornadiene **20** and norbornene **22** however, afforded products **21** and **23** solely as *exo*-isomers.^{6a} The use of *trans*-diesters such as **24** resulted in mixtures of diastereomers.^{7a} More recently, allenes (e.g., **26**) have been demonstrated to engage in [5 + 2] cycloadditions, as in the synthesis of enol ether **27**.^{7b}



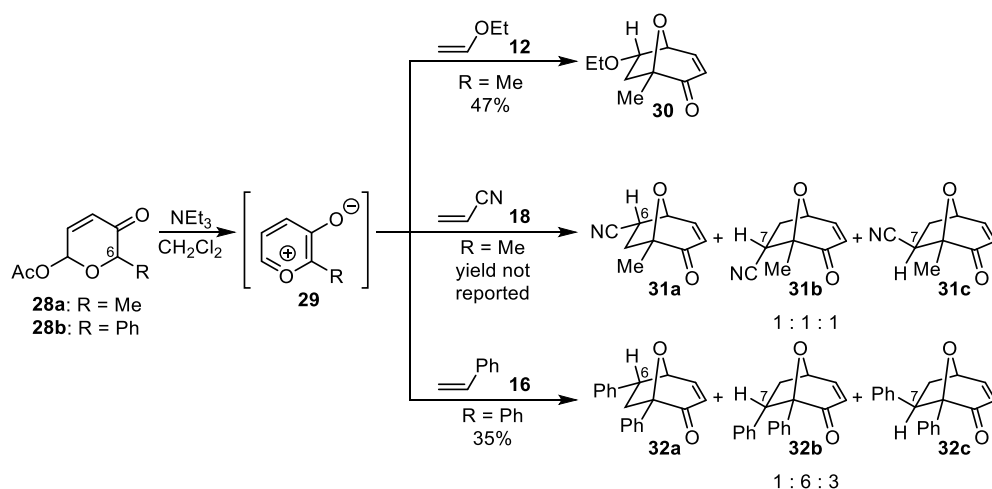
Scheme 1.4. Expansion of the dipolarophile scope.

No clear trends for predicting *endo/exo*-selectivity can be gleaned from the data presented so far, and regioselectivity becomes a complicating factor when substituted acetoxyfuranones are considered as well. For instance, although the reaction of 6-methyl substrate **28a** (Scheme 1.5) with ethyl vinyl ether gave the same stereo- and regioselectivity in product **30** as observed for unsubstituted product **13**,^{6a} acrylonitrile afforded a 1:1:1 mixture of three possible isomers (**31a–c**, compare to **19**, Scheme 1.4).^{6c} Similarly, reaction of 6-phenyl **28b** with styrene resulted in three

⁶ (a) Sammes, P. G.; Street, L. J. *J. Chem. Soc., Perkin Trans. 1* **1983**, 1261–1265. (b) Sammes, P. G.; Street, L. J.; Kirby, P. *J. Chem. Soc., Perkin Trans. 1* **1983**, 2729–2734. (c) Sammes, P. G.; Street, L. J. *J. Chem. Res., Synop.* **1984**, 196–197.

⁷ (a) Ohmori, N.; Miyazaki, T.; Kojima, S.; Ohkata, K. *Chem. Lett.* **2001**, *30*, 906–907. (b) Lee, H.-Y.; Sohn, J.-H.; Kim, H. Y. *Tetrahedron Lett.* **2001**, *42*, 1698–1698.

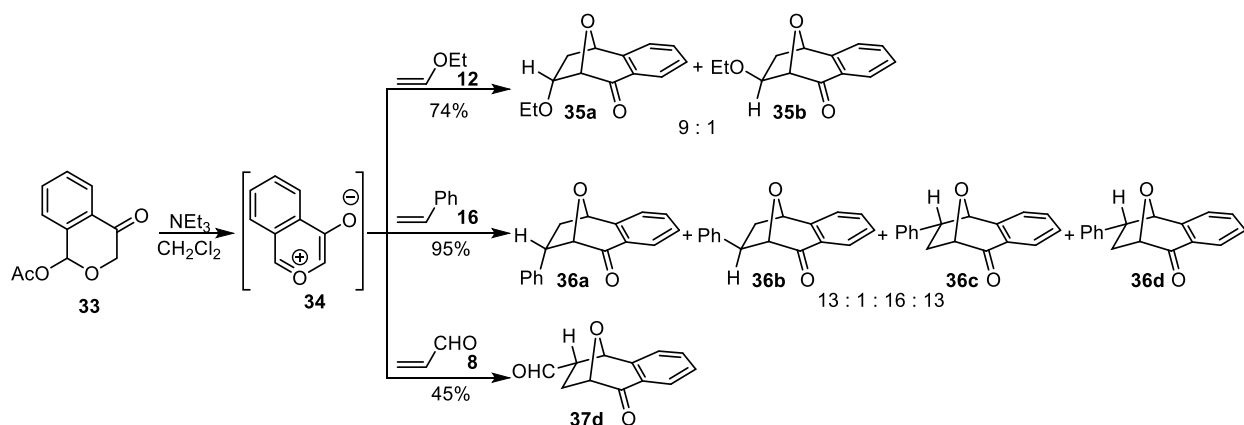
isomeric products (**32a–c**, compare to **17**, Scheme 1.4),^{6c} strongly favoring the new regioisomer. Sammes and Street invoked FMO theory to rationalize the observed switch in regioselectivity. As true dipolar cycloadditions, either the HOMO or the LUMO of the oxidopyrylium intermediate **29** could react with either the HOMO or the LUMO of the 2π dipolarophile. One HOMO–LUMO pair would result in one outcome (C6 regioselectivity, note the different numbering standard for cycloadducts relative to pyranone starting materials) and the opposite LUMO–HOMO pair would result in the opposite outcome (C7 regioselectivity). In the latter two reactions in Scheme 1.5, both pathways are accessible.



Scheme 1.5. Reactions with more substituted pyranone substrates.

Sammes and Whitby analyzed this FMO phenomenon more rigorously in the context of reactions with 2-benzopyrylium-4-oxide **34**.⁸ Selected examples of these cycloadditions appear in Scheme 1.6. Ethyl vinyl ether gives the opposite regioselectivity (C7) in **35a** and **35b** from that seen in products **13** and **30** (C6). Styrene gives all four possible isomers **36a–d**, and reaction with acrolein results in the same regioselectivity (**37d**, C6) as observed for the parent oxidopyrylium (**9a,b**, Scheme 1.3).

⁸ (a) Sammes, P. G.; Whitby, R. J. *J. Chem. Soc., Chem. Commun.* **1984**, 702–703. (b) Sammes, P. G.; Whitby, R. J. *J. Chem. Soc., Perkin Trans. 1* **1987**, 195–202.



Scheme 1.6. Reactions with the 2-benzopyrylium-4-oxide (**34**) intermediate.

Using published Hückel methods,⁹ the authors calculated the HOMO and LUMO energies for all reacting species (Figure 1.2).^{8b} The calculated energies predict that the HOMO of ethyl vinyl ether will interact with the LUMO of benzopyrylium **34**, resulting in the observed C7 selectivity (based on calculated orbital coefficients). Conversely, reaction between acrolein **8** and **34** is predicted to occur predominantly through a HOMO₃₄–LUMO₈ interaction, giving rise to the opposite C6 regioselectivity. Both HOMO–LUMO energy differences for reaction with styrene **16** are calculated to be approximately equivalent, explaining the energetic accessibility of both regiochemical outcomes.

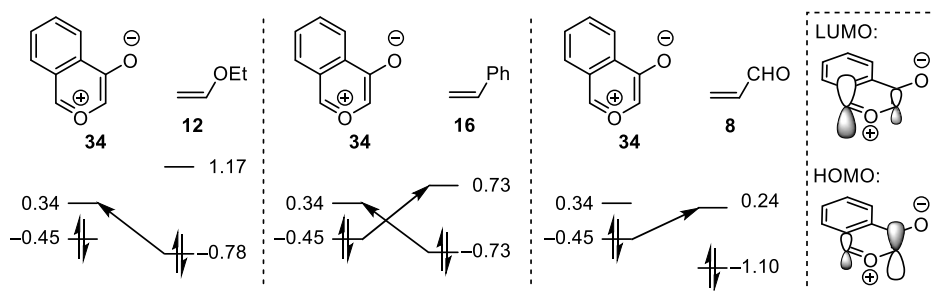
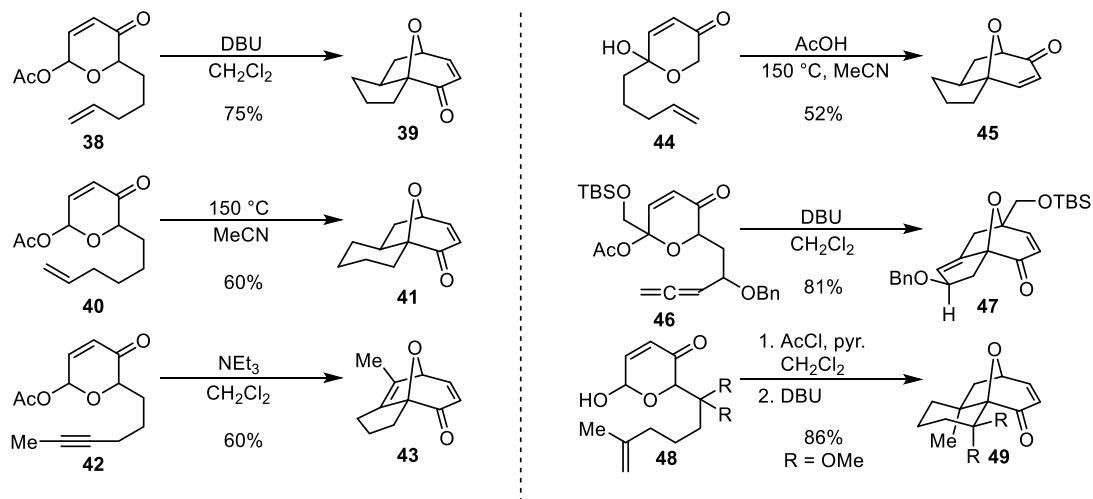


Figure 1.2. Predicted HOMO–LUMO interactions. Energies in terms of $-\beta$ relative to α . In the inset, calculated orbital coefficients are depicted to scale on the reactive atoms of **34**.

⁹ Houk, K. N.; Sims, J.; Duke, Jr., R. E.; Strozier, R. W.; George, J. K. *J. Am. Chem. Soc.* **1973**, *95*, 7287–7301.

1.2.2 Intramolecular Oxidopyrylium Cycloadditions from Acetoxypyranones

Given the challenges associated with stereo- and regioselectivity in intermolecular [5 + 2] cycloadditions, many research groups quickly turned to the related intramolecular transformations. By tethering the 5 π dipole to the 2 π dipolarophile in acetoxypyranone **38**, Sammes and Street were able to restrict the possible orientations of reaction and form a single cycloadduct (**39**, Scheme 1.7).¹⁰ Homologue **40**, and alkyne **42** also afforded single products, bicyclooctenones **41** and **43** respectively. These authors also demonstrated that the tether could be moved from the C2 to C6, and hydroxypyranone **44** could be cyclized in the presence of catalytic acetic acid to form product **45** in moderate yield. The Lee group later reported that the intramolecular reaction could be expanded to allene substrates such as **46**, with an ether substituent on the tether.^{7b} The Williams lab could also perform the transformation with a tethered disubstituted olefin (**48**).¹¹



Scheme 1.7. Selected intramolecular [5 + 2] cycloadditions of acetoxypyranones.

Other examples of intramolecular cycloadditions have been reported in the context of

¹⁰ (a) Sammes, P. G.; Street, L. J. *J. Chem. Soc., Chem. Commun.* **1982**, 1056–1057. (b) Sammes, P. G. *Gazz. Chim. Ital.* **1986**, *119*, 109–114.

¹¹ (a) Williams, D. R.; Benbow, J. W.; Allen, E. E. *Tetrahedron Lett.* **1990**, *31*, 6769–6772. (b) Williams, D. R.; Benbow, J. W.; McNutt, J. G.; Allen, E. E. *J. Org. Chem.* **1995**, *60*, 833–843.

asymmetric reactions and natural product total syntheses. They will be discussed in Sections 1.4 and 1.5 respectively.

1.3 Oxidopyrylium Generation from Alternate Starting Materials

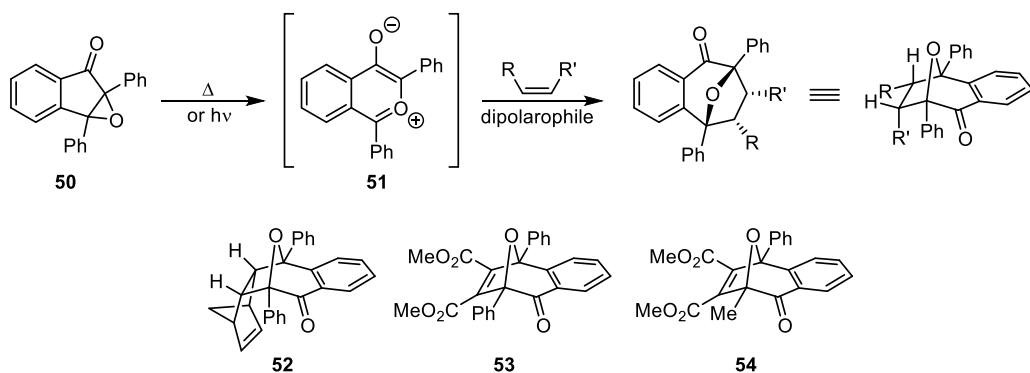
Although acetoxypranones have traditionally been the most common oxidopyrylium precursors studied in the literature, epoxyindanones and β -hydroxy- γ -pyrones have also seen limited use. While the original research described in Chapters 2 and 3 of this dissertation does not deal specifically with these starting materials, important developments will briefly be summarized in the following two subsections in order to familiarize the reader with their usage.

1.3.1 Epoxyindanones as Oxidopyrylium Precursors

The first reported oxidopyrylium ylides were derived from epoxyindanone starting materials. In 1962, Ullman and Milks described the simple generation of a red-colored, aromatic dipole (**51**, Scheme 1.8) from epoxide **50** upon heating or photolysis.¹² Benzopyrylium **51** is structurally related to intermediate **34** (Scheme 1.6) but is derived from a distinct precursor. In this initial publication, two adducts of **51** were reported; products **52** and **53** were formed from reactions with norbornadiene **20** and dicarboxylate **10** respectively. Zimmerman and Simkin later demonstrated that 2,3-epoxy-2-methyl-3-phenylindanone was also a viable precursor for formation of product **54** with **10**.¹³

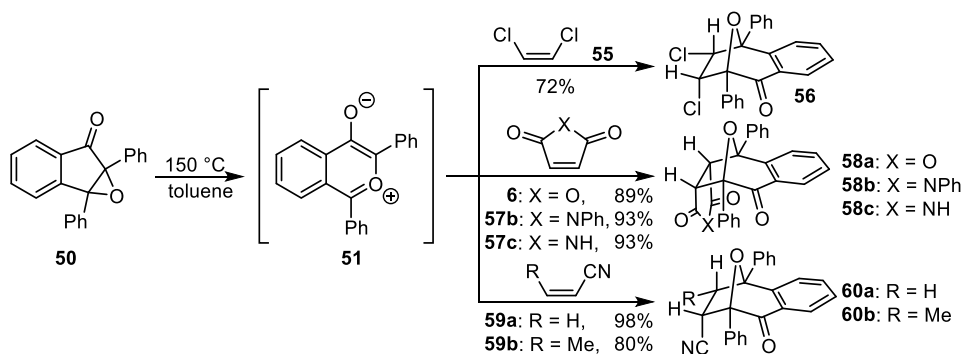
¹² (a) Ullman, E. F.; Milks, J. E. *J. Am. Chem. Soc.* **1962**, *84*, 1315–1316. (b) Ullman, E. F.; Henderson, Jr., W. A. *J. Am. Chem. Soc.* **1966**, *88*, 4942–4960.

¹³ Zimmerman, H. E.; Simkin, R. D. *Tetrahedron Lett.* **1964**, *5*, 1847–1851.



Scheme 1.8. The [5 + 2] cycloaddition of benzoperilyliums derived from epoxyindanones.

In 1971, Lown and Matsumoto greatly elaborated on previous work through a systematic screen of disubstituted dipolarophiles in reactions with intermediate **51** (Scheme 1.9).¹⁴ 1,2-dichloroethene **55**, maleic anhydride **6**, and maleimides **57b** and **57c** all provided exclusively *endo*-adducts in good yields. However, other *cis*-olefins and *trans*-olefins gave more complicated mixtures of diastereomers (Table 1.1). With the exception of *cis*-stilbene **61** (entries 1 and 2), other *cis*-olefins (entries 3–8) favored predominant formation of the *endo*-products. *Trans*-olefins showed variable diastereomer ratios, but generally favored C6-*exo*/C7-*endo* orientations (entries 9–16).



Scheme 1.9. Lown and Matsumoto's *cis*-dipolarophile screen.

¹⁴ Lown, J. W.; Matsumoto, K. *Can. J. Chem.* **1971**, *49*, 3443–3455.

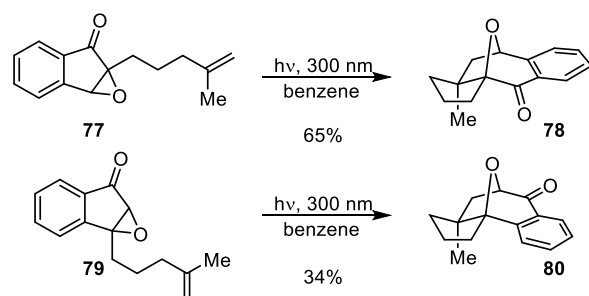
Table 1.1. Summary of Lown and Matsumoto's results.

Entry	Dipolarophile	Product	R ¹	R ²	R ³	R ⁴	Yield (%)	Ratio ^a
1		69a	Ph	Ph	H	H	72	1:1.5
2	61	69b	H	H	Ph	Ph		
3		70a	CO ₂ Me	CO ₂ Me	H	H	94	3.5:1
4	62	70b	H	H	CO ₂ Me	CO ₂ Me		
5		71a	-OC(O)O-		H	H	87	3:1
6	63	71b	H	H	-OC(O)O-			
7		72a	-1,8-naphthyl-		H	H	93	1.7:1
8	64	72b	H	H	-1,8-naphthyl-			
9		73a	H	Cl	Cl	H	69	1:4.9
10	65	73b	Cl	H	H	Cl		
11		74a	H	CN	CN	H	85	1:6.7
12	66	74b	CN	H	H	CN		
13		75a	H	Ph	Ph	H	93	1:2.3
14	67	75b	Ph	H	H	Ph		
15		76a	H	CO ₂ Me	CO ₂ Me	H	92	1:3
16	68	76b	CO ₂ Me	H	H	CO ₂ Me		

^a Determined by NMR analysis.

Two examples of intramolecular [5 + 2] epoxyindanone cycloadditions were reported in 1983 (Scheme 1.10).¹⁵ Irradiation of compound **77** to form cycloadduct **78** proceeded smoothly, but synthesis of **80** was hampered by the formation of byproducts associated with radical recombination pathways.

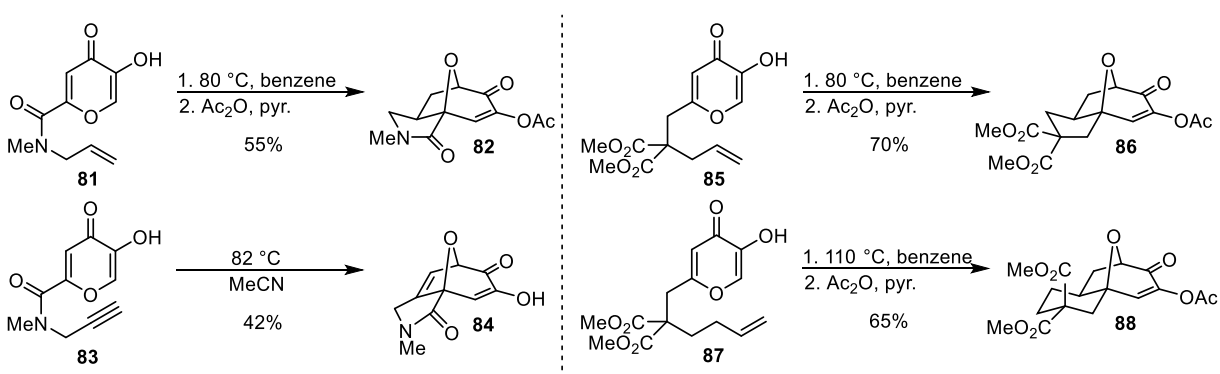
¹⁵ Feldman, K. S. *Tetrahedron Lett.* **1983**, 24, 5585–5586.



Scheme 1.10. Intramolecular [5 + 2] cycloadditions of benzopyryliums derived from epoxyindanones.

1.3.2 β -Hydroxy- γ -pyrones as Oxidopyrylium Precursors

The most recent class of oxidopyrylium precursors to be thoroughly described consists of derivatives of kojic acid. In 1983, the Garst group reported four new pyrolysis-promoted intramolecular [5 + 2] cycloaddition reactions (Scheme 1.11).¹⁶ Tethered olefins (**81**, **85**, **87**) and alkynes (**83**) participated in these transformation to generate cycloadducts bearing five-membered (**82**, **84**, **86**) and six-membered (**88**) product rings. In most cases, isolation required acetylation of the initially formed enol intermediate, but amide **84** could be characterized without this extra step.



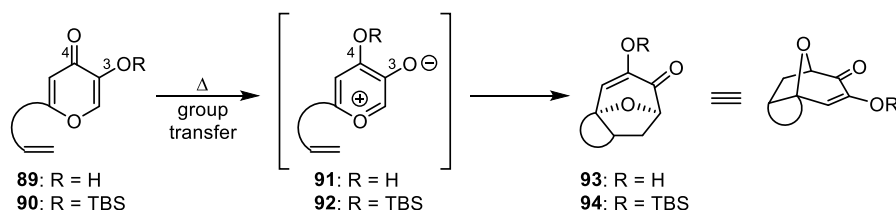
Scheme 1.11. The first [5 + 2] cycloadditions of β -hydroxy- γ -pyrones.

Mechanistically, these reactions were inspired by the group transfer step of the perezzone-pipitzol transformation¹⁷ and contemporary analysis of related kojic acid cycloadditions.¹⁸ Upon

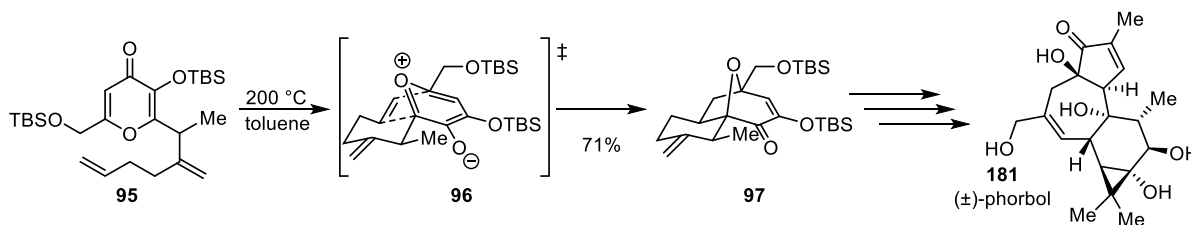
¹⁶ Garst, M. E.; McBride, B. J.; Douglass III, J. G. *Tetrahedron Lett.* **1983**, *24*, 1675–1678.

¹⁷ Sánchez, I. H.; Yáñez, R.; Enríquez, R.; Joseph-Nathan, P. *J. Org. Chem.* **1981**, *46*, 2818–2819.

heating, a β -hydroxy- γ -pyrone (e.g., **89**, Scheme 1.12) undergoes a proton migration from O3 to O4, generating the zwitterionic oxidopyrylium heterocycle **91**, which is trapped by the tethered dipolarophile to afford cycloadduct **93**.¹⁹ As an alternative to the proton transfer from **89** to **91**, the Wender group introduced silyl transfer (e.g., **90** to **92**) in their second generation synthesis of phorbol (Scheme 1.13).^{20,21} β -Silyloxy- γ -pyrone **95** undergoes a TBS-migration at 200 °C, which produces cycloadduct **97** as a single diastereomer. This excellent selectivity is implemented by a chair like transition state (**96**) in which the methyl-group on the forming six-membered ring preferentially adopts an equatorial orientation.



Scheme 1.12. Group transfer mechanism of β -hydroxy- γ -pyrone cycloadditions.



Scheme 1.13. Wender's silyl-migration method.

Building off of a curious result reported by Garst,¹⁶ Wender and Mascareñas formalized an

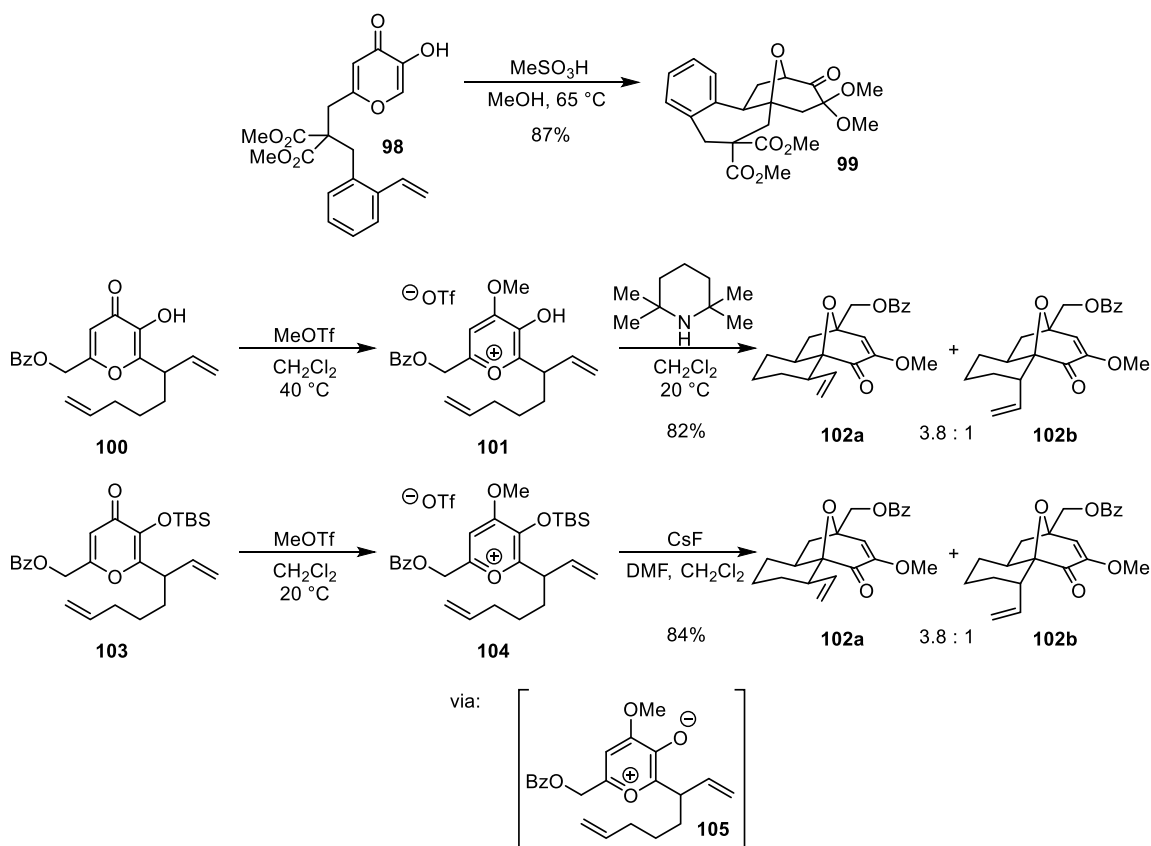
¹⁸ Volkmann, R. A.; Weeks, P. D.; Kuhla, D. E.; Whipple, E. B.; Chmurny, G. N. *J. Org. Chem.* **1977**, *42*, 3976–3978.

¹⁹ This mechanism has been rigorously analyzed by DFT calculations: (a) Domingo, L. R.; Zaragoza, R. J. *J. Org. Chem.* **2000**, *65*, 5480–5486. (b) Domingo, L. R.; Zaragoza, R. J. *Tetrahedron* **2001**, *57*, 5597–5606. (c) Zaragoza, R. J.; Aurell, M. J.; Domingo, L. R. *J. Phys. Org. Chem.* **2005**, *18*, 610–615.

²⁰ Wender, P. A.; McDonald, F. E. *J. Am. Chem. Soc.* **1990**, *112*, 4956–4958.

²¹ A more detailed outline of [5 + 2] oxidopyrylium cycloadditions in total syntheses is presented in Section 1.5.

alternative, lower temperature activation strategy (Scheme 1.14).²² Garst reported that olefin **98**, when heated with methanesulfonic acid in methanol, cyclized to 8-oxabicyclooctanone **99**. Akin to their previously reported synthesis of cycloadduct **97**, Wender and Mascareñas treated benzoate **100** with methyl triflate in order to methylate the carbonyl oxygen. Deprotonation of cationic intermediate **101** with TMP generated oxidopyrylium **105**, which rapidly reacted with the distal tethered olefin to form products **102a** and **102b** in a 3.8:1 ratio of diastereomers. Likewise, methylation of compound **103** afforded **104**, and desilylation of this intermediate produced the same oxidopyrylium **105**, which cyclized to **102a** and **102b** with the same stereoselectivity.

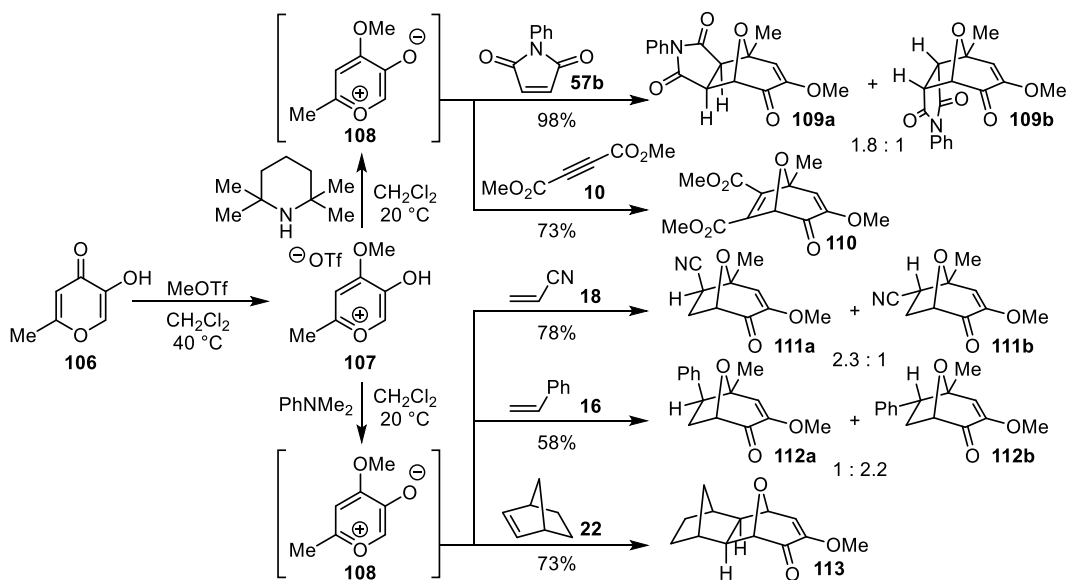


Scheme 1.14. Methylation-induced [5 + 2] cycloadditions.

Although intramolecular [5 + 2] cycloadditions of oxidopyryliums derived from γ -pyrones

²² Wender, P. A.; Mascareñas, J. L. *J. Org. Chem.* **1991**, *56*, 6267–6269.

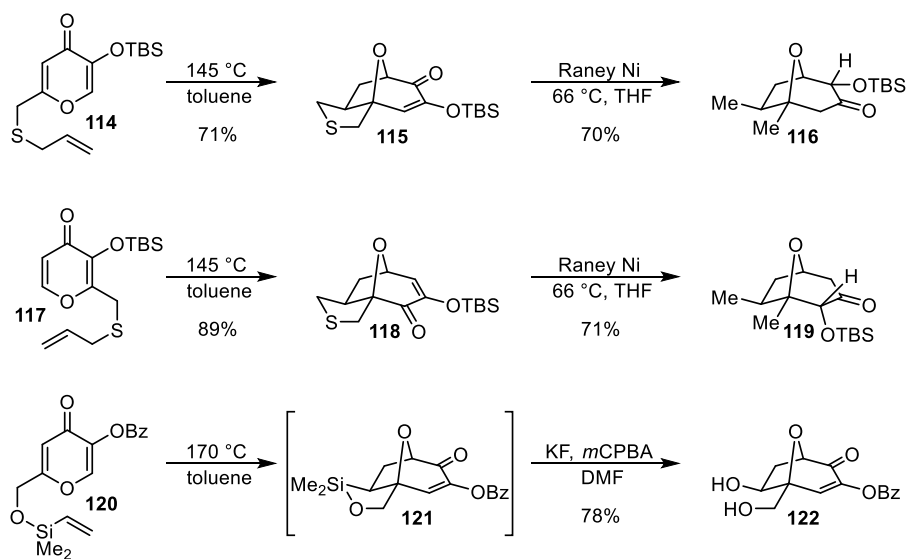
afford their desired products in high yields and predictable diastereoselectivities, analogous intermolecular reactions have been plagued by high failure rates or poor stereoselectivities. Wender and Mascareñas reported two methyl triflate/TMP-activated intermolecular reactions in 1992 (Scheme 1.15).²³ Oxiopyrylium **108** was successfully cyclized with *N*-phenylmaleimide **57b** to afford products *exo*-**109a** and *endo*-**109b** in low diastereoselectivity. Acetylene **10** provided cycloadduct **110** in reasonable yield under the same conditions. However, reactions with less reactive dipolarophiles such as acrylonitrile **18**, styrene **16**, and norbornene **22** resulted in the predominant dimerization of **108**. The authors reasoned that use of the less basic amine *N,N*-dimethylaniline would result in a lower concentration of reactive ylide **108** and thus decelerate dimerization. Under these gentler conditions, products **111**–**113** were synthesized in good yields. Norbornene adds to **108** with exclusively *exo*-selectivity, likely due to steric hindrance in the alternative *endo*-approach.



Scheme 1.15. Intermolecular [5 + 2] cycloadditions of β -hydroxy- γ -pyrones.

²³ Wender, P. A.; Mascareñas, J. L. *Tetrahedron Lett.* **1992**, 33, 2115–2118.

Mascareñas continued to study [5 + 2] oxidopyrylium cycloadditions during his independent career.²⁴ In 1993, his group reported temporary tethering strategies for producing intermolecular-type products from intramolecular reactions (Scheme 1.16).^{24a} Thioethers **114** and **117** underwent silyl-migration, oxidopyrylium formation, and cyclization at 145 °C. Treatment of adducts **115** and **118** with Raney nickel in refluxing THF effected desulfurization as well as an unexpected reduction/silyl-migration to afford products **116** and **119** respectively. Similarly, vinyl silyl ether **120** underwent one-pot [5 + 2] cycloaddition and desilylation to provide diol **122** in 78% yield overall.



Scheme 1.16. Temporary tethers in β -hydroxy- γ -pyrone [5 + 2] cycloadditions.

1.4 Asymmetric Access to the 8-Oxabicyclo[3.2.1]octane Core

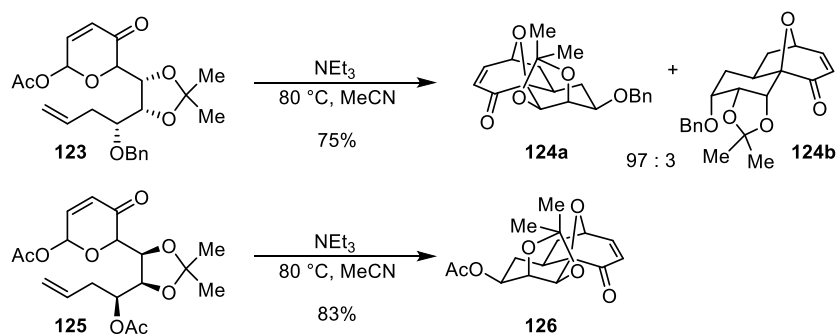
To this point, all reactions discussed have generated racemic mixtures of products. The vast majority of asymmetric [5 + 2] cycloadditions have utilized diastereoselective methods based on preinstalled chirality. In the following subsections, these will be discussed first. Next, a

²⁴ (a) Rumbo, A.; Castedo, L.; Mourino, A.; Mascareñas, J. L. *J. Org. Chem.* **1993**, *58*, 5585–5586. (b) Mascareñas, J. L.; Pérez, I.; Rumbo, A.; Castedo, L. *Synlett* **1997**, 81–82. (c) Rumbo, A.; Castedo, L. Mascareñas, J. L. *Tetrahedron Lett.* **1997**, *38*, 5885–5886.

summary of exceptional examples of catalytic asymmetric [3 + 2] cycloadditions toward related product scaffolds will be presented. This section will close with the two examples of modestly enantioselective catalytic [5 + 2] oxidopyrylium cycloadditions (prior to our work in Chapters 2 and 3). Examination of diastereoselective reactions in the context of natural product total syntheses will be deferred until Section 1.5.

1.4.1 Diastereoselective [5 + 2] Oxidopyrylium Cycloadditions

Trivedi and coworkers utilized D-ribose as a precursor for acetoxypyranones **123** and **125** (Scheme 1.17).²⁵ The necessity for a sugar starting material resulting in triol functionality on the tether certainly limits the generality of this method. Nonetheless, benzoate **123** could be cyclized to afford enantiomerically pure **124a** and **124b** as an inseparable mixture of diastereomers favoring a diequatorial orientation of substituents on the product cyclohexane ring, rather than diaxial. Similarly, acetate **125** reacted in refluxing acetonitrile, in the presence of triethylamine, to generate the pseudoenantiomer **126** in diastereomerically pure form.

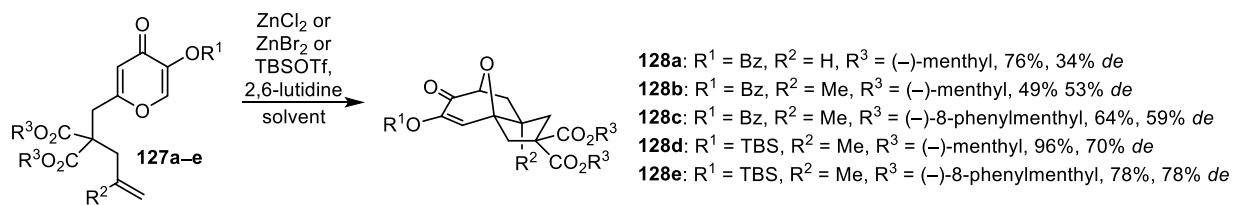


Scheme 1.17. Diastereoselective [5 + 2] cycloadditions of ribose-derived acetoxypyranones.

Capitalizing on the group transfer type mechanism, Ohmori and coworkers used menthol-based chiral auxiliaries on a tether diester to effect diastereoselective [5 + 2] cycloadditions,

²⁵ (a) Krishna, U. M.; Srikanth, G. S. C.; Trivedi, G. K.; Deodhar, K. D. *Synlett* **2003**, 2383–2385. (b) Krishna, U. M.; Deodhar, K. D.; Trivedi, G. K. *Tetrahedron* **2004**, *60*, 4829–4836.

generating products **128a–e** with moderate selectivity (Scheme 1.18).²⁶ These transformations proceeded through TBSOTf–lutidine or zinc activation.



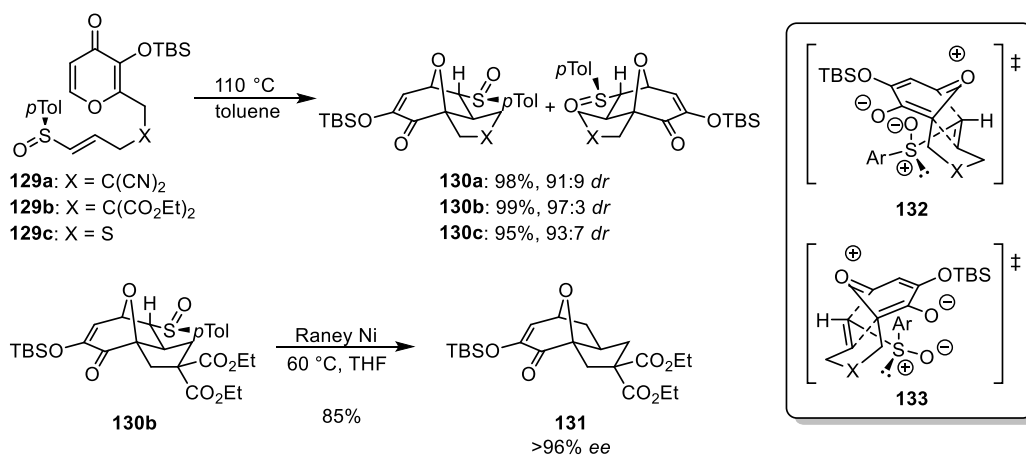
Scheme 1.18. Diastereoselective [5 + 2] cycloadditions of menthol diesters.

The most successful work on diastereoselective [5 + 2] oxidopyrylium cycloadditions was pioneered by the Mascareñas group. Building off of preliminary results,^{24c} Mascareñas and coworkers reported asymmetric reactions directed by an enantiopure sulfinyl auxiliary (Scheme 1.19).²⁷ Oxidopyrylium intermediates were generated by pyrolysis of γ -pyrones **129a–c** and captured by tethered sulfoxide-substituted olefins in up to 97:3 *dr* (**130b**). The diastereomers could be chromatographically separated and desulfinylation with Raney nickel afforded adduct **131** with near perfect retention of stereochemistry. The sense of diastereoselection was rationalized based on the proposal that the sulfoxide adopts a *syn*-coplanar conformation between its lone pair and the adjacent olefin. In the predominant transition state structure **132**, the sulfoxide auxiliary projects its oxygen substituent under the oxidopyrylium ring. In minor transition state **133**, the auxiliary must project the larger *p*-tolyl group against the ring, resulting in a substantial steric penalty for adopting this structure. This hypothesis was later supported by DFT calculations.²⁸

²⁶ Ohmori, N.; Yoshimura, M.; Ohkata, K. *Heterocycles* **1997**, *45*, 2097–2100.

²⁷ López, F.; Castedo, L.; Mascareñas, J. L. *Org. Lett.* **2000**, *2*, 1005–1007.

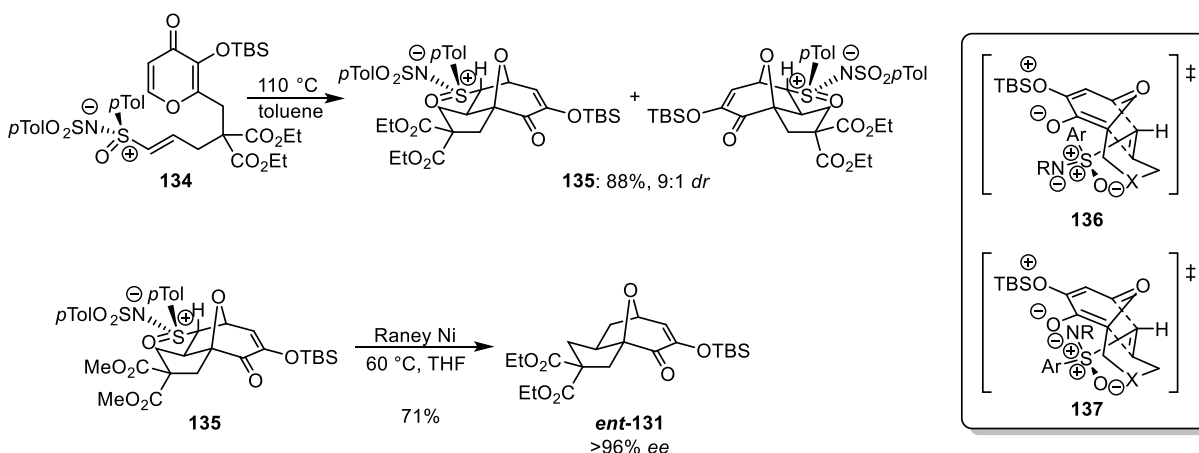
²⁸ López, F.; Castedo, L.; Mascareñas, J. L. *J. Org. Chem.* **2003**, *68*, 9780–9786.



Scheme 1.19. Sulfinyl-directed [5 + 2] oxidopyrylium cycloadditions.

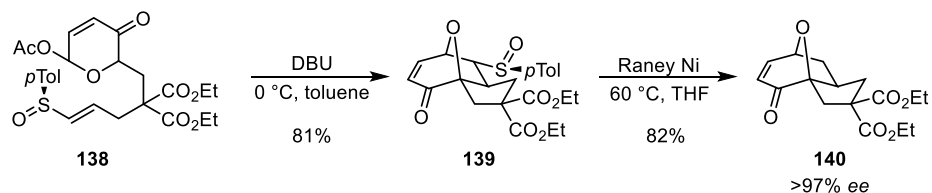
The following year, the Mascareñas group disclosed a procedure to synthesize the opposite enantiomer of **131** by using a related sulfoximine auxiliary (Scheme 1.20)²⁹ Although the sulfoximine in substrate **134** derives from the same sulfoxide used in **129**, it favors the opposite sense of diastereoselectivity in product **135** by a ratio of 9:1. This result originates from a change in major (**136**) and minor (**137**) transition states. The sulfoximine no longer has a lone pair, so the oxygen substituent adopts the *syn*-coplanar orientation with the olefin. As such, the preferred transition state (**136**) is now the one with the *p*-tolyl projected into the ring, as this group is smaller than the sulfonamide that clashes with the ring in **137**. Again, this hypothesis has been borne out by DFT calculations.²⁸

²⁹ López, F.; Castedo, L.; Mascareñas, J. L. *Org. Lett.* **2001**, *3*, 623–625.



Scheme 1.20. Sulfoximine-directed [5 + 2] oxidopyrylium cycloadditions.

Finally, Mascareñas and coworkers expanded their sulfinyl-directed asymmetric reactions to an acetoxy pyranone starting material (Scheme 1.21).³⁰ Upon treatment with DBU, compound **138** undergoes ionization and intramolecular cycloaddition to generate adduct **139** as a single diastereomer, via a transition state analogous to **132**. Desulfinylation affords **140** in nearly complete enantiopurity. This represents the only reported example of this type of transformation.



Scheme 1.21. Sulfinyl-directed [5 + 2] oxidopyrylium cycloaddition of an acetoxy pyranone.

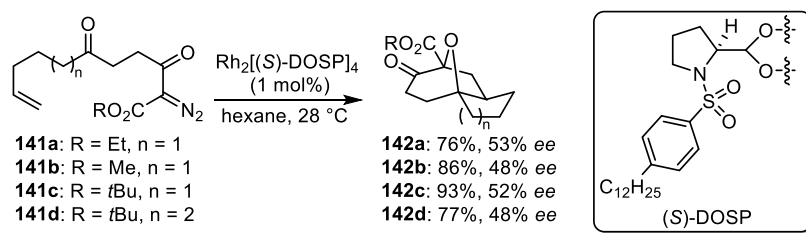
1.4.2 Catalytic Enantioselective [3 + 2] Carbonyl Ylide Cycloadditions

Based on seminal work on rhodium catalysis by Padwa and coworkers,³¹ the Hodgson group has contributed several chiral catalysts for enantioselective [3 + 2] cycloaddition reactions. In 1997, they reported the first such intramolecular reaction, utilizing an *N*-[(4-dodecylphenyl)]

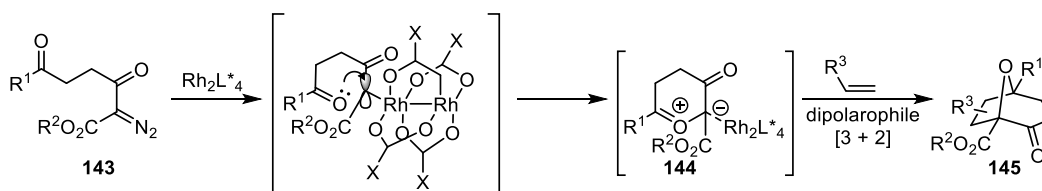
³⁰ López, F.; Castedo, L.; Mascareñas, J. L. *Org. Lett.* **2002**, *4*, 3683–3685.

³¹ For a review, see: Padwa, A.; Weingarten, M. D. *Chem. Rev.* **1996**, *96*, 223–270.

sulphonyl]proline (DOSP) ligand (Scheme 1.22).³² Cycloadditions proceed in high yields and moderate enantioselectivities. However, an important mechanistic distinction must be highlighted between these reactions and the previously discussed [5 + 2] transformations. Hodgson's Rh-catalyzed reactions proceed through a carbonyl ylide (i.e., **144**, Scheme 1.23) rather than an oxidopyrylium ylide. The π -system in these reactions does not extend all the way around the six-membered ring. As such, the final products lack the α,β -unsaturation found in oxidopyrylium cycloaddition products; this functional handle is often used for subsequent complexity-generating modifications.³³



Scheme 1.22. Hodgson's first catalytic asymmetric [3 + 2] cycloaddition.



Scheme 1.23. Distinct mechanism of rhodium-catalyzed [3 + 2] cycloadditions.

Later catalyst developments led to improved levels of selectivity,³⁴ ultimately culminating in a wider examination of the substrate scope (Scheme 1.24).³⁵ Alkenes (**146a–d**) and alkynes

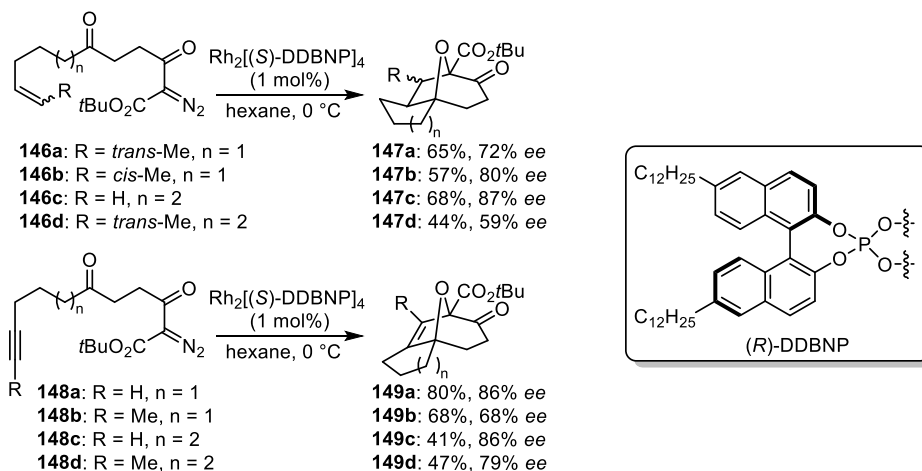
³² Hodgson, D. M.; Stupple, P. A.; Johnstone, C. *Tetrahedron Lett.* **1997**, *38*, 6471–6472.

³³ See Section 3.6.

³⁴ (a) Hodgson, D. M.; Stupple, P. A.; Johnstone, C. *Chem. Commun.* **1999**, 2185–2186. (b) Hodgson, D. M.; Stupple, P. A.; Pierard, F. Y. T. M.; Labande, A. H.; Johnstone, C. *Chem.–Eur. J.* **2001**, *7*, 4465–4476.

³⁵ (a) Hodgson, D. M.; Labande, A. H.; Pierard, F. Y. T. M. *Synlett* **2003**, 59–62. (b) Hodgson, D. M.; Labande, A. H.; Pierard, F. Y. T. M.; Expósito Castro, M. Á. *J. Org. Chem.* **2003**, *68*, 6153–6159.

(**148a–d**) both proved to be viable dipolarophiles, affording cycloadducts in a maximum of 87% *ee*. More recent efforts have pushed the limits of the substrate scope even further, but with no additional improvement in enantioselectivities.³⁶ Another limitation of this methodology lies in the fact that an electron-withdrawing ester group is required adjacent to the substrate's diazoketone.



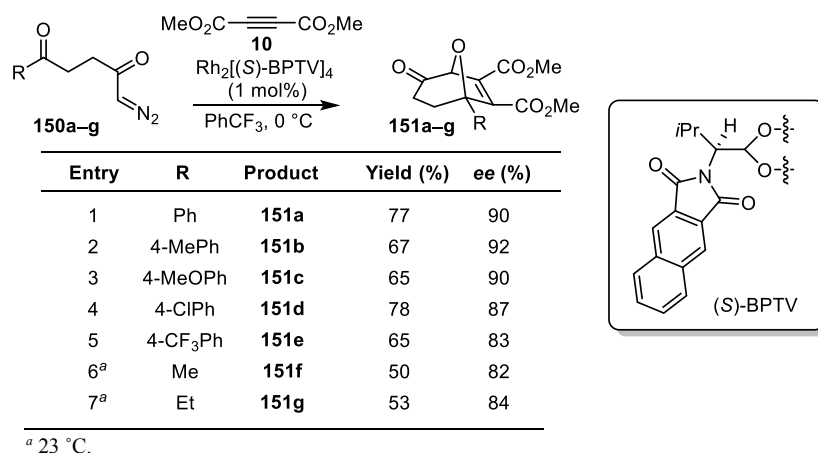
Scheme 1.24. Substrate scope of intramolecular rhodium-catalyzed [3 + 2] cycloadditions.

Research into the analogous intermolecular reaction was initiated by the Hashimoto group.³⁷ In these transformations, high enantioselectivity was observed with substrate diazoketones (**150a–g**) lacking an adjacent ester, when acetylene **10** was probed as an electrophile (Table 1.2). Cycloadducts were isolated in up to 92% *ee*.

³⁶ (a) Hodgson, D. M.; Selden, D. A.; Dossetter, A. G. *Tetrahedron: Asymmetry* **2003**, *14*, 3841–3849. (b) Hodgson, D. M.; Angrish, D.; Labande, A. H. *Chem. Commun.* **2006**, 627–628. (c) Hodgson, D. M.; Angrish, D. *Adv. Synth. Catal.* **2006**, *348*, 2509–2514.

³⁷ Kitagaki, S.; Anada, M.; Kataoka, O.; Matsuno, K.; Umeda, C.; Watanabe, N.; Hashimoto, S. *J. Am. Chem. Soc.* **1999**, *121*, 1417–1418.

Table 1.2. Intermolecular catalytic asymmetric [3 + 2] cycloadditions.

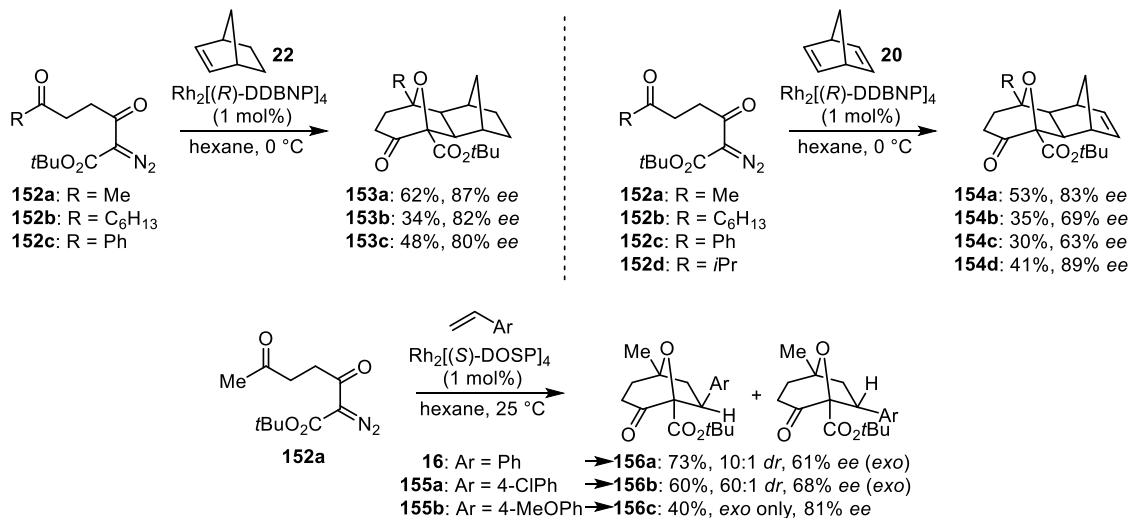


Following some preliminary work with monosubstituted alkynes, resulting in *ee*'s below 50%,³⁸ the Hodgson group experienced more success in the intermolecular reactions of olefins (Scheme 1.25).³⁹ Norbornene **22** and norbornadiene **20** afforded cycloadducts in up to 89% *ee*, with DDBNP ligands on rhodium. Monosubstituted styrenes (**16**, **155a**, and **155b**) also underwent reactions under these conditions, although higher enantio- and diastereoselectivities were observed after a ligand switch. These methodologies were later applied to syntheses of nemorensic acids.⁴⁰

³⁸ (a) Hodgson, D. M.; Glen, R.; Redgrave, A. J. *Tetrahedron Lett.* **2002**, *43*, 3927–3930. (b) Hodgson, D. M.; Glen, R.; Grant, G. H.; Redgrave, A. J. *J. Org. Chem.* **2003**, *68*, 581–586.

³⁹ (a) Hodgson, D. M.; Labande, A. H.; Glen, R.; Redgrave, A. J. *Tetrahedron: Asymmetry* **2003**, *14*, 921–924. (b) Hodgson, D. M.; Brückl, T.; Glen, R.; Labande, A. H.; Selden, D. A.; Dossetter, A. G.; Redgrave, A. J. *Proc. Natl. Acad. Sci. U.S.A.* **2004**, *101*, 5450–5454.

⁴⁰ Hodgson, D. M.; Le Strat, F.; Avery, T. D.; Donohue, A. C.; Brückl, T. *J. Org. Chem.* **2004**, *69*, 8796–8803.



Scheme 1.25. Expansion of the intermolecular substrate scope.

More recently, Iwasawa and coworkers used a platinum Walphos catalyst to effect a related [3 + 2] cycloaddition of ynone substrates (i.e., **157**, Table 1.3).⁴¹ These reactions are also mechanistically distinct from [5 + 2] cycloadditions in that—as in Hodgson and Hashimoto’s work—the key intermediate (**159**) is a carbonyl ylide rather than an oxidopyrylium ylide. Products **161a–k** are less functionally rich than oxidopyrylium cycloadducts in that they lack the carbonyl handle for further derivatizations.

Table 1.3. Iwasawa’s platinum-catalyzed [3 + 2] cycloadditions.

158

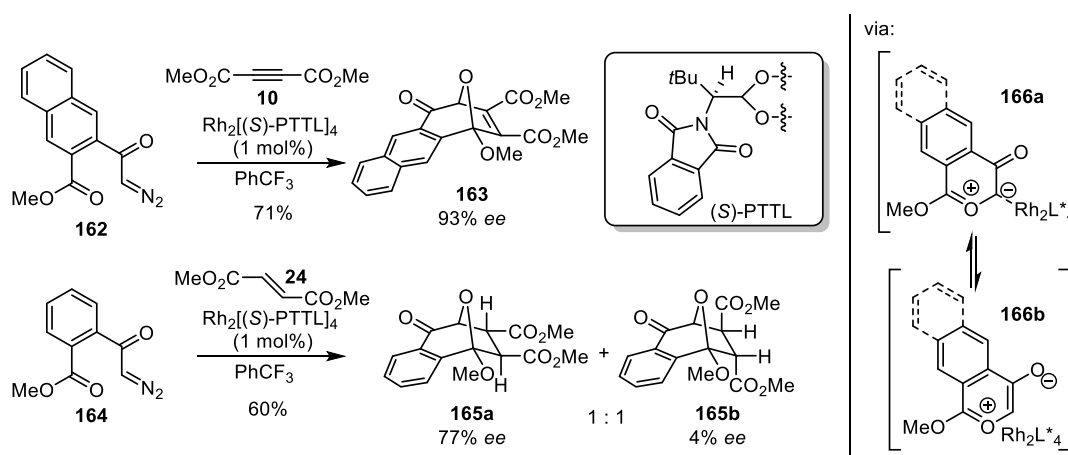
Entry	R ¹	R ²	R ³	Product	Yield (%)	ee (%)
1	Ph	Me	Bn	161a	70	91
2	4-MePh	Me	Bn	161b	70	91
3	4-CF ₃ Ph	Me	Bn	161c	79	89
4	CH ₂ CH ₂ Ph	Me	Bn	161d	80	91
5	CH ₂ CH ₂ Ph	Me	TIPS	161e	68	94
6	<i>i</i> Pr	Me	Bn	161f	89	90

Entry	R ¹	R ²	R ³	Product	Yield (%)	ee (%)
7	<i>i</i> Pr	Me	PMB	161g	69	91
8	(CH ₂) ₃ OTIPS	Me	Bn	161h	83	93
9	CH ₂ CH ₂ Ph	Bu	Bn	161i	50	96
10	Ph	CH ₂ OBn	Bn	161j	51	97
11	Ph	CH=CH ₂	TIPS	161k	65	97

⁴¹ Ishida, K.; Kusama, H.; Iwasawa, N. *J. Am. Chem. Soc.* **2010**, *132*, 8842–8843.

1.4.3 Catalytic Enantioselective [5 + 2] Benzopyrylium Cycloadditions

Aside from the research described in Chapters 2 and 3 of this dissertation, there have been only two reports of catalytic asymmetric [5 + 2] oxidopyrylium cycloadditions, both closely related to the rhodium-catalyzed [3 + 2] cycloadditions summarized in Section 1.4.2. In 2000, Hashimoto and coworkers expanded their intermolecular [3 + 2] cycloaddition reactions to diazoketone substrates containing benzene rings (Scheme 1.26).⁴² In these reactions, acetylene **10** provides product **163** in high yield and enantioselectivity. Olefin **24** could also act as the dipolarophile; although this reaction showed no diastereoselectivity, 77% *ee* was observed for one of the diastereomers.



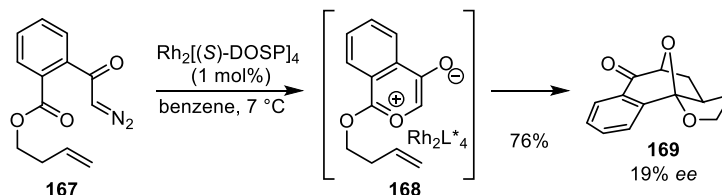
Scheme 1.26. A rhodium-catalyzed asymmetric [5 + 2] cycloaddition.

Despite the fact that carbonyl ylide **166a** (analogous to **144**, Scheme 1.23) is initially formed upon extrusion of N₂, it exists in equilibrium with oxidobenzopyrylium ylide **166b** (analogous to **34** and **51**, Schemes 1.6 and 1.8) in which the rhodium complex must still be sufficiently associated with the organic zwitterion to induce enantioselectivity. As such, the π -system extends around the entire ring and these reactions can formally be classified as [5 + 2]

⁴² Kitagaki, S.; Yasugahira, M.; Anada, M.; Nakajima, M.; Hashimoto, S. *Tetrahedron Lett.* **2000**, *41*, 5931–5935.

cycloadditions.

Similarly, the Hodgson group has studied the benzene containing diazoketone **167** in an intramolecular [5 + 2] benzopyrylium cycloaddition reaction (Scheme 1.27).⁴³ Although this transformation proceeds in 76% yield, an extensive ligand screen only engendered a maximum *ee* of 19%. Given the utility of oxidopyrylium-derived 8-oxabicyclo[3.2.1]oct-3-en-2-ones, as will be demonstrated in the subsequent section of this chapter, more efficient and selective methods for catalytic asymmetric [5 + 2] cycloadditions of this type would be highly valuable. Moreover, the ambiguous nature of catalyst/pyrylium association depicted in structures **166b** and **168** does not provide a satisfactory rationale for enantioselectivity. A more clearly defined mechanistic strategy for directly engaging these important intermediates through specific interactions was still lacking at the outset of our own research in this area.



Scheme 1.27. An intramolecular rhodium-catalyzed asymmetric [5 + 2] cycloaddition.

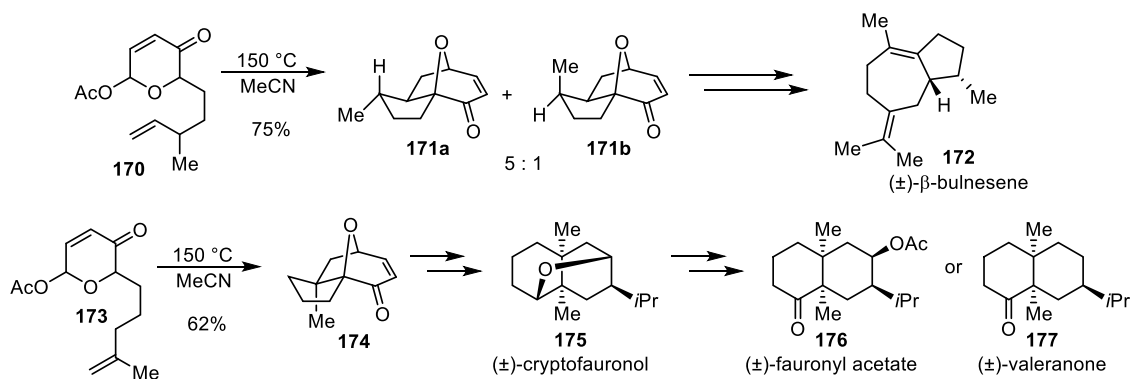
1.5 [5 + 2] Oxidopyrylium Cycloadditions in Total Syntheses

Since the 1980's, the [5 + 2] oxidopyrylium cycloaddition reaction has seen extensive application in the total synthesis of natural products and related cores bearing oxygenated seven-membered rings. This section by no measure represents an exhaustive survey of such work. Instead, the most remarkable examples of oxidopyrylium intermediates in total synthesis will be summarized herein, as a means to demonstrate the synthetic potential of a catalytic asymmetric variant of this powerful transformation. More comprehensive reviews have been published on the

⁴³ Hodgson, D. M.; Stupple, P. A.; Johnstone, C. *ARKIVOC* **2003**, 49–58.

subject.¹

Soon after they first explored the reactivity pattern of oxidopyrylium ylides, Sammes and Street applied this procedure to the total synthesis of four natural products in racemic form (Scheme 1.28).⁴⁴ Heat-promoted intramolecular cycloaddition of acetoxypyranone **170** afforded a 5:1 *dr* of intermediate **171a** and **171b**. The minor isomer was then elaborated in six steps to β -bulnesene **172**. Reaction of **173** under the same conditions efficiently generated common intermediate **174**, which could be transformed into cryptofauronol **175** in three steps. This natural product served as a precursor towards fauronyl acetate **176** and valeranone **177**.



Scheme 1.28. Four related total syntheses.

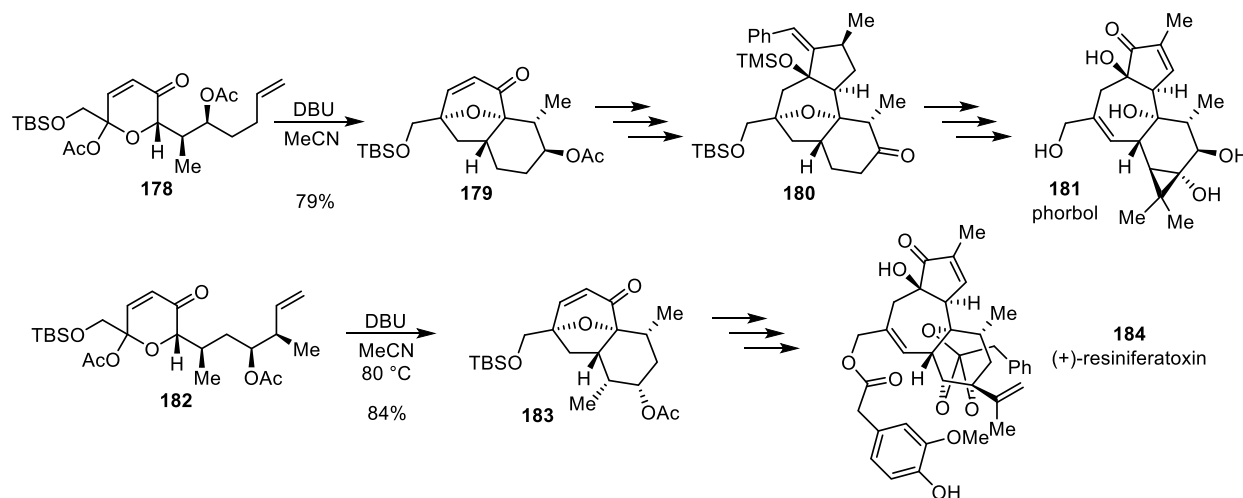
After several racemic synthetic routes,^{20,22,45} the Wender group reported the first formal asymmetric total synthesis of phorbol (**181**, Scheme 1.29) in 1997.⁴⁶ The key step of this landmark sequence relied upon the base-promoted [5 + 2] cycloaddition of acetate **178** to bicyclooctenone **179**, a reaction which proceeded with nearly perfect diastereoselectivity. Pyranone **178** was

⁴⁴ (a) Sammes, P. G.; Street, L. J. *J. Chem. Soc., Chem. Commun.* **1983**, 666–668. (b) Bromidge, S. M.; Sammes, P. G.; Street, L. J. *J. Chem. Soc., Perkin Trans. 1* **1985**, 1725–1730. (c) Sammes, P. G.; Street, L. J.; Whitby, R. J. *J. Chem. Soc., Perkin Trans. 1* **1986**, 281–289. See also related routes towards (\pm) -copaene and (\pm) -ylangene: (d) Archer, D. A.; Bromidge, S. M.; Sammes, P. G. *J. Chem. Soc., Perkin Trans. 1* **1988**, 3223–3228.

⁴⁵ Wender, P. A.; Kogen, H.; Lee, H. Y.; Munger, Jr., J. D.; Wilhelm, R. S.; Williams, P. D. *J. Am. Chem. Soc.* **1989**, *111*, 8957–8958.

⁴⁶ Wender, P. A.; Rice, K. D.; Schnute, M. E. *J. Am. Chem. Soc.* **1997**, *119*, 7897–7898.

synthesized in enantiomerically pure form via a chiral auxiliary-mediated aldol condensation. Cycloadduct **179** was then elaborated to intermediate **180** as a single enantiomer. The racemic conversion of **180** to the potent antitumor and anti-HIV natural product (**181**) had previously been accomplished.⁴⁶



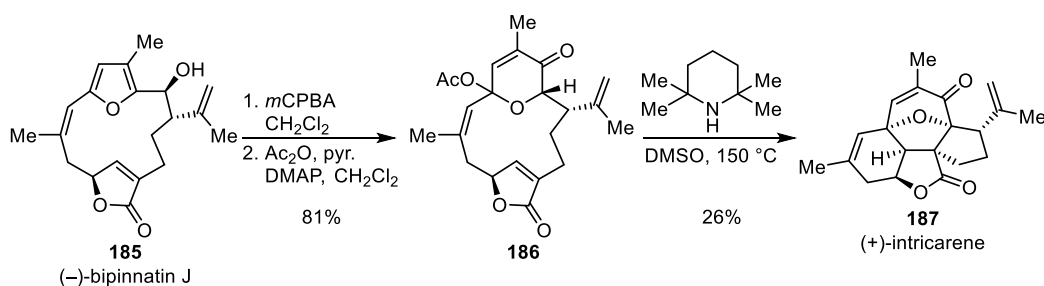
Scheme 1.29. Wender's asymmetric total syntheses of phorbol and resiniferatoxin.

In a subsequent publication, Wender and coworkers reported the first asymmetric total synthesis of the daphnane diterpine resiniferatoxin (**184**) utilizing a similar strategy.⁴⁷ Precursor **182** was derived as a single enantiomer from an enantiopure chiral epoxide, then underwent completely diastereoselective cycloaddition to afford intermediate **183**. This compound was carried through to the natural product. In the years since, the Wender group has continued to study [5 + 2] oxidopyrylium cycloadditions as a general strategy towards the synthesis of tiglianes, daphnanes, and ingenanes.⁴⁸

⁴⁷ Wender, P. A.; Jesudason, C. D.; Nakahira, H.; Tamura, N.; Tebbe, A. L.; Ueno, Y. *J. Am. Chem. Soc.* **1997**, *119*, 12976–12977.

⁴⁸ (a) Wender, P. A.; Lee, H. Y.; Wilhelm, R. S.; Williams, P. D. *J. Am. Chem. Soc.* **1989**, *111*, 8954–8957. (b) Wender, P. A.; Bi, F. C.; Buschmann, N.; Gosselin, F.; Kan, C.; Kee, J.-M.; Ohmura, H. *Org. Lett.* **2006**, *8*, 5373–5376. (c) Wender, P. A.; D'Angelo, N. D.; Elitzin, V. I.; Ernst, M.; Jackson-Ugueto, E. E.; Kowalski, J. A.; McKendry, S.; Rehfeuter, M.; Sun, R.; Voigtlaender, D. *Org. Lett.* **2007**, *9*, 1829–1832. (d) Wender, P. A.; Buschmann, N.; Cardin, N. B.; Jones, L. R.; Kan, C.; Kee, J.-M.; Kowalski, J. A.; Longcore, K. E. *Nat. Chem.* **2011**, *3*, 615–619.

In 2006, the groups of Trauner⁴⁹ and Pattenden⁵⁰ independently reported conversions of the natural product (–)-bipinnatin J (**185**, Scheme 1.30) into (+)-intricarene (**187**). Although the key cycloaddition only occurred in 26% and 10% yields respectively, it served to corroborate a longstanding biosynthetic hypothesis that enzymatic oxidation followed by dehydration of bipinnatin J could form an oxidopyrylium, which would then undergo cycloaddition. DFT calculations by the Tantillo group demonstrated that enzymatic intervention would be necessary for formation of the putative oxidopyrylium, but that the preorganization of this scaffold would provide a significant energetic benefit for the subsequent transannular cycloaddition.⁵¹ This [5 + 2] step, they propose, could occur without the assistance of an enzyme.



Scheme 1.30. Trauner's conversion of bipinnatin J to intricarene.

More recently, the Pattenden group has utilized a [5 + 2] cycloaddition reaction in their total synthesis of racemic anthecularin (**191**, Scheme 1.31).⁵² The previously described asymmetric strategies would not work in this sequence. Even if the authors had used an enantiopure acetate (**188**) as substrate, all stereochemical information would have been lost in oxidopyrylium intermediate **189**. Only a catalytic enantioselective reaction, a stoichiometric reagent, or the use of

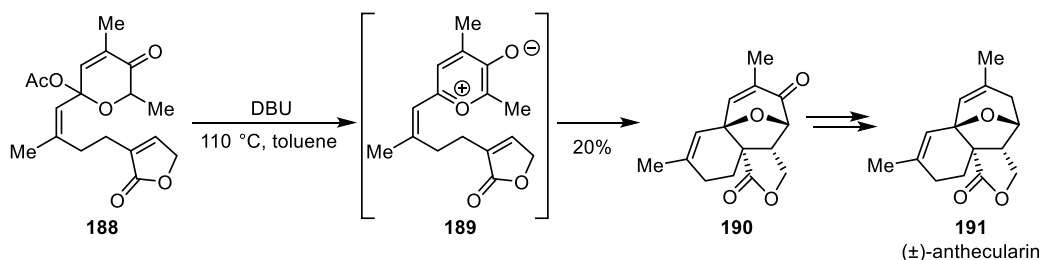
⁴⁹ Roethle, P. A.; Hernandez, P. T.; Trauner, D. *Org. Lett.* **2006**, *8*, 5901–5904.

⁵⁰ (a) Tang, B.; Bray, C. D.; Pattenden, G. *Tetrahedron Lett.* **2006**, *47*, 6401–6404. (b) Tang, B.; Bray, C. D.; Pattenden, G. *Org. Biomol. Chem.* **2009**, *7*, 4448–4457.

⁵¹ Wang, S. C.; Tantillo, D. J. *J. Org. Chem.* **2008**, *73*, 1516–1523.

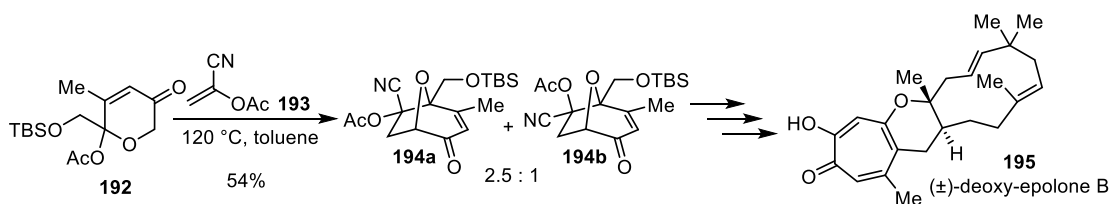
⁵² Li, Y.; Nawrat, C. C.; Pattenden, G.; Winne, J. M. *Org. Biomol. Chem.* **2009**, *7*, 639–640.

a chiral auxiliary to be removed later, could afford **190** in non-racemic form.



Scheme 1.31. Pattenden's total synthesis of anthecularin.

Baldwin and coworkers have leveraged both intermolecular⁵³ and intramolecular⁵⁴ [5 + 2] cycloadditions towards the synthesis of tropolone skeletons, including a total synthesis of deoxy-epolone B (**195** Scheme 1.32).^{53a} Thermal cycloaddition of acetoxytropolone **192** with α -acetoxyacrylonitrile **193** afforded **194a** and **194b** in a 2.5:1 ratio of diastereomers. Again, since neither the 5π nor the 2π component possesses stereogenicity, this reaction could not be rendered asymmetric without the aid of a chiral catalyst, auxiliary, or stoichiometric reagent. Both diastereomers of **194** were then elaborated to deoxy-epolone B through a sequence involving a final-step hetero-Diels–Alder reaction with the sesquiterpene natural product humulene.



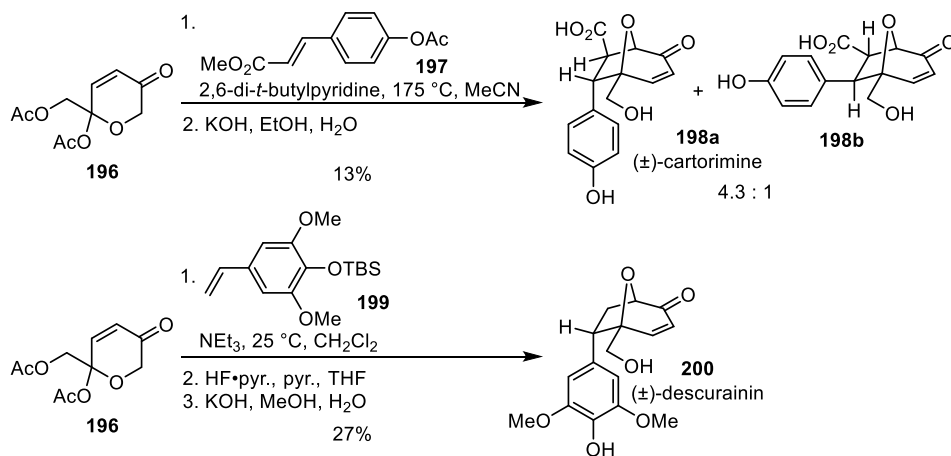
Scheme 1.32. Baldwin's total synthesis of deoxy-epolone B.

Snider and Grabowski recently reported the total syntheses of racemic cartormine (**198a**) and descurainin (**201**, Scheme 1.33) using styrenes as dipolarophiles in [5 + 2] cycloaddition

⁵³ (a) Adlington, R. M.; Baldwin, J. E.; Mayweg, A. V. W.; Pritchard, G. J. *Org. Lett.* **2002**, *4*, 3009–3011. (b) Baldwin, J. E.; Mayweg, A. V. W.; Pritchard, G. J.; Adlington, R. M. *Tetrahedron Lett.* **2003**, 4543–4545.

⁵⁴ Celanire, S.; Marlin, F.; Baldwin, J. E.; Adlington, R. M. *Tetrahedron* **2005**, *61*, 3025–3032.

reactions.⁵⁵ Cycloaddition of diacetate **196** with **197** required both high temperature as well as a bulky pyridine base. Ester hydrolysis of the cycloadduct afforded cartormine in a 4.3:1 *dr* with **198b**. Diacetate **196** underwent completely diastereoselective cycloaddition with **199** to afford, after two deprotection steps, descurainin in 27% yield. The groups of Snider and Hashimoto later collaborated to use this approach for a formal total synthesis of racemic polygaloides.⁵⁶



Scheme 1.33. Snider's total syntheses of cartormine and descurainin.

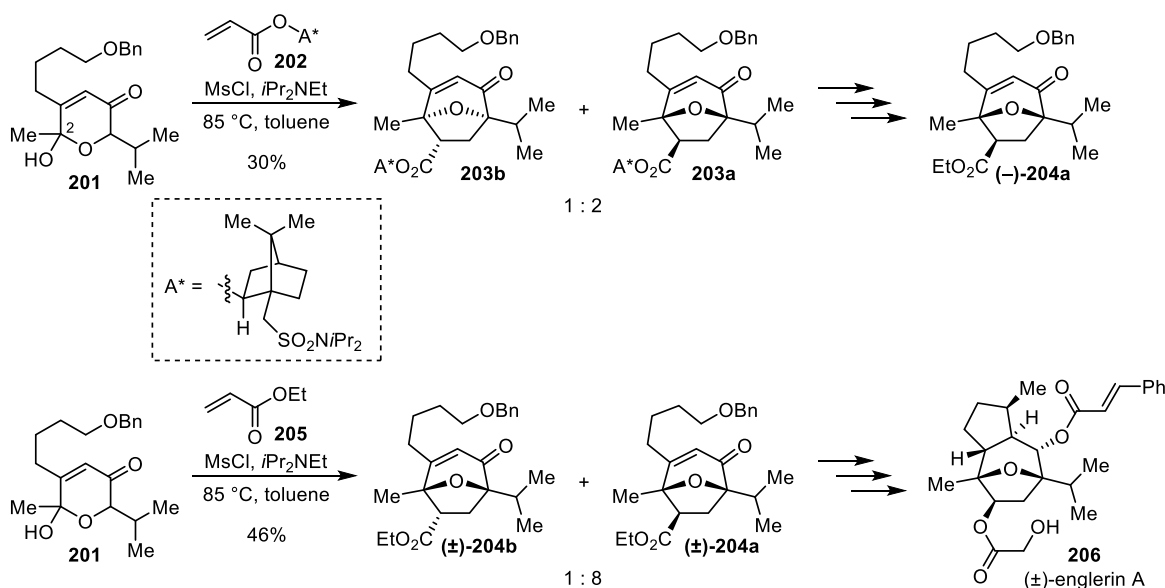
In 2010, the Nicolaou and Chen groups reported a formal asymmetric total synthesis of englerin A (**206**, Scheme 1.34).⁵⁷ After extensive screening of conditions, the researchers found that placing a sulfonamide-derived chiral auxiliary (A*) onto their acrylate dipolarophile (**202**) and performing a one-pot mesylation/elimination of the C2 hydroxyl-group provided optimal yield and diastereoselectivity in favor of the desired cycloadduct (**203a**). Instead of proceeding to the natural product from this enantiopure intermediate, they transesterified the major diastereomer to (–)-**204a**, a compound they could generate more efficiently in racemic form using ethyl acrylate **205**

⁵⁵ (a) Snider, B. B.; Grabowski, J. F. *Tetrahedron Lett.* **2005**, *46*, 823–825. (b) Snider, B. B.; Grabowski, J. F. *Tetrahedron* **2006**, *62*, 5171–5177.

⁵⁶ Snider, B. B.; Wu, X.; Nakamura, S.; Hashimoto, S. *Org. Lett.* **2007**, *9*, 873–874.

⁵⁷ Nicolaou, K. C.; Kang, Q.; Ng, S. Y.; Chen, D. Y.-K. *J. Am. Chem. Soc.* **2010**, *132*, 8219–8222.

as a dipolarophile. This cycloaddition demonstrated an 8:1 *dr* in favor of the desired *exo*-isomer **204a**, which was then elaborated to racemic englerin A. As in the previous three total syntheses discussed, there is no stereochemical information retained in the transition state for cycloaddition of **201** with **205**. Absent methods for asymmetric catalysis, this necessitated the use of a chiral auxiliary in **202** to effect an asymmetric reaction. To date, this is the only instance of this auxiliary strategy appearing in a total synthesis.



Scheme 1.34. Nicolaou and Chen's total synthesis of englerin A.

Aside from the aforementioned total syntheses, several synthetic studies and partial syntheses merit mention. The Magnus group has developed [5 + 2] oxidopyrylium cycloadditions as a means to construct the BC-ring system of taxol.⁵⁸ Hoffmann and Heathcock have studied the

⁵⁸ (a) Bauta, W.; Booth, J.; Bos, M. E.; DeLuca, M.; Diorazio, L.; Donohoe, T.; Magnus, N.; Magnus, P.; Mendoza, J.; Pye, P.; Tarrant, J.; Thom, S.; Ujjainwalla, F. *Tetrahedron Lett.* **1995**, *36*, 5327–5330. (b) Bauta, W. E.; Booth, J.; Bos, M. E.; DeLuca, M.; Diorazio, L.; Donohoe, T. J.; Frost, C.; Magnus, N.; Magnus, P.; Mendoza, J.; Pye, P.; Tarrant, J. G.; Thom, S.; Ujjainwalla, F. *Tetrahedron* **1996**, *52*, 14081–14102. See also: (c) Magnus, P.; Shen, L. *Tetrahedron* **1999**, *55*, 3553–3560. (d) Magnus, P.; Waring, M. J.; Ollivier, C.; Lynch, V. *Tetrahedron Lett.* **2001**, *42*, 4947–4950.

transformation in the context of the dioxatricyclic core of dictyoxetane.⁵⁹ Ohmori has extensively explored [5 + 2] cycloadditions as a means to approach the ring system of phomoidride B.⁶⁰ Krishna and Trivedi have also used indene as a dipolarophile in studies towards the 7-5-6 fused ring system of FCRR toxin.⁶¹

Finally, Krishna has used ring-opening strategies to approach the furopyran core of natural products such as dysiherbaine, neodysiherbaine A, and malayamicin A (Scheme 1.35).⁶² In 2007, Trivedi and Salunkhe reported a Beckmann fragmentation procedure to open oximes **207** to oxocarbeniums **208**, which are then stereospecifically trapped by solvent on the more exposed face, to afford tetrahydrofurans **209**.⁶³ Similarly, the Fishwick group described an ozonolytic approach to tetrahydrofurans **211** following stereospecific Luche reduction of cycloadducts such as **2**.⁶⁴ Krishna utilized a variation on the former methodology to achieve the synthesis of furopyrans **215a–c**.⁶²

⁵⁹ (a) Reinecke, J.; Hoffmann, H. M. R. *Chem.–Eur. J.* **1995**, *1*, 368–373. (b) Marshall, K. A.; Mapp, A. K.; Heathcock, C. H. *J. Org. Chem.* **1996**, *61*, 9135–9145.

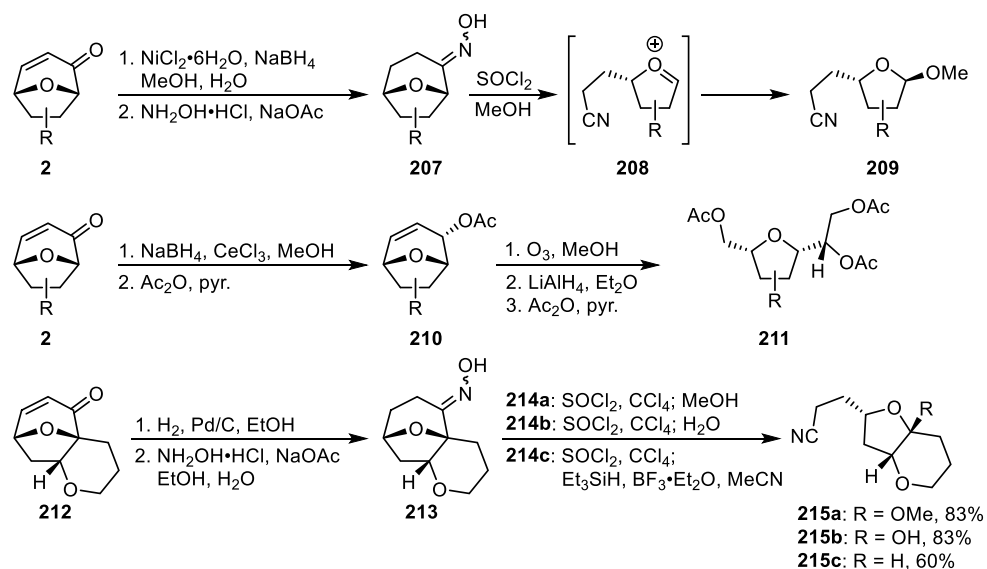
⁶⁰ Ohmori, N. *J. Chem. Soc., Perkin Trans. 1*, **2002**, 755–767.

⁶¹ Krishna, U. M.; Trivedi, G. K. *Tetrahedron Lett.* **2004**, *45*, 257–259.

⁶² Krishna, U. M. *Tetrahedron Lett.* **2010**, *51*, 2148–2150.

⁶³ Yadav, A. A.; Sarang, P. S.; Trivedi, G. K.; Salunkhe, M. M. *Synlett* **2007**, 989–991.

⁶⁴ Fishwick, C. W. G.; Mitchell, G.; Pang, P. F. W. *Synlett* **2005**, 285–286.



Scheme 1.35. Conversion of 8-oxabicyclo[3.2.1]oct-3-en-2-one cycloadducts to tetrahydrofurans.

1.6 Outlook

The [5 + 2] cycloaddition reactions of oxidopyrylium ylides are powerful means to rapidly generate a great deal of molecular complexity in chiral 8-oxabicyclo[3.2.1]oct-3-en-2-one scaffolds. These structures bear various functional handles (e.g., ether, enone) for further diversification, making them valuable intermediates for the construction of manifold downstream derivatives. Although a few asymmetric methods using chiral auxiliaries or chiral pool starting materials have been reported—and despite pervasive use of these reactions in total syntheses—no general catalytic asymmetric approaches for employing these versatile dipoles had been reported as of 2009. Since then, we have reported the only such methodologies, in research that will be described in the following two chapters.

Hydrogen-Bonding and Primary Amine Catalysis in Enantioselective [5 + 2] Pirylium Cycloadditions¹

2.1 Introduction

The [5 + 2] dipolar cycloaddition of oxidopyrylium ylides (i.e., **2**, Scheme 2.1) and two-carbon dipolarophiles generates complex, chiral 8-oxabicyclo[3.2.1]octane architectures **3**.² In addition to bearing a structural motif common to numerous natural products,³ such cycloadducts have proven to be highly valuable intermediates in the synthesis of functionalized seven-membered carbocycles⁴ and tetrahydrofuran derivatives.⁵ Despite the utility of this [5 + 2]

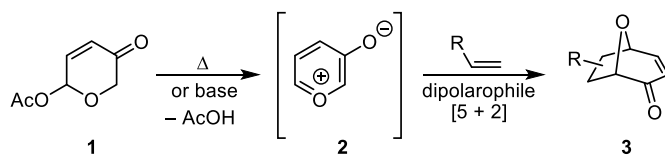
¹ Portions of this chapter have been published: Burns, N. Z.; Witten, M. R.; Jacobsen, E. N. *J. Am. Chem. Soc.* **2011**, *133*, 14578–14581. Adapted with permission. Copyright 2011 American Chemical Society.

² For recent reviews, see: (a) Singh, V.; Krishna, U. M.; Vikrant; Trivedi, G. K. *Tetrahedron* **2008**, *64*, 3405–3428. (b) Pellissier, H. *Adv. Synth. Catal.* **2011**, *353*, 189–218. (c) Ylijoki, K. E. O.; Stryker, J. M. *Chem. Rev.* **2013**, *113*, 2244–2266.

³ For example, Englerin A: (a) Ratnayake, R.; Covell, D.; Ransom, T. T.; Gustafson, K. R.; Beutler, J. A. *Org. Lett.* **2009**, *11*, 57–60. Phorbol: (b) Hecker, E.; Schmidt, R. *Fortschr. Chem. Org. Naturst.* **1974**, *31*, 377–467. Secodolastanes: (c) Teixeira, V. L.; Tomassini, T.; Fleury, B. G.; Kelecom, A. *J. Nat. Prod.* **1986**, *49*, 570–575. Cortistatin A: (d) Aoki, S.; Watanabe, Y.; Sanagawa, M.; Setiawan, A.; Kotoku, N.; Kobayashi, M. *J. Am. Chem. Soc.* **2006**, *128*, 3148–3149. Anthecularin: (e) Karioti, A.; Skaltsa, H. Linden, A.; Perozzo, R.; Brun, R.; Tasdemi, D. *J. Org. Chem.* **2007**, *72*, 8103–8106. Intricarene: (f) Marrero, J.; Rodríguez, A. D.; Barnes, C. L. *Org. Lett.* **2005**, *7*, 1877–1880. Komaroviquinone: (g) Uchiyama, N.; Kiuchi, F.; Ito, M.; Honda, G.; Takeda, Y.; Khodzhimatov, O. K.; Ashurmetov, O. A. *J. Nat. Prod.* **2003**, *66*, 128–131. Descurainin: (h) Sun, K.; Li, X.; Li, W.; Wang, J.; Liu, J.; Sha, Y. *Chem. Pharm. Bull.* **2004**, *52*, 1483–1486. Cartorimine: (i) Yin, H.-B.; He, Z.-S.; Ye, Y. *J. Nat. Prod.* **2000**, *63*, 1164–1165.

⁴ (a) Wender, P. A.; Lee, H. Y.; Wilhelm, R. S.; Williams, P. D. *J. Am. Chem. Soc.* **1989**, *111*, 8954–8957. (b) Bromidge, S. M.; Sammes, P. G.; Street, L. J. *J. Chem. Soc., Perkin Trans. 1* **1985**, 1725–1730.

cycloaddition and its widespread use in organic synthesis,⁶ asymmetric examples to date have been limited to diastereoselective variants,⁷ and there are currently no catalytic enantioselective methods that engage reactive pyrylium intermediates in cycloaddition chemistry.^{8,9}



Scheme 2.1. The [5 + 2] oxidopyrylium cycloaddition.

Our group has recently demonstrated that small-molecule chiral hydrogen-bond donor catalysts can serve as anion abstractors and binders in the generation and enantioselective transformation of highly reactive cationic intermediates.¹⁰ For example, in 2007, we reported that

⁵ (a) Krishna, U. M. *Tetrahedron Lett.* **2010**, *51*, 2148–2150. (b) Yadav, A. A.; Sarang, P. S.; Trivedi, G. K.; Salunkhe, M. M. *Synlett* **2007**, 989–991. (c) Fishwick, C. W. G.; Mitchell, G.; Pang, P. F. W. *Synlett* **2005**, 285–286.

⁶ (a) Wender, P. A.; Kogen, H.; Lee, H. Y.; Munger, Jr., J. D.; Wilhelm, R. S.; Williams, P. D. *J. Am. Chem. Soc.* **1989**, *111*, 8957–8958. (b) Wender, P. A.; Jesudason, C. D.; Nakahira, H.; Tamura, N.; Tebbe, A. L.; Ueno, Y. *J. Am. Chem. Soc.* **1997**, *119*, 12976–12977. (c) Ali, M. A.; Bhogal, N.; Findlay, J. B. C.; Fishwick, C. W. G. *J. Med. Chem.* **2005**, *48*, 5655–5658. (d) Roethle, P. A.; Hernandez, P. T.; Trauner, D. *Org. Lett.* **2006**, *8*, 5901–5904. (e) Li, Y.; Nawrat, C. C.; Pattenden, G.; Winne, J. M. *Org. Biomol. Chem.* **2009**, *7*, 639–640. (f) Nicolaou, K. C.; Kang, Q.; Ng, S. Y.; Chen, D. Y.-K. *J. Am. Chem. Soc.* **2010**, *132*, 8219–8222.

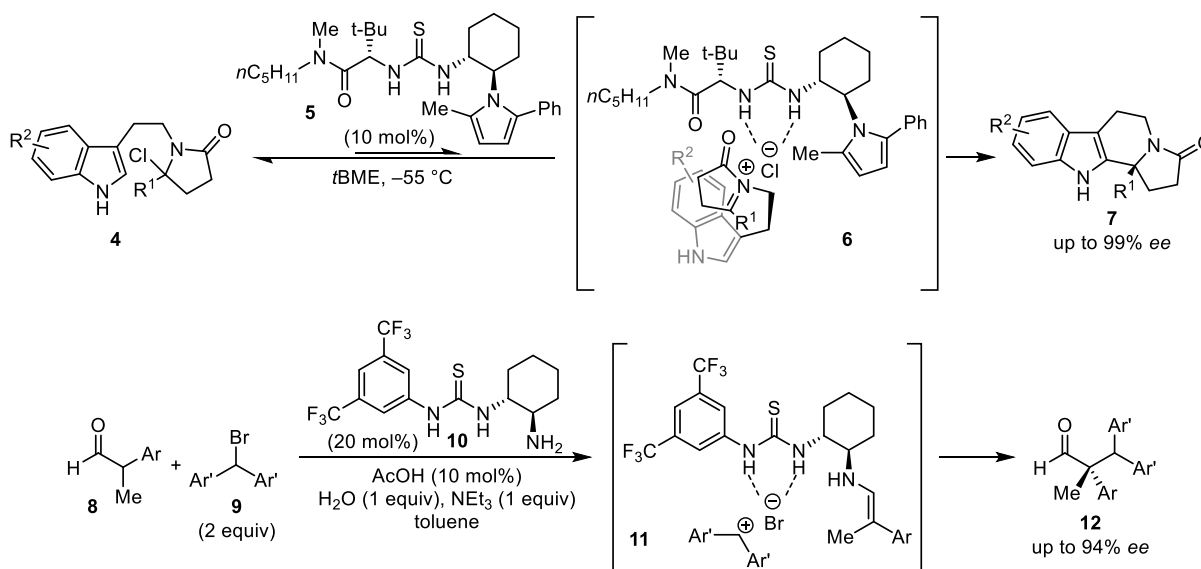
⁷ (a) Wender, P. A.; Rice, K. D.; Schnute, M. E. *J. Am. Chem. Soc.* **1997**, *119*, 7897–7898. (b) López, F.; Castedo, L.; Mascareñas, J. L. *Org. Lett.* **2000**, *2*, 1005–1007. (c) López, F.; Castedo, L.; Mascareñas, J. L. *Org. Lett.* **2002**, *4*, 3683–3685. (d) Wender, P. A.; Bi, F. C.; Buschmann, N.; Gosselin, F.; Kan, C.; Kee, J.-M.; Ohmura, H. *Org. Lett.* **2006**, *8*, 5373–5376. (e) Garnier, E. C.; Liebeskind, L. S. *J. Am. Chem. Soc.* **2008**, *130*, 7449–7458.

⁸ For isolated examples of Rh-catalyzed benzopyrylium cycloadditions, see: (a) Hodgson, D. M.; Stuppel, P. A.; Johnstone, C. *ARKIVOC* **2003**, 49–58. (b) Kitagaki, S.; Yasugahira, M.; Anada, M.; Nakajima, M.; Hashimoto, S. *Tetrahedron Lett.* **2000**, *41*, 5931–5935.

⁹ Transition-metal-catalyzed asymmetric 1,3-dipolar cycloadditions of carbonyl ylides to access similar products have been reported. See: (a) Kitagaki, S.; Anada, M.; Kataoka, O.; Matsuno, K.; Umeda, C.; Watanabe, N.; Hashimoto, S. *J. Am. Chem. Soc.* **1999**, *121*, 1417–1418. (b) Hodgson, D. M.; Labande, A. H.; Pierard, F. Y. T. M.; Expósito Castro, M. Á. *J. Org. Chem.* **2003**, *68*, 6153–6159. (c) Hodgson, D. M.; Brückl, T.; Glen, R.; Labande, A. H.; Selden, D. A.; Dossetter, A. G.; Redgrave, A. J. *Proc. Natl. Acad. Sci. U.S.A.* **2004**, *101*, 5450–5454. (d) Shimada, N.; Anada, M.; Nakamura, S.; Nambu, H.; Tsutsui, H.; Hashimoto, S. *Org. Lett.* **2008**, *10*, 3603–3606. (e) Ishida, K.; Kusama, H.; Iwasawa, N. *J. Am. Chem. Soc.* **2010**, *132*, 8842–8843.

¹⁰ (a) Raheem, I. T.; Thiara, P. S.; Peterson, E. A.; Jacobsen, E. N. *J. Am. Chem. Soc.* **2007**, *129*, 13404–13405. (b) Reisman, S. E.; Doyle, A. G.; Jacobsen, E. N. *J. Am. Chem. Soc.* **2008**, *130*, 7198–7199. (c) Klausen, R. S.; Jacobsen, E. N. *Org. Lett.* **2009**, *11*, 887–890. (d) Zuend, S. J.; Jacobsen, E. N. *J. Am. Chem. Soc.* **2009**, *131*, 15358–15374. (e) Xu, H.; Zuend, S. J.; Woll, M. G.; Tao, Y.; Jacobsen, E. N. *Science* **2010**, *327*, 986–990. (f) Knowles, R. R.; Lin, S.; Jacobsen, E. N. *J. Am. Chem. Soc.* **2010**, *132*, 5030–5032. (g) Brown, A. R.; Kuo, W.-H.; Jacobsen, E. N. *J. Am.*

thiourea **5** (Scheme 2.2) could catalyze the enantioselective Pictet–Spengler reactions of hydroxylactams to tetracyclic products such as **7**.^{10a} DFT calculations supported a mechanism by which the catalyst promotes the dissociation of chloride from chlorolactam **4** (generated *in situ* from the corresponding hydroxylactam), to form catalyst-associated *N*-acyliminium/chloride ion pair **6**. This iminium then undergoes cyclization in up to 99% *ee*, with stereochemical information relayed from the chiral catalyst. As in oxidopyrylium cycloadditions, these transformations proceed through a prochiral reactive intermediate, generated here by abstraction of the anion from a stereogenic carbon.



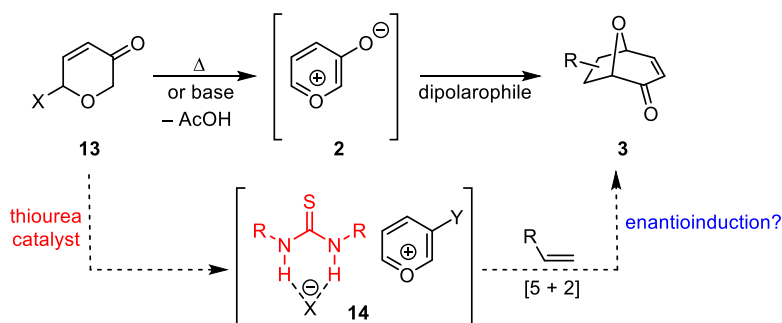
Scheme 2.2. Examples of hydrogen-bond donors as anion abstractors in enantioselective catalysis.

Similarly, we reported a primary aminothiourea-catalyzed α -alkylation of α -branched aldehydes in 2010.^{10g} In this transformation, both the nucleophile and the electrophile are activated by a single catalyst. The thiourea portion of catalyst **10** induces ionization of benzhydryl bromide **9** to form the cationic electrophile, and the amine condenses with aldehyde **8** to generate the

Chem. Soc. **2010**, 132, 9286–9288. See also: (h) De, C. K.; Klauber, E. G.; Seidel, D. *J. Am. Chem. Soc.* **2009**, 131, 17060–17061. For recent reviews, see: (i) Zhang, Z.; Schreiner, P. R. *Chem. Soc. Rev.* **2009**, 38, 1187–1198. (j) Brak, K.; Jacobsen, E. N. *Angew. Chem. Int. Ed.* **2013**, 52, 534–561.

enamine nucleophile in intermediate **11**. S_N1 reaction between the separate components yields aldehydes **12** in up to 94% *ee*.

We became interested in the potential application of anion-binding catalysis to oxidopyrylium formation and cycloaddition. Pyrylium intermediates are generally accessed by thermolysis of the corresponding acetoxyranone **1** (Scheme 2.1)¹¹ or by reaction of **1** with an amine base.¹² Upon elimination of acetic acid, reactive intermediate **2** has been shown to undergo [5 + 2] cycloadditions with both electron-rich and electron-poor dipolarophiles.^{13,14} We hypothesized that a urea or thiourea catalyst could induce ionization of an appropriate leaving group in **13** (Scheme 2.3) or a tautomeric form thereof, giving pyrylium **14**, in which the nature of Y was as yet undetermined (*vide infra*). Thus, our initial efforts focused on identifying an appropriate precursor to this species (i.e., with regards to X in **13**) as well as the optimal mode for activation and asymmetric induction in subsequent [5 + 2] cycloadditions.



Scheme 2.3. Proposed mode of catalysis for a catalytic asymmetric [5 + 2] oxidopyrylium cycloaddition.

¹¹ Hendrickson, J. B.; Farina, J. S. *J. Org. Chem.* **1980**, *45*, 3359–3361.

¹² (a) Sammes, P. G.; Street, L. J. *J. Chem. Soc., Chem. Commun.* **1982**, 1056–1057. (b) Sammes, P. G.; Street, L. J. *J. Chem. Soc., Perkin Trans. 1* **1983**, 1261–1265.

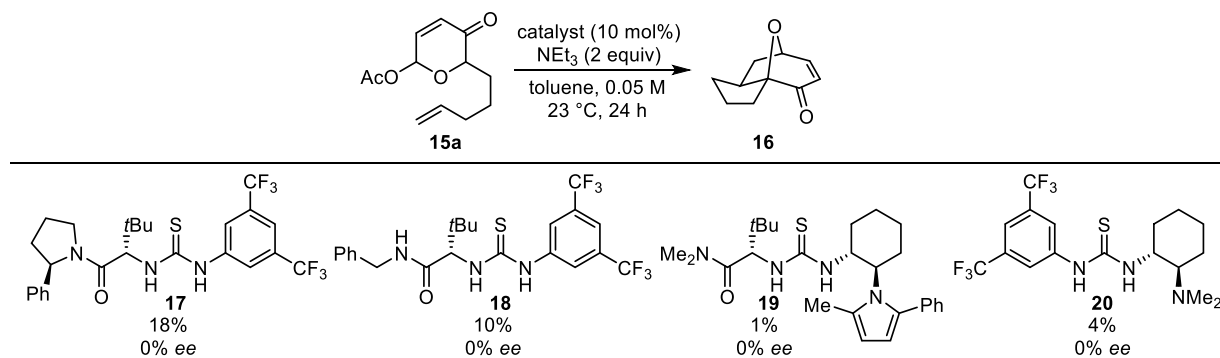
¹³ Sammes, P. G.; Street, L. J. *J. Chem. Res., Synop.* **1984**, 196–197.

¹⁴ See complete discussion in Section 1.2.

2.2 Reaction Development¹⁵

Racemic acetoxypyranone **15a**^{12a} (Table 2.1) was chosen for preliminary exploratory and ensuing optimization studies. Several thiourea catalysts were initially tested, but none provided desired product **16**. Stoichiometric triethylamine promoted the reaction in the presence of a variety of chiral thiourea derivatives, but no stereoselection was observed.

Table 2.1. Initial catalyst screen with triethylamine (Dr. Noah Z. Burns).^a



^a Reactions performed on 0.05 mmol scale. Yields determined by NMR analysis using 1,3,5-trimethoxybenzene as an internal standard. Enantioselectivities determined by HPLC using commercial columns with chiral stationary phases.

In contrast, bifunctional primary aminothiourea **10**¹⁶ (Table 2.2) induced formation of **16** in low yield and with measurable levels of enantioselectivity in the absence of exogenous base (entry 1). The related urea catalyst **21** provided cycloadduct **16** in much lower yield (entry 2). An increase in temperature to 40 °C improved reactivity significantly, but resulted in a drop in *ee* (entry 3). An unexpected but ultimately significant observation resulted from a broad screen of additives, with achiral thiourea catalyst **23**¹⁷ dramatically improving the reaction enantioselectivity (entry 4). The addition of acetic acid as a second cocatalyst provided a measurable yield

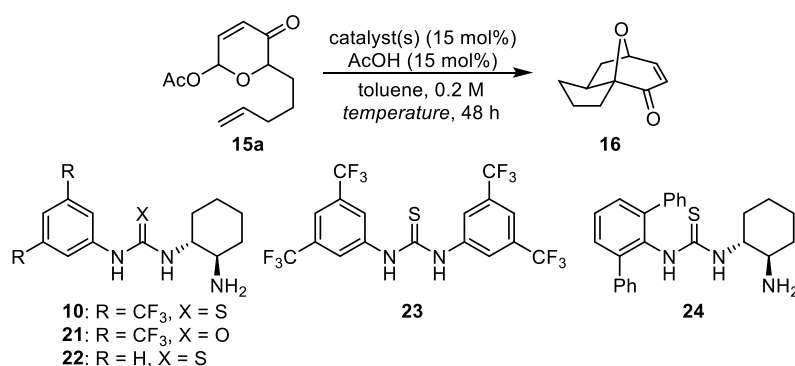
¹⁵ This project was devised and initiated by Dr. Noah Z. Burns, who was kind enough to let this author ride on his coattails at first. His intellectual and experimental contributions will be explicitly noted, when appropriate, on graphics in this and subsequent sections.

¹⁶ For preparation and use, see ref. 10g.

¹⁷ (a) Schreiner, P. R.; Wittkopp, A. *Org. Lett.* **2002**, *4*, 217–220. (b) Wittkopp, A.; Schreiner, P. R. *Chem.–Eur. J.* **2003**, *9*, 407–414.

enhancement with no effect on the product *ee* (entry 5). Other achiral or chiral hydrogen-bond donors (including the urea analogue of **23**) proved less beneficial as additives. Whereas the electron-poor bis(trifluoromethyl)anilide group has been found to be an optimal chiral catalyst feature in a growing number of enantioselective thiourea-promoted reactions,¹⁸ phenylthiourea **22** (entry 6) was found to be comparable to **10**. This prompted an exhaustive examination of the effect of aryl substitution on the aminothiourea catalyst¹⁹ that led to the identification of **24**, which bears a 2,6-diphenylanilide component, as the most enantioselective aminothiourea catalyst (entry 7).

Table 2.2. Optimization of catalytic asymmetric [5 + 2] cycloaddition (Dr. Noah Z. Burns).^a



Entry	Catalyst(s)	Temperature (°C)	Yield (%) ^b	<i>ee</i> (%) ^c
1 ^d	10	23	12	54
2 ^d	21	23	9	15
3 ^d	10	40	37	21
4 ^d	10 + 23	40	44	67
5	10 + 23	40	53	67
6	22 + 23	40	41	66
7	24 + 23	40	30	88

^a Reactions performed on 0.05 mmol scale. ^b Yields determined by NMR analysis using 1,3,5-trimethoxybenzene as an internal standard. ^c Enantioselectivities determined by HPLC using commercial columns with chiral stationary phases. ^d No added AcOH.

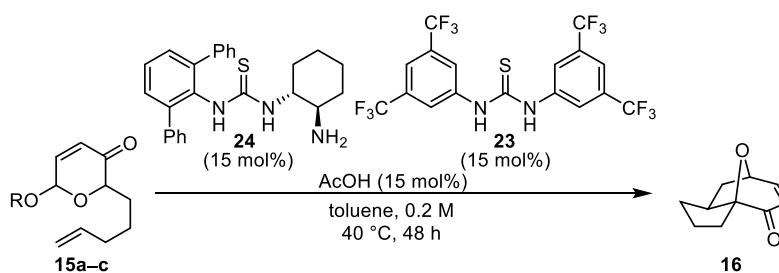
The diminished reactivity displayed by **24** was overcome by utilizing substrate **15b** containing a benzoate leaving group (Table 2.3, entry 2). Upon exploration of various substituents

¹⁸ For examples, see refs. 10b–10d, 10g, 10h and 24.

¹⁹ See Section 2.6 for full details.

on the benzoate,¹⁹ further enhancement was observed with *p*-thiomethylbenzoyl substrate **15c** (entry 3). This improved reactivity is unlikely to result from better leaving group or hydrogen-bond accepting ability, as *p*-thiomethyl substitution has no effect on the acidity of benzoic acid ($\sigma_{\text{para}} = 0.0$ ²⁰). This effect instead seems to be the result of the lower solubility in toluene of the *p*-thiomethylbenzoic acid byproduct (relative to benzoic or acetic acid), which precipitates over the course of the reaction. Finally, increasing the reaction concentration further improved the rate, allowing the loadings of **24** and **23** to be reduced with this parent substrate (entry 4).

Table 2.3. Effect of leaving group on cycloaddition (Dr. Noah Z. Burns).^a



Entry	Substrate (R)	Yield (%) ^b	ee (%) ^c
1	15a (Ac)	30	88
2	15b (Bz)	56	91
3	15c (<i>p</i> -MeSBz)	72	91
4 ^d	15c (<i>p</i> -MeSBz)	76	91

^a Reactions performed on 0.05 mmol scale. ^b Yields determined by NMR analysis using 1,3,5-trimethoxybenzene as an internal standard. ^c Enantioselectivities determined by HPLC using commercial columns with chiral stationary phases. ^d Conditions: 10 mol% **24** + **23**, 0.4 M.

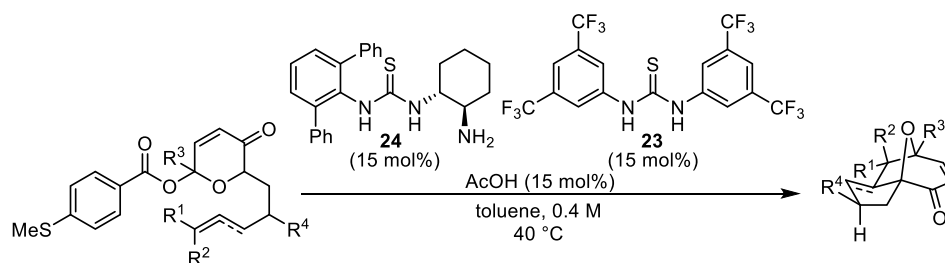
2.3 Substrate Scope

With optimal catalytic conditions established, an examination of the substrate scope was undertaken (Table 2.4). Substitutions at the olefin terminus were tolerated (entries 2–7), despite diminished reactivity upon increased substitution (entries 4 and 7). Allenes were viable cycloaddition substrates (entries 8 and 9), but alkyne-bearing substrates proved unreactive under the current set of conditions.¹⁹ Other viable substrates included those bearing substitution on the

²⁰ McDaniel, D. H.; Brown, H. C. *J. Org. Chem.* **1958**, *23*, 420–427.

tether connecting the dipole and dipolarophile, as in diallyl substrate **41** (entry 10), or on the pyranone ring, as in **43** (entry 11). Product **44** bears a siloxymethylene unit commonly found in synthetically useful oxidopyrylium cycloadducts.²¹ Substrate variations that were not tolerated included methylation at the internal position of the olefin as well as a homologue of substrate **15c** containing an additional methylene in the tether.

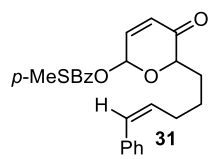
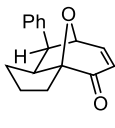
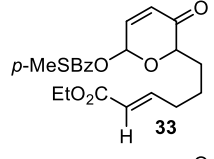
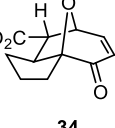
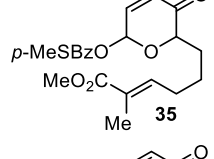
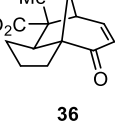
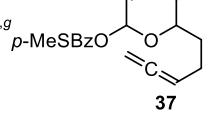
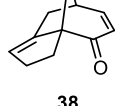
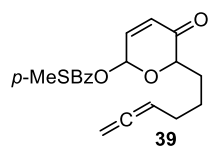
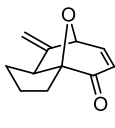
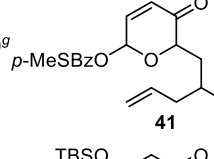
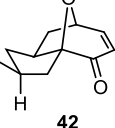
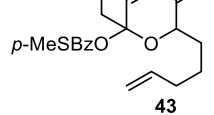
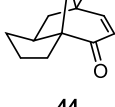
Table 2.4. Substrate scope of intramolecular [5 + 2] cycloaddition (with Dr. Noah Z. Burns).^a



Entry	Substrate	Product	Time (h)	Yield (%) ^b	ee (%) ^c
1 ^{d,g}	<p>15c</p>	<p>16</p>	48	74	91
2	<p>25</p>	<p>26</p>	72	70	90
3	<p>27</p>	<p>28</p>	72	66	89
4	<p>29</p>	<p>30</p>	96	51	89

²¹ See refs. 4a, 6b, 7a, 7d, and Section 1.5 for examples.

Table 2.4 (continued).

Entry	Substrate	Product	Time (h)	Yield (%) ^b	ee (%) ^c
5			72	48	86
6			72	66	90
7 ^e			96	37	80
8 ^{d,g}			72	54	95
9			72	42	88
10 ^g			72	77	90
11			72	70 ^f	89 ^f

^a Reactions performed on 0.3 mmol scale. ^b Yields of isolated products after column chromatography. ^c Enantioselectivities determined by HPLC using commercial columns with chiral stationary phases. ^d 10 mol% **24** + **23**. ^e 20 mol% **24** + **23**. ^f Determined on free alcohol. ^g The absolute stereochemical configurations of **38** and derivatives of **16** and **42** were determined by X-ray crystallography, and those of all other products were assigned by analogy.

We were able to obtain an x-ray crystal structure of cycloadduct **38** as well as a *para*-bromobenzoate derivative of **16** (Figure 2.1), in order to determine the stereochemical configuration of these products. The absolute sense of enantioselectivity for all other products was assigned by comparison.

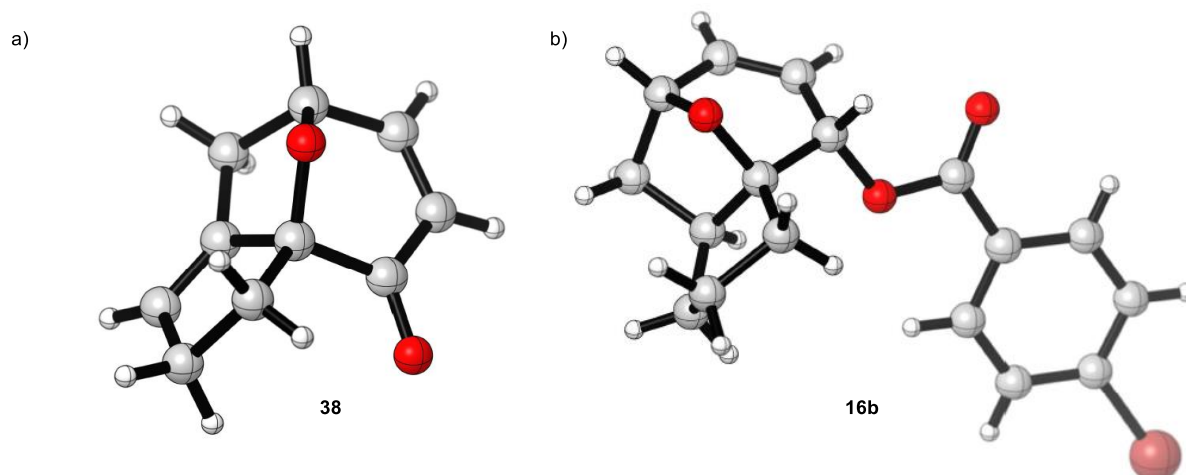


Figure 2.1. X-ray crystal structures of (a) **38** and (b) a *para*-bromobenzoate derivative of **16** (Noah Z. Burns).

2.4 Mechanistic Studies

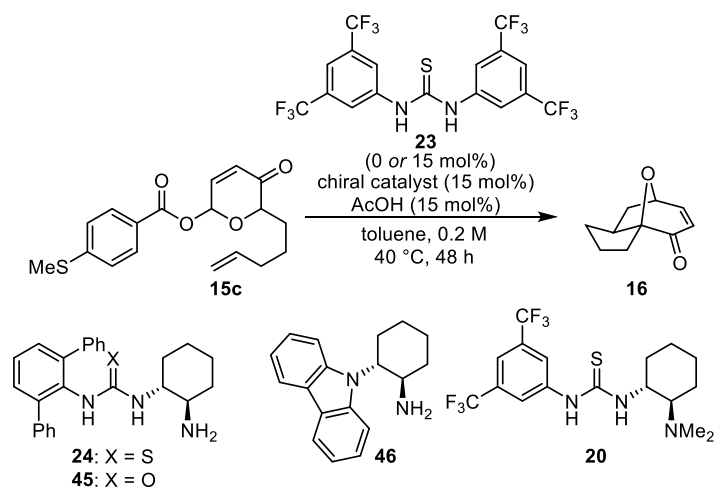
In order to better understand the observed effect that two separate catalysts have on the cycloaddition, experimental and computational tools were employed to investigate each of the reaction components individually. The results of these studies implicate a new type of cooperative catalysis, with each catalyst species necessary for generation of the reactive pyrylium intermediate. First, a catalyst structure–activity study revealed discrete functions for each of the two catalysts. Next, a computational FMO analysis was carried out to determine the exact nature (with respect to **14**, Scheme 2.3) of the cycloaddition participants in the key [5 + 2] step. Finally, DFT methods were utilized to understand the origin of enantioselectivity.

2.4.1 Catalyst Structure–Activity Study

In order to probe the possible roles of each thiourea in this dual catalyst system, a series of reactions was carried out with different bifunctional chiral catalysts in the presence and absence of thiourea **23** (Table 2.5). A clear and dramatic cooperative effect between the optimal catalysts was observed, as evidenced by the poorer results obtained without achiral catalyst **23** (entry 1). A beneficial effect of **23** has also been reported recently in proline-catalyzed transformations, in

which it appears to serve as a phase-transfer catalyst to solubilize proline in nonpolar media.²² Such a role is unlikely in the present system, as all components of this oxidopyrylium-based cycloaddition reaction are initially soluble in toluene (*vide supra*).

Table 2.5. Catalyst structure–activity relationship study (with Dr. Noah Z. Burns).^a



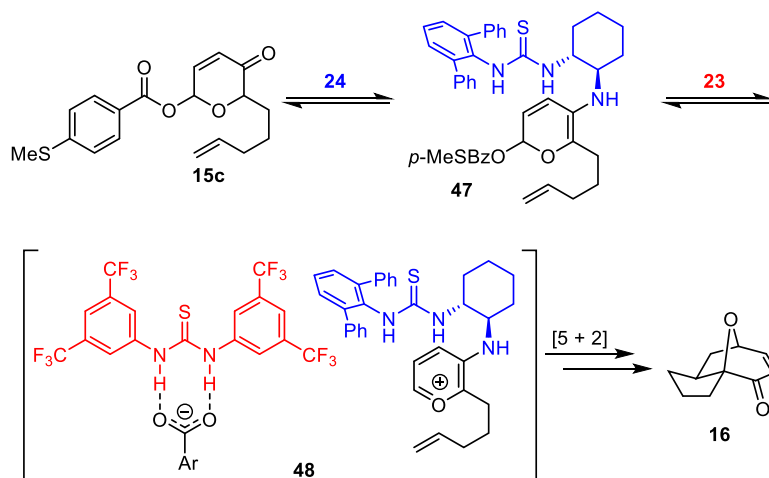
Entry	Catalyst	0 mol% 23		15 mol% 23	
		Yield (%) ^b	ee (%) ^c	Yield (%) ^b	ee (%) ^c
1	24	32	72	72	91
2	45	7	n.d.	58	71
3	46	7	n.d.	58	–85
4	20	10	n.d.	11	n.d.

^a Reactions performed on 0.05 mmol scale. ^b Yields determined by NMR analysis using 1,3,5-trimethoxybenzene as an internal standard. ^c Enantioselectivities determined by HPLC using commercial columns with chiral stationary phases.

Instead, we propose that catalyst **23** acts as a carboxylate-binding agent in the pyrylium cycloaddition reaction (Scheme 2.4), functioning cooperatively with **24** to generate the reactive ion pair **48**. Therefore, we suggest the intermediacy of the cationic aminopyrylium depicted in Scheme 2.4, rather than a traditional zwitterionic oxidopyrylium (e.g., **2**, Scheme 2.1). Evidence provided in this and the subsequent two subsections supports this proposal.

²² (a) Reis, Ö.; Eymur, S.; Reis, B.; Demir, A. S. *Chem. Commun.* **2009**, 1088–1090. (b) Companyó, X.; Valero, G.; Crovetto, L.; Moyano, A.; Rios, R. *Chem.–Eur. J.* **2009**, *15*, 6564–6568. (c) Demir, A. S.; Eymur, S. *Tetrahedron: Asymmetry* **2010**, *21*, 112–115. (d) Demir, A. S.; Eymur, S. *Tetrahedron: Asymmetry* **2010**, *21*, 405–409.

Catalyst **45**, the urea analogue of **24** exhibits very low reactivity in the absence of **23**²³ but does serve as a moderately enantioselective cocatalyst in conjunction with **23** (Table 2.5, entry 2). This indicates that the thiourea component of the optimal catalyst **24** indeed influences the reaction enantioselectivity even in the presence of **23** (compare entries 1 and 2); however it is not necessary for obtaining reactivity or high *ee*. Thus, the combination of primary aminocarbazole **46**, which possesses no hydrogen-bond donor functionality, and thiourea **23** is an effective catalyst system, promoting the selective formation of **16** with 85% *ee* (entry 3). It is significant that catalysts **24** and **46** induce cycloaddition with opposite senses of enantiocontrol (*vide infra*). Consistent with the notion that a hydrogen-bond donor catalyst is needed to induce ionization to the pyrylium ion, primary aminocarbazole **46** is virtually unreactive in the absence of **23** (entry 3). Tertiary aminothiourea **20**²⁴ is unreactive in both the presence and absence of **23** (entry 4), pointing to the necessity of a primary amine for catalytic activity.



Scheme 2.4. Proposed role for thiourea catalysts **23** and **24**.

²³ In general, ureas are substantially weaker Brønsted acids than the corresponding thioureas, and accordingly, they are also poorer H-bond donors. For example, the pK_a of *N,N'*-diphenylthiourea in DMSO is 13.5, while that of *N,N'*-diphenylurea is 19.5. See: Bordwell, F. G.; Algrim, D. J.; Harrelson, Jr., J. A. *J. Am. Chem. Soc.* **1988**, *110*, 5903–5904.

²⁴ Okino, T.; Hoashi, Y.; Takemoto, Y. *J. Am. Chem. Soc.* **2003**, *125*, 12672–12673.

These observations with basic tertiary aminothiourea **20**, as well as the fact that acetic acid increases the rate of reaction, are consistent with an operative enamine catalysis mechanism. Condensation between the amine of the catalyst and the ketone of the substrate is expected to yield a dienamine (**47**, Scheme 2.4) after tautomerization. Hydrogen-bond donor-mediated benzoate abstraction would then generate a catalyst•pyrylium adduct **48** poised to undergo the intramolecular cycloaddition.

2.4.2 An FMO Analysis to Support an Aminopyrylium Intermediate

To evaluate the viability of aminopyrylium **48** in the cycloaddition chemistry induced by the catalyst combination of **23** and **24**, a computational FMO analysis²⁵ of a variety of dipolarophiles as well as oxido-, amido-, and aminopyryliums (**49–51** Figure 2.2) was performed. The dominant HOMO–LUMO interactions between each pyrylium-dipolarophile pair were thereby predicted, then compared with observed trends in intermolecular cycloadditions. With an oxidopyrylium (**49**) or amidopyrylium (**50**), either the HOMO or the LUMO of the dipole can be more relevant to cycloaddition depending on the dipolarophile, consistent with the experimental observation that oxidopyrylium dipolar intermediates can undergo reactions with both electron-rich and electron-deficient alkenes.^{12b,13,14}

²⁵ Zhang, G.; Musgrave, C. B. *J. Phys. Chem. A* **2007**, *111*, 1554–1561.

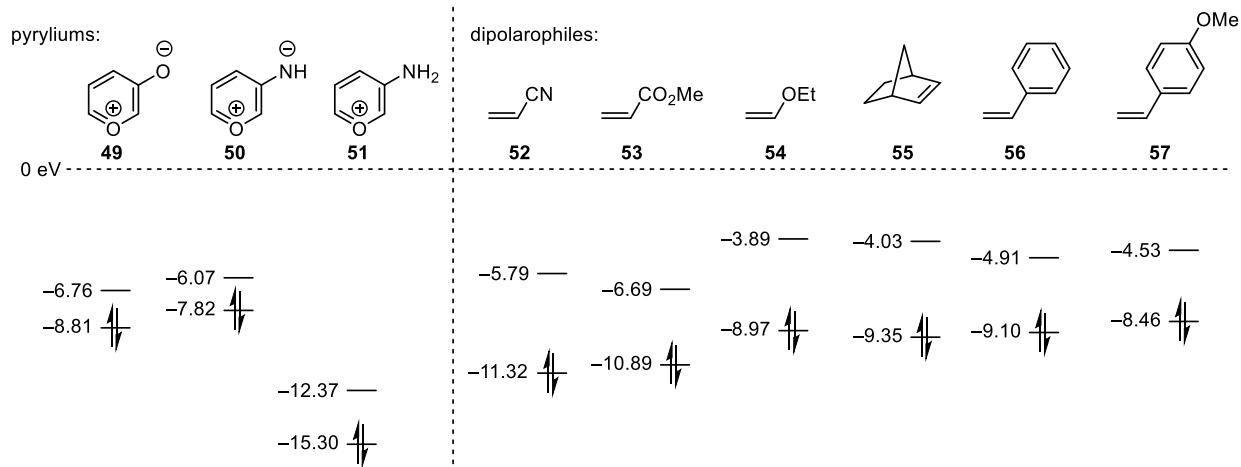
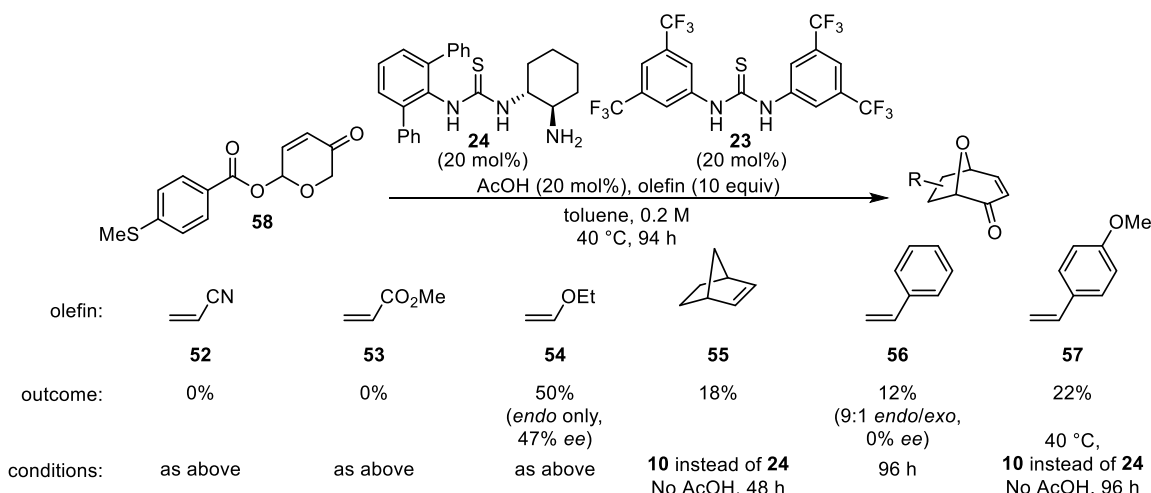


Figure 2.2. Predicted HOMO–LUMO interactions (Dr. Noah Z. Burns). Energies in terms of eV.

In a preliminary attempt to extend the thiourea-catalyzed [5 + 2] cycloaddition to an intermolecular variant²⁶ a variety of dipolarophiles were examined under catalytic conditions (Scheme 2.5). In no case was a reaction found to occur between pyranone **58** and an electron-deficient alkene (acrylonitrile **52** or methyl acrylate **53**). On the other hand, more electron-rich olefins, ethyl vinyl ether **54**, norbornene **55**, styrene **56**, and *para*-methoxystyrene **57**, all yielded cycloadducts under these non-basic conditions, albeit with low reactivity.



Scheme 2.5. Preliminary intermolecular reactions.

²⁶ See Chapter 3 for complete report.

If the catalytic reaction under investigation were proceeding via an oxidopyrylium intermediate (i.e., **49**), similar trends to reported triethylamine-promoted reactions (i.e., reactivity with both electron-rich and electron-deficient dipolarophiles) would be expected. This is not the case, allowing us to infer that an oxidopyrylium is not the species undergoing cycloaddition.

Based on computed FMO energy values, the hypothetical amidopyrylium (**50**) is predicted to have similar reactivity to oxidopyrylium **49**: Either the HOMO or the LUMO of an amidopyrylium can participate in cycloaddition, depending on the electronic nature of the partner dipolarophile. In fact, the slightly increased HOMO energy value of the amidopyrylium indicates that it should be more reactive than an oxidopyrylium with electron-deficient dipolarophiles. This also contrasts with the observed reactivity trends in Scheme 2.5, and we therefore conclude that an amidopyrylium is not the species undergoing cycloaddition either.

The computed FMO energy values of an aminopyrylium (**51**) reveal that the LUMO of this species should be most relevant to cycloaddition with all examined dipolarophiles. This is consistent with the data presented in Scheme 2.5, which demonstrate that only dipolarophiles with high-lying HOMOs react under our conditions. These results, in conjunction with the structure–activity relationship studies, have led us to propose that an aminopyrylium (as in **48**, Scheme 2.4) is the active species undergoing cycloaddition in the present catalytic reaction. The oxygen-analogue of this species, a 3-hydroxypyrylium, has calculated HOMO and LUMO values (–16.7 eV and –12.9 eV, respectively) similar to that of the aminopyrylium, but was eliminated as a likely intermediate due to its anticipated high acidity (estimated to be similar to that of a protonated carbonyl), and because tertiary aminothiourea **20** is not an active catalyst (Table 2.5).

In order to examine the effect of a thiourea-bound counteranion, an FMO analysis of ion-pair **58** was also performed (Figure 2.3). Although both the HOMO and the LUMO of **58** are higher

in energy than those of free aminopyrylium **51**, their values are such that the predicted interaction should still be the same with the examined series of dipolarophiles. Therefore, our experimental results are still consistent with an aminopyrylium undergoing cycloaddition. Since an overall cationic aminopyrylium would be expected to have lower-lying frontier MOs as compared to its neutral counterpart, it is not surprising that the introduction of a counteranion to give a neutral ion pair would then raise the energy values of these orbitals. The fact that **58** nonetheless has lower FMO energy values than the oxido- and aminopyrylium can be accounted for by the greater charge separation in this ion pair relative to the zwitterions.

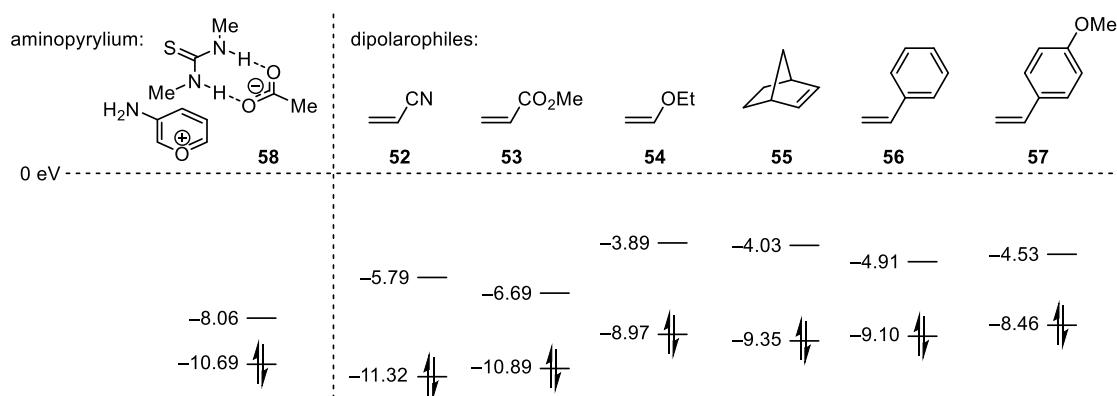


Figure 2.3. Predicted HOMO–LUMO interactions of an aminopyrylium ion pair (Dr. Noah Z. Burns). Energies in terms of eV.

2.4.3 Rationalization of Stereoselectivity by DFT Calculations

While the unprecedented intermediacy of an aminopyrylium such as **48** agrees with the experimental and computational data described above, the reversal in the sense of enantioinduction observed using primary amine catalysts **24** and **46** (derived from the same enantiomer of 1,2-*trans*-cyclohexyldiamine) in conjunction with achiral thiourea **23** was difficult to reconcile by any simple means. A computational analysis of transition structures for cycloadditions of the proposed

24•pyrylium and **46•pyrylium** ions was therefore undertaken.²⁷ Although these simplified models did not take into account the thiourea-bound carboxylate, good correlation with the experimental results was obtained. Of the multiple first-order saddle points that were located for each complex, the lowest energy transition structure leads to the observed major enantiomer of the product (Figure 2.4), and the second-lowest-energy transition structure corresponds to the observed minor enantiomer in each case.

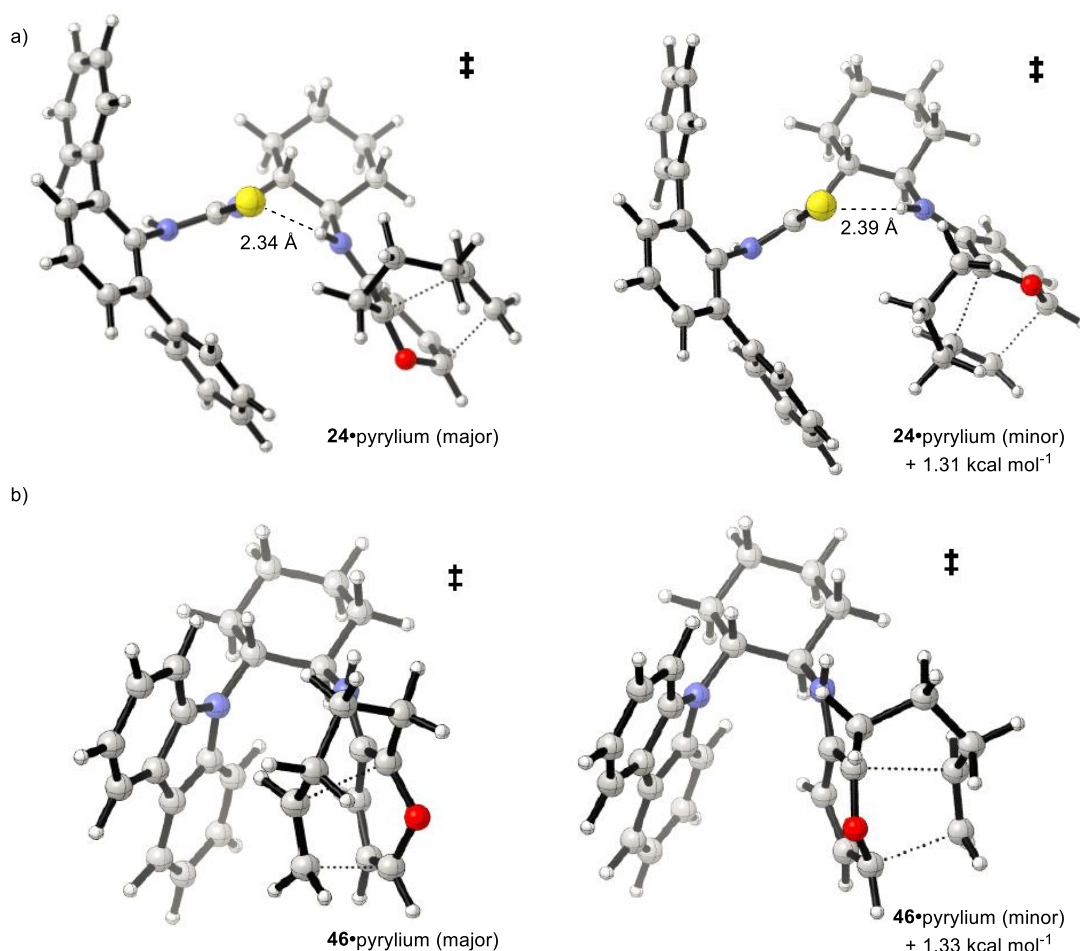


Figure 2.4. The two lowest energy cycloaddition transition structures calculated at the B3LYP/6-31G(d) level of theory for (a) **24•pyrylium** and (b) **46•pyrylium** (Noah Z. Burns).

²⁷ B3LYP/6-31G(d) has been established as an appropriate level of theory for studying oxidopyrylium [5 + 2] cycloadditions. See: (a) López, F.; Castedo, L.; Mascareñas, J. L. *J. Org. Chem.* **2003**, *68*, 9780–9786. (b) Wang, S. C.; Tantillo, D. J. *J. Org. Chem.* **2008**, *73*, 1516–1523.

Although the exact origin of selectivity for each catalyst is not yet fully understood, some speculation is possible based on the structures shown in Figure 2.4. The two lowest energy transition structures of **24**•pyrylium both contain an interaction between the N–H of the pyrylium and the sulfur of the thiourea (H–S distance = 2.34 Å and 2.39 Å for the structures leading to the major and minor enantiomers, respectively). This may serve to rigidify the structure and control the orientation of the aminopyrylium with respect to the cyclohexyl unit. The tethered alkene may then approach the pyrylium on either the more exposed outer face, as in the structure leading to the major enantiomer, or on the inner face, as in the structure leading to the minor enantiomer. One of the *ortho*-phenyl substituents on the *m*-terphenyl of the thiourea may serve to block this inner face of the pyrylium, raising the energy of cycloaddition on this face due to destabilizing steric interactions.

In each of the two lowest energy transition structures for **46**•pyrylium, the carbazole and the pyrylium are both essentially perpendicular to the cyclohexane plane. In contrast to the case with **24**•pyrylium, approach of the alkene to the more exposed outer face now leads to the observed minor enantiomer of product. A structure wherein cycloaddition occurs onto the inner face is actually lower in energy and leads to the observed major enantiomer of product. In this structure, the pyrylium is in closer proximity to the carbazole, suggesting that this heterocycle may engage in a stabilizing cation- π interaction with the alkene dipolarophile as it accumulates cationic character in the transition state. This interaction is absent from the transition structure leading to the minor enantiomer of product.

2.5 Conclusions and Outlook

In this chapter, the identification of a dual thiourea catalyst system for intramolecular pyrylium [5 + 2] cycloadditions has been described. This innovative methodology provides

enantioselective access to valuable tricyclic structures. The reaction system demonstrates a unique mode of cooperative catalysis in which an achiral thiourea (**23**) functions as an anion abstractor and a chiral primary aminothiourea (**24**) activates the ketone substrate via enamine catalysis. Although the hydrogen-bond donating ability of **24** does not appear to participate in the traditional sense of thiourea catalysis, we have not found an alternate primary amine scaffold that provides superior results.

Furthermore, we have shown that rather than a traditional zwitterionic oxidopyrylium intermediate (e.g., **2**), these reactions proceed through a cationic aminopyrylium intermediate (**48**). Qualitatively, the fact that only electron-rich olefins react through an intermolecular manifold, but electron-deficient olefins do not, supports this conclusion (Scheme 2.5). Additionally, quantitative FMO calculations have been presented to provide further support.

Extension of this dual catalysis principle to other transformations remains the subject of ongoing investigations. In Section 2.4.2, preliminary examples of intermolecular reactions were introduced. The following chapter will describe in detail our research efforts to optimize these related cycloadditions.

2.6 Experimental Details

2.6.1 General Information

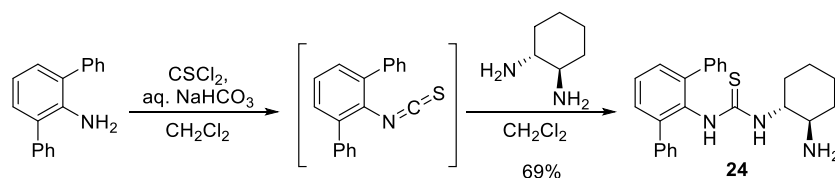
Cycloaddition reactions were performed in oven-dried 0.5-dram vials; all other reactions were performed in oven- or flame-dried round bottom flasks unless otherwise noted. The vials and flasks were fitted with rubber septa and reactions were conducted under air unless noted. Stainless steel syringes were used to transfer air- and moisture-sensitive liquids. Flash chromatography was performed using silica gel 60 (230-400 mesh) from EM Science or Davisil® (Grade 643, pore size 150Å, 200-425 mesh) from Sigma-Aldrich. Commercial reagents were purchased from Sigma-Aldrich, Alfa Aesar, or TCI, and used as received with the following exceptions: dichloromethane, toluene, tetrahydrofuran, diethyl ether, 1,4-

dioxane, and methanol were dried by passing through columns of activated alumina. Triethylamine and pyridine were distilled from CaH₂ at 760 torr. Furfural was distilled at 20 torr. *n*-Butyllithium was titrated using *N*-benzylbenzamide as an indicator.

Proton nuclear magnetic resonance (¹H NMR) spectra and carbon nuclear magnetic resonance (¹³C NMR) spectra were recorded on Varian-Mercury-400 (400 MHz), Inova-500 (500 MHz), or Inova-600 (600 MHz) spectrometers. Chemical shifts for protons are reported in parts per million downfield from tetramethylsilane and are referenced to residual protium in the NMR solvent (CHCl₃ = δ 7.27). Chemical shifts for carbon are reported in parts per million downfield from tetramethylsilane and are referenced to the carbon resonances of the solvent (CDCl₃ = δ 77.0). Data are represented as follows: chemical shift (multiplicity (br. = broad, s = singlet, d = doublet, t = triplet, q = quartet, quin = quintet, m = multiplet), coupling constants in Hertz (Hz), integration).

Infrared (IR) spectra were obtained using a Bruker Optics Tensor 27 FTIR spectrometer. Optical rotations were measured using a Jasco DIP 370 digital polarimeter. The mass spectral data were obtained on an Agilent Technologies 6120 quadrupole LC/MS spectrometer (when designated ESI, APCI, or ESI-APCI) or on a Bruker micrOTOF-Q II time-of-flight LC/MS spectrometer (when designated ESI-TOF). Chiral HPLC analysis was performed using an Agilent analytical chromatograph with commercial ChiralPak or ChiralCel columns.

2.6.2 Synthesis and Characterization of Catalysts



Scheme 2.6. Synthesis of catalyst 24.

1-([1,1':3',1''-terphenyl]-2'-yl)-3-((1*R*,2*R*)-2-aminocyclohexyl)thiourea (24):

2,6-diphenylaniline²⁸ (150.0 mg, 0.611 mmol) was dissolved in CH₂Cl₂ (3.1 mL) and sat. aq. NaHCO₃ (3.1

²⁸ 2,6-diphenylaniline synthesized according to: Miura, Y.; Oka, H.; Momoki, M. *Synthesis* **1995**, 1419–1422.

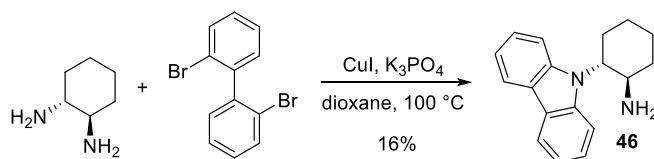
mL) was added. The resulting biphasic solution was cooled to 0 °C and thiophosgene (0.061 mL, 0.795 mmol, 1.3 equiv) was then carefully added via syringe. The reaction was allowed to warm to 23 °C and stirred for 5 h. The layers were separated and the aqueous layer was extracted with CH₂Cl₂ (3 x 20 mL). The combined organic layers were dried over Na₂SO₄, filtered, and concentrated. The crude product was then redissolved in hexanes and minimal CH₂Cl₂ and filtered through a plug of silica gel, eluting with hexanes, to afford 2,6-diphenylphenylisothiocyanate as a white solid (170.0 mg, 97%) which was used directly in the subsequent reaction.

(*R,R*)-1,2-*trans*-diaminocyclohexane²⁹ (203.0 mg, 1.78 mmol, 3.0 equiv) was dissolved in CH₂Cl₂ (2.0 mL) and the resulting solution was cooled to 0 °C. To this was added dropwise a solution of 2,6-diphenylphenylisothiocyanate (170.0 mg, 0.592 mmol, 1.0 equiv) in CH₂Cl₂ (2 mL). The resulting reaction mixture was allowed to warm to 23 °C and stir for 3 h. The solution was then concentrated and loaded directly onto silica gel. Column chromatography (silica gel, 95:5 CH₂Cl₂/MeOH) afforded clean primary aminothiourea as a slightly yellow foam. This was redissolved in minimal benzene and triturated with hexanes. Filtration and further washing of the solid with hexanes afforded **24** as a white solid (170 mg, 71%).

R_f = 0.44 (silica gel, 90:10 CH₂Cl₂/MeOH); **IR** (film) ν_{max} 3237, 3054, 2926, 2854, 2360, 2341, 1692, 1522, 755, 700, 613 cm⁻¹; **¹H NMR** (400 MHz, CD₃OD) δ 7.64 – 7.29 (br. m, 13H), 4.03 – 3.83 (br. s, 1H), 2.24 – 2.12 (br. ap. tr, 1H), 1.90 – 1.76 (br. ap. d, 1H), 1.70 – 1.46 (2 br. s, 3H), 1.25 – 1.09 (br. s, 2H), 1.09 – 1.94 (br. m, 2H); **¹³C NMR**³⁰ (100 MHz, CDCl₃) δ 180.3, 140.5, 138.3, 131.1, 129.1 (br. s), 128.9 (br. s), 128.5 (br. s), 62.3, 56.3, 34.8, 32.3, 25.2; **MS** (ESI-TOF) calcd. for C₂₅H₂₇N₃S [M + H⁺] 402.2004, found 402.1995; $[\alpha]_D^{22} = +38.4$ ($c = 1.0$, CHCl₃).

²⁹ (*R,R*)-1,2-*trans*-diaminocyclohexane was resolved according to: (a) Larrow, J. F.; Jacobsen, E. N.; Gao, Y.; Hong, Y.; Nie, X.; Zepp, C. M. *J. Org. Chem.* **1994**, *59*, 1939–1942. (b) Larrow, J. F.; Jacobsen, E. N. *Org. Synth.* **1998**, *75*, 1–6.

³⁰ ¹³C NMR spectra of **24** in a variety of solvents at room or elevated temperature all showed broad signals preventing the observation of distinct peaks for all carbons. The obtained X-ray crystal structure also exhibits whole molecular disorder.



Scheme 2.7. Synthesis of catalyst **46**.

(1*R*,2*R*)-2-(9*H*-carbazol-9-yl)cyclohexanamine (46**):**

A flame-dried vial was charged sequentially with 2,2'-dibromobiphenyl (500 mg, 1.60 mmol), (*R,R*)-1,2-*trans*-diaminocyclohexane²⁹ (220 mg, 1.92 mmol, 1.2 equiv), copper iodide (152 mg, 0.80 mmol, 0.5 equiv), and potassium phosphate (747 mg, 3.52 mmol, 2.2 equiv). The vial was sealed and then evacuated and backfilled with N₂ three times. 1,4-Dioxane (3.2 mL, 0.5 M) was added, the sealed vessel was placed in a 100 °C oil bath, and the reaction mixture was stirred vigorously for 24 h. The reaction mixture was allowed to cool to 23 °C and then diluted with EtOAc (20 mL), filtered through a pad of celite, and concentrated. Purification by column chromatography (silica gel, 95:5 CH₂Cl₂/MeOH) afforded **46** as an off-white solid (67.2 mg, 16%, unoptimized).

R_f = 0.45 (silica gel, 90:10 CH₂Cl₂/MeOH); **IR** (film) ν_{\max} 2936, 2858, 1594, 1482, 1453, 1329, 1221, 910, 750, 724 cm⁻¹; **¹H NMR** (500 MHz, CDCl₃) δ 8.14 (dd, *J* = 7.3, 16.5 Hz, 2H), 7.67 (d, *J* = 8.2 Hz, 1H), 7.56 – 7.40 (m, 3H), 7.25 (t, *J* = 7.6 Hz, 2H), 4.23 (ddd, *J* = 3.9, 10.5, 12.6 Hz, 1H), 3.77 (td, *J* = 3.9, 10.6 Hz, 1H), 2.47 – 2.38 (m, 1H), 2.23 – 2.17 (m, 1H), 2.02 – 1.92 (m, 3H), 1.61 – 1.52 (m, 2H), 1.44 (dq, *J* = 3.2, 12.8 Hz, 1H), 1.26 (br. s, 2H); **¹³C NMR** (125 MHz, CDCl₃) 126.1, 125.5, 120.8, 120.3, 119.2, 111.9, 109.3, 63.4, 52.2, 35.6, 29.6, 26.4, 25.4; **MS** (ESI-TOF) calcd. for C₁₈H₂₀N₂ [M + H⁺] 265.1699, found 265.1691; $[\alpha]_D^{25}$ = +66.8 (*c* = 0.9, CHCl₃).

2.6.3 Synthesis and Characterization of Substrates



Scheme 2.8. Synthesis of substrate **15c**.

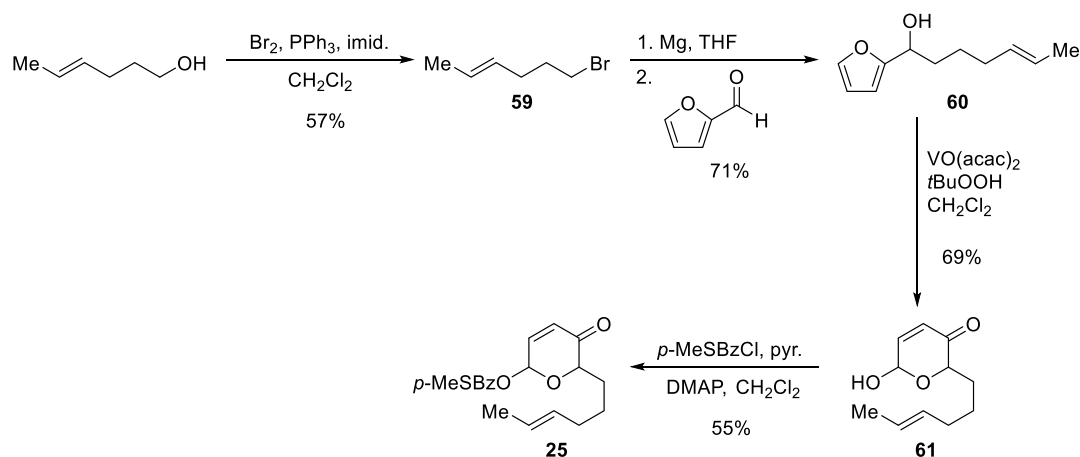
5-oxo-6-(pent-4-en-1-yl)-5,6-dihydro-2H-pyran-2-yl 4-(methylthio)benzoate (15c):

6-Hydroxy-2-(pent-4-en-1-yl)-2H-pyran-3(6H)-one³¹ (700 mg, 3.84 mmol) was dissolved in CH₂Cl₂ (15.4 mL, 0.25 M) and the flask was cooled to 0 °C. To this solution was added sequentially 4-methylthiobenzoic acid (775 mg, 4.61 mmol, 1.2 equiv), EDC (884 mg, 4.61 mmol, 1.2 equiv), and DMAP (563 mg, 4.61 mmol, 1.2 equiv). The reaction mixture was stirred at 0 °C for 30 min and then allowed to warm to 23 °C and stirred a further 30 min. The reaction mixture was then diluted with Et₂O (60 mL) and quenched with 1N HCl (25 mL). The layers were separated and the organic layer was washed successively with 1N HCl (25 mL), sat. aq. NaHCO₃ (25 mL), water (25 mL), and brine (25 mL). The organic layer was dried over Na₂SO₄, filtered, concentrated and purified by column chromatography (silica gel, 95:5 to 5:1 hexanes, Et₂O) to afford **15c** as a yellow oil as a 3:2 mixture of diastereomers which solidified upon storage at -30 °C (798 mg, 63%).³²

R_f = 0.37, 0.44 (silica gel, 5:1 hexanes/EtOAc); **IR** (film) ν_{\max} 3079, 2924, 2866, 1721, 1693, 1595, 1263, 1095, 1072, 907, 754 cm⁻¹; **¹H NMR** (500 MHz, CDCl₃) δ 7.93 (d, *J* = 8.3 Hz, 2H), 7.27 – 7.23 (m, 2H), 7.02 – 6.95 (m, 1H), 6.78 (minor diast., dd, *J* = 1.0, 2.9, 0.4H), 6.73 (major diast., d, *J* = 3.4 Hz, 0.6H), 6.28 – 6.27 (m, 1H), 5.81 – 5.71 (major diast., m, 0.6H), 5.69 – 5.59 (minor diast., m, 0.4H), 5.00 – 4.84 (m, 2H), 4.57 (major diast., dd, *J* = 3.9, 7.3 Hz, 0.6H), 4.27 (minor diast., dd, *J* = 4.6, 9.5 Hz, 0.4H), 2.51 (s, 3H), 2.04 (q, *J* = 7.3 Hz, 1H), 2.01 – 1.82 (m, 2H), 1.81 – 1.72 (m, 1H), 1.54 – 1.47 (m, 2H); **¹³C NMR** (100 MHz, CDCl₃) δ 196.0, 195.9, 165.0, 164.9, 147.1, 147.0, 142.8, 142.0, 138.5, 138.2, 130.4, 129.0, 128.4, 125.3, 125.2, 115.2, 115.1, 88.0, 87.7, 79.8, 76.1, 33.6, 33.5, 33.2, 29.3, 24.9, 24.1, 15.0; **MS** (ESI-TOF) calcd. for C₁₈H₂₀O₄S [M + Na⁺] 355.0975, found 355.0994.

³¹ 6-Hydroxy-2-(pent-4-en-1-yl)-2H-pyran-3(6H)-one synthesized according to: Sammes, P. G.; Street, L. J.; Kirby, P. J. *Chem. Soc., Perkin Trans. 1* **1983**, 2729–2734.

³² In some instances 4-methylthiobenzoic anhydride was found to coelute with the desired product upon column chromatography. Treatment of this mixture with 1 equiv DMAP (relative to anhydride) in a 1:1 mixture of CH₂Cl₂ and MeOH (0.2 M relative to anhydride) instantaneously converted the anhydride to the methyl ester, which could be separated from the desired product under the same chromatography conditions as before.



Scheme 2.9. Synthesis of substrate **25**.

(E)-6-bromohex-2-ene (59):

Triphenylphosphine (20.058 g, 76.5 mmol, 1.8 equiv) and imidazole (8.688 g, 128 mmol, 3 equiv) were dissolved in CH₂Cl₂ (150 mL, 0.28 M) and the resulting solution was cooled to 0 °C. To this mixture was slowly added bromine (3.7 mL, 71.8 mmol, 1.7 equiv) by syringe and the resulting solution was stirred for 15 min at 0 °C under an atmosphere of N₂. (E)-4-hexen-1-ol³³ (5.0 mL, 42.5 mmol) was then added neat by syringe, and the solution was stirred under N₂ for a further 45 min at 0 °C. The resulting suspension was washed with 3% aq. hydrogen peroxide (25 mL), then 1M Na₂S₂O₃ (2 x 50 mL). The thiosulfate layers were extracted with CH₂Cl₂ (70 mL). The pooled organic layers were dried over Na₂SO₄, filtered, and concentrated. The resultant crude white paste was then redissolved in hexanes and minimal CH₂Cl₂ and filtered through a plug of silica gel, eluting with hexanes, to afford **59** as a pale yellow oil (3.926 g, 57%). Spectroscopic data agree with previously reported data.³⁴

(E)-1-(furan-2-yl)hept-5-en-1-ol (60):

Magnesium turnings (374 mg, 15.4 mmol, 5 equiv) were rigorously flame-dried under vacuum in a round bottom flask attached with a condenser. Once the magnesium had cooled, it was exposed to an atmosphere

³³ (E)-4-Hexen-1-ol was purchased from Sigma-Aldrich as a “predominantly *trans*” mixture. A small amount (approx. 4%) of inseparable (*Z*)-4-Hexen-1-ol impurity was carried through the synthesis of substrate **25** and subsequent cycloaddition to **26**.

³⁴ Oppolzer, W.; Siles, S.; Snowden, R. L.; Bakker, B. H.; Petrzilka, M. *Tetrahedron* **1985**, *41*, 3497–3509.

of N₂ and suspended in THF (7.7 mL, 0.4 M). To this suspension was added sequentially 1,2-dibromoethane activator (0.01 mL, 0.12 mmol) then **59** (503 mg, 3.09 mmol). This was stirred and gently heated (approx. 40 °C) until an exotherm was observed. The suspension was then stirred for a further 30 min at 23 °C, after which the dark suspension was cannulated into a solution of furfural (0.26 mL, 3.1 mmol, 1 equiv) in THF (7.7 mL 0.4 M), pre-cooled to 0 °C. This reaction mixture was stirred under an atmosphere of N₂ at 0 °C for 1 h. The resulting solution was then washed with sat. aq. NH₄Cl (2 x 15 mL), and the pooled aqueous layers were extracted with EtOAc (2 x 10 mL). The combined organic layers were dried over Na₂SO₄, filtered, and concentrated. The crude product was purified by flash chromatography (silica gel, 9:1 to 3:2 hexanes/EtOAc) to afford **60** as a colorless oil (393 mg, 71%).

R_f = 0.37 (silica gel, 2:1 hexanes/EtOAc); **IR** (film) ν_{\max} 3375 (br), 2938, 1505, 1453, 1149, 1008, 967, 914, 736 cm⁻¹; **¹H NMR** (500 MHz, CDCl₃) δ 7.35 (d, *J* = 2.0 Hz, 1H), 6.30 (dd, *J* = 1.7, 3.2 Hz, 1H), 6.20 (d, *J* = 3.4 Hz, 1H), 5.46 – 5.35 (m, 2H), 4.67 – 4.60 (m, 1H), 2.27 (d, *J* = 4.4 Hz, 1H), 2.03 – 1.97 (m, 3H), 1.85 – 1.79 (m, 2H), 1.63 (d, *J* = 4.4 Hz, 2H), 1.52 – 1.42 (m, 1H), 1.40 – 1.29 (m, 1H); **¹³C NMR** (125 MHz, CDCl₃) δ 157.1, 142.0, 131.2, 125.4, 110.3, 106.0, 67.9, 35.2, 32.5, 25.7, 18.1; **MS** (ESI-APCI) calcd. for C₁₁H₁₆O₂ [M – OH]⁺ 163.1, found 163.2.

(E)-2-(hex-4-en-1-yl)-6-hydroxy-2H-pyran-3(6H)-one (61):

Alcohol **60** (521 mg, 2.89 mmol) was dissolved in CH₂Cl₂ (10 mL, 0.3 M), and the resulting solution was cooled to 0 °C. To this solution was added solid vanadyl acetylacetonate (77 mg, 0.29 mmol, 0.1 equiv), then *tert*-butyl hydroperoxide (0.79 mL of a 5.5 M solution in dodecane, 4.35 mmol, 1.5 equiv) by syringe. The reaction was stirred at 0 °C for 1 h, before it was quenched with 1M Na₂S₂O₃ (20 mL) and stirred for a further 30 min. The aqueous layer was extracted with CH₂Cl₂ (2 x 20 mL) and the pooled organic layers were dried over Na₂SO₄, filtered, and concentrated. The crude product was purified by flash chromatography (silica gel, 9:1 to 3:2 hexanes/EtOAc) to afford **61** as a colorless oil as a 2:1 mixture of diastereomers (389 mg, 69%).

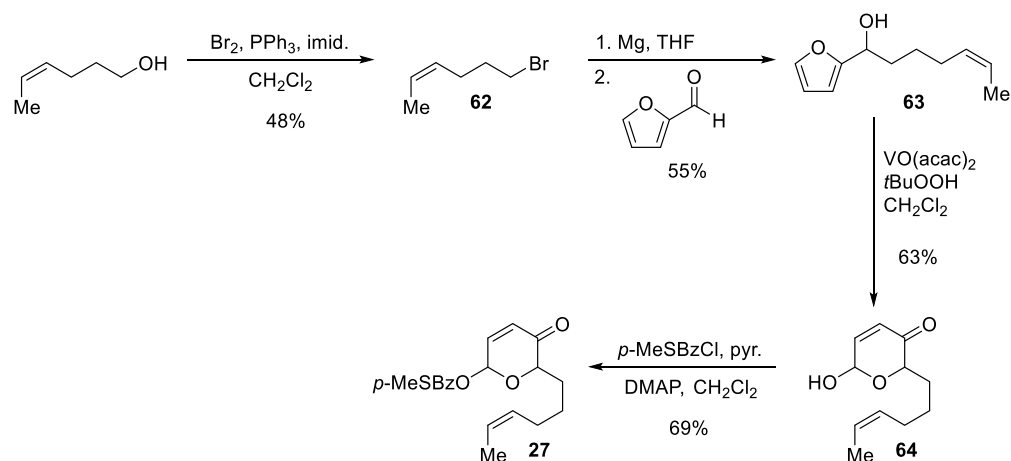
R_f = 0.31 (silica gel, 2:1 hexanes/EtOAc); **IR** (film) ν_{\max} 3398 (br), 2929, 1687, 1438, 1375, 1241, 1153, 1089, 1027, 967, 911, 732 cm⁻¹; **¹H NMR** (500 MHz, CDCl₃) δ 6.94 (minor diast., dd, *J* = 1.4, 10.5 Hz,

0.33H), 6.90 (major diast., dd, $J = 3.7, 10.5$ Hz, 0.67H), 6.15 (minor diast., dd $J = 1.4, 10.5$ Hz, 0.33H), 6.10 (major diast., d, $J = 10.5$ Hz, 0.67H), 5.67 – 5.62 (m, 1H), 5.48 – 5.37 (m, 2H), 4.56 (major diast., dd, $J = 3.9, 8.0$ Hz, 0.67H), 4.08 (minor diast., dd, $J = 3.4, 8.0$ Hz, 0.33H), 3.81 (minor diast., dd, $J = 1.8, 7.3$ Hz, 0.33H), 3.54 (major diast., dd, $J = 1.8, 5.0, 0.67$ H), 2.05 – 1.88 (m, 3H), 1.82 – 1.42 (m, 6H); $^{13}\text{C NMR}$ (500 MHz, CDCl_3) δ 197.1, 196.6, 148.1, 144.8, 131.0, 129.0, 127.8, 125.6, 125.5, 91.1, 87.8, 79.1, 74.4, 32.5, 30.4, 29.4, 25.3, 25.1, 18.1; **MS** (ESI-TOF) calcd. for $\text{C}_{11}\text{H}_{16}\text{O}_3$ $[\text{M} + \text{Na}]^+$ 219.0992, found 219.1005.

(E)-6-(hex-4-en-1-yl)-5-oxo-5,6-dihydro-2H-pyran-2-yl 4-(methylthio)benzoate (25):

Hemiacetal **61** (1.330 g, 6.78 mmol) was dissolved in CH_2Cl_2 (34 mL, 0.2 M) and the resulting solution was cooled to 0 °C. To this solution was added sequentially, 4-thiomethylbenzoyl chloride (1.464 g, 7.45 mmol, 1.1 equiv), pyridine (0.88 mL, 10.88 mmol, 1.6 equiv), and DMAP (250 mg, 2.05 mmol, 0.3 equiv). The reaction was stirred under N_2 and allowed to warm to 23 °C overnight. The solution was diluted with ethyl acetate (60 mL), then washed with 1N HCl (2 x 50 mL), saturated NaHCO_3 (50 mL), and brine (50 mL). The organic layer was dried over Na_2SO_4 , filtered, and concentrated. The crude product was purified by flash chromatography (silica gel, 9:1 to 3:1 hexanes/ Et_2O) to afford **25** as a white powder as a 2:1 mixture of diastereomers (1.286 g, 55%).³²

$R_f = 0.15, 0.19$ (silica gel, 4:1 hexanes/ Et_2O); **IR** (film) ν_{max} 2920, 2361, 1721, 1695, 1593, 1437, 1401, 1327, 1261, 1178, 1094, 1067, 1013, 967, 922, 841, 757, 689 cm^{-1} ; **$^1\text{H NMR}$** (500 MHz, CDCl_3) δ 7.96 – 7.91 (m, 2H), 7.28 – 7.24 (m, 2H), 7.02 – 6.95 (m, 1H), 6.79 (minor diast., dd, $J = 1.5, 2.9$ Hz, 0.33H), 6.74 (major diast., d, $J = 3.9$ Hz, 0.67H), 6.28 – 6.24 (m, 1H), 5.40 – 5.26 (m, 2H), 4.56 (major diast., dd, $J = 3.9, 7.8$ Hz, 0.67H), 4.27 (minor diast., dd, $J = 4.9, 9.8$ Hz, 0.33H), 2.53 – 2.51 (m, 3H), 2.00 – 1.41 (m, 9H); **$^{13}\text{C NMR}$** (125 MHz, CDCl_3) δ 196.0, 165.0, 147.1, 147.0, 142.7, 142.0, 131.0, 130.7, 130.4, 129.1, 128.4, 125.6, 125.5, 125.2, 88.0, 87.7, 79.9, 76.2, 33.3, 32.5, 32.3, 29.4, 25.5, 24.8, 18.1, 15.0; **MS** (ESI-TOF) calcd. for $\text{C}_{19}\text{H}_{22}\text{O}_4\text{S}$ $[\text{M} + \text{Na}]^+$ 369.1131, found 369.1127.



Scheme 2.10. Synthesis of substrate **27**.

(Z)-6-bromohex-2-ene (62):

Reaction of triphenylphosphine (20.204 g, 77.0 mmol, 1.8 equiv), imidazole (8.745 g, 128 mmol, 3 equiv), and bromine (3.8 mL, 73.8 mmol, 1.7 equiv) in CH₂Cl₂ (160 mL, 0.27 M) followed by (Z)-4-hexen-1-ol (5.0 mL, 42.8 mmol) according to **59** above afforded **62** as a pale yellow oil (3.341 g, 48%).

R_f = 0.87 (silica gel, hexanes); **IR** (film) ν_{\max} 3014, 2928, 2855, 1436, 1245, 700, 565 cm⁻¹; **¹H NMR** (500 MHz, CDCl₃) 5.56 – 5.47 (m, 1H), 5.37 – 5.29 (m, 1H), 3.40 (t, J = 6.6 Hz, 2H), 2.20 (q, J = 7.3 Hz, 2H), 1.91 (quin, J = 7.0 Hz, 2H), 1.63 (d, J = 6.8 Hz, 3H); **¹³C NMR** (125 MHz, CDCl₃) δ 126.6, 125.7, 33.6, 32.7, 25.5, 13.1.

(Z)-1-(furan-2-yl)hept-5-en-1-ol (63):

Grignard formation between magnesium turnings (2.498 g, 103 mmol, 5 equiv) and **62** (3.341 g, 20.5 mmol) with 1,2-dibromoethane (0.05 mL, 0.58 mmol) was carried out in THF (50 mL, 0.41 M) according to **60** above. Addition of this Grignard reagent to furfural (1.70 mL, 20.5 mmol, 1 equiv) in THF (50 mL) according to **60** above afforded **63** as a colorless oil after column chromatography (silica gel, 9:1 to 3:2 hexanes/EtOAc) (2.031 g, 55%).

R_f = 0.37 (silica gel, 2:1 hexanes/EtOAc); **IR** (film) ν_{\max} 3375 (br), 3013, 2936, 2862, 2360, 2341, 1505, 1443, 1404, 1231, 1148, 1006 cm⁻¹; **¹H NMR** (500 MHz, CDCl₃) δ 7.36 – 7.34 (m, 1H), 6.31 (dd, J = 2.1, 3.0 Hz, 1H), 6.21 (d, J = 3.2 Hz, 1H), 5.52 – 5.42 (m, 1H), 5.42 – 5.34 (m, 1H), 4.67 – 4.60 (m, 1H), 2.56

(br. s., 1H), 2.07 (q, $J = 7.3$ Hz, 2H), 1.92 – 1.78 (m, 2H), 1.60 (dd, $J = 0.9, 7.3$ Hz, 3H), 1.54 – 1.44 (m, 1H), 1.43 – 1.33 (m, 1H); ^{13}C NMR (125 MHz, CDCl_3) δ 157.2, 142.0, 130.4, 124.4, 110.3, 106.0, 67.9, 35.3, 26.7, 25.7, 13.0; MS (ESI-APCI) calcd. for $\text{C}_{11}\text{H}_{16}\text{O}_2$ $[\text{M} - \text{OH}]^+$ 163.1, found 163.1.

(Z)-2-(hex-4-en-1-yl)-6-hydroxy-2H-pyran-3(6H)-one (64):

Reaction of **63** (2.031 g, 11.3 mmol), vanadyl acetylacetonate (300 mg, 1.13 mmol, 0.1 equiv), and *tert*-butyl hydroperoxide (3.1 mL of a 5.5 M solution in dodecane, 17.1 mmol, 1.5 equiv) in CH_2Cl_2 (38 mL, 0.3 M) according to **61** above afforded **64** as a colorless oil after column chromatography (silica gel, 9:1 to 3:2 hexanes/EtOAc) as a 2:1 mixture of diastereomers (1.402 g, 63%).

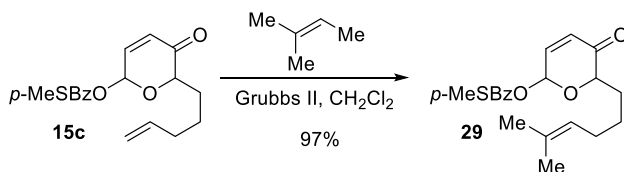
$R_f = 0.37$ (silica gel, 2:1 hexanes/EtOAc); IR (film) ν_{max} 3401 (br), 2929, 1694, 1438, 1373, 1241, 1143, 1091, 1033, 964, 913, 737 cm^{-1} ; ^1H NMR (500 MHz, CDCl_3) δ 6.94 (minor diast., dd, $J = 1.4, 10.1$ Hz, 0.33H), 6.91 (major diast., dd, $J = 3.2, 10.3$ Hz, 0.67H), 6.18 (minor diast., dd, $J = 1.6, 10.3$ Hz, 0.33H), 6.13 (major diast., d, $J = 10.1$ Hz, 0.67H), 5.70 – 5.65 (m, 1H), 5.52 – 5.45 (m, 1H), 5.43 – 5.37 (m, 1H), 4.59 (major diast., dd, $J = 4.1, 8.4$ Hz, 0.67H), 4.11 (minor diast., dd, $J = 4.1, 8.2$ Hz, 0.33H), 3.10 (minor diast., d, $J = 7.3$ Hz, 0.33H), 2.89 (major diast., d, $J = 5.0$ Hz, 0.67H), 2.10 (q, $J = 7.0$ Hz, 2H), 2.02 – 1.94 (m, 1H), 1.86 – 1.78 (minor diast., m, 0.33H), 1.78 – 1.69 (major diast., m, 0.67H), 1.62 (d, $J = 6.4$ Hz, 3H), 1.56 – 1.47 (m, 2H); ^{13}C NMR (125 MHz, CDCl_3) δ 198.5, 147.7, 144.3, 130.3, 130.2, 129.06, 128.0, 124.6, 91.1, 87.9, 79.1, 74.4, 30.5, 29.5, 26.38, 25.3, 25.2, 13.0; MS (ESI-TOF) calcd. for $\text{C}_{11}\text{H}_{16}\text{O}_3$ $[\text{M} + \text{Na}]^+$ 219.0992, found 219.1004.

(Z)-6-(hex-4-en-1-yl)-5-oxo-5,6-dihydro-2H-pyran-2-yl 4-(methylthio)benzoate (27):

Reaction of **64** (687 mg, 3.50 mmol), 4-thiomethylbenzoyl chloride (756 mg, 3.85 mmol, 1.1 equiv), pyridine (0.45 mL, 5.56 mmol, 1.59 equiv), and DMAP (130 mg, 1.06 mmol, 0.3 equiv) in CH_2Cl_2 (18 mL, 0.19 M) according to **25** above afforded **27** as a white gel after column chromatography (silica gel, 9:1 to 3:1 hexanes/Et₂O) as a 2:1 mixture of diastereomers (835 mg, 69%).

$R_f = 0.15, 0.19$ (silica gel, 4:1 hexanes/Et₂O); IR (film) ν_{max} 2924, 1720, 1695, 1593, 1491, 1437, 1402, 1327, 1262, 1177, 1094, 1067, 1013, 922, 840, 756, 689 cm^{-1} ; ^1H NMR (500 MHz, CDCl_3) δ 7.96 – 7.89 (m, 2H), 7.27 – 7.24 (m, 2H), 7.03 – 6.94 (m, 1H), 6.78 (minor diast., d, $J = 2.4$ Hz, 0.33H), 6.73 (major

diast., d, $J = 3.4$ Hz, 0.67H), 6.28 – 6.24 (m, 1H), 5.46 – 5.17 (m, 2H), 4.56 (major diast., dd, $J = 3.7, 7.6$ Hz, 0.67H), 4.27 (minor diast., dd, $J = 4.4, 9.8$ Hz, 0.33H), 2.50 (s, 3H), 2.08 – 1.80 (m, 4H), 1.76 (dq, $J = 7.5, 14.7$ Hz, 1H), 1.54 (d, $J = 6.3$ Hz, 2H), 1.51 – 1.43 (m, 2H); $^{13}\text{C NMR}$ (125 MHz, CDCl_3) δ 196.1, 196.0, 165.0, 164.9, 147.1, 147.0, 142.8, 142.0, 130.4, 130.2, 129.9, 129.1, 128.4, 125.2, 124.6, 124.5, 88.0, 87.7, 79.9, 76.1, 33.4, 29.5, 26.7, 26.5, 25.5, 24.7, 15.0, 13.0; **MS** (ESI-TOF) calcd. for $\text{C}_{19}\text{H}_{22}\text{O}_4\text{S}$ [$\text{M} + \text{Na}$] $^+$ 369.1131, found 369.1133.

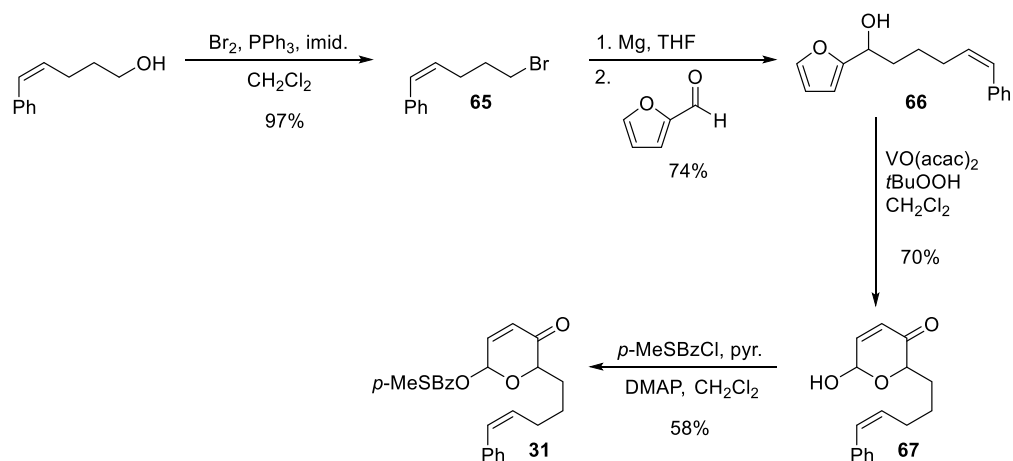


Scheme 2.11. Synthesis of substrate **29**.

6-(5-methylhex-4-en-1-yl)-5-oxo-5,6-dihydro-2H-pyran-2-yl 4-(methylthio)benzoate (29):

Grubbs' Catalyst, 2nd Generation (29 mg, 0.034 mmol, 0.03 equiv) was dissolved in CH_2Cl_2 (2.0 mL) in a sealed tube. To the solution was added by syringe **15c** (378 mg, 1.14 mmol), dissolved in CH_2Cl_2 (2.0 mL) then 2-methyl-2-butene (3.3 mL, 31.1 mmol, 27 equiv). The reaction was stirred at 39 °C overnight. The crude mixture was concentrated and purified by flash chromatography (silica gel, 9:1 to 3:2 hexanes/ Et_2O) to afford **29** as a colorless oil as a 2:1 mixture of diastereomers (397 mg, 97%).

$R_f = 0.13, 0.17$ (silica gel, 4:1 hexanes/ Et_2O); **IR** (film) ν_{max} 2925, 1725, 1698, 1594, 1438, 1402, 1328, 1235, 1177, 1095, 1071, 1013, 930, 841, 758, 690 cm^{-1} ; $^1\text{H NMR}$ (500 MHz, CDCl_3) δ 7.97 – 7.92 (m, 2H), 7.29 – 7.24 (m, 2H), 7.02 – 6.95 (m, 1H), 6.79 (minor diast., dd, $J = 1.5, 2.9$ Hz, 0.33H), 6.74 (major diast., d, $J = 3.9$ Hz, 0.67H), 6.29 – 6.25 (m, 1H), 5.12 – 5.05 (major diast., m, 0.67H), 5.01 – 4.95 (minor diast., m, 0.33H), 4.56 (major diast., dd, $J = 3.9, 7.8$ Hz, 0.67H), 4.30 (minor diast., dd, $J = 4.6, 9.5$ Hz, 0.33H), 2.54 – 2.51 (m, 3H), 2.02 – 1.81 (m, 3H), 1.80 – 1.71 (m, 1H), 1.69 – 1.60 (m, 3H), 1.58 – 1.53 (m, 2H), 1.52 – 1.41 (m, 3H); $^{13}\text{C NMR}$ (125 MHz, CDCl_3) δ 196.0, 165.0, 147.0, 142.8, 141.9, 132.0, 130.4, 129.1, 128.5, 125.2, 124.3, 124.0, 88.0, 87.7, 80.0, 79.2, 33.4, 29.5, 27.9, 27.7, 25.9, 25.8, 25.1, 17.9, 17.8, 15.0; **MS** (ESI-TOF) calcd. for $\text{C}_{20}\text{H}_{24}\text{O}_4\text{S}$ [$\text{M} + \text{Na}$] $^+$ 383.1293, found 383.1276.



Scheme 2.12. Synthesis of substrate **31**.

(Z)-(5-bromopent-1-en-1-yl)benzene (65):

Reaction of triphenylphosphine (10.006 g, 38.1 mmol, 1.8 equiv), imidazole (4.319 g, 63.4 mmol, 3 equiv), and bromine (1.9 mL, 36.9 mmol, 1.7 equiv) in CH_2Cl_2 (71 mL, 0.30 M) followed by (Z)-5-phenylpent-4-en-1-ol³⁵ (3.435 g, 21.2 mmol) according to **59** above afforded **65** as a pale yellow oil (4.646 g, 97%).

Spectroscopic data agree with previously reported data.³⁶

(Z)-1-(furan-2-yl)-6-phenylhex-5-en-1-ol (66):

Grignard formation between magnesium turnings (2.514 g, 103 mmol, 8 equiv) and **65** (2.910 g, 12.9 mmol) with 1,2-dibromoethane (0.05 mL, 0.58 mmol) was carried out in THF (32 mL, 0.40 M) according to **60** above. Addition of this Grignard reagent to furfural (1.07 mL, 12.9 mmol, 1 equiv) in THF (32 mL) according to **60** above afforded **66** as a yellow oil after column chromatography (silica gel, 9:1 to 3:2 hexanes/ Et_2O) (2.307 g, 74%).

$R_f = 0.43$ (silica gel, 2:1 hexanes/ EtOAc); **IR** (film) ν_{max} 3355 (br), 3009, 2939, 2862, 1599, 1494, 1447, 1151, 1170, 1070, 1008, 915, 807, 767, 737, 699 cm^{-1} ; **$^1\text{H NMR}$** (500 MHz, CDCl_3) δ 7.41 – 7.26 (m, 6H), 6.47 (d, $J = 11.7$ Hz, 1H), 6.35 (dd, $J = 2.0, 3.4$ Hz, 1H), 6.24 (d, $J = 2.9$ Hz, 1H), 5.68 (dt, $J = 7.3, 11.7$ Hz, 1H), 4.71 – 4.65 (m, 1H), 2.41 (qd, $J = 1.7, 7.4$ Hz, 2H), 1.95 – 1.88 (m, 2H), 1.69 – 1.59 (m, 1H), 1.56

³⁵ (Z)-5-phenylpent-4-en-1-ol synthesized according to: Liu, G.; Stahl, S. S. *J. Am. Chem. Soc.* **2007**, *129*, 6328–6335.

³⁶ Feltenberger, J. B.; Hayashi, R.; Tang, Y.; Babiash, E. S. C.; Hsung, R. P. *Org. Lett.* **2009**, *11*, 3666–3669.

– 1.46 (m, 1H); ^{13}C NMR (125 MHz, CDCl_3) δ 157.0, 142.2, 137.9, 132.7, 129.5, 129.0, 128.4, 126.8, 110.4, 106.1, 67.8, 35.4, 28.5, 26.1; MS (ESI-APCI) calcd. for $\text{C}_{16}\text{H}_{18}\text{O}_2$ $[\text{M} - \text{OH}]^+$ 225.1, found 225.2.

(Z)-6-hydroxy-2-(5-phenylpent-4-en-1-yl)-2H-pyran-3(6H)-one (67):

Reaction of **66** (325 mg, 1.34 mmol), vanadyl acetylacetonate (37 mg, 0.13 mmol, 0.1 equiv), and *tert*-butyl hydroperoxide (0.37 mL of a 5.5 M solution in dodecane, 2.04 mmol, 1.5 equiv) in CH_2Cl_2 (4.5 mL, 0.3 M) according to **61** above afforded **67** as a colorless oil after column chromatography (silica gel, 9:1 to 3:2 hexanes/EtOAc) as a 9:1 mixture of diastereomers (245 mg, 70%).

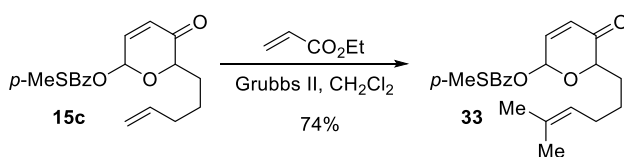
R_f = 0.26 (silica gel, 2:1 hexanes/EtOAc); IR (film) ν_{max} 3400 (br), 3009, 2927, 2862, 1687, 1494, 1446, 1371, 1237, 1150, 1092, 1027, 917, 801, 769, 699 cm^{-1} ; ^1H NMR (500 MHz, CDCl_3) δ 7.36 – 7.31 (m, 2H), 7.27 (d, J = 21.5 Hz, 2H), 7.22 (t, J = 7.32 Hz, 1H), 6.89 (minor diast., dd, J = 1.5, 10.4 Hz, 0.11H), 6.85 (major diast., dd, J = 3.4, 10.3 Hz, 0.89H), 6.44 (major diast., d, J = 11.2 Hz, 0.89H), 6.40 (minor diast., d, J = 15.6 Hz, 0.11H), 6.12 (minor diast., dd, J = 1.5, 10.3 Hz, 0.11H), 6.08 (major diast., d, J = 10.3 Hz, 0.89H), 5.66 (dt, J = 7.2, 11.5 Hz, 1H), 5.57 (dd, J = 3.7, 4.6 Hz, 1H), 4.60 (minor diast., dd, J = 3.9, 7.8 Hz, 0.11H), 4.54 (major diast., dd, J = 3.9, 8.3 Hz, 0.89H), 2.44 – 2.30 (m, 2H), 2.03 – 1.92 (m, 1H), 1.85 – 1.70 (m, 1H), 1.65 – 1.55 (m, 2H); ^{13}C NMR (125 MHz, CDCl_3) δ 197.1, 196.7, 148.3, 144.9, 137.9, 137.8, 132.6, 132.5, 129.6, 129.5, 129.0, 128.9, 128.8, 128.4, 127.7, 126.8, 126.2, 91.1, 87.8, 78.8, 74.1, 33.0, 30.3, 29.4, 28.4, 25.6.

(Z)-5-oxo-6-(5-phenylpent-4-en-1-yl)-5,6-dihydro-2H-pyran-2-yl 4-(methylthio)benzoate (31):

Reaction of **67** (1.107 g, 4.29 mmol), 4-thiomethylbenzoyl chloride (926 mg, 4.71 mmol, 1.1 equiv), pyridine (0.56 mL, 6.92 mmol, 1.62 equiv), and DMAP (157 mg, 1.29 mmol, 0.3 equiv) in CH_2Cl_2 (21 mL, 0.2 M) according to **25** above afforded **31** as a yellow oil after column chromatography (silica gel, 9:1 to 3:1 hexanes/ Et_2O) as a 9:1 mixture of diastereomers (1.010 g, 58%).

R_f = 0.15, 0.20 (silica gel, 4:1 hexanes/ Et_2O); IR (film) ν_{max} 2924, 1721, 1698, 1593, 1492, 1402, 1328, 1264, 1177, 1094, 1069, 1013, 928, 915, 841, 757, 700, 631 cm^{-1} ; ^1H NMR (500 MHz, CDCl_3) δ 7.99 – 7.94 (m, 2H), 7.38 – 7.17 (m, 7H), 7.15 (major diast., dd, J = 3.3, 10.6 Hz, 0.89H), 7.00 (minor diast., dd, J = 3.9, 10.4 Hz, 0.11H), 6.76 (major diast., d, J = 3.9 Hz, 0.89H), 6.74 (minor, diast., d, J = 3.9 Hz, 0.11H),

6.41 (minor diast., d, $J = 11.2$ Hz, 0.11H), 6.35 (major diast., d, $J = 15.6$ Hz, 0.89H), 6.33 (major diast., m, 0.89H), 6.26 (d, $J = 10.3$ Hz, 0.11H), 5.64 (dt, $J = 7.1, 11.6$ Hz, 1H), 4.61 (major diast., dd, $J = 3.9, 7.4$ Hz, 0.89H), 4.57 (minor, diast., dd, $J = 3.9, 7.3$ Hz, 0.11H), 2.51 (s, 3H), 2.41 – 2.31 (m, 2H), 2.06 – 1.77 (m, 2H), 1.77 – 1.60 (m, 2H); $^{13}\text{C NMR}$ (125 MHz, CDCl_3) δ 195.9, 195.8, 164.9, 147.1, 147.0, 142.9, 142.0, 137.8, 132.5, 132.2, 130.4, 130.3, 129.6, 129.5, 129.0, 128.9, 128.5, 128.4, 126.8, 126.7, 126.2, 125.3, 125.2, 88.1, 87.7, 79.7, 76.1, 33.2, 29.6, 28.5, 28.2, 25.9, 25.1, 15.0; **MS** (ESI-TOF) calcd. for $\text{C}_{24}\text{H}_{24}\text{O}_4\text{S}$ $[\text{M} + \text{Na}]^+$ 431.1288, found 431.1289.



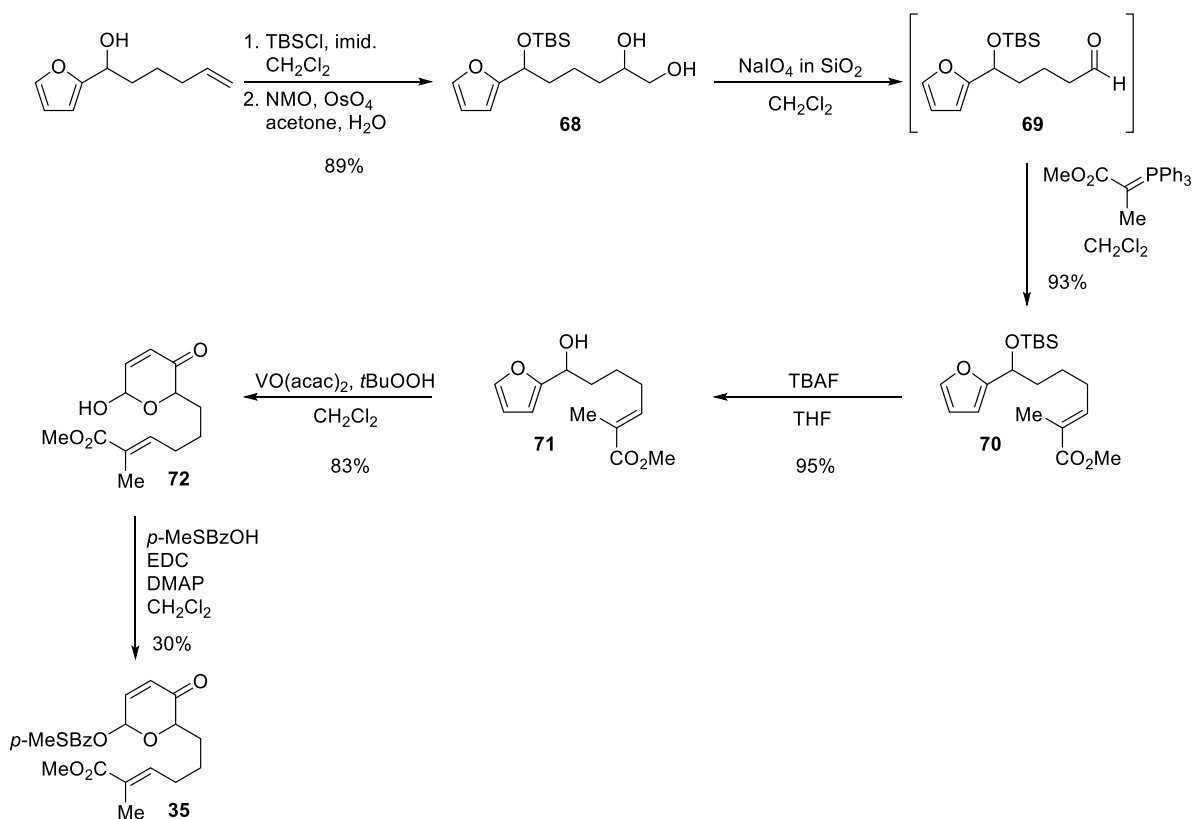
Scheme 2.13. Synthesis of substrate **33**.

(E)-6-(6-ethoxy-6-oxohex-4-en-1-yl)-5-oxo-5,6-dihydro-2H-pyran-2-yl 4-(methylthio)benzoate (33):

A microwave vial was charged with **15c** (199.0 mg, 0.599 mmol) and Grubbs' Catalyst, 2nd Generation (25.0 mg, 0.03 mmol, 0.05 equiv). The vial was capped and then purged with N_2 before the addition of CH_2Cl_2 (3.0 mL, 0.2 M). Ethyl acrylate (0.260 mL, 2.40 mmol, 4.0 equiv) was introduced via syringe and the vial was then placed in a $40\text{ }^\circ\text{C}$ oil bath and stirred for 22 h. The reaction mixture was then concentrated and chromatographed on silica gel to afford **33** as a slightly dark oil as a 3:2 mixture of diastereomers (180.0 mg, 74%).

$R_f = 0.11, 0.17$ (silica gel, 5:1 hexanes/EtOAc); **IR** (film) ν_{max} 2926, 2867, 1714, 1593, 1262, 1176, 1094, 1067, 924, 757 cm^{-1} ; $^1\text{H NMR}$ (500 MHz, CDCl_3) δ 7.95 – 7.89 (m, 2H), 7.28 – 7.22 (m, 2H), 7.02 – 6.96 (m, 1H), 6.90 (major diast., dt, $J = 6.8, 15.6$ Hz, 0.6H), 6.81 (minor diast., dt, $J = 6.8, 15.6$ Hz, 0.4H), 6.79 – 6.71 (m, 1H), 6.28 – 6.24 (m, 1H), 5.77 (major diast., dt, $J = 1.5, 15.6$ Hz, 0.6H), 5.71 – 5.66 (minor diast., m, 0.4H), 4.55 (major diast., dd, $J = 3.9, 7.8$ Hz, 0.6H), 4.26 (minor diast., dd, $J = 5.1, 9.0$ Hz, 0.4H), 4.17 – 4.11 (m, 2H), 2.51 (s, 3H), 2.21 – 2.16 (m, 1H), 2.14 – 1.73 (m, 3H), 1.61 – 1.54 (m, 2H), 1.25 (dt, $J = 2.0, 6.8$ Hz, 3H); $^{13}\text{C NMR}$ (100 MHz, CDCl_3) δ 195.6, 166.8, 166.7, 165.0, 164.8, 148.6, 148.2, 147.3, 147.1, 143.1, 142.1, 130.4, 129.0, 128.6, 125.2, 122.1, 122.0, 88.1, 87.6, 79.5, 75.9, 60.4, 32.9, 32.0, 31.9,

29.3, 24.1, 23.4, 14.9, 14.5; **MS** (ESI-TOF) calcd. for C₂₁H₂₄O₆S [M + Na⁺] 427.1186, found 427.1190.



Scheme 2.14. Synthesis of substrate **35**.

6-((*tert*-butyldimethylsilyloxy)-6-(furan-2-yl)hexane-1,2-diol (68):

1-(furan-2-yl)hex-5-en-1-ol³⁷ (2.096 g, 12.6 mmol) was dissolved in CH₂Cl₂ (63 mL, 0.2 M) under a N₂ atmosphere and cooled to 0 °C. Imidazole (2.06g, 30.3 mmol, 2.4 equiv) was added to the reaction mixture followed by *tert*-butyldimethylsilyl chloride (2.28 g, 15.1 mmol, 1.2 equiv). The reaction mixture was allowed to warm to 23 °C and stirred for 30 min. Sat. aq. NH₄Cl (50 mL) and Et₂O (100 mL) were added and the layers were separated. The organic layer was washed sequentially with water (50 mL) and brine (50 mL) and the organic layer was then dried over Na₂SO₄, filtered, and concentrated to afford the silyl ether as a slightly yellow oil (3.398 g, 96%). This material was dissolved in acetone/H₂O (9:1, 61 mL total volume, 0.2 M) and cooled to 0 °C. *N*-Methylmorpholine-*N*-oxide (2.129 g, 18.2 mmol, 1.5 equiv) was

³⁷ 1-(furan-2-yl)hex-5-en-1-ol was synthesized according to: Sammes, P. G.; Street, L. J.; Kirby, P. *J. Chem. Soc., Perkin Trans. 1* **1983**, 2729–2734.

added followed by osmium tetroxide (1.52 mL of a 2.5 wt% solution in *tert*-butanol, 0.121 mmol, 0.01 equiv). The reaction mixture was kept at 0 °C for 30 min then allowed to warm to 23 °C. After stirring for 3 h, 1M Na₂S₂O₃ (30 mL) was added and the mixture was stirred overnight. Sat. aq. NaHCO₃ (30 mL) and EtOAc (150 mL) were added and the layers were separated. The aqueous layer was further extracted with EtOAc (3 x 100 mL), and the combined organic layers were dried over Na₂SO₄, filtered, and concentrated. Purification by column chromatography (silica gel, 2:1 to 1:1 hexanes/EtOAc) then afforded **68** as a clear oil (3.55 g, 89% overall).

R_f = 0.08 (silica gel, 2:1 hexanes/EtOAc); **IR** (film) ν_{\max} 3368 (br), 2930, 2858, 2360, 1462, 1361, 1344, 1254, 1075, 1006, 835, 776, 734 cm⁻¹; **¹H NMR** (500 MHz, CDCl₃) δ 7.34 – 7.31 (m, 1H), 6.31 – 6.28 (m, 1H), 6.15 (d, J = 2.9 Hz, 1H), 4.68 (td, J = 1.5, 7.1 Hz, 1H), 3.73 – 3.66 (m, 1H), 3.65 – 3.59 (m, 1H), 3.44 – 3.37 (m, 1H), 1.89 – 1.73 (m, 3H), 1.57 – 1.47 (m, 1H), 1.47 – 1.37 (m, 3H), 1.37 – 1.28 (m, 1H), 0.87 (s, 9H), 0.04 (s, 3H), –0.08 (s, 3H); **¹³C NMR** (125 MHz, CDCl₃) δ 157.4, 141.5, 110.2, 106.0, 72.4, 68.6, 67.0, 37.0, 33.1, 26.0, 21.6, 18.4, –4.7; **MS** (ESI-TOF) calcd. for C₁₆H₃₀O₄Si [M + Na⁺] 337.1806, found 337.1820.

5-((*tert*-butyldimethylsilyl)oxy)-5-(furan-2-yl)pentanal (69**):**

Diol **68** (1.003 g, 3.19 mmol) was dissolved in CH₂Cl₂ (32 mL, 0.1 M) and to this solution was added sodium periodate immobilized on silica gel³⁸ (6.36 g, 2 g per mmol substrate). The reaction was vigorously stirred under N₂ for 30 minutes. The resulting suspension was filtered through a sintered glass funnel, and the silica gel was washed with CH₂Cl₂ (3 x 25 mL). The filtrate was concentrated to afford **69** as a colorless oil which was used immediately in the subsequent Wittig olefination (848 mg, 94%).

¹H NMR (500 MHz, CDCl₃) δ 9.74 (t, J = 1.4 Hz, 1H), 7.33 (dd, J = 0.9, 1.8 Hz, 1H), 6.30 (dd, J = 1.6, 3.0 Hz, 1H), 6.17 (d, J = 3.2 Hz, 1H), 4.71 (dd, J = 5.3, 7.1 Hz, 1H), 2.42 (td, J = 1.6, 7.2 Hz, 2H), 1.91 – 1.57 (m, 4H), 0.87 (s, 9H), 0.05 (s, 3H), –0.08 (s, 3H).

³⁸ Silica gel-supported sodium periodate prepared and used according to: Zhong, Y.-L.; Shing, T. K. M. *J. Org. Chem.* **1997**, *62*, 2622–2624.

(E)-methyl 7-((tert-butyldimethylsilyloxy)-7-(furan-2-yl)-2-methylhept-2-enoate (70):

Aldehyde **69** (848 mg, 3.00 mmol) was dissolved in CH₂Cl₂ (11.5 mL, 0.26 M) and the resulting solution was cooled to 0 °C. To this solution was added known ylide methyl 2-(triphenylphosphoranylidene)propanoate³⁹ (1.361 g, 3.91 mmol, 1.3 equiv) and the solution was allowed to warm to 23 °C. The reaction was stirred under N₂ for 4 h until TLC indicated complete disappearance of **69**. The resulting solution was concentrated and purified by flash chromatography (silica gel, 9:1 to 3:1 hexanes/EtOAc) to afford **70** as a colorless oil (1.048 g, 99%).

R_f = 0.15 (silica gel, hexanes); **IR** (film) ν_{\max} 2930, 2361, 1715, 1256, 1089, 1006, 835, 776, 734 cm⁻¹; **¹H NMR** (500 MHz, CDCl₃) δ 7.33 (t, *J* = 0.92, 1H), 6.75 (td, *J* = 1.4, 7.5 Hz, 1H), 6.30 (dd, *J* = 2.1, 3.0 Hz, 1H), 6.16 (d, *J* = 3.2 Hz, 1H), 4.69 (dd, *J* = 5.7, 7.1 Hz, 1H), 3.73 (s, 3H), 2.18 (q, *J* = 7.8 Hz, 2H), 1.91 – 1.74 (m, 5H), 1.60 – 1.50 (m, 1H), 1.49 – 1.39 (m, 1H), 0.88 (s, 9H), 0.06 (s, 3H), –0.07 (s, 3H); **¹³C NMR** (125 MHz, CDCl₃) δ 168.8, 157.4, 142.5, 141.5, 127.9, 110.2, 105.9, 68.5, 51.9, 36.8, 28.7, 26.0, 24.6, 18.4, 12.6, –4.7, –4.9; **MS** (ESI) calcd. for C₁₉H₃₂O₄Si [M + Na]⁺ 375.2, found 375.2.

(E)-methyl 7-(furan-2-yl)-7-hydroxy-2-methylhept-2-enoate (71):

Ester **70** (1.096 g, 3.11 mmol) was dissolved in THF (21 mL, 0.15 M) and the resulting solution was cooled to 0 °C. To this solution was added by syringe TBAF (1.0 M in THF, 4.7 mL, 4.7 mmol, 1.5 equiv). The reaction was stirred under N₂ for 2 h, until TLC indicated complete disappearance of **70**. The solution was diluted with EtOAc (40 mL), then washed with sat. aq. NH₄Cl (40 mL). The aqueous layer was then extracted with EtOAc (2 x 30 mL), and the pooled organic layers were washed with brine (40 mL), dried over Na₂SO₄, filtered, and concentrated. The crude product was purified by flash chromatography (silica gel, 9:1 to 3:2 hexanes/EtOAc) to afford **71** as a colorless oil (707 mg, 95%).

R_f = 0.11 (silica gel, 4:1 hexanes/EtOAc); **IR** (film) ν_{\max} 3435 (br), 2949, 1709, 1648, 1436, 1259, 1090, 1008, 737 cm⁻¹; **¹H NMR** (500 MHz, CDCl₃) δ 7.33 (dd, *J* = 1.0, 2.0, 1H), 6.72 (td, *J* = 1.2, 7.4 Hz, 1H), 6.29 (dd, *J* = 2.0, 2.9 Hz, 1H), 6.19 (d, *J* = 3.4 Hz, 1H), 4.64 (t, *J* = 6.8 Hz, 1H), 3.69 (s, 3H), 2.44 (br. s,

³⁹ Methyl 2-(triphenylphosphoranylidene)propanoate synthesized according to: Eey, S. T.-C.; Lear, M. J. *Org. Lett.* **2010**, *12*, 5510–5513.

1H), 2.18 (q, $J = 7.3$ Hz, 2H), 1.84 (q, $J = 7.4$ Hz, 2H), 1.79 (s, 3H), 1.62 – 1.52 (m, 1H), 1.49 – 1.39 (m, 1H); ^{13}C NMR (125 MHz, CDCl_3) δ 168.9, 159.9, 142.3, 142.1, 128.0, 110.3, 106.1, 67.7, 51.9, 35.3, 28.5, 24.8, 12.5; MS (APCI) calcd. for $\text{C}_{13}\text{H}_{18}\text{O}_4$ $[\text{M} - \text{OH}]^+$ 221.1, found 221.1.

(E)-methyl 6-(6-hydroxy-3-oxo-3,6-dihydro-2H-pyran-2-yl)-2-methylhex-2-enoate (72):

Reaction of **71** (707 mg, 2.97 mmol), vanadyl acetylacetonate (80 mg, 0.30 mmol, 0.1 equiv), and *tert*-butyl hydroperoxide (0.81 mL of a 5.5 M solution in dodecane, 1.50 mmol, 1.5 equiv) in CH_2Cl_2 (10 mL, 0.3 M) according to **61** above afforded **72** as a colorless oil after column chromatography (silica gel, 4:1 to 1:1 hexanes/EtOAc) as a 2:1 mixture of diastereomers (623 mg, 83%).

$R_f = 0.37$ (silica gel, 1:1 hexanes/EtOAc); IR (film) ν_{max} 3412 (br), 2952, 1690, 1648, 1437, 1370, 1264, 1090, 1029, 746 cm^{-1} ; ^1H NMR (500 MHz, CDCl_3) δ 6.93 (minor diast., dd, $J = 0.9, 9.8$ Hz, 0.33H), 6.90 (major diast., dd, $J = 3.2, 10.1$ Hz, 0.67H), 6.78 – 6.71 (m, 1H), 6.11 (minor diast., dd, $J = 1.1, 10.3$ Hz, 0.33H), 6.06 (major diast., d, $J = 10.5$ Hz, 0.67H), 5.65 – 5.59 (m, 1H), 4.56 (dd, $J = 3.9, 8.0$ Hz, 1H), 4.34 (br. s, 1H), 3.71 (s, 3H), 2.19 (q, $J = 7.3$ Hz, 2H), 1.99 – 1.90 (m, 1H), 1.80 (s, 3H), 1.75 – 1.66 (m, 1H), 1.61 – 1.53 (m, 2H); ^{13}C NMR (125 MHz, CDCl_3) δ 197.0, 196.5, 169.3, 148.7, 145.2, 142.8, 142.6, 128.8, 127.9, 127.5, 91.1, 87.8, 78.7, 73.8, 52.1, 30.4, 29.5, 28.6, 24.4, 24.2, 12.6; MS (ESI-TOF) calcd. for $\text{C}_{13}\text{H}_{18}\text{O}_5$ $[\text{M} + \text{Na}^+]$ 277.1046, found 277.1073.

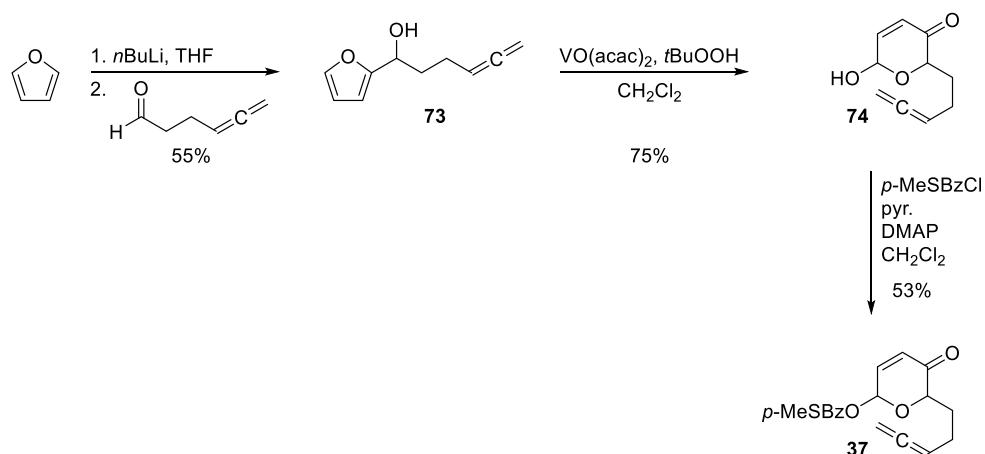
(E)-6-(6-methoxy-5-methyl-6-oxohex-4-en-1-yl)-5-oxo-5,6-dihydro-2H-pyran-2-yl

4-(methylthio)benzoate (35):

Reaction of **72** (623 mg, 2.45 mmol), 4-methylthiobenzoic acid (536 mg, 3.19 mmol, 1.3 equiv), EDC (661 mg, 3.45 mmol, 1.4 equiv), and DMAP (391 mg, 3.20 mmol, 1.3 equiv) in CH_2Cl_2 (12 mL, 0.2 M) according to **15c** above afforded **35** as a colorless oil after column chromatography (silica gel, 9:1 to 3:2 hexanes/EtOAc) as a 2:1 mixture of diastereomers (293 mg, 30%).

$R_f = 0.22$ (silica gel, 4:1 hexanes/EtOAc); IR (film) ν_{max} 2951, 2360, 1709, 1650, 1593, 1436, 1260, 1178, 1094, 1069, 924, 758 cm^{-1} ; ^1H NMR (500 MHz, CDCl_3) δ 7.94 (dd, $J = 0.9, 8.7$ Hz, 2H), 7.29 – 7.25 (m, 2H), 7.01 (major diast., td, $J = 3.2, 10.6$ Hz, 0.67H), 6.89 (minor diast., dd, $J = 3.7, 10.2$ Hz, 0.33H), 6.81 (major diast., dd, $J = 1.4, 2.7$ Hz, 0.67H), 6.76 – 6.70 (minor diast. x 2, m, 0.66H), 6.65 (major diast., td, J

= 1.4, 7.3 Hz, 0.67H), 6.31 – 6.26 (m, 1H), 4.57 (minor diast., dd, $J = 3.9, 7.6$ Hz, 0.33H), 4.29 (major diast., dd, $J = 5.0, 9.2$ Hz, 0.67H), 3.72 (major diast., s, 2H), 3.71 (minor diast., s, 1H), 2.53 (d, $J = 2.3$ Hz, 3H), 2.22 – 1.54 (m, 9H); ^{13}C NMR (125 MHz, CDCl_3) δ 201.9, 195.7, 174.9, 171.8, 168.7, 164.9, 147.3, 147.1, 143.1, 142.1, 141.9, 141.6, 130.3, 129.0, 128.6, 128.2, 125.2, 88.1, 87.6, 87.3, 79.6, 76.0, 53.3, 51.9, 47.3, 47.2, 45.8, 35.4, 33.1, 29.5, 28.5, 28.4, 24.6, 24.0, 21.3, 14.9, 12.5; **MS** (ESI-TOF) calcd. for $\text{C}_{21}\text{H}_{24}\text{O}_6\text{S}$ [$\text{M} + \text{Na}^+$] 427.1186, found 427.1184.



Scheme 2.15. Synthesis of substrate 37.

1-(furan-2-yl)hexa-4,5-dien-1-ol (73):

Freshly distilled furan (0.952 mL, 13.0 mmol, 1.3 equiv) was dissolved in THF (15 mL, 0.87 M relative to furan) under an atmosphere of N_2 and the resulting mixture was cooled to -78 °C. $n\text{BuLi}$ (5.71 mL of a 2.1 M solution in hexanes, 12.0 mmol, 1.2 equiv) was introduced dropwise via syringe. After addition, the reaction mixture was allowed to warm to 0 °C and stirred at that temperature for 30 min. A separate flask was charged with a solution of 4,5-hexadien-1-al⁴⁰ (0.961 g, 10.0 mmol) in THF (15 mL, 0.67 M in aldehyde) and this mixture was cooled to 0 °C. The furan-2-yllithium solution was then added via cannula. An additional amount of THF (3 mL) was used in order to ensure a quantitative transfer. The solution was stirred at 0 °C for 30 min before the careful addition of sat. aq. NH_4Cl (20 mL). EtOAc (50 mL) was added

⁴⁰ 4,5-Hexadien-1-al synthesized according to: Tsukamoto, H.; Matsumoto, T.; Kondo, Y. *J. Am. Chem. Soc.* **2008**, *130*, 388–389.

and the layers were separated. The organic layer was washed with brine (20 mL), and the combined aqueous layers were extracted with EtOAc (2 x 50 mL). The combined organic layers were then dried over MgSO₄, filtered, and concentrated. Purification by column chromatography (silica gel, 95:5 hexanes/EtOAc) afforded **73** as a clear oil (910 mg, 55%).

R_f = 0.37 (silica gel, 4:1 hexanes/EtOAc); **IR** (film) ν_{\max} 3468 (br), 2931, 2859, 1955, 1760, 1698, 1010, 842, 787, 738 cm⁻¹; **¹H NMR** (500 MHz, CDCl₃) δ 7.40 (d, J = 1.5 Hz, 1H), 6.35 (dd, J = 1.7, 3.2 Hz, 1H), 6.26 (d, J = 3.4 Hz, 1H), 5.16 (quin, J = 6.7 Hz, 1H), 4.79 – 4.74 (m, 1H), 4.72 (quin, J = 3.4 Hz, 2H), 2.20 – 2.06 (m, 2H), 2.00 (q, J = 7.3 Hz, 2H), 1.93 – 1.87 (m, 1H); **¹³C NMR** (125 MHz, CDCl₃) δ 208.8, 156.7, 142.2, 110.4, 106.2, 89.5, 75.6, 67.4, 34.9, 24.4.

6-hydroxy-2-(penta-3,4-dien-1-yl)-2H-pyran-3(6H)-one (74):

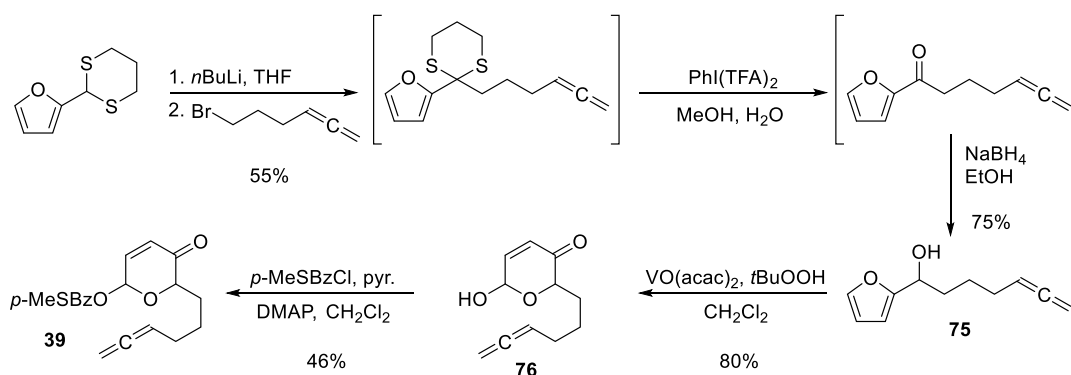
Reaction of **73** (900 mg, 5.48 mmol), vanadyl acetylacetonate (145 mg, 0.548 mmol, 0.1 equiv), and *tert*-butyl hydroperoxide (1.5 mL of a 5.5 M solution in dodecane, 8.22 mmol, 1.5 equiv) in CH₂Cl₂ (27 mL, 0.2 M) according to **61** above afforded **73** as a colorless oil after column chromatography (silica gel, 9:1 to 7:3 hexanes/EtOAc) as a 7:3 mixture of diastereomers (745 mg, 75%).

R_f = 0.13 (silica gel, 4:1 hexanes/EtOAc); **IR** (film) ν_{\max} 3431 (br), 2926, 1726, 1065, 995, 913, 848, 731 cm⁻¹; **¹H NMR** (600 MHz, CDCl₃) δ 7.00 (minor diast., dd, J = 1.8, 10.3 Hz, 0.3H), 6.95 (major diast., dd, J = 3.5, 10.3 Hz, 0.7H), 6.21 (minor diast., dd, J = 1.5, 10.3 Hz, 0.3H), 6.17 (major diast., dd, J = 0.6, 10.3 Hz, 0.7H), 5.73 – 5.69 (m, 1H), 5.20 – 5.15 (m, 1H), 4.77 – 4.72 (m, 2H), 4.69 (major diast., dd, J = 3.7, 8.3 Hz, 0.7H), 4.20 (minor diast., ddd, J = 1.2, 3.7, 8.6 Hz, 0.3H), 3.36 (minor diast., br. s, 0.3H), 3.10 (major diast., br. s, 0.7H), 2.31 – 2.18 (m, 2H), 2.17 – 2.10 (m, 1H), 2.01 – 1.92 (minor diast., m, 0.3H), 1.88 (dtd, J = 5.7, 8.1, 13.9 Hz, 0.7H), ; **¹³C NMR** (125 MHz, CDCl₃) δ 208.9, 196.6, 196.2, 147.8, 144.4, 129.0, 127.9, 91.1, 89.3, 87.9, 78.2, 75.5, 73.5, 30.2, 29.2, 23.8.

5-oxo-6-(penta-3,4-dien-1-yl)-5,6-dihydro-2H-pyran-2-yl 4-(methylthio)benzoate (37):

Reaction of **74** (656 mg, 3.64 mmol), 4-thiomethylbenzoyl chloride (1.019 g, 5.46 mmol, 1.5 equiv), pyridine (294 μ L, 3.64 mmol, 1.0 equiv), and DMAP (222 mg, 1.82 mmol, 0.5 equiv) in CH₂Cl₂ (18 mL, 0.2 M) according to **25** above afforded **37** as a slightly yellow oil after purification by column

chromatography (silica gel, 95:5 to 5:1 hexanes/EtOAc) as a 2:1 mixture of diastereomers (637 mg, 53%). $R_f = 0.33, 0.38$ (silica gel, 4:1 hexanes/EtOAc); **IR** (film) ν_{\max} 2924, 2857, 1954, 1720, 1693, 1593, 1261, 1179, 1094, 1066, 1012, 921, 839, 756, 688 cm^{-1} ; **$^1\text{H NMR}$** (500 MHz, CDCl_3) δ 7.96 – 7.91 (m, 2H), 7.25 (d, $J = 8.3$ Hz, 2H), 7.02 – 6.97 (m, 1H), 6.80 (minor diast., dd, $J = 1.0, 2.9$ Hz, 0.33H), 6.74 (major diast., d, $J = 3.4$ Hz, 0.67H), 6.29 – 6.25 (m, 1H), 5.09 – 5.01 (m, 1H), 4.64 – 4.55 (m, 2H), 4.54 – 4.48 (major diast., m, 0.67H), 4.34 (minor diast., dd, $J = 4.4, 9.3$ Hz, 0.33H), 2.52 (s, 3H), 2.21 – 2.04 (m, 3H), 2.03 – 1.94 (minor diast., m, 0.33H), 1.91 – 1.82 (major diast., m, 0.67H); **$^{13}\text{C NMR}$** (125 MHz, CDCl_3) δ 195.9, 165.0, 164.9, 147.1, 147.0, 142.8, 141.9, 130.4, 129.0, 128.6, 128.4, 125.2, 89.1, 89.0, 88.1, 87.6, 79.1, 75.8, 75.4, 75.2, 32.9, 29.2, 24.0, 23.6, 15.0; **MS** (ESI-TOF) calcd. for $\text{C}_{18}\text{H}_{18}\text{O}_4\text{S}$ [$\text{M} + \text{Na}^+$] 353.0818, found 353.0809.



Scheme 2.16. Synthesis of substrate **39**.

1-(furan-2-yl)hepta-5,6-dien-1-ol (**75**):

2-(2-(hexa-4,5-dien-1-yl)-1,3-dithian-2-yl)furan⁴¹ (1.437 g, 7.71 mmol) was placed in a round bottom flask and azeotroped with benzene (10 mL). Under an atmosphere of N_2 , THF (19.3 mL, 0.4 M) was added and the solution was cooled to -78 °C. $n\text{BuLi}$ (3.84 mL of a 2.01 M solution in hexanes, 7.71 mmol, 1.0 equiv) was introduced dropwise via syringe and the resulting mixture was stirred at -78 °C for 1 h. A solution of

⁴¹ 2-(2-(hexa-4,5-dien-1-yl)-1,3-dithian-2-yl)furan synthesized according to: De, S. K. *Tetrahedron Lett.* **2004**, *45*, 2339–2341.

6-bromohexa-1,2-diene⁴² (1.366 g, 8.48 mmol) in THF (10 mL) at 0 °C was then added via cannula to the lithiated dithiane at –78 °C. An additional amount of THF (5 mL) was used to ensure quantitative transfer. The reaction mixture was then allowed to warm to 23 °C and stir for 30 min. The reaction mixture was then cooled to 0 °C and quenched with the careful addition of sat. aq. NH₄Cl (20 mL). Et₂O (50 mL) was added and the layers were separated. The organic layer was washed with brine (20 mL), and the combined aqueous layers were extracted again with Et₂O (50 mL). The combined organic layers were dried over MgSO₄, filtered, and concentrated. Purification by column chromatography (silica gel, 1:0 to 95:5 hexanes/Et₂O) afforded the allenyldithiane (1.68 g, 82%). A portion of this dithiane (1.62 g, 6.08 mmol) was then dethioacetalized according to the method of Stork and Zhao⁴³ with bis(trifluoroacetoxy)iodobenzene (3.92 g, 9.12 mmol, 1.5 equiv) to give the ketone (~quantitative) which was immediately dissolved in EtOH (20 mL, 0.3 M) under N₂ and cooled to 0 °C. Sodium borohydride (230 mg, 6.08 mmol, 1.0 equiv) was added portionwise and the resultant mixture was allowed to warm to 23 °C. Stirring was continued for 2 h before the careful addition of sat. aq. NaHCO₃ (15 mL). EtOAc (50 mL) and H₂O (30 mL) were added and the layers were then separated. The aqueous layer was further extracted with EtOAc (2 x 50 mL), dried over Na₂SO₄, filtered, and concentrated. Purification by column chromatography (silica gel, 95:5 to 5:1 hexanes/EtOAc) then afforded **75** as a clear oil (989 mg, 91%).

R_f = 0.40 (silica gel, 4:1 hexanes/EtOAc); **IR** (film) ν_{max} 3414 (br), 2934, 2861, 1955, 1718, 1150, 1073, 1010, 883, 842, 789, 739 cm⁻¹; **¹H NMR** (500 MHz, CDCl₃) δ 7.39 (dd, *J* = 1.0, 2.0 Hz, 1H), 6.35 (dd, *J* = 2.0, 2.9 Hz, 1H), 6.25 (d, *J* = 2.9 Hz, 1H), 5.11 (quin, *J* = 6.8 Hz, 1H), 4.73 – 4.66 (m, 3H), 2.10 – 2.03 (m, 2H), 1.95 – 1.88 (m, 2H), 1.86 (d, *J* = 5.4 Hz, 1H), 1.65 – 1.55 (m, 1H), 1.52 – 1.42 (m, 1H); **¹³C NMR** (125 MHz, CDCl₃) δ 208.8, 157.0, 142.2, 110.4, 106.1, 89.9, 75.1, 67.9, 35.2, 28.2, 25.2.

2-(hexa-4,5-dien-1-yl)-6-hydroxy-2H-pyran-3(6H)-one (76):

Reaction of **75** (983 mg, 5.52 mmol), vanadyl acetylacetonate (146 mg, 0.552 mmol, 0.1 equiv), and *tert*-

⁴² 6-Bromohexa-1,2-diene synthesized according to: Molander, G. A.; Cormier, E. P. *J. Org. Chem.* **2005**, *70*, 2622–2626.

⁴³ Stork, G.; Zhao, K. *Tetrahedron Lett.* **1989**, *30*, 287–290.

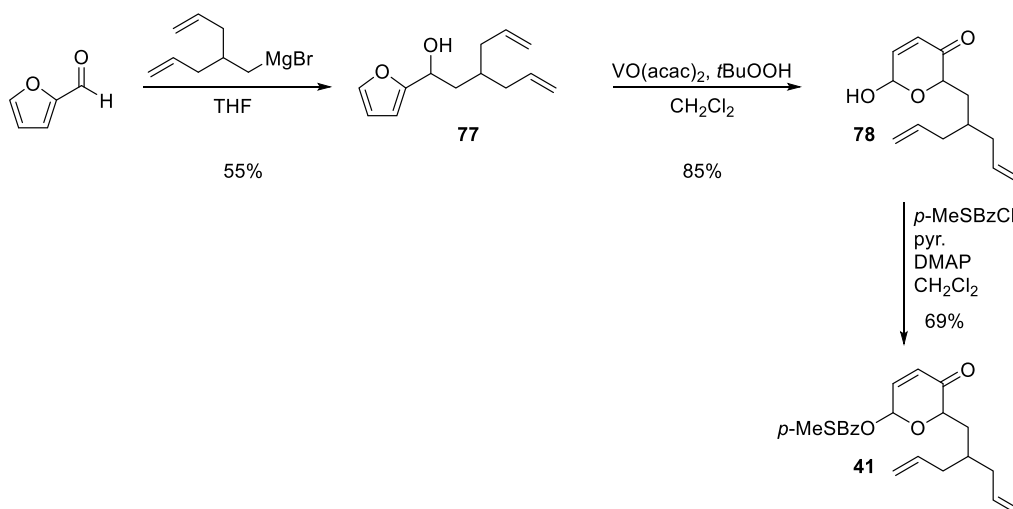
butyl hydroperoxide (1.5 mL of a 5.5 M solution in dodecane, 8.25 mmol, 1.5 equiv) in CH₂Cl₂ (18 mL, 0.3 M) according to **61** above afforded **76** as a yellow oil after column chromatography (silica gel, 9:1 to 7:3 hexanes/EtOAc) as a 17:3 mixture of diastereomers (858 mg, 80%).

R_f = 0.17 (silica gel, 4:1 hexanes/EtOAc); **IR** (film) ν_{\max} 3393 (br), 2932, 2863, 2361, 2341, 1955, 1686, 1092, 1028, 846 cm⁻¹; **¹H NMR** (400 MHz, CDCl₃) δ 6.92 (minor diast., dd, J = 1.5, 10.2 Hz, 0.15H), 6.89 (major diast., dd, J = 3.7, 10.3 Hz, 0.85H), 6.14 (minor diast., dd, J = 1.5, 10.2 Hz, 0.15H), 6.09 (major diast., d, J = 10.3 Hz, 0.85H), 5.64 (d, J = 3.3 Hz, 1H), 5.08 (quin, J = 6.8 Hz, 1H), 4.65 (dt, J = 3.3, 6.6 Hz, 2H), 4.56 (major diast., dd, J = 4.0, 8.1 Hz, 0.85H), 4.10 – 4.05 (minor diast., m, 0.15H), 3.41 (br. s, 1H), 2.08 – 1.92 (m, 3H), 1.80 – 1.68 (m, 1H), 1.61 – 1.49 (m, 2H); **¹³C NMR** (100 MHz, CDCl₃) δ 208.8, 196.8, 196.4, 148.0, 144.7, 129.0, 127.8, 91.1, 89.8, 87.8, 79.0, 75.1, 74.2, 30.3, 29.3, 28.3, 24.9, 24.7.

6-(hexa-4,5-dien-1-yl)-5-oxo-5,6-dihydro-2H-pyran-2-yl 4-(methylthio)benzoate (39):

Reaction of **76** (823 mg, 4.24 mmol), 4-thiomethylbenzoyl chloride (1.028 g, 5.51 mmol, 1.3 equiv), pyridine (480 μ L, 5.93 mmol, 1.4 equiv), and DMAP (518 mg, 4.24 mmol, 1.0 equiv) in CH₂Cl₂ (14 mL, 0.3 M) according to **25** above afforded **39** as a slightly yellow oil after purification by column chromatography (silica gel, 95:5 to 5:1 hexanes/EtOAc) as a 3:1 mixture of diastereomers (665 mg, 46%).

R_f = 0.34, 0.42 (silica gel, 4:1 hexanes/EtOAc); **IR** (film) ν_{\max} 2924, 2861, 1955, 1720, 1695, 1592, 1262, 1177, 1094, 1067, 1012, 923, 840, 756 cm⁻¹; **¹H NMR** (500 MHz, CDCl₃) δ 7.95 – 7.90 (m, 2H), 7.25 (dt, J = 1.6, 8.5 Hz, 2H), 7.02 – 6.95 (m 1H), 6.80 – 6.78 (minor diast., m, 0.25H), 6.74 (major diast., d, J = 3.4 Hz, 0.75H), 6.29 – 6.24 (m, 1H), 5.05 (major diast., quin, J = 6.8 Hz, 0.75H), 4.94 (minor diast., quin, J = 6.8 Hz, 0.25H), 4.64 – 4.55 (m, 2.75H), 4.28 (minor diast., dd, J = 4.9, 9.8 Hz, 0.25H), 2.51 (s, 3H), 2.04 – 1.88 (m, 3H), 1.83 – 1.74 (m, 1H), 1.54 (quin, J = 7.7 Hz, 1H); **¹³C NMR** (125 MHz, CDCl₃) δ 196.0, 195.9, 165.0, 147.1, 147.0, 142.8, 142.0, 130.4, 130.3, 129.0, 128.4, 125.3, 125.2, 89.7, 89.5, 88.1, 87.7, 79.7, 76.0, 75.1, 33.1, 29.3, 28.2, 28.1, 25.1, 24.4, 15.0; **MS** (ESI-TOF) calcd. for C₁₉H₂₀O₄S [M + Na⁺] 367.0975, found 367.0967.



Scheme 2.17. Synthesis of substrate **41**.

3-allyl-1-(furan-2-yl)hex-5-en-1-ol (77):

Freshly distilled furfural (704 mg, 7.33 mmol, 1.1 equiv) was dissolved in THF (24.4 mL, 0.3 M in furfural) under an atmosphere of N₂ and cooled to 0 °C. A solution of (2-allylpent-4-en-1-yl)magnesium bromide⁴⁴ (13.3 mL of a 0.5 M solution in THF, 6.66 mmol) was added dropwise and the resulting reaction mixture was stirred for 20 min. Sat. aq. NH₄Cl (20 mL) was carefully added followed by Et₂O (50 mL). The organic layer was washed with brine (20 mL), and the combined aqueous layers were extracted with Et₂O (2 x 50 mL). The combined organic layers were dried over MgSO₄, filtered, and concentrated. Purification by column chromatography (silica gel, 95:5 to 9:1 hexanes/Et₂O) afforded **77** as a clear oil (755 mg, 55%).

R_f = 0.39 (silica gel, 5:1 hexanes/EtOAc); **IR** (film) ν_{\max} 3390 (br), 3075, 2976, 2919, 1697, 1639, 1505, 1442, 1150, 995, 910, 734 cm⁻¹; **¹H NMR** (500 MHz, CDCl₃) δ 7.40 – 7.38 (m, 1H), 6.35 (dd, J = 2.0, 3.4 Hz, 1H), 6.25 (d, J = 2.9 Hz, 1H), 5.84 – 5.73 (m, 2H), 5.09 – 5.02 (m, 4H), 4.82 (dt, J = 5.6, 8.3 Hz, 1H), 2.18 – 2.04 (m, 4H), 1.90 – 1.70 (m, 3H); **¹³C NMR** (125 MHz, CDCl₃) δ 157.1, 142.2, 136.9, 136.7, 116.8, 110.4, 106.1, 66.0, 39.3, 38.4, 37.8, 33.9.

2-(2-allylpent-4-en-1-yl)-6-hydroxy-2H-pyran-3(6H)-one (78):

Reaction of **77** (745 mg, 3.61 mmol), vanadyl acetylacetonate (96 mg, 0.36 mmol, 0.1 equiv), and *tert*-butyl

⁴⁴ (2-Allylpent-4-en-1-yl)magnesium bromide synthesized according to: Krech, F.; Issleib, K. *Z. Anorg. Allg. Chem.* **1988**, 557, 143–152.

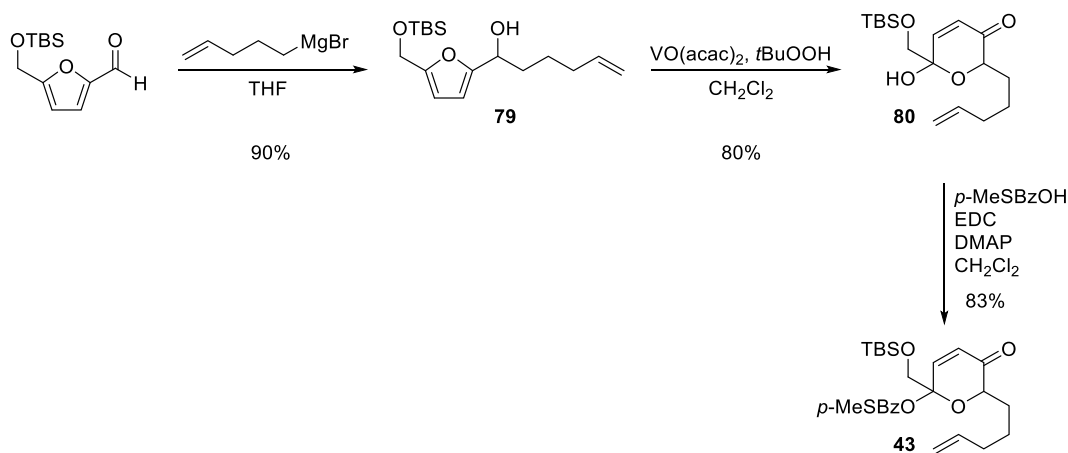
hydroperoxide (1.5 mL of a 5.5 M solution in dodecane, 5.42 mmol, 1.5 equiv) in CH₂Cl₂ (18.1 mL, 0.2 M) according to **61** above afforded **78** as a yellow oil after column chromatography (silica gel, 9:1 to 7:3 hexanes/EtOAc) as a 7:3 mixture of diastereomers (680 mg, 85%).

R_f = 0.28 (silica gel, 5:1 hexanes/EtOAc); **IR** (film) ν_{\max} 3408 (br), 3076, 2976, 2919, 1686, 1638, 1087, 1028, 995, 911 cm⁻¹; **¹H NMR** (500 MHz, CDCl₃) δ 6.94 (minor diast., dd, *J* = 1.5, 10.3, 0.3H), 6.90 (major diast., dd, *J* = 3.4, 10.3 Hz, 0.7H), 6.12 (minor diast., dd, *J* = 2.0, 10.3 Hz, 0.3H), 6.11 (major diast., dd, *J* = 1.0, 10.3 Hz, 0.7H), 5.84 – 5.72 (m, 2H), 5.65 (d, *J* = 2.9 Hz, 1H), 5.08 – 5.01 (m, 4H), 4.67 (major diast., dd, *J* = 3.4, 4.8 Hz, 0.7H), 4.22 – 4.18 (minor diast., m, 0.3H), 3.72 (minor diast., br. s, 0.3H), 3.48 (major diast., br. s, 0.7H), 2.21 – 2.12 (m, 2H), 2.11 – 1.98 (m, 2H), 1.95 – 1.88 (m, 1H), 1.87 – 1.78 (m, 1H), 1.65 (ddd, *J* = 4.2, 10.0, 14.2, 1H); **¹³C NMR** (125 MHz, CDCl₃) δ 197.2, 196.8, 147.9, 144.6, 136.9, 136.8, 136.6, 136.5, 128.9, 127.8, 116.9, 116.8, 91.0, 87.8, 72.6, 38.6, 38.5, 37.2, 37.1, 34.5, 33.4, 33.3, 33.2.

6-(2-allylpent-4-en-1-yl)-5-oxo-5,6-dihydro-2H-pyran-2-yl 4-(methylthio)benzoate (41):

Reaction of **78** (600 mg, 2.70 mmol), 4-thiomethylbenzoyl chloride (756 mg, 4.05 mmol, 1.5 equiv), pyridine (218 μ L, 2.70 mmol, 1.0 equiv), and DMAP (518 mg, 4.24 mmol, 1.0 equiv) in CH₂Cl₂ (14 mL, 0.3 M) according to **25** above afforded **41** as a slightly yellow oil after purification by column chromatography (silica gel, 95:5 to 5:1 hexanes/EtOAc) as a 3:1 mixture of diastereomers (690 mg, 69%).

R_f = 0.37, 0.43 (silica gel, 4:1 hexanes/EtOAc); **IR** (film) ν_{\max} 3074, 2975, 2920, 1721, 1697, 1593, 1261, 1175, 1094, 1066, 1013, 913, 840, 756 cm⁻¹; **¹H NMR** (500 MHz, CDCl₃) δ 7.97 – 7.92 (m, 2H), 7.29 – 7.25 (m, 2H), 7.02 – 6.96 (m, 1H), 6.79 (minor diast., dd, *J* = 1.2, 2.7 Hz, 0.25H), 6.73 (major diast., d, *J* = 3.4 Hz, 0.75H), 6.30 – 6.24 (m, 1H), 5.79 – 5.66 (m, 1.75H), 5.59 – 5.49 (minor diast., m, 0.25H), 5.06 – 4.85 (m, 4H), 4.69 (major diast. dd, *J* = 3.4, 9.8 Hz, 0.75H), 4.44 (minor diast., dd, *J* = 3.9, 10.3 Hz, 0.25H), 2.53 (s, 3H), 2.15 – 2.04 (m, 2H), 2.04 – 1.93 (m, 2H), 1.90 – 1.78 (m, 2H), 1.69 (ddd, *J* = 3.9, 10.0, 14.4 Hz, 1H); **¹³C NMR** (125 MHz, CDCl₃) δ 196.2, 196.1, 165.0, 147.1, 142.9, 141.7, 136.8, 136.6, 136.5, 136.2, 130.5, 130.3, 129.0, 128.6, 125.3, 125.2, 117.1, 116.8, 88.0, 87.8, 74.3, 38.8, 38.4, 37.3, 37.2, 36.5, 33.2, 33.1, 15.0; **MS** (ESI-TOF) calcd. for C₂₁H₂₄O₄S [M + Na⁺] 395.1288, found 395.1290.



Scheme 2.18. Synthesis of substrate **43**.

1-(5-(((*tert*-butyldimethylsilyloxy)methyl)furan-2-yl)hex-5-en-1-ol (79**):**

5-(((*tert*-Butyldimethylsilyloxy)methyl)furan-2-carbaldehyde⁴⁵ (1.0 g, 4.16 mmol) was dissolved in THF (21 mL, 0.2 M) under an atmosphere of N₂ and cooled to 0 °C. A solution of pent-4-en-1-ylmagnesium bromide (10.0 mL of a 0.5 M solution in THF, 5.0 mmol, 1.2 equiv) was added dropwise and the resulting reaction mixture was stirred for 20 min. Sat. aq. NH₄Cl (20 mL) was then carefully added followed by Et₂O (50 mL). The organic layer was washed with brine (20 mL), and the combined aqueous layers were extracted with Et₂O (2 x 50 mL). The combined organic layers were dried over MgSO₄, filtered, and concentrated. Purification by column chromatography (silica gel, 95:5 to 9:1 hexanes/EtOAc) afforded **79** as a clear oil (1.16 g, 90%).

R_f = 0.25 (silica gel, 9:1 hexanes/EtOAc); **IR** (film) ν_{\max} 3374, 2930, 2858, 1255, 1075, 834, 776 cm⁻¹; **¹H NMR** (500 MHz, CDCl₃) δ 6.18 – 6.16 (m, 2H), 5.85 – 5.76 (m, 1H), 5.02 (dq, *J* = 5.0, 17.1 Hz, 1H), 4.99 – 4.95 (m, 1H), 4.67 (dd, *J* = 5.4, 4.8, 1H), 4.63 (s, 2H), 2.11 (q, *J* = 7.2 Hz, 2H), 1.91 – 1.84 (m, 3H), 1.61 – 1.51 (m, 1H), 1.48 – 1.39 (m, 1H), 0.92 (s, 9H), 0.10 – 0.08 (m, 6H); **¹³C NMR** (125 MHz, CDCl₃) δ 156.6, 153.9, 138.7, 115.0, 108.1, 106.7, 68.0, 58.4, 35.2, 33.7, 26.1, 25.0, 18.6, –5.0; **MS** (ESI-TOF) calcd. for C₁₇H₃₀O₃Si [M + Na⁺] 333.1856, found 333.1866.

⁴⁵ 5-(((*tert*-Butyldimethylsilyloxy)methyl)furan-2-carbaldehyde prepared according to: Celanire, S.; Marlin, F.; Baldwin, J. E.; Adlington, R. M. *Tetrahedron* **2005**, *61*, 3025–3032.

6-(((*tert*-butyldimethylsilyl)oxy)methyl)-6-hydroxy-2-(pent-4-en-1-yl)-2*H*-pyran-3(6*H*)-one (80):

Reaction of **79** (608 mg, 1.96 mmol), vanadyl acetylacetonate (52 mg, 0.20 mmol, 0.1 equiv), and *tert*-butyl hydroperoxide (534 μ L of a 5.5 M solution in dodecane, 2.94 mmol, 1.5 equiv) in CH₂Cl₂ (9.8 mL, 0.2 M) according to **61** above afforded **80** as a yellow oil after column chromatography (silica gel, 95:5 to 9:1 hexanes/EtOAc) (512 mg, 80%).

R_f = 0.50 (silica gel, 5:1 hexanes/EtOAc); **IR** (film) ν_{\max} 3466 (br), 2954, 2930, 2858, 1694, 1254, 1101, 1059, 912, 836, 779 cm⁻¹; **¹H NMR** (400 MHz, CDCl₃) δ 6.73 (d, *J* = 10.2 Hz, 1H), 6.08 (d, *J* = 10.2 Hz, 1H), 5.85 – 5.73 (m, 1H), 4.99 (dq, *J* = 1.8, 16.8 Hz, 1H), 4.96 – 4.92 (m, 1H), 4.53 (dd, *J* = 3.8, 7.9 Hz, 1H), 3.76 – 3.64 (m, 3H), 2.10 – 2.02 (m, 2H), 2.00 – 1.90 (m, 1H), 1.72 – 1.61 (m, 1H), 1.56 – 1.46 (m, 2H), 0.92 (s, 9H), 0.11 (d, *J* = 2.6 Hz, 6H); **¹³C NMR** (100 MHz, CDCl₃) δ 197.3, 145.2, 138.7, 128.8, 114.8, 92.8, 74.5, 68.5, 33.7, 29.3, 26.0, 24.4, 18.6, –5.0, –5.2.

2-(((*tert*-butyldimethylsilyl)oxy)methyl)-5-oxo-6-(pent-4-en-1-yl)-5,6-dihydro-2*H*-pyran-2-yl

4-(methylthio)benzoate (43):

Reaction of **80** (355 mg, 1.09 mmol), EDC (417 mg, 2.18 mmol, 2.0 equiv), 4-methylthiobenzoic acid (366 mg, 2.18 mmol, 2.0 equiv), and DMAP (266 mg, 2.18 mmol, 2.0 equiv) in CH₂Cl₂ (5.4 mL, 0.2 M) according to **15c** above afforded **43** as a clear oil after column chromatography (Davisil®, 1:0 to 99:1 toluene/EtOAc) as a single diastereomer (431 mg, 83%). Decomposition and conversion to **43** was observed to occur upon prolonged exposure of **43** to silica gel; this occurs to a lesser degree with Davisil®.

R_f = 0.60 (silica gel, 5:1 hexanes/EtOAc); **IR** (film) ν_{\max} 2928, 2857, 1716, 1594, 1272, 1109, 911, 836, 778, 757, 732 cm⁻¹; **¹H NMR** (400 MHz, CDCl₃) δ 7.89 – 7.85 (m, 2H), 7.37 (d, *J* = 10.2 Hz, 1H), 7.25 – 7.21 (m, 2H), 6.19 (d, *J* = 10.2 Hz, 1H), 5.86 – 5.74 (m, 1H), 5.01 (dd, *J* = 2.0, 17.0 Hz, 1H), 4.95 (dt, *J* = 1.1, 10.2 Hz, 1H), 4.61 (dd, *J* = 3.7, 7.7 Hz, 1H), 4.27 (d, *J* = 10.6 Hz, 1H), 3.92 (d, *J* = 10.6 Hz, 1H), 2.50 (s, 3H), 2.09 (q, *J* = 6.6 Hz, 2H), 2.03 – 1.95 (m, 1H), 1.83 – 1.71 (m, 1H), 1.57 (quin, *J* = 7.7 Hz, 2H), 0.85 (s, 9H), 0.07 – 0.04 (m, 6H); **¹³C NMR** (100 MHz, CDCl₃) δ 196.5, 164.8, 146.5, 144.7, 138.6, 130.3, 127.6, 126.1, 125.1, 115.0, 100.1, 77.6, 66.5, 33.7, 29.7, 25.9, 24.2, 18.4, 15.0, –5.2; **MS** (ESI-TOF) calcd. for C₂₅H₃₆O₅SSi [M + Na⁺] 499.1945, found 499.1938.

2.6.4 Procedures for Cycloadditions and Characterization of Products

General Procedure for Thiourea-Catalyzed Cycloadditions (Optimization and Structure–Activity Relationship Studies):

An oven-dried 0.5-dram vial was charged with the specified urea, thiourea, or carbazole catalyst(s) (0.10 or 0.15 equiv as indicated). To these catalysts was added a stock solution of substrate **15** (0.05 mmol) and AcOH (0 or 0.15 equiv as indicated) in toluene (0.2 M or 0.4 M in **15** as indicated). No special precautions were taken to exclude air or moisture. The vial was sealed, placed in a 40 °C oil bath, and allowed to stir for the designated length of time. The reaction was then removed from heating and quenched with 1N HCl (10 mL). The aqueous layer was extracted with CH₂Cl₂ (3 x 10 mL), which was added to a flask containing 1,3,5-trimethoxybenzene (0.0119 M in benzene, 0.10 equiv relative to substrate). The combined organic layers were dried over Na₂SO₄, filtered, and concentrated. A yield was then determined by ¹H NMR of this crude reaction mixture in CDCl₃. Enantiomeric excess was determined by HPLC on commercial chiral columns after chromatographic purification on silica gel.

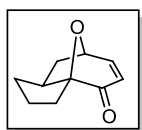
General Procedure for Thiourea-Catalyzed Cycloadditions (Substrate Scope):

An oven-dried 0.5-dram vial was charged with *para*-thiomethylbenzoyl substrate (≥ 50.0 mg). To this vial was then added a stock solution of AcOH (0.15 eq) in toluene such that the final substrate concentration was 0.4 M. To this solution was added chiral primary aminothiourea catalyst **24** (0.10, 0.15, or 0.20 equiv as indicated) and achiral thiourea catalyst **23** (0.10, 0.15, or 0.20 equiv as indicated). No special precautions were taken to exclude air or moisture. The vial was sealed, placed in a 40 °C oil bath, and allowed to stir for the designated length of time. The reaction was then removed from the bath and transferred with CH₂Cl₂ to a separatory funnel containing 1N HCl (15 mL). The aqueous layer was then extracted with CH₂Cl₂ (4 x 15 mL). The combined organic layers were dried over Na₂SO₄, filtered, and concentrated. The crude product was purified by silica gel flash chromatography. Some products required a second purification by silica gel flash chromatography eluting with toluene/EtOAc in order to remove unreacted starting material. A byproduct was observed arising from presumed decomposition of catalyst **23** and conjugate addition of 3,5-

bis(trifluoromethyl)aniline to the enone of the product. The yield of this byproduct was $\leq 4\%$ in all cases. An X-ray crystal structure of this byproduct was obtained from the reaction with product **42**.

General Procedure for Preparation of Racemic Products:

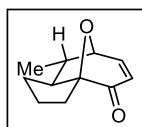
An oven-dried 2.0-dram vial was charged with substrate (≥ 0.5 mmol) and dissolved in CH_2Cl_2 (0.05 M). To this solution was added DBU (1.5 equiv) via syringe. The vial was sealed and allowed to stir overnight at 23°C . The reaction mixture was then concentrated and the racemic product purified by silica gel flash chromatography.



(3aS,7R,8aS)-2,3,8,8a-tetrahydro-1H-3a,7-epoxyazulen-4(7H)-one (**16**):

According to the general procedure, **15c** (102.4 mg, 0.308 mmol), **24** (12.4 mg, 0.031 mmol, 0.10 equiv), and **23** (15.4 mg, 0.031 mmol, 0.10 equiv) were allowed to react in a toluene solution (770 μL , 0.4 M) containing AcOH (2.7 μL , 0.046 mmol, 0.15 equiv) for 48 h to afford **16** (37.3 mg, 74%) as a colorless oil after column chromatography (silica gel, 9:1 to 3:2 hexanes/ Et_2O) followed by subsequent column chromatography (silica gel, 98:2 toluene/ EtOAc). This material was determined to be 91% *ee* by chiral HPLC analysis (ChiralPak AS-H, 2% *i*PrOH in hexanes, 1 mL/min, 218 nm, t_{R} (major) = 23.4 min, t_{R} (minor) = 17.8 min).

R_f = 0.24 (silica gel, 95:5 toluene/ EtOAc); IR (film) ν_{max} 2954, 2868, 1689, 1165, 1038, 789 cm^{-1} ; $^1\text{H NMR}$ (500 MHz, CDCl_3) δ 7.12 (dd, J = 4.4, 9.8 Hz, 1H), 5.95 (d, J = 9.8 Hz, 1H), 4.87 (dd, J = 4.6, 6.6 Hz, 1H), 2.44 – 2.36 (m, 1H), 2.23 – 2.26 (m, 1H), 2.15 (dd, J = 8.8, 11.7 Hz, 1H), 1.95 – 1.75 (m, 4H), 1.73 – 1.67 (m, 1H), 1.61 – 1.55 (m, 1H); $^{13}\text{C NMR}$ (125 MHz, CDCl_3) δ 197.7, 152.2, 126.4, 98.3, 76.3, 44.8, 36.9, 32.6, 30.3, 26.3; MS (ESI-TOF) calcd. for $\text{C}_{10}\text{H}_{12}\text{O}_2$ [$\text{M} + \text{H}^+$] 165.0916, found 165.0794; $[\alpha]_D^{23} = -155.4$ (c = 1.4, CHCl_3).

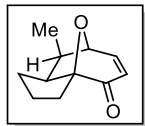


(3aS,7S,8aS)-8-methyl-2,3,8,8a-tetrahydro-1H-3a,7-epoxyazulen-4(7H)-one (**26**):

According to the general procedure, **25** (100.0 mg, 0.29 mmol), **24** (17.4 mg, 0.043 mmol, 0.15 equiv), and **23** (21.7 mg, 0.043 mmol, 0.15 equiv) were allowed to react in a toluene solution (722 μL , 0.4 M) containing AcOH (2.5 μL , 0.043 mmol, 0.15 equiv) for 72 h to afford **26** (35.9 mg, 70%) as a colorless oil after column chromatography (silica gel, 9:1 to 3:2 hexanes/ Et_2O) followed by subsequent

column chromatography (silica gel, 98:2 toluene/EtOAc). This material was determined to be 90% *ee* by chiral HPLC analysis (ChiralPak AS-H, 5% *i*PrOH in hexanes, 1 mL/min, 218 nm, $t_{\text{R}}(\text{major}) = 16.7$ min, $t_{\text{R}}(\text{minor}) = 9.1$ min).

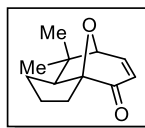
$R_f = 0.52$ (silica gel, 4:1 hexanes/EtOAc); **IR** (film) ν_{max} 2959, 2871, 1694, 1457, 1380, 1265, 1160, 1050, 929, 669 cm^{-1} ; **$^1\text{H NMR}$** (500 MHz, CDCl_3) δ 7.10 (dd, $J = 4.4, 9.8$ Hz, 1H), 6.09 (d, $J = 9.8$ Hz, 1H), 4.67 (dd, $J = 4.4, 5.9$ Hz, 1H), 2.25 – 2.14 (m, 2H), 1.96 – 1.90 (m, 1H), 1.88 – 1.77 (m, 3H), 1.72 – 1.61 (m, 2H), 1.07 (d, $J = 6.8$ Hz, 3H); **$^{13}\text{C NMR}$** (125 MHz, CDCl_3) δ 197.7, 150.7, 128.1, 98.3, 79.4, 52.7, 45.8, 30.8, 30.3, 25.7, 15.8; **MS** (ESI-TOF) calcd. for $\text{C}_{11}\text{H}_{14}\text{O}_2$ [$\text{M} + \text{Na}^+$] 201.0886, found 201.0887; $[\alpha]_{\text{D}}^{23} = -143.5$ ($c = 2.0$, CHCl_3).



(3aS,7S,8R,8aS)-8-methyl-2,3,8,8a-tetrahydro-1H-3a,7-epoxyazulen-4(7H)-one (28):

According to the general procedure, **27** (100.0 mg, 0.29 mmol), **24** (17.4 mg, 0.043 mmol, 0.15 equiv), and **23** (21.7 mg, 0.043 mmol, 0.15 equiv) were allowed to react in a toluene solution (722 μL , 0.4 M) containing AcOH (2.5 μL , 0.043 mmol, 0.15 equiv) for 72 h to afford **28** (33.8 mg, 66%) as a colorless oil after column chromatography (silica gel, 9:1 to 3:2 hexanes/ Et_2O) followed by subsequent column chromatography (silica gel, 98:2 toluene/EtOAc). This material was determined to be 89% *ee* by chiral HPLC analysis (ChiralPak AS-H, 5% *i*PrOH in hexanes, 1 mL/min, 220 nm, $t_{\text{R}}(\text{major}) = 12.4$ min, $t_{\text{R}}(\text{minor}) = 8.7$ min).

$R_f = 0.48$ (silica gel, 4:1 hexanes/EtOAc); **IR** (film) ν_{max} 2962, 2873, 1692, 1461, 1377, 1270, 1171, 1009, 912, 794, 669 cm^{-1} ; **$^1\text{H NMR}$** (500 MHz, CDCl_3) δ 7.18 (dd, $J = 4.3, 9.8$ Hz, 1H), 5.98 (d, $J = 10.1$ Hz, 1H), 4.44 (d, $J = 4.1$ Hz, 1H), 2.45 (td, $J = 3.4, 8.8$ Hz, 1H), 2.38 – 2.27 (m, 2H), 1.88 – 1.81 (m, 1H), 1.80 – 1.65 (m, 4H), 1.16 (d, $J = 7.3$ Hz, 3H); **$^{13}\text{C NMR}$** (125 MHz, CDCl_3) δ 198.0, 151.7, 125.8, 99.3, 83.0, 47.5, 38.4, 30.1, 27.9, 26.6, 16.7; **MS** (ESI-TOF) calcd. for $\text{C}_{11}\text{H}_{14}\text{O}_2$ [$\text{M} + \text{Na}^+$] 201.0886, found 201.0876; $[\alpha]_{\text{D}}^{24} = -43.0$ ($c = 0.8$, CHCl_3).

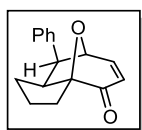


(3aS,7S,8aS)-8,8-dimethyl-2,3,8,8a-tetrahydro-1H-3a,7-epoxyazulen-4(7H)-one (30):

According to the general procedure, **29** (100.0 mg, 0.28 mmol), **24** (16.7 mg, 0.042 mmol, 0.15 equiv), and **23** (20.8 mg, 0.042 mmol, 0.15 equiv) were allowed to react in a toluene solution (694 μL ,

0.4 M) containing AcOH (2.4 μ L, 0.042 mmol, 0.15 equiv) for 96 h to afford **30** (27.0 mg, 51%) as a colorless oil after column chromatography (silica gel, 9:1 to 3:2 hexanes/Et₂O) followed by subsequent column chromatography (silica gel, 98:2 toluene/EtOAc). This material was determined to be 89% *ee* by chiral HPLC analysis (ChiralPak AD-H, 5% *i*PrOH in hexanes, 1 mL/min, 220 nm, $t_{\text{R}}(\text{major}) = 6.5$ min, $t_{\text{R}}(\text{minor}) = 5.9$ min).

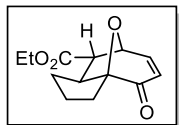
$R_f = 0.50$ (silica gel, 4:1 hexanes/EtOAc); **IR** (film) ν_{max} 2963, 1696, 1162, 1036, 900, 795, 669 cm^{-1} ; **¹H NMR** (500 MHz, CDCl₃) δ 7.17 (dd, $J = 4.6, 10.1$ Hz, 1H), 6.10 (d, $J = 9.6$ Hz, 1H), 4.31 (d, $J = 4.6$ Hz, 1H), 2.27 (ddd, $J = 6.9, 1.03, 13.5$ Hz, 1H), 2.10 (dd, $J = 2.5, 9.7$ Hz, 1H), 1.88 – 1.73 (m, 3H), 1.71 – 1.62 (m, 2H), 1.23 (s, 3H), 1.09 (s, 3H); **¹³C NMR** (125 MHz, CDCl₃) δ 197.7, 151.4, 127.1, 99.4, 85.4, 54.8, 45.3, 30.1, 27.5, 26.6, 26.5, 25.2; **MS** (ESI-TOF) calcd. for C₁₂H₁₆O₂ [M + Na⁺] 215.1043, found 215.1056; $[\alpha]_D^{23} = -86.9$ ($c = 1.4$, CHCl₃).



(3aS,7S,8S,8aS)-8-phenyl-2,3,8,8a-tetrahydro-1H-3a,7-epoxyazulen-4(7H)-one (32):

According to the general procedure, **31** (100.0 mg, 0.25 mmol), **24** (14.7 mg, 0.037 mmol, 0.15 equiv), and **23** (18.4 mg, 0.037 mmol, 0.15 equiv) were allowed to react in a toluene solution (612 μ L, 0.4 M) containing AcOH (2.1 μ L, 0.037 mmol, 0.15 equiv) for 72 h to afford **32** (28.4 mg, 48%) as a colorless oil after column chromatography (silica gel, 9:1 to 3:2 hexanes/Et₂O). This material was determined to be 86% *ee* by chiral HPLC analysis (ChiralPak AS-H, 5% *i*PrOH in hexanes, 1 mL/min, 206 nm, $t_{\text{R}}(\text{major}) = 14.7$ min, $t_{\text{R}}(\text{minor}) = 13.5$ min).

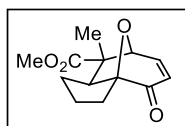
$R_f = 0.50$ (silica gel, 4:1 hexanes/EtOAc); **IR** (film) ν_{max} 2960, 1695, 1494, 1454, 1267, 1168, 1039, 794, 704 cm^{-1} ; **¹H NMR** (500 MHz, CDCl₃) δ 7.39 – 7.25 (m, 6H), 6.08 (d, $J = 10.1$ Hz, 1H), 5.05 (d, $J = 4.6$ Hz, 1H), 3.47 (d, $J = 9.6$ Hz, 1H), 2.81 (td, $J = 3.9, 9.7$ Hz, 1H), 2.36 (ddd, $J = 7.3, 10.1, 13.7$ Hz, 1H), 1.84 – 1.77 (m, 1H), 1.69 – 1.56 (m, 2H), 1.54 – 1.47 (m, 1H), 1.07 – 1.00 (m, 1H); **¹³C NMR** (125 MHz, CDCl₃) δ 198.1, 151.5, 140.9, 128.8, 128.5, 127.0, 126.2, 99.3, 82.2, 50.5, 49.8, 30.2, 27.9, 27.1; **MS** (ESI-TOF) calcd. for C₁₆H₁₆O₂ [M + H⁺] 241.1229, found 241.1247; $[\alpha]_D^{24} = -79.7$ ($c = 1.4$, CHCl₃).



(3a*S*,7*S*,8*S*,8a*S*)- ethyl 4-oxo-2,3,4,7,8,8a-hexahydro-1*H*-3a,7-epoxyazulene-8-carboxylate (34**):**

According to the general procedure, **33** (100.0 mg, 0.247 mmol), **24** (14.9 mg, 0.037mmol, 0.15 equiv), and **23** (18.6 mg, 0.037 mmol, 0.15 equiv) were allowed to react in a toluene solution (618 μ L, 0.4 M) containing AcOH (2.1 μ L, 0.037 mmol, 0.15 equiv) for 72 h to afford **20** (38.8 mg, 66%) as a colorless oil after column chromatography (silica gel, 9:1 to 5:1 hexanes/Et₂O). This material was determined to be 90% *ee* by chiral HPLC analysis (ChiralPak AS-H, 5% *i*PrOH in hexanes, 1 mL/min, 220 nm, t_R (major) = 22.7 min, t_R (minor) = 15.9 min).

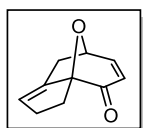
R_f = 0.35 (silica gel, 5:1 hexanes/EtOAc); **IR** (film) ν_{\max} 2961, 2872, 1732, 1694, 1374, 1192, 1166, 1048, 1034, 1019, 929 cm^{-1} ; **¹H NMR** (500 MHz, CDCl₃) δ 7.15 (dd, J = 4.4, 9.8 Hz, 1H), 6.06 (d, J = 9.8 Hz, 1H), 5.00 (dd, J = 4.4, 6.3 Hz, 1H), 4.14 (dq, J = 1.5, 7.3 Hz, 2H), 3.11 (t, J = 6.6 Hz, 1H), 2.71 (ddd, J = 2.9, 6.3, 9.3 Hz, 1H), 2.29 – 2.21 (m, 1H), 2.01 – 1.92 (m, 1H), 1.90 – 1.80 (m, 2H), 1.75 – 1.66 (m, 2H), 1.25 (t, J = 7.3 Hz, 3H); **¹³C NMR** (125 MHz, CDCl₃) δ 196.6, 170.9, 149.5, 127.9, 98.5, 76.4, 61.4, 56.0, 48.3, 31.7, 30.3, 25.8, 14.4; **MS** (ESI-APCI) calcd. for C₁₃H₁₆O₄ [M + H⁺] 237.1, found 237.1; $[\alpha]_D^{23}$ = – 272.2 (c = 1.21, CHCl₃).



(3a*S*,7*S*,8*S*,8a*S*)-methyl 8-methyl-4-oxo-2,3,4,7,8,8a-hexahydro-1*H*-3a,7-epoxyazulene-8-carboxylate (36**):**

According to the general procedure, **35** (63.1 mg, 0.16 mmol), **24** (12.5 mg, 0.031 mmol, 0.20 equiv), and **23** (15.6 mg, 0.031 mmol, 0.20 equiv) were allowed to react in a toluene solution (390 μ L, 0.4 M) containing AcOH (1.3 μ L, 0.023 mmol, 0.15 equiv) for 96 h to afford **36** (13.8 mg, 37%) as a colorless oil after column chromatography (silica gel, 9:1 to 3:2 hexanes/Et₂O). This material was determined to be 80% *ee* by chiral HPLC analysis (ChiralCel OC-H, 5% *i*PrOH in hexanes, 1 mL/min, 218 nm, t_R (major) = 19.6 min, t_R (minor) = 15.7 min).

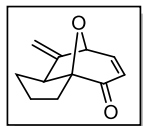
R_f = 0.45 (silica gel, 4:1 hexanes/EtOAc); **IR** (film) ν_{\max} 2958, 1736, 1698, 1277, 1247, 1139, 1122, 1036, 914, 734, 650 cm^{-1} ; **$^1\text{H NMR}$** (500 MHz, CDCl_3) δ 7.22 (dd, J = 4.6, 9.7 Hz, 1H), 6.04 (d, J = 10.1 Hz, 1H), 4.59 (d, J = 4.1 Hz, 1H), 3.70 (s, 3H), 2.88 (dd, J = 3.2, 8.7 Hz, 1H), 2.35 – 2.27 (m, 1H), 1.90 – 1.76 (m, 4H), 1.69 (dd, J = 4.6, 14.4 Hz, 1H), 1.52 (s, 3H); **$^{13}\text{C NMR}$** (125 MHz, CDCl_3) δ 196.9, 175.2, 150.1, 127.1, 99.3, 82.8, 56.6, 52.5, 50.0, 30.1, 27.7, 26.7, 21.8; **MS** (ESI-TOF) calcd. for $\text{C}_{13}\text{H}_{16}\text{O}_4$ [$\text{M} + \text{H}^+$] 237.1127, found 237.1151; $[\alpha]_D^{23} = -100.7$ (c = 0.8, CHCl_3).



(3aS,7R)-7,8-dihydro-2H-3a,7-epoxyazulen-4(3H)-one (38):

According to the general procedure, **37** (107.4 mg, 0.325 mmol), **24** (19.6 mg, 0.049 mmol, 0.15 equiv), and **23** (24.4 mg, 0.049 mmol, 0.15 equiv) were allowed to react in a toluene solution (813 μL , 0.4 M) containing AcOH (2.8 μL , 0.049 mmol, 0.15 equiv) for 72 h to afford **38** (28.5 mg, 54%) as a white solid after column chromatography (silica gel, 9:1 to 5:1 hexanes/ Et_2O) followed by subsequent column chromatography (silica gel, 98:2 toluene/EtOAc). This material was determined to be 95% *ee* by chiral HPLC analysis (ChiralPak AS-H, 3% *i*PrOH in hexanes, 1 mL/min, 218 nm, t_R (major) = 21.0 min, t_R (minor) = 18.0 min).

R_f = 0.44 (silica gel, 5:1 hexanes/EtOAc); **IR** (film) ν_{\max} 2981, 2935, 2855, 1684, 1376, 1167, 1096, 1016, 987, 904, 814, 790, 648 cm^{-1} ; **$^1\text{H NMR}$** (500 MHz, CDCl_3) δ 7.34 (dd, J = 4.4, 9.8 Hz, 1H), 6.01 (d, J = 9.8 Hz, 1H), 5.76 (dq, J = 1.9, 3.7 Hz, 1H), 5.15 – 5.11 (m, 1H), 3.04 – 2.94 (m, 1H), 2.80 – 2.73 (m, 2H), 2.73 – 2.66 (m, 1H), 2.33 – 2.27 (m, 1H), 1.84 (dt, J = 9.0, 12.2 Hz, 1H); **$^{13}\text{C NMR}$** (125 MHz, CDCl_3) δ 195.2, 153.4, 142.5, 127.6, 126.6, 101.0, 79.3, 38.9, 32.5, 30.0; **MS** (ESI-TOF) calcd. for $\text{C}_{10}\text{H}_{10}\text{O}_2$ [$\text{M} + \text{H}^+$] 163.0759, found 163.0628; $[\alpha]_D^{23} = +56.6$ (c = 1.07, CHCl_3).

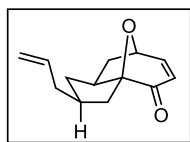


(3aS,7S,8aS)-8-methylene-2,3,8,8a-tetrahydro-1H-3a,7-epoxyazulen-4(7H)-one (40):

According to the general procedure, **39** (107.4 mg, 0.266 mmol), **24** (16.0 mg, 0.040 mmol, 0.15 equiv), and **23** (20.0 mg, 0.040 mmol, 0.15 equiv) were allowed to react in a toluene solution (665 μL , 0.4 M) containing AcOH (2.3 μL , 0.040 mmol, 0.15 equiv) for 72 h to afford **40** (19.7 mg, 54%) as a clear oil after column chromatography (silica gel, 9:1 to 5:1 hexanes/ Et_2O) followed by subsequent column chromatography (silica gel, 98:2 toluene/EtOAc). This material was determined to be 88% *ee* by chiral

HPLC analysis (ChiralPak AS-H, 10% *i*PrOH in hexanes, 1 mL/min, 222 nm, $t_R(\text{major}) = 24.1$ min, $t_R(\text{minor}) = 10.9$ min).

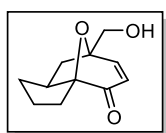
$R_f = 0.45$ (silica gel, 4:1 hexanes/EtOAc); **IR** (film) ν_{max} 2958, 2870, 1690, 1267, 1163, 1031, 934, 897, 817, 79, 782, 627 cm^{-1} ; **$^1\text{H NMR}$** (500 MHz, CDCl_3) δ 7.17 (dd, $J = 4.4, 9.8$ Hz, 1H), 6.00 (d, $J = 9.8$ Hz, 1H), 5.17 (d, $J = 2.4$ Hz, 1H), 5.02 – 4.99 (m, 2H), 2.84 – 2.78 (m, 1H), 2.34 (ddd, $J = 7.6, 9.3, 13.4$ Hz, 1H), 2.13 – 2.04 (m, 1H), 1.92 – 1.81 (m, 2H), 1.81 – 1.71 (m, 2H); **$^{13}\text{C NMR}$** (125 MHz, CDCl_3) δ 196.4, 150.6, 150.5, 126.6, 107.3, 98.9, 79.9, 48.4, 32.2, 30.7, 26.1; **MS** (ESI-TOF) calcd. for $\text{C}_{11}\text{H}_{12}\text{O}_2$ [$\text{M} + \text{Na}^+$] 199.0735, found 199.0723; $[\alpha]_D^{23} = -526.0$ ($c = 0.4$, CHCl_3).



(2*S*,3*aS*,7*R*,8*aS*)-2-allyl-2,3,8,8*a*-tetrahydro-1*H*-3*a*,7-epoxyazulen-4(7*H*)-one (42):

According to the general procedure, **41** (111.7 mg, 0.300 mmol), **24** (12.0 mg, 0.030 mmol, 0.10 equiv), and **23** (15.0 mg, 0.049 mmol, 0.10 equiv) were allowed to react in a toluene solution (750 μL , 0.4 M) containing AcOH (2.6 μL , 0.045 mmol, 0.15 equiv) for 72 h to afford **42** (47.0 mg, 77%) as a clear oil after column chromatography (silica gel, 9:1 to 5:1 hexanes/ Et_2O) followed by subsequent column chromatography (silica gel, 98:2 toluene/EtOAc). This material was determined to be 90% *ee* by chiral HPLC analysis (ChiralPak AS-H, 4% *i*PrOH in hexanes, 1 mL/min, 230 nm, $t_R(\text{major}) = 15.5$ min, $t_R(\text{minor}) = 12.9$ min).

$R_f = 0.37$ (silica gel, 5:1 hexanes/EtOAc); **IR** (film) ν_{max} 3075, 2971, 2925, 1691, 1166, 1024, 909, 803 cm^{-1} ; **$^1\text{H NMR}$** (500 MHz, CDCl_3) δ 7.16 (dd, $J = 4.4, 9.8$ Hz, 1H), 5.96 (d, $J = 9.8$ Hz, 1H), 5.79 (ddt, $J = 6.9, 10.1, 17.1$ Hz, 1H), 5.02 (dd, $J = 1.5, 17.1$ Hz, 1H), 4.99 – 4.94 (m, 2H), 2.75 (ddd, $J = 1.5, 7.8, 13.4$ Hz, 1H), 2.36 – 2.28 (m, 1H), 2.28 – 2.11 (m, 4H), 2.01 (dd, $J = 8.3, 11.7$ Hz, 1H), 1.95 – 1.89 (m, 1H), 1.31 – 1.18 (m, 2H); **$^{13}\text{C NMR}$** (125 MHz, CDCl_3) δ 197.8, 152.6, 137.4, 125.8, 115.8, 98.4, 77.7, 46.1, 44.6, 40.6, 39.5, 36.4, 35.6; **MS** (ESI-TOF) calcd. for $\text{C}_{13}\text{H}_{16}\text{O}_2$ [$\text{M} + \text{Na}^+$] 227.1048, found 227.1069; $[\alpha]_D^{23} = -91.8$ ($c = 1.2$, CHCl_3).



(3*aS*,7*R*)-7-(hydroxymethyl)-2,3,8,8*a*-tetrahydro-1*H*-3*a*,7-epoxyazulen-4(7*H*)-one (81):

According to the general procedure, **43** (124.0 mg, 0.260 mmol), **24** (15.7 mg, 0.039 mmol, 0.15 equiv),

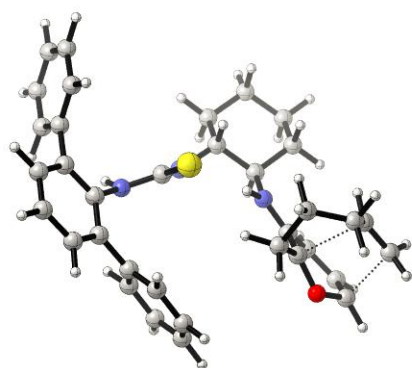
and **23** (19.5 mg, 0.039 mmol, 0.15 equiv) were allowed to react in a toluene solution (650 μL , 0.4 M) containing AcOH (2.2 μL , 0.039 mmol, 0.15 equiv) for 72 h to afford **44** after column chromatography (silica gel, 98:2 toluene/EtOAc). The silyl ether was then immediately dissolved in THF (1.0 mL) at 23 °C. H₂O (400 μL), AcOH (500 μL), and conc. HCl (100 μL) were subsequently added, and the reaction mixture was stirred for 2 h at 23 °C. Sat. aq. NaHCO₃ (10 mL) was then carefully added. The mixture was transferred to a separatory funnel with EtOAc (20 mL). An additional portion of sat. aq. NaHCO₃ (10 mL) was then added and the layers were separated. The organic layer was washed with brine (15 mL) and the combined aqueous layers were further extracted with EtOAc (2 x 20 mL). The combined organic layers were dried over Na₂SO₄, filtered, and concentrated. Purification by column chromatography (silica gel, 2:1 hexanes/EtOAc) afforded **81** as a clear oil (35.7 mg, 70% overall). This material was determined to be 89% *ee* by chiral HPLC analysis (ChiralPak AD-H, 10% *i*PrOH in hexanes, 1 mL/min, 210 nm, $t_{\text{R}}(\text{major}) = 13.6$ min, $t_{\text{R}}(\text{minor}) = 14.9$ min).

R_f = 0.35 (silica gel, 1:1 hexanes/EtOAc); **IR** (film) ν_{max} 3442, 2952, 2869, 2360, 1688, 1382, 1270, 1169, 1085, 1066, 813 cm^{-1} ; **¹H NMR** (500 MHz, CDCl₃) δ 7.09 (d, $J = 9.8$ Hz, 1H), 6.06 (d, $J = 9.3$ Hz, 1H), 3.91 (dd, $J = 5.4, 11.7$ Hz, 1H), 3.80 (dd, $J = 5.4, 11.7$ Hz, 1H), 2.50 – 2.43 (m, 1H), 2.34 – 2.27 (m, 1H), 2.11 (dd, $J = 8.8, 12.2$ Hz, 1H), 1.98 – 1.85 (m, 2H), 1.84 – 1.77 (m, 1H), 1.75 – 1.69 (m, 2H), 1.64 – 1.58 (m, 1H); **¹³C NMR** (100 MHz, CDCl₃) δ 197.4, 152.4, 127.6, 98.5, 86.0, 65.6, 46.1, 38.2, 32.7, 30.4, 26.4; **MS** (ESI-TOF) calcd. for C₁₁H₁₄O₃ [M + Na⁺] 217.0841, found 217.0790; $[\alpha]_{\text{D}}^{23} = -55.2$ ($c = 0.47$, CHCl₃).

2.6.5 Computational Procedures and Results

Calculations were performed at Harvard University using Gaussian 09⁴⁶ at the B3LYP⁴⁷ level of density functional theory with the 6-31G(d)⁴⁸ basis set. Transition structures were fully optimized and verified to be first-order saddle points by frequency calculations showing the existence of a single imaginary frequency. Relative energies between diastereomeric transition structures are for uncorrected electronic energy differences.

Transition structure leading to the observed major enantiomer of product with **24**•pyrylium:



E(RB+HF-LYP): -1994.03711612

Zero-point correction= 0.661700 (Hartree/Particle)

Thermal correction to Energy= 0.696396

Thermal correction to Enthalpy= 0.697340

⁴⁶ Gaussian 09, Revision A.1, Frisch, M. J.; Trucks, G. W.; Schlegel, H. B.; Scuseria, G. E.; Robb, M. A.; Cheeseman, J. R.; Scalmani, G.; Barone, V.; Mennucci, B.; Petersson, G. A.; Nakatsuji, H.; Caricato, M.; Li, X.; Hratchian, H. P.; Izmaylov, A. F.; Bloino, J.; Zheng, G.; Sonnenberg, J. L.; Hada, M.; Ehara, M.; Toyota, K.; Fukuda, R.; Hasegawa, J.; Ishida, M.; Nakajima, T.; Honda, Y.; Kitao, O.; Nakai, H.; Vreven, T.; Montgomery, Jr., J. A.; Peralta, J. E.; Ogliaro, F.; Bearpark, M.; Heyd, J. J.; Brothers, E.; Kudin, K. N.; Staroverov, V. N.; Kobayashi, R.; Normand, J.; Raghavachari, K.; Rendell, A.; Burant, J. C.; Iyengar, S. S.; Tomasi, J.; Cossi, M.; Rega, N.; Millam, N. J.; Klene, M.; Knox, J. E.; Cross, J. B.; Bakken, V.; Adamo, C.; Jaramillo, J.; Gomperts, R.; Stratmann, R. E.; Yazyev, O.; Austin, A. J.; Cammi, R.; Pomelli, C.; Ochterski, J. W.; Martin, R. L.; Morokuma, K.; Zakrzewski, V. G.; Voth, G. A.; Salvador, P.; Dannenberg, J. J.; Dapprich, S.; Daniels, A. D.; Farkas, Ö.; Foresman, J. B.; Ortiz, J. V.; Cioslowski, J.; Fox, D. J. Gaussian, Inc., Wallingford CT, 2009.

⁴⁷ B3LYP = Becke-3-Lee-Yang-Parr density functional theory: (a) Becke, A. D. *J. Chem. Phys.* **1993**, *98*, 1372–1377. (b) Lee, C.; Yang, W.; Parr, R. G. *Phys. Rev. B* **1988**, *37*, 785–789.

⁴⁸ (a) Ditchfield, R.; Hehre, W. J.; Pople, J. A. *J. Chem. Phys.* **1971**, *54*, 724–728. (b) Hehre, W. J.; Ditchfield, R.; Pople, J. A. *J. Chem. Phys.* **1972**, *56*, 2257–2261. (c) Hariharan, P. C.; Pople, J. A. *Theor. Chim. Acta.* **1973**, *28*, 213–222.

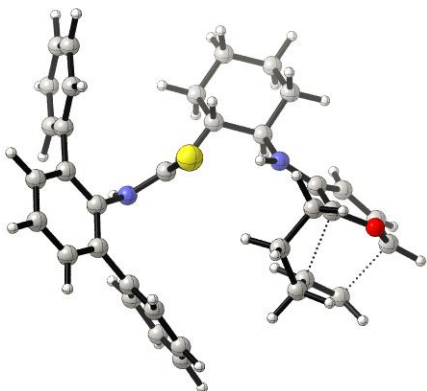
Thermal correction to Gibbs Free Energy= 0.591999

Cartesian coordinates:

C	2.42811600	3.51378200	-0.12486000	C	-4.48395000	-3.36208000	1.01529100
C	1.61112100	2.32480800	-0.67184800	H	-5.98928000	-1.86965200	1.41351600
C	0.10634300	2.53168400	-0.37176500	H	-2.85506800	-4.63433500	0.42180900
C	-0.37782100	3.86957800	-0.95937400	H	-5.04471100	-4.16890700	1.47805000
C	0.45222100	5.05848000	-0.45474100	H	-1.08714800	1.56566700	-1.81812400
C	1.94855300	4.84665500	-0.71740600	H	-2.78717100	0.31552900	-1.46152900
H	1.72586600	2.27421400	-1.76445700	N	2.05236700	1.04438200	-0.09750800
H	2.32110000	3.53012100	0.96829800	C	3.18365600	0.39689200	-0.41378300
H	3.49421600	3.36268700	-0.33367400	C	4.07124100	0.84130600	-1.44526200
H	-0.31813200	3.82350700	-2.05813900	C	3.58053100	-0.77799000	0.31115600
H	-1.43480700	4.00014200	-0.70229300	H	3.79901800	1.67907700	-2.07481200
H	0.10538000	5.97929700	-0.93617000	C	5.62621900	-0.85485000	-0.74495000
H	0.28409600	5.18632600	0.62327000	H	6.45469900	-1.51334500	-0.97892400
H	2.13860700	4.85732000	-1.80038200	C	5.29883200	0.24969400	-1.57239800
H	2.53217700	5.67012400	-0.29140800	H	6.04486300	0.63428200	-2.26057500
H	-0.02583000	2.54383400	0.71522200	O	4.59253400	-1.52633000	-0.18467700
N	-0.72363200	1.44013700	-0.87942100	S	-0.70899400	0.03920000	1.41773500
C	-1.27302400	0.43976300	-0.12818900	H	1.38646100	0.60810400	0.55581600
N	-2.29805700	-0.20979800	-0.74459900	C	-4.88329300	0.34858400	0.35151900
C	-3.04072900	-1.30163900	-0.17605300	C	-5.32321600	0.91079700	-0.85811500
C	-4.30264500	-1.02756900	0.38418800	C	-5.02352200	1.09248700	1.53148000
C	-2.50463600	-2.60410400	-0.18642100	C	-5.88368100	2.18875700	-0.88824200
C	-5.01415700	-2.07459500	0.98192600	H	-5.26448800	0.32502300	-1.77399700
C	-3.24697500	-3.62181800	0.43174100	C	-5.58454300	2.37043800	1.50102700

H	-4.68365600	0.66725600	2.47145900	H	2.12163400	-4.06612400	-2.54163100
C	-6.01337900	2.92259400	0.29265300	C	2.76982300	-1.48332700	1.35245100
H	-6.23411400	2.60319100	-1.82973000	H	1.69732500	-1.45312200	1.13387900
H	-5.68881500	2.93384100	2.42421800	H	3.08021000	-2.53242800	1.34727500
H	-6.45575900	3.91462300	0.27239200	C	3.06985000	-0.85029900	2.73690400
C	-1.20521900	-2.94809000	-0.82800600	H	2.51979200	0.09371400	2.83440700
C	-0.92200600	-2.58791500	-2.15571700	H	2.71317300	-1.50762000	3.53612400
C	-0.25974900	-3.71820000	-0.13127800	C	4.57794800	-0.58861600	2.84486800
C	0.26868100	-2.98154100	-2.76547000	H	4.80390800	-0.12012900	3.81371700
H	-1.65475100	-2.02304100	-2.72391700	H	5.13346200	-1.53463800	2.81785300
C	0.93098700	-4.11481200	-0.74160700	C	5.06441300	0.32414900	1.74445700
H	-0.46272000	-4.00286100	0.89728700	C	6.25837300	0.13551900	1.04783100
C	1.20127800	-3.74589000	-2.06069000	H	6.76713300	0.98903800	0.61138200
H	0.45822500	-2.70951200	-3.80061000	H	6.91002300	-0.68514000	1.34156200
H	1.64167000	-4.72403900	-0.18883600	H	4.60844100	1.31257900	1.71813400

Transition structure leading to the observed minor enantiomer of product with **24**•pyrylium:



E(RB+HF-LYP): -1994.03502204

Zero-point correction= 0.662040 (Hartree/Particle)

Thermal correction to Energy= 0.696602

Thermal correction to Enthalpy= 0.697546

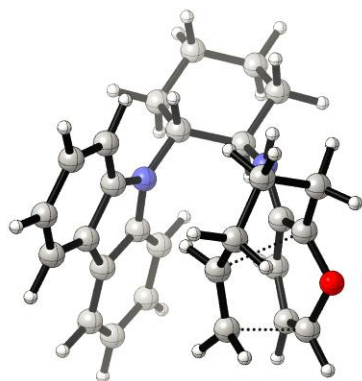
Thermal correction to Gibbs Free Energy= 0.593406

Cartesian coordinates:

C	-1.93555900	4.09210000	-0.18219800	C	3.31804900	-3.64494200	-0.59327200
C	-1.52336800	2.71653900	0.38743400	C	4.50336100	-3.18086100	-1.15451500
C	0.01822800	2.60495400	0.39617700	H	5.79308800	-1.47740500	-1.44443500
C	0.63849000	3.75597200	1.20948200	H	3.06755900	-4.69949700	-0.65377500
C	0.19799000	5.13256000	0.69232800	H	5.16548500	-3.87142600	-1.66866700
C	-1.33044200	5.24355300	0.63288100	H	0.80848000	1.36021700	1.88566300
H	-1.87624800	2.62385200	1.42510100	H	2.21756000	-0.15760700	1.72638700
H	-1.59025100	4.14722400	-1.22346400	N	-2.09853400	1.61006000	-0.39386400
H	-3.02741000	4.17809100	-0.21589500	C	-3.38413500	1.22890500	-0.35815300
H	0.34331500	3.65093900	2.26554600	C	-4.34107200	1.83320600	0.51825000
H	1.72967700	3.65989600	1.16849200	C	-3.86225800	0.15106900	-1.18178000
H	0.61550000	5.91683200	1.33326800	H	-4.05852100	2.67256100	1.13998700
H	0.61585700	5.29229700	-0.31083200	C	-5.94918500	0.19717600	-0.20217100
H	-1.74208600	5.22930300	1.65262300	H	-6.98250400	-0.09511200	-0.34811000
H	-1.62727700	6.20134900	0.19170300	C	-5.58815600	1.27989200	0.63501300
H	0.36609700	2.67146500	-0.64005600	H	-6.29386800	1.62787000	1.38252900
N	0.49988700	1.32165100	0.91925800	O	-5.20604100	0.00416300	-1.31299300
C	1.07280700	0.34949400	0.14080100	S	0.71423700	0.17337600	-1.50373500
N	1.92120700	-0.47570200	0.81035100	H	-1.43143700	1.10491600	-0.99136300
C	2.80424400	-1.42121100	0.17267200	C	4.42019000	0.49035000	-0.23103800
C	4.01720100	-0.94084700	-0.36144400	C	4.65242200	1.06467400	1.02944500
C	2.44483200	-2.77927800	0.08589900	C	4.60869300	1.28123400	-1.37382000
C	4.85517600	-1.83858500	-1.03346700	C	5.04990000	2.39713000	1.14600200

H	4.56561200	0.45021400	1.92381000	H	-1.30837100	-5.52348000	-0.10348700
C	5.00578400	2.61433900	-1.25845200	H	-1.92120400	-5.07294000	2.26883700
H	4.42684400	0.84963000	-2.35369900	C	-3.09602400	-0.53722200	-2.27075800
C	5.22367800	3.17754500	0.00010300	H	-3.80661400	-0.74586600	-3.07699800
H	5.24567400	2.81875400	2.12841100	H	-2.30750500	0.10234400	-2.68100000
H	5.14706300	3.21235700	-2.15449200	C	-2.49636500	-1.86681100	-1.73383800
H	5.54149800	4.21272700	0.08797400	H	-1.54405600	-1.65955000	-1.23439200
C	1.20095600	-3.34188700	0.68058700	H	-2.27444700	-2.54022500	-2.56781400
C	0.84192100	-3.09878900	2.01672100	C	-3.47863700	-2.49747100	-0.74229700
C	0.39966200	-4.21562100	-0.07312100	H	-3.02413900	-3.39844400	-0.30785900
C	-0.27831100	-3.70799900	2.58097400	H	-4.40051600	-2.81358400	-1.24716900
H	1.46835500	-2.46117600	2.63311000	C	-3.81304200	-1.54547200	0.38052500
C	-0.71703500	-4.83293300	0.49245900	C	-5.08929800	-1.43993400	0.93220600
H	0.65833200	-4.41222600	-1.10967100	H	-5.21414500	-1.06927700	1.94452400
C	-1.06171000	-4.58053200	1.82216400	H	-5.86540600	-2.12328300	0.59366700
H	-0.52401000	-3.52245700	3.62325500	H	-2.96728000	-1.18046400	0.96098200

Transition structure leading to the observed major enantiomer of product with **46**•pyrylium:



E(RB+HF-LYP): -1270.12693678

Zero-point correction= 0.535358 (Hartree/Particle)

Thermal correction to Energy= 0.560440

Thermal correction to Enthalpy= 0.561384

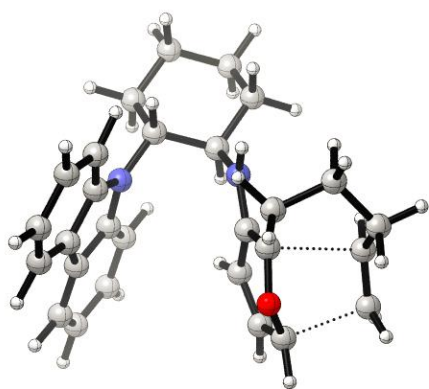
Thermal correction to Gibbs Free Energy= 0.481163

Cartesian coordinates:

C	2.25419200	-3.15363000	0.07750200	H	-3.83950100	-0.54322400	-3.06575600
C	1.58970400	-1.78859600	-0.18746700	H	-0.16012000	-2.48210400	0.74441700
C	2.13488500	-0.70631800	0.78838500	C	-1.67127600	-0.34944900	-2.82257000
C	3.67759900	-0.64611200	0.78361600	H	-1.52822600	0.31690600	-3.66690700
C	4.29766500	-2.02307400	1.05647700	O	-3.13578400	-1.72858600	-1.58364800
C	3.78696300	-3.06735300	0.05599000	N	1.50885900	0.59398100	0.57667000
H	1.80622800	-1.49001500	-1.21490700	C	0.65779900	1.21814900	1.49548800
H	1.92985300	-3.51725200	1.06527900	C	1.59800100	1.40462600	-0.56148700
H	1.89093400	-3.87758100	-0.66087100	C	0.18805800	2.43729300	0.94117000
H	4.03918300	-0.26741900	-0.17858200	C	0.78374800	2.55394800	-0.37226800
H	3.98998800	0.08248500	1.53949100	C	2.31550000	1.22639100	-1.75376200
H	5.38950800	-1.95057900	1.00844800	C	0.69074700	3.52089000	-1.38041100
H	4.05210700	-2.34456900	2.07885500	C	1.39846900	3.34013400	-2.56493200
H	4.12563900	-2.80723600	-0.95683300	H	1.34168300	4.08742300	-3.35039400
H	4.20700200	-4.05408400	0.27915800	C	2.20297300	2.20309000	-2.74361800
H	1.83369200	-1.02206900	1.79283300	H	2.76399400	2.08379000	-3.66616100
N	0.13117800	-1.94094000	-0.05994300	C	-0.68854900	3.24591100	1.67578900
C	-0.84640900	-1.55972800	-0.91000000	C	0.26147700	0.80693000	2.77445000
C	-0.60370000	-0.83917900	-2.11925000	C	-1.08906000	2.83564100	2.94392000
C	-2.21081200	-1.85957900	-0.60219200	H	-1.76104900	3.45758300	3.52723900
H	0.40376100	-0.58702900	-2.42244600	C	-0.61386500	1.62858400	3.48470300
C	-2.99010400	-0.66167700	-2.40291800	H	-0.92050700	1.33298600	4.48402700

H	0.63308300	-0.10621700	3.22965500	H	-2.01648800	-1.46307000	2.24835700
H	-1.04497700	4.18594600	1.26338100	C	-3.65880100	-0.47207700	1.26168600
H	0.07882300	4.40709200	-1.23480100	H	-4.64183700	-0.71367100	0.83808000
H	2.96802800	0.37511700	-1.91417400	H	-3.83516800	0.20798200	2.10715200
C	-2.69172600	-2.67687200	0.55852600	C	-2.81137500	0.25251400	0.24493800
H	-3.62281200	-3.16199700	0.24989300	H	-1.83314400	0.57641600	0.59170100
H	-1.98985100	-3.47852700	0.82130300	C	-3.31762800	0.83471800	-0.91716100
C	-2.96322000	-1.74238600	1.76886600	H	-2.78388500	1.66538900	-1.36784100
H	-3.56347600	-2.26437500	2.52099200	H	-4.39399300	0.83257000	-1.07931100

Transition structure leading to the observed minor enantiomer of product with **46**•pyrylium:



E(RB+HF-LYP): -1270.12481009

Zero-point correction= 0.534791 (Hartree/Particle)

Thermal correction to Energy= 0.560053

Thermal correction to Enthalpy= 0.560998

Thermal correction to Gibbs Free Energy= 0.478788

Cartesian coordinates:

C	0.24084100	3.53137800	0.03668700	C	-2.62580000	2.75828600	0.22743000
C	-0.18428800	2.06924200	-0.19149500	C	-2.16415400	4.20206900	0.47210800
C	-1.50872200	1.74821700	0.56271500	C	-0.88415800	4.51712000	-0.31283600

H	-0.32785100	1.90507500	-1.26201700	C	-2.53983500	0.23324300	-2.06051500
H	0.51436100	3.65879500	1.09567400	C	-2.93328800	-2.52334800	-1.52333200
H	1.14303900	3.74090200	-0.54976800	C	-3.14918700	-2.01328100	-2.80006400
H	-2.94163900	2.64951200	-0.81510000	H	-3.48036900	-2.67087100	-3.59792000
H	-3.49895800	2.51557500	0.84247400	C	-2.95125700	-0.64823000	-3.06127300
H	-2.96332500	4.89608500	0.19037900	H	-3.13300900	-0.26188300	-4.06022600
H	-1.98273200	4.35631300	1.54544600	C	-2.18397000	-2.99867000	1.72010100
H	-1.09066100	4.46965600	-1.39146200	C	-1.43291900	-0.46580900	2.75589300
H	-0.54686000	5.53869500	-0.10660200	C	-1.80280400	-2.86132800	3.05118200
H	-1.28937100	1.87343400	1.62878000	H	-1.79928100	-3.72755800	3.70559000
N	0.88949900	1.17124000	0.26112100	C	-1.43330000	-1.60526300	3.56009300
C	1.38929200	0.07240000	-0.33960500	H	-1.15309600	-1.51339200	4.60565000
C	0.99164200	-0.37245400	-1.63709700	H	-1.17063400	0.49721700	3.18468600
C	2.42319100	-0.67630700	0.30965900	H	-2.47829800	-3.96873800	1.32903100
H	0.13741400	0.06479200	-2.13745600	H	-3.08972500	-3.57905500	-1.31907600
C	2.81324900	-1.94860300	-1.56139700	H	-2.41523300	1.28536200	-2.29189900
H	3.25038000	-2.88039000	-1.90134000	C	2.89122700	-0.47547700	1.71926000
H	1.19294200	1.33767600	1.21289700	H	3.26752600	-1.43908800	2.07541200
C	1.74204900	-1.33335200	-2.26002300	H	2.06909800	-0.19099300	2.38792800
H	1.55276000	-1.61412400	-3.29107200	C	4.03779600	0.57155300	1.72955200
O	2.78304000	-1.87046400	-0.21038400	H	4.58377200	0.52706100	2.67709100
N	-1.90239800	0.35551400	0.40216800	H	3.62277700	1.58482500	1.64953400
C	-1.81368600	-0.60798400	1.41632700	C	4.95546100	0.30099900	0.52873600
C	-2.32637200	-0.27974200	-0.77241800	H	5.76230300	1.04726000	0.50520700
C	-2.18994800	-1.87000500	0.89192900	H	5.43811600	-0.67885400	0.63182600
C	-2.51499500	-1.66219500	-0.50258800	C	4.19726000	0.36596700	-0.77720500

H	3.71461000	1.31792700	-0.99375200	H	5.16636200	-1.28158300	-1.74586200
C	4.38957200	-0.52453100	-1.83428400	H	4.17417600	-0.20657100	-2.84925000

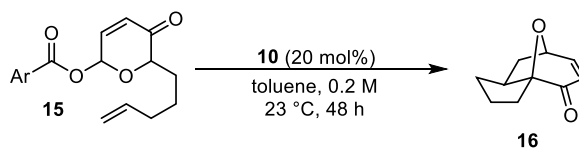
2.6.6 Frontier Molecular Orbital Methods

Frontier molecular orbital energies were calculated according to the DFT-based method of Musgrave²⁵ wherein the excitation energy of the first singlet excited state is used as an approximation of the HOMO–LUMO energy gap; the authors also provide linear correction factors to improve the accuracy of computed values. Structures were first fully optimized at the B3LYP/6-311+G(d,p) level of density functional theory and verified to be local minima by the existence of no imaginary frequencies. HOMO energy values were then linearly corrected. A time-dependent DFT (TD–DFT) calculation was then performed on each optimized structure in order to determine the excitation energy of the first singlet excited state, and this value was then linearly corrected and added to the corrected HOMO energy to give a LUMO energy value.

For ion pair **58** a TD–DFT calculation was not possible owing to the fact that the Kohn-Sham orbitals taken into consideration in such a calculation are not those relevant to cycloaddition. This was determined through visualization of the HOMO and LUMO surfaces. Visualization of other MO surfaces allowed for the identification of a reasonable “HOMO” and “LUMO” that would be involved in cycloaddition of **58** through analogy to visualized HOMO and LUMO surfaces of the other pyryliums. The identified “HOMO” was linearly corrected as before. Musgrave also provides linear corrections for LUMO values from DFT calculations and shows these to give comparable yet slightly less accurate results than with TD-DFT calculations. This was used to determine an energy value for the “LUMO” of **58**.

2.6.7 Additional Optimization Studies

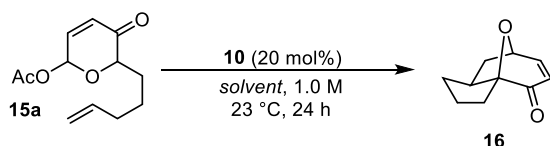
Table 2.6. Benzoate leaving group screen (with Dr. Noah Z. Burns).^a



Entry	Ar	Yield (%) ^b	ee (%) ^c
1	Ph	36	58
2	<i>p</i> -Me ₂ NPh	15	55
3	<i>p</i> -MeOPh	40	61
4	<i>o</i> -MeOPh	13	75
5	<i>p</i> - <i>t</i> BuPh	26	58
6	<i>p</i> -NO ₂ Ph	12	43
7	2-naphthyl	36	46

^a Reactions performed on 0.05 mmol scale. ^b Yields determined by NMR analysis using 1,3,5-trimethoxybenzene as an internal standard. ^c Enantioselectivities determined by HPLC using commercial columns with chiral stationary phases.

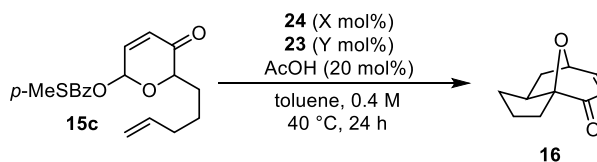
Table 2.7. Solvent screen (with Dr. Noah Z. Burns).^a



Entry	Solvent	ee (%) ^b
1	CH ₂ Cl ₂	46
2	<i>t</i> BME	20
3	hexanes	30
4	Et ₂ O	22
5	THF	-
6	H ₂ O	6
7	MeCN	18
8	MeOH	-
9	toluene	54
10	-	28

^a Reactions performed on 0.05 mmol scale. ^b Enantioselectivities determined by HPLC using commercial columns with chiral stationary phases.

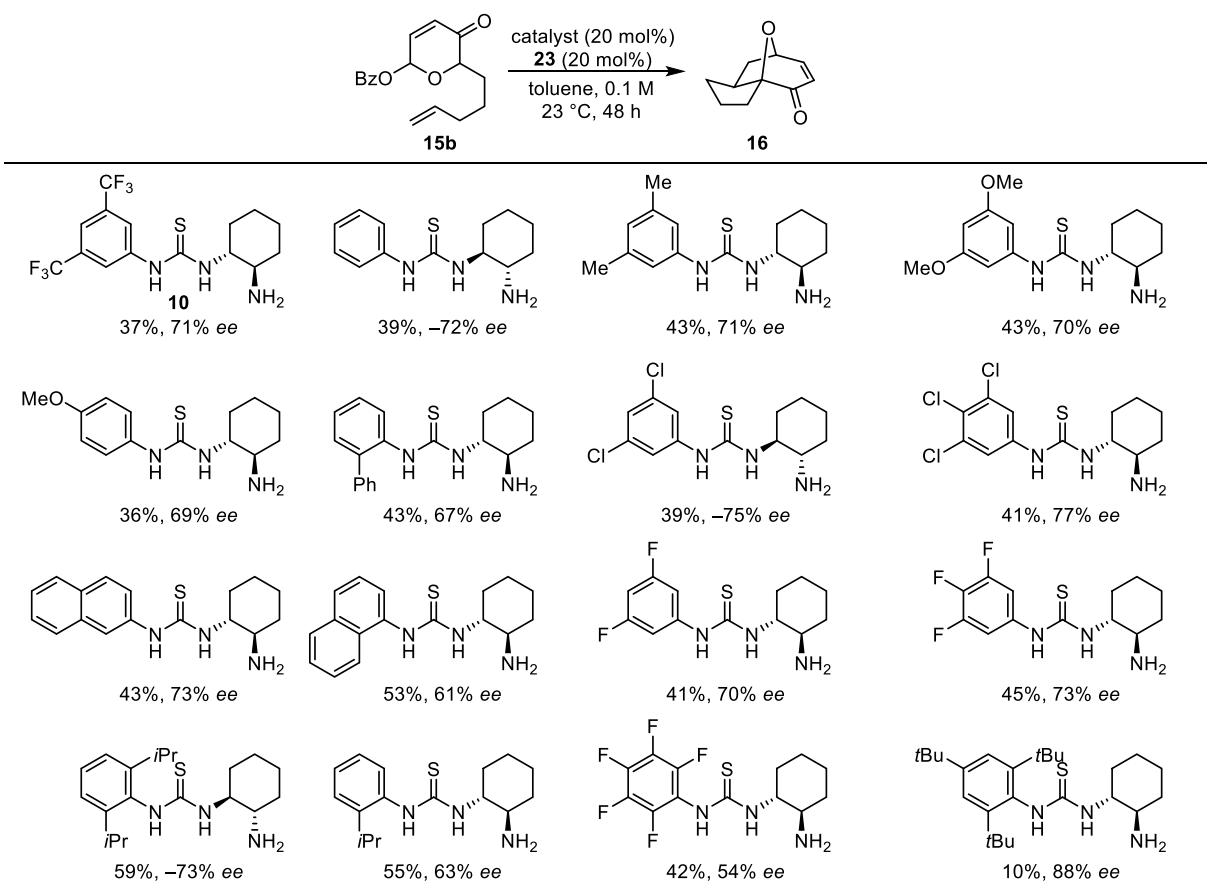
Table 2.8. Catalyst loading (with Dr. Noah Z. Burns).^a



Entry	mol% 24	mol% 23	Yield (%) ^b	ee (%) ^c
1	20	20	69	91
2	20	15	68	92
3	20	10	71	90
4	20	5	70	90
5	20	2.5	66	90
6	20	1	63	87
7	15	20	59	92
8	10	20	43	91

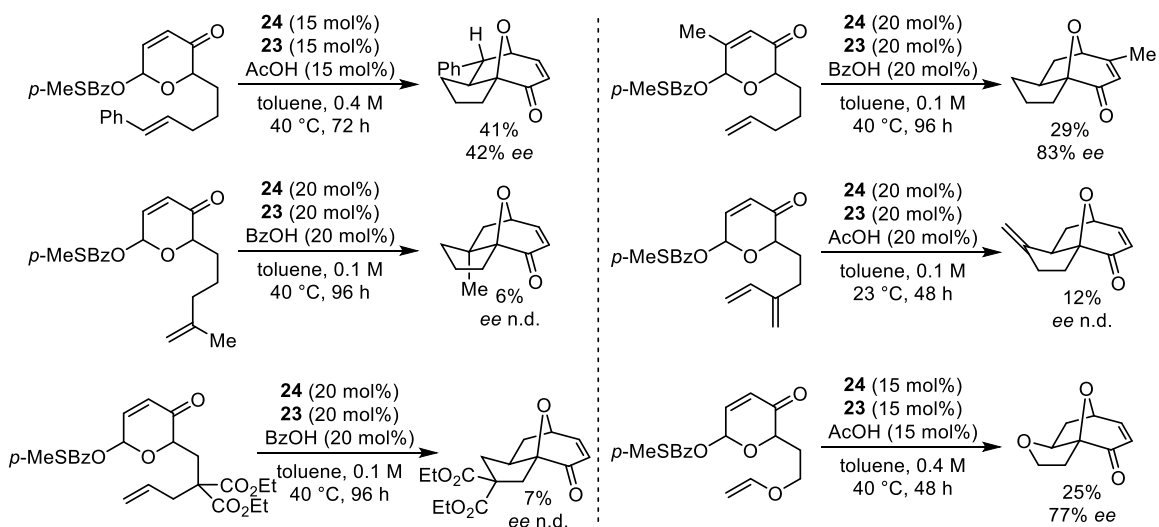
^a Reactions performed on 0.05 mmol scale. ^b Yields determined by NMR analysis using 1,3,5-trimethoxybenzene as an internal standard. ^c Enantioselectivities determined by HPLC using commercial columns with chiral stationary phases.

Table 2.9. Full catalyst screen (with Dr. Noah Z. Burns).^a

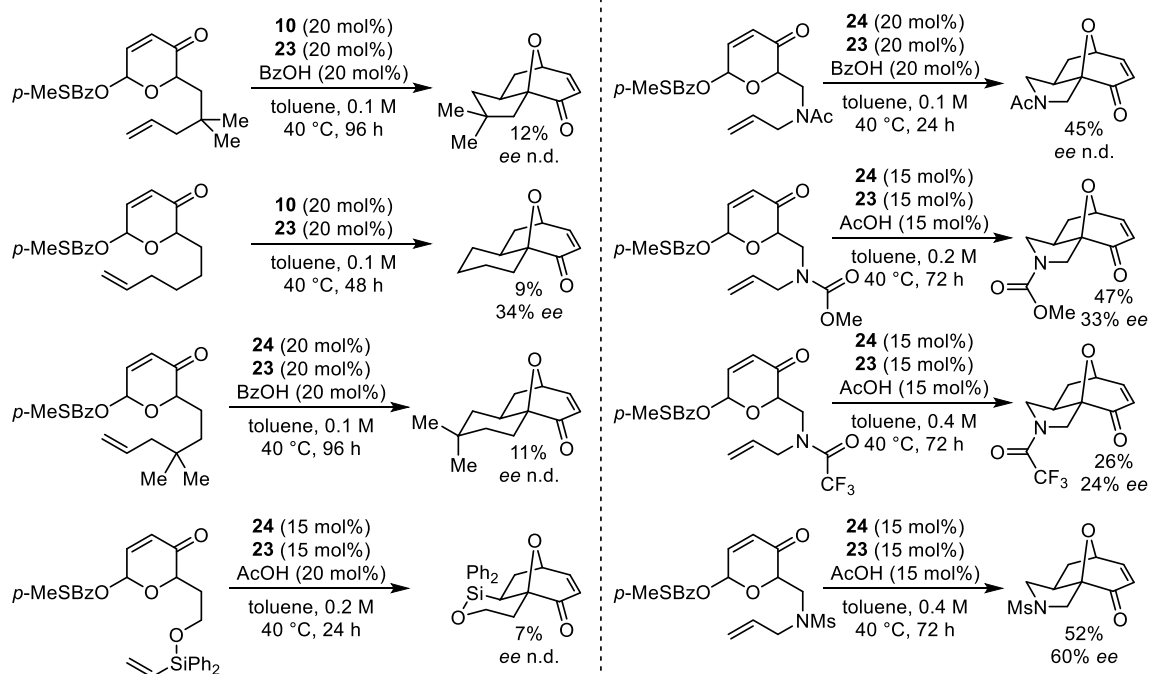


^a Reactions performed on 0.05 mmol scale. Yields determined by NMR analysis using 1,3,5-trimethoxybenzene as an internal standard. Enantioselectivities determined by HPLC using commercial columns with chiral stationary phases.

2.6.8 Results with Sub-Optimal and Unreactive Substrates



Scheme 2.19. Results with additional substrates.



Scheme 2.19 (continued).

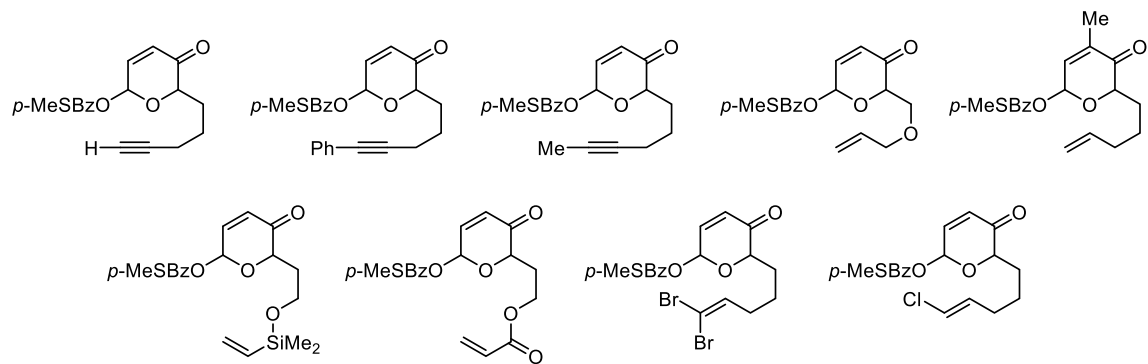
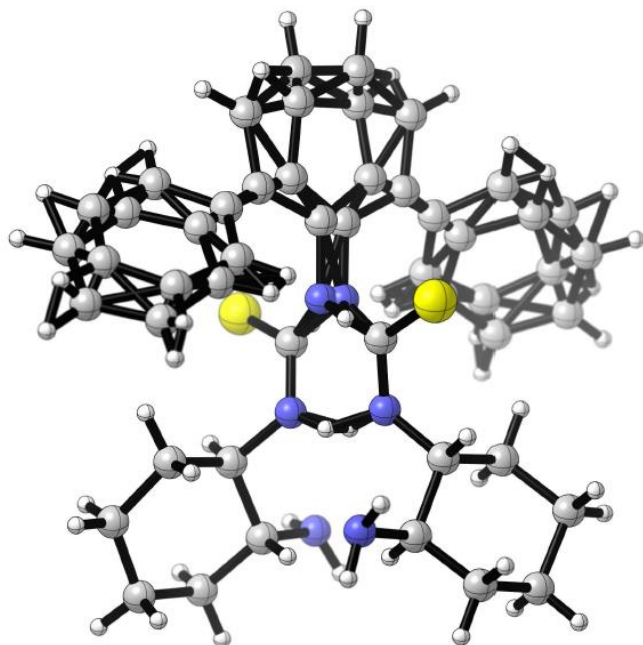


Figure 2.5. Unreactive substrates.

2.6.9 Crystallographic Information⁴⁹

Catalyst 24:

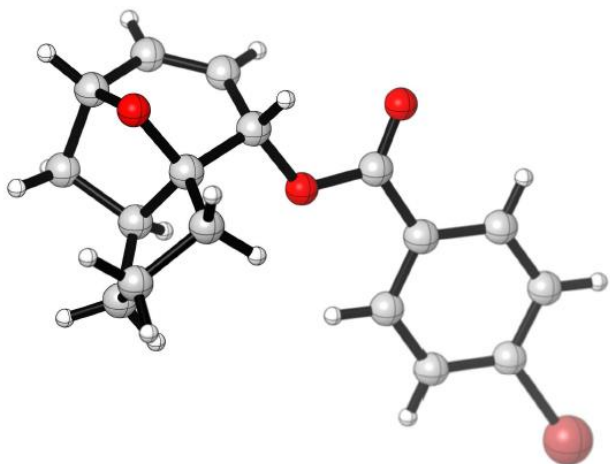


Crystal data	
Chemical formula	C ₂₅ H ₂₇ N ₃ S
<i>M</i> _r	401.56
Crystal system, space group	Trigonal, <i>P</i> 3 ₁
Temperature (K)	100
<i>a</i> , <i>b</i> , <i>c</i> (Å)	11.4229 (4), 11.4229 (4), 14.1312 (5)
α , β , γ (°)	90, 90, 120
<i>V</i> (Å ³)	1596.84 (10)
<i>Z</i>	3
Radiation type	Cu <i>K</i> α
μ (mm ⁻¹)	1.46
Crystal size (mm)	0.26 × 0.14 × 0.12
Data collection	
Diffractometer	CCD area detector diffractometer
Absorption correction	Multi-scan <i>SADABS</i>

⁴⁹ Crystal structures solved by Dr. Shao-Liang Zheng.

T_{\min}, T_{\max}	0.703, 0.845
No. of measured, independent and observed [$I > 2\sigma(I)$] reflections	32886, 3653, 3637
R_{int}	0.048
Refinement	
$R[F^2 > 2\sigma(F^2)], wR(F^2), S$	0.090, 0.178, 1.02
No. of reflections	3653
No. of parameters	249
No. of restraints	6
H-atom treatment	H-atom parameters constrained
$\Delta\rho_{\max}, \Delta\rho_{\min}$ (e \AA^{-3})	0.41, -0.33
Absolute structure	Flack, H. D. <i>Acta Cryst.</i> 1983 , <i>A39</i> , 876–881.
Flack parameter	-10 (10)

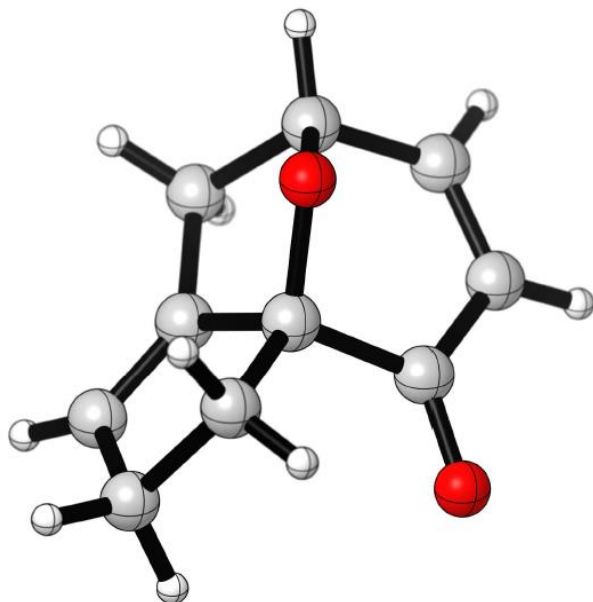
para-Bromobenzoate of cycloadduct **16**:



Crystal data	
Chemical formula	$\text{C}_{17}\text{H}_{17}\text{BrO}_3$
M_r	349.22
Crystal system, space group	Monoclinic, $P2_1$
Temperature (K)	100
a, b, c (\AA)	6.9456 (3), 6.6693 (3), 16.2697 (7)
β ($^\circ$)	95.464 (2)

V (Å ³)	750.23 (6)
Z	2
Radiation type	Mo $K\alpha$
μ (mm ⁻¹)	2.75
Crystal size (mm)	0.24 × 0.18 × 0.16
Data collection	
Diffractometer	Bruker D8 goniometer with CCD area detector diffractometer
Absorption correction	Multi-scan <i>SADABS</i>
T_{\min}, T_{\max}	0.559, 0.668
No. of measured, independent and observed [$I > 2\sigma(I)$] reflections	20486, 3847, 3623
R_{int}	0.030
Refinement	
$R[F^2 > 2\sigma(F^2)], wR(F^2), S$	0.020, 0.046, 1.08
No. of reflections	3847
No. of parameters	190
No. of restraints	1
H-atom treatment	H-atom parameters constrained
$\Delta\rho_{\max}, \Delta\rho_{\min}$ (e Å ⁻³)	0.31, -0.28
Absolute structure	Flack, H. D. <i>Acta Cryst.</i> 1983 , <i>A39</i> , 876–881.
Flack parameter	-0.004 (5)

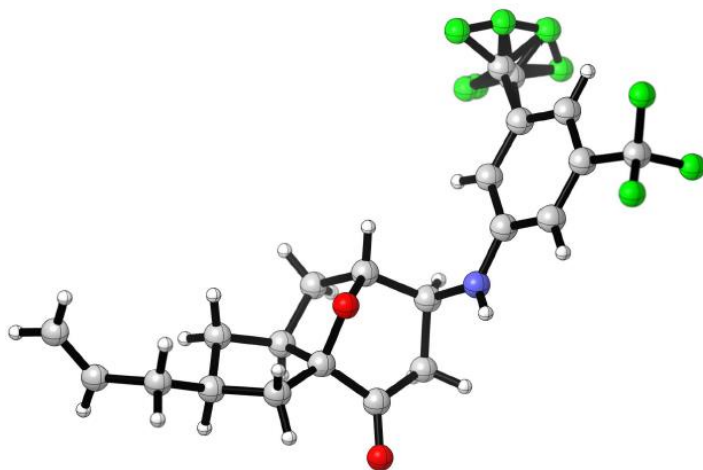
Cycloadduct **38**:



Crystal data	
Chemical formula	C ₁₀ H ₁₀ O ₂
<i>M_r</i>	162.18
Crystal system, space group	Orthorhombic, <i>P</i> 2 ₁ 2 ₁ 2 ₁
Temperature (K)	100
<i>a</i> , <i>b</i> , <i>c</i> (Å)	7.2085 (1), 7.8988 (1), 13.8528 (2)
<i>V</i> (Å ³)	788.76 (2)
<i>Z</i>	4
Radiation type	Cu <i>K</i> α
μ (mm ⁻¹)	0.77
Crystal size (mm)	0.28 × 0.16 × 0.12
Data collection	
Diffractometer	Bruker D8 goniometer with CCD area detector diffractometer
Absorption correction	Multi-scan <i>SADABS</i>
<i>T_{min}</i> , <i>T_{max}</i>	0.814, 0.914
No. of measured, independent and observed [<i>I</i> > 2σ(<i>I</i>)] reflections	13604, 1387, 1378
<i>R_{int}</i>	0.031

Refinement	
$R[F^2 > 2\sigma(F^2)], wR(F^2), S$	0.029, 0.073, 1.15
No. of reflections	1387
No. of parameters	109
No. of restraints	0
H-atom treatment	H-atom parameters constrained
$\Delta\rho_{\max}, \Delta\rho_{\min}$ (e Å ⁻³)	0.12, -0.21
Absolute structure	Flack, H. D. <i>Acta Cryst.</i> 1983 , <i>A39</i> , 876–881.
Flack parameter	0.1 (2)

Byproduct of cycloadduct **42**:



Crystal data	
Chemical formula	C ₂₁ H ₂₁ F ₆ NO ₂
M_r	433.39
Crystal system, space group	Monoclinic, <i>C2</i>
Temperature (K)	100
a, b, c (Å)	29.9461 (7), 5.0733 (1), 15.3388 (4)
β (°)	90.381 (2)
V (Å ³)	2330.30 (9)
Z	4
Radiation type	Cu $K\alpha$
μ (mm ⁻¹)	0.97
Crystal size (mm)	0.22 × 0.18 × 0.08

Data collection	
Diffractionmeter	Bruker D8 goniometer with CCD area detector diffractometer
Absorption correction	Multi-scan <i>SADABS</i>
T_{\min}, T_{\max}	0.814, 0.926
No. of measured, independent and observed [$I > 2\sigma(I)$] reflections	3818, 3818, 3728
R_{int}	0.0000
Refinement	
$R[F^2 > 2\sigma(F^2)], wR(F^2), S$	0.035, 0.094, 1.09
No. of reflections	3818
No. of parameters	288
No. of restraints	26
H-atom treatment	H atoms treated by mixture of independent and constrained refinement
$\Delta\rho_{\max}, \Delta\rho_{\min}$ (e Å ⁻³)	0.20, -0.19
Absolute structure	Flack, H. D. <i>Acta Cryst.</i> 1983 , <i>A39</i> , 876–881.
Flack parameter	0.11 (13)

Expansion of Catalytic Asymmetric [5 + 2] Cycloadditions to Intermolecular Reactions¹

3.1 Introduction

Chiral 8-oxabicyclo[3.2.1]octane architectures reside at the core of numerous natural products and biologically significant compounds (Figure 3.1).^{2,3} Heterocycles of this class have also proven to be valuable intermediates in the stereoselective synthesis of oxygenated seven-

¹ Portions of this chapter have been published: Witten, M. R.; Jacobsen, E. N. *Angew. Chem. Int. Ed.* **2014**, *53*, 5912–5916. Adapted with permission. Copyright 2014 Wiley-VCH.

² For example, Englerin A: (a) Ratnayake, R.; Covell, D.; Ransom, T. T.; Gustafson, K. R.; Beutler, J. A. *Org. Lett.* **2009**, *11*, 57–60. Phorbol: (b) Hecker, E.; Schmidt, R. *Fortschr. Chem. Org. Naturst.* **1974**, *31*, 377–467. Secodolastanes: (c) Teixeira, V. L.; Tomassini, T.; Fleury, B. G.; Kelecom, A. *J. Nat. Prod.* **1986**, *49*, 570–575. Cortistatin A: (d) Aoki, S.; Watanabe, Y.; Sanagawa, M.; Setiawan, A.; Kotoku, N.; Kobayashi, M. *J. Am. Chem. Soc.* **2006**, *128*, 3148–3149. Anthecularin: (e) Karioti, A.; Skaltsa, H.; Linden, A.; Perozzo, R.; Brun, R.; Tasdemir, D. *J. Org. Chem.* **2007**, *72*, 8103–8106. Intricarene: (f) Marrero, J.; Rodríguez, A. D.; Barnes, C. L. *Org. Lett.* **2005**, *7*, 1877–1880. Komaroviquinone: (g) Uchiyama, N.; Kiuchi, F.; Ito, M.; Honda, G.; Takeda, Y.; Khodzhimatov, O. K.; Ashurmetov, O. A. *J. Nat. Prod.* **2003**, *66*, 128–131. Descurainin: (h) Sun, K.; Li, X.; Li, W.; Wang, J.; Liu, J.; Sha, Y. *Chem. Pharm. Bull.* **2004**, *52*, 1483–1486. Cartorimine: (i) Yin, H.-B.; He, Z.-S.; Ye, Y. *J. Nat. Prod.* **2000**, *63*, 1164–1165.

³ Compounds containing the chiral 8-oxabicyclo[3.2.1]octane core have been identified recently as psychoactive analogues of the tropane alkaloids with promising therapeutic potential: (a) Meltzer, P. C.; Liang, A. Y.; Blundell, P.; Gonzalez, M. D.; Chen, Z.; George, C.; Madras, B. K. *J. Med. Chem.* **1997**, *40*, 2661–2673. (b) Meltzer, P. C.; Liu, S.; Blanchette, H. S.; Blundell, P.; Madras, B. K. *Bioorg. Med. Chem.* **2002**, *10*, 3583–3591. (c) Meltzer, P. C.; Kryatova, O.; Pham-Huu, D.-P.; Donovan, P.; Janowsky, A. *Bioorg. Med. Chem.* **2008**, *16*, 1832–1841.

membered carbocycles⁴ and tetrahydrofuran derivatives.⁵ Successful stereoselective approaches to the 8-oxabicyclo[3.2.1]octane framework have previously relied on transition metal-catalyzed [3 + 2] cycloadditions,⁶ [4 + 3] cycloadditions,⁷ diastereoselective [5 + 2] cycloadditions,⁸ and diastereoselective cascade cyclizations.⁹ Much of this precedent has been summarized in Chapter 1. Three examples most relevant to this chapter will be discussed in Section 3.1.2.

⁴ (a) Wender, P. A.; Lee, H. Y.; Wilhelm, R. S.; Williams, P. D. *J. Am. Chem. Soc.* **1989**, *111*, 8954–8957. (b) Wender, P. A.; Kogen, H.; Lee, H. Y.; Munger, Jr., J. D.; Wilhelm, R. S.; Williams, P. D. *J. Am. Chem. Soc.* **1989**, *111*, 8957–8958. (c) Bromidge, S. M.; Sammes, P. G.; Street, L. J. *J. Chem. Soc., Perkin Trans. 1* **1985**, 1725–1730. (d) Wender, P. A.; Jesudason, C. D.; Nakahira, H.; Tamura, N.; Tebbe, A. L.; Ueno, Y. *J. Am. Chem. Soc.* **1997**, *119*, 12976–12977. (e) Roethle, P. A.; Hernandez, P. T.; Trauner, D. *Org. Lett.* **2006**, *8*, 5901–5904. (f) Li, Y.; Nawrat, C. C.; Pattenden, G.; Winne, J. M. *Org. Biomol. Chem.* **2009**, *7*, 639–640. (g) Nicolaou, K. C.; Kang, Q.; Ng, S. Y.; Chen, D. Y.-K. *J. Am. Chem. Soc.* **2010**, *132*, 8219–8222.

⁵ (a) Fishwick, C. W. G.; Mitchell, G.; Pang, P. F. W. *Synlett* **2005**, 285–286. (b) Krishna, U. M. *Tetrahedron Lett.* **2010**, *51*, 2148–2150. (c) Yadav, A. A.; Sarang, P. S.; Trivedi, G. K.; Salunkhe, M. M. *Synlett*, **2007**, 989–991. (d) Ali, M. A.; Bhogal, N.; Findlay, J. B. C.; Fishwick, C. W. G. *J. Med. Chem.* **2005**, *48*, 5655–5658.

⁶ (a) Kitagaki, S.; Anada, M.; Kataoka, O.; Matsuno, K.; Umeda, C.; Watanabe, N.; Hashimoto, S. *J. Am. Chem. Soc.* **1999**, *121*, 1417–1418. (b) Hodgson, D. M.; Labande, A. H.; Pierard, F. Y. T. M.; Expósito Castro, M. Á. *J. Org. Chem.* **2003**, *68*, 6153–6159. (c) Hodgson, D. M.; Brückl, T.; Glen, R.; Labande, A. H.; Selden, D. A.; Dossetter, A. G.; Redgrave, A. J. *Proc. Natl. Acad. Sci. U.S.A.* **2004**, *101*, 5450–5454. (d) Shimada, N.; Anada, M.; Nakamura, S.; Nambu, H.; Tsutsui, H.; Hashimoto, S. *Org. Lett.* **2008**, *10*, 3603–3606. (e) Ishida, K.; Kusama, H.; Iwasawa, N. *J. Am. Chem. Soc.* **2010**, *132*, 8842–8843.

⁷ (a) Harmata, M.; Ghosh, S. K.; Hong, X.; Wacharasindhu, S.; Kirchhoefer, P. *J. Am. Chem. Soc.* **2003**, *125*, 2058–2059. (b) Huang, J.; Hsung, R. P. *J. Am. Chem. Soc.* **2005**, *127*, 50–51.

⁸ (a) Wender, P. A.; Rice, K. D.; Schnute, M. E. *J. Am. Chem. Soc.* **1997**, *119*, 7897–7898. (b) López, F.; Castedo, L.; Mascareñas, J. L. *Org. Lett.* **2000**, *2*, 1005–1007. (c) López, F.; Castedo, L.; Mascareñas, J. L. *Org. Lett.* **2002**, *4*, 3683–3685. (d) Krishna, U. M.; Deodhar, K. D.; Trivedi, G. K. *Tetrahedron* **2004**, *60*, 4829–4836. (e) Wender, P. A.; Bi, F. C.; Buschmann, N.; Gosselin, F.; Kan, C.; Kee, J.-M.; Ohmura, H. *Org. Lett.* **2006**, *8*, 5373–5376. (f) Wender, P. A.; Buschmann, N.; Cardin, N. B.; Jones, L. R.; Kan, C.; Kee, J.-M.; Kowalski, J. A.; Longcore, K. E. *Nat. Chem.* **2011**, *3*, 615–619.

⁹ Li, B.; Zhao, Y.-J.; Lai, Y.-C.; Loh, T.-P. *Angew. Chem. Int. Ed.* **2012**, *51*, 8041–8045.

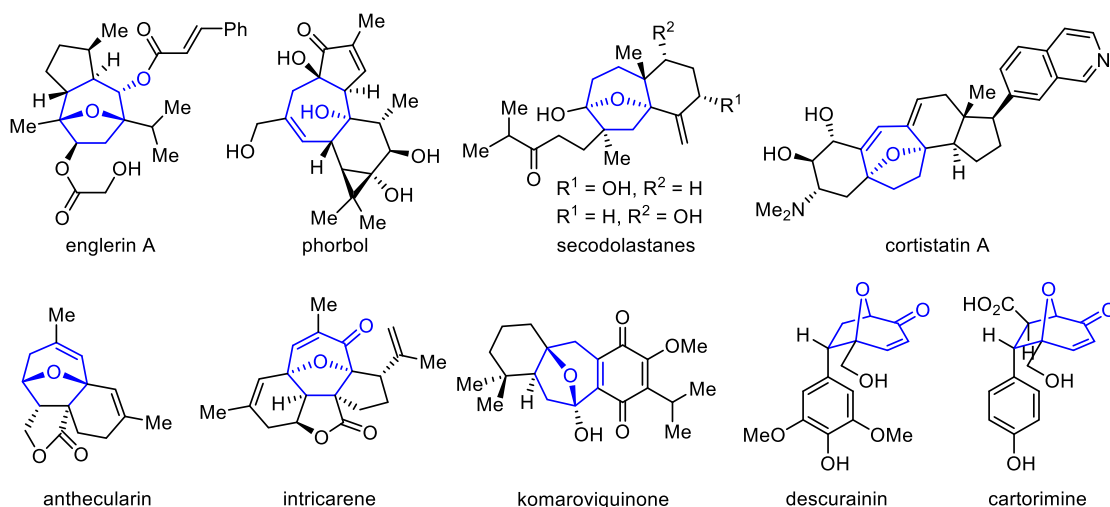


Figure 3.1. The 8-oxabicyclo[3.2.1]octane core in selected natural products.

3.1.1 The Catalytic Asymmetric [5 + 2] Pirylium Cycloaddition

The [5 + 2] cycloaddition of a pyrylium ylide precursor with a two-carbon dipolarophile (e.g., **1** to **2**, Scheme 3.1) provides a concise approach to the 8-oxabicyclo[3.2.1]octane framework, while also embedding a reactive α,β -unsaturated ketone in the bicyclic core.^{10,11} The products can thus be subjected to stereoselective elaboration to afford a diverse array of chiral structures in just one or two steps (*vide infra*). In Chapter 2, a dual catalyst system consisting of the chiral primary amine **4** and the achiral thiourea **5** was introduced (Scheme 3.2).^{12,13} These thioureas catalyze enantioselective intramolecular [5 + 2] cycloadditions of alkenylpyranones of structure **3** through the proposed intermediacy of thiourea-complexed aminopyrylium salts (i.e., **6**). While this

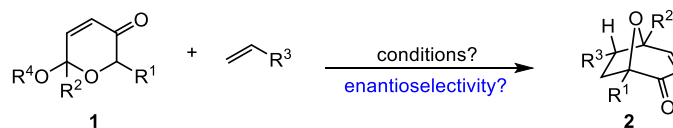
¹⁰ For recent reviews, see: (a) Singh, V.; Krishna, U. M.; Vikrant; Trivedi, G. K. *Tetrahedron* **2008**, *64*, 3405–3428. (b) Pellissier, H. *Adv. Synth. Catal.* **2011**, *353*, 189–218. (c) Ylijoki, K. E. O.; Stryker, J. M. *Chem. Rev.* **2013**, *113*, 2244–2266.

¹¹ For pioneering reports, see: (a) Hendrickson, J. B.; Farina, J. S. *J. Org. Chem.* **1980**, *45*, 3359–3361. (b) Sammes, P. G.; Street, L. J. *J. Chem. Soc., Chem. Commun.* **1982**, 1056–1057. (c) Sammes, P. G.; Street, L. J. *J. Chem. Soc., Perkin Trans. 1* **1983**, 1261–1265. (d) Sammes, P. G.; Street, L. J. *J. Chem. Res., Synop.* **1984**, 196–197.

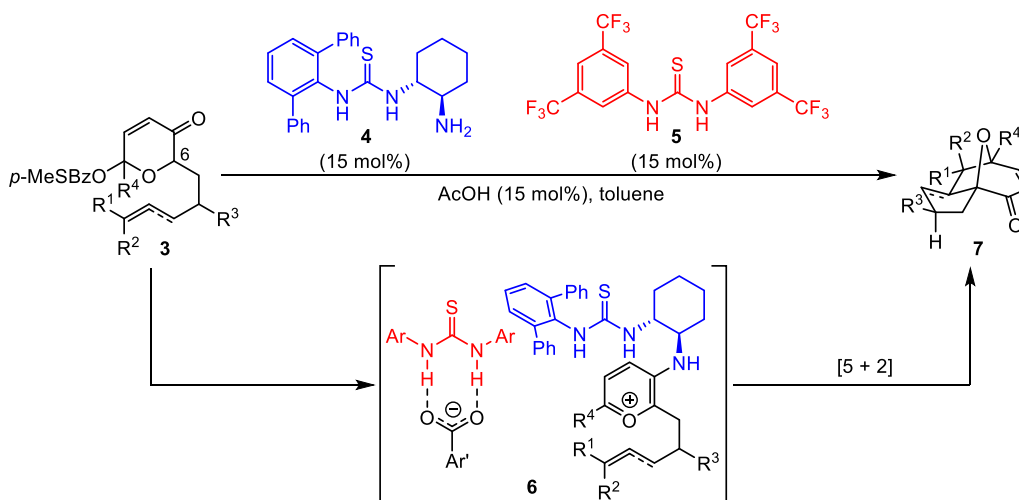
¹² For a review of anion-binding asymmetric catalysis, see: Brak, K.; Jacobsen, E. N. *Angew. Chem. Int. Ed.* **2013**, *52*, 534–561.

¹³ For preparation and use of thiourea **5**, see: (a) Schreiner, P. R.; Wittkopp, A. *Org. Lett.* **2002**, *4*, 217–220. (b) Wittkopp, A.; Schreiner, P. R. *Chem.–Eur. J.* **2003**, *9*, 407–414.

methodology enables the preparation of a range of complex tricyclic products, we reasoned that the corresponding intermolecular reaction (Scheme 3.1) would provide more general access to 8-oxabicyclo[3.2.1]octane derivatives from simpler and more accessible starting materials.



Scheme 3.1. The intermolecular [5 + 2] cycloaddition of an acetoxy-pyrone and an olefin.



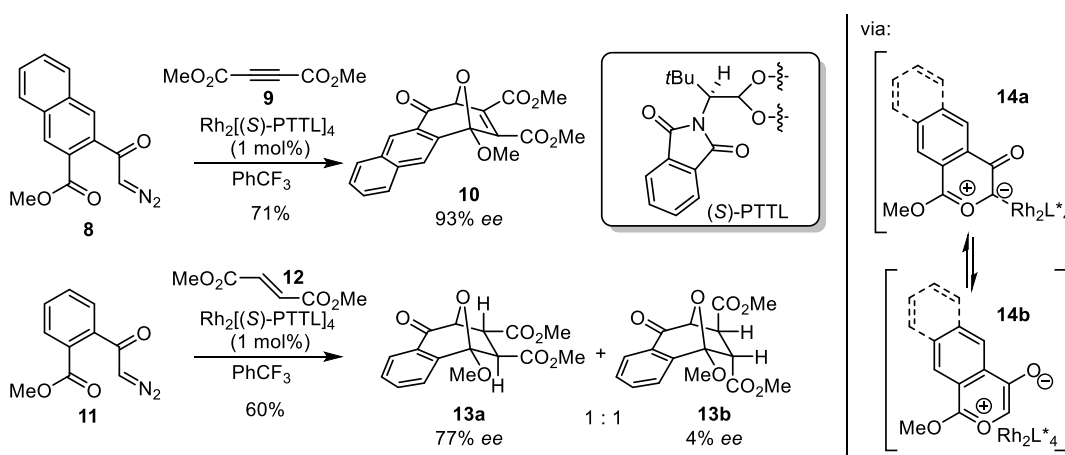
Scheme 3.2. The intramolecular [5 + 2] cycloaddition described in Chapter 2.

As described in Section 2.4.2, initial efforts to effect intermolecular variants of these reactions proved unsuccessful. Upon closer examination of the reaction system, the observance of striking substrate structure–enantioselectivity effects led to the successful development of highly enantioselective intermolecular [5 + 2] cycloadditions. This work will be described in the present chapter.

3.1.2 Asymmetric Intermolecular [5 + 2] Pirylium Cycloadditions

At the outset of this project, three asymmetric intermolecular [5 + 2] oxipyrylium cycloaddition methodologies had been reported previously. The first, by the Hashimoto group in 2000, utilized diazoketone starting materials and a rhodium catalyst to generate ylides such as **14a**,

which are thought to equilibrate with benzopyrylium isomers such as **14b** (Scheme 3.3).¹⁴ In these transformations, it is unknown whether the reactive dipole is carbonyl ylide **14a** (which would participate in a [3 + 2] cycloaddition) or oxipyrylium **14b** (which would react via a [5 + 2] manifold). Furthermore, the nature of the association between the chiral ligand/catalyst and the prochiral pyrylium in **14b** remains undefined. Nonetheless, reaction of ester **8** with dimethyl acetylenedicarboxylate **9** provided cycloadduct **10** in 93% *ee*. However, reactions with olefins, such as that between substrate **11** and dimethyl fumarate **12**, exhibited no diastereoselectivity. Hashimoto's report remains the only intermolecular example of a catalytic asymmetric [5 + 2] pyrylium cycloaddition outside of the original research described in this chapter.



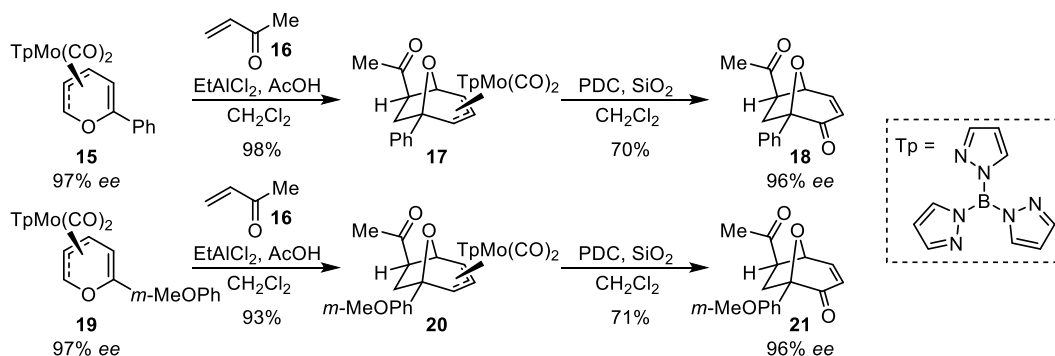
Scheme 3.3. A rhodium-catalyzed asymmetric [5 + 2] cycloaddition.

The other two examples of asymmetric intermolecular [5 + 2] oxidopyrylium cycloadditions deal with diastereoselective reactions of enantiopure chiral 5 π and 2 π components. In 2008, the Liebeskind group reported the synthesis of η^3 -pyranyl scaffolds such as **15** and **19** in very high *ee*.¹⁵ They further demonstrated [5 + 2] cycloaddition reactions of these substrates with methyl vinyl ketone **16** to afford cycloadducts **17** and **20**. Oxidative demetalation of these

¹⁴ Kitagaki, S.; Yasugahira, M.; Anada, M.; Nakajima, M.; Hashimoto, S. *Tetrahedron Lett.* **2000**, *41*, 5931–5935.

¹⁵ Garnier, E. C.; Liebeskind, L. S. *J. Am. Chem. Soc.* **2008**, *130*, 7449–7458.

intermediates provided compounds **18** and **21** respectively. This sequence ultimately forms 8-oxabicyclo[3.2.1]oct-3-en-2-one products complete with α,β -unsaturated ketone functionality. Nevertheless, the requirement for molybdenum-containing starting materials, generated in six steps from D-arabinose, limits the practicality of this methodology.



Scheme 3.4. Molybdenum scaffolds in asymmetric [5 + 2] cycloadditions.

In 2012, inspired by Nicolau and Chen's total synthesis of englerin A,^{4g,16} Tchabanenko and coworkers reported asymmetric [5 + 2] oxidopyrylium cycloadditions using chiral enamide dipolarophiles (Table 3.1).¹⁷ Reactions of pyrones **22a–c** with enamides **23a–d** afforded products **24a–f** as single diastereomers in moderate yields. The enamides were synthesized as single enantiomers utilizing palladium-catalyzed vinylations or copper-catalyzed cross-couplings. Reductive cleavage of the chiral auxiliary from cycloadduct **24c** proceeded in 50% yield.

¹⁶ See Section 1.5.

¹⁷ Tchabanenko, K.; Sloan, C.; Bunetel, Y.-M.; Mullen, P. *Org. Biomol. Chem.* **2012**, *10*, 4215–4219.

Table 3.1. Substrate scope of Tchababenko's intermolecular [5 + 2] cycloaddition.

Entry	Pyrone	Enamide	Product	Yield (%)
1 ^a				59
2				45
3				51
4 ^b				63
5 ^a				87
6				21

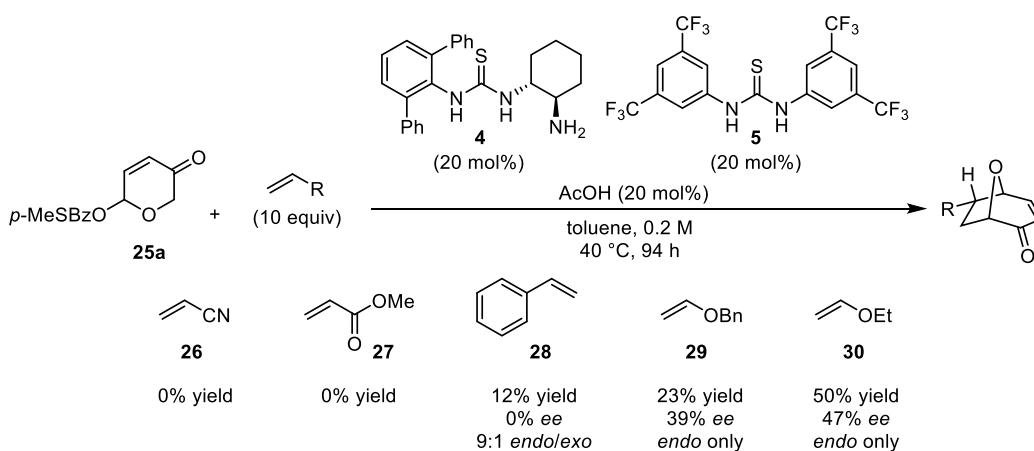
^a 24 h. ^b 50 °C.

3.2 Reaction Development

The racemic pyranone **25a** (Scheme 3.5), which is superficially analogous to pyranone substrates (**3**) identified as optimal for the intramolecular reaction,¹⁸ was examined initially as a model substrate for the study of the intermolecular cycloaddition. Treatment of **25a** with a series of terminal alkenes under the dual catalyst conditions developed in the original study revealed that the electronic properties of the 2π component exerted a strong effect on reactivity. Electron-

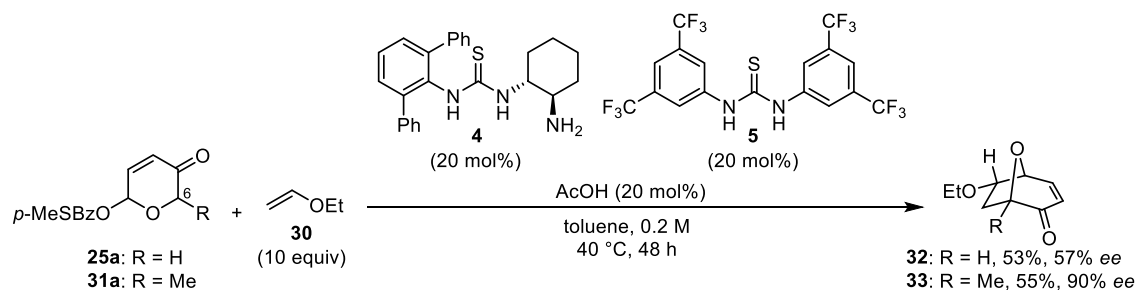
¹⁸ Refer to Chapter 2 for complete discussion.

deficient olefins such as acrylonitrile **26** and methyl acrylate **27** were completely inert; styrene **28** displayed measurable but low reactivity to afford racemic product; electron-rich olefins such as benzyl vinyl ether **29** and ethyl vinyl ether **30** underwent cycloaddition with higher conversions and encouraging enantioselectivity. The observation that a nucleophilic 2π component is required in the catalytic reaction is consistent with a mechanism involving a cationic, electron-poor aminopyrylium intermediate analogous to **6** (Scheme 3.2) rather than an ambiphilic, zwitterionic oxidopyrylium intermediate.¹¹



Scheme 3.5. Survey of 2π components.

It proved possible to affect the enantioselectivity of the intermolecular cycloaddition reaction to a remarkable degree through relatively subtle modifications to the structure of the pyrylium precursor. All substrates shown to undergo intramolecular cycloadditions with high enantioselectivity in the original study had possessed a linkage to the 2π component through the 6-position of the pyranone (e.g., **3**, Scheme 3.2). The possibility that the presence of a 6-substituent might affect enantioselectivity in the intermolecular reaction was evaluated by comparing the reaction of **25a** with that of methylated pyranone **31a** (Scheme 3.6). The dramatic improvement in enantioselectivity observed with methylated derivative **31a** suggests a critical role of that substituent in controlling the transition structure geometry in the catalytic reaction (*vide infra*).



Scheme 3.6. Effect of a 6-substituent on enantioselectivity.

Although the enantioselectivity of the transformation had been dramatically improved, the yield still required enhancement. Investigation of related chiral primary amine catalysts, other acid additives, and various solvents and concentrations failed to provide increased reactivity.¹⁹ However, electronic tuning of the leaving group on the pyranone allowed for further improvement in both enantioselectivity and yield. While the *p*-thiomethylbenzoate leaving group had been identified as optimal in the intramolecular reaction, a screen of alternative benzoate leaving groups (Table 3.2) revealed that analogs with electron-withdrawing substituents at the *para*-position (entries 7 and 12) were advantageous in terms of rate. In particular, 3,4,5-trifluorobenzoate derivative **31p** (entry 16) provided the best balance of reactivity and enantioselectivity.

In the intramolecular reaction,¹⁸ we proposed that the low solubility of the *p*-thiomethylbenzoic acid byproduct represented a crucial driving force. In contrast, both *p*-thiomethylbenzoic and 3,4,5-trifluorobenzoic acid are fully soluble under the reaction conditions employed in this study, likely due the presence of excess vinyl ether. The improved reactivity imparted by the 3,4,5-trifluorobenzoate group in **31p** relative to more electron-rich analogs may be ascribed simply to its superior properties as a leaving group. Fortuitously, further improvement in *ee* could be achieved by carrying out the reaction at ambient temperature and decreasing the amount of ethyl vinyl ether from 10 to 5 equivalents relative to pyranone (entry 17).

¹⁹ For details, see Section 3.8.

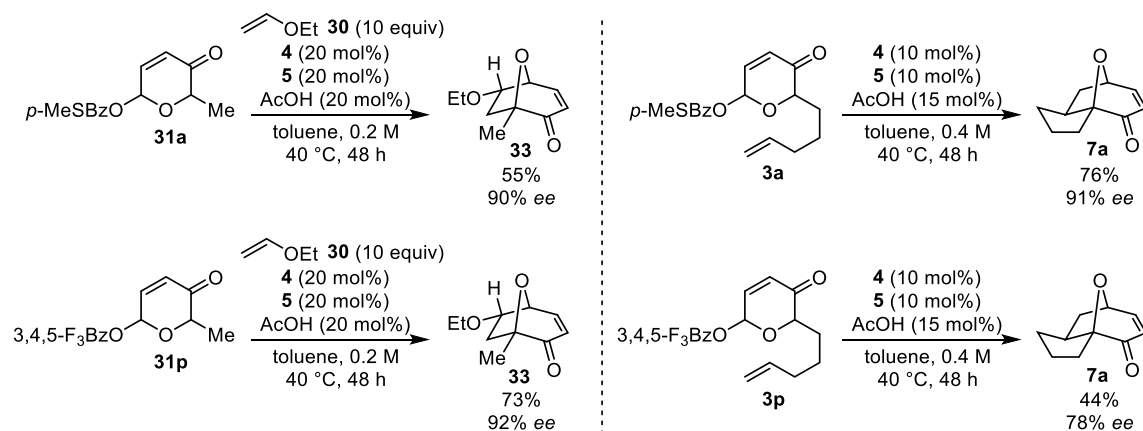
Table 3.2. Optimization of the benzoate leaving group.^a

Reaction scheme: **31a-p** + **30** (10 equiv) $\xrightarrow[\text{toluene, 0.2 M, 40 } ^\circ\text{C, 48 h}]{\text{AcOH (20 mol\%), 4 (20 mol\%), 5 (20 mol\%)}}$ **33**

Entry	X	Yield (%) ^b	ee (%) ^c	Entry	X	Yield (%) ^b	ee (%) ^c
1		55	90	10		31	70
2		15	n.d.	11		52	92
3		22	n.d.	12		65	93
4		50	n.d.	13		32	84
5		59	n.d.	14		25	n.d.
6		56	n.d.	15		62	n.d.
7		63	94	16		73	92
8		11	n.d.	17 ^d		75	96
9		7	n.d.				

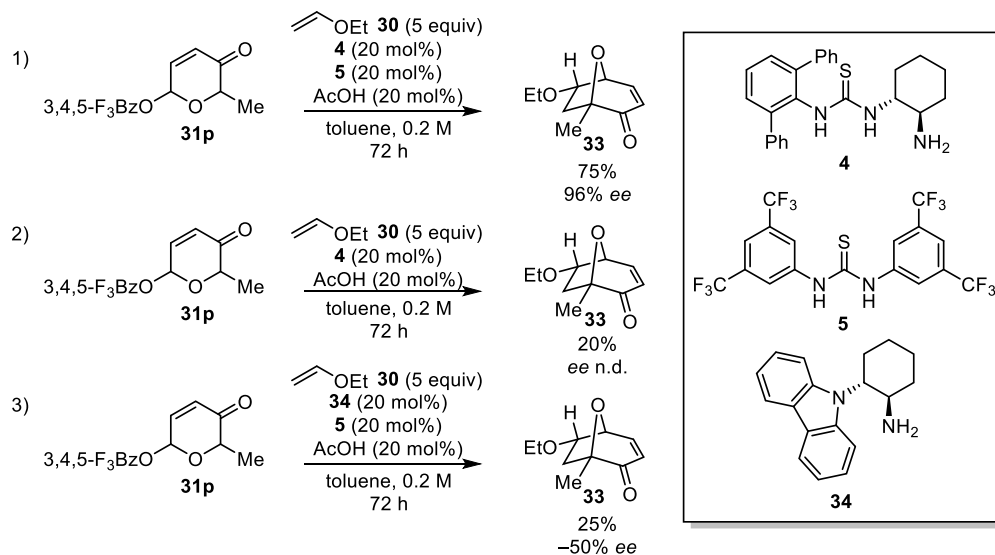
^a Reactions performed on 0.07 mmol scale. ^b Yields determined by NMR analysis using 1,3,5-trimethoxybenzene as an internal standard. ^c Enantioselectivities determined by HPLC using commercial columns with chiral stationary phases. ^d Conditions: 5 equiv **30**, 23 °C, 72 h.

The superiority of the 3,4,5-trifluorobenzoate leaving group in the intermolecular cycloaddition raised the question of how it would perform in the previously studied intramolecular reactions (Scheme 3.7). Despite the present results, 3,4,5-trifluorobenzoate proved to be an inferior nucleofuge in the intramolecular reaction. Thus, tricycle **7a** was isolated in higher yield and *ee* when derived from *p*-thiomethylbenzoate **3a** rather than 3,4,5-trifluorobenzoate **3p**.



Scheme 3.7. Comparison of optimal leaving groups in intermolecular and intramolecular reactions.

Similar to the structure–activity studies discussed in Section 2.4.1, we also confirmed that achiral catalyst **5** indeed provides significant rate enhancements over just thiourea **4** alone in this transformation (Scheme 3.8, eq. 1 and 2, compare to Table 2.5). Also, when carbazole catalyst **34** was used instead of thiourea **4** in the intramolecular reaction, we observed lower yields and a switch in the sense of enantioselectivity. The same held true for the intermolecular cycloaddition (eq. 3), with a much more precipitous drop in the absolute value of the *ee*. In the intramolecular reaction the *ee* of **7a** changed from 91% to –85% upon exchanging catalyst **34** for **4**. In the intermolecular reaction, the *ee* changed from 96% to –50%.



Scheme 3.8. Comparison of catalytic conditions from Chapter 2.

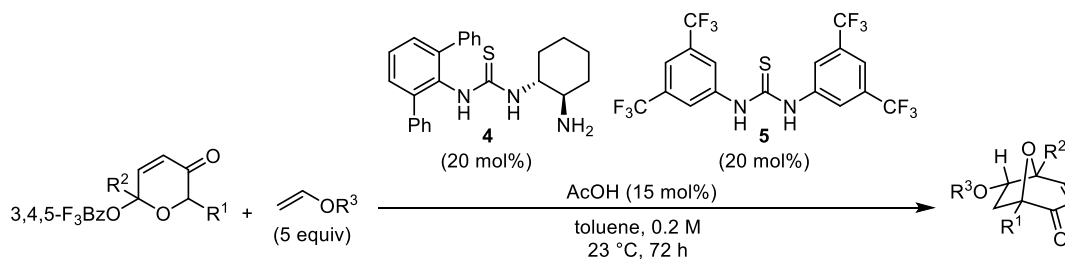
3.3 Substrate Scope

Having thus established viable parameters for effecting highly enantioselective intermolecular [5 + 2] cycloadditions of a pyrylium ion precursor, an investigation of the reaction substrate scope was carried out (Table 3.3).²⁰ Cooling to 0 °C improved the *ee* of unsubstituted product **32** to 84% (entry 2). Pyranones bearing longer alkyl chains at the 6-position also undergo cycloaddition with ethyl vinyl ether with high enantioselectivity (entry 3); however β -branching in the side chain has a deleterious effect on reactivity (entries 4 and 5). Cycloadducts bearing siloxymethylene groups could also be accessed in moderate-to-good enantioselectivity under the catalytic conditions (entries 6–8). Products of this type have found extensive synthetic applications.^{4a,d,8a,e,f,16} Benzyl vinyl ether (entry 9) and (methoxymethoxy)ethene (entry 10) were also used successfully as 2π components in the cycloaddition reaction, affording products with readily cleavable ethers. However, styrene derivatives remain poorly reactive in reactions with

²⁰ For certain indicated substrates, catalyst loading could be reduced to 15 mol% **4** and 15 mol% **5** without detrimental effect on yield or enantioselectivity. In all other cases, this reduction in catalyst resulted in significantly diminished yields.

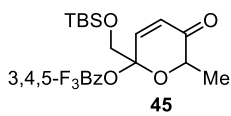
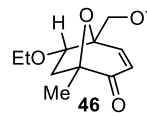
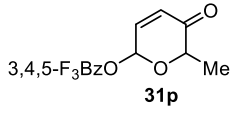
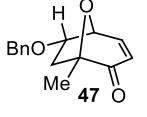
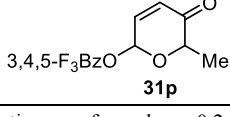
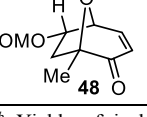
31p, with the resultant cycloadducts formed in very low *ee*'s. Enamines and polysubstituted vinyl ethers also proved to be poor substrates, the former undergoing hydrolysis under the reaction conditions and the latter exhibiting very low reactivity.¹⁹

Table 3.3. Substrate scope of intermolecular [5 + 2] cycloaddition.^a



Entry	Substrate	R ³	Product	Yield (%) ^b	ee (%) ^c
1 ^{d,g}	 31p	Et	 33	69	96
2 ^e	 25p	Et	 32	51	84
3	 35	Et	 36	59	90
4 ^d	 37	Et	 38	22	88
5	 39	Et	 40	26	67
6	 41	Et	 42	64	86
7 ^{d,e}	 43	Et	 44	95	64

Table 3.3 (continued).

Entry	Substrate	R ³	Product	Yield (%) ^b	ee (%) ^c
8	 45	Et	 46	75	89
9 ^d	 31p	Bn	 47	88	89
10 ^f	 31p	MOM	 48	54	91

^a Reactions performed on 0.2 mmol scale. ^b Yields of isolated products after column chromatography. ^c Enantioselectivities determined by HPLC using commercial columns with chiral stationary phases. ^d 15 mol% **4** + **5**. ^e 96 h at 0 °C. ^f 10 equiv vinyl ether. ^g The absolute stereochemical configuration of a derivative of **33** was determined by X-ray crystallography, and those of all other products were assigned by analogy.

3.4 An Asymmetric Total Synthesis of (–)-Descurainin

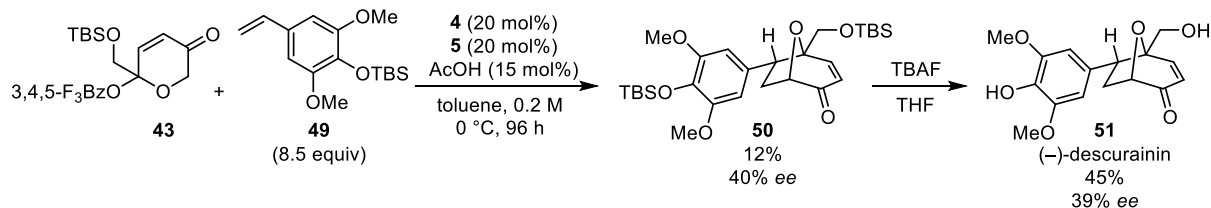
An example of the challenges associated with styrene 2π components is demonstrated by a catalytic asymmetric total synthesis of (–)-descurainin. The natural product was initially isolated from the seeds of *Descurainia sophia*,^{2h} which are used in traditional Chinese medicines. A total synthesis of racemic descurainin utilizing a [5 + 2] cycloaddition was reported by the Snider group in 2006.^{16,21} More recently, Hashimoto and coworkers published a 17-step asymmetric total synthesis using a catalytic enantioselective [3 + 2] cycloaddition in the key step towards (+)-descurainin.²²

When cycloaddition of pyranone **43** and styrene **49**²¹ was attempted under the conditions in Table 3.3, cycloadduct **50** was isolated in 19% yield and 16% *ee*. Cooling the reaction mixture to 0 °C resulted in lower quantities of recovered product, but an increase in enantioselectivity to 40%. Removal of the silyl protecting groups afforded (–)-descurainin in 39% *ee* and 5% yield over

²¹ Snider, B. B.; Grabowski, J. F. *Tetrahedron* **2006**, *62*, 5171–5177.

²² Shimada, N.; Hanari, T.; Kurosaki, Y.; Anada, M.; Nambu, H.; Hashimoto, S. *Tetrahedron Lett.* **2010**, *51*, 6572–6575.

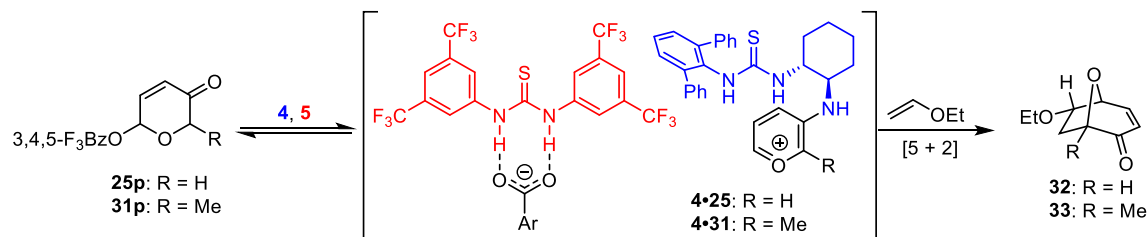
two steps (seven linear steps from commercial materials).



Scheme 3.9. Asymmetric total synthesis of (-)-descurainin.

3.5 Mechanistic Studies

We sought to elucidate the basis for the significant difference in enantioselectivity between the reactions of pyranones **25** and **31** (Scheme 3.6) as a possible path toward gaining insight into the origin of stereoinduction in these reactions. By analogy to the intramolecular reaction, which is thought to proceed through an aminopyrylium intermediate, the formation of the adduct **4•31** (Scheme 3.10) was confirmed by mass spectrometric analysis of a reaction mixture sampled prior to addition of the vinyl ether component.



Scheme 3.10. Formation of the intermediate aminopyrylium ion pair.

The lowest energy structures of the two aminopyrylium ions **4•25** and **4•31** were located computationally (Figure 3.2).²³ Rotation about the C(sp²)-N bond was scanned for each, allowing the models to relax to a minimum energy at intervals of 10 degrees. Thus, graphs of calculated electronic energies versus C–N dihedral angle were generated (Figures 3.3 and 3.4). These graphs

²³ B3LYP/6-31G(d) has been established as an appropriate level of theory for studying oxidopyrylium [5 + 2] cycloadditions. See: (a) López, F.; Castedo, L.; Mascareñas, J. L. *J. Org. Chem.* **2003**, *68*, 9780–9786. (b) Wang, S. C.; Tantillo, D. J. *J. Org. Chem.* **2008**, *73*, 1516–1523.

reveal several key features pertaining to this bond rotation. Notably, for both pyrylium ions, the absolute barrier for rotation is approximately equal (14.72 kcal mol⁻¹ for **4•25** and 15.24 kcal mol⁻¹ for **4•31**). The difference between the two local energy minima for each pyrylium however (1.21 kcal mol⁻¹ for **4•25** and 6.39 kcal mol⁻¹ for **4•31**), represents a much more substantial discrepancy.

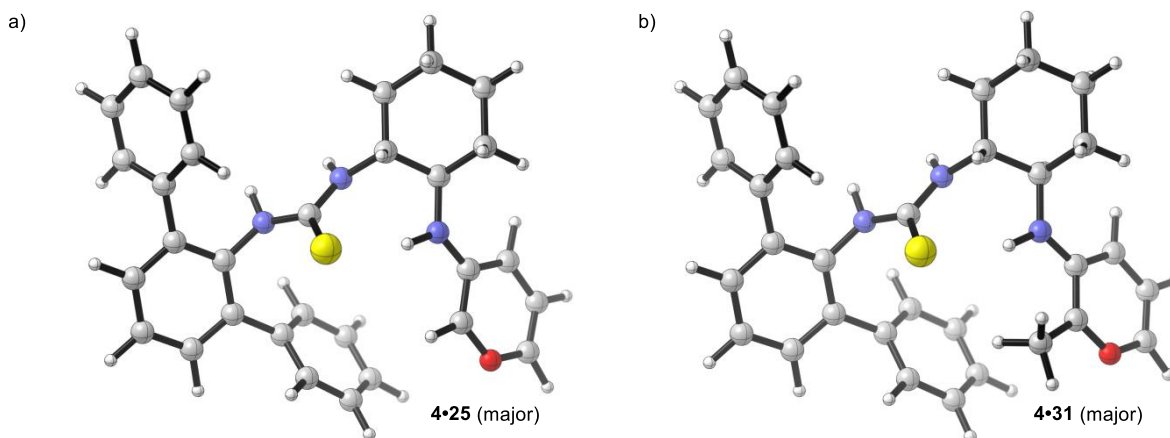


Figure 3.2. Lowest energy structures leading to the major enantiomer of cycloadduct calculated at the B3LYP/6-31G(d) level of theory for proposed aminopyrylium intermediates (a) **4•25** and (b) **4•31**.

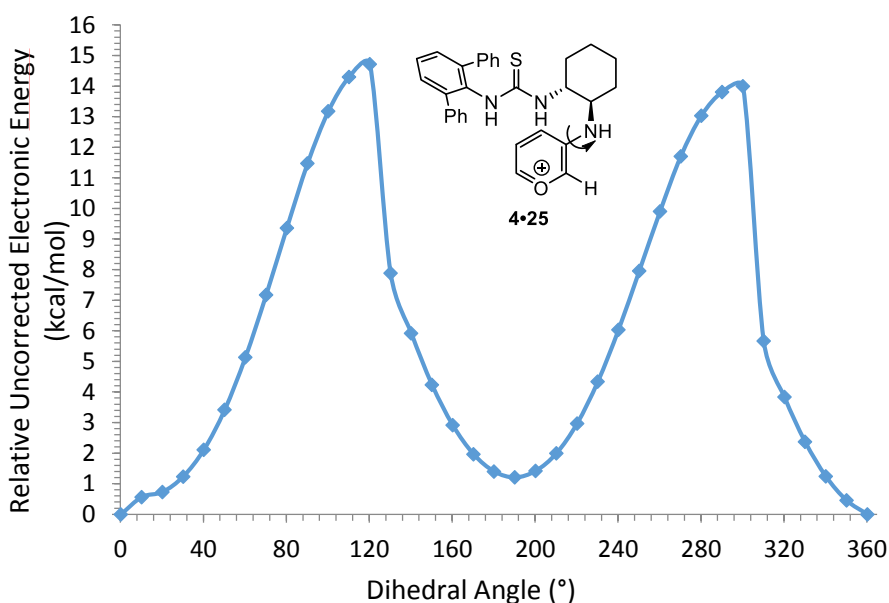


Figure 3.3. Dihedral angle versus relative uncorrected electronic energy graph for C(sp²)-N rotation of **4•25**.

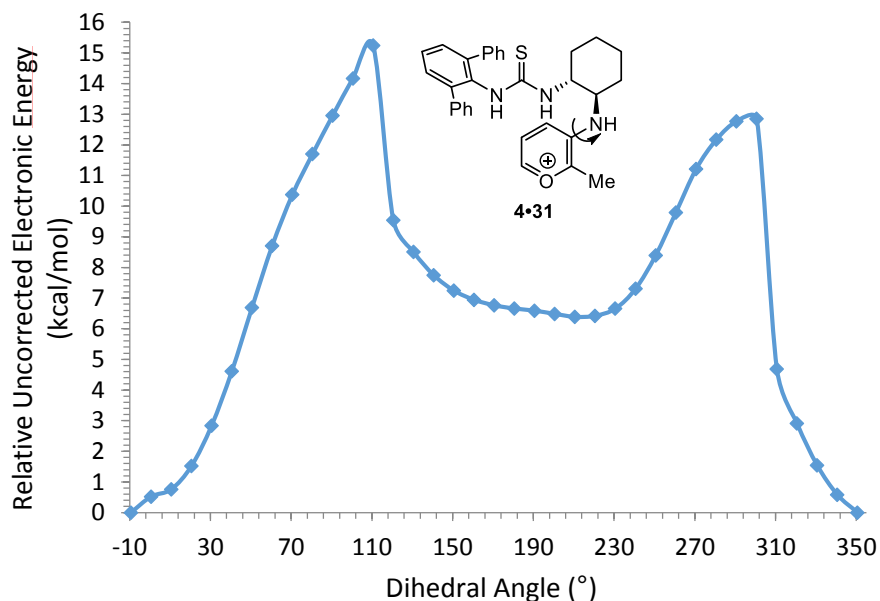


Figure 3.4. Dihedral angle versus relative uncorrected electronic energy graph for C(sp²)-N rotation of **4•31**.

The disfavored structures represented by these higher energy local minima are those wherein the pyrylium face to which cycloaddition would lead to the minor enantiomer of product is exposed (Figure 3.5). In the minor structure of **4•31**, a steric clash between the additional methyl substituent and the cyclohexyl backbone has caused the pyrylium portion of the adduct to swing under the thiourea and in turn displace the diphenylaniline moiety. Without that methyl substituent (**4•25**), there is no such steric clash and therefore a much less substantial destabilization of the adduct leading to the minor enantiomer. This accounts for a much smaller energy difference between minimum pyrylium conformations, and consequently lower *ee* for cycloadduct **32** than for **33**.

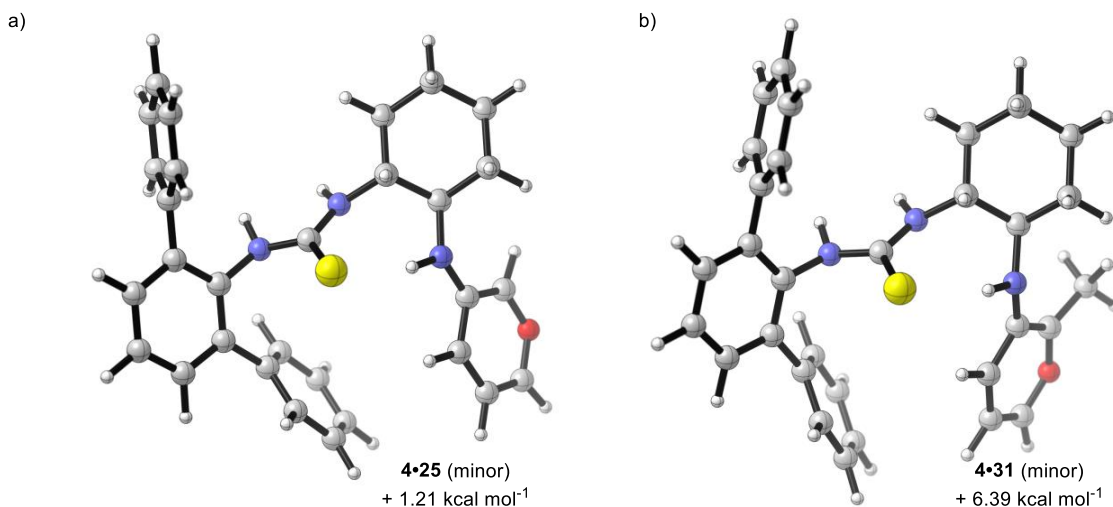


Figure 3.5. Local minimum energy structures leading to the minor enantiomer of cycloadduct calculated at the B3LYP/6-31G(d) level of theory for proposed aminopyrylium intermediates (a) **4•25** and (b) **4•31**.

Of course, these calculations apply to the conformations of the aminopyrylium ground states prior to the cycloaddition step, rather than to the actual transition structures for cycloaddition. They are further simplified in that they omit the thiourea **5**•benzoate counteranion. Nonetheless, we propose that the pronounced energy difference calculated for the conformations of **4•31** is expected to translate to the relevant cycloaddition transition structures that lead to the two enantiomers of **33**.

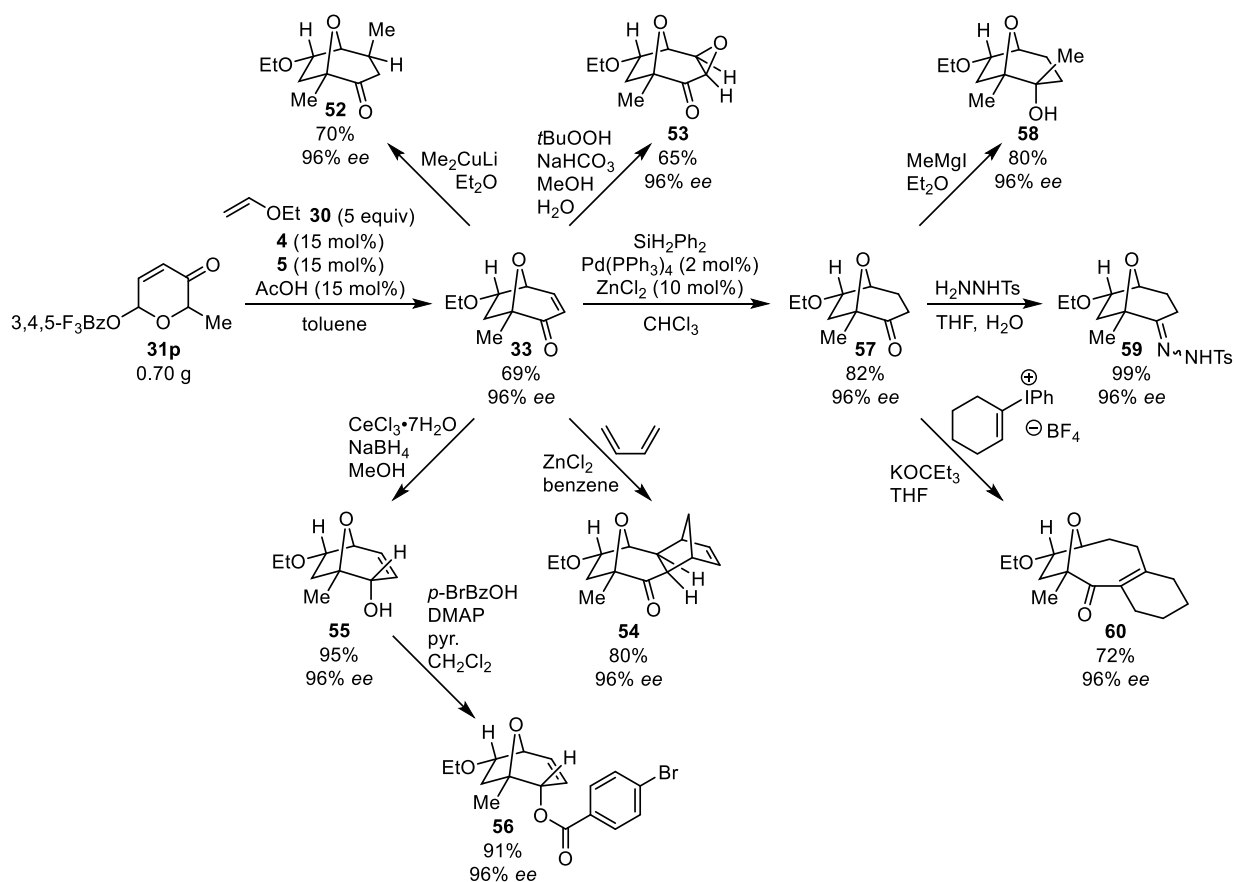
3.6 Derivatization of Cycloadducts

The 8-oxabicyclooctenone cycloadducts possess several functional group handles for potential elaboration (Scheme 3.11). The synthesis of **33** was carried out successfully on a 0.70 g scale under the conditions described in Table 3.3 above to give cycloadduct in 69% yield and 96% *ee*. Products resulting from conjugate addition (**52**), epoxidation (**53**),²⁴ Diels–Alder reaction (**54**),²⁵ or Luche reduction (**55**) and subsequent acylation (**56**) were all generated as single

²⁴ Marshall, K. A.; Mapp, A. K.; Heathcock, C. H. *J. Org. Chem.* **1996**, *61*, 9135–9145.

²⁵ Nair, V.; Anilkumar, G.; Sujatha, T. S.; Nair, J. S. *Synth. Commun.* **1998**, *28*, 2549–2557.

diastereomers within detection limits. The cycloadduct **33** could also be subjected to hydrogenation to another key intermediate, saturated ketone **57**.²⁶ This heterocycle underwent Grignard addition stereoselectively to afford tertiary alcohol **58**. Tosylhydrazone **59**, which is primed to undergo Shapiro or Bamford-Stevens reactions, was also readily synthesized from intermediate **57**. Finally, σ -bond insertion of cyclohexyne yielded an unusual 9,6-fused ring system (**60**) in a single step.²⁷



Scheme 3.11. Derivatization of cycloadduct **33**.

Tosylhydrazone **59** proved to be a crystalline solid. X-ray diffraction of a single crystal (Figure 3.6) allowed for the determination of the absolute stereochemical configuration of

²⁶ Archer, D. A.; Bromidge, S. M.; Sannes, P. G. *J. Chem. Soc., Perkin Trans. 1* **1988**, 3223–3228.

²⁷ Gampe, C. M.; Boulos, S.; Carreira, E. M. *Angew. Chem. Int. Ed.* **2010**, *49*, 4092–4095.

cycloadduct **33**. This configuration corresponds to that observed in the intramolecular reactions described in Chapter 2, as well as the known structure of (–)-descurainin, which was synthesized through this methodology (Section 3.4). The configuration of all other cycloadducts was assigned by comparison.

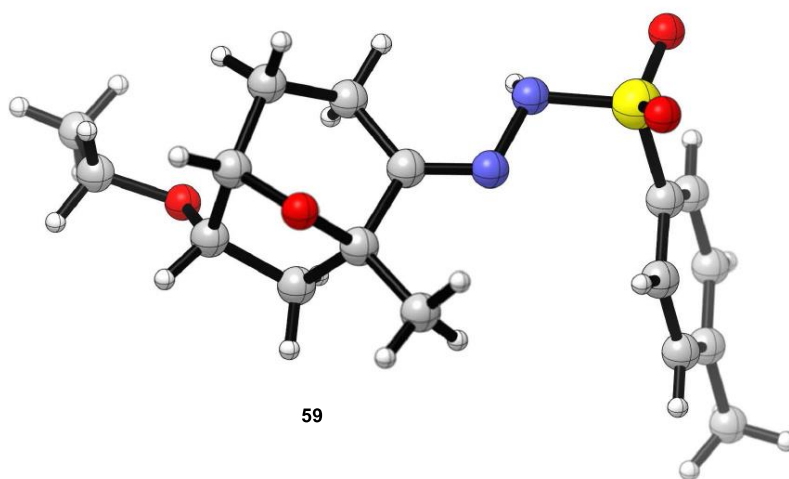
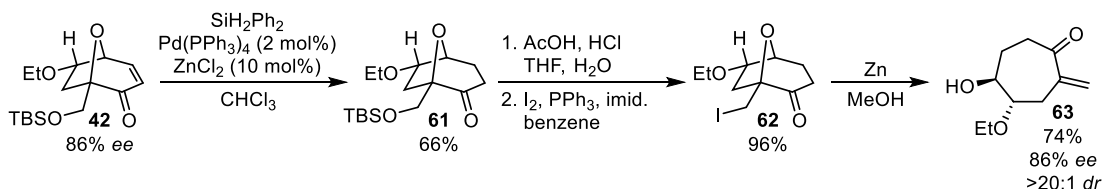


Figure 3.6. X-ray crystal structure of **59**.

The oxygen bridge of the 8-oxabicyclo[3.2.1]oct-3-en-2-one framework can also be cleaved reductively. Cycloadduct **42** was hydrogenated to ketone **61**,²⁶ then the silyl ether was replaced by an iodide in two steps (Scheme 3.12). Opening of the cyclic ether in iodide **62** resulted in the formation of an interesting 7-membered product (**63**) possessing an exocyclic enone.²⁸ As in all of the previous examples, the product was generated as a single diastereomer and without compromise of the optical purity of the initial cycloadduct.



Scheme 3.12. Stereocontrolled preparation of cycloheptanone **63**.

²⁸ Ohmori, N. *J. Chem. Soc., Perkin Trans. 1* **2002**, 755–767.

3.7 Conclusions and Outlook

The catalytic, asymmetric, intermolecular [5 + 2] pyrylium cycloadditions developed in this study provide multifunctional chiral building blocks that are immediate precursors to a wide range of compound classes accessible through simple manipulations. In addition to the cycloaddition itself, we have demonstrated many of these complexity-generating transformations, which operate in good to excellent yields, high diastereoselectivities, and without erosion of *ee*.

The presence of a substituent at the 6-position of the substrate pyranone ring exerts a significant impact on the overall enantioselectivity of the cycloaddition. This effect has been probed computationally in order to better understand the overall mechanistic consequences of this phenomenon. The additional substituent destabilizes the enamine conformation that leads to the minor diastereomer of cycloadduct, but does not exert such an effect on the conformation that leads to the major enantiomer.

To date, the dual catalysis principle described in this and the preceding chapter has only been applied to [5 + 2] cycloadditions. Ongoing research efforts seek to expand the utility of this mechanistic system to other transformations.

3.8 Experimental Details

3.8.1 General Information

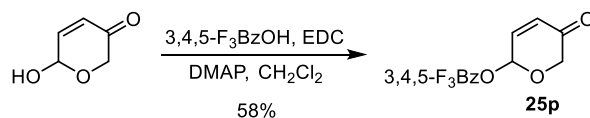
Cycloaddition reactions were performed in oven-dried 1.0-dram vials; all other reactions were performed in oven- or flame-dried round-bottom flasks unless otherwise noted. The vials were capped and flasks were fitted with rubber septa. Reactions were conducted under air unless noted. Stainless steel syringes were used to transfer air- and moisture-sensitive liquids. Flash chromatography was performed using silica gel 60 (230–400 mesh) from EM Science. Commercial reagents were purchased from Sigma-Aldrich, Alfa Aesar, Oakwood Chemical, or TCI, and used as received with the following exceptions: dichloromethane, chloroform, toluene, acetonitrile, tetrahydrofuran, *N,N*-dimethylformamide, and diethyl

ether were dried by passing through columns of activated alumina. Triethylamine and pyridine were distilled from CaH₂ at 760 torr. Furfural was distilled at 20 torr. Ethyl vinyl ether was distilled at atmospheric pressure. *n*-Butyllithium was titrated using *N*-benzylbenzamide as an indicator.

Proton nuclear magnetic resonance (¹H NMR) spectra and carbon nuclear magnetic resonance (¹³C NMR) spectra were recorded on Varian-Mercury-400 (400 MHz) or Inova-500 (500 MHz) spectrometers. Chemical shifts for protons are reported in parts per million downfield from tetramethylsilane and are referenced to residual protium in the NMR solvent (CHCl₃ = δ 7.27, (CD₃)₂SO = δ 2.50). Chemical shifts for carbon are reported in parts per million downfield from tetramethylsilane and are referenced to the carbon resonances of the solvent (CDCl₃ = δ 77.0). Data are represented as follows: chemical shift (multiplicity (br. = broad, s = singlet, d = doublet, t = triplet, q = quartet, quin = quintet, m = multiplet), coupling constants in Hertz (Hz), integration).

Infrared (IR) spectra were obtained using a Bruker Optics Tensor 27 FTIR spectrometer. Optical rotations were measured using a Jasco DIP 370 digital polarimeter. The mass spectral data were obtained on a Bruker micrOTOF-Q II time-of-flight LC/MS spectrometer (ESI-TOF). Chiral HPLC analysis was performed using an Agilent analytical chromatograph with commercial ChiralPak or ChiralCel columns. Chiral GC analysis was performed using an Agilent analytical chromatograph with a commercial chiral column. Chiral SFC analysis was performed on a Berger analytical chromatograph with a commercial ChiralPak column.

3.8.2 Synthesis and Characterization of Substrates

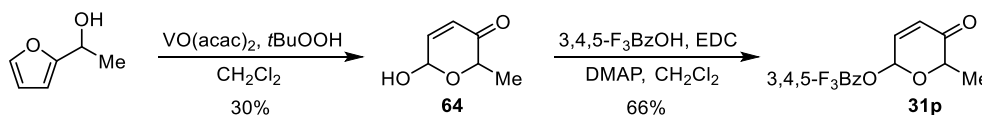


Scheme 3.13. Synthesis of substrate **25p**.

5-oxo-5,6-dihydro-2H-pyran-2-yl 3,4,5-trifluorobenzoate (**25p**):

6-Hydroxy-2H-pyran-3(6H)-one²⁹ (1.003 g, 8.79 mmol) was dissolved in CH₂Cl₂ in a round-bottom flask (44 mL, 0.20 M) and the flask was cooled to 0 °C. To this solution was added sequentially 3,4,5-trifluorobenzoic acid (2.312 g, 13.1 mmol, 1.5 equiv), EDC (2.531 g, 13.2 mmol, 1.5 equiv), and DMAP (1.606 g, 13.1 mmol, 1.5 equiv). The reaction mixture was stirred at 0 °C for 90 min. The reaction mixture was then diluted with EtOAc (120 mL) and quenched with 1N HCl (60 mL). The layers were separated and the organic layer was washed successively with 1N HCl (60 mL), sat. aq. NaHCO₃ (60 mL), and brine (60 mL). The organic layer was dried over Na₂SO₄, filtered, concentrated and purified by column chromatography (silica gel, 95:5 to 3:1 hexanes/EtOAc) to afford **25p** as a white solid (1.385 g, 58%).

R_f = 0.61 (silica gel, 2:1 hexanes/EtOAc); **IR** (film) ν_{\max} 1739, 1710, 1530, 1442, 1363, 1214, 1174, 1049, 943, 913, 714 cm⁻¹; **¹H NMR** (500 MHz, CDCl₃) δ 7.72 (t, *J* = 6.8 Hz, 2H), 7.05 – 7.02 (m, 1H), 6.73 (d, *J* = 3.91 Hz, 1H), 6.39 – 6.37 (m, 1H), 4.58 (d, *J* = 17.1 Hz, 1H), 4.32 (d, *J* = 17.1 Hz, 1H); **¹³C NMR** (126 MHz, CDCl₃) δ 193.0, 141.5, 129.6, 111.9, 111.9, 114.8, 114.7, 88.3, 67.8; **MS** (ESI-TOF) calcd. for C₁₂H₇F₃O₄ [M + H]⁺ 273.0369, found 273.0369.



Scheme 3.14. Synthesis of substrate **31p**.

6-hydroxy-2-methyl-2H-pyran-3(6H)-one (**64**):

1-(Furan-2-yl)ethanol³⁰ (4.487 g, 40.0 mmol) was dissolved in CH₂Cl₂ (133 mL, 0.30 M), and the resulting solution was cooled to 0 °C. To this solution was added solid vanadyl acetylacetonate (1.058 g, 3.99 mmol, 0.1 equiv), then *tert*-butyl hydroperoxide (10.9 mL of a 5.5 M solution in dodecane, 60.0 mmol, 1.5 equiv) by syringe. The reaction was stirred at 0 °C for 2 h, before it was quenched with 1M Na₂S₂O₃ (300 mL) and

²⁹ 6-hydroxy-2H-pyran-3(6H)-one synthesized according to: Brescia, M.-R.; Shimshock, Y. C.; DeShong, P. *J. Org. Chem.* **1997**, *62*, 1257–1263.

³⁰ 1-(furan-2-yl)ethanol synthesized according to: Jones, R. A.; Krische, M. *J. Org. Lett.* **2009**, *11*, 1849–1851.

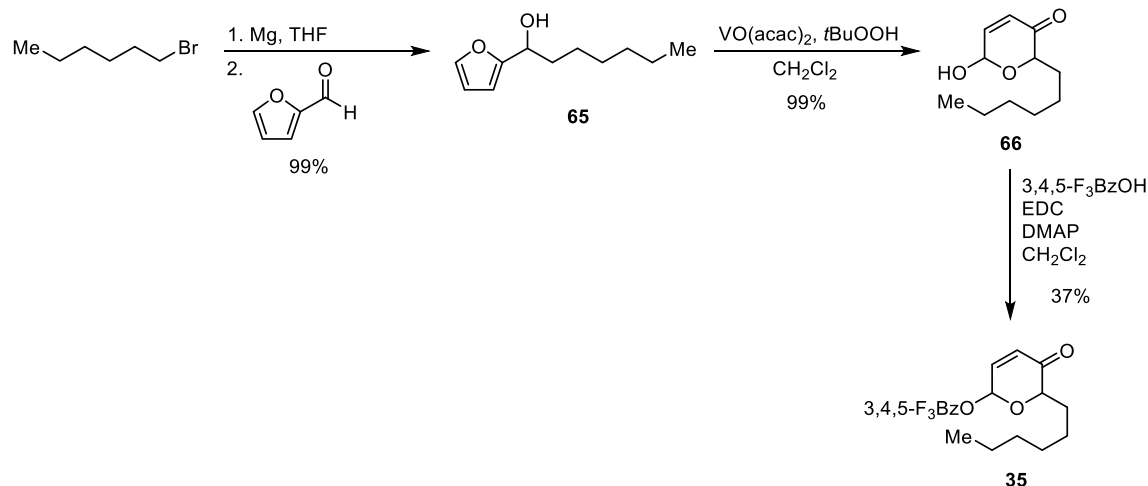
stirred for a further 30 min. The aqueous layer was extracted with CH₂Cl₂ (2 x 300 mL) and the pooled organic layers were dried over Na₂SO₄, filtered, and concentrated. The crude product was purified by flash chromatography (silica gel, 95:5 to 4:1 hexanes/EtOAc) to afford **64** as a colorless oil in a 2.3:1 mixture of diastereomers which solidified upon storage at -30 °C (1.544 g, 30%).

R_f = 0.38 (silica gel, 2:1 hexanes/EtOAc); **IR** (film) ν_{\max} 3399 (br), 1700, 1375, 1236, 1102, 1074, 1030 cm⁻¹; **¹H NMR** (500 MHz, CDCl₃) δ 6.87 (minor diast., d, J = 10.3 Hz, 0.30H), 6.82 (major diast., dd, J = 3.4, 10.3 Hz, 0.70H), 6.03 (minor diast., d, J = 10.3 Hz, 0.30H), 5.97 (major diast., d, J = 10.3 Hz, 0.70H), 5.57 (minor diast., d, J = 5.4 Hz, 0.30H), 5.50 (major diast., br. s, 0.70H), 5.32 (minor diast., d, J = 6.3 Hz, 0.30H), 5.00 (major diast., br. s, 0.70H), 4.60 (major diast., q, J = 6.8 Hz, 0.70H), 4.11 (minor diast., q, J = 6.8 Hz, 0.30H), 1.31 (minor diast., d, J = 6.8 Hz, 0.9H), 1.25 (major diast., d, J = 6.8 Hz, 2.1H); **¹³C NMR** (126 MHz, CDCl₃) δ 197.4, 196.8, 148.9, 145.2, 128.0, 126.5, 90.7, 87.2, 74.8, 70.0, 15.8, 15.0; **MS** (ESI-TOF) calcd. for C₆H₈O₃ [M + Na]⁺ 151.0366, found 151.0341.

6-methyl-5-oxo-5,6-dihydro-2H-pyran-2-yl 3,4,5-trifluorobenzoate (31p):

Reaction of **64** (607 mg, 4.74 mmol), 3,4,5-trifluorobenzoic acid (1.237 g, 7.02 mmol, 1.5 equiv), EDC (1.342 g, 7.00 mmol, 1.5 equiv), and DMAP (856 mg, 7.00 mmol, 1.5 equiv) in CH₂Cl₂ (23 mL, 0.21 M) according to **25p** above afforded **31p** as a white solid after column chromatography (silica gel, 9:1 to 2:1 hexanes/EtOAc) in a 5:1 mixture of diastereomers (894 mg, 66%).

R_f = 0.55, 0.65 (silica gel, 2:1 hexanes/Et₂O); **IR** (film) ν_{\max} 1739, 1704, 1626, 1601, 1529, 1443, 1360, 1212, 1049, 911, 767, 733 cm⁻¹; **¹H NMR** (500 MHz, CDCl₃) δ 7.75 - 7.70 (m, 2H), 6.99 (dd, J = 3.4, 10.3 Hz, 1H), 6.80 (minor diast., dd, J = 1.2, 2.7 Hz, 0.17H), 6.73 - 6.71 (major diast., 0.83H), 6.34 - 6.30 (m, 1H), 4.71 - 4.66 (major diast., m, 0.83H), 4.50 - 4.46 (minor diast., m, 0.17H), 1.57 - 1.54 (minor diast., m, 0.51H), 1.47 - 1.43 (major diast., m, 2.49H); **¹³C NMR** (126 MHz, CDCl₃) δ 195.3, 140.7, 128.9, 114.6, 114.6, 114.5, 114.5, 89.0, 88.5, 75.9, 72.7, 18.9, 15.4; **MS** (ESI-TOF) calcd. for C₁₃H₉F₃O₄ [M + Na]⁺ 309.0345, found 309.0301.



Scheme 3.15. Synthesis of substrate **35**.

1-(furan-2-yl)heptan-1-ol (65):

Magnesium turnings (3.395 g, 140 mmol, 7.7 equiv) were rigorously flame-dried under vacuum in a round-bottom flask attached with a condenser. Once the magnesium had cooled, it was exposed to an atmosphere of N₂ and suspended in THF (70 mL, 0.4 M). To this suspension was added sequentially 1,2-dibromoethane activator (0.05 mL, 0.58 mmol) then 1-bromohexane (3.9 mL, 27.9 mmol, 1.5 equiv). This mixture was stirred and gently heated (approx. 40 °C) until an exotherm was observed. The suspension was then stirred for a further 45 min at 23 °C, after which the dark suspension was cannulated into a solution of furfural (1.50 mL, 18.1 mmol) in THF (35 mL 0.52 M), pre-cooled to –20 °C. This reaction mixture was stirred under an atmosphere of N₂ at –20 °C for 40 min. The resulting solution was then quenched with sat. aq. NH₄Cl (40 mL), and the aqueous layer was extracted with EtOAc (3 x 20 mL). The combined organic layers were washed with brine (30 mL). The organic phase was dried over Na₂SO₄, filtered, and concentrated. The crude product was purified by flash chromatography (silica gel, 9:1 to 2:1 hexanes/EtOAc) to afford **65** as a yellow oil (3.277 g, 99%).

R_f = 0.70 (silica gel, 2:1 hexanes/EtOAc); **IR** (film) ν_{max} 3349 (br), 2929, 2858, 1458, 1150, 1009, 735 cm⁻¹; **¹H NMR** (500 MHz, CDCl₃) δ 7.36 (dd, *J* = 0.9, 1.8 Hz, 1H), 6.32 (dd, *J* = 1.8, 3.2 Hz, 1H), 6.21 (d, *J* = 3.2 Hz, 1H), 4.64 (dd, *J* = 6.9, 11.5 Hz, 1H), 2.28 (d, *J* = 4.6 Hz, 1H), 1.87 – 1.79 (m, 2H), 1.45 – 1.24 (m, 8H), 0.91 – 0.87 (m, 3H); **¹³C NMR** (126 MHz, CDCl₃) δ 157.0, 141.7, 110.0, 105.6, 67.7, 35.5, 31.7,

29.0, 25.4, 22.5, 14.0; **MS** (ESI-TOF) calcd. for C₁₁H₁₈O₂ [M + Na]⁺ 205.1199, found 205.1184.

2-hexyl-6-hydroxy-2H-pyran-3(6H)-one (66):

Reaction of **65** (2.007 g, 11.0 mmol), vanadyl acetylacetonate (298 mg, 1.13 mmol, 0.1 equiv), and *tert*-butyl hydroperoxide (3.0 mL of a 5.5 M solution in dodecane, 16.5 mmol, 1.5 equiv) in CH₂Cl₂ (37 mL, 0.3 M) according to **64** above afforded **66** as a white powder after column chromatography (silica gel, 9:1 to 5:1 hexanes/EtOAc) in a 2.1:1 mixture of diastereomers (2.161 g, 99%).

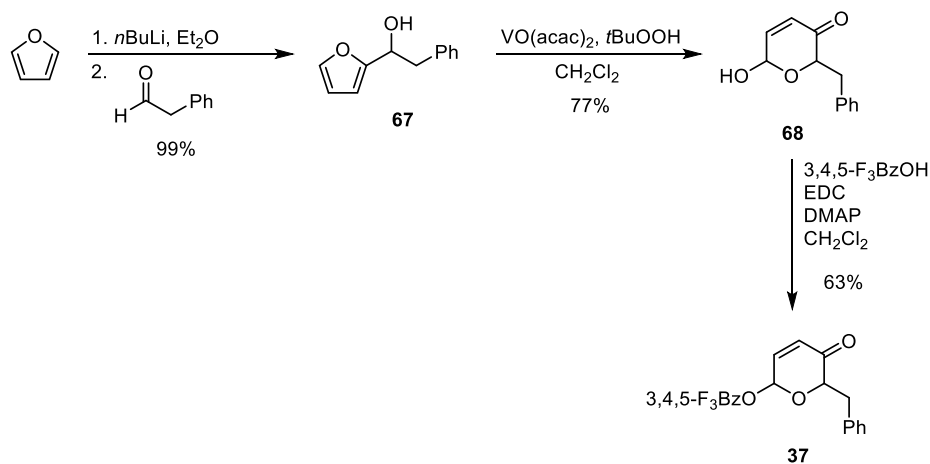
R_f = 0.24 (silica gel, 4:1 hexanes/EtOAc); **IR** (film) ν_{\max} 3400 (br), 2929, 2955, 2927, 2858, 1686, 1090, 1033, 735 cm⁻¹; **¹H NMR** (500 MHz, CDCl₃) δ 6.92 (minor diast., dd, *J* = 1.5, 10.3 Hz, 0.32H), 6.89 (major diast., dd, *J* = 3.4, 10.3 Hz, 0.68H), 6.15 – 6.12 (minor diast., m, 0.32H), 6.09 (major diast., dd, *J* = 2.4, 10.3 Hz, 0.68H), 5.64 (br. s, 1H), 4.55 (major diast., dt, *J* = 1.8, 4.2 Hz, 0.68H), 4.07 – 4.06 (minor diast., m, 0.32H), 3.66 (br. s, 1H), 1.96 – 1.86 (m, 1H), 1.79 – 1.65 (m, 1H), 1.45 – 1.40 (m, 2H), 1.35 – 1.21 (m, 6H), 0.89 – 0.84 (m, 3H); **¹³C NMR** (126 MHz, CDCl₃) δ 148.2, 144.8, 128.9, 127.8, 91.1, 87.8, 79.2, 74.5, 31.9, 30.8, 29.9, 29.3, 29.3, 25.3, 25.1, 22.8, 14.3; **MS** (ESI-TOF) calcd. for C₁₁H₁₈O₃ [M + Na]⁺ 221.1148, found 221.1207.

6-hexyl-5-oxo-5,6-dihydro-2H-pyran-2-yl 3,4,5-trifluorobenzoate (35):

Reaction of **66** (2.500 g, 12.6 mmol), 3,4,5-trifluorobenzoic acid (3.356 g, 19.1 mmol, 1.5 equiv), EDC (3.6262 g, 18.9 mmol, 1.5 equiv), and DMAP (2.299 g, 18.8 mmol, 1.5 equiv) in CH₂Cl₂ (63 mL, 0.20 M) according to **25p** above afforded **35** as a colorless oil after column chromatography (silica gel, 9:1 to 2:1 hexanes/EtOAc) in a >25:1 mixture of diastereomers (1.942 g, 37%).

R_f = 0.63, 0.69 (silica gel, 2:1 hexanes/Et₂O); **IR** (film) ν_{\max} 2931, 2860, 1739, 1700, 1626, 1530, 1442, 1361, 1213, 1186, 1049, 914, 765, 736 cm⁻¹; **¹H NMR** (500 MHz, CDCl₃) δ 7.68 (t, *J* = 6.8, 2H), 6.98 (dd, *J* = 3.9, 10.3 Hz, 1H), 6.72 (d, *J* = 3.4 Hz, 1H), 6.28 (d, *J* = 10.3 Hz, 1H), 4.53 (dd, *J* = 3.7, 7.6 Hz, 1H), 1.97 – 1.90 (m, 1H), 1.77 – 1.70 (m, 1H), 1.38 (quin, *J* = 7.2 Hz, 2H), 1.26 – 1.17 (m, 6H), 0.83 – 0.80 (m, 3H); **¹³C NMR** (126 MHz, CDCl₃) δ 125.2, 162.3, 152.0, 150.0, 140.6, 129.2, 125.1, 114.5, 114.3, 85.6, 76.1, 31.5, 29.5, 28.9, 24.4, 22.5, 13.9; **MS** (ESI-TOF) calcd. for C₁₈H₁₉F₃O₄ [M + K – H₂O]⁺ 433.0884,

found 433.0882.



Scheme 3.16. Synthesis of substrate 37.

1-(furan-2-yl)-2-phenylethanol (67):

Freshly distilled furan (2.7 mL, 36.9 mmol, 1.9 equiv) was dissolved in Et₂O (20 mL, 1.84 M relative to furan) under an atmosphere of N₂ and the resulting mixture was cooled to -20 °C. *n*-BuLi (11.0 mL of a 1.73 M solution in hexanes, 19.0 mmol) was introduced dropwise via syringe. After addition, the reaction mixture was allowed to warm to 0 °C and stirred at that temperature for 4 h. The reaction was then re-cooled to -20 °C and phenylacetaldehyde (4.3 mL, 33.1 mmol, 1.7 equiv) was added dropwise by syringe. The solution was stirred at -20 °C for 3 h before the careful addition of sat. aq. NH₄Cl (8 mL). The aqueous layer was extracted with Et₂O (2 x 10 mL). The combined organic layers were then dried over NaSO₄, filtered, and concentrated. Purification by column chromatography (silica gel, 9:1 to 2:1 hexanes/EtOAc) afforded **67** as a yellow oil (3.544 g, 99%).

Spectroscopic data agree with previously reported data.³¹

2-benzyl-6-hydroxy-2H-pyran-3(6H)-one (68):

Reaction of **67** (2.517 g, 13.4 mmol), vanadyl acetylacetonate (356 mg, 1.34 mmol, 0.1 equiv), and *tert*-butyl hydroperoxide (3.7 mL of a 5.5 M solution in dodecane, 20.4 mmol, 1.5 equiv) in CH₂Cl₂ (45 mL, 0.3 M) according to **64** above afforded **68** as a yellow oil after column chromatography (silica gel, 9:1 to

³¹ Zhou, C.; Wang, Z. *Synthesis* **2005**, 1649–1655.

5:1 hexanes/EtOAc) in a 2.7:1 mixture of diastereomers which solidified upon storage at $-30\text{ }^{\circ}\text{C}$ (2.090 g, 77%).

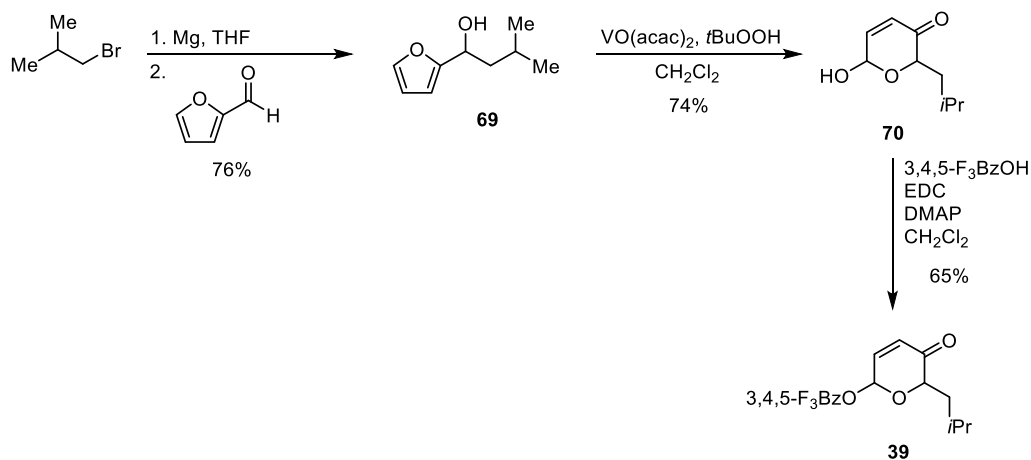
$R_f = 0.15$ (silica gel, 4:1 hexanes/EtOAc); **IR** (film) ν_{max} 3423 (br), 2361, 1693, 1267, 1090, 1031, 742, 701 cm^{-1} ; **$^1\text{H NMR}$** (500 MHz, CDCl_3) δ 7.30 – 7.20 (m, 5H), 6.84 (minor diast., dd, $J = 1.5, 10.3\text{ Hz}$, 0.27H), 6.79 (major diast., $J = 3.4, 10.3\text{ Hz}$, 0.73H), 6.11 (minor diast., dd, $J = 1.5, 10.3\text{ Hz}$, 0.27H), 6.06 (major diast., d, $J = 10.3\text{ Hz}$, 0.73H), 5.43 (major diast., d, $J = 3.4\text{ Hz}$, 0.73H), 5.38 (minor diast., d, $J = 4.9\text{ Hz}$, 0.27H), 4.71 (major diast., dd, $J = 3.2, 9.0\text{ Hz}$, 0.73H), 4.25 – 4.23 (minor diast., m, 0.27H), 3.8 (br. s, 1H), 3.38 – 3.32 (m, 1H), 2.94 (minor diast., dd, $J = 9.3, 14.6\text{ Hz}$, 0.27H), 2.86 (major diast., dd, $J = 9.3, 14.6\text{ Hz}$, 0.73H); **$^{13}\text{C NMR}$** (126 MHz, CDCl_3) δ 195.8, 148.1, 144.7, 137.7, 129.4, 129.3, 128.3, 128.2, 127.2, 126.5, 126.4, 90.7, 87.4, 79.7, 74.7, 36.5, 35.6; **MS** (ESI-TOF) calcd. for $\text{C}_{12}\text{H}_{12}\text{O}_3$ $[\text{M} + \text{Na}]^+$ 227.0679, found 227.0644.

6-benzyl-5-oxo-5,6-dihydro-2H-pyran-2-yl 3,4,5-trifluorobenzoate (37):

Reaction of **68** (1.001 g, 4.90 mmol), 3,4,5-trifluorobenzoic acid (1.295 g, 7.35 mmol, 1.5 equiv), EDC (1.396 g, 7.28 mmol, 1.5 equiv), and DMAP (897 mg, 7.34 mmol, 1.5 equiv) in CH_2Cl_2 (25 mL, 0.20 M) according to **25p** above afforded **37** as a pale yellow solid after column chromatography (silica gel, 9:1 to 2:1 hexanes/EtOAc) in a 2.7:1 mixture of diastereomers (1.111 g, 63%).

$R_f = 0.38, 0.48$ (silica gel, 4:1 hexanes/EtOAc); **IR** (film) ν_{max} 1736, 1698, 1529, 1441, 1360, 1214, 1046, 764, 734, 700 cm^{-1} ; **$^1\text{H NMR}$** (500 MHz, CDCl_3) δ 7.67 (minor diast. t, $J = 6.9\text{ Hz}$, 0.54H), 7.63 (major diast., t, $J = 6.9\text{ Hz}$, 1.46H), 7.25 – 7.17 (m, 5H), 6.99 (minor diast., dd, $J = 2.7, 10.5\text{ Hz}$, 0.27H), 6.96 (major diast., dd, $J = 3.4, 10.3\text{ Hz}$, 0.73H), 6.77 (minor diast., m, 0.27H), 6.71 (major diast., d, $J = 3.4\text{ Hz}$, 0.73H), 6.36 (minor diast., dd, $J = 1.0, 10.3\text{ Hz}$, 0.27H), 6.28 (major diast., d, $J = 9.8\text{ Hz}$, 0.73H), 4.83 (major diast., dd, $J = 3.7, 7.6\text{ Hz}$, 0.73H), 4.63 (minor diast., dd, $J = 4.2, 9.5\text{ Hz}$, 0.27H), 3.34 (major diast., dd, $J = 3.7, 14.9\text{ Hz}$, 0.73H), 3.28 (minor diast., dd, $J = 4.4, 15.1\text{ Hz}$, 0.27H), 3.17 (minor diast., dd, $J = 9.5, 14.9\text{ Hz}$, 0.27H), 3.09 (major diast., dd, $J = 7.6, 14.9\text{ Hz}$, 0.73H); **$^{13}\text{C NMR}$** (126 MHz, CDCl_3) δ 194.1, 162.3, 152.1, 152.0, 150.1, 150.0, 142.1, 140.7, 136.7, 136.5, 129.6, 129.1, 129.0, 128.4, 128.2, 126.7,

126.6, 125.0, 114.5, 114.5, 114.4, 114.4, 89.0, 88.7, 80.1, 77.0, 38.6, 35.5; **MS** (ESI-TOF) calcd. for C₁₉H₁₃F₃O₄ [M + Na]⁺ 385.0669, found 385.0658.



Scheme 3.17. Synthesis of substrate **39**.

1-(furan-2-yl)-3-methylbutan-1-ol (69):

Grignard formation between magnesium turnings (2.910 g, 120 mmol, 6.6 equiv) and 1-bromo-2-methylpropane (2.6 mL, 24.0 mmol, 1.3 equiv) with 1,2-dibromoethane (0.05 mL, 0.58 mmol) was carried out in THF (60 mL, 0.4 M) according to **65** above. Addition of this Grignard reagent to furfural (1.50 mL, 18.1 mmol) in THF (45 mL) according to **65** above afforded **69** as a pale yellow oil after column chromatography (silica gel, 9:1 to 2:1 hexanes/EtOAc) (2.136 g, 76%).

R_f = 0.65 (silica gel, 2:1 hexanes/EtOAc); **IR** (film) ν_{\max} 3382 (br), 2956, 2930, 2859, 1471, 1367, 1256, 1079, 837, 778 cm⁻¹; **¹H NMR** (500 MHz, CDCl₃) δ 7.36 - 7.35 (m, 1H), 6.32 – 6.31 (m, 1H), 6.21 (d, *J* = 3.2 Hz, 1H), 4.74 – 4.71 (m, 1H), 2.31 (d, *J* = 4.6 Hz, 1H), 1.79 – 1.64 (m, 2H), 0.94 (dd, *J* = 6.4, 7.8 Hz, 6H); **¹³C NMR** (126 MHz, CDCl₃) δ 157.1, 141.7, 110.0, 105.6, 65.8, 44.4, 24.5, 22.9, 22.1; **MS** (ESI-TOF) calcd. for C₉H₁₄O₂ [M + Na]⁺ 177.0886, found 177.1004.

6-hydroxy-2-isobutyl-2H-pyran-3(6H)-one (70):

Reaction of **69** (2.136 g, 13.9 mmol), vanadyl acetylacetonate (371 mg, 1.40 mmol, 0.1 equiv), and *tert*-butyl hydroperoxide (3.8 mL of a 5.5 M solution in dodecane, 20.9 mmol, 1.5 equiv) in CH₂Cl₂ (46 mL, 0.3 M) according to **64** above afforded **70** as a yellow oil after column chromatography (silica gel, 9:1 to

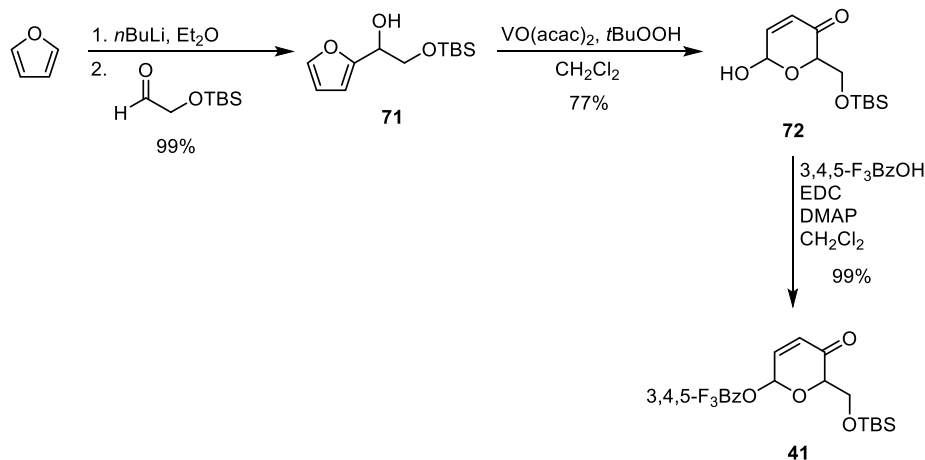
5:1 hexanes/EtOAc) in a 2.2:1 mixture of diastereomers which solidified upon storage at $-30\text{ }^{\circ}\text{C}$ (1.746 g, 74%).

$R_f = 0.19$ (silica gel, 4:1 hexanes/EtOAc); **IR** (film) ν_{max} 3414 (br), 2958, 2871, 1687, 1469, 1370, 1270, 1158, 1089, 1031, 908, 737 cm^{-1} ; **$^1\text{H NMR}$** (500 MHz, CDCl_3) δ 6.91 (minor diast., dd, $J = 1.4, 10.1$ Hz, 0.31H), 6.86 (major diast., dd, $J = 3.4, 10.3$ Hz, 0.69H), 6.11 – 6.08 (minor diast., m, 0.31H), 6.07 – 6.04 (major diast., m, 0.69H), 5.59 (br. s, 1H), 4.58 – 4.55 (m, 1H), 4.37 (br. s, 1H), 1.86 – 1.70 (m, 2H), 1.67 – 1.62 (minor diast., m, 0.31H), 1.56 – 1.50 (major diast., m, 0.69H), 0.91 – 0.87 (m, 6H); **$^{13}\text{C NMR}$** (126 MHz, CDCl_3) δ 197.9, 197.5, 148.5, 145.2, 128.7, 127.5, 91.0, 87.7, 77.5, 72.9, 39.4, 38.2, 24.4, 24.3, 23.6, 23.5, 21.6; **MS** (ESI-TOF) calcd. for $\text{C}_9\text{H}_{14}\text{O}_3$ $[\text{M} + \text{Na}]^+$ 193.0835, found 193.2882.

6-isobutyl-5-oxo-5,6-dihydro-2H-pyran-2-yl 3,4,5-trifluorobenzoate (39):

Reaction of **70** (1.668 g, 9.80 mmol), 3,4,5-trifluorobenzoic acid (2.594 g, 14.7 mmol, 1.5 equiv), EDC (2.820 g, 14.7 mmol, 1.5 equiv), and DMAP (1.795 g, 14.7 mmol, 1.5 equiv) in CH_2Cl_2 (49 mL, 0.20 M) according to **25p** above afforded **39** as a white paste after column chromatography (silica gel, 9:1 to 2:1 hexanes/EtOAc) in a 2.3:1 mixture of diastereomers (2.102 g, 65%).

$R_f = 0.63, 0.69$ (silica gel, 2:1 hexanes/EtOAc); **IR** (film) ν_{max} 1742, 1700, 1531, 1442, 1362, 1210, 1178, 1049, 924 cm^{-1} ; **$^1\text{H NMR}$** (500 MHz, CDCl_3) δ 7.73 – 7.69 (m, 2H), 6.99 – 6.95 (m, 1H), 6.78 (minor diast., d, $J = 2.9$ Hz, 0.30H), 6.72 (major diast., d, $J = 3.9$ Hz, 0.70H), 6.32 – 6.30 (m, 1H), 4.59 (major diast., dd, $J = 2.9, 9.8$ Hz, 0.70H), 4.40 (minor diast., dd, $J = 3.7, 11.0$ Hz, 0.30H), 1.92 – 1.81 (m, 2H), 1.68 – 1.58 (m, 1H), 0.94 – 0.92 (m, 3H), 0.87 – 0.84 (m, 3H); **$^{13}\text{C NMR}$** (126 MHz, CDCl_3) δ 195.4, 152.1, 141.2, 140.4, 129.2, 128.6, 114.6, 114.4, 88.7, 88.6, 78.1, 74.7, 42.1, 37.7, 24.1, 24.0, 23.2, 23.1, 20.3, 21.0; **MS** (ESI-TOF) calcd. for $\text{C}_{16}\text{H}_{15}\text{F}_3\text{O}_4$ $[\text{M} + \text{Na}]^+$ 351.0815, found 351.0848.



Scheme 3.18. Synthesis of substrate **41**.

2-(((tert-butyldimethylsilyl)oxy)-1-(furan-2-yl)ethanol (71**):**

Freshly distilled furan (1.5 mL, 20.5 mmol, 1.5 equiv) was dissolved in Et₂O (20 mL, 1.0 M relative to furan) under an atmosphere of N₂ and the resulting mixture was cooled to -20 °C. *n*-BuLi (6.5 mL of a 2.10 M solution in hexanes, 13.7 mmol) was introduced dropwise via syringe. After addition, the reaction mixture was allowed to warm to 0 °C and stirred at that temperature for 3 h. The reaction was then recooled to -20 °C and 2-(((tert-butyldimethylsilyl)oxy)acetaldehyde (4.3 mL, 20.3 mmol, 1.5 equiv, 90 wt%) was added dropwise by syringe. The solution was stirred at -20 °C for 2 h before the careful addition of sat. aq. NH₄Cl (4 mL). The aqueous layer was extracted with Et₂O (2 x 10 mL). The combined organic layers were then dried over NaSO₄, filtered, and concentrated. Purification by column chromatography (silica gel, 9:1 to 5:1 hexanes/EtOAc) afforded **71** as a colorless oil (3.277 g, 99%).

R_f = 0.56 (silica gel, 4:1 hexanes/EtOAc); **IR** (film) ν_{max} 3446 (br), 2955, 2930, 2886, 2858, 1472, 1257, 1118, 1007, 839, 779, 738 cm⁻¹; **¹H NMR** (500 MHz, CDCl₃) δ 7.36 – 7.35 (m, 1H), 6.32 (dd, *J* = 1.7, 2.7 Hz, 1H), 6.30 (d, *J* = 10.7 Hz, 1H), 4.76 – 4.73 (m, 1H), 3.88 – 3.81 (m, 2H), 2.99 – 2.96 (m, 1H), 0.89 (s, 9H), 0.06 (d, *J* = 5.9 Hz, 6H); **¹³C NMR** (100 MHz, CDCl₃) δ 153.7, 141.8, 110.1, 106.9, 68.3, 65.6, 25.7, -5.6; **MS** (ESI-TOF) calcd. for C₁₂H₂₂O₃Si [M + Na]⁺ 265.1230, found 265.1231.

2-(((tert-butyldimethylsilyl)oxy)methyl)-6-hydroxy-2H-pyran-3(6H)-one (72**):**

Reaction of **71** (4.292 g, 17.7 mmol), vanadyl acetylacetonate (473 mg, 1.79 mmol, 0.1 equiv), and *tert*-

butyl hydroperoxide (4.8 mL of a 5.5 M solution in dodecane, 26.4 mmol, 1.5 equiv) in CH₂Cl₂ (59 mL, 0.3 M) according to **64** above afforded **72** as a pale yellow oil after column chromatography (silica gel, 9:1 to 5:1 hexanes/EtOAc) in a 1.9:1 mixture of diastereomers (3.525 g, 77%).

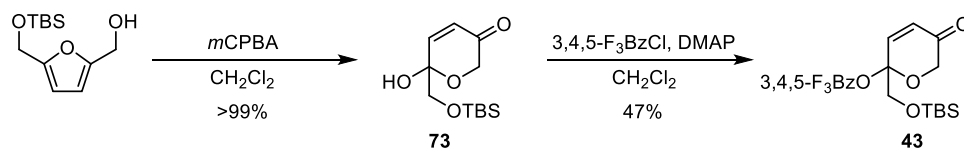
R_f = 0.33 (silica gel, 4:1 hexanes/EtOAc); **IR** (film) ν_{\max} 3378 (br), 2955, 2931, 2885, 2859, 1696, 1473, 1258, 1121, 1084, 1025, 837, 783 cm⁻¹; **¹H NMR** (500 MHz, CDCl₃) δ 6.91 – 6.86 (m, 1H), 6.10 (minor diast., d, *J* = 10.7 Hz, 0.34H), 6.04 (major diast., d, *J* = 10.3 Hz, 0.66H), 5.71 (major diast., br. s, 0.66H), 5.50 – 5.39 (m, 1H), 4.76 (minor diast., br. s, 0.34H), 4.50 (major diast., t, *J* = 3.7 Hz, 0.66H), 4.31 (minor diast., t, *J* = 2.4 Hz, 0.34H), 4.01 – 3.85 (m, 2H), 0.79 (s, 9H), 0.01 – -0.03 (m, 6H); **¹³C NMR** (126 MHz, CDCl₃) δ 194.6, 147.0, 145.8, 127.8, 127.2, 87.8, 86.6, 79.6, 76.5, 65.4, 63.2, 34.5, 31.5, 25.7, 25.5, 25.1, 22.5, 18.2, 18.1, 14.0, -5.5, -5.6, -5.9, -6.0; **MS** (ESI-TOF) calcd. for C₁₂H₂₂O₄Si [M + Na]⁺ 281.1180, found 281.1189.

6-(((*tert*-butyldimethylsilyl)oxy)methyl)-5-oxo-5,6-dihydro-2*H*-pyran-2-yl 3,4,5-trifluorobenzoate (41):

Reaction of **72** (2.116 g, 8.19 mmol), 3,4,5-trifluorobenzoic acid (2.162 g, 12.3 mmol, 1.5 equiv), EDC (1.919 g, 10.0 mmol, 1.2 equiv), and DMAP (1.498 g, 12.3 mmol, 1.5 equiv) in CH₂Cl₂ (41 mL, 0.20 M) according to **25p** above afforded **41** as a yellow oil after column chromatography (silica gel, 9:1 to 2:1 hexanes/EtOAc) in a 1.7:1 mixture of diastereomers (3.376 g, 99%).

R_f = 0.36, 0.50 (silica gel, 4:1 hexanes/EtOAc); **IR** (film) ν_{\max} 2957, 2932, 2860, 1739, 1704, 1531, 1464, 1363, 1212, 1050, 913, 839, 765 cm⁻¹; **¹H NMR** (500 MHz, CDCl₃) δ 7.75 – 7.69 (m, 2H), 7.02 (major diast., ddd, *J* = 1.7, 3.2, 10.3 Hz, 0.37H), 6.99 – 6.96 (minor diast., m, 0.63H), 6.85 – 6.84 (major diast., m, 0.63H), 6.81 – 6.80 (minor diast., m, 0.37H), 6.34 (dd, *J* = 2.4, 10.3 Hz, 1H), 4.58 – 4.57 (major diast., m, 0.63H), 4.43 – 4.40 (minor diast., m, 0.37H), 4.14 – 4.00 (m, 2H), 0.85 (major diast., s, 5.67H), 0.81 (minor diast., s, 3.33H), 0.07 – 0.05 (major diast., m, 3.78H), 0.02 – -0.02 (minor diast., m, 2.22H); **¹³C NMR** (126 MHz, CDCl₃) δ 193.3, 193.2, 141.8, 141.2, 129.7, 129.4, 114.7, 114.6, 114.5, 114.4, 88.7, 88.4, 78.2,

64.3, 62.8, 31.6, 25.7, 25.7, 18.2, -5.4; **MS** (ESI-TOF) calcd. for C₁₉H₂₃F₃O₅Si [M + Na]⁺ 439.1159, found 439.1201.



Scheme 3.19. Synthesis of substrate **43**.

6-(((tert-butyldimethylsilyloxy)methyl)-6-hydroxy-2H-pyran-3(6H)-one (73):

(5-(((tert-Butyldimethylsilyloxy)methyl)furan-2-yl)methanol³² (1.3403 g, 5.53 mmol) was dissolved in CH₂Cl₂ (37 mL, 0.15 M). To this solution was added solid *m*-chloroperoxybenzoic acid (1.495 g, 6.67 mmol, 1.2 equiv, 77 wt%). The reaction was stirred under an atmosphere of N₂ at 23 °C for 3 h, before it was quenched with sat. aq. Na₂S₂O₃ (8 mL), sat. aq. NaHCO₃ (8 mL), and 10% aq. Na₂CO₃ (8 mL). The quenched reaction was allowed to stir for a further 30 min. The aqueous layer was extracted with CH₂Cl₂ (3 x 15 mL). The pooled organic layers were then washed with brine (25 mL), dried over Na₂SO₄, filtered, and concentrated. The resultant white powder (**73**) was used without further purification (1.429 g, 100%).

R_f = 0.32 (silica gel, 4:1 hexanes/EtOAc); **IR** (film) ν_{\max} 3255 (br), 2952, 2930, 2886, 2858, 1681, 1252, 1119, 1063, 841, 778, 737 cm⁻¹; **¹H NMR** (500 MHz, CDCl₃) δ 6.80 (d, *J* = 10.5 Hz, 1H), 6.16 (d, *J* = 10.1 Hz, 1H), 4.61 (d, *J* = 16.9 Hz, 1H), 4.15 (d, *J* = 16.9 Hz, 1H), 3.78 (d, *J* = 10.5 Hz, 1H), 3.70 – 3.68 (m, 2H), 0.94 (s, 9H), 0.13 (d, *J* = 1.4 Hz, 6H); **¹³C NMR** (126 MHz, CDCl₃) δ 195.1, 145.7, 128.6, 92.5, 67.9, 66.6, 25.8, 18.4, -5.2, -5.5; **MS** (ESI-TOF) calcd. for C₁₂H₂₂O₄Si [M + Na]⁺ 281.1180, found 281.1162.

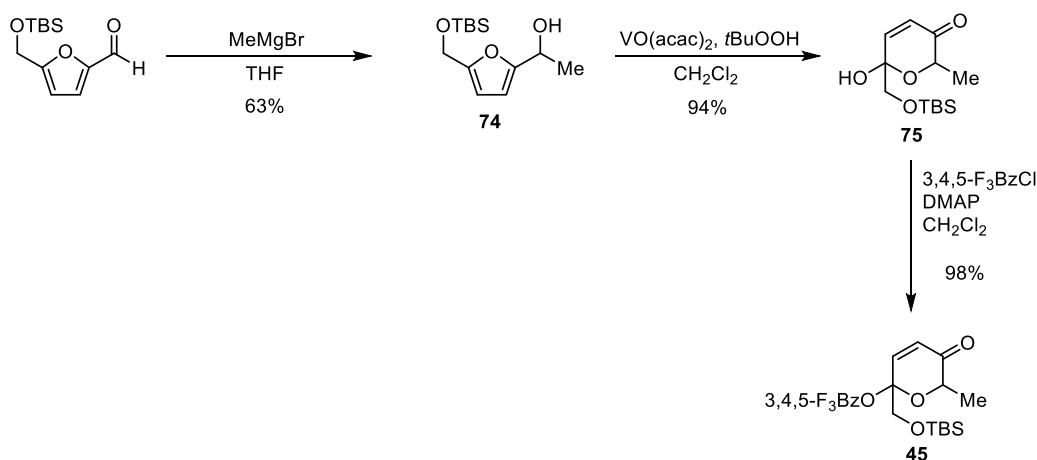
2-(((tert-butyldimethylsilyloxy)methyl)-5-oxo-5,6-dihydro-2H-pyran-2-yl 3,4,5-trifluorobenzoate (43):

Hemiketal **73** (253 mg, 0.98 mmol) was dissolved in CH₂Cl₂ (3.2 mL, 0.31 M) and the flask was cooled to 0 °C. To this solution was added sequentially 3,4,5-trifluorobenzoyl chloride (0.19 mL, 1.45 mmol, 1.5 equiv) and solid DMAP (185 mg, 1.51 mmol, 1.5 equiv). The reaction mixture was stirred at 0 °C for 30

³² (5-(((tert-Butyldimethylsilyloxy)methyl)furan-2-yl)methanol synthesized according to: Celanire, S.; Marlin, F.; Baldwin, J. E.; Adlington, R. M. *Tetrahedron* **2005**, *61*, 3025–3032.

min under an atmosphere of N₂. The reaction mixture was then quenched with H₂O (3 mL) and allowed to warm to 23 °C. The organic phase was washed with 1N HCl (2 x 3 mL). The pooled aqueous layers were then extracted with CH₂Cl₂ (2 x 3 mL). The combined organic layers were dried over Na₂SO₄, filtered, concentrated and purified by column chromatography (silica gel, 95:5 to 2:1 hexanes/Et₂O) to afford **43** as a colorless oil (192 mg, 47%).

R_f = 0.66 (silica gel, 2:1 hexanes/Et₂O); **IR** (film) ν_{\max} 2956, 2931, 2859, 1733, 1705, 1626, 1528, 1440, 1358, 1254, 1227, 1121, 1047, 956, 837, 779, 763 cm⁻¹; **¹H NMR** (500 MHz, CDCl₃) δ 7.65 (dd, *J* = 6.3, 7.8 Hz, 2H), 7.32 (d, *J* = 10.7 Hz, 1H), 6.3 (d, *J* = 10.3 Hz, 1H), 4.64 (d, *J* = 17.1 Hz, 1H), 4.34 (d, *J* = 17.1 Hz, 1H), 4.23 (d, *J* = 10.7 Hz, 1H), 3.93 (d, *J* = 10.7 Hz, 1H), 0.86 (s, 9H), 0.07 (d, *J* = 2.4 Hz, 6H); **¹³C NMR** (126 MHz, CDCl₃) δ 193.3, 143.7, 127.9, 114.5, 114.3, 106.8, 100.2, 68.3, 66.1, 34.6, 31.6, 29.0, 25.6, 22.6, 18.1, 14.1, -5.5, -5.5; **MS** (ESI-TOF) calcd. for C₁₉H₂₃F₃O₅Si [M + Na]⁺ 439.1159, found 439.1204.



Scheme 3.20. Synthesis of substrate **45**.

1-(5-(((*tert*-butyldimethylsilyl)oxy)methyl)furan-2-yl)ethanol (74**):**

5-(((*tert*-Butyldimethylsilyl)oxy)methyl)furan-2-carbaldehyde³³ (7.525 g, 31.3 mmol) was dissolved in THF (157 mL, 0.20 M) in a flame-dried round-bottom flask and the resultant solution was cooled to -20

³³ 5-(((*tert*-Butyldimethylsilyl)oxy)methyl)furan-2-carbaldehyde synthesized according to: Celanire, S.; Marlin, F.; Baldwin, J. E.; Adlington, R. M. *Tetrahedron* **2005**, *61*, 3025–3032.

°C and stirred under an atmosphere of N₂. Dropwise by syringe, methylmagnesium bromide (15.5 mL of a 3.0 M solution in THF, 46.5 mmol, 1.5 equiv) was added to the cooled reaction mixture. The resultant solution was allowed to stir for 40 min at -20 °C under an atmosphere of N₂. The reaction was quenched with sat. aq. NH₄Cl (60 mL) and warmed to 23 °C. The phases were separated and the aqueous layer was extracted with EtOAc (3 x 40 mL). The combined organic phases were washed with brine (60 mL), dried over Na₂SO₄, filtered, concentrated and purified by column chromatography (silica gel, 95:5 to 2:1 hexanes/Et₂O) to afford **74** as a brown oil (5.083 g, 63%).

R_f = 0.26 (silica gel, 2:1 hexanes/Et₂O); **IR** (film) ν_{\max} 3389 (br), 2955, 2931, 2858, 1473, 1373, 1256, 1078, 1016, 837, 778 cm⁻¹; **¹H NMR** (400 MHz, CDCl₃) δ 6.15 (d, *J* = 1.1 Hz, 1H), 4.86 – 4.79 (m, 1H), 4.61 (s, 2H), 2.33 – 2.26 (m, 1H), 1.51 (d, *J* = 6.6 Hz, 3H), 0.90 (s, 9H), 0.09 – 0.07 (m, 6H); **¹³C NMR** (100 MHz, CDCl₃) δ 157.2, 153.6, 107.8, 105.7, 63.6, 58.2, 31.5, 25.8, 21.2, -5.28; **MS** (ESI-TOF) calcd. for C₁₃H₂₄O₃Si [M + Na]⁺ 279.1387, found 279.1550.

6-(((*tert*-butyldimethylsilyl)oxy)methyl)-6-hydroxy-2-methyl-2*H*-pyran-3(6*H*)-one (75):

Reaction of **74** (5.083 g, 19.8 mmol), vanadyl acetylacetonate (526 mg, 1.98 mmol, 0.1 equiv), and *tert*-butyl hydroperoxide (5.4 mL of a 5.5 M solution in dodecane, 29.7 mmol, 1.5 equiv) in CH₂Cl₂ (66 mL, 0.3 M) according to **64** above afforded **75** as a yellow oil after column chromatography (silica gel, 9:1 to 5:1 hexanes/EtOAc) in a 6.2:1 mixture of diastereomers (5.088 g, 94%).

R_f = 0.26 (silica gel, 2:1 hexanes/EtOAc); **IR** (film) ν_{\max} 3443 (br), 2956, 2932, 2858, 1699, 1257, 1121, 1061, 839, 780 cm⁻¹; **¹H NMR** (500 MHz, CDCl₃) δ 6.80 (minor diast., d, *J* = 10.5 Hz, 0.14H), 6.76 (major diast., d, *J* = 10.5 Hz, 0.86H), 6.11 (minor diast., d, *J* = 10.5 Hz, 0.14H), 6.06 (major diast., d, *J* = 10.1 Hz, 0.86H), 4.64 (major diast., q, *J* = 6.9 Hz, 0.86H), 4.41 (minor diast., q, *J* = 6.5 Hz, 0.14H), 3.72 – 3.63 (m, 2H), 1.33 (d, *J* = 6.9 Hz, 3H), 0.90 – 0.87 (m, 9H), 0.09 – 0.07 (m, 6H); **¹³C NMR** (126 MHz, CDCl₃) δ 197.4, 145.3, 127.8, 92.6, 70.7, 68.3, 25.7, 18.3, 15.2, -5.24, -5.47; **MS** (ESI-TOF) calcd. for C₁₃H₂₄O₄Si [M + Na]⁺ 295.1336, found 295.1344.

2-(((*tert*-butyldimethylsilyl)oxy)methyl)-6-methyl-5-oxo-5,6-dihydro-2*H*-pyran-2-yl 3,4,5-trifluorobenzoate (45):

Reaction of **75** (754 mg, 2.77 mmol), 3,4,5-trifluorobenzoyl chloride (0.36 mL, 2.75 mmol, 1.0 equiv), and DMAP (375 mg, 3.07 mmol, 1.1 equiv) in CH₂Cl₂ (9.2 mL, 0.30 M) according to **43** above afforded **45** as a brown oil in a 5.4:1 mixture of diastereomers (1.167 g, 98%). **45** rapidly decomposes on silica, Davisil®, or alumina. On the benchtop, it decomposes within hours, and cannot even be stored at –80 °C overnight without significant decomposition. The reaction goes to complete conversion within 30 min and the crude material is ~95% pure. This crude material was immediately carried forward to the cycloaddition step.

R_f = 0.65 (silica gel, 4:1 hexanes/EtOAc); **IR** (film) ν_{\max} 2956, 2933, 2859, 1735, 1701, 1529, 1440, 1359, 1256, 1211, 1125, 1049, 840 cm⁻¹; **¹H NMR** (500 MHz, CDCl₃) δ 7.65 (dd, *J* = 6.6, 7.6 Hz, 2H), 7.31 (d, *J* = 10.5 Hz, 1H), 6.27 (minor diast., d, *J* = 10.5, 0.16H), 6.24 (major diast., d, *J* = 10.5 Hz, 0.84H), 4.72 (major diast., q, *J* = 6.9 Hz, 0.84H), 4.64 – 4.58 (minor diast., m, 0.16H), 4.28 (minor diast., d, *J* = 10.5 Hz, 0.16H), 4.24 (major diast., d, *J* = 11.0 Hz, 0.84H), 3.95 (minor diast., d, *J* = 10.5 Hz, 0.16H), 3.90 (major diast., d, *J* = 10.5 Hz, 0.84H), 1.45 (d, *J* = 6.9 Hz, 3H), 0.86 – 0.85 (m, 9H), 0.07 – 0.06 (m, 6H); **¹³C NMR** (126 MHz, CDCl₃) δ 195.9, 143.3, 127.4, 114.4, 114.3, 100.7, 76.0, 73.3, 66.3, 53.4, 40.5, 25.6, 18.1, 15.7, –5.5; **MS** (ESI-TOF) calcd. for C₂₀H₂₅F₃O₅Si [M + Na]⁺ 453.1332, found 453.1316.

3.8.3 Procedures for Cycloadditions and Characterization of Products

General Procedure for Thiourea-Catalyzed Cycloadditions (Optimization Studies):

An oven-dried 0.5-dram vial was charged with thioureas **4** and **5** (0.20 equiv). To these catalysts was added a stock solution of pyranone **25** or **31** (0.07 mmol) and AcOH (0.20 equiv as indicated) in toluene (0.2 M in pyranone as indicated). Last, the olefin (acrylonitrile, methyl acrylate, styrene, benzyl vinyl ether³⁴, or ethyl vinyl ether—10 equiv) was added by syringe. No special precautions were taken to exclude air or moisture. The vial was sealed and allowed to stir for the designated length of time at 40 °C. The reaction

³⁴ Benzyl vinyl ether synthesized according to: Okimoto, Y.; Sakaguchi, S.; Ishii, Y, *J. Am. Chem. Soc.* **2002**, *124*, 1590–1591.

was then quenched with 1N HCl (10 mL). The aqueous layer was extracted with CH₂Cl₂ (3 x 10 mL), which was added to a flask containing 1,3,5-trimethoxybenzene (0.012 M in benzene, 0.10 equiv relative to substrate). The combined organic layers were dried over Na₂SO₄, filtered, and concentrated. Yield was then determined by ¹H NMR of this crude reaction mixture. Enantiomeric excess was determined by chiral HPLC after chromatographic purification on silica gel.

General Procedure for Thiourea-Catalyzed Cycloadditions (Substrate Scope):

An oven-dried 1.0-dram vial was charged with 3,4,5-trifluorobenzoyl pyranone substrate **25p**, **31p**, **35**, **37**, **39**, **41**, **43**, or **45** (≥50.0 mg). To this vial was then added a stock solution of AcOH (0.15 equiv) in toluene such that the substrate concentration was 0.2 M. To the resulting solution was added catalysts **4** and **5** (0.15 or 0.20 equiv as indicated). Last, the vinyl ether (ethyl vinyl ether, benzyl vinyl ether, or (methoxymethoxy)ethene³⁵—5 or 10 equiv as indicated) was added by syringe. No special precautions were taken to exclude air or moisture. The vial was sealed and allowed to stir for the designated length of time at the designated temperature. The reaction was then transferred with CH₂Cl₂ to a separatory funnel containing 1N HCl (30 mL). The aqueous layer was extracted with CH₂Cl₂ (4 x 30 mL). The combined organic layers were dried over Na₂SO₄, filtered, and concentrated. The crude product was purified by silica gel flash chromatography.

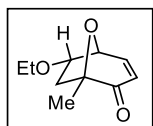
General Procedure for Preparation of Racemic Products 32, 33, 36, 40, 44, 46, 47, and 48:

An oven-dried 1.0-dram vial was charged with 3,4,5-trifluorobenzoyl pyranone substrate (≥ 0.5 mmol) which was then dissolved in CH₂Cl₂ (0.5 M). To this solution was added NEt₃ (3.0 equiv) by syringe, then vinyl ether (10.0 equiv). The vial was sealed and allowed to stir for 72 hours. The crude product was concentrated and purified by silica gel flash chromatography.

³⁵ (Methoxymethoxy)ethene synthesized according to: Tamao, K.; Nakagawa, Y.; Ito, Y. *Org. Synth.* **1996**, 73, 94–102.

General Procedure for Preparation of Racemic Products 38 and 42:

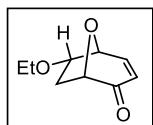
A 5.0 mL pressure tube was charged with 3,4,5-trifluorobenzoyl pyranone substrate (≥ 0.5 mmol) which was then dissolved in MeCN (0.17 M). To this solution was added vinyl ether (15.0 equiv). The tube was sealed and allowed to stir at 80 °C for 16 hours. The crude product was concentrated and purified by silica gel flash chromatography.



(1S,5S,6S)-6-ethoxy-1-methyl-8-oxabicyclo[3.2.1]oct-3-en-2-one (33):

According to the general procedure, **31p** (700 mg, 2.45 mmol), **4** (147 mg, 0.37 mmol, 0.15 equiv), **5** (184 mg, 0.37 mmol, 0.15 equiv), and ethyl vinyl ether (1.17 mL, 12.23 mmol, 5 equiv) were allowed to react in a toluene solution (12.2 mL, 0.2 M) containing AcOH (21 μ L, 0.37 mmol, 0.15 equiv) for 72 h to afford **33** (309 mg, 69%) as a colorless oil after column chromatography (silica gel, 9:1 to 3:2 hexanes/Et₂O). This material was determined to be 96% *ee* by chiral HPLC analysis (ChiralCel OD-H, 5% *i*PrOH in hexanes, 1 mL/min, 220 nm, t_R (major) = 7.0 min, t_R (minor) = 9.4 min). The relative stereochemistry and identification of the *endo* diastereomer were determined by comparison to the previously reported racemic material.^{11c} The relative stereochemistry of all other ethyl ether products was assigned by analogy.

R_f = 0.24 (silica gel, 2:1 hexanes/Et₂O); **IR** (film) ν_{\max} 2980, 1696, 1375, 1156, 739, 699 cm⁻¹; **¹H NMR** (500 MHz, CDCl₃) δ 7.19 (ddd, J = 1.0, 4.4, 9.8 Hz, 1H), 6.17 (dd, J = 1.0, 9.8 Hz, 1H), 4.83 – 4.81 (m, 1H), 4.47 – 4.43 (m, 1H), 3.55 – 3.47 (m, 2H), 2.25 (dd, J = 8.8, 13.2 Hz, 1H), 1.76 (dd, J = 4.6, 13.4 Hz, 1H), 1.44 (s, 3H), 1.18 (t, J = 7.3 Hz, 3H); **¹³C NMR** (126 MHz, CDCl₃) δ 197.9, 150.4, 127.5, 85.6, 81.0, 74.5, 66.3, 36.6, 19.9, 15.3; **MS** (ESI-TOF) calcd. for C₁₀H₁₄O₃ [M + Na⁺] 205.0835, found 205.0832; $[\alpha]_D^{24}$ = -188.6 (c = 0.1, CHCl₃).

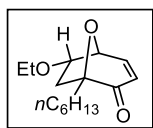


(1S,5S,6S)-6-ethoxy-8-oxabicyclo[3.2.1]oct-3-en-2-one (32):

According to the general procedure, **25p** (80.0 mg, 0.294 mmol), **4** (23.6 mg, 0.059 mmol, 0.20 equiv), **5** (29.4 mg, 0.059 mmol, 0.20 equiv), and ethyl vinyl ether (141 μ L, 1.470 mmol, 5 equiv) were allowed to react in a toluene solution (1.47 mL, 0.2 M) containing AcOH (2.5 μ L, 0.044 mmol, 0.15

equiv) for 96 h at 0 °C to afford **32** (24.9 mg, 51%) as a colorless oil after column chromatography (silica gel, 9:1 to 3:2 hexanes/Et₂O) followed by subsequent column chromatography (silica gel, 98:2 to 92:8 toluene/EtOAc). This material was determined to be 84% *ee* by chiral HPLC analysis (ChiralCel OB-H, 5% *i*PrOH in hexanes, 1 mL/min, 218 nm, *t*_R(major) = 15.3 min, *t*_R(minor) = 13.2 min).

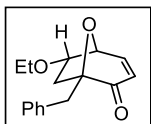
R_f = 0.16 (silica gel, 2:1 hexanes/Et₂O); **IR** (film) ν_{\max} 2978, 2881, 1706, 1690, 1383, 1249, 1122, 1107, 1056, 920, 870 cm⁻¹; **¹H NMR** (500 MHz, CDCl₃) δ 7.19 (dd, *J* = 4.4, 9.8 Hz, 1H), 6.15 (d, *J* = 10.3 Hz, 1H), 4.79 (t, *J* = 5.1 Hz, 1H), 4.41 (d, *J* = 8.8 Hz, 1H), 4.38 – 4.36 (m, 1H), 3.54 – 3.43 (m, 2H), 2.66 (dt, *J* = 8.8, 13.7 Hz, 1H), 1.59 – 1.55 (m, 1H), 1.15 (t, *J* = 6.8 Hz, 3H); **¹³C NMR** (126 MHz, CDCl₃) δ 196.6, 150.6, 127.5, 81.0, 80.7, 73.6, 66.4, 31.9, 15.2; **MS** (ESI-TOF) calcd. for C₉H₁₂O₃ [M + Na⁺] 191.0679, found 191.0676; **[α]_D²³** = -28.1 (*c* = 0.3, CHCl₃).



(1S,5S,6S)-6-ethoxy-1-hexyl-8-oxabicyclo[3.2.1]oct-3-en-2-one (36):

According to the general procedure, **35** (97.8 mg, 0.274 mmol), **4** (22.0 mg, 0.055 mmol, 0.20 equiv), **5** (27.4 mg, 0.055 mmol, 0.20 equiv), and ethyl vinyl ether (131 μ L, 1.372 mmol, 5 equiv) were allowed to react in a toluene solution (1.37 mL, 0.2 M) containing AcOH (2.4 μ L, 0.041 mmol, 0.15 equiv) for 72 h to afford **36** (40.7 mg, 59%) as a colorless oil after column chromatography (silica gel, 9:1 to 2:1 hexanes/Et₂O). This material was determined to be 90% *ee* by chiral HPLC analysis (ChiralCel OB-H, 2% *i*PrOH in hexanes, 1 mL/min, 210 nm, *t*_R(major) = 8.1 min, *t*_R(minor) = 10.2 min).

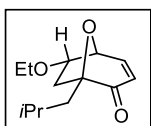
R_f = 0.39 (silica gel, 2:1 hexanes/EtOAc); **IR** (film) ν_{\max} 2930, 1697, 1125, 1056, 909, 738 cm⁻¹; **¹H NMR** (500 MHz, CDCl₃) δ 7.18 (dd, *J* = 4.6, 9.6 Hz, 1H), 6.17 (d, *J* = 9.6 Hz, 1H), 4.81 (dd, *J* = 4.6, 6.0 Hz, 1H), 4.39 (ddd, *J* = 4.8, 6.1, 8.8 Hz, 1H), 3.53 – 3.46 (m, 2H), 2.30 (dd, *J* = 8.9, 13.5 Hz, 1H), 2.06 – 2.00 (m, 1H), 1.66 – 1.59 (m, 2H), 1.41 – 1.28 (m, 8H), 1.17 (t, *J* = 6.9 Hz, 3H), 0.87 (t, *J* = 6.6 Hz, 3H); **¹³C NMR** (126 MHz, CDCl₃) δ 198.0, 150.1, 128.2, 88.2, 80.2, 74.2, 66.3, 37.0, 33.3, 31.7, 29.7, 23.1, 22.5, 15.3, 14.0; **MS** (ESI-TOF) calcd. for C₁₅H₂₄O₃ [M + Na⁺] 275.1618, found 275.1615; **[α]_D²⁴** = -234.3 (*c* = 1.2, CHCl₃).



(1S,5S,6S)-1-benzyl-6-ethoxy-8-oxabicyclo[3.2.1]oct-3-en-2-one (38):

According to the general procedure, **37** (100.0 mg, 0.276 mmol), **4** (16.6 mg, 0.041 mmol, 0.15 equiv), **5** (20.7 mg, 0.041 mmol, 0.15 equiv), and ethyl vinyl ether (132 μ L, 1.380 mmol, 5 equiv) were allowed to react in a toluene solution (1.38 mL, 0.2 M) containing AcOH (2.4 μ L, 0.041 mmol, 0.15 equiv) for 72 h to afford **38** (15.5 mg, 22%) as a colorless oil after column chromatography (silica gel, 9:1 to 3:2 hexanes/Et₂O). This material was determined to be 88% *ee* by chiral HPLC analysis (ChiralCel OD-H, 4% *i*PrOH in hexanes, 1 mL/min, 208 nm, t_R (major) = 8.4 min, t_R (minor) = 7.7 min).

R_f = 0.28 (silica gel, 2:1 hexanes/Et₂O); **IR** (film) ν_{\max} 1695, 1119, 1056, 1037, 912, 737, 701 cm^{-1} ; **¹H NMR** (500 MHz, CDCl₃) δ 7.31 – 7.23 (m, 5H), 7.20 (dd, J = 4.3, 9.8 Hz, 1H), 6.20 (d, J = 9.6 Hz, 1H), 4.82 (dd, J = 4.6, 6.0 Hz, 1H), 4.17 (ddd, J = 4.8, 6.1, 8.8 Hz, 1H), 3.44 (qq, J = 7.0, 9.2 Hz, 2H), 3.26 (d, J = 15.1 Hz, 1H), 3.10 (d, J = 14.7 Hz, 1H), 2.29 (dd, J = 8.9, 13.5 Hz, 1H), 1.61 (dd, J = 4.8, 13.5 Hz, 1H), 1.14 (t, J = 7.1 Hz, 3H); **¹³C NMR** (126 MHz, CDCl₃) δ 197.4, 150.4, 136.1, 130.9, 128.0, 127.9, 126.5, 87.9, 81.0, 74.1, 66.3, 37.6, 35.3, 15.3; **MS** (ESI-TOF) calcd. for C₁₆H₁₈O₃ [M + Na⁺] 281.1148, found 281.1137; $[\alpha]_D^{24}$ = -54.2 (c = 0.8, CHCl₃).

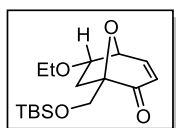


(1S,5S,6S)-6-ethoxy-1-isobutyl-8-oxabicyclo[3.2.1]oct-3-en-2-one (40):

According to the general procedure, **39** (101.1 mg, 0.308 mmol), **4** (24.7 mg, 0.062 mmol, 0.20 equiv), **5** (30.8 mg, 0.062 mmol, 0.20 equiv), and ethyl vinyl ether (147 μ L, 1.540 mmol, 5 equiv) were allowed to react in a toluene solution (1.54 mL, 0.2 M) containing AcOH (2.6 μ L, 0.046 mmol, 0.15 equiv) for 72 h to afford **40** (18.1 mg, 26%) as a colorless oil after column chromatography (silica gel, 9:1 to 4:1 hexanes/Et₂O) followed by subsequent column chromatography (silica gel, 98:2 to 92:8 toluene/EtOAc). This material was determined to be 67% *ee* by chiral HPLC analysis (ChiralCel OC-H, 2% *i*PrOH in hexanes, 1 mL/min, 210 nm, t_R (major) = 8.2 min, t_R (minor) = 9.5 min).

R_f = 0.24 (silica gel, 4:1 hexanes/Et₂O); **IR** (film) ν_{\max} 2957, 2873, 1696, 1125, 1052, 911, 737 cm^{-1} ; **¹H NMR** (500 MHz, CDCl₃) δ 7.18 (dd, J = 4.6, 10.1 Hz, 1H), 6.19 (d, J = 1.9 Hz, 1H), 4.83 (dd, J = 5.1, 5.5

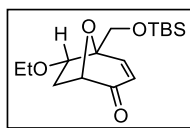
Hz, 1H), 4.42 – 4.38 (m, 1H), 3.54 – 3.44 (m, 2H), 2.30 (dd, $J = 8.9, 13.5$ Hz, 1H), 2.08 (dd, $J = 6.9, 14.7$ Hz, 1H), 1.83 (tt, $J = 6.8, 13.2$ Hz, 1H), 1.65 (dd, $J = 4.8, 13.5$ Hz, 1H), 1.56 – 1.51 (m, 1H), 1.18 (t, $J = 7.1$ Hz, 3H), 0.95 (d, $J = 6.9$ Hz, 3H), 0.90 (d, $J = 6.9$ Hz, 3H); ^{13}C NMR (100 MHz, CDCl_3) δ 198.0, 150.0, 128.2, 88.7, 80.8, 74.2, 66.3, 41.6, 38.5, 24.4, 24.1, 24.0, 15.3; **MS** (ESI-TOF) calcd. for $\text{C}_{13}\text{H}_{20}\text{O}_3$ [$\text{M} + \text{Na}^+$] 247.1305, found 247.1287; $[\alpha]_D^{24} = -77.0$ ($c = 0.7$, CHCl_3).



(1R,5S,6S)-1-(((*tert*-butyldimethylsilyl)oxy)methyl)-6-ethoxy-8-oxabicyclo[3.2.1]oct-3-en-2-one (42):

According to the general procedure, **41** (303.6 mg, 0.729 mmol), **4** (58.6 mg, 0.146 mmol, 0.20 equiv), **5** (73.0 mg, 0.146 mmol, 0.20 equiv), and ethyl vinyl ether (349 μL , 3.64 mmol, 5 equiv) were allowed to react in a toluene solution (3.64 mL, 0.2 M) containing AcOH (6.3 μL , 0.109 mmol, 0.15 equiv) for 72 h to afford **42** (146.2 mg, 64%) as a colorless oil after column chromatography (silica gel, 9:1 to 3:2 hexanes/EtOAc). This material was determined to be 86% *ee* by chiral HPLC analysis (ChiralCel OD-H, 2% *i*PrOH in hexanes, 1 mL/min, 216 nm, $t_{\text{R}}(\text{major}) = 5.9$ min, $t_{\text{R}}(\text{minor}) = 4.9$ min).

$R_f = 0.59$ (silica gel, 2:1 hexanes/EtOAc); **IR** (film) ν_{max} 2930, 2858, 1696, 1257, 1112, 912, 839, 780, 736 cm^{-1} ; ^1H NMR (500 MHz, CDCl_3) δ 7.20 (dd, $J = 4.6, 10.1$ Hz, 1H), 6.16 (d, $J = 10.1$ Hz, 1H), 4.86 (t, $J = 5.0$ Hz, 1H), 4.40 – 4.36 (m, 1H), 3.95 (d, $J = 3.2$ Hz, 2H), 3.58 – 3.46 (m, 2H), 2.65 (dd, $J = 8.9, 13.0$, 1H), 1.49 (dd, $J = 4.8, 13.0$ Hz, 1H), 1.19 (t, $J = 6.9$ Hz, 3H), 0.91 (s, 9H), 0.09 (s, 3H), 0.07 (s, 3H); ^{13}C NMR (126 MHz, CDCl_3) δ 196.8, 150.4, 128.0, 88.2, 81.1, 74.4, 66.4, 61.7, 32.1, 25.9, 18.4, 15.3, -5.2, -5.4; **MS** (ESI-TOF) calcd. for $\text{C}_{16}\text{H}_{28}\text{O}_4\text{Si}$ [$\text{M} + \text{Na}^+$] 335.1649, found 335.1636; $[\alpha]_D^{24} = -84.4$ ($c = 1.1$, CHCl_3).

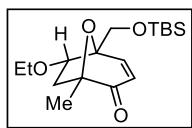


(1S,5R,6S)-5-(((*tert*-butyldimethylsilyl)oxy)methyl)-6-ethoxy-8-oxabicyclo[3.2.1]oct-3-en-2-one (44):

According to the general procedure, **43** (68.1 mg, 0.164 mmol), **4** (9.9 mg, 0.025 mmol, 0.15 equiv), **5** (12.3 mg, 0.025 mmol, 0.15 equiv), and ethyl vinyl ether (78 μL , 0.818 mmol, 5 equiv) were allowed to react in a toluene solution (818 μL , 0.2 M) containing AcOH (1.4 μL , 0.025 mmol, 0.15 equiv) for 96 h at 0 $^\circ\text{C}$ to

afford **44** (48.5 mg, 95%) as a colorless oil after column chromatography (silica gel, 19:1 to 3:1 hexanes/Et₂O). This material was determined to be 64% *ee* by chiral HPLC analysis (ChiralPak AS-H, 3% *i*PrOH in hexanes, 1 mL/min, 208 nm, *t*_R(major) = 9.7 min, *t*_R(minor) = 5.3 min).

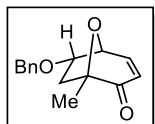
R_f = 0.28 (silica gel, 4:1 hexanes/Et₂O); **IR** (film) ν_{\max} 2931, 2858, 1703, 1252, 1112, 911, 838, 779, 735 cm⁻¹; **¹H NMR** (500 MHz, CDCl₃) δ 7.11 (d, *J* = 9.6 Hz, 1H), 6.18 (dd, *J* = 1.4, 10.1 Hz, 1H), 4.44 (d, *J* = 8.7 Hz, 1H), 4.14 (dd, *J* = 4.1, 8.7 Hz, 1H), 3.98 (d, *J* = 11.4 Hz, 1H), 3.87 (d, *J* = 11.0 Hz, 1H), 3.52 – 3.47 (m, 2H), 2.73 – 2.66 (m, 1H), 1.66 – 1.62 (m, 1H), 1.15 (t, *J* = 6.9 Hz, 3H), 0.92 (s, 9H), 0.10 (d, *J* = 0.9 Hz, 6H); **¹³C NMR** (125 MHz, CDCl₃) δ 197.2, 151.1, 127.781.2, 80.4, 66.5, 64.4, 33.5, 25.8, 18.4, 15.3, –5.4; **MS** (ESI-TOF) calcd. for C₁₆H₂₈O₄Si [M + Na⁺] 335.1649, found 335.1635; **[α]_D²⁴** = –25.1 (*c* = 3.6, CHCl₃).



(1*S*,5*R*,6*S*)-5-(((*tert*-butyldimethylsilyl)oxy)methyl)-6-ethoxy-1-methyl-8-oxabicyclo[3.2.1]oct-3-en-2-one (46**):**

According to the general procedure, **45** (104.0 mg, 0.242 mmol), **4** (19.4 mg, 0.048 mmol, 0.20 equiv), **5** (24.2 mg, 0.048 mmol, 0.20 equiv), and ethyl vinyl ether (116 μ L, 1.208 mmol, 5 equiv) were allowed to react in a toluene solution (1.2 mL, 0.2 M) containing AcOH (2.1 μ L, 0.036 mmol, 0.15 equiv) for 72 h to afford **46** (59.5 mg, 75%) as a colorless oil after column chromatography (silica gel, 19:1 to 3:1 hexanes/Et₂O). This material was determined to be 89% *ee* by chiral HPLC analysis (ChiralPak AD-H, 0.2% *i*PrOH in hexanes, 1 mL/min, 206 nm, *t*_R(major) = 8.4 min, *t*_R(minor) = 7.4 min).

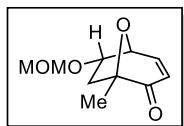
R_f = 0.34 (silica gel, 4:1 hexanes/Et₂O); **IR** (film) ν_{\max} 2934, 2859, 1699, 1279, 1122, 1082, 912, 839, 780, 736 cm⁻¹; **¹H NMR** (500 MHz, CDCl₃) δ 7.09 (d, *J* = 9.6 Hz, 1H), 6.17 (d, *J* = 9.6 Hz, 1H), 4.20 (dd, *J* = 4.3, 8.9 Hz, 1H), 3.94 (d, *J* = 11.5 Hz, 1H), 3.86 (d, *J* = 11.5 Hz, 1H), 3.50 – 3.46 (m, 2H), 2.26 (dd, *J* = 8.7, 13.3 Hz, 1H), 1.79 (dd, *J* = 4.3, 13.5 Hz, 1H), 1.42 (s, 3H), 1.14 (t, *J* = 6.9 Hz, 3H), 0.92 – 0.88 (m, 9H), 0.09 (s, 6H); **¹³C NMR** (126 MHz, CDCl₃) δ 198.5, 151.8, 127.5, 81.6, 66.4, 64.5, 40.3, 31.6, 25.8, 22.6, 20.0, 15.3, 14.1, –5.3; **MS** (ESI-TOF) calcd. for C₁₇H₃₀O₄Si [M + Na⁺] 349.1806, found 349.1794; **[α]_D²⁵** = –21.5 (*c* = 3.9, CHCl₃).



(1S,5S,6S)-6-(benzyloxy)-1-methyl-8-oxabicyclo[3.2.1]oct-3-en-2-one (47):

According to the general procedure, **31p** (100.0 mg, 0.349 mmol), **4** (21.0 mg, 0.052 mmol, 0.15 equiv), **5** (26.2 mg, 0.052 mmol, 0.15 equiv), and benzyl vinyl ether (24.5 μ L, 1.747 mmol, 5 equiv) were allowed to react in a toluene solution (1.75 mL, 0.2 M) containing AcOH (3.0 μ L, 0.052 mmol, 0.15 equiv) for 72 h to afford **47** (75.1 mg, 88%) as a colorless oil after column chromatography (silica gel, 19:1 to 3:1 hexanes/EtOAc). This material was determined to be 89% *ee* by chiral HPLC analysis (ChiralCel OB-H, 4% *i*PrOH in hexanes, 1 mL/min, 208 nm, 206 nm, t_R (major) = 29.8 min, t_R (minor) = 39.7 min). The relative stereochemistry and identification of the *endo* diastereomer was made by comparison to previously reported racemic material from reaction of **25** with benzyl vinyl ether.³⁶

R_f = 0.32 (silica gel, 4:1 hexanes/EtOAc); **IR** (film) ν_{\max} 2935, 1695, 1455, 1374, 1153, 1129, 1116, 911, 818, 738 cm^{-1} ; **¹H NMR** (500 MHz, CDCl_3) δ 7.39 – 7.30 (m, 5H), 7.16 (dd, J = 4.3, 9.8 Hz, 1H), 6.18 (d, J = 10.1 Hz, 1H), 4.75 (dd, J = 4.6, 6.0 Hz, 1H), 4.57 (d, J = 11.9 Hz, 1H), 4.53 (ddd, J = 4.6, 6.1, 9.0 Hz, 1H), 4.49 (d, J = 11.9 Hz, 1H), 2.24 (dd, J = 8.9, 13.5 Hz, 1H), 1.82 (dd, J = 4.8, 13.5 Hz, 1H), 1.43 (s, 3H); **¹³C NMR** (126 MHz, CDCl_3) δ 197.9, 150.4, 137.4, 128.6, 128.1, 127.8, 127.5, 85.6, 80.7, 74.5, 73.0, 38.6, 19.8; **MS** (ESI-TOF) calcd. for $\text{C}_{15}\text{H}_{16}\text{O}_3$ [$\text{M} + \text{Na}^+$] 267.0992, found 267.3383; $[\alpha]_D^{25} = -45.7$ ($c = 1.1$, CHCl_3).



(1S,5S,6S)-6-(methoxymethoxy)-1-methyl-8-oxabicyclo[3.2.1]oct-3-en-2-one (48):

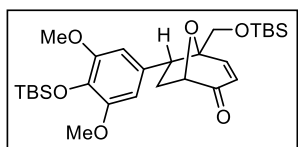
According to the general procedure, **31p** (205.0 mg, 0.716 mmol), **4** (57.5 mg, 0.143 mmol, 0.20 equiv), **5** (71.8 mg, 0.144 mmol, 0.20 equiv), and (methoxymethoxy)ethene (632 mg, 7.18 mmol, 10 equiv) were allowed to react in a toluene solution (3.6 mL, 0.2 M) containing AcOH (6.2 μ L, 0.108 mmol, 0.15 equiv) for 72 h to afford **48** (76.8 mg, 54%) as a colorless oil after column chromatography (silica gel, 9:1 to 1:1 hexanes/Et₂O). This material was determined to be 91% *ee* by chiral HPLC analysis (ChiralPak AD-H, 4% *i*PrOH in hexanes, 1 mL/min, 220 nm, t_R (major) = 11.0 min,

³⁶ Sammes, P. G.; Street, L. J.; Kirby, P. J. *Chem. Soc., Perkin Trans. 1* **1983**, 2729–2734.

$t_{\text{R}}(\text{minor}) = 15.5$ min). The relative stereochemistry and identification of the *endo* diastereomer was made by comparison of J coupling constants to ethyl ether products.

$R_f = 0.16$ (silica gel, 2:1 hexanes/Et₂O); **IR** (film) ν_{max} 2937, 1697, 1376, 1280, 1154, 1139, 1117, 1047, 915, 738 cm⁻¹; **¹H NMR** (500 MHz, CDCl₃) δ 7.22 (dd, $J = 4.6, 10.1$ Hz, 1H), 6.18 (d, $J = 9.6$ Hz, 1H), 4.81 (dd, $J = 4.6, 6.0$ Hz, 1H), 4.64 (s, 2H), 4.58 (ddd, $J = 4.8, 6.2, 9.2$ Hz, 1H), 3.37 (s, 3H), 2.32 (dd, $J = 9.2, 13.7$ Hz, 1H), 1.80 (dd, $J = 5.0, 13.7$ Hz, 1H), 1.44 (s, 3H); **¹³C NMR** (126 MHz, CDCl₃) δ 198.0, 150.8, 127.3, 97.2, 85.4, 79.5, 74.7, 56.0, 38.8, 19.7; **MS** (ESI-TOF) calcd. for C₁₀H₁₄O₄ [M + Na⁺] 221.0784, found 221.0763; $[\alpha]_D^{25} = -103.7$ ($c = 2.2$, CHCl₃).

3.8.4 Synthesis and Characterization of Product Derivatives

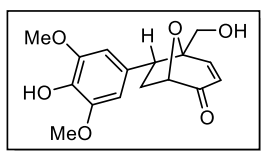


(1*S*,5*S*,6*R*)-6-(4-(((*tert*-butyldimethylsilyl)oxy)-3,5-dimethoxyphenyl)-5-(((*tert*-butyldimethylsilyl)oxy)methyl)-8-oxabicyclo[3.2.1]oct-3-en-2-one (50):

An oven-dried 1.0-dram vial was charged with pyranone substrate **43** (49.4 mg, 0.119 mmol) and styrene **49**³⁷ (29.5 mg, 1.00 mmol, 8.5 equiv). To this vial was then added a stock solution of AcOH (1.0 μ L, 1.1 mg, 0.018 mmol, 0.15 equiv) in toluene (0.59 mL, 0.2 M). To the resulting solution was added catalyst **4** (9.53 mg, 0.024 mmol, 0.20 equiv) and catalyst **5** (12.0 mg, 0.024 mmol, 0.20 equiv). No special precautions were taken to exclude air or moisture. The vial was sealed and allowed to stir for 96 h at 0 °C. The reaction was then transferred with CH₂Cl₂ to a separatory funnel containing 1N HCl (15 mL). The aqueous layer was extracted with CH₂Cl₂ (3 x 20 mL). The combined organic layers were dried over Na₂SO₄, filtered, and concentrated. The crude product was purified by column chromatography (silica gel, 95:5 to 2:1 hexanes/Et₂O) to afford **50** (7.8 mg, 12%). This material was determined to be 40% *ee* by chiral HPLC analysis (ChiralPak AD-H, 0.5% *i*PrOH in hexanes, 1 mL/min, 210 nm, $t_{\text{R}}(\text{major}) = 6.1$ min, $t_{\text{R}}(\text{minor}) = 12.9$ min).

³⁷ *tert*-Butyl(2,6-dimethoxy-4-vinylphenoxy)dimethylsilane synthesized according to: Snider, B. B.; Grabowski, J. F. *Tetrahedron* **2006**, *62*, 5171–5177.

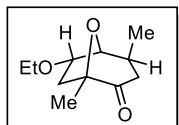
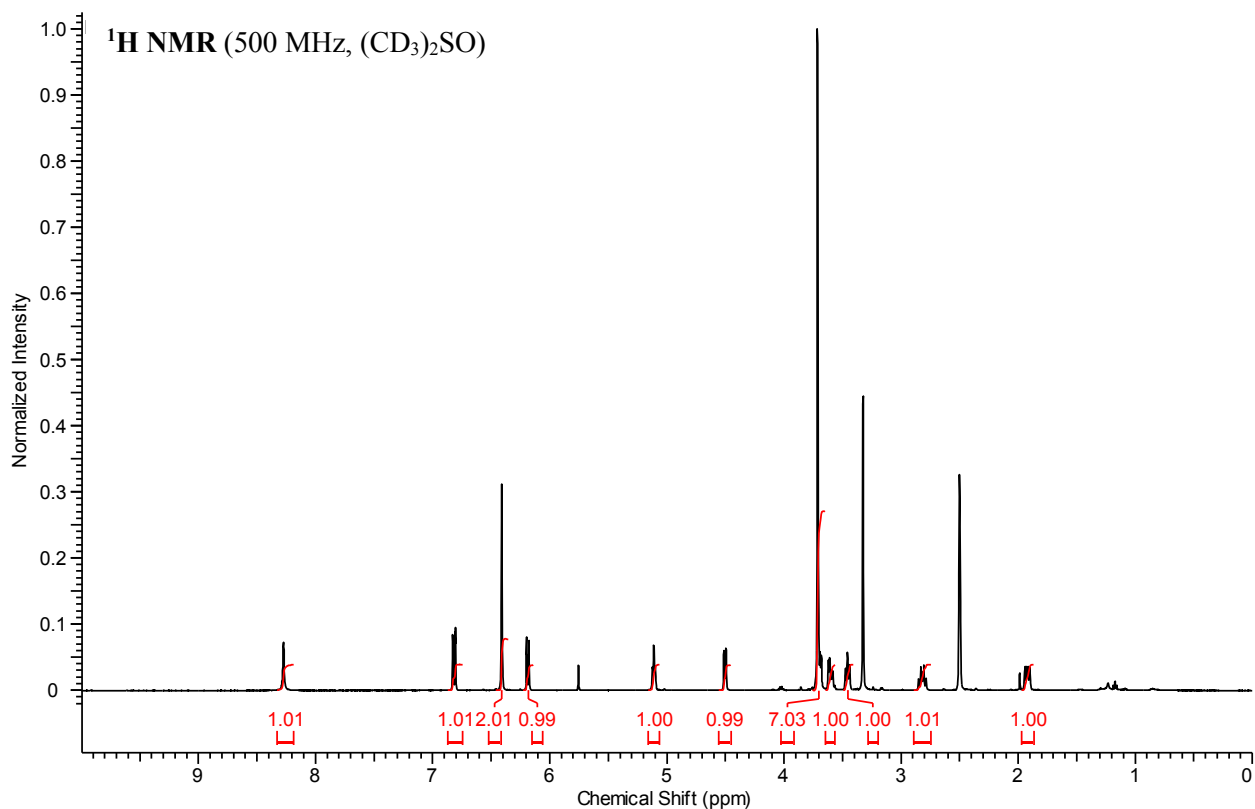
R_f = 0.61 (silica gel, 4:1 hexanes/EtOAc); IR (film) ν_{\max} 2954, 2931, 2857, 1699, 1589, 1517, 1464, 1333, 1252, 1133, 911, 839 cm^{-1} ; $^1\text{H NMR}$ (500 MHz, CDCl_3) δ 6.64 (d, J = 9.6 Hz, 1H), 6.35 (s, 2H), 6.21 (dd, J = 10.1, 1.4 Hz, 1H), 4.63 (d, J = 8.2 Hz, 1H), 3.94 (d, J = 11.4 Hz, 1H), 3.79 (d, J = 11.9 Hz, 1H), 3.75 (s, 6H), 3.62 (dd, J = 10.1, 7.3 Hz, 1H), 2.95 – 2.88 (m, 1H), 1.97 (ddd, J = 13.7, 6.9, 1.4 Hz, 1H), 1.00 (s, 9H), 0.91 (s, 9H), 0.12 (s, 6H), 0.09 (s, 6H); $^{13}\text{C NMR}$ (126 MHz, CDCl_3) δ 197.4, 153.0, 151.3, 133.7, 129.5, 127.8, 105.8, 85.7, 80.5, 63.8, 55.8, 47.6, 33.8, 25.83, 25.75, 18.7, 18.3, -4.6, -5.3, -5.4; MS (ESI-TOF) calcd. for $\text{C}_{28}\text{H}_{46}\text{O}_6\text{Si}_2$ [$\text{M} + \text{Na}^+$] 535.2906, found 535.2917.



(1*S*,5*S*,6*R*)-6-(4-hydroxy-3,5-dimethoxyphenyl)-5-(hydroxymethyl)-8-oxabicyclo[3.2.1]oct-3-en-2-one ((-)-Descurainin, **51):**

Cycloadduct **50** (41.6 mg, 0.078 mmol) was dissolved in anhydrous THF (0.43 mL, 0.18 M) in a 20-mL vial. To this solution was added by syringe TBAF (1.0 M in THF, 0.24 mL, 0.24 mmol, 3.1 equiv). The reaction was stirred under N_2 for 2 h, until TLC indicated complete disappearance of **50**. The mixture was then quenched with H_2O (2 mL). The aqueous layer was extracted with EtOAc (2 x 5 mL). Then the pooled organic layers were washed with brine (2 mL), dried over Na_2SO_4 , filtered, and concentrated. The crude product was purified by flash chromatography (silica gel, 9:1 to 2:1 hexanes/EtOAc) to afford **51** as a white solid (10.7 mg, 45%). This material was determined to be 39% *ee* by chiral SFC analysis (ChiralPak AD-H, 10% MeOH in CO_2 , 3 mL/min, 206 nm).

Spectroscopic data agree with previously reported data.^{21,22}

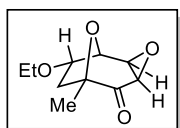


(1*S*,4*S*,5*S*,6*S*)-6-ethoxy-1,4-dimethyl-8-oxabicyclo[3.2.1]octan-2-one (52):

Copper(I) iodide (115 mg, 0.60 mmol, 2.1 equiv) was suspended in Et₂O (3.0 mL, 0.20 M relative to copper(I) iodide) in a flame-dried round-bottom flask under an atmosphere of N₂. The suspension was then cooled to 0 °C. Dropwise by syringe, methyllithium (1.1 mL of a 1.6 M solution in Et₂O, 1.76 mmol, 6.1 equiv) was added to the stirring suspension. The resultant mixture was stirred at 0 °C under an atmosphere of N₂ for 15 min in order to form Me₂CuLi. In a separate flame-dried flask, cycloadduct **33** (52 mg, 0.29 mmol) was dissolved in Et₂O. The Me₂CuLi solution was cooled to –20 °C and the **33** solution was added dropwise by syringe, under an atmosphere of N₂. An additional amount of Et₂O (0.2 mL) was used to ensure quantitative transfer of **33**. The resultant solution was warmed to 23 °C and allowed to stir under an atmosphere of N₂ for 1 h. The reaction was then quenched with sat. aq. NH₄Cl (3 mL). The layers were separated and the aqueous phase was extracted with Et₂O (3 x 10 mL). The combined organic layers were then washed with brine (5 mL) and H₂O (5 mL). The organic layer was dried

over Na₂SO₄, filtered, concentrated and purified by column chromatography (silica gel, 95:5 to 3:1 hexanes/Et₂O) to afford diastereomerically pure **52** as a colorless oil (40 mg, 70%). This material was determined to be 96% *ee* by chiral GC analysis (γ -TA, 120 °C, 7 psi, t_R (major) = 20.7 min, t_R (minor) = 24.2 min). The stereochemistry of methyl addition was assigned by analogy to ref. 11c.

R_f = 0.41 (silica gel, 2:1 hexanes/Et₂O); **IR** (film) ν_{\max} 2970, 2879, 1724, 1138, 737 cm⁻¹; **¹H NMR** (500 MHz, CDCl₃) δ 4.31 (ddd, J = 4.2, 6.3, 10.0 Hz, 1H), 4.14 (d, J = 6.3 Hz, 1H), 3.58 – 3.44 (m, 2H), 2.87 (dd, J = 7.6, 16.4 Hz, 1H), 2.57 – 2.51 (m, 1H), 2.17 (dd, J = 10.0, 13.9 Hz, 1H), 2.11 – 2.07 (m, 1H), 1.82 (dd, J = 3.9, 14.2 Hz, 1H), 1.32 (s, 3H), 1.21 (t, J = 7.1 Hz, 3H), 1.16 (d, J = 7.3 Hz, 3H); **¹³C NMR** (126 MHz, CDCl₃) δ 188.1, 84.7, 81.2, 79.5, 66.3, 41.7, 41.1, 30.6, 19.9, 19.3, 15.4; **MS** (ESI-TOF) calcd. for C₁₁H₁₈O₃ [M + H⁺] 199.1329, found 199.1330; **[α]_D²⁴** = -15.4 (c = 1.8, CHCl₃).

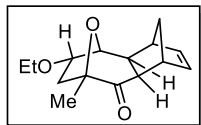


(1R,2R,4R,6S,8S)-8-ethoxy-6-methyl-3,9-dioxatricyclo[4.2.1.0^{2,4}]nonan-5-one (53**):**

Following a procedure by Marshall *et al.*,²⁴ cycloadduct **33** (40.0 mg, 0.220 mmol) was dissolved in a 3:1 mixture of MeOH (1.0 mL) and H₂O (0.34 mL, 0.16 M overall) and the flask was cooled to 0 °C. Slowly, *tert*-butyl hydroperoxide (50 μ L of a 90% aqueous solution in dodecane, 0.450 mmol, 2.05 equiv) was added to the stirring solution by syringe. Then sat. aq. NaHCO₃ (0.34 mL) was also added by syringe. The resulting reaction mixture was allowed to stir at 0 °C under an atmosphere of N₂ for 90 min. The mixture was then warmed to 23 °C and quenched with sat. aq. NaHSO₃ (2 mL). The layers were separated and the aqueous phase was extracted with EtOAc (2 x 10 mL). The combined organic layers were dried over Na₂SO₄, filtered, concentrated and purified by column chromatography (silica gel, 95:5 to 2:1 hexanes/Et₂O) to afford diastereomerically pure **53** as a white powder (28.4 mg, 65%). This material was determined to be 96% *ee* by chiral GC analysis (γ -TA, 120 °C, 7 psi, t_R (major) = 26.3 min, t_R (minor) = 38.6 min). The stereochemistry of epoxidation was assigned by analogy to ref. 24.

R_f = 0.19 (silica gel, 2:1 hexanes/Et₂O); **IR** (film) ν_{\max} 2983, 2884, 1729, 1121, 1109, 737 cm⁻¹; **¹H NMR** (500 MHz, CDCl₃) δ 4.74 (dd, J = 1.5, 5.9 Hz, 1H), 4.45 – 4.41 (m, 1H), 3.62 (dd, J = 1.7, 3.7 Hz, 1H), 3.58 – 3.47 (m, 2H), 3.37 (d, J = 3.9 Hz, 1H), 2.15 (dd, J = 9.3, 14.2 Hz, 1H), 1.76 (dd, J = 3.9, 14.2 Hz,

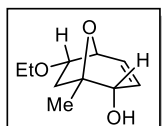
1H), 1.41 (s, 3H), 1.20 (t, $J = 7.1$ Hz, 3H); ^{13}C NMR (126 MHz, CDCl_3) δ 202.6, 86.0, 79.8, 72.6, 66.6, 50.1, 41.8, 19.5, 15.3; MS (ESI-TOF) calcd. for $\text{C}_{10}\text{H}_{14}\text{O}_4$ [$\text{M} + \text{Na}^+$] 221.0784, found 221.0782; $[\alpha]_D^{25} = -25.4$ ($c = 0.5$, CHCl_3).



(1R,4S,4aS,5S,6S,8S,9aR)-6-ethoxy-8-methyl-4,4a,5,6,7,8-hexahydro-1H-5,8-epoxy-1,4-methano-benzo[7]annulen-9(9aH)-oneone (54):

Following a procedure by Nair *et al.*,²⁵ cycloadduct **33** (24.4 mg, 0.134 mmol) was dissolved in benzene (1.3 mL, 0.10 M) in a flame-dried round-bottom flask. To this solution was added sequentially, freshly cracked (from dicyclopentadiene) and distilled cyclopentadiene (74 μL , 0.880 mmol, 6.5 equiv) and zinc chloride (49.7 mg, 0.365 mmol, 2.7 equiv). The reaction was allowed to stir at 23 $^\circ\text{C}$ under an atmosphere of N_2 for 37 h. Then, the reaction mixture was extracted with CH_2Cl_2 (3 x 10 mL). The combined organic layers were washed with sat. aq. NaHCO_3 (2 x 5 mL) and brine (2 x 5 mL). The organic phase was dried over Na_2SO_4 , filtered, concentrated and purified by column chromatography (silica gel, 95:5 to 2:1 hexanes/ Et_2O) to afford diastereomerically pure **54** as a colorless oil (26.4 mg, 80%). This material was determined to be 96% *ee* by chiral GC analysis (γ -TA, 130 $^\circ\text{C}$, 7 psi, $t_{\text{R}}(\text{major}) = 69.7$ min, $t_{\text{R}}(\text{minor}) = 65.3$ min). The stereochemistry of diene cycloaddition was assigned by analogy to ref. 25.

$R_f = 0.34$ (silica gel, 2:1 hexanes/ Et_2O); IR (film) ν_{max} 2976, 2936, 2874, 1716, 1143, 1194, 1044, 739 cm^{-1} ; ^1H NMR (500 MHz, CDCl_3) δ 6.25 (dd, $J = 2.9, 5.9$ Hz, 1H), 6.01 (dd, $J = 2.9, 5.4$ Hz, 1H), 4.3d (d, $J = 5.9$ Hz, 1H), 4.12 (dt, $J = 5.9, 9.6$ Hz, 1H), 3.55 – 3.46 (m, 2H), 3.38 (br. s, 1H), 2.97 – 2.94 (m, 2H), 2.79 (dd, $J = 3.4, 9.3$ Hz, 1H), 2.09 (dd, $J = 9.8, 13.7$ Hz, 1H), 1.59 (dd, $J = 5.9, 13.7$ Hz, 1H), 1.42 – 1.40 (m, 1H), 1.36 – 1.34 (m, 1H), 1.24 – 1.21 (m, 3H), 1.19 (s, 3H); ^{13}C NMR (126 MHz, CDCl_3) δ 136.2, 135.0, 82.1, 79.4, 77.7, 66.0, 49.6, 48.0, 47.4, 47.3, 20.3, 36.0, 19.5, 15.4; MS (ESI-TOF) calcd. for $\text{C}_{15}\text{H}_{20}\text{O}_3$ [$\text{M} + \text{H}^+$] 249.1485, found 249.1521; $[\alpha]_D^{25} = -48.3$ ($c = 0.5$, CHCl_3).

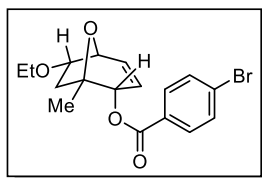


(1S,2S,5S,6S)-6-ethoxy-1-methyl-8-oxabicyclo[3.2.1]oct-3-en-2-ol (55):

Cycloadduct **33** (20.0 mg, 0.110 mmol) was dissolved in MeOH (1.1 mL, 0.10 M) in a round-bottom flask. To the resultant solution was added solid cerium trichloride heptahydrate (84.3 mg,

0.226 mmol, 2.06 equiv), then, portionwise, sodium borohydride (17.1 mg, 0.452 mmol, 4.12 equiv). The reaction was stirred at 23 °C under an atmosphere of N₂, with an outlet for venting gas evolved, for 30 min. The reaction was quenched with sat. aq. NH₄Cl (5 mL). The aqueous phase was separated and extracted with EtOAc (5 x 5 mL). The combined organic fractions were washed with brine (5 mL) and the brine layer was further extracted with EtOAc (7 x 5 mL). All combined organic layers were dried over Na₂SO₄, filtered, concentrated and purified by column chromatography (silica gel, 95:5 to 2:1 hexanes/EtOAc) to afford diastereomerically pure **55** as a white powder (19.1 mg, 95%). This material was determined to be 96% *ee* by chiral GC analysis (γ -TA, 120 °C, 7 psi, t_R (major) = 28.5 min, t_R (minor) = 32.1 min). The stereochemistry of reduction was assigned by analogy to crystallographic data from our previous report described in Chapter 2.³⁸

R_f = 0.20 (silica gel, 2:1 hexanes/EtOAc); **IR** (film) ν_{\max} 3434 (br), 2977, 2875, 1449, 1374, 1127, 1099, 1061, 889, 738, 720 cm⁻¹; **¹H NMR** (500 MHz, CDCl₃) δ 6.00 – 5.97 (m, 1H), 5.70 (d, *J* = 9.8 Hz, 1H), 4.41 (t, *J* = 4.6 Hz, 1H), 4.37 (d, *J* = 5.4 Hz, 1H), 4.21 – 4.17 (m, 1H), 3.55 – 3.44 (m, 2H), 2.19 (dd, *J* = 6.3, 13.2 Hz, 1H), 1.91 (dd, *J* = 9.0, 12.9 Hz, 1H), 1.70 (d, *J* = 6.8 Hz, 1H), 1.38 (s, 3H), 1.20 (td, *J* = 1.0, 7.1 Hz, 3H); **¹³C NMR** (126 MHz, CDCl₃) δ 130.6, 129.1, 82.4, 81.9, 74.3, 74.1, 65.9, 35.5, 24.5, 15.4; **MS** (ESI-TOF) calcd. for C₁₀H₁₆O₃ [M + Na⁺] 207.0992, found 207.0985; **[α]_D²⁴** = -45.2 (*c* = 0.9, CHCl₃).



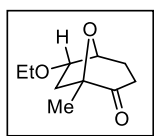
(1*S*,2*S*,5*S*,6*S*)-6-ethoxy-1-methyl-8-oxabicyclo[3.2.1]oct-3-en-2-yl 4-bromobenzoate (56**):**

Alcohol **55** (5.5 mg, 0.030 mmol) was dissolved in CH₂Cl₂ (750 μ L, 0.40 M) in a 2.0-dram vial. To this solution was added sequentially *para*-bromobenzoyl chloride (8.7 mg, 0.040 mmol, 1.33 equiv), pyridine (3.6 μ L, 0.045 mmol, 1.50 equiv), and DMAP (5.3 mg, 0.043 mmol, 1.45 equiv). The reaction mixture was stirred at 23 °C for 21 h. The solution was then diluted with EtOAc (10 mL). The organic solution was washed sequentially with 1N HCl (2 x 10 mL), sat. aq. NaHCO₃ (10 mL), and brine (10 mL). The organic layer was dried over Na₂SO₄, filtered, concentrated and purified by column

³⁸ Burns, N. Z.; Witten, M. R.; Jacobsen, E. N. *J. Am. Chem. Soc.* **2011**, *133*, 14578–14581.

chromatography (silica gel, 95:5 to 4:1 hexanes/Et₂O) to afford diastereomerically pure **56** as a colorless oil (10.0 mg, 91%). This material was determined to be 96% *ee* by chiral HPLC analysis (ChiralCel OD-H, 2% *i*PrOH in hexanes, 1 mL/min, 244 nm, *t*_R(major) = 8.7 min, *t*_R(minor) = 14.7 min).

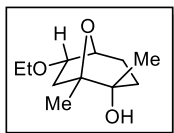
R_f = 0.23 (silica gel, 2:1 hexanes/Et₂O); **IR** (film) ν_{\max} 1722, 1591, 1268, 1101, 757, 734 cm⁻¹; **¹H NMR** (500 MHz, CDCl₃) δ 7.91 – 7.88 (m, 2H), 7.61 – 7.58 (m, 2H), 6.12 (ddd, *J* = 1.7, 4.0, 9.9 Hz, 1H), 5.79 (dd, *J* = 2.0, 9.8 Hz, 1H), 5.74 (br. s, 1H), 4.52 (t, *J* = 4.6 Hz, 1H), 4.29 – 4.25 (m, 1H), 3.60 – 3.48 (m, 2H), 2.47 (dd, *J* = 6.6, 12.9 Hz, 1H), 2.08 (ddd, *J* = 1.0, 9.3, 13.2 Hz, 1H), 1.36 (s, 3H), 1.23 (t, *J* = 7.1 Hz, 3H); **¹³C NMR** (126 MHz, CDCl₃) δ 132.3, 131.8, 131.2, 125.5, 82.5, 80.3, 76.5, 74.5, 66.1, 37.0, 24.6, 15.5; **MS** (ESI-TOF) calcd. for C₁₇H₁₉BrO₄ [M + Na⁺] 1:1 389.0364 & 391.0344, found 1:1 389.0307 & 391.0288; **[α]_D²⁴** = -4.4 (*c* = 1.7, CHCl₃).



(1S,5S,6S)-6-ethoxy-1-methyl-8-oxabicyclo[3.2.1]octan-2-one (57):

Following a procedure by Archer *et al.*,²⁶ cycloadduct **33** (278 mg, 1.54 mmol) was dissolved in CHCl₃ (9.6 mL, 0.16 M) in a flame-dried round-bottom flask. To this solution was added sequentially, diphenylsilane (0.34 mL, 1.83 mmol, 1.2 equiv), zinc chloride (21 mg, 0.16 mmol, 0.10 equiv), and Pd(PPh₃)₄ (37 mg, 0.03 mmol, 0.02 equiv). The solution was stirred at 23 °C for 4 h, then filtered through a plug of silica gel, eluting with CH₂Cl₂. Purification by column chromatography (silica gel, 95:5 to 2:1 hexanes/Et₂O) afforded diastereomerically pure **57** as a pale yellow oil (233 mg, 82%). This material was determined to be 96% *ee* by chiral GC analysis (γ -TA, 120 °C, 7 psi, *t*_R(major) = 19.6 min, *t*_R(minor) = 28.7 min).

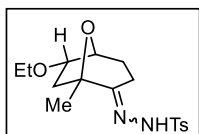
R_f = 0.35 (silica gel, 2:1 hexanes/Et₂O); **IR** (film) ν_{\max} 2982, 1725, 1125, 1098 cm⁻¹; **¹H NMR** (500 MHz, CDCl₃) δ 4.46 (t, *J* = 5.6 Hz, 1H), 4.29 (dd, *J* = 3.9, 6.3, 10.3 Hz, 1H), 3.56 – 3.43 (m, 2H), 2.74 – 2.67 (m, 1H), 2.37 (ddd, *J* = 1.0, 7.8, 17.1 Hz, 1H), 2.24 – 2.08 (m, 3H), 1.80 (dd, *J* = 3.9, 14.2 Hz, 1H), 1.31 (s, 3H), 1.19 (t, *J* = 6.8 Hz, 3H); **¹³C NMR** (126 MHz, CDCl₃) δ 208.7, 84.8, 79.5, 76.0, 66.2, 42.2, 33.2, 26.1, 19.4, 15.4; **MS** (ESI-TOF) calcd. for C₁₀H₁₆O₃ [M + Na⁺] 207.0992, found 207.0972; **[α]_D²⁵** = -12.0 (*c* = 8.5, CHCl₃).



(1S,2S,5S,6S)-6-ethoxy-1,2-dimethyl-8-oxabicyclo[3.2.1]octan-2-ol (58):

Ketone **57** (33.7 mg, 0.183 mmol) was dissolved in Et₂O (1.6 mL, 0.11 M) in a flame-dried round-bottom flask and the resultant solution was cooled to 0 °C and stirred under an atmosphere of N₂. Dropwise by syringe, methylmagnesium iodide (111 μL of a 3.0 M solution in Et₂O, 0.330 mmol, 1.8 equiv) was added to the cooled reaction mixture. The resultant solution was allowed to stir for 90 min at 0 °C under an atmosphere of N₂. The reaction was quenched with sat. aq. NH₄Cl (1 mL) and warmed to 23 °C. The phases were separated and the aqueous layer was extracted with EtOAc (3 x 40 mL). The combined organic phases were dried over Na₂SO₄, filtered, concentrated and purified by column chromatography (silica gel, 95:5 to 2:1 hexanes/EtOAc) to afford diastereomerically pure **58** as a white powder (29.4 mg, 80%). This material was determined to be 96% *ee* by chiral GC analysis (γ -TA, 120 °C, 7 psi, t_R (major) = 22.6 min, t_R (minor) = 24.8 min). The stereochemistry of methyl addition was assigned by analogy to ref. 26.

R_f = 0.30 (silica gel, 2:1 hexanes/EtOAc); **IR** (film) ν_{\max} 3445, 2973, 2944, 2871, 1374, 1353, 1128, 1081, 1009, 978 cm⁻¹; **¹H NMR** (500 MHz, CDCl₃) δ 4.19 – 4.15 (m, 2H), 3.55 – 3.41 (m, 2H), 2.09 (dd, J = 3.9, 13.7 Hz, 1H), 1.96 (dd, J = 9.0, 11.5 Hz, 1H), 1.91 – 1.86 (m, 1H), 1.78 – 1.74 (m, 2H), 1.60 – 1.56 (m, 1H), 1.36 (s, 3H), 1.25 (s, 3H), 1.19 (t, J = 6.8 Hz, 3H); **¹³C NMR** (126 MHz, CDCl₃) δ 83.7, 80.0, 76.2, 72.2, 65.9, 39.8, 34.6, 25.5, 22.8, 20.5, 15.5; **MS** (ESI-TOF) calcd. for C₁₁H₂₀O₃ [M + Na⁺] 223.1305, found 223.1270; **[α]_D²⁵** = +10.0 (c = 0.4, CHCl₃).

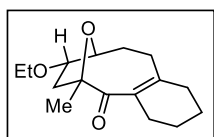


N'-((1S,5S,6S)-6-ethoxy-1-methyl-8-oxabicyclo[3.2.1]octan-2-ylidene)-4-methylbenzenesulfonohydrazide (59):

Ketone **57** (40.0 mg, 0.183 mmol) was dissolved in a 1:1 mixture of THF (0.68 mL) and H₂O (0.68 mL, 0.16 M overall) in a 20 mL vial. To the resultant solution was added *p*-toluenesulfonyl hydrazide (61.2 mg, 0.329 mmol, 1.5 equiv) and the mixture was stirred at 23 °C for 90 min. The reaction mixture was then concentrated and purified by column chromatography (silica gel, 95:5 to 2:1 hexanes/EtOAc) to afford diastereomerically pure **59** as a colorless oil (76.1 mg, 99%). This material was determined to be 96% *ee*

by chiral HPLC analysis (ChiralCel OD-H, 10% *i*PrOH in hexanes, 1 mL/min, 210 nm, $t_R(\text{major}) = 11.0$ min, $t_R(\text{minor}) = 15.5$ min).

$R_f = 0.29$ (silica gel, 2:1 hexanes/EtOAc); **IR** (film) ν_{max} 3213, 2981, 1348, 1167, 731, 669 cm^{-1} ; **$^1\text{H NMR}$** (500 MHz, CDCl_3) δ 7.82 (d, $J = 8.3$ Hz, 2H), 7.62 (s, 1H), 7.30 (d, $J = 7.8$ Hz, 2H), 4.35 (t, $J = 5.4$ Hz, 1H), 4.19 (ddd, $J = 3.9, 6.3, 10.3$ Hz, 1H), 3.50 – 3.37 (m, 2H), 2.45 – 2.41 (m, 4H), 2.37 – 2.29 (m, 1H), 2.11 (dd, $J = 10.3, 13.7$ Hz, 1H), 1.99 (dd, $J = 8.3, 13.7$ Hz, 1H), 1.85 – 1.80 (m, 1H), 1.69 (dd, $J = 3.4, 13.7$ Hz, 1H), 1.37 (s, 3H), 1.16 (t, $J = 6.8$ Hz, 3H); **$^{13}\text{C NMR}$** (126 MHz, CDCl_3) δ 159.2, 144.0, 135.1, 129.4, 128.1, 81.9, 79.3, 76.0, 66.1, 43.7, 24.6, 21.7, 21.6, 19.6, 15.4; **MS** (ESI-TOF) calcd. for $\text{C}_{17}\text{H}_{24}\text{N}_2\text{O}_4\text{S}$ [$\text{M} + \text{H}^+$] 353.1530, found 353.1510; $[\alpha]_D^{25} = -0.7$ ($c = 6.1$, CHCl_3).

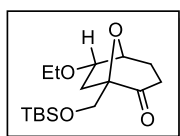


(6S,8S,9S)-8-ethoxy-3,4,6,7,8,9,10,11-octahydro-1H-6,9-epoxybenzo[9]annulen-5(2H)-one (60):

Following a procedure by Gampe *et al.*,²⁷ ketone **57** (29.5 mg, 0.160 mmol) was dissolved in THF (8.0 mL, 0.02 M) in a flame-dried round-bottom flask. To this solution was added cyclohexenylphenyl iodonium tetrafluoroborate and the flask was cooled to -78 °C. Over the course of 5 min, KOEt_3 (1.6 mL of a 0.25 M solution in THF, 0.400 mmol, 2.5 equiv) was allowed to stream down the sides of the flask as the solution was stirred under an atmosphere of N_2 . The mixture continued to stir at -78 °C for 30 min before being warmed to 23 °C and stirred for an additional 25 min. The reaction mixture was then partitioned between Et_2O (10 mL) and phosphate buffer (1M, pH = 7.0, 10 mL). The aqueous layer was extracted with Et_2O (2 x 10 mL) and the combined organic phases were dried over Na_2SO_4 , filtered, concentrated and purified by column chromatography (silica gel, 95:5 to 2:1 hexanes/ Et_2O) to afford **60** and its deconjugated enone isomer. The mixture was then dissolved in MeOH (2 mL) and treated with NaOMe (1 mL of a 1M solution in MeOH). This mixture was stirred in a pressure tube at 50 °C for 10 hours, then quenched with H_2O (5 mL) and cooled to 23 °C. The aqueous phase was extracted with Et_2O (3 x 15 mL) and the pooled organic layers were dried over Na_2SO_4 , filtered, concentrated and purified by column chromatography as before to afford conjugated **60** as a colorless oil (30.1 mg, 72%). This material was determined to be 96% *ee* by chiral

HPLC analysis (ChiralPak AS-H, 2% *i*PrOH in hexanes, 1 mL/min, 248 nm, $t_R(\text{major}) = 6.6$ min, $t_R(\text{minor}) = 6.1$ min).

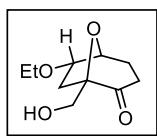
$R_f = 0.30$ (silica gel, 2:1 hexanes/EtOAc); **IR** (film) ν_{max} 2936, 1677, 1121, 739, 669 cm^{-1} ; **$^1\text{H NMR}$** (500 MHz, CDCl_3) δ 4.22 – 4.14 (m, 2H), 3.54 – 3.35 (m, 2H), 2.54 – 2.49 (m, 2H), 2.32 – 2.28 (m, 1H), 2.21 – 2.11 (m, 3H), 1.99 – 1.89 (m, 2H), 1.76 – 1.49 (m, 6H), 1.27 (s, 3H), 1.17 (t, $J = 6.9$ Hz, 3H); **$^{13}\text{C NMR}$** (126 MHz, CDCl_3) δ 217.1, 86.2, 80.6, 80.2, 65.7, 40.0, 34.4, 31.7, 30.0, 25.6, 23.3, 22.6, 22.3, 15.4; **MS** (ESI-TOF) calcd. for $\text{C}_{16}\text{H}_{24}\text{O}_3$ [$\text{M} + \text{H}^+$] 265.1798, found 265.1832; $[\alpha]_D^{24} = +136.3$ ($c = 0.6$, CHCl_3).



(1R,5S,6S)-1-(((*tert*-butyldimethylsilyl)oxy)methyl)-6-ethoxy-8-oxabicyclo[3.2.1]octan-2-one (61):

Reaction of **42** (0.100 g, 0.322 mmol), SiH_2Ph_2 (72 μL , 0.388 mmol, 1.2 equiv), ZnCl_2 (4.4 mg, 0.03 mmol, 0.10 equiv) and $\text{Pd}(\text{PPh}_3)_4$ (6.0 mg, 5 μmol) in CHCl_3 (2.0 mL, 0.16 M) according to **57** above afforded **61** as a colorless oil after column chromatography (silica gel, 9:1 to 4:1 hexanes/ Et_2O) as a single diastereomer (67 mg, 66%).

$R_f = 0.32$ (silica gel, 4:1 hexanes/ Et_2O); **IR** (film) ν_{max} 2955, 2929, 2857, 1724, 1254, 1110, 839, 779, 739 cm^{-1} ; **$^1\text{H NMR}$** (400 MHz, CDCl_3) δ 4.52 (t, $J = 5.9$ Hz, 1H), 4.23 – 4.18 (m, 1H), 3.83 (s, 2H), 3.58 – 3.43 (m, 2H), 2.69 – 2.60 (m, 1H), 2.51 (dd, $J = 9.9, 13.7$ Hz, 1H), 2.40 (dddd, $J = 0.8, 3.9, 8.2, 16.8$ Hz, 1H), 2.25 – 2.09 (m, 2H), 1.56 (dd, $J = 3.9, 13.7$ Hz, 1H), 1.21 (t, $J = 7.0$ Hz, 3H), 0.89 (s, 9H), 0.07 – 0.05 (m, 6H); **$^{13}\text{C NMR}$** (100 MHz, CDCl_3) δ 209.1, 87.4, 79.1, 75.5, 66.2, 62.0, 35.8, 33.6, 25.9, 24.3, 18.4, 15.4, –5.3, –5.5; **MS** (ESI-TOF) calcd. for $\text{C}_{16}\text{H}_{30}\text{O}_4\text{Si}$ [$\text{M} + \text{H}^+$] 315.1986, found 315.1987; $[\alpha]_D^{24} = -1.2$ ($c = 0.5$, CHCl_3).

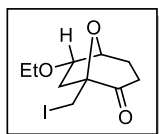


(1R,5S,6S)-6-ethoxy-1-(hydroxymethyl)-8-oxabicyclo[3.2.1]octan-2-one (76):

Following a procedure by Ohmori,²⁸ ketone **61** (17.6 mg, 0.056 mmol) was dissolved in a 2:1 mixture of THF (0.42 mL) and H_2O (0.21 mL, 0.09M overall) in a 20 mL vial. To this solution was added sequentially acetic acid (200 μL , 3.49 mmol, 62 equiv) and conc. HCl (40 μL , 0.48 mmol, 8.6 equiv). The reaction mixture was stirred at 23 $^\circ\text{C}$ for 1 h then neutralized with sat. aq. NaHCO_3 . The phases were

separated and the aqueous layer was extracted with EtOAc (3 x 5mL). The combined organic layers were dried over Na₂SO₄, filtered, concentrated and purified by column chromatography (silica gel, 10:1 to 1:1 hexanes/EtOAc) to afford diastereomerically pure **76** as a colorless oil (10.7 mg, 98%).

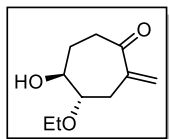
R_f = 0.28 (silica gel, 1:1 hexanes/EtOAc); **IR** (film) ν_{\max} 1721, 1113, 1044, 738, 669 cm⁻¹; **¹H NMR** (400 MHz, CDCl₃) δ 4.54 (t, *J* = 5.3 Hz, 1H), 4.28 (ddd, *J* = 3.9, 6.2, 10.1 Hz, 1H), 3.83 – 3.71 (m, 2H), 3.60 – 3.45 (m, 2H), 2.75 (dt, *J* = 8.9, 17.4 Hz, 1H), 2.44 – 2.37 (m, 2H), 2.29 – 2.24 (m, 1H), 2.21 – 2.13 (m, 2H), 1.74 (dd, *J* = 3.9, 14.0 Hz, 1H), 1.22 (t, *J* = 7.2 Hz, 3H); **¹³C NMR** (100 MHz, CDCl₃) δ 209.6, 86.1, 78.9, 76.2, 66.4, 63.3, 37.5, 33.7, 25.6, 15.4; **MS** (ESI-TOF) calcd. for C₁₀H₁₆O₄ [M + H⁺] 201.1121, found 201.1120; **[α]_D²³** = -1.4 (*c* = 0.1, CHCl₃).



(1S,5S,6S)-6-ethoxy-1-(iodomethyl)-8-oxabicyclo[3.2.1]octan-2-one (62**):**

Alcohol **76** (25.9 mg, 0.129 mmol) was dissolved in benzene (3.2 mL, 0.04 M) in a thick-walled pressure tube. To the resultant solution was added sequentially, triphenylphosphine (94.3 mg, 0.360 mmol, 2.8 equiv), imidazole (23.5 mg, 0.345 mmol, 2.7 equiv), and iodine (72.1 mg, 0.284 mmol, 2.2 equiv). The tube was sealed and the reaction mixture was stirred at 80 °C for 2 h. The mixture was then cooled to 23 °C and quenched with sat. aq. Na₂S₂O₃ (10 mL). The aqueous layer was extracted with CH₂Cl₂ (3 x 20 mL) and the combined organic layers were dried over Na₂SO₄, filtered, concentrated and purified by column chromatography (silica gel, 95:5 to 4:1 hexanes/EtOAc) to afford diastereomerically pure **62** as a colorless oil (39.3 mg, 98%).

R_f = 0.48 (silica gel, 4:1 hexanes/EtOAc); **IR** (film) ν_{\max} 2973, 2879, 1724, 1105, 738, 719 cm⁻¹; **¹H NMR** (500 MHz, CDCl₃) δ 4.57 (t, *J* = 5.9 Hz, 1H), 4.28 (ddd, *J* = 4.2, 6.2, 10.1 Hz, 1H), 3.58 – 3.45 (m, 3H), 3.37 (d, *J* = 10.7 Hz, 1H), 2.72 (dt, *J* = 8.7, 17.2 Hz, 1H), 2.48 – 2.43 (m, 1H), 2.40 (dd, *J* = 10.3, 14.2 Hz, 1H), 2.27 – 2.14 (m, 2H), 1.81 (dd, *J* = 4.1, 14.2 Hz, 1H), 1.21 (t, *J* = 6.9 Hz, 3H); **¹³C NMR** (126 MHz, CDCl₃) δ 84.7, 79.2, 76.3, 66.3, 40.7, 33.6, 25.1, 15.4, 7.5; **MS** (ESI-TOF) calcd. for C₁₀H₁₅IO₃ [M + H⁺] 311.0139, found 311.0151; **[α]_D²⁴** = +3.6 (*c* = 0.1, CHCl₃).



(4*S*,5*S*)-4-ethoxy-5-hydroxy-2-methylenecycloheptanone (63):

Iodide **62** (39.3 mg, 0.13 mmol) was dissolved in MeOH (4.1 mL, 0.03 M) in a thick-walled pressure tube. To the resultant solution was added zinc powder (36.8 mg, 0.56 mmol, 4.4 equiv),³⁹ and the tube was sealed. The suspension was stirred at 65 °C for 6 h before it was cooled to 23 °C and quenched with solid NH₄Cl. This material was then filtered through a plug of celite, concentrated and purified by column chromatography (silica gel, 95:5 to 2:1 hexanes/EtOAc) to afford diastereomerically pure **63** as a colorless oil (16.9 mg, 74%). This material was determined to be 86% *ee* by chiral GC analysis (γ -TA, 120 °C, 7 psi, t_R (major) = 62.0 min, t_R (minor) = 68.3 min).

R_f = 0.19 (silica gel, 2:1 hexanes/EtOAc); **IR** (film) ν_{\max} 3460 (br), 2924, 1686, 1614, 1106, 741, 669 cm⁻¹; **¹H NMR** (500 MHz, CDCl₃) δ 6.15 (d, J = 2.0 Hz, 1H), 5.42 (s, 1H), 3.82 – 3.76 (m, 1H), 3.69 – 3.64 (m, 1H), 3.53 – 3.45 (m, 1H), 3.11 (ddd, J = 2.0, 8.4, 10.6 Hz, 1H), 2.86 – 2.80 (m, 2H), 2.65 – 2.60 (m, 2H), 2.49 – 2.43 (m, 1H), 2.21 – 2.15 (m, 1H), 1.63 – 1.55 (m, 1H), 1.27 – 1.24 (m, 3H); **¹³C NMR** (126 MHz, CDCl₃) δ 201.4, 142.1, 125.9, 84.6, 75.5, 64.6, 37.6, 34.2, 27.3, 15.4; **MS** (ESI-TOF) calcd. for C₁₀H₁₆O₃ [M + H⁺] 207.0992, found 207.3023; $[\alpha]_D^{24}$ = -9.6 (c = 1.6, CHCl₃).

3.8.5 Computational Procedures and Results

Calculations were performed at Harvard University using Gaussian 09⁴⁰ at the B3LYP⁴¹ level of

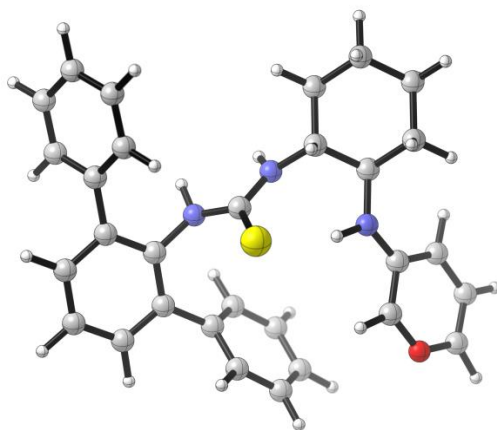
³⁹ Zinc activated according to: Wender, P. A.; Buschmann, N.; Cardin, N. B.; Jones, L. R.; Kan, C.; Kee, J.-M.; Kowalski, J. A.; Longcore, K. E. *Nat. Chem.* **2011**, 3, 615–619.

⁴⁰ Gaussian 09, Revision A.1, Frisch, M. J.; Trucks, G. W.; Schlegel, H. B.; Scuseria, G. E.; Robb, M. A.; Cheeseman, J. R.; Scalmani, G.; Barone, V.; Mennucci, B.; Petersson, G. A.; Nakatsuji, H.; Caricato, M.; Li, X.; Hratchian, H. P.; Izmaylov, A. F.; Bloino, J.; Zheng, G.; Sonnenberg, J. L.; Hada, M.; Ehara, M.; Toyota, K.; Fukuda, R.; Hasegawa, J.; Ishida, M.; Nakajima, T.; Honda, Y.; Kitao, O.; Nakai, H.; Vreven, T.; Montgomery, Jr., J. A.; Peralta, J. E.; Ogliaro, F.; Bearpark, M.; Heyd, J. J.; Brothers, E.; Kudin, K. N.; Staroverov, V. N.; Kobayashi, R.; Normand, J.; Raghavachari, K.; Rendell, A.; Burant, J. C.; Iyengar, S. S.; Tomasi, J.; Cossi, M.; Rega, N.; Millam, N. J.; Klene, M.; Knox, J. E.; Cross, J. B.; Bakken, V.; Adamo, C.; Jaramillo, J.; Gomperts, R.; Stratmann, R. E.; Yazyev, O.; Austin, A. J.; Cammi, R.; Pomelli, C.; Ochterski, J. W.; Martin, R. L.; Morokuma, K.; Zakrzewski, V. G.; Voth, G. A.; Salvador, P.; Dannenberg, J. J.; Dapprich, S.; Daniels, A. D.; Farkas, Ö.; Foresman, J. B.; Ortiz, J. V.; Cioslowski, J.; Fox, D. J. Gaussian, Inc., Wallingford CT, 2009.

⁴¹ B3LYP = Becke-3-Lee-Yang-Parr density functional theory: (a) Becke, A. D. *J. Chem. Phys.* **1993**, 98, 1372–1377. (b) Lee, C.; Yang, W.; Parr, R. G. *Phys. Rev. B* **1988**, 37, 785–789.

density functional theory with the 6-31G(d)⁴² basis set. Relative energies are for uncorrected electronic energy differences.

4•25 (major):



E(RB3LYP): -1798.71062514

Zero-point correction: 0.542101 (Hartree/Particle)

Thermal correction to Energy: 0.572191

Thermal correction to Enthalpy: 0.573135

Thermal correction to Gibbs Free Energy: 0.477708

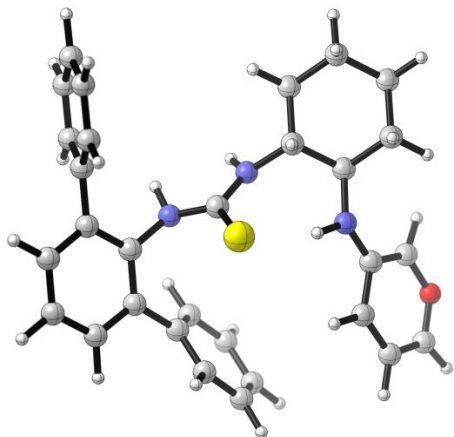
Cartesian coordinates:

C	-3.03509900	3.54186600	-0.60395600	H	-2.78235100	3.57867900	-1.67187800
C	-2.29236200	2.34736300	0.02795500	H	-4.11932800	3.38265600	-0.54938200
C	-0.75921400	2.56615600	-0.04615600	H	-0.58414400	3.82591800	1.70692100
C	-0.36975200	3.89228200	0.62856900	H	0.71181100	4.03402000	0.52553300
C	-1.13092900	5.08462000	0.03025400	H	-0.86140200	5.99912500	0.56964300
C	-2.64848700	4.86308100	0.07663800	H	-0.81376200	5.23046900	-1.01120100
H	-2.57047300	2.26473500	1.09082900	H	-2.98708100	4.85133100	1.12287000

⁴² (a) Ditchfield, R.; Hehre, W. J.; Pople, J. A. *J. Chem. Phys.* **1971**, *54*, 724–728. (b) Hehre, W. J.; Ditchfield, R.; Pople, J. A. *J. Chem. Phys.* **1972**, *56*, 2257–2261. (c) Hariharan, P. C.; Pople, J. A. *Theor. Chim. Acta.* **1973**, *28*, 213–222.

H	-3.17057900	5.69422400	-0.40964900	S	0.21766900	0.03104100	-1.72270800
H	-0.47515000	2.60077700	-1.10376300	H	-1.83546300	0.67092100	-1.18844600
N	-0.00807800	1.46115200	0.55245100	C	4.28321900	0.22499900	0.06369000
C	0.59782800	0.43891200	-0.12229400	C	4.55832000	0.70092800	1.35652500
N	1.52288700	-0.23162000	0.62140700	C	4.61778300	1.02661700	-1.03673800
C	2.30419700	-1.34470900	0.15880800	C	5.14898000	1.95215500	1.54389500
C	3.66256800	-1.12062200	-0.13433200	H	4.34454800	0.06952800	2.21723000
C	1.72040500	-2.61863800	0.01392000	C	5.20975100	2.27671900	-0.84826900
C	4.43129300	-2.18417400	-0.62126400	H	4.40720400	0.66778000	-2.04017200
C	2.52335200	-3.65311800	-0.48954900	C	5.47457100	2.74354200	0.44072800
C	3.86154200	-3.44092300	-0.80956900	H	5.37013100	2.29989600	2.54941400
H	5.47971000	-2.01516700	-0.84775500	H	5.46700600	2.88504700	-1.71097100
H	2.09240900	-4.64385500	-0.59739000	H	5.94126000	3.71391900	0.58459400
H	4.46510700	-4.26106400	-1.18692300	C	0.30922200	-2.92203900	0.38202800
H	0.24428900	1.58104600	1.52763700	C	-0.20732000	-2.59603800	1.64658200
H	1.95790800	0.30419500	1.36590400	C	-0.51515600	-3.62391100	-0.51343400
N	-2.60860700	1.07733500	-0.63231700	C	-1.50479200	-2.96084000	2.00586500
C	-3.66105800	0.28967800	-0.36615400	H	0.42410800	-2.08264100	2.36503000
C	-4.76927300	0.64002100	0.45704900	C	-1.81208500	-3.99416900	-0.15424100
C	-3.71509100	-1.00638400	-0.92572400	H	-0.13256700	-3.87803800	-1.49764600
H	-4.79803900	1.60965400	0.94005600	C	-2.31237700	-3.66339900	1.10812200
C	-5.79500600	-1.48009800	0.01801000	H	-1.87444400	-2.72191400	2.99977800
H	-6.54329400	-2.25907600	0.05807300	H	-2.42325600	-4.55847700	-0.85442900
C	-5.82365100	-0.24880900	0.63751000	H	-3.31183500	-3.97581500	1.40054900
H	-6.67527300	0.01304900	1.25540300	H	-2.93269800	-1.45220900	-1.52775600
O	-4.74359000	-1.80748300	-0.73204500				

4•25 (minor):



E(RB3LYP): -1798.70959964

Zero-point correction: 0.542076 (Hartree/Particle)

Thermal correction to Energy: 0.572188

Thermal correction to Enthalpy: 0.573133

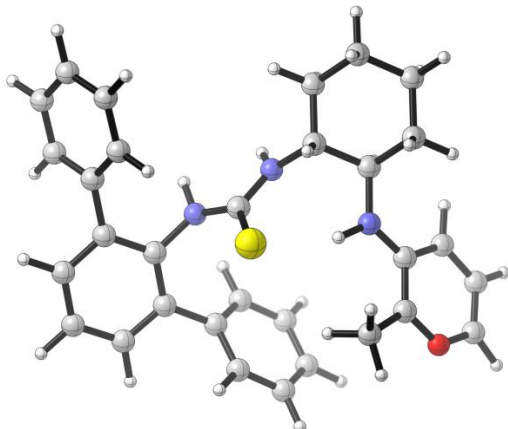
Thermal correction to Gibbs Free Energy: 0.477421

Cartesian coordinates:

C	-3.04638200	3.51584300	-0.60366400	H	-0.88802900	5.95737600	0.62727800
C	-2.31464700	2.31296400	0.02538100	H	-0.81906000	5.20519200	-0.96076100
C	-0.78051300	2.53027200	-0.02259600	H	-3.02265000	4.80595900	1.13833800
C	-0.40013400	3.84932500	0.67115400	H	-3.18374100	5.66597100	-0.38722400
C	-1.15103100	5.04895400	0.07456800	H	-0.48059700	2.57477700	-1.07546500
C	-2.66934700	4.82897600	0.09717200	N	-0.03919900	1.41916500	0.57791600
H	-2.60778000	2.21836000	1.08380200	C	0.58598900	0.41044000	-0.10105500
H	-2.77736900	3.56442000	-1.66709200	N	1.51462200	-0.25507400	0.64206000
H	-4.13191100	3.35806200	-0.56848400	C	2.33469600	-1.33224000	0.15866900
H	-0.63064600	3.77200200	1.74546600	C	3.67846100	-1.04976400	-0.15149400
H	0.68297100	3.99090500	0.58555000	C	1.79980000	-2.62624200	0.00631000

C	4.48201600	-2.07602600	-0.66171900	C	4.55818500	1.13090200	-1.04833100
C	2.63669200	-3.62219200	-0.51959100	C	5.04539400	2.07438900	1.53431900
C	3.96045700	-3.35262400	-0.85574100	H	4.30878700	0.16330200	2.20425700
H	5.51953800	-1.86280600	-0.90074200	C	5.10352800	2.40171800	-0.85743900
H	2.24419400	-4.62812400	-0.63308900	H	4.36443700	0.76505500	-2.05261400
H	4.59109400	-4.14372100	-1.25051500	C	5.34607100	2.87762200	0.43255000
H	0.21393200	1.54121900	1.55269700	H	5.25048100	2.42930600	2.54074700
H	1.92568300	0.27399200	1.40458100	H	5.34190900	3.01914000	-1.71911400
N	-2.62468000	1.05119300	-0.65298700	H	5.77672900	3.86423900	0.57838000
C	-3.68482100	0.26642300	-0.41704300	C	0.40667100	-2.99005700	0.38798800
C	-3.77280900	-1.04372200	-0.98236200	C	-0.10592700	-2.70058200	1.66303700
C	-4.77599800	0.64571200	0.38747900	C	-0.39893500	-3.71700200	-0.50419700
H	-2.94407400	-1.40958700	-1.58159300	C	-1.38044800	-3.12670200	2.03594700
C	-5.90691600	-1.36900800	0.04232700	H	0.51246200	-2.16790400	2.37884300
H	-6.82454700	-1.87858200	0.30348400	C	-1.67252300	-4.14856000	-0.13064300
C	-4.88005900	-1.84327900	-0.75414000	H	-0.01965100	-3.94335700	-1.49645900
H	-4.95108100	-2.83752000	-1.17959500	C	-2.16843400	-3.85542800	1.14197400
O	-5.81396300	-0.16259500	0.58020700	H	-1.74660400	-2.91440500	3.03714700
S	0.22087700	0.01055100	-1.70652800	H	-2.26600700	-4.73411200	-0.82897300
H	-1.84499800	0.64069500	-1.19661300	H	-3.14907300	-4.21355600	1.44533500
C	4.24808200	0.31738800	0.05051600	H	-4.89200800	1.58735500	0.90405800
C	4.50122900	0.80272000	1.34433000				

4•31 (major):



E(RB3LYP): -1838.03924556

Zero-point correction: 0.569780 (Hartree/Particle)

Thermal correction to Energy: 0.601491

Thermal correction to Enthalpy: 0.602435

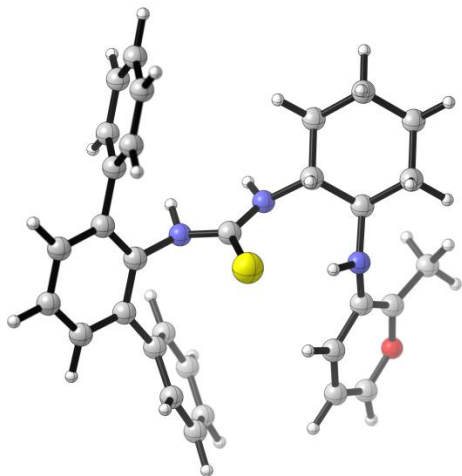
Thermal correction to Gibbs Free Energy: 0.503467

Cartesian coordinates:

C	-2.91586500	3.57114600	-0.47598100	H	-0.68675500	6.00332700	0.63936700
C	-2.16854600	2.36262900	0.12595900	H	-0.69471400	5.23754500	-0.94370500
C	-0.63721000	2.56611900	0.01802500	H	-2.80736000	4.87435200	1.25334000
C	-0.21941700	3.89105200	0.68072400	H	-3.02869600	5.72329800	-0.27075000
C	-0.98244300	5.09305100	0.10648400	H	-0.36923300	2.59099300	-1.04365300
C	-2.49953100	4.88624900	0.19758900	N	0.11394800	1.46126100	0.61425500
H	-2.41322700	2.27765400	1.19644500	C	0.72532700	0.44667300	-0.06438600
H	-2.69123100	3.61133900	-1.55017000	N	1.64647200	-0.22912800	0.67846500
H	-3.99955600	3.42181600	-0.39321800	C	2.42743800	-1.34169000	0.21281300
H	-0.40570000	3.82620900	1.76449300	C	3.77088500	-1.10656400	-0.13367500
H	0.86068700	4.02020900	0.55000500	C	1.85636800	-2.62665900	0.12136300

C	4.53836400	-2.17183100	-0.61878500	C	5.27931700	2.02452700	1.41145700
C	2.65855500	-3.66374800	-0.37897400	H	4.52861300	0.14825000	2.16017700
C	3.98154300	-3.44155900	-0.75069200	C	5.23619400	2.29445000	-0.98784100
H	5.57560200	-1.99454100	-0.88661600	H	4.40864700	0.64753100	-2.10857500
H	2.24054900	-4.66369900	-0.44337700	C	5.54746700	2.79445100	0.27803300
H	4.58438800	-4.26381500	-1.12469800	H	5.53660500	2.39849900	2.39881400
H	0.36450100	1.57928800	1.59011100	H	5.44873700	2.88608800	-1.87402300
H	2.06863400	0.29478000	1.43829900	H	6.00572500	3.77409900	0.38041000
N	-2.54059100	1.10705200	-0.53692600	C	0.46014300	-2.93698100	0.53740800
C	-3.65872500	0.40034300	-0.27472000	C	-0.04158400	-2.54973000	1.79104300
C	-4.64185000	0.77949500	0.67243200	C	-0.36629100	-3.70660200	-0.29928700
C	-3.91542300	-0.80297900	-0.99403700	C	-1.32608200	-2.91548100	2.19256400
H	-4.52555400	1.70060700	1.23000100	H	0.59144400	-1.98611600	2.46897600
C	-5.92085500	-1.17716400	0.18811100	C	-1.65028300	-4.07776900	0.10356100
H	-6.72883100	-1.89248300	0.24860600	H	0.00481800	-4.01437800	-1.27278700
C	-5.76228100	-0.01829800	0.90379800	C	-2.13697800	-3.68077800	1.35092500
H	-6.50966600	0.26519000	1.63604200	H	-1.68396500	-2.62512300	3.17705500
O	-5.00320900	-1.51142300	-0.72597500	H	-2.26308100	-4.69036300	-0.55302000
S	0.35329100	0.05688200	-1.66958800	H	-3.12803300	-3.98722300	1.67582500
H	-1.80156800	0.68229500	-1.11532600	C	-3.06164200	-1.36242900	-2.06994300
C	4.37789900	0.25232200	0.00814300	H	-2.85113600	-0.59663000	-2.82663800
C	4.69918300	0.76170200	1.27714500	H	-2.09255800	-1.68630400	-1.66672500
C	4.65522200	1.03232400	-1.12317900	H	-3.55727100	-2.21333100	-2.54048700

4•31 (minor):



E(RB3LYP): -1838.02989839

Zero-point correction: 0.570413 (Hartree/Particle)

Thermal correction to Energy: 0.602040

Thermal correction to Enthalpy: 0.602985

Thermal correction to Gibbs Free Energy: 0.504193

Cartesian coordinates:

C	-2.80974300	3.65390300	-0.89983000	H	-0.65362600	5.90876700	0.65641300
C	-2.27630400	2.39350400	-0.19290000	H	-0.42459200	5.17422000	-0.92509000
C	-0.73300700	2.49673200	-0.06076500	H	-2.92206400	4.93819800	0.84190800
C	-0.33942400	3.76708000	0.71274400	H	-2.79968900	5.80891100	-0.68048900
C	-0.90718700	5.03153200	0.05123200	H	-0.31769400	2.55344100	-1.07299100
C	-2.42630200	4.93236300	-0.13989900	N	-0.13283500	1.31649100	0.57026500
H	-2.69674200	2.32550600	0.81688100	C	0.56699700	0.34848100	-0.10031600
H	-2.39442100	3.68084300	-1.91651000	N	1.41675900	-0.36952600	0.68781900
H	-3.89705000	3.58539800	-1.02020100	C	2.39810000	-1.29234200	0.17373900
H	-0.71355700	3.69357200	1.74623300	C	3.68635500	-0.79516800	-0.10460200
H	0.75397100	3.82078900	0.76968300	C	2.06302600	-2.63983700	-0.05396600

C	4.63710500	-1.66071500	-0.65754300	C	4.47085400	2.43840900	1.74075000
C	3.04473000	-3.47170500	-0.61608300	H	3.98251500	0.42155100	2.31821700
C	4.31397900	-2.98964200	-0.92118400	C	4.64373200	2.84270300	-0.63384300
H	5.63253500	-1.28330400	-0.87150100	H	4.23582200	1.15266500	-1.91063400
H	2.80943500	-4.51804600	-0.78478300	C	4.72289700	3.31056100	0.67916400
H	5.05847100	-3.65613200	-1.34657900	H	4.55527400	2.78823400	2.76619600
H	0.09160000	1.43277700	1.55336700	H	4.84820000	3.51323500	-1.46394400
H	1.68264400	0.07754200	1.55918600	H	4.99338700	4.34429600	0.87528000
N	-2.61124600	1.15911700	-0.92537100	C	0.74052700	-3.23381000	0.28781400
C	-3.40785600	0.13392200	-0.52413300	C	0.18080700	-3.09528100	1.56872600
C	-3.12025400	-1.17939000	-0.99199400	C	0.07426400	-4.04553100	-0.64552900
C	-4.56752400	0.26177500	0.28183700	C	-0.99604200	-3.76032000	1.91136500
H	-2.23306900	-1.32159400	-1.60312200	H	0.69447700	-2.49640700	2.31439700
C	-5.00498900	-2.06099100	0.15084500	C	-1.10085500	-4.71612000	-0.30262000
H	-5.71731300	-2.79437800	0.50400200	H	0.48915600	-4.15659800	-1.64317300
C	-3.91212000	-2.26878800	-0.65676100	C	-1.63808100	-4.58003200	0.97985000
H	-3.66491300	-3.26671300	-0.99633000	H	-1.39445000	-3.66381200	2.91804800
O	-5.28063000	-0.83261000	0.57444900	H	-1.58057100	-5.36485600	-1.03175900
S	0.36770500	0.04331200	-1.75467200	H	-2.53510900	-5.12670000	1.25992700
H	-1.82521300	0.84096400	-1.50765000	C	-5.18011000	1.49346200	0.86090700
C	4.04145900	0.62983000	0.16892500	H	-6.23842600	1.31022700	1.06178800
C	4.13398500	1.10806300	1.48665800	H	-4.70571800	1.78055600	1.80739800
C	4.30602200	1.51208900	-0.88806900	H	-5.09050300	2.33372300	0.16887900

3.8.6 Additional Optimization Studies

Table 3.4. Full catalyst screen.^a

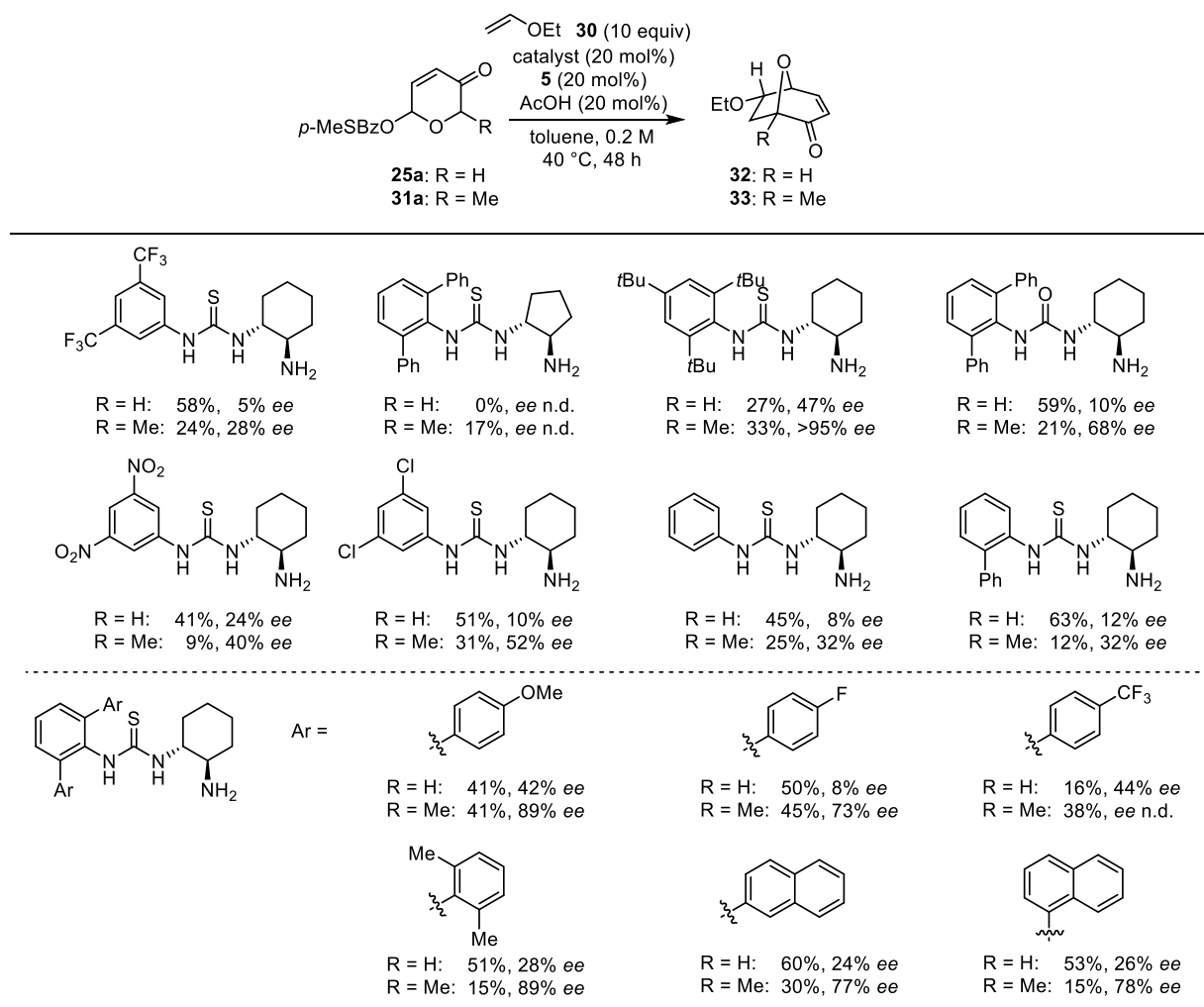
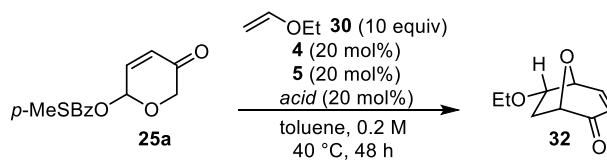
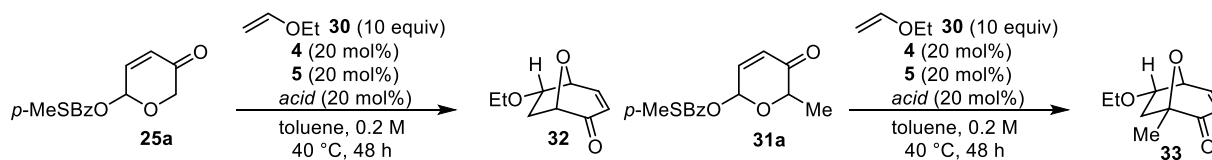


Table 3.5. Acid additive screen.^a



Entry	Acid	Yield (%) ^b	ee (%) ^c
1	AcOH	53	47
2	BzOH	41	40
3	<i>p</i> -MeOBzOH	23	44
4	<i>p</i> -MeSBzOH	26	44
5	TCA	0	-
6	TFA	0	-
7	MsOH	0	-
8	PPTS	0	-

^a Reactions performed on 0.07 mmol scale. ^b Yields determined by NMR analysis using 1,3,5-trimethoxybenzene as an internal standard. ^c Enantioselectivities determined by HPLC using commercial columns with chiral stationary phases.



Entry	Acid	Yield (%) ^b	ee (%) ^c
1	AcOH	53	47
2	HCOOH	17	n.d.
3	MIA	11	n.d.
4	MCA	8	n.d.
5		43	40
6		14	n.d.

Entry	Acid	Yield (%) ^b	ee (%) ^c
1	AcOH	55	90
2	HCOOH	63	89
3	MIA	0	-
4	MCA	14	n.d.
5		43	88
6		33	85

^a Reactions performed on 0.07 mmol scale. ^b Yields determined by NMR analysis using 1,3,5-trimethoxybenzene as an internal standard. ^c Enantioselectivities determined by HPLC using commercial columns with chiral stationary phases.

Table 3.6. Solvent screen.^a

25a

31a

Entry	Solvent	Yield (%) ^b	ee (%) ^c
1	toluene	53	47
2	PhBr	49	46
3	PhCl	43	40
4	PhEt	49	42
5	<i>o</i> -xylene	18	40
6	<i>m</i> -xylene	60	42
7	<i>p</i> -xylene	53	40
8	PhNO ₂	14	n.d.
9	PhCF ₃	33	30
10	anisole	23	40

Entry	Solvent	Yield (%) ^b	ee (%) ^c
1	toluene	55	90
2	PhBr	37	90
3	PhCl	35	90
4	PhEt	45	84
5	<i>o</i> -xylene	49	90
6	<i>m</i> -xylene	45	90
7	<i>p</i> -xylene	43	89
8	PhNO ₂	9	n.d.
9	PhCF ₃	25	86
10	anisole	33	94

^a Reactions performed on 0.07 mmol scale. ^b Yields determined by NMR analysis using 1,3,5-trimethoxybenzene as an internal standard. ^c Enantioselectivities determined by HPLC using commercial columns with chiral stationary phases.

Table 3.7. Medium effects screen.^a

25a

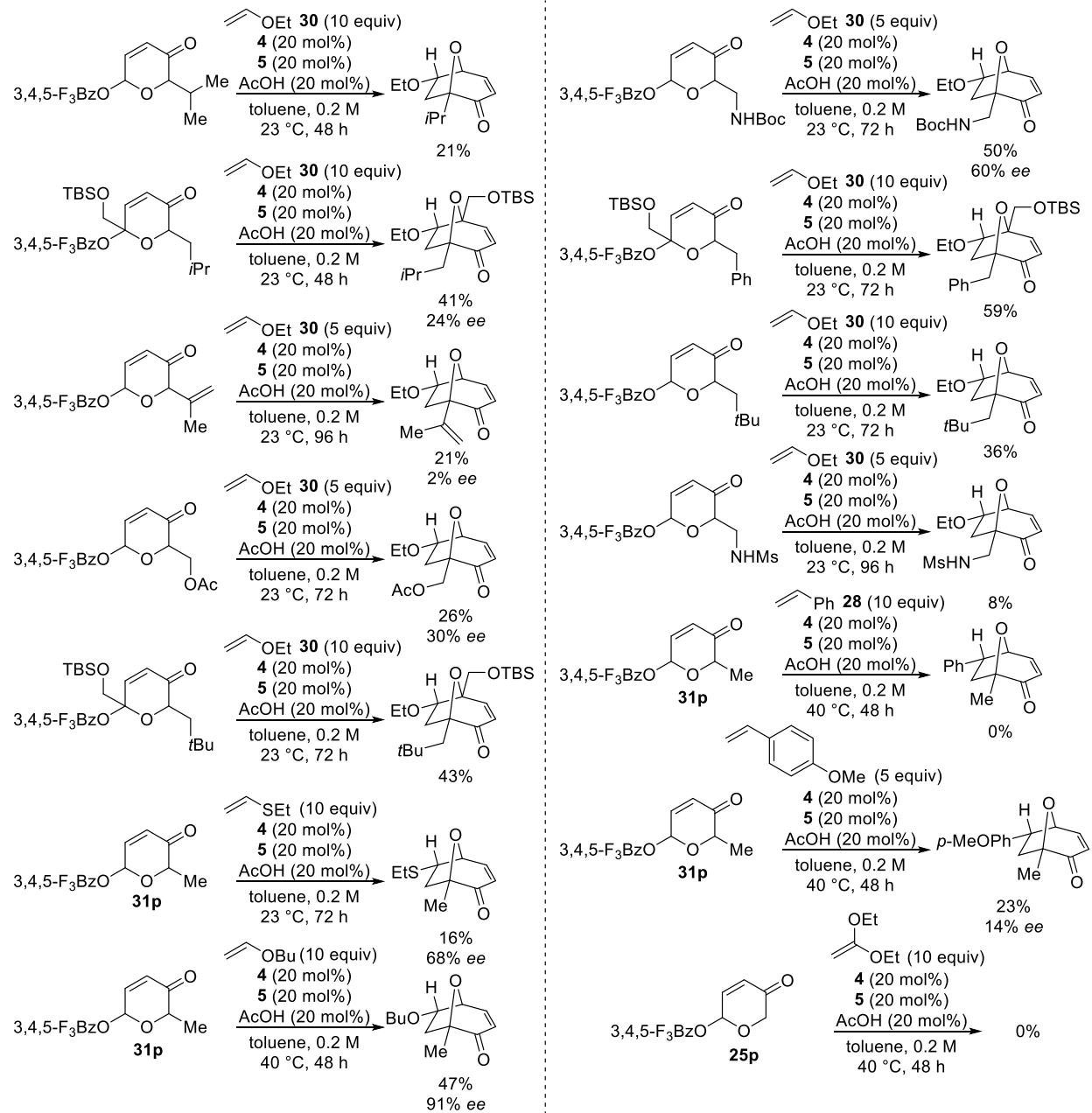
31a

Entry	Conc.	X	20 mol% AcOH		0 mol% AcOH	
			Yield (%) ^b	ee (%) ^c	Yield (%) ^b	ee (%) ^c
1	0.2	10	53	47	-	-
2	0.15	2	26	n.d.	29	38
3	0.15	3	35	38	15	30
4	0.3	2	24	42	19	30
5	0.3	3	16	42	16	34
6	0.4	2	32	42	33	38
7	0.4	3	22	44	21	37

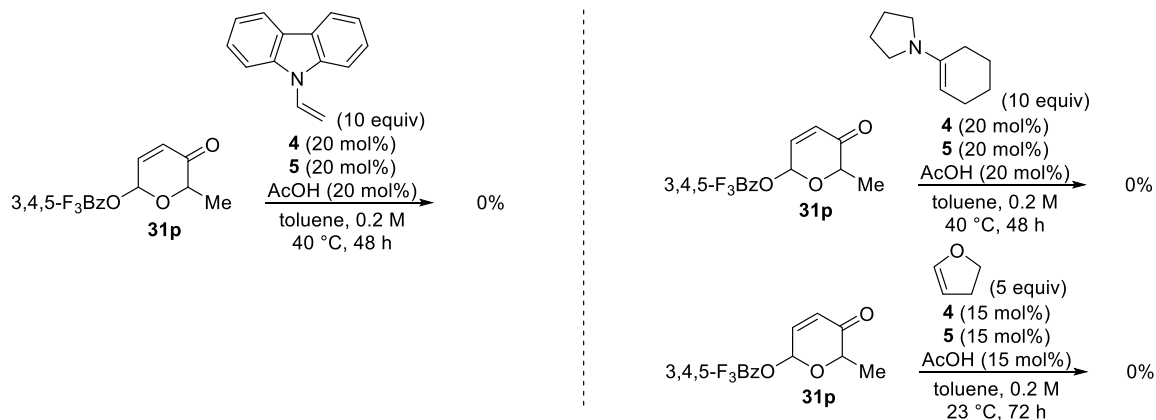
Entry	Conc.	X	20 mol% AcOH		0 mol% AcOH	
			Yield (%) ^b	ee (%) ^c	Yield (%) ^b	ee (%) ^c
1	0.2	10	55	90	-	-
2	0.15	2	39	89	40	86
3	0.15	3	35	89	38	87
4	0.3	2	26	89	15	84
5	0.3	3	26	89	15	88
6	0.4	2	29	90	31	88
7	0.4	3	19	89	17	86

^a Reactions performed on 0.07 mmol scale. ^b Yields determined by NMR analysis using 1,3,5-trimethoxybenzene as an internal standard. ^c Enantioselectivities determined by HPLC using commercial columns with chiral stationary phases.

3.8.7 Results with Sub-Optimal and Unreactive Substrates



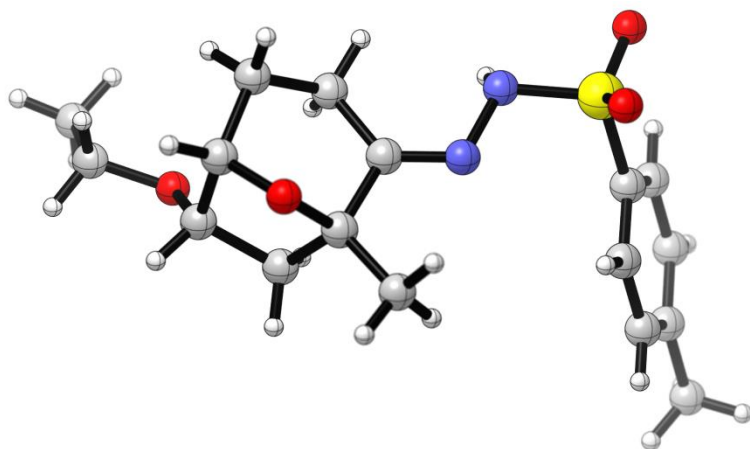
Scheme 3.21. Results with additional substrates.



Scheme 3.21 (continued).

3.8.8 Crystallographic Information⁴³

Tosylhydrazone **59**:



Tosylhydrazone **59** was crystallized by vapor diffusion of hexanes into a solution of **59** in benzene. The hexane layer was then allowed to slowly evaporate at 23 °C to afford X-ray quality crystals. A crystal was mounted on a diffractometer and data was collected at 100 K. The intensities of the reflections were collected by means of a Bruker APEX II CCD diffractometer (MoK α radiation, $\lambda=0.71073$ Å), and equipped with an Oxford Cryosystems nitrogen flow apparatus. The collection method involved 0.5° scans in ω at 28° in 2θ . Data integration down to 0.82 Å resolution was carried out using SAINT V7.46 A⁴⁴ with

⁴³ Crystal structure solved by Dr. Shao-Liang Zheng.

⁴⁴ Bruker AXS APEX II, Bruker AXS, Madison, Wisconsin, 2009.

reflection spot size optimization. Absorption corrections were made with the program SADABS.⁴⁴ The structure was solved by the direct methods procedure and refined by least-squares methods again F^2 using SHELXS-97 and SHELXL-97⁴⁵ with OLEX 2 interface.⁴⁶ Non-hydrogen atoms were refined anisotropically, and hydrogen atoms were allowed to ride on the respective atoms.

Crystal data	
Chemical formula	C ₁₇ H ₂₄ N ₂ O ₄ S
M_r	352.44
Crystal system, space group	Orthorhombic, $P2_12_12_1$
Temperature (K)	100
a, b, c (Å)	9.7352 (7), 9.8178 (7), 18.7447 (13)
V (Å ³)	1791.6 (2)
Z	4
Radiation type	Mo $K\alpha$
μ (mm ⁻¹)	0.20
Crystal size (mm)	0.24 × 0.12 × 0.10
Data collection	
Diffractometer	Bruker D8 goniometer with CCD area detector diffractometer
Absorption correction	Multi-scan <i>SADABS</i>
T_{\min}, T_{\max}	0.953, 0.980
No. of measured, independent and observed [$I > 2\sigma(I)$] reflections	17108, 3966, 3466
R_{int}	0.046
$(\sin \theta/\lambda)_{\text{max}}$ (Å ⁻¹)	0.642
Refinement	
$R[F^2 > 2\sigma(F^2)], wR(F^2), S$	0.035, 0.078, 1.03
No. of reflections	3966
No. of parameters	224

⁴⁵ Sheldrick, G. M. *Acta Cryst.* **2008**, *A64*, 112–122.

⁴⁶ Dolomanov, O. V.; Bourhis, L. J.; Gildea, R. J.; Howard, J. A. K.; Puschmann, H. *J. Appl. Cryst.* **2009**, *42*, 339–341.

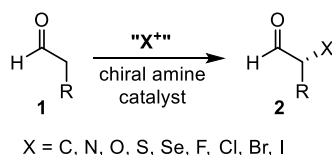
No. of restraints	0
H-atom treatment	H atoms treated by a mixture of independent and constrained refinement
$\Delta\rho_{\max}, \Delta\rho_{\min}$ (e Å ⁻³)	0.21, -0.32
Absolute structure	Flack, H. D. <i>Acta Cryst.</i> 1983 , <i>A39</i> , 876–881.
Flack parameter	0.03 (7)

Chapter Four

An Overview of Amine-Catalyzed α -Functionalizations of Branched Aldehydes

4.1 Introduction

The asymmetric construction of new bonds at the α -position of aldehydes permits the synthesis of enantioenriched products containing stereogenic carbon centers. This type of transformation has been thoroughly investigated over the past several decades, resulting in various carbon–X (X = C, N, chalcogen, halogen) bond formations of α -unbranched aldehydes, such as **1** to **2**, which proceed in high yields and selectivities (Scheme 4.1). These reactions are typically mediated by cyclic secondary amine catalysts, such as proline (**3**, Figure 4.1) derivatives, MacMillan's imidazolidinones (e.g., **4**), and Jørgensen and Hayashi's pyrrolidines (e.g., **5**).¹



Scheme 4.1. Amine-catalyzed α -functionalizations of linear aldehydes.

¹ See the following reviews and references therein: (a) Marigo, M.; Jørgensen, K. A. *Chem. Commun.* **2006**, 2001–2011. (b) Vilaivan, T.; Bhanthumnavin, W. *Molecules* **2010**, *15*, 917–958. (c) Bertelsen, S.; Jørgensen, K. A. *Chem. Soc. Rev.* **2009**, *38*, 2178–2189. (d) Nielsen, M.; Worgull, D.; Zweifel, T.; Gschwend, B.; Bertelsen, S.; Jørgensen, K. A. *Chem. Commun.* **2011**, 632–649. (e) *Comprehensive Enantioselective Organocatalysis*; Dalko, P. I., Ed.; Wiley: Weinheim, Germany, 2013.

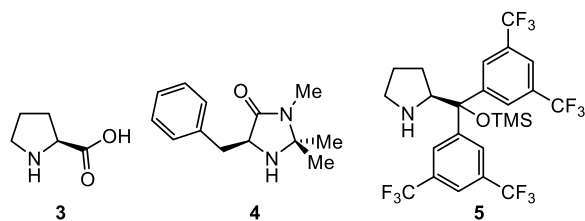
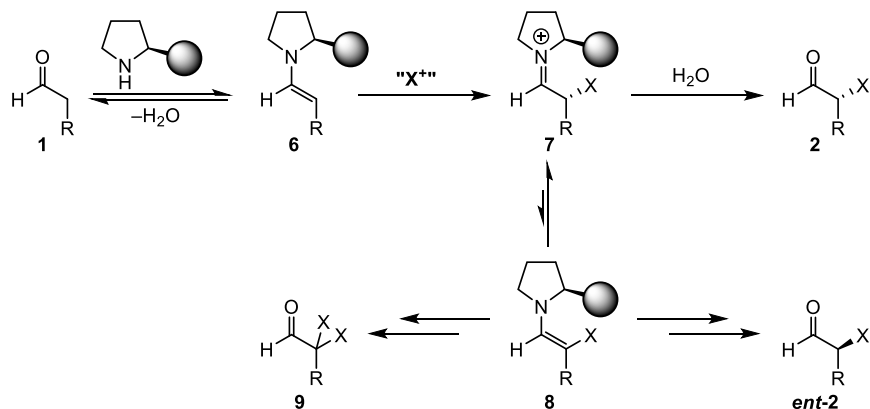


Figure 4.1. Common secondary amine catalysts.

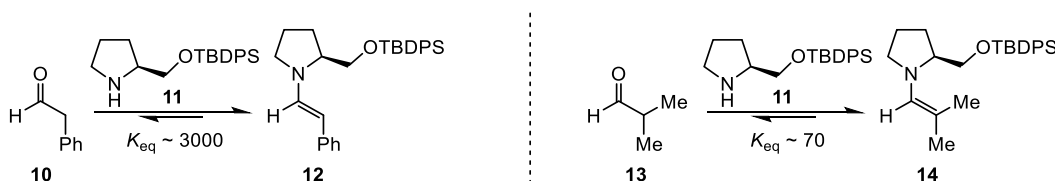
One reason that these catalysts are so effective is that they typically do not overfunctionalize the aldehyde products **2** (Scheme 4.2). Following attack of enamine **6** onto electrophile “X⁺,” iminium **7** is rapidly hydrolyzed to product. This final step is essentially irreversible due to the increased steric hindrance of the product, which prevents the recondensation of the amine catalyst onto the more congested aldehyde. This prohibits formation of any appreciable quantity of enamine **8**, thus precluding racemization of **2** or difunctionalization to aldehyde **9**. As such, while these catalysts have proven to be extremely useful for the α -functionalization of linear aldehyde substrates, they tend to fail in the context of forming tetrasubstituted centers on α,α -disubstituted aldehydes.



Scheme 4.2. Prevention of overfunctionalization with secondary amine catalysts.

In fact, several challenges associated with enamine catalysis of α -branched aldehydes exist. The Vilarrasa group has studied the propensity of several different types of carbonyl groups to form enamines with pyrrolidine **11** (Scheme 4.3), a compound which bears significant structural

similarity with several of the most common secondary amine catalysts.² The equilibrium constants for condensation encompass a wide range of values, with formation of **14** from branched aldehyde **13** being less thermodynamically favored than formation of **12** from linear aldehyde **10** by two orders of magnitude, due to the increased steric hindrance of the branched substrate.



Scheme 4.3. Thermodynamics of condensation.

Tetrasubstituted enamines are also less nucleophilic than their disubstituted counterparts. Mayr and coworkers have calculated the nucleophilicity parameters for several morpholine-based enamines, dependent upon the second-order rate constants of their reactions with benzhydrylium cation **18** (Figure 4.2).³ The nucleophilicity parameters N and rate constants k_2 for three representative enamines are collected in Figure 4.2. Trisubstituted enamine **17**, which comes from branched isobutyraldehyde, reacts with cation **18** two orders of magnitude more slowly than *trans*- and *cis*-disubstituted enamines **15** and **16**. Thus, in addition to existing at a lower equilibrium concentration, the enamines of branched aldehydes also react more slowly with electrophiles.

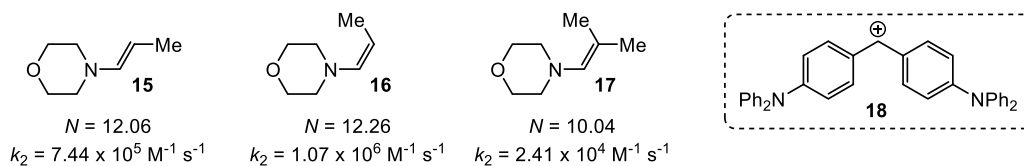


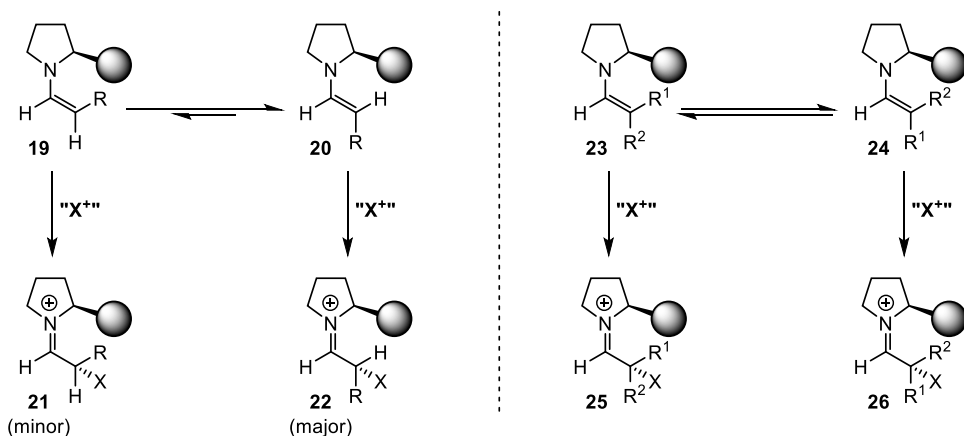
Figure 4.2. Nucleophilicity parameters of representative enamines.

Outside of thermodynamic and kinetic barriers to reaction, in the realm of asymmetric catalysis, one must also consider the stereoselectivity of the overall process. Here, too, α,α -

² Sánchez, D.; Bastida, D.; Burés, J.; Isart, C.; Pineda, O.; Vilarrasa, J. *Org. Lett.* **2012**, *14*, 536–539.

³ Kempf, B.; Hampel, N.; Ofial, A. R.; Mayr, H. *Chem.–Eur. J.* **2003**, *9*, 2209–2218.

disubstituted aldehydes present a unique challenge. Hypothetical *Z*-enamine intermediate **19** (Scheme 4.4), which results from the condensation of a linear aldehyde with a typical secondary amine catalyst, should be strongly disfavored relative to *E*-enamine **20** at equilibrium. Assuming the front face of the enamine nucleophile is sterically blocked by the catalyst substituent, then the electrophilic reaction component is expected to approach from the rear face of both enamine isomers. Thus, provided that α -functionalization is rapid relative to enamine formation, the *ee* of the reaction depends on the *E/Z* ratio of enamine intermediates. This ratio is quite high for unbranched aldehyde substrates. On the other hand, enamines **23** and **24**, which come from an α -branched aldehyde starting material, should not demonstrate such a strong preference at equilibrium, resulting in significant formation of both iminiums **25** and **26**, and therefore low enantioselectivity in the overall process.⁴

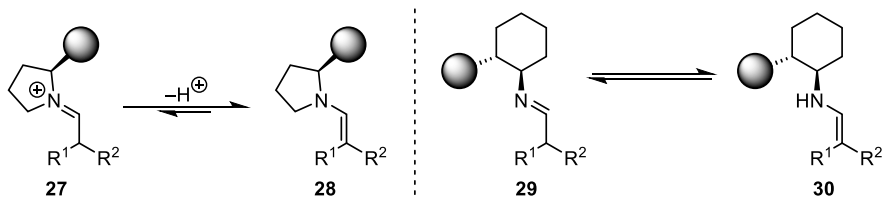


Scheme 4.4. *E/Z*-equilibrium of enamines.

Despite these obstacles, several groups have experienced success in enamine catalyzed α -functionalizations of branched aldehyde substrates. Many advances in this area have involved the use of primary amine catalysts, rather than the traditional secondary amines such as those in Figure 4.1. Primary amine catalysts, being less sterically congested than secondary amines, undergo less

⁴ Burés, J.; Armstrong, A.; Blackmond, D. G. *Chem. Sci.* **2012**, 3, 1273–1277.

hindered approaches to aldehydes and experience more favorable thermodynamics and kinetics of condensation.⁵ However, once condensation occurs, there is another step to be considered. The iminium/enamine equilibrium for a secondary amine (e.g., **27** to **28**, Scheme 4.5) is markedly more favorable than the imine/enamine equilibrium for a primary amine (e.g., **29** to **30**) due to the loss of charge upon going from **27** to **28**.⁶



Scheme 4.5. Secondary and primary amines in enamine catalysis.

Regardless of this added complication, primary amines generally perform better in α -functionalizations of α,α -disubstituted aldehydes. As an introduction to our own contributions to this field, presented in Chapter 5 of this dissertation, several key examples of previous work will be highlighted in the present chapter. Discussion here will be limited to α -heterofunctionalizations. Carbon–carbon bond formations (conjugate additions, aldol/Mannich reactions, and alkylations) represent the most well-precedented area of research in this field. As they are fundamentally distinct from the heterofunctionalizations in our original research, they are best left to their own review.⁷ Specific carbon–carbon formations from our laboratory will be highlighted in Chapter 5.

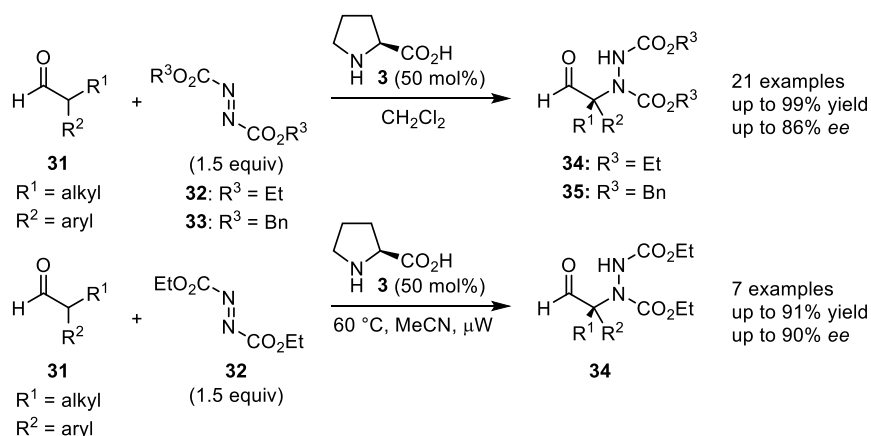
⁵ Henderson, Jr., W. A.; Schultz, C. J. *J. Org. Chem.* **1962**, *27*, 4643–4646.

⁶ (a) Bergmann, E. D.; Zimkin, E.; Pinchas, S. *Rec. Trav. Chim.* **1952**, *71*, 168–191. (b) Bergmann, E. D.; Hirshberg, Y.; Pinchas, S.; Zimkin, E. *Rec. Trav. Chim.* **1952**, *71*, 192–199. (c) Bergmann, E. D.; Meeron, E.; Hirschberg, Y.; Pinchas, S. *Rec. Trav. Chim.* **1952**, *71*, 200–212. (d) Witkop, B. *J. Am. Chem. Soc.* **1956**, *78*, 2873–2882. (e) Pfau, M.; Ribière, C. *J. Chem. Soc. D* **1970**, 66–67. (f) Clark, R. A.; Parker, D. C. *J. Am. Chem. Soc.* **1971**, *93*, 7257–7261. (g) de Jaso, B.; Pommier, J.-C. *J. Chem. Soc., Chem. Commun.* **1977**, 565–566. (h) Knorr, R.; Weiß, A.; Löw, P.; Rappé, E. *Chem. Ber* **1980**, *113*, 2462–2489. (i) Boyd, D. R.; Jennings, W. B.; Waring, L. C. *J. Org. Chem.* **1986**, *51*, 992–995. (j) Capon, B.; Wu, Z. P. *J. Org. Chem.* **1990**, *55*, 2317–2324.

⁷ For a comprehensive review, see: Desmarchelier, A.; Coeffard, V.; Moreau, X.; Greck, C. *Tetrahedron* **2014**, *70*, 2491–2513.

4.2 α -Amination Reactions

α -Aminations constitute the most widely reported α -functionalization reactions in the literature. In 2003, the Bräse group reported the first amine-catalyzed electrophilic amination of α -branched aldehydes.⁸ With α,α -dialkyl aldehyde substrates, dialkyl azodicarboxylate electrophiles (**32** and **33**, Scheme 4.6) and 50 mol% proline **3** as catalyst, these authors observed a maximum of 39% *ee*. However, upon switching to α -alkyl- α -aryl aldehydes **31**, they could achieve up to 86% enantioselectivity for hydrazinoaldehydes **34** and **35**. The same group later discovered that microwave irradiation provided improvements in both yield and enantioselectivity.⁹



Scheme 4.6. Preliminary α -aminations.

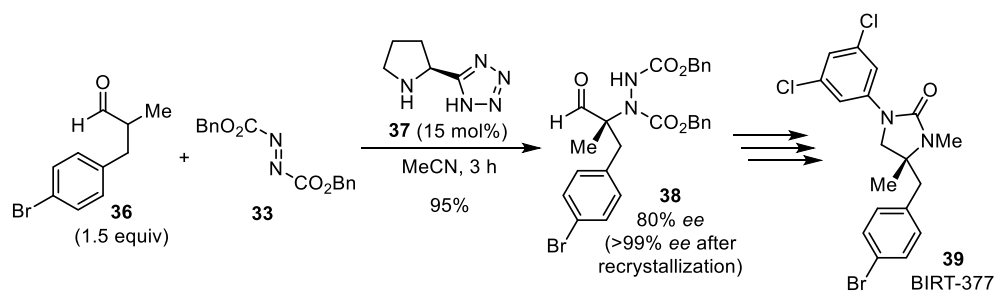
In their total synthesis of BIRT-377, Chowdari and Barbas screened several pyrrolidine-based catalysts for the asymmetric amination of branched aldehyde **36**, ultimately arriving at tetrazole **37**, which afforded the desired hydrazinoaldehyde **38** in 80% *ee* (Scheme 4.7).¹⁰ This could be improved to >99% *ee* upon recrystallization. Compound **38** was then elaborated to the

⁸ (a) Vogt, H.; Vanderheiden, S.; Bräse, S. *Chem. Commun.* **2003**, 2448–2449. (b) Baumann, T.; Vogt, H.; Bräse, S. *Eur. J. Org. Chem.* **2007**, 266–282.

⁹ (a) Baumann, T.; Bächle, M.; Hartmann, C.; Bräse, S. *Eur. J. Org. Chem.* **2008**, 2207–2212. (b) Hartmann, C. E.; Baumann, T.; Bächle, M.; Bräse, S. *Tetrahedron: Asymmetry* **2010**, *21*, 1341–1349.

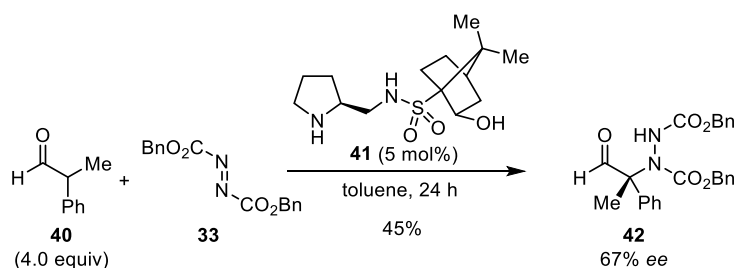
¹⁰ Chowdari, N. S.; Barbas III, C. F. *Org. Lett.* **2005**, *7*, 867–870.

cell adhesion inhibitor. The Barbas group later used (*R*)-proline (*ent*-**3**) as an α -amination catalyst in the synthesis of the glutamate receptor ligand (*S*)-AIDA to similar effect.¹¹



Scheme 4.7. Total synthesis of BIRT-377.

The field remained relatively quiet until a series of reports at the beginning of this decade explored alternative amine catalysts. In 2010, Chen and coworkers disclosed a camphor-derived pyrrolidine (**41**, Scheme 4.8) which could effectively catalyze the α -amination of aldehyde **40** at loadings as low as 5 mol%. However, the enantioselectivity of this process topped out at 67%.¹²



Scheme 4.8. Chen's camphor-derived catalyst.

The first report of a primary amine catalyst in the α -amination of branched aldehydes came from the Lu group in 2011.¹³ These authors found that cinchona alkaloid-derived diamine **44**, in conjunction with (–)-camphorsulfonic acid **45** could effect α -aminations in high yields and enantioselectivities within 24 hours (Table 4.1). The acid was not entirely necessary, but served to

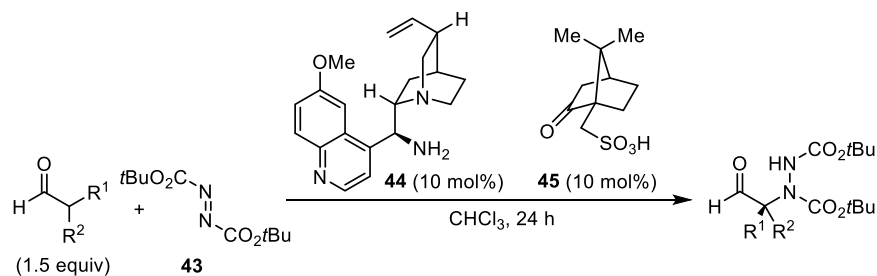
¹¹ Suri, J. T.; Steiner, D. D.; Barbas III, C. F. *Org. Lett.* **2005**, *7*, 3885–3888.

¹² Liu, P.-M.; Magar, D. R.; Chen, K. *Eur. J. Org. Chem.* **2010**, 5705–5713.

¹³ Liu, C.; Zhu, Q.; Huang, K.-W.; Lu, Y. *Org. Lett.* **2011**, *13*, 2638–2641.

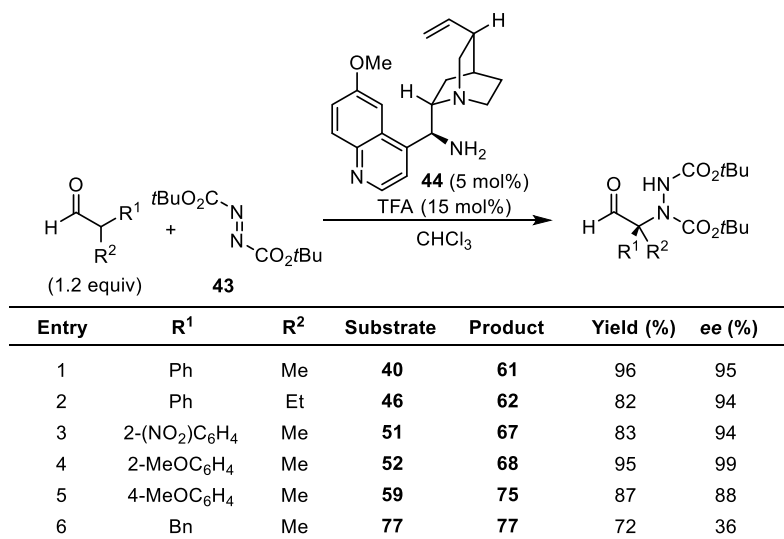
increase the reaction rate and selectivity. α,α -Dialkyl aldehydes still presented a liability, as 2-methylpentanal **60** could only be aminated in 68% *ee* (entry 16). A few months later, Greck's group demonstrated that the same catalyst, with achiral trifluoroacetic acid, could achieve similar yields and *ee*'s, although reaction times were not reported (Table 4.2).¹⁴ Once again, α,α -dialkylaldehydes presented a challenge for selectivity (entry 6).

Table 4.1. The first primary amine catalyst in α -aminations of branched aldehydes.

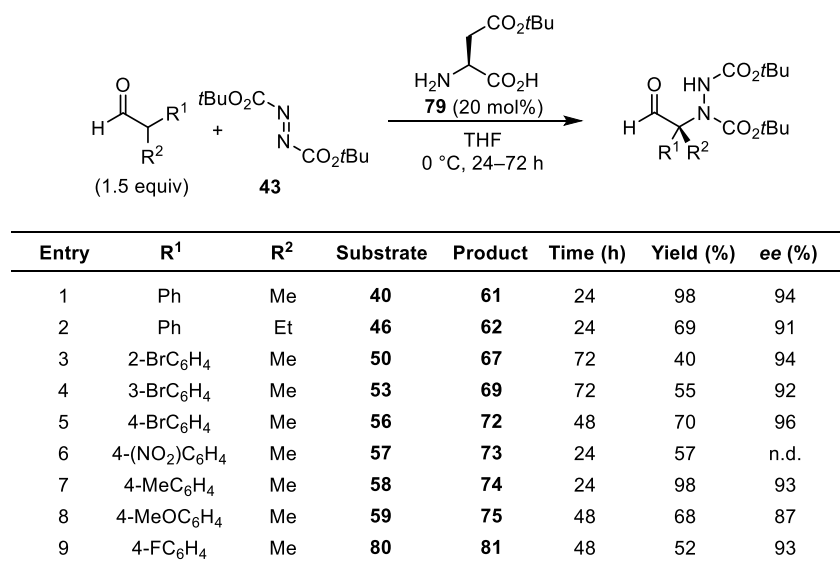


Entry	R ¹	R ²	Substrate	Product	Yield (%)	<i>ee</i> (%)
1	Ph	Me	40	61	99	97
2	Ph	Et	46	62	91	99
3	Ph	<i>i</i> Pr	47	63	95	96
4	1-naphthyl	Me	48	64	97	98
5	2-naphthyl	Me	49	65	97	97
6	2-BrC ₆ H ₄	Me	50	66	92	99
7	2-(NO ₂)C ₆ H ₄	Me	51	67	80	96
8	2-MeOC ₆ H ₄	Me	52	68	99	99
9	3-BrC ₆ H ₄	Me	53	69	83	97
10	3-(NO ₂)C ₆ H ₄	Me	54	70	99	95
11	3,5-(MeO) ₂ C ₆ H ₄	Me	55	71	99	99
12	4-BrC ₆ H ₄	Me	56	72	99	96
13	4-(NO ₂)C ₆ H ₄	Me	57	73	82	96
14	4-MeC ₆ H ₄	Me	58	74	85	99
15	4-MeOC ₆ H ₄	Me	59	75	99	97
16	<i>n</i> Pr	Me	60	76	99	68

¹⁴ Desmarchelier, A.; Yalgin, H.; Coeffard, V.; Moreau, X.; Greck, C. *Tetrahedron Lett.* **2011**, 52, 4430–4432.

Table 4.2. TFA and primary amine catalyst **44** in the α -amination of branched aldehydes.

The simplest primary amine catalyst to be described for this transformation, β -*tert*-butyl aspartate **79**, was reported by Kokotos and coworkers in 2013 (Table 4.3).¹⁵ Here, the catalyst acts as both primary amine and acid. Products are obtained in generally high yields and enantioselectivities within 1 to 3 days.

Table 4.3. β -*tert*-butyl aspartate as a catalyst for the α -amination of branched aldehydes.

¹⁵ Theodorou, A.; Papadopoulos, G. N.; Kokotos, C. G. *Tetrahedron* **2013**, *69*, 5438–5443.

Beginning in 2010, Xu, Wang, and coworkers have examined several amine catalysts for asymmetric α -aminations of α -branched aldehydes (Figure 4.3).¹⁶ Thiourea-based secondary amine catalyst **82** affords products in up to 97% *ee*, when combined with *o*-hydroxybenzoic acid.^{16a} Simpler primary amines **83**^{16b} and **84**^{16c} also aminate α -alkyl- α -aryl aldehydes in greater than 90% *ee*, with HCl and TFA additives respectively. Benzamide **85**, the most structurally similar scaffold to the new benzamide catalyst described in Chapter 5, can perform this transformation, with TFA, in as a little as 2 hours. However, other substrates require up to six days to reach high conversion (Table 4.4).^{16d} Lower enantioselectivities were observed for aldehyde substrates with electron-withdrawing groups (entry 4) or *ortho*-substitution (entries 9 and 11) on the aryl ring.

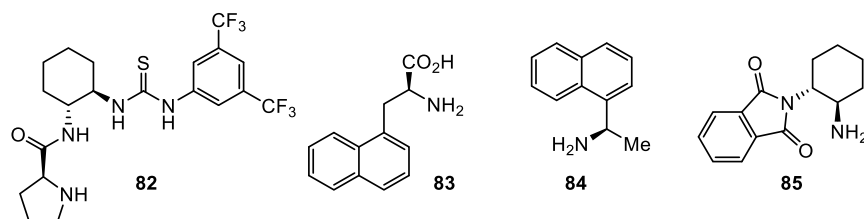


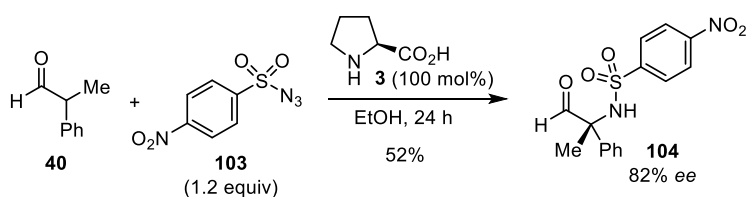
Figure 4.3. Xu and Wang's α -amination catalysts.

¹⁶ (a) Fu, J.-Y.; Xu, X.-Y.; Li, Y.-C.; Huang, Q.-C.; Wang, L.-X. *Org. Biomol. Chem.* **2010**, *8*, 4524–4526. (b) Fu, J.-Y.; Yang, Q.-C.; Wang, Q.-L.; Ming, J.-N.; Wang, F.-Y.; Xu, X.-Y.; Wang, L.-X. *J. Org. Chem.* **2011**, *76*, 4661–4664. (c) Fu, J.-Y.; Wang, Q.-L.; Peng, L.; Gui, Y.-Y.; Wang, F.; Tian, F.; Xu, X.-Y.; Wang, L.-X. *Eur. J. Org. Chem.* **2013**, 2864–2868. (d) Fu, J.-Y.; Wang, Q.-L.; Peng, L.; Gui, Y.-Y.; Xu, X.-Y.; Wang, L.-X. *Chirality* **2013**, *25*, 668–672.

Table 4.4. Benzimide catalyst **85** in the α -amination of branched aldehydes.

Entry	Ar	Substrate	Product	Time (h)	Yield (%)	ee (%)
1	Ph	40	91	5	96	91
2	4-MeOC ₆ H ₄	59	92	48	88	91
3	4-MeC ₆ H ₄	58	93	155	38	97
4	4-(NO ₂)C ₆ H ₄	57	94	48	94	54
5	4-BrC ₆ H ₄	56	95	3	99	95
6	4-FC ₆ H ₄	80	96	18	62	93
7	4-ClC ₆ H ₄	86	97	144	38	81
8	3-ClC ₆ H ₄	87	98	3	94	89
9	2-ClC ₆ H ₄	88	99	24	47	78
10	2-naphthyl	49	100	3	95	93
11	2-MeC ₆ H ₄	89	101	48	75	76
12	3-MeOC ₆ H ₄	90	102	90	90	90

In addition to the above aminations with dialkyl azodicarboxylates, the Bräse group has also explored sulfonyl azides as electrophiles.¹⁷ After screening various azides with parent substrate **40** and proline **3**, *p*-nosyl azide **103** proved to give product **104** with the highest enantioselectivity, 82% (Scheme 4.9). All reactions reported in this work required stoichiometric quantities of the amine promoter.



Scheme 4.9. An α -amination with a sulfonyl azide.

Gong, Jiang, and coworkers also explored nitrosobenzene **105** as an aminating reagent in

¹⁷ (a) Baumann, T.; Bächle, M.; Bräse, S. *Org. Lett.* **2006**, *8*, 3797–3800. (b) Vogt, H.; Baumann, T.; Nieger, M.; Bräse, S. *Eur. J. Org. Chem.* **2006**, 5315–5338.

prolinamide **106**-catalyzed nitrosoaldol reactions (Table 4.5).¹⁸ In five reactions of α,α -dialkyl aldehydes, followed by *in situ* reduction for ease of characterization, these authors observed no *ee*'s greater than 60%, with the most successful reactions being those of α -alkyl- α -benzyl aldehydes (entries 1, 4, and 5). Strangely, unlike the early dialkyl azodicarboxylate reactions that had already been reported by this time,^{8a,11} Gong and Jiang did not explore α -alkyl- α -aryl aldehydes as substrates. As will be discussed in the next section of this chapter, other catalysts provided more complicated results in reactions with nitrosobenzene **105**.

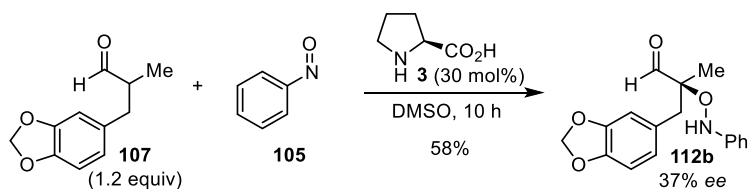
Table 4.5. Catalytic asymmetric nitrosoaldol reactions.

Entry	R	Substrate	Product	Yield (%)	ee (%)
1		107	112a	74	59
2	Me	108	113a	53	46
3	Et	109	114a	55	46
4	4- <i>t</i> BuC ₆ H ₄	110	115a	69	59
5	4- <i>i</i> BuC ₆ H ₄	111	116a	71	53

4.3 α -Oxygenation Reactions

When Gong and Jiang utilized proline **3** instead of amide **106** as catalyst in the reaction of aldehyde **107** with **105**, rather than the expected nitrosoaldol reaction, they observed an oxyamination to **112b** (Scheme 4.10).¹⁸ They hypothesized that the higher acidity of catalyst **3** relative to **106** influenced the overall regioselectivity of the process, an effect that had not been observed in previous reactions with linear aldehydes.¹⁹

¹⁸ Guo, H.-M.; Cheng, L.; Cun, L.-F.; Gong, L.-Z.; Mi, A.-Q.; Jiang, Y.-Z. *Chem. Commun.* **2006**, 429–431.



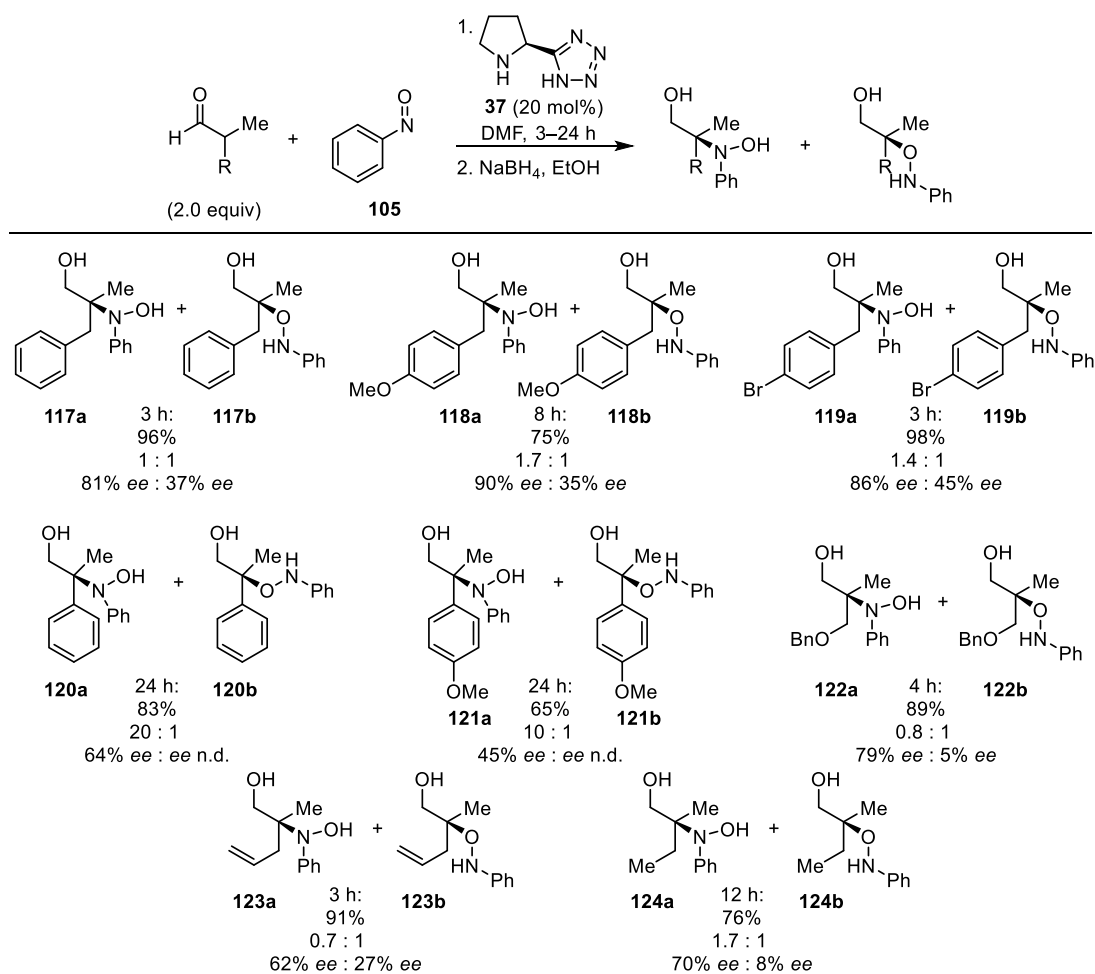
Scheme 4.10. Regioselectivity change with nitrosobenzene **105**.

Ultimately, predictable regiocontrol in this transformation would prove elusive. Kim and Park later attempted to probe the scope of this oxyamination using acidic tetrazole catalyst **37** (Table 4.6).²⁰ α -Benzyl- α -methyl aldehydes showed almost no regioselectivity in the reaction (products **117–119**), but nitrosoaldol products exhibited much higher enantioselectivities than the corresponding α -aminoxyalcohols (obtained after *in situ* reduction). In the case of α -aryl- α -methyl substrates, the nitrosoaldol products were heavily favored (**120** and **121**), but with lower *ee*'s. Substrate aldehydes bearing ether (products **122**), allyl (products **123**), or simple alkyl (products **124**) substitution also showed poor regioselectivities and even lower enantioselectivities for the oxyaminated products. The reactivity of branched aldehydes with nitrosobenzene has not been further studied since 2006.

¹⁹ For example: (a) Zhong G. *Angew. Chem. Int. Ed.* **2003**, *42*, 4247–4250. (b) Brown, S. P.; Brochu, M. P.; Sinz, C. J.; MacMillan, D. W. C. *J. Am. Chem. Soc.* **2003**, *125*, 10808–10809. (c) Hayashi, Y.; Yamaguchi, J.; Hibino, K.; Shoji, M. *Tetrahedron Lett.* **2003**, *44*, 8293–8296. (d) Córdova, A.; Sundén, H.; Bøgevig, A.; Johansson, M.; Himo, F. *Chem.–Eur. J.* **2004**, *10*, 3673–3684. (e) Kumarn, S.; Shaw, D. M.; Longbottom, D. A.; Ley, S. V. *Org. Lett.* **2005**, *7*, 4189–4191.

²⁰ Kim, S.-G.; Park, T.-H. *Tetrahedron Lett.* **2006**, *47*, 9067–9071.

Table 4.6. Oxyamination and nitrosoaldol reactions.



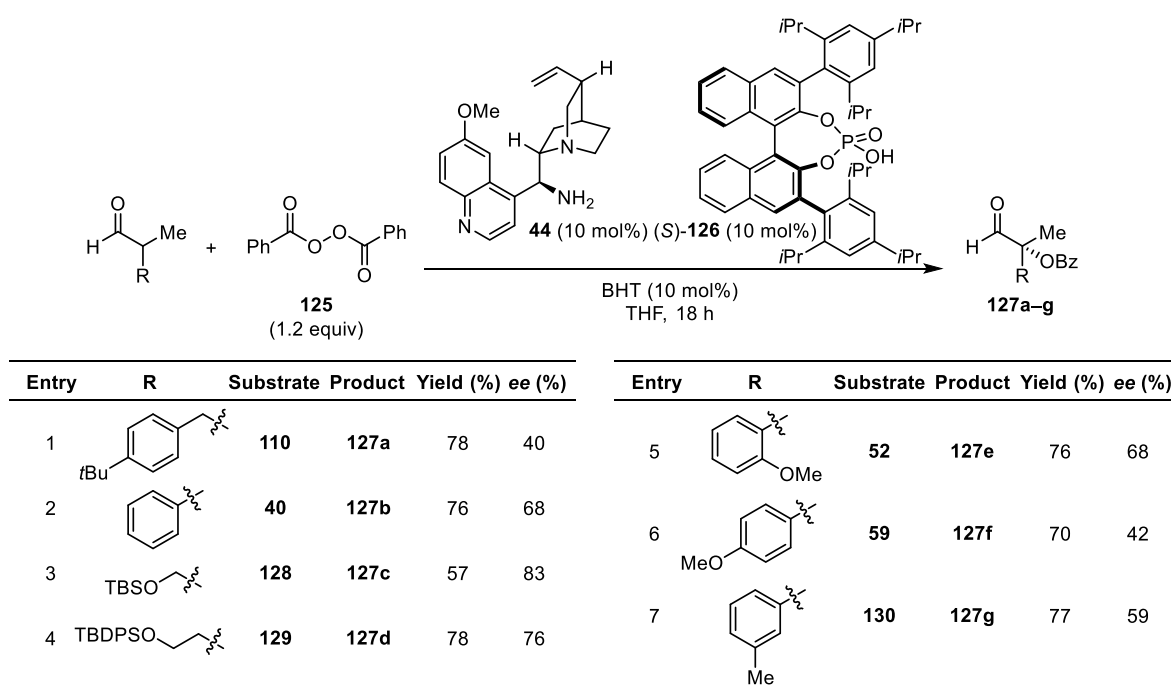
In order to bypass the problem of selectivity in α -oxyaminations, the List group developed an enamine-catalyzed α -benzoyloxylation of α -branched aldehydes.^{21,22} After screening several pyrrolidine-based secondary amine catalysts, these researchers began to explore cinchona alkaloid-derived primary amines, eventually arriving at catalyst **44**, which provided improved reactivity but poor enantioselectivity. Several achiral acid additives were also screened, but List and coworkers

²¹ Demoulin, N.; Lifchits, O.; List, B. *Tetrahedron* **2012**, *68*, 7568–7574.

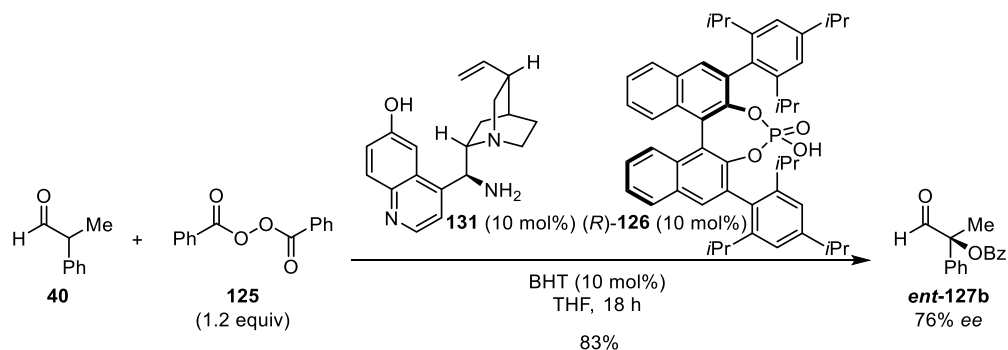
²² For preliminary reports with unbranched aldehydes, see: (a) Kano, T.; Mii, H.; Maruoka, K. *J. Am. Chem. Soc.* **2009**, *131*, 3450–3451. (b) Gotoh, H.; Hayashi, Y. *Chem. Commun.* **2009**, 3083–3085. (c) Vaismaa, M. J. P.; Yau, S. C.; Tomkinson, N. C. O. *Tetrahedron Lett.* **2009**, *50*, 3625–3627. For ketones, see: (d) Lifchits, O.; Demoulin, N.; List, B. *Angew. Chem. Int. Ed.* **2011**, *50*, 9680–9683.

still achieved low enantioselectivities with their model substrates. Only after switching to chiral phosphoric acid cocatalyst (*S*)-**126** did the researchers obtain products in high *ee* (Table 4.7). Butylated hydroxytoluene was also required in order to scavenge radicals. In conjunction with catalyst **44**, (*R*)-**126** provided the opposite enantiomer of product esters **127**, but typically in slightly lower *ee*. Thus the amine catalyst does not determine the stereochemical outcome of the reaction, but instead the acid cocatalyst does.

Table 4.7. Catalytic asymmetric α -benzoyloxylation.



Substrates with silyl ether components on the larger (non-methyl) α -substituent provided products with the highest enantioselectivities (entries 3 and 4). α -Aryl- α -methyl substrates generally provided lower *ee*'s (entries 2 and 5–7), with a maximum of 68% for products **127b** and **127e**. However, *ent*-**127b** could be synthesized in higher yield and *ee* by replacing the methoxy-substituent on amine **44** with an alcohol and using (*R*)-**126** (Scheme 4.11). Under these conditions, ester *ent*-**127b** was isolated in 76% *ee*.



Scheme 4.11. Improved α -benzoyloxylation of **40**.

For practical purposes, the scalability of these α -benzoyloxylation is limited by the cost of phosphoric acid cocatalyst **126** (TRIP).²³ Furthermore, these reactions provide ester products **127**. Conditions for deprotecting to the more versatile α -hydroxyaldehyde products were not provided in List's manuscript, nor have they been reported elsewhere. Given the steric congestion around the α -carbon, hydrolysis of the benzoate is expected to be nontrivial. To date, the direct catalytic asymmetric α -hydroxylation of α -branched aldehydes has not been reported. In Chapter 5, our own efforts towards this transformation will be presented.

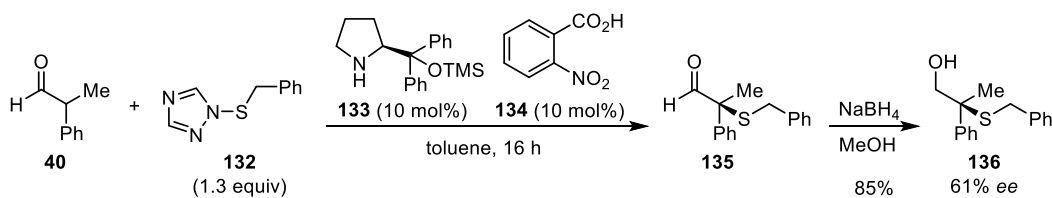
4.4 α -Sulfonylation Reactions

In 2005, the Jørgensen group reported the pyrrolidine-catalyzed α -sulfonylation of unbranched aldehydes.²⁴ This publication contains the only example of the complementary reaction of an α -branched aldehyde, to date (Scheme 4.12).²⁵ Sulfonylation of aldehyde **40** requires an acid cocatalyst and, after *in situ* reduction, affords alcohol product **136** in 85% yield overall and 61% *ee*. For comparison, sulfonylation of unbranched aldehydes did not require benzoic acid cocatalyst **134**, took only 3 hours, and proceeded with over 90% *ee* for all substrates.

²³ Sigma-Aldrich: \$1,275 for 500 mg of (*S*)-TRIP and \$1,210 for 500 mg of (*R*)-TRIP as of January 2015.

²⁴ Marigo, M.; Wabnitz, T. C.; Fielenbach, D.; Jørgensen, K. A. *Angew. Chem. Int. Ed.* **2005**, *44*, 794–797.

²⁵ For a related racemic reaction, see: Enders, D.; Rembiak, A.; Liebich, J. X. *Synthesis* **2011**, 281–286.



Scheme 4.12. Pyrrolidine-catalyzed α -sulfenylation.

4.5 α -Fluorination Reactions

Nitrogen, oxygen, and sulfur are commonly found atoms in natural products. Fluorine, on the other hand, has only been identified in a handful of naturally occurring molecules, despite its abundance in the earth's crust.²⁶ Nonetheless, its incorporation into organic scaffolds has grown profoundly important over the past several years, due to the atom's unique electronic and polar characteristics.²⁷ In medicinal chemistry, for example, the substitution of a C–H bond with C–F can significantly improve its biological properties, such as enhancing bioavailability or preventing metabolic oxidation.²⁸ To provide some perspective, in the first decade of this century, 38 fluorine-containing pharmaceuticals reached the market.²⁹ It is therefore no surprise that fluorination reactions in asymmetric catalysis have received considerable attention.

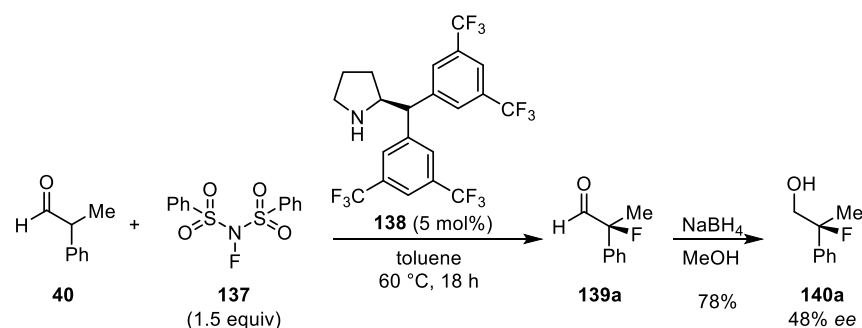
²⁶ Harper, D. B.; O'Hagan, D.; Murphy, C. D. In *The Handbook of Environmental Chemistry*; Gribble, G. W., Ed.; Springer: Berlin, 2003; Vol. 3 Part P, pp 141–169.

²⁷ For recent reviews, see: (a) Ma, J.-A.; Cahard, D. *Chem. Rev.* **2008**, *108*, PR1–PR43. (b) Lectard, S.; Hamashima, Y.; Sodeoka, M. *Adv. Synth. Catal.* **2010**, *352*, 2708–2732. (c) Furuya, T.; Kamlet, A. S.; Ritter, T. *Nature* **2011**, *473*, 470–477. (d) Cahard, D.; Bizet, V. *Chem. Soc. Rev.* **2014**, *43*, 135–147.

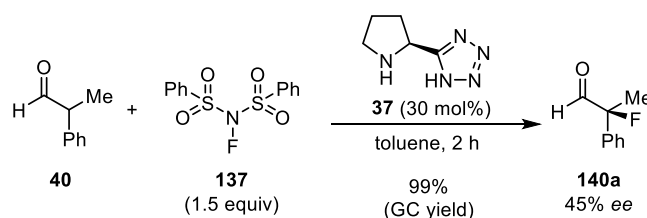
²⁸ (a) Müller, K.; Faeh, C.; Diederich, F. *Science* **2007**, *317*, 1881–1886. (b) Purser, S.; Moore, P. R.; Swallow, S.; Gouverneur, V. *Chem. Soc. Rev.* **2008**, *37*, 320–330. (c) Tredwell, M.; Gouverneur V. In *Comprehensive Chirality*; Carreira, E. M., Yamamoto H., Eds.; Elsevier: Amsterdam, 2012; Vol. 1, pp 70–85.

²⁹ Wang, J.; Sánchez-Roselló, M.; Aceña, J. L.; del Pozo, C.; Sorochinsky, A. E.; Fustero, S.; Soloshonok, V. A.; Liu, H. *Chem. Rev.* **2014**, *114*, 2432–2506.

In 2005, the groups of Enders,³⁰ Jørgensen,³¹ Barbas,³² and MacMillan³³ published secondary amine-catalyzed α -functionalizations of linear aldehydes almost simultaneously. Despite achieving up to 97% *ee* for linear substrates, with branched aldehyde **40**, Jørgensen and coworkers only reached 48% *ee* of alcohol **140a** (Scheme 4.13). *In situ* reduction was necessitated by the volatility and instability of fluoroaldehyde **139a** on silica gel. Likewise, Barbas and coworkers observed up to 96% *ee* in the fluorination of linear aldehydes, but **40** only provided them with 45% *ee* in product **140a** (Scheme 4.14). (Barbas reported the GC yield of aldehyde **139a** prior to reduction.) Both authors used commercially available, bench-stable NFSI **137** as their fluorinating reagent.



Scheme 4.13. Jørgensen's first α -fluorination of a branched aldehyde.



Scheme 4.14. Barbas's α -fluorination of a branched aldehyde.

³⁰ Enders, D.; Hüttl, M. R. M. *Synlett* **2005**, 991–993.

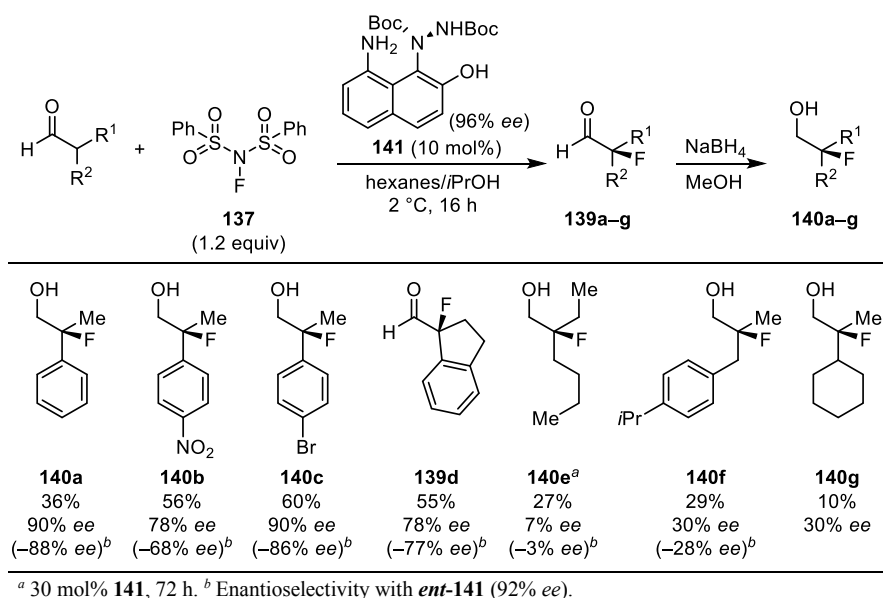
³¹ Marigo, M.; Fielenbach, D.; Braunton, A.; Kjærsgaard, A.; Jørgensen, K. A. *Angew. Chem. Int. Ed.* **2005**, *44*, 3703–3706.

³² Steiner, D. D.; Mase, N.; Barbas III, C. F. *Angew. Chem. Int. Ed.* **2005**, *44*, 3706–3710.

³³ Beeson, T. D.; MacMillan, D. W. C. *J. Am. Chem. Soc.* **2005**, *127*, 8826–8828.

In the subsequent year, Jørgensen and coworkers followed up on their original fluorination report with the publication of a unique, new, axially chiral primary amine catalyst.³⁴ These authors, based on the more favorable condensation of a primary amine with a branched aldehyde than a secondary amine such as **138**, studied catalyst **141** in the α -fluorination of α,α -disubstituted aldehydes (Table 4.8). α -Alkyl, α -aryl aldehydes provided the highest enantioselectivities (products **140a–c** and **139d**), while α,α -dialkyl aldehydes only showed low *ee* (products **140e–g**). In general, the yields were moderate at best after 16 hours.

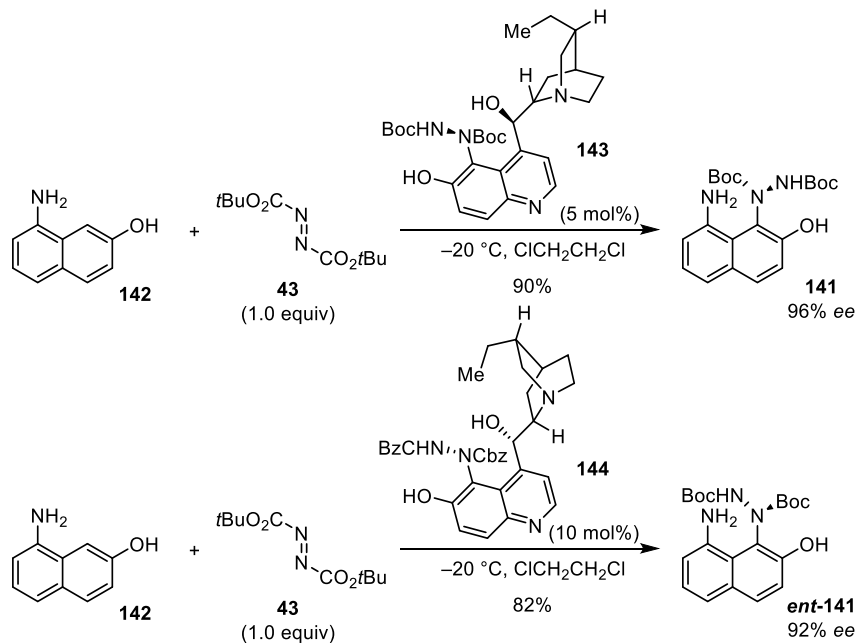
Table 4.8. Catalytic asymmetric α -fluorinations of branched aldehydes.



One potential limitation of this methodology lies in the catalyst itself. The synthesis of amine **141** requires a more complicated axially chiral catalyst (**143**, Scheme 4.15). This catalyst, and its Cbz-substituted pseudoenantiomer **144** are derived from common cinchona alkaloid catalysts (compare to **131**, Scheme 4.11). Although **141** has been produced in up to 96% *ee*, *ent*-**141** has only been made in a maximum of 92% *ee*, resulting in lower enantioselectivity in the synthesis of the opposite enantiomers of aldehydes **139** and fluorohydrins **140**. Enantioselectivities

³⁴ Brandes, S.; Niess, B.; Bella, M.; Prieto, A.; Overgaard, J.; Jørgensen, K. A. *Chem.–Eur. J.* **2006**, *12*, 6039–6052.

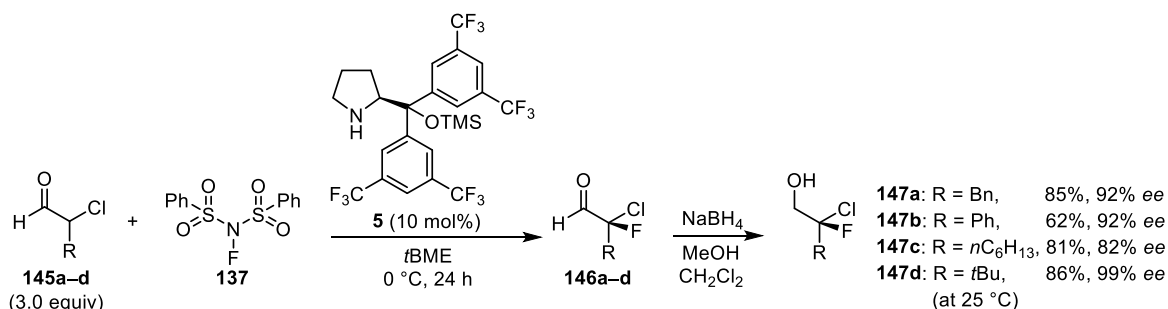
for reactions in Table 4.8 using **ent-141** are presented in parentheses where data is available.



Scheme 4.15. Synthesis of catalyst **141**.

In 2008, Shibatomi and Yamamoto utilized Jørgensen's earlier conditions³¹ in the α -fluorination of α -chloroaldehydes **145** (Scheme 4.16).³⁵ Although only four different reactions were reported, they all proceeded to α -chloro- α -fluoroalcohol products **147** with good yields and high *ee*'s, even using cyclic secondary amine **5**. Evidently, branched α -chloroaldehydes achieve more favorable rates and selectivities with these catalysts than do branched substrate aldehydes bearing two carbon substituents.

³⁵ Shibatomi, K.; Yamamoto, H. *Angew. Chem. Int. Ed.* **2008**, *47*, 5796–5798.



Scheme 4.16. α -Fluorination of α -chloroaldehydes.

To date, no other catalytic asymmetric α -fluorinations of α -branched aldehydes have been reported.³⁶ Although Jørgensen's results with catalyst **141** (Table 4.8) were quite promising in terms of enantioselectivity,³⁴ no further efforts to improve the rate of catalysis or to develop simpler, more accessible catalyst structures have been published. In Chapter 5, our work towards improving the practicality of these α -fluorination reactions will be presented.

4.6 Outlook

Several catalytic enantioselective difunctionalization reactions of α -alkyl- α,β -unsaturated aldehydes have also been reported to form epoxides, aziridines, and cyclopropanes, but as these transformations are mechanistically distinct from those discussed above, they are best classified on their own and reviewed separately.⁷ Although asymmetric α -iodinations,³⁷ α -brominations,³⁸ α -chlorinations,³⁹ and α -selenylations⁴⁰ of linear aldehydes have been catalyzed by amines, the corresponding transformations of α -branched aldehydes have never been reported. Undoubtedly,

³⁶ For an asymmetric catalytic α -fluorination of branched cyclic ketones, see: Yang, X.; Phipps, R. J.; Toste, F. D. *J. Am. Chem. Soc.* **2014**, *136*, 5225–5228.

³⁷ Kano, T.; Ueda, M.; Maruoka, K. *J. Am. Chem. Soc.* **2008**, *130*, 3728–3729.

³⁸ (a) Bertelsen, S.; Halland, N.; Bachmann, S.; Marigo, M.; Branton, A.; Jørgensen, K. A. *Chem. Commun.* **2005**, 4821–4823. (b) Kano, T.; Shirozu, F.; Maruoka, K. *Chem. Commun.* **2010**, *46*, 7590–7592.

³⁹ Brochu, M. P.; Brown, S. P.; MacMillan, D. W. C. *J. Am. Chem. Soc.* **2004**, *126*, 4108–4109.

⁴⁰ (a) Giacalone, F.; Gruttadauria, M.; Marculescu, A. M.; Noto, R. *Tetrahedron Lett.* **2007**, *48*, 255–259. (b) Kamlar, M.; Veselý, J. *Tetrahedron: Asymmetry* **2013**, *24*, 254–259.

the field of asymmetric enamine catalysis with α,α -disubstituted aldehydes remains in its infancy.

Stereoselective α -functionalizations of α -branched aldehydes provide complex, chiral products bearing fully tetrasubstituted α -carbons. All known heterofunctionalizations of this type have been summarized in this chapter. Despite the fact that general secondary amine scaffolds (i.e., **3–5**, Figure 4.1) have been identified for α -functionalizations of unbranched aldehydes, no such simple structures have emerged for the more challenging branched substrates. Typically, primary amines serve as the catalysts of choice, but even this can hardly be considered a compulsory rule. In Chapter 5, our steps toward a new, simple, general primary amine catalyst for asymmetric catalysis with α -branched aldehydes will be detailed.

**A New Primary Amine Catalyst for Efficient
Asymmetric α -Functionalizations of Branched Aldehydes¹**

5.1 Introduction

The enantioselective incorporation of heteroatoms such as oxygen or fluorine at the α -position of α -branched aldehydes allows for the synthesis of complex products containing tetrasubstituted, stereogenic carbon centers. The α -hydroxycarbonyl motif, with its differentiated oxygen atoms, represents a valuable precursor to manifold natural and bioactive compounds (Figure 5.1).² Alternatively, although fluorine is rarely found in natural products, its synthetic incorporation into organic scaffolds has recently developed into an active field of research, as evidenced by the fact that approximately 30% of all agrochemicals and 20% of all pharmaceuticals

¹ Portions of this chapter have been prepared for publication: Witten, M. R.; Jacobsen, E. N. *Manuscript in preparation*.

² For example, Doxorubicin: (a) DiMarco, A.; Gaetani, M.; Scarpinato, B. *Cancer Chemother. Rep.* **1969**, *1*, 33–37. Streptomycin: (b) Waksman, S. A.; Woodruff, H. B. *Proc. Soc. Exp. Biol. Med.* **1942**, *49*, 207–209. Rotenolone: (c) LaForge, F. B.; Smith, L. E. *J. Am. Chem. Soc.* **1930**, *52*, 1091–1098. Convolutamydine A: (d) Kamano, Y.; Zhang, H.-p.; Ichihara, Y.; Kizu, H.; Komiyama, K.; Pettit, G. R. *Tetrahedron Lett.* **1995**, *36*, 2783–2784. Danshenol A: (e) Kasimu, R.; Basnet, P.; Tezuka, Y.; Kadota, S.; Namba, T. *Chem. Pharm. Bull.* **1997**, *45*, 564–566. Forskolin: (f) Bhat, S. V.; Bajqwa, B. S.; Dornauer, H.; doScusa, N. J.; Fehlhaber, H.-W. *Tetrahedron Lett.* **1977**, *18*, 1669–1672. Okadaic acid: (g) Tachibana, K.; Scheuer, P. J.; Tsukitani, Y.; Kikuchi, H.; Van Engen, D.; Clardy, J.; Gopichand, Y.; Schmitz, F. J. *J. Am. Chem. Soc.* **1981**, *103*, 2469–2471.

contain a fluorine atom.³ The substitution of a C–H bond with C–F in an organic molecule can significantly alter its chemical and biological properties, such as improving bioavailability or preventing metabolic oxidation.⁴

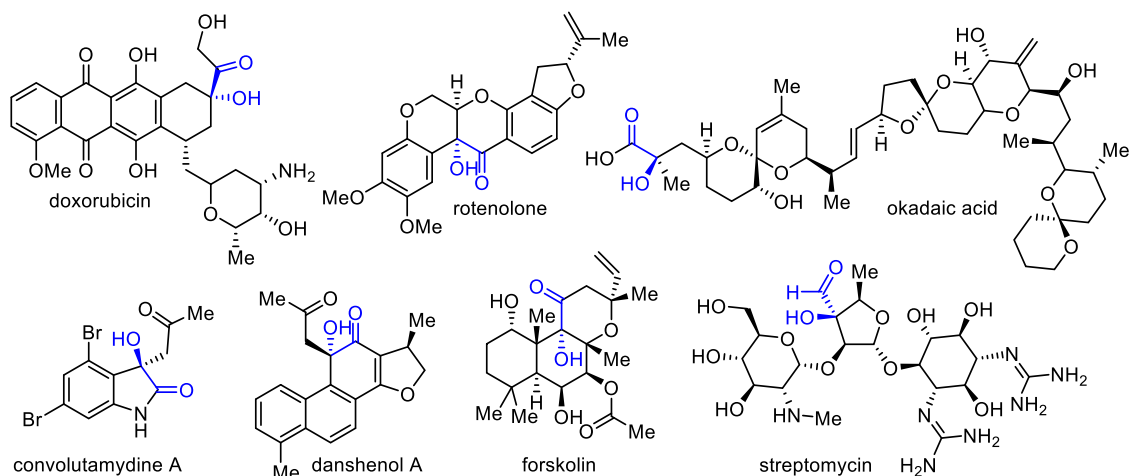


Figure 5.1. Tetrasubstituted α -hydroxycarbonyls in selected natural products.

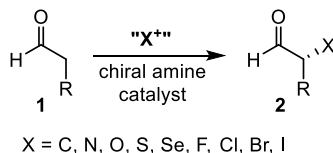
Enamine-catalyzed asymmetric α -functionalizations of carbonyl-containing compounds have proven to be effective means for generating complex, chiral products bearing C–C, C–N, and C–X (X = halogen or chalcogen) bonds. Although such reactions of α -unbranched aldehyde substrates to form products with trisubstitution at the α -position have been well developed (Scheme 5.1),⁵ related transformations of branched α,α -disubstituted aldehydes have thus far been

³ For recent reviews, see: (a) Ma, J.-A.; Cahard, D. *Chem. Rev.* **2008**, *108*, PR1–PR43. (b) Lectard, S.; Hamashima, Y.; Sodeoka, M. *Adv. Synth. Catal.* **2010**, *352*, 2708–2732. (c) Furuya, T.; Kamlet, A. S.; Ritter, T. *Nature* **2011**, *473*, 470–477. (d) Cahard, D.; Bizet, V. *Chem. Soc. Rev.* **2014**, *43*, 135–147.

⁴ (a) Müller, K.; Faeh, C.; Diederich, F. *Science* **2007**, *317*, 1881–1886. (b) Purser, S.; Moore, P. R.; Swallow, S.; Gouverneur, V. *Chem. Soc. Rev.* **2008**, *37*, 320–330. (c) Tredwell, M.; Gouverneur, V. In *Comprehensive Chirality*; Carreira, E. M., Yamamoto H., Eds.; Elsevier: Amsterdam, 2012; Vol. 1, pp 70–85.

⁵ See the following reviews and references therein: (a) Marigo, M.; Jørgensen, K. A. *Chem. Commun.* **2006**, 2001–2011. (b) Vilaivan, T.; Bhanthumnavin, W. *Molecules* **2010**, *15*, 917–958. (c) Bertelsen, S.; Jørgensen, K. A. *Chem. Soc. Rev.* **2009**, *38*, 2178–2189. (d) Nielsen, M.; Worgull, D.; Zweifel, T.; Gschwend, B.; Bertelsen, S.; Jørgensen, K. A. *Chem. Commun.* **2011**, 632–649. (e) *Comprehensive Enantioselective Organocatalysis*; Dalko, P. I., Ed.; Wiley: Weinheim, Germany, 2013.

primarily limited to aminations and C–C bond formations.⁶ Unique challenges associated with activation of these more sterically-encumbered carbonyl substrates, such as disfavored condensation⁷ and reduced reactivity of enamine intermediates⁸ have precluded their general application in asymmetric catalysis.⁹ In this section, the most relevant precedent to our own research will be recapitulated.



Scheme 5.1. Amine-catalyzed α -functionalizations of linear aldehydes.

5.1.1 α -Oxygenation Reactions

Amine-catalyzed asymmetric syntheses of α -oxygenated aldehydes and ketones have traditionally utilized oxygen sources such as nitrosobenzene or TEMPO for oxyamination.¹⁰ When α -branched aldehydes have been explored as substrates in reactions with nitrosobenzene **4**, products have typically been isolated with moderate *ee* and as regioisomeric mixtures representing enamine addition to either the oxygen or nitrogen atom of the electrophile (Scheme 5.2).^{11,12} In

⁶ For a comprehensive review, see: Desmarchelier, A.; Coeffard, V.; Moreau, X.; Greck, C. *Tetrahedron* **2014**, *70*, 2491–2513.

⁷ Sánchez, D.; Bastida, D.; Burés, J.; Isart, C.; Pineda, O.; Vilarrasa, J. *Org. Lett.* **2012**, *14*, 536–539.

⁸ Kempf, B.; Hampel, N.; Ofial, A. R.; Mayr, H. *Chem.–Eur. J.* **2003**, *9*, 2209–2218.

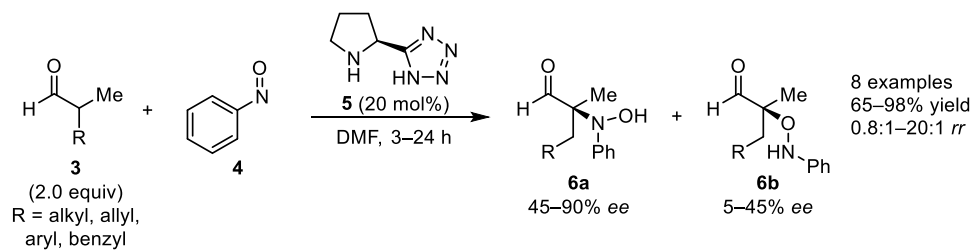
⁹ For a full analysis, see Section 4.1.

¹⁰ For pioneering reports, see: (a) Zhong G. *Angew. Chem. Int. Ed.* **2003**, *42*, 4247–4250. (b) Brown, S. P.; Brochu, M. P.; Sinz, C. J.; MacMillan, D. W. C. *J. Am. Chem. Soc.* **2003**, *125*, 10808–10809. (c) Hayashi, Y.; Yamaguchi, J.; Hibino, K.; Shoji, M. *Tetrahedron Lett.* **2003**, *44*, 8293–8296. (d) Córdova, A.; Sundén, H.; Bøgevig, A.; Johansson, M.; Himo, F. *Chem.–Eur. J.* **2004**, *10*, 3673–3684. (e) Simonovich, S. P.; Van Humbeck, J. F.; MacMillan, D. W. C. *Chem. Sci.* **2012**, *3*, 58–61. (f) Kumarn, S.; Shaw, D. M.; Longbottom, D. A.; Ley, S. V. *Org. Lett.* **2005**, *7*, 4189–4191. (g) Fan, X.; Alza, E.; Pericàs, M. A. *RSC Adv.* **2012**, *2*, 6164–6166.

¹¹ (a) Guo, H.-M.; Cheng, L.; Cun, L.-F.; Gong, L.-Z.; Mi, A.-Q.; Jiang, Y.-Z. *Chem. Commun.* **2006**, 429–431. (b) Kim, S.-G.; Park, T.-H. *Tetrahedron Lett.* **2006**, *47*, 9067–9071.

¹² For full description, see Section 4.3.

cases where one aldehyde is strongly favored, nitrosoaldol product **6a** predominates.



Scheme 5.2. Catalytic asymmetric α -oxyaminations.

The majority of enamine-promoted reactions to date have used secondary amines as catalysts, owing to their thermodynamically favorable iminium/enamine equilibria.¹³ Conversely, primary amines have only recently experienced a complementary spate of study, despite the fundamental role of lysine as Nature's enamine catalyst in aldolases, decarboxylases, and dehydratases.¹⁴ For example, List and coworkers found primary amine catalysts to perform better than pyrrolidines in the α -benzoyloxylation of cyclic ketones and α -branched aldehydes, likely due to a less sterically hindered condensation with the substrate carbonyl groups.^{15,16} Primary amine **8**, in conjunction with a chiral TRIP phosphoric acid cocatalyst (**9**) and benzoyl peroxide **7** as electrophile, successfully α -benzoyloxyated branched aldehydes **3** in up to 83% *ee* (Scheme 5.3). However, conditions for hydrolyzing ester products **10** to the free α -hydroxyaldehyde have not

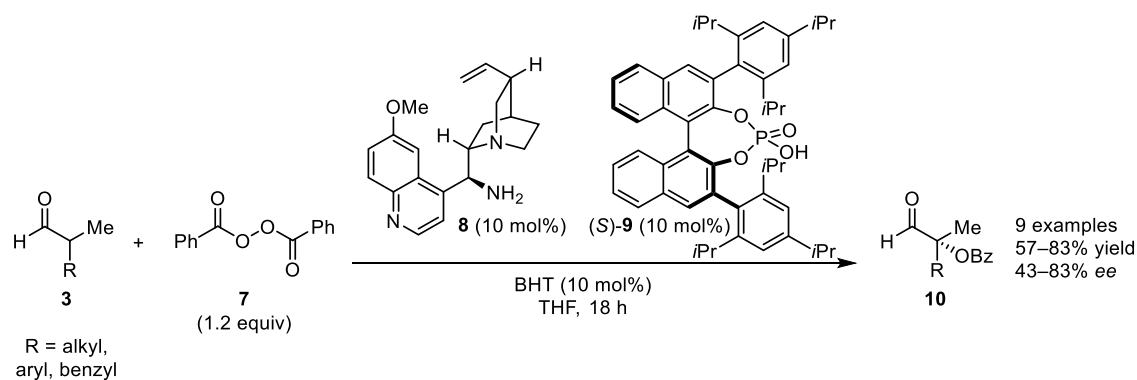
¹³ (a) Bergmann, E. D.; Zimkin, E.; Pinchas, S. *Rec. Trav. Chim.* **1952**, *71*, 168-191. (b) Bergmann, E. D.; Hirshberg, Y.; Pinchas, S.; Zimkin, E. *Rec. Trav. Chim.* **1952**, *71*, 192-199. (c) Bergmann, E. D.; Meeron, E.; Hirschberg, Y.; Pinchas, S. *Rec. Trav. Chim.* **1952**, *71*, 200-212. (d) Witkop, B. *J. Am. Chem. Soc.* **1956**, *78*, 2873-2882. (e) Pfau, M.; Ribière, C. *J. Chem. Soc. D* **1970**, 66-67. (f) Clark, R. A.; Parker, D. C. *J. Am. Chem. Soc.* **1971**, *93*, 7257-7261. (g) de Jaso, B.; Pommier, J.-C. *J. Chem. Soc., Chem. Commun.* **1977**, 565-566. (h) Knorr, R.; Weiß, A.; Löw, P.; Rappé, E. *Chem. Ber* **1980**, *113*, 2462-2489. (i) Boyd, D. R.; Jennings, W. B.; Waring, L. C. *J. Org. Chem.* **1986**, *51*, 992-995. (j) Capon, B.; Wu, Z. P. *J. Org. Chem.* **1990**, *55*, 2317-2324.

¹⁴ Hupe, D. J. In *New Comprehensive Biochemistry*; Page, M. I., Eds.; Elsevier: Amsterdam, 1984; Vol. 6, pp. 271-301.

¹⁵ Demoulin, N.; Lifchits, O.; List, B. *Tetrahedron* **2012**, *68*, 7568-7574.

¹⁶ For preliminary reports with unbranched aldehydes, see: (a) Kano, T.; Mii, H.; Maruoka, K. *J. Am. Chem. Soc.* **2009**, *131*, 3450-3451. (b) Gotoh, H.; Hayashi, Y. *Chem. Commun.* **2009**, 3083-3085. (c) Vaismaa, M. J. P.; Yau, S. C.; Tomkinson, N. C. O. *Tetrahedron Lett.* **2009**, *50*, 3625-3627. For ketones, see: (d) Lifchits, O.; Demoulin, N.; List, B. *Angew. Chem. Int. Ed.* **2011**, *50*, 9680-9683.

been disclosed and the direct catalytic asymmetric α -hydroxylation of branched aldehydes to generate unprotected α -hydroxy products has not been reported.



Scheme 5.3. Catalytic asymmetric α -benzoyloxylation.

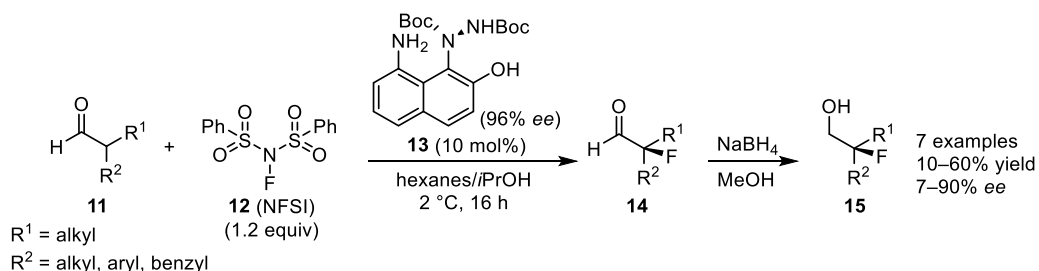
5.1.2 α -Fluorination Reactions

Similarly, the Jørgensen¹⁷ and Barbas¹⁸ groups were unable to use secondary amine catalysts to effect the α -fluorination of branched aldehydes in greater than 50% *ee*. However, Jørgensen and coworkers later demonstrated that an exotic, axially chiral primary amine catalyst (**13**, Scheme 5.4) could be employed to access tertiary fluorohydrins **15** in up to 90% *ee*, albeit with low to moderate yields.¹⁹ Catalyst **13** is itself synthesized by asymmetric catalysis, and can be obtained in 96% *ee*. However, the opposite enantiomer of **13**, which would be used to produce the opposite enantiomers of fluorides **15**, can only be formed in 92% *ee*.

¹⁷ Marigo, M.; Fielenbach, D.; Braunton, A.; Kjærsgaard, A.; Jørgensen, K. A. *Angew. Chem. Int. Ed.* **2005**, *44*, 3703–3706.

¹⁸ Steiner, D. D.; Mase, N.; Barbas III, C. F. *Angew. Chem. Int. Ed.* **2005**, *44*, 3706–3710.

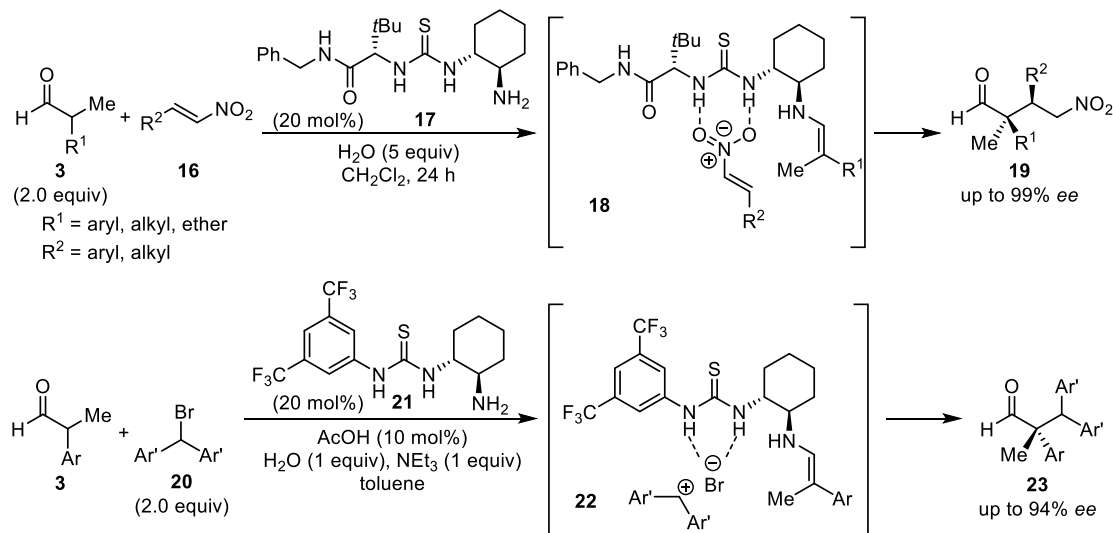
¹⁹ Brandes, S.; Niess, B.; Bella, M.; Prieto, A.; Overgaard, J.; Jørgensen, K. A. *Chem.–Eur. J.* **2006**, *12*, 6039–6052.



Scheme 5.4. Catalytic asymmetric α -fluorinations of branched aldehydes.

5.1.3 α -Functionalization Reactions from the Jacobsen Lab

Our group has also previously utilized primary amine catalysts for α -functionalizations of α,α -disubstituted aldehydes, specifically conjugate additions²⁰ and alkylations,²¹ to construct C–C bonds (Scheme 5.5). In 2006, we reported a conjugate addition of branched aldehydes **3** to nitroolefins **16**, catalyzed by primary aminothiourea **17**. These reactions proceeded in up to 99% *ee* through the putative intermediacy of enamine **18**, in which the electrophilic nitroolefin is templated by the hydrogen-bond donor portion of the catalyst.



Scheme 5.5. Examples of aldehyde α -functionalizations from our group.

²⁰ Lalonde, M. P.; Chen, Y.; Jacobsen, E. N. *Angew. Chem. Int. Ed.* **2006**, *45*, 6366–6370.

²¹ Brown, A. R.; Kuo, W.-H.; Jacobsen, E. N. *J. Am. Chem. Soc.* **2010**, *132*, 9286–9288.

In 2010, we published a related α -alkylation of branched aldehydes using similar catalyst **21**. The primary amine functional group is thought to activate aldehydes **3** through enamine catalysis. However, in this case, the catalyst thiourea ionizes the electrophilic benzhydryl bromides **20**. Product aldehydes **23** were isolated in up to 94% *ee*. Given the dearth of general solutions for efficient heteroatom incorporation at the α -position of branched aldehydes, we became interested in examining our chiral, cyclohexyldiamine-derived catalysts in other transformations of this type.

5.2 Reaction Development

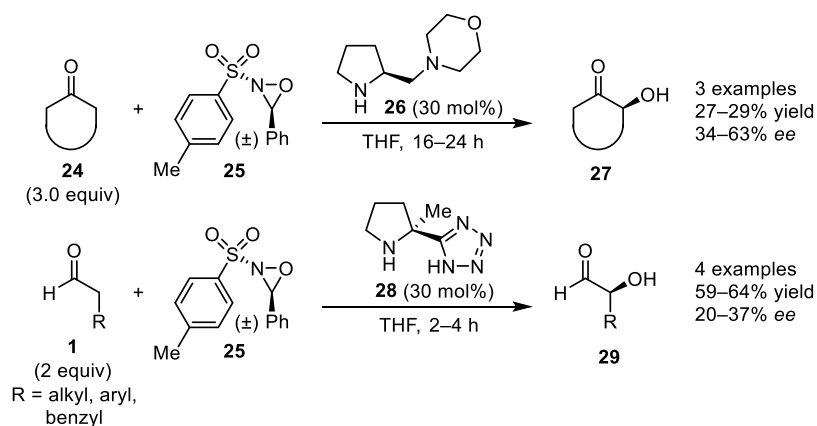
We chose to study two reactions simultaneously—hydroxylations and fluorinations—in order to enhance the likelihood of arriving at a general system with broad electrophile scope. Specifically, with regard to the hydroxylation, we intended to develop a methodology that would directly afford unprotected tertiary alcohols, an unknown transformation for branched aldehydes.²² A simple, new, primary amine catalyst that effectively promotes highly enantioselective α -hydroxylations and α -fluorinations of α,α -disubstituted aldehydes under operationally simple conditions will be described in this chapter.

5.2.1 An *N*-Sulfonyloxaziridine Hydroxylating Reagent

Although the α -hydroxylation of branched aldehydes has not previously been described, the related reaction of unbranched aldehydes and ketones has been achieved with moderate enantioselectivity using a racemic *N*-sulfonyloxaziridine (**25**) as the electrophilic oxygenating reagent (Scheme 5.6). Córdova and coworkers first studied this type of reactivity with cyclic ketones **24** in 2005, achieving low to moderate enantioselectivity for a very limited number of

²² For examples with unbranched aldehydes and ketones, see: (a) Córdova, A.; Sundén, H.; Engqvist, M.; Ibrahim, I.; Casas, J. *J. Am. Chem. Soc.* **2004**, *126*, 8914–8915. (b) Sundén, H.; Engqvist, M.; Casas, J.; Ibrahim, I.; Córdova, A. *Angew. Chem. Int. Ed.* **2004**, *43*, 6532–6535. (c) Engqvist, M.; Casas, J.; Sundén, H.; Ibrahim, I.; Córdova, A. *Tetrahedron Lett.* **2005**, *46*, 2053–2057. (d) Ibrahim, I.; Zhao, G.-L.; Sundén, H.; Córdova, A. *Tetrahedron Lett.* **2006**, *47*, 4659–4663. (e) Tong, S.-T.; Brimble, M. A.; Barker, D. *Tetrahedron* **2009**, *65*, 4801–4807.

substrates.^{22c} In 2009, the Barker group explored the related reaction of unbranched aldehydes **1**, attaining a maximum of 37% *ee* among four hydroxyaldehyde products **29**.^{22e}

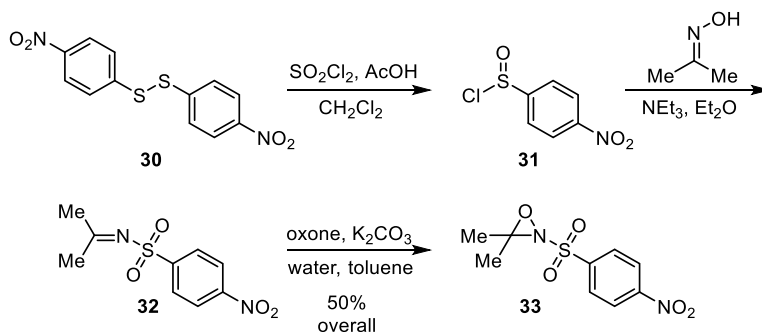


Scheme 5.6. Oxaziridines in asymmetric α -hydroxylations.

Conversely, molecular oxygen has also been investigated as an electrophilic hydroxylating reagent in α -hydroxylations of unbranched substrates, with marginally higher success.^{22a,b,d} As reactions which require bubbling gaseous O_2 through solution can be practically challenging, as well as difficult and dangerous to scale up, we chose instead to utilize a simple *N*-sulfonyloxaziridine as our oxygenating reagent. Oxaziridine **33** (Scheme 5.7), which was previously described by the Yoon group, is crystalline, bench-stable, and readily accessible on multigram scale.^{23,24} Furthermore, their reported synthesis requires no purification between steps, and the final oxaziridine product is isolated following a simple silica plug and recrystallization.

²³ Benkovics, T.; Du, J.; Guzei, I. A.; Yoon, T. P. *J. Org. Chem.* **2009**, *74*, 5545–5552.

²⁴ Oxaziridine **33** is stereogenic at its nitrogen atom. NMR experiments reveal saturation exchange of the diastereotopic methyl proton peaks within 5 seconds. Thus inversion is rapid on the timescale of α -functionalization reactions.



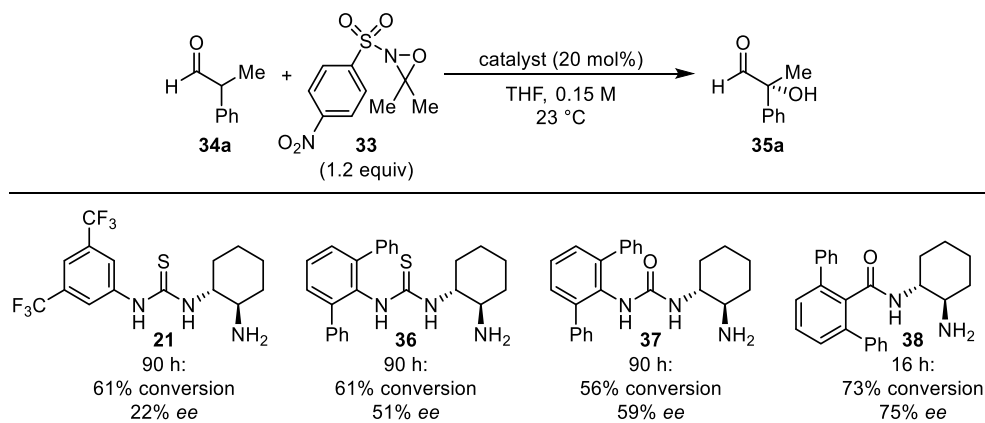
Scheme 5.7. Yoon's synthesis of *N*-sulfonyloxaziridine **33**.

5.2.2 Condition Optimization

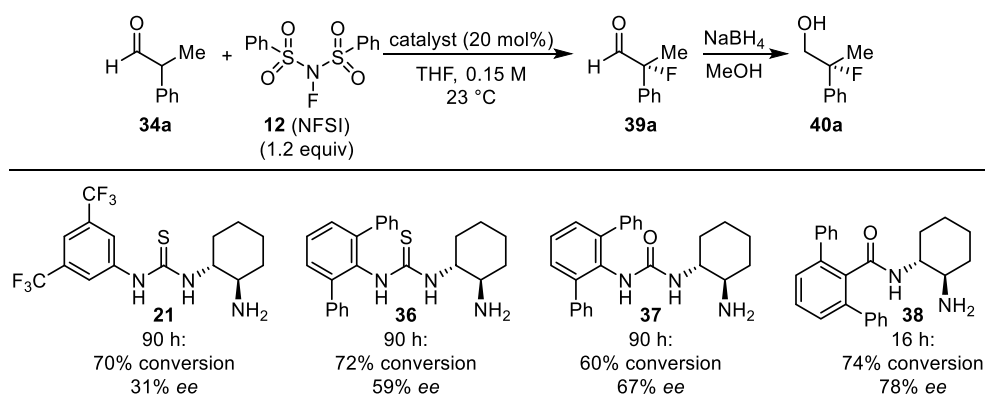
Initial exploration of both the α -hydroxylation (Table 5.1) and α -fluorination (Table 5.2) commenced with racemic aldehyde **34a** as substrate. Commercially available NFSI (**12**) was selected as the fluorinating reagent. Volatility and instability of fluoroaldehyde **39a** on silica gel necessitated its *in situ* reduction to fluorohydrin **40a** for isolation and analysis.^{17,19,25} Primary aminothiourea **21**, which we had previously employed in an asymmetric α -alkylation,²¹ provided reasonable conversions to both products **35a** and **40a** in modest enantioselectivities within four days. The use of primary amine **36**, which had proven successful in the enamine-catalyzed [5 + 2] cycloadditions discussed in Chapters 2 and 3,²⁶ resulted in an enhancement in *ee* for both reaction products. Urea analogue **37**, provided another small increase in reaction enantioselectivities. Finally, by simplifying the urea to benzamide catalyst **38**, hydroxyaldehyde **35a** and fluorohydrin **40a** could be formed in greater than 70% *ee* in significantly shortened reaction times.

²⁵ Beeson, T. D.; MacMillan, D. W. C. *J. Am. Chem. Soc.* **2005**, *127*, 8826–8828.

²⁶ (a) Burns, N. Z.; Witten, M. R.; Jacobsen, E. N. *J. Am. Chem. Soc.* **2011**, *133*, 14578–14581. (b) Witten, M. R.; Jacobsen, E. N. *Angew. Chem. Int. Ed.* **2014**, *53*, 5912–5916.

Table 5.1. Catalyst optimization for the α -hydroxylation.^a

^a Reactions performed on 0.15 mmol scale. Conversions determined by GC analysis. Enantioselectivities determined by HPLC analysis of reduced diol using commercial columns with chiral stationary phases.

Table 5.2. Catalyst optimization for the α -fluorination.^a

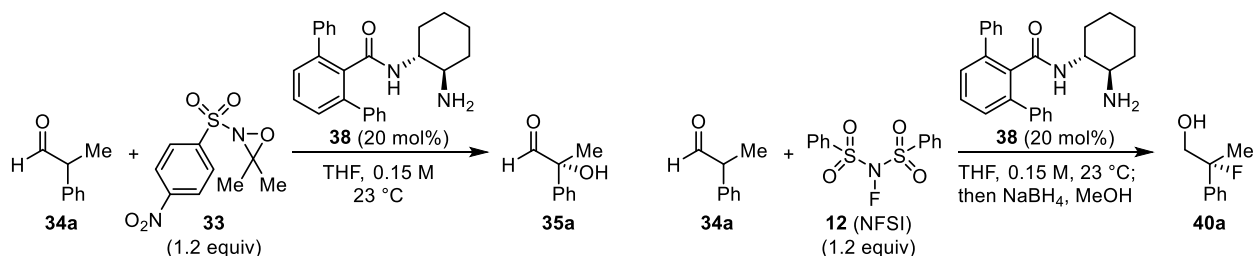
^a Reactions performed on 0.15 mmol scale. Conversions determined by GC analysis. Enantioselectivities determined by HPLC analysis of fluorohydrin using commercial columns with chiral stationary phases.

Acid and base additives are well-precedented promoters of enamine-catalyzed transformations due to their effects on the kinetics and thermodynamics of condensation and hydrolysis.^{5,6,16d,21,25–27} Water alone had almost no effect on either reaction (Tables 5.3 and 5.4, entries 2). Weak carboxylic acids also had little effect on rate, but a slightly positive effect on the enantioselectivities (entries 3 and 4). Stronger carboxylic acids such as trifluoroacetic, trichloroacetic, and dichloroacetic acid significantly enhanced the rates of both reactions (entries 5–7). Carboxylate bases proved detrimental to the hydroxylation yet had little effect on the

²⁷ Kwiatkowski, P.; Beeson, T. D.; Conrad, J. C.; MacMillan, D. W. C. *J. Am. Chem. Soc.* **2011**, *133*, 1738–1741.

fluorination (entries 8 and 9). Carbonate bases, on the other hand, diminished the rate and enantioselectivity of the hydroxylation to a lesser extent, and sodium bicarbonate even improved the rate of fluorination (entries 10 and 11). Finally, evaluation of additives alone and in combinations revealed a striking cooperative enhancement in rate and enantioselectivity for both reactions when TFA and NaHCO₃ were used together (entries 12).²⁸

Table 5.3. Additive screen in the α -hydroxylation.^a **Table 5.4.** Additive screen in the α -fluorination.^a



Entry	Additive(s)	Time (h)	Conversion (%) ^b	ee (%) ^c
1	none	16	73	75
2	1 equiv H ₂ O	19	77	72
3	20 mol% AcOH	19	72	79
4	20 mol% BzOH	17	61	81
5	20 mol% DCA	2	91	80
6	20 mol% TCA	2	64	70
7	20 mol% TFA	2	87	73
8	0.5 equiv NaOAc	160	54	42
9	0.5 equiv NaOBz	160	66	42
10	1.5 equiv Na ₂ CO ₃	92	52	57
11	1.5 equiv NaHCO ₃	48	72	71
12	20 mol% TFA + 1.5 equiv NaHCO ₃	4	85	87

^a Reactions performed on 0.15 mmol scale. ^b Conversions determined by GC analysis. ^c Enantioselectivities determined by HPLC analysis of reduced diol using commercial columns with chiral stationary phases.

Entry	Additive(s)	Time (h)	Conversion (%) ^b	ee (%) ^c
1	none	16	74	78
2	1 equiv H ₂ O	19	71	77
3	20 mol% AcOH	19	80	77
4	20 mol% BzOH	17	79	81
5	20 mol% DCA	2	63	80
6	20 mol% TCA	2	68	80
7	20 mol% TFA	2	64	80
8	0.5 equiv NaOAc	16	89	78
9	0.5 equiv NaOBz	16	95	78
10	1.5 equiv Na ₂ CO ₃	19	87	79
11	1.5 equiv NaHCO ₃	4	82	79
12	20 mol% TFA + 1.5 equiv NaHCO ₃	4	83	83

^a Reactions performed on 0.15 mmol scale. ^b Conversions determined by GC analysis. ^c Enantioselectivities determined by HPLC analysis of fluorohydrin using commercial columns with chiral stationary phases.

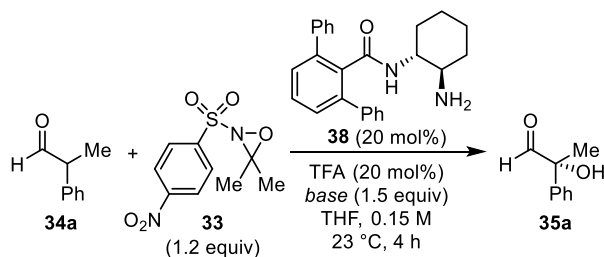
While the effect of acid and base additives on the rates of enamine catalysis are well precedented,²⁹ the curious dependence of the enantioselectivity on the nature of the base additive is more puzzling. We believe the remarkable effect of additives on reaction enantioselectivity

²⁸ See Section 5.7 for full details.

²⁹ For example, Chapter 2.

results from their influence on the equilibrium *E/Z* ratio of the proposed enamine intermediate (*vide infra*). Different carbonate bases behave quite differently, indicating a significant dependence on the identity of the counteranion in addition to the anion (Tables 5.5 and 5.6).

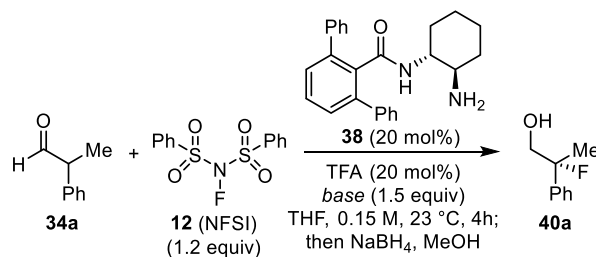
Table 5.5. Base screen in the α -hydroxylation.^a



Entry	Base	Conversion (%) ^b	ee (%) ^c
1	NaHCO ₃	85	87
2	Na ₂ CO ₃	87	88
3	K ₂ CO ₃	29	60
4	Li ₂ CO ₃	82	80
5	Cs ₂ CO ₃	31	47
6	BaCO ₃	87	83
7	CaCO ₃	86	79

^a Reactions performed on 0.15 mmol scale. ^b Conversions determined by GC analysis. ^c Enantioselectivities determined by HPLC analysis of reduced diol using commercial columns with chiral stationary phases.

Table 5.6. Base screen in the α -fluorination.^a



Entry	Base	Conversion (%) ^b	ee (%) ^c
1	NaHCO ₃	83	83
2	Na ₂ CO ₃	79	81
3	K ₂ CO ₃	74	73
4	Li ₂ CO ₃	78	73
5	Cs ₂ CO ₃	56	74
6	BaCO ₃	80	82
7	CaCO ₃	80	82

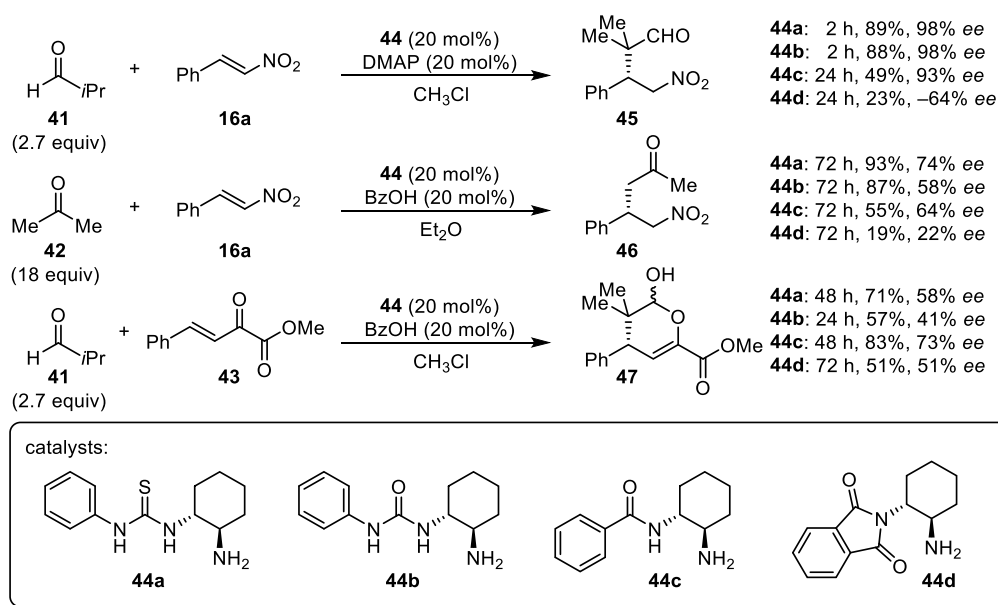
^a Reactions performed on 0.15 mmol scale. ^b Conversions determined by GC analysis. ^c Enantioselectivities determined by HPLC analysis of fluorohydrin using commercial columns with chiral stationary phases.

5.3 Regarding Benzamide Catalysts

Cyclohexyldiamine-derived benzamide catalysts such as **38** have only been investigated sporadically over the past few years. In 2009, the Yan group attempted to comprehensively correlate the catalytic efficiency of hydrogen-bond donors **44a** and **44b** (compare to **36** and **37** respectively) with benzamide **44c** (compare to **38**) and benzimide **44d** in conjugate addition reactions similar to that in Scheme 5.5 (Scheme 5.8).³⁰ For additions to nitrostyrene **16a**, the catalysts with dual hydrogen-bond donors are more effective in terms of rate, although amide **44c** provides product **46** in higher *ee* than urea **44b**. In the case of conjugate addition to enone **43**, **44c**

³⁰ Lao, J.-h.; Zhang, X.-j.; Wang, J.-j.; Li, X.-m.; Yan, M.; Luo, H.-b. *Tetrahedron: Asymmetry* **2009**, *20*, 2818–2822.

actually proved to be a higher-yielding and more enantioselective catalyst than thiourea **44a**. It should be noted that the purpose of this study was to compare dual hydrogen-bonding catalysts (**44a** and **44b**) with those which can only contribute one (**44c**) or zero (**44d**) hydrogen bonds. Benzamide **38** should not be considered a hydrogen-bond donor insofar as its amide NH is effectively blocked by one of the phenyl substituents on the terphenyl system. Nonetheless, this work was the first to study primary amines similar to **38** in enamine-catalyzed processes. Later, attempted benzamide-catalyzed additions of cyclohexanone to nitrostyrene **16a** resulted in the observation of only trace product.³¹



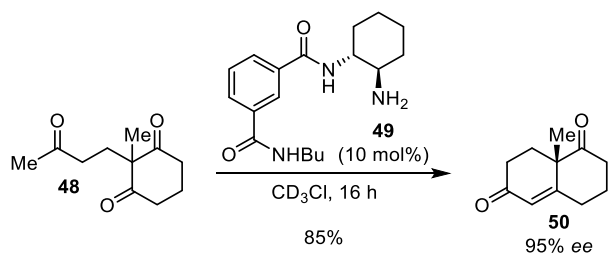
Scheme 5.8. Yan's investigation of catalytic asymmetric conjugate additions.

More recently, Morán and coworkers have used a benzamide catalyst (**49**) to effect the intramolecular aldol condensation of triketone **48** (Scheme 5.9).³² The Goldfuss group also used lithium sulfonate salts of cyclohexyldiamine-derived benzamide catalysts in asymmetric Michael

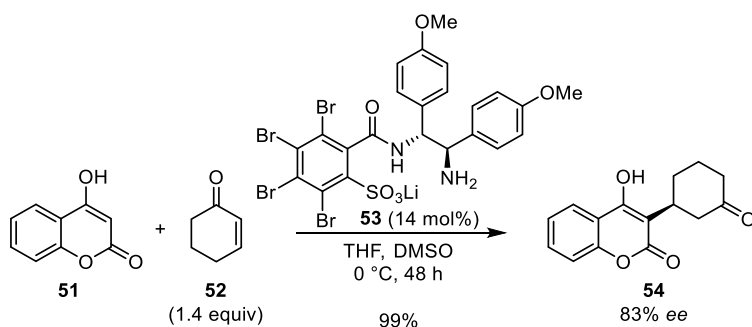
³¹ Zhong, J.; Guan, Z.; He, Y.-H. *Catal. Commun.* **2013**, *32*, 18–22.

³² Fuentes de Arriba, Á. L.; Seisdedos, D. G.; Simón, L.; Alcázar, V.; Raposo, C.; Morán, J. R. *J. Org. Chem.* **2010**, *75*, 8303–8306.

additions, but they ultimately settled on a different chiral diamine scaffold (**53**) which provided superior results (Scheme 5.10).³³



Scheme 5.9. Morán's benzamide-catalyzed aldol reaction.

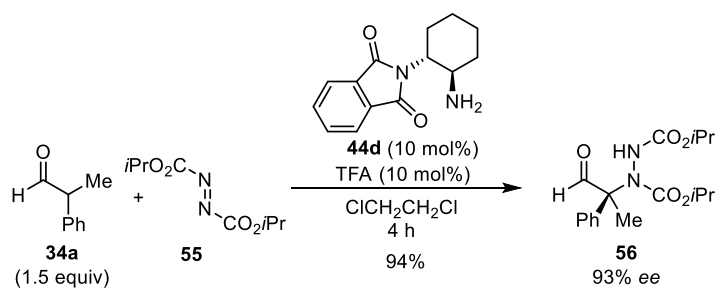


Scheme 5.10. Goldfuss's benzamide-catalyzed Michael reaction.

To date, no related primary aminobenzamides have been utilized for enamine catalysis. However, the Xu and Wang groups have used benzimide **44d** in an α -amination of branched aldehydes.³⁴ Although catalyst **44d** provides product **56** in 93% *ee*, we found it to be vastly inferior to benzamide **38** in the α -fluorination (61% *ee*) and α -hydroxylation (66% *ee*) reactions of the same substrate (**34a**).

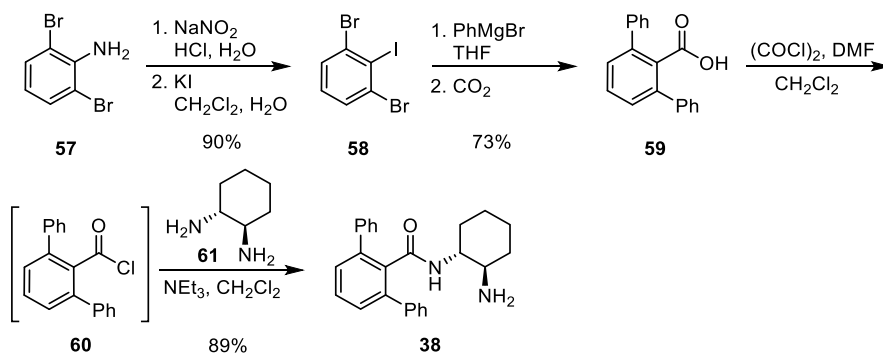
³³ Leven, M.; Neudörfl, J. M.; Goldfuss, B. *Beilstein J. Org. Chem.* **2013**, *9*, 155–165.

³⁴ Fu, J.-Y.; Wang, Q.-L.; Peng, L.; Gui, Y.-Y.; Xu, X.-Y.; Wang, L.-X. *Chirality* **2013**, *25*, 668–672.



Scheme 5.11. Xu and Wang's benzimide-catalyzed α -amination reaction.

Benzamide **38** is synthesized from inexpensive dibromoaniline **57** in four steps. Sandmeyer reaction with potassium iodide affords trihalobenzene **58**,³⁵ which is then converted to benzoic acid **59** in a single step.³⁶ Excess phenylmagnesium bromide displaces the bromide substituents on compound **58** and metallates at the *ortho*-iodide. Bubbling carbon dioxide into the solution results in efficient formation of acid **59**, which is converted to benzoyl chloride **60** then coupled with diamine **61**.³⁷ Chloride **60** does not need to be purified, and is sufficiently hindered to avoid double acylation of free diamine **61**. Catalyst **38** has been synthesized on a 3 gram scale.



Scheme 5.12. Synthesis of catalyst **38**.

³⁵ Mao, G.; Orita, A.; Matsuo, D.; Hirate, T.; Iwanaga, T.; Toyota, S.; Otera, J. *Tetrahedron Lett.* **2009**, *50*, 2860–2864.

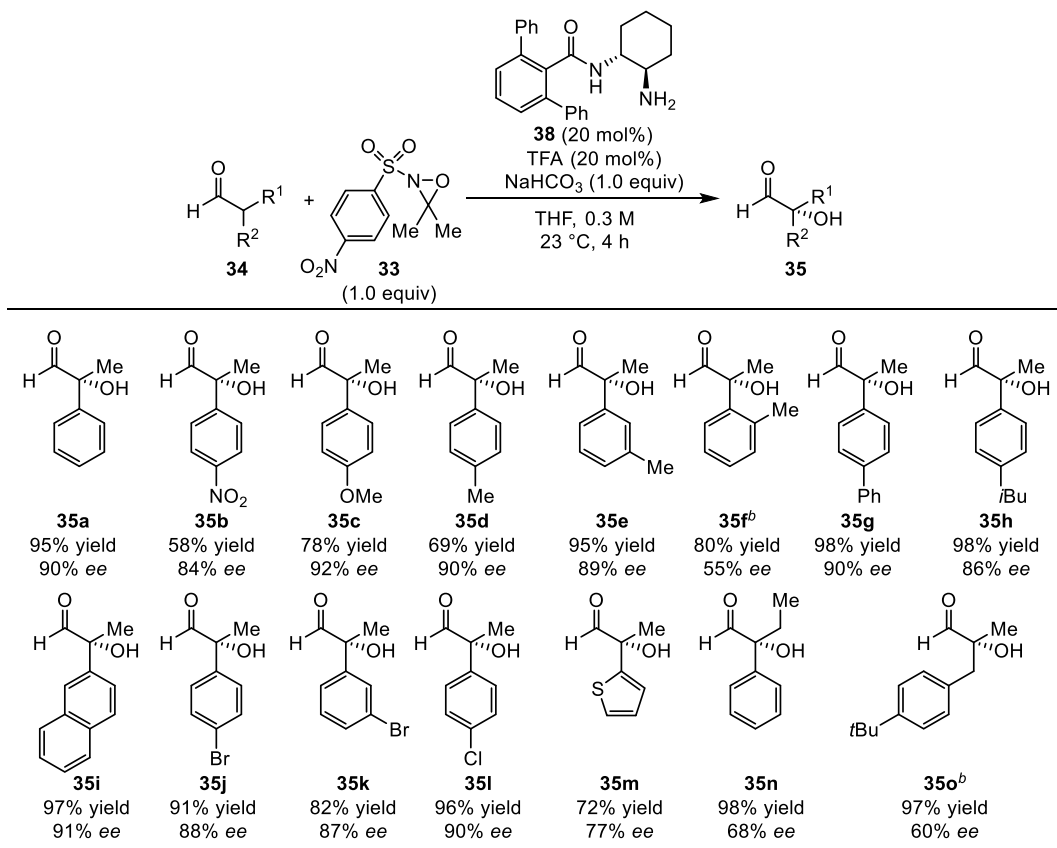
³⁶ Dickie, D. A.; Chan, A. Y. C.; Jalali, H.; Jenkins, H. A.; Yu, H.-Z.; Clyburne, J. A. C. *Chem. Commun.* **2004**, 2432–2433.

³⁷ Branca, M.; Pena, S.; Guillot, R.; Gori, D.; Alezra, V.; Kouklovsky, C. *J. Am. Chem. Soc.* **2009**, *131*, 10711–10718.

5.4 Substrate Scope

In order to demonstrate the synthetic utility of our α -functionalizations, reactions were scaled up to 1 mmol of aldehyde for examination of the substrate scope. In adjusting our reaction conditions for scale-up, we discovered that we could double the overall reaction concentration and decrease the amount of electrophile and NaHCO_3 to 1.0 equivalent each, thus reducing waste generated from these processes.²⁸ With this optimized protocol, which requires no extraction/wash procedure, we isolated a 95% yield of hydroxyaldehyde **35a** in 90% *ee* (Table 5.7). An aldehyde with an electron-deficient aromatic ring afforded the desired tertiary alcohol (**35b**) product in slightly decreased enantioselectivity and diminished yield due to instability. However, electron-donating substituents were well tolerated in both the *para*- and *meta*-positions (**35c–e**). *Ortho*-substitution on the substrate ring resulted in slower reaction rates and lower enantioselectivity (**35f**). Larger carbon substituents and halogens could be incorporated onto the aldehyde's benzene ring to generate products **35g–l**, with **35j** and **35k** representing potential cross-coupling substrates for further diversification. The presence of smaller heteroaromatic rings (**35m**), longer alkyl chains (**35n**), and α,α -dialkyl substitution (**35o**) represent limitations which remain to be addressed.

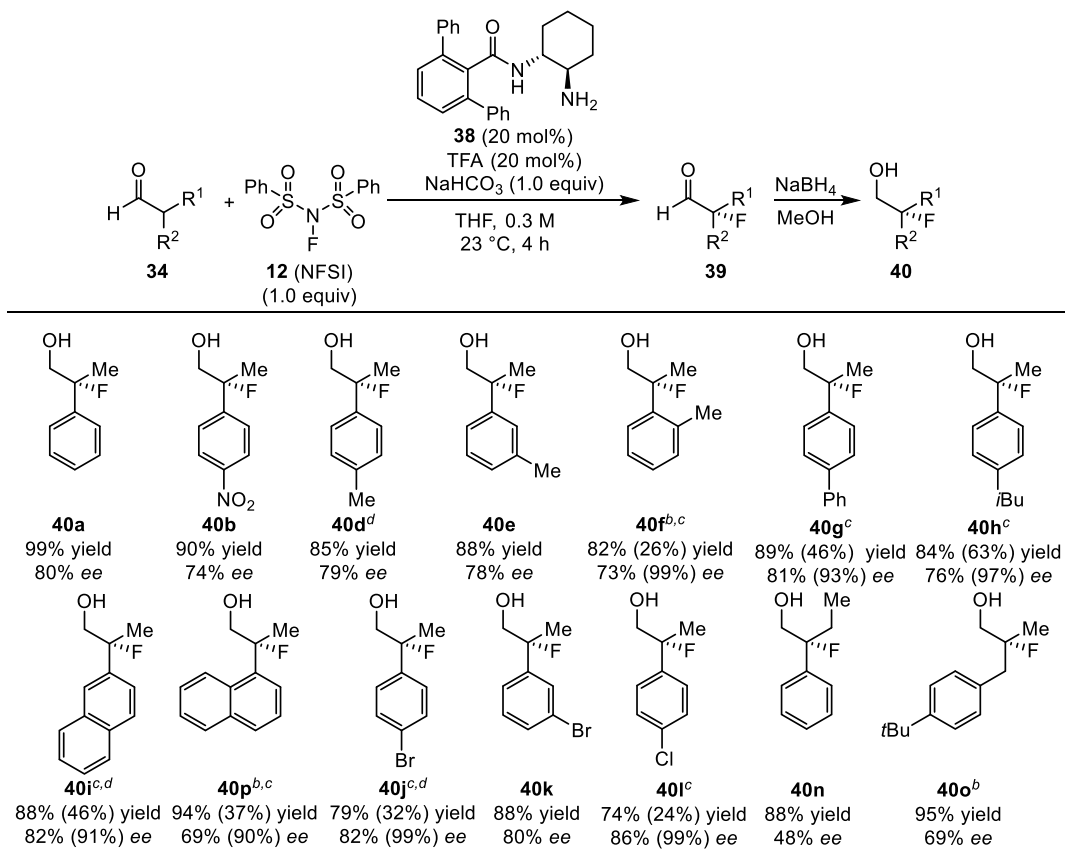
Table 5.7. Substrate scope of α -hydroxylation.^a



^a Reactions performed on 1.00 mmol scale. Yields of isolated products after column chromatography. Enantioselectivities determined by HPLC analysis of reduced diol using commercial columns with chiral stationary phases. Absolute configurations assigned based on comparison of optical rotations to published data.²⁸ ^b 20 h.

The α -fluorination was also scaled up successfully to 1 mmol of aldehyde, although we observed a small reduction in *ee* of isolated fluorohydrin **40a** (Table 5.8). This transformation demonstrated a similar substrate scope to the α -hydroxylation with electron-deficient (**40b**), *para*- (**40d,g,h**), and *meta*-substitution (**40e**) permitted on the aryl ring. As for the hydroxylation, *ortho*-substitution resulted in longer reaction times, but the diminution in enantioselectivity was not as substantial as in the hydroxylation (**40f,p**). Bromo- and chloro-substituents could be incorporated onto the aromatic ring (**40j-l**), but longer alkyl chains (**40n**) and dialiphatic aldehydes (**40o**) resulted in lower *ee*'s as observed for the α -hydroxylation.

Table 5.8. Substrate scope of α -fluorination.^a



^a Reactions performed on 1.00 mmol scale. Yields of isolated products after column chromatography. Enantioselectivities determined by HPLC analysis of fluorohydrin using commercial columns with chiral stationary phases. Absolute configurations assigned based on comparison of optical rotations to published data.²⁸ ^b 20 h. ^c Numbers in parentheses correspond to isolated yield and ee after recrystallization. ^d The absolute stereochemical configurations of **40d**, **40i**, and **40j** were confirmed by X-ray crystallography.

Notably, hydroxyaldehyde **35h** and fluoroaldehyde **39h**, bear the same α -(4-isobutylphenyl), α -methyl substitution pattern as ibuprofen. In fact, 2-arylpropionic acids define a general class of nonsteroidal anti-inflammatory drugs known as profens (Figure 5.2).³⁸ Thus, our methodology allows for simple access to fluorinated congeners of these compounds. Furthermore, the carboxylic acids of α -hydroxylated compounds such as **35a**, atrolactic acids, are often used as

³⁸ (a) *Ibuprofen: A Critical Bibliographic Review*; Rainsford, K. D., Ed.; Taylor & Francis: London, 1999. (b) Kourist, R.; de Maria, P. D.; Miyamoto, K. *Green Chem.* **2011**, *13*, 2607–2618.

configurationally stable, non-enolizable substitutes for mandelic acid.³⁹ Finally, despite lower enantioselectivities for the fluorination chemistry, many of the fluorohydrins could be recrystallized to enhanced enantiopurities.²⁸

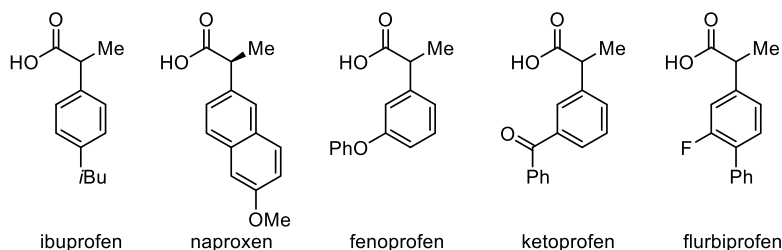


Figure 5.2. Selected profen nonsteroidal anti-inflammatory drugs.

X-ray quality crystals of fluorohydrins **40d**, **40i**, and **40j** were grown from hexanes and ether (Figure 5.3). The absolute stereochemical configurations of these compounds matches that assigned to all other fluorohydrins and all hydroxyaldehydes based on optical rotations.²⁸

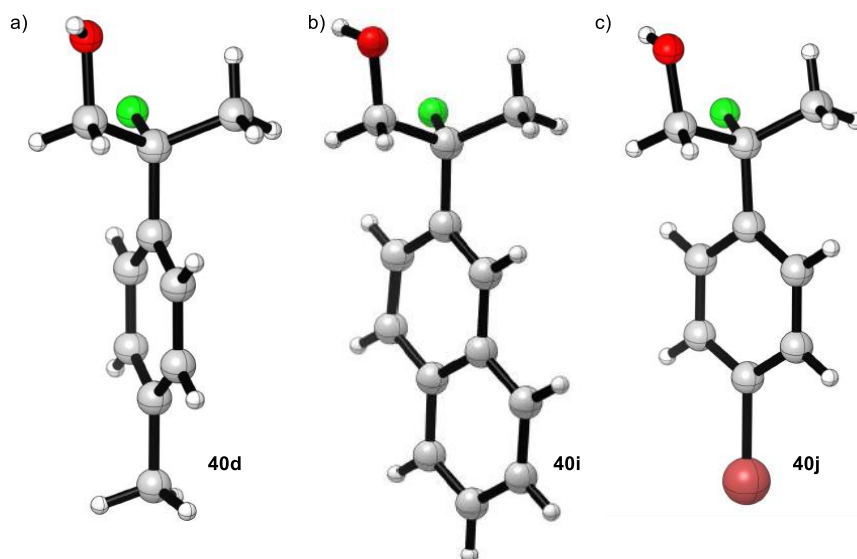
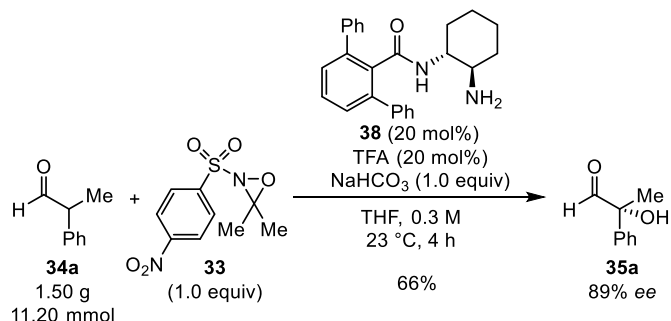


Figure 5.3. X-ray crystal structures of (a) **40d**, (b) **40i**, and (c) **40j**.

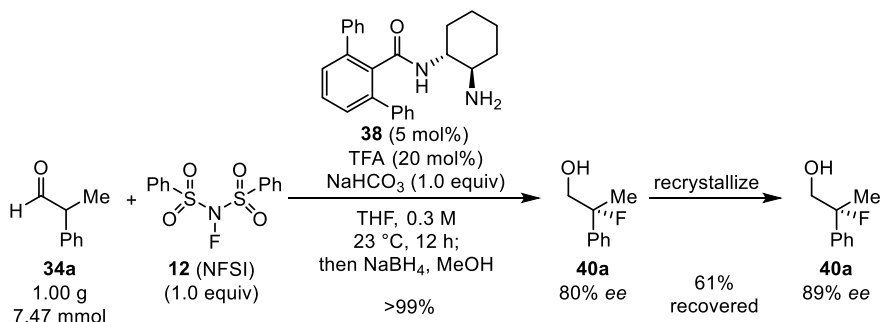
Both reactions can be scaled up even further to generate greater than one gram of

³⁹ Oxidation of aldehydes such as **35a** to the corresponding atrolactic acids has been described: Pérez-Estrada, S.; Lagunas-Rivera, S.; Vargas-Díaz, M. E.; Velázquez-Ponce, P.; Joseph-Nathan, P.; Zepeda, L. G. *Tetrahedron: Asymmetry* **2005**, *16*, 1837–1843.

hydroxyaldehyde **35a** (Scheme 5.13) or fluoroalcohol **40a** (Scheme 5.14). In the case of the fluorination, the loading of catalyst **38** could be reduced to 5 mol% to generate quantitative yield of fluorohydrin **40a** within 12 hours.⁴⁰ Recrystallization from hexanes provided the tertiary fluoride in improved 89% *ee*.²⁸ Higher enantioselectivities can also be achieved in the α -hydroxylation when the reaction is performed at lower temperature (Scheme 5.15).⁴¹



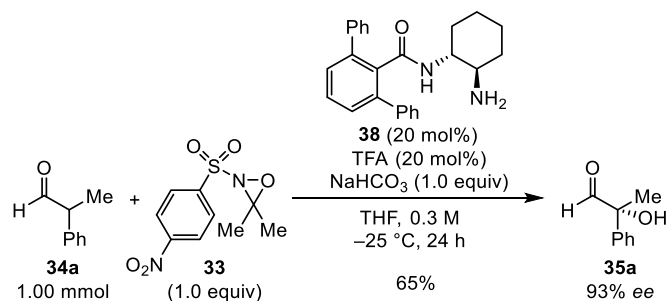
Scheme 5.13. Gram-scale α -hydroxylation.



Scheme 5.14. Gram-scale α -fluorination.

⁴⁰ Reduction in catalyst loading below 20 mol% in the α -hydroxylation resulted in diminished yields. See Section 5.7 for details.

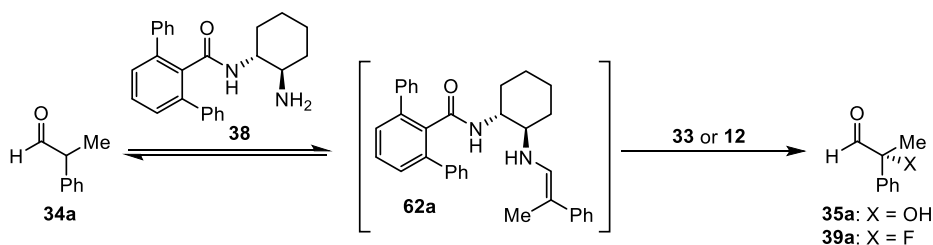
⁴¹ The α -fluorination does not exhibit increased enantioselectivities when cooled as low as -25 °C.



Scheme 5.15. Low temperature α -hydroxylation.

5.5 Mechanistic Studies

The viability of putative enamine intermediate **62a** (Scheme 5.16) was confirmed by mass spectrometric analysis of a reaction mixture lacking oxaziridine **33** or NFSI (**12**). However, we anticipated that a more detailed structural understanding of this key nucleophile would elucidate a clearer model for stereoselection and inform further reaction design. To this end, a computational examination of the key enamine **62a** was undertaken.



Scheme 5.16. Formation of proposed intermediate **62a**.

5.5.1 A DFT Model for Enantioinduction

Computational analysis of enamine **62a** revealed a lowest energy structure in which a crucial intramolecular hydrogen bond between the benzamide carbonyl and the enamine NH rigidifies the catalyst backbone (*E*-**62a**, Figure 5.4). This stabilizing interaction appears to stiffen the catalyst backbone and cause the terphenyl moiety to project one of its aryl rings directly behind one face of the reactive nucleophile. Although the origin of stereoselectivity in these α -functionalization reactions is not fully understood, we speculate that it is primarily determined by

the *E/Z* ratio of intermediate **62a**, with the electrophilic component of the reaction approaching the enamine almost exclusively from the exposed front face.

The lowest energy calculated structures for *E*-**62a** and *Z*-**62a** are separated by a difference of 1.28 kcal mol⁻¹, owing to a steric clash between substrate and catalyst phenyl rings in *Z*-**62a**. At room temperature, this would correspond to an 8.8:1 ratio of *E*-**62a** to *Z*-**62a**, or approximately 90% *ee*, which is precisely what we observe in the α -hydroxylation of substrate **34a** to product **35a**. This revelation necessitates a revision of Scheme 5.16 to Scheme 5.17, with a more schematic depiction of intermediate enamine **62a**.

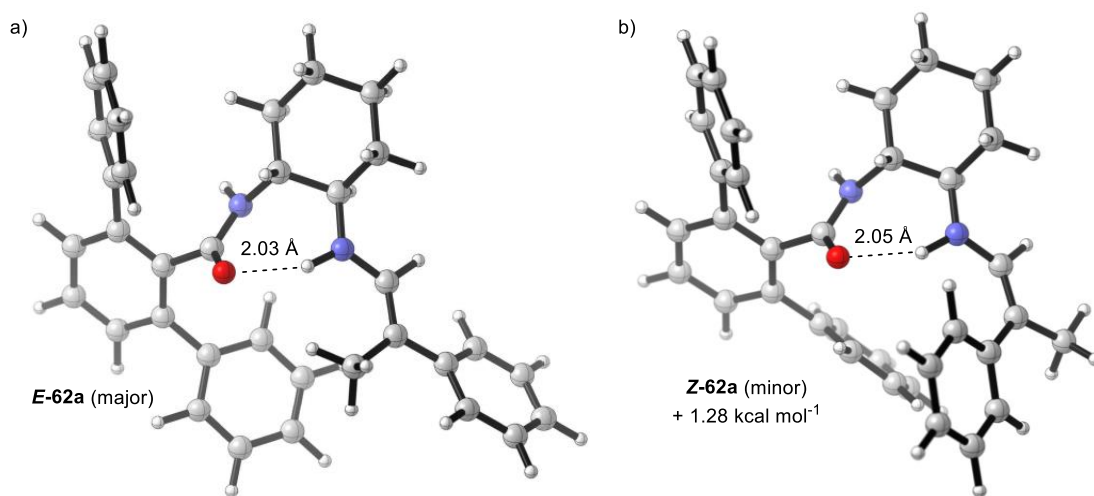
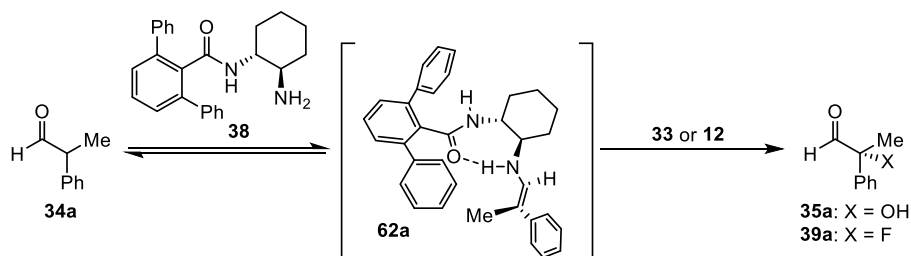


Figure 5.4. Lowest energy structures calculated at the B3LYP/6-31G(d) level of theory for (a) *E*-**62a** leading to the major enantiomers of products (*R*)-**35a** and (*R*)-**39a** and (b) *Z*-**62a** leading to the minor enantiomers of products (*S*)-**35a** and (*S*)-**39a**.



Scheme 5.17. Revised scheme for formation of intermediate **62a**.

It should be considered that these calculations represent enamine ground states. Although

the steric destabilization of **Z-62a** almost certainly still exists in the subsequent transition state for nucleophilic attack, the identity of the electrophile must also play a role in the location of this saddle point along a reaction coordinate. Different electrophiles, much like different acids, bases, and solvents, may also influence the partitioning of enamine **62a** between *E* and *Z* isomers. Therefore, as will be discussed in the following subsection, enantioselectivities do not remain constant with different classes of electrophiles, although they are generally high.

Finally, we have located a third enamine **62a** structure by rotating the C–N bond between catalyst **38** and substrate **34a** in **E-62a** (Figure 5.5). This intermediate (**ZE-62a**), which would also provide minor enantiomers of products **35a** and **39a**, maintains an *E*-geometry on the enamine bond, but has a *Z*-geometry on the C–N bond. This stationary point lies 4.06 kcal mol⁻¹ above **E-62a**, and is therefore not considered a significant component in the overall mechanism.

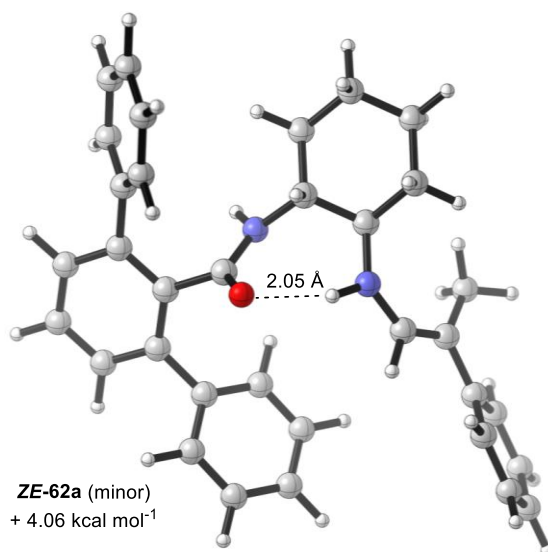
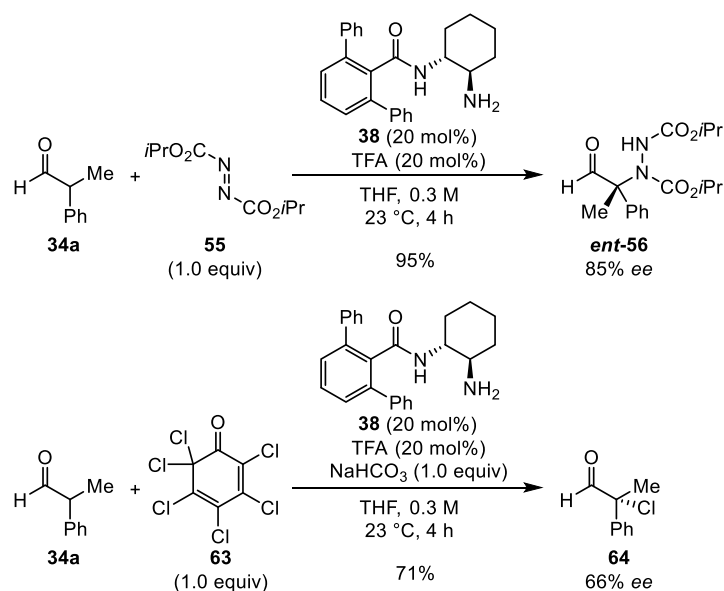


Figure 5.5. Lowest energy structure calculated at the B3LYP/6-31G(d) level of theory for **ZE-62a** leading to the minor enantiomers of products (*S*)-**35a** and (*S*)-**39a**.

5.5.2 Investigation of Other α -Functionalizations

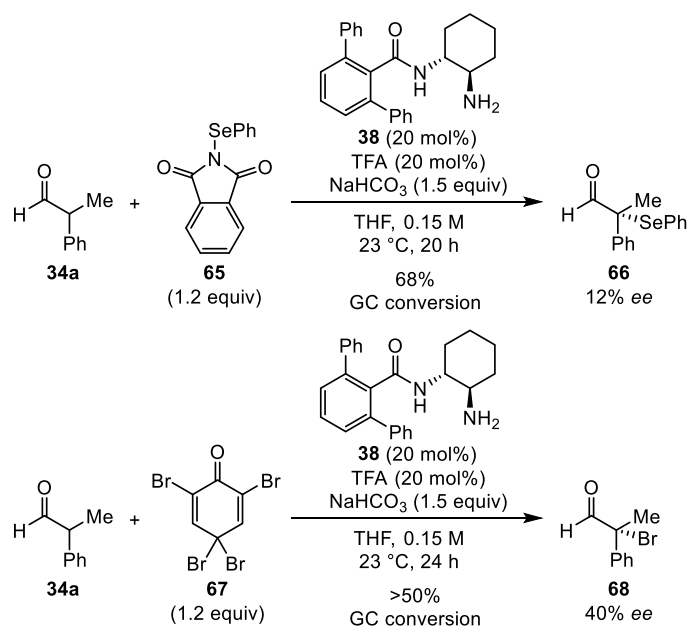
The stereochemical model illustrated above suggests a possible general mode of enamine catalysis with primary amine **38** in which several electrophiles or oxidants could be expected to

preferentially add to the exposed face of enamine **62a**, with enantioselectivity predominantly determined by the equilibrium *E/Z* ratio of this intermediate. Preliminary results for an α -amination and the first asymmetric α -chlorination (Scheme 5.18) of a branched aldehyde support this hypothesis. Both of these reactions use commercially available electrophiles. Aldehydes **ent-56** and **64** were isolated in 85% and 66% *ee* respectively; these are encouraging starting points for future improvement, accounting for the fact that the overall conditions were not optimized for these electrophiles.



Scheme 5.18. Catalytic asymmetric α -amination and α -chlorination.

However, preliminary attempts at an α -selenylation and an α -bromination were met with lower *ee*'s of isolated products **66** and **68** respectively, demonstrating the influence of the electrophile on enantiodetermination in the overall reaction (Scheme 5.19). Nonetheless, the general benzamide catalyst **38** discovered in this work appears to be compatible with a range of electrophiles, and future optimization around this skeleton, coupled with greater mechanistic understanding, should provide improved results in these and other α -functionalization reactions.



Scheme 5.19. Catalytic asymmetric α -selenylation and α -bromination.

One mechanistic possibility for decreased enantioselectivities with electrophiles such as **65** and **67**, as mentioned in Section 5.5.1, would be that they alter the ratio of intermediates *E*-**62a** and *Z*-**62a**. Alternatively, the selenylation and bromination reactions may operate under Curtin-Hammett control. Presumably, for the hydroxylations, fluorinations, and amination, good agreement between the enamine energy differences and ultimate product *ee*'s implies that formation of enamines **62** is slow relative to α -functionalization and that the *E*- and *Z*-isomers are formed in a thermodynamic ratio (Figure 5.6). Subsequently, the enamine intermediates are rapidly converted to the desired products, and the ultimate enantioselectivity—which reflects the thermodynamic enamine ratio—is not affected by the relative activation barriers for α -functionalization.

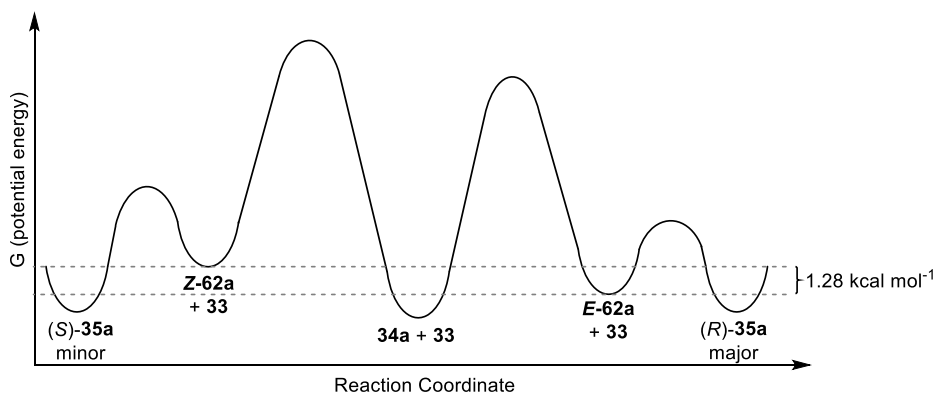


Figure 5.6. Possible energy diagram for α -hydroxylation of **34a** to **35a**, in which the ratio of enamine intermediates **62a** determines the overall enantioselectivity. Note that the conversion from aldehyde **34a** to enamines **62a** represents several elementary condensation steps, with the largest single activation barrier represented on the diagram.

Under Curtin-Hammett conditions, however, the enamines **Z-62a** and **E-62a** would form and equilibrate rapidly relative to the rate of α -functionalization (Figure 5.7). In this case, the enamine isomers would continue to interconvert over the course of the entire reaction and the *ee* would depend primarily on the relative activation energies for α -functionalizations of **Z-62a** and **E-62a**. Given the overall longer reaction times necessary for α -selenylation to **66** and α -bromination to **68**, this could explain the observed drop in enantioselectivity for these transformations.

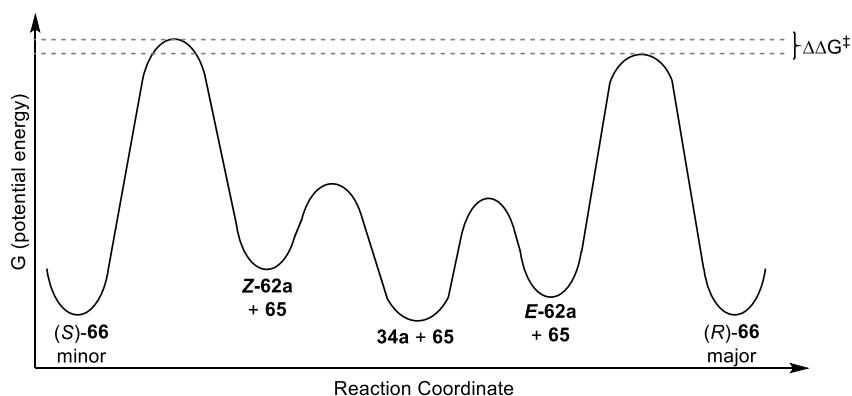


Figure 5.7. Possible energy diagram for α -selenylation of **34a** to **66**, under Curtin-Hammett control, in which the relative heights of the barriers to α -functionalization determine the overall enantioselectivity. Note that the conversion from aldehyde **34a** to enamines **62a** represents several elementary condensation steps, with the largest single activation barrier represented on the diagram.

5.6 Conclusions and Outlook

In conclusion, we have identified a simple, powerful primary aminobenzamide catalyst that efficiently performs both α -hydroxylations and α -fluorinations of α,α -disubstituted aldehyde substrates in excellent yields, high stereoselectivities and short reaction times. Computational findings and initial experiments probing other α -functionalizations support the feasibility of expanding this catalytic system to various alternative transformations of branched aldehydes. Ongoing endeavors in our laboratory seek to widen the presently described principles to other reactions, in an effort to define a broadly general engine for α -functionalizations.

5.7 Experimental Details

5.7.1 General Information

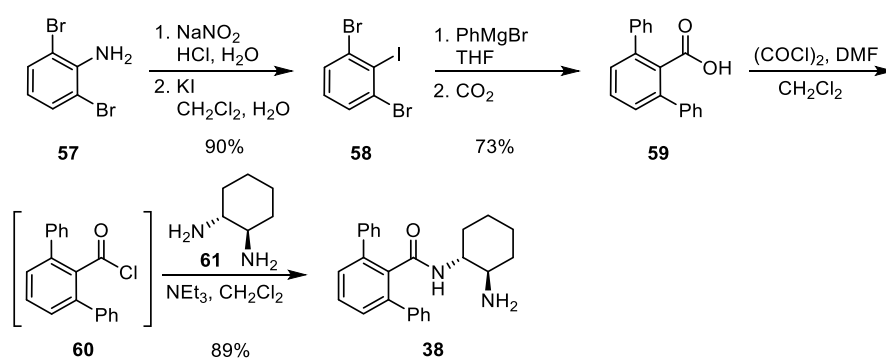
Unless otherwise noted, all reactions were performed in oven- or flame-dried round-bottom flasks. Vials were capped and flasks were fitted with rubber septa. Reactions were conducted under air unless noted. Stainless steel syringes were used to transfer air- and moisture-sensitive liquids. Flash chromatography was performed using silica gel 60 (230-400 mesh) from EM Science. Commercial reagents were purchased from Sigma-Aldrich, Alfa Aesar, Oakwood Chemical, Matrix Chemical, or TCI America, and used as received with the following exceptions: dichloromethane, toluene, tetrahydrofuran, *N,N*-dimethylformamide, and diethyl ether were dried by passing through columns of activated alumina. Triethylamine was distilled from CaH₂ at 760 torr. 2-phenylpropionaldehyde (**34a**) and 3-(4-*tert*-butylphenyl)isobutyraldehyde (**34o**) were purchased from Sigma-Aldrich and TCI America respectively, and distilled from CaH₂ at 50 torr prior to use. *n*-Butyllithium was titrated using *N*-benzylbenzamide as an indicator.

Proton nuclear magnetic resonance (¹H NMR) spectra, fluorine nuclear magnetic resonance (¹⁹F NMR) spectra, and carbon nuclear magnetic resonance (¹³C NMR) spectra were recorded on Varian-Mercury-300 (300 MHz), Varian-Mercury-400 (400 MHz), or Inova-500 (500 MHz) spectrometers. Chemical shifts for protons are reported in parts per million downfield from tetramethylsilane and are

referenced to residual protium in the NMR solvent ($\text{CHCl}_3 = \delta 7.27$). Chemical shifts for carbon are reported in parts per million downfield from tetramethylsilane and are referenced to the carbon resonances of the solvent ($\text{CDCl}_3 = \delta 77.0$). Data are represented as follows: chemical shift (multiplicity (br = broad, s = singlet, d = doublet, t = triplet, q = quartet, quin = quintet, m = multiplet), coupling constants in Hertz (Hz), integration).

Infrared (IR) spectra were obtained using a Bruker Alpha Platinum ATR FTIR spectrometer. Optical rotations were measured using a Jasco DIP 370 digital polarimeter. The mass spectral data were obtained on a Bruker micrOTOF-Q II time-of-flight LC/MS spectrometer (ESI-TOF). Chiral HPLC analysis was performed using an Agilent analytical chromatograph with commercial ChiralPak or ChiralCel columns.

5.7.2 Synthesis and Characterization of Catalyst **38**



Scheme 5.20. Synthesis of catalyst **38**.

1,3-dibromo-2-iodobenzene (58):

Following a reported procedure,³⁵ 2,6-dibromoaniline (**57**, 5.002 g, 19.93 mmol) was dissolved in 37% HCl (10 mL) and H₂O (27 mL) in a 500-mL round-bottom flask. The reaction mixture was cooled to 0 °C in an ice bath then a solution of sodium nitrite (1.435 g, 20.79 mmol, 1.04 equiv) in H₂O (22 mL) was slowly added. The flask was sealed with a septum under an atmosphere of N₂, and the mixture was stirred at 0 °C. After 1 h of stirring, the flask was opened again, and an ice cold solution of potassium iodide (33.10 g, 199 mmol, 10.0 equiv) in H₂O (46 mL) was slowly and carefully added at 0 °C. The yellow mixture rapidly turned red and began to bubble. If potassium iodide is added too quickly, the solution will bubble over.

After addition of all potassium iodide, CH₂Cl₂ (40 mL) was also added to the reaction and the biphasic mixture was stirred under an atmosphere of N₂ at 23 °C for 4.5 h. Then, solid sodium sulfite (0.750 g, 5.95 mmol, 0.3 equiv) was added to quench the oxidant and the red color rapidly dissipated. This mixture was stirred at 23 °C under an atmosphere of N₂ for an additional 15 min, then the phases were separated. The aqueous phase was extracted with CH₂Cl₂ (2 x 25 mL) and the pooled organic layers were washed with brine (30 mL). The organic phase was dried over Na₂SO₄, filtered, and concentrated. The crude orange powder was dissolved in hexanes with minimal CH₂Cl₂, and purified by silica plug, eluting with hexanes to afford **58** as a white powder (6.457 g, 90%).

Spectroscopic results agree with previously reported data.³⁵

[1,1':3',1''-terphenyl]-2'-carboxylic acid (59):

Following a reported procedure,³⁶ aryl iodide **58** (5.919 g, 16.36 mmol) was dissolved in anhydrous THF (12 mL). Dropwise by syringe, under an atmosphere of N₂, phenylmagnesium bromide (49 mL of a 1.0 M solution in THF, 49 mmol, 3.0 equiv) was added to the stirring **58** solution at 23 °C. The reaction began to get cloudy. After 2.5 h, dry CO₂ gas was bubbled from a balloon directly into the stirring reaction mixture by needle, with a gas outlet line from the flask attached to an oil bubbler to prevent moisture from entering the reaction. The solution rapidly clarified. The balloon was refilled as necessary, and after 3.5 h, the reaction was quenched with H₂O (50 mL) and 1M aq. HCl (10 mL). The aqueous layer was extracted with Et₂O (4 x 50 mL). Then the pooled organic layers were washed with H₂O (50 mL). The organic solution was dried over Na₂SO₄, filtered, and concentrated. The crude product was purified by flash chromatography (silica gel, 19:1 to 3:2 hexanes/EtOAc) to afford **59** as a white powder (3.257g, 73%).

R_f = 0.22 (silica gel, 2:1 hexanes/EtOAc); **IR** (film) ν_{\max} 1695, 1458, 1292, 1275, 909, 757, 732, 699 cm⁻¹; **¹H NMR** (500 MHz, CDCl₃) δ 7.53 (dd, *J* = 7.3, 8.3 Hz, 1H), 7.45 – 7.38 (m, 12H); **¹³C NMR** (126 MHz, CDCl₃) δ 174.5, 140.3, 140.2, 131.6, 129.6, 128.9, 128.4, 128.3, 127.6; **MS** (ESI-TOF) calcd. for C₁₉H₁₄O₂ [M + H]⁺ 275.1067, found 275.1067.

[1,1':3',1''-terphenyl]-2'-carbonyl chloride (60):

Following a reported procedure,³⁷ benzoic acid **59** (3.257 g, 11.87 mmol) was dissolved in anhydrous CH₂Cl₂ (16 mL, 0.74 M) and the resultant mixture was cooled to 0 °C in an ice bath. Under an atmosphere of N₂, oxalyl chloride (2.8 mL, 4.06 g, 32.0 mmol, 2.7 equiv) was then added by syringe to the stirring solution, followed by catalytic anhydrous DMF (0.05 mL, 0.047 g, 0.646 mmol, 5 mol%). The reaction was stirred under an atmosphere of N₂ for 90 min, and slowly allowed to warm to 23 °C. The organic solution was then washed sequentially with 5% aq. NaHCO₃ (2 x 10 mL) and H₂O (2 x 10 mL). The organic solution was dried over Na₂SO₄, filtered, and concentrated to afford **60** as a fluffy, pale yellow powder which was used without further purification (3.504 g, 100%).

¹H NMR (400, CDCl₃) δ 7.64 – 7.59 (m, 1H), 7.52 – 7.45 (m, 12H).

***N*-((1*R*,2*R*)-2-aminocyclohexyl)-[1,1':3',1''-terphenyl]-2'-carboxamide (38):**

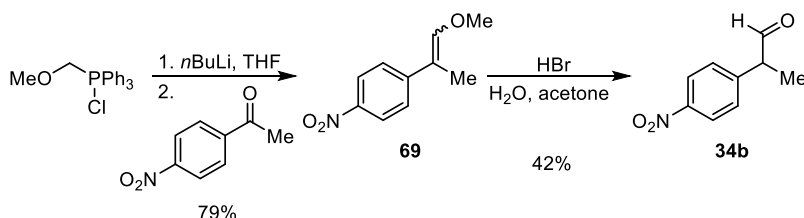
(*R,R*)-1,2-*trans*-diaminocyclohexane⁴² (**61**, 2.781 g, 24.36 mmol, 4.0 equiv) was dissolved in anhydrous CH₂Cl₂ (30 mL, 0.2 M) and the resultant mixture was cooled to 0 °C in an ice bath. Under an atmosphere of N₂, NEt₃ (0.83 mL, 0.603 g, 5.95 mol, 1.0 equiv) was added by syringe, followed by benzoyl chloride **60** (1.752 g, 5.98 mmol) in minimal anhydrous CH₂Cl₂ (~5 mL). Complete transfer of acyl chloride was ensured with an additional aliquot of CH₂Cl₂ (~5 mL). The reaction was stirred under an atmosphere of N₂ for 12 h, during which time it was slowly allowed to warm to 23 °C. The mixture was then concentrated by rotary evaporation and the crude white residue was purified by flash chromatography (silica gel, 99:1 to 9:1 CH₂Cl₂/MeOH) to afford **38** as a white powder (1.7306g, 78%).

R_f = 0.31 (silica gel, 9:1 CH₂Cl₂/MeOH); **IR** (film) ν_{\max} 3251, 2932, 2855, 1623, 1549, 1328, 758, 730, 699 cm⁻¹; ¹H NMR (500 MHz, CDCl₃) δ 7.50 (d, *J* = 7.8 Hz, 4H), 7.47 (d, *J* = 6.8 Hz, 1H), 7.42 – 7.38 (m, 4H), 7.37 – 7.34 (m, 4H), 5.20 (d, *J* = 8.8 Hz, 1H), 3.24 – 3.15 (m, 1H), 1.98 (td, *J* = 10.5, 3.9 Hz, 1H), 1.78 (d, *J* = 12.2 Hz, 1H), 1.58 (d, *J* = 10.2 Hz, 1H), 1.53 – 1.47 (m, 1H), 1.31 – 1.21 (m, 2H), 1.12 – 1.01

⁴² (*R,R*)-1,2-*trans*-diaminocyclohexane was resolved according to: (a) Larrow, J. F.; Jacobsen, E. N.; Gao, Y.; Hong, Y.; Nie, X.; Zepp, C. M. *J. Org. Chem.* **1994**, *59*, 1939–1942. (b) Larrow, J. F.; Jacobsen, E. N. *Org. Synth.* **1998**, *75*, 1–6.

(m, 2H), 0.93 – 0.86 (m, 2H), 0.63 (qd, $J = 12.2, 3.4$ Hz, 1H); ^{13}C NMR (126 MHz, CDCl_3) δ 168.9, 140.4, 139.8, 136.3, 129.0, 128.9, 128.8, 128.2, 127.7, 56.4, 54.9, 34.2, 31.4, 24.9, 24.8; MS (ESI-TOF) calcd. for $\text{C}_{25}\text{H}_{26}\text{N}_2\text{O}$ [$\text{M} + \text{H}^+$] 371.2118, found 371.2121; $[\alpha]_D^{25} = -36.0$ ($c = 2.0, \text{CHCl}_3$).

5.7.3 Synthesis and Characterization of Substrates



Scheme 5.21. Synthesis of substrate **34b**.

1-(1-methoxyprop-1-en-2-yl)-4-nitrobenzene (**69**):

Following a general procedure,⁴³ (methoxymethyl)triphenylphosphonium chloride (6.231 g, 18.18 mmol, 1.5 equiv) was suspended in anhydrous THF (144 mL, 0.084 M) and the resultant mixture was cooled to -78 °C in a dry ice/acetone bath. Slowly by syringe, *n*BuLi (9.5 mL of a 1.92 M solution in hexanes, 18.24 mmol, 1.5 equiv) was added to the stirring phosphonium chloride solution under an atmosphere of N_2 . The reaction was allowed to stir under N_2 at -78 °C for 30 min, then at 23 °C for 30 min, at which point the solution turned deep red. Then, the mixture was re-cooled to -78 °C, and 4'-nitroacetophenone (2.001 g, 12.11 mmol) in minimal anhydrous THF (~5 mL) was added dropwise by syringe. After stirring under N_2 for 16 h, the reaction was quenched with H_2O (75 mL). The layers were separated and the aqueous phase was extracted with Et_2O (2 x 45 mL). The pooled organic solutions were washed with brine (60 mL), dried over Na_2SO_3 , filtered, and concentrated. The crude product was purified by flash chromatography (silica gel, 19:1 to 2:1 hexanes/EtOAc) to afford **69** as an orange oil (1.850 g, 79%) in a 1.35:1 ratio of *E/Z*-enol ether isomers.

Spectroscopic results agree with previously reported data.⁴⁴

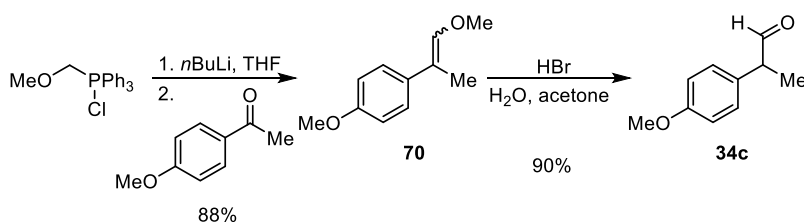
⁴³ Fu, J.-Y.; Xu, X.-Y.; Li, Y.-C.; Huang, Q.-C.; Wang, L.-X. *Org. Biomol. Chem.* **2010**, *8*, 4524–4526.

⁴⁴ Baumann, T.; Vogt, H.; Bräse, S. *Eur. J. Org. Chem.* **2007**, *2007*, 266–282.

2-(4-nitrophenyl)propanal (34b):

Following a general procedure,⁴³ enol ether **69** (0.810 g, 4.19 mmol) was dissolved in a 4:1 mixture of acetone and H₂O (4.9 mL, 0.86 M) and the resultant solution was cooled to 0 °C in an ice bath. Conc. HBr (48%, 0.45 mL) was added to the solution and the reaction mixture was stirred at 23 °C for 46 h. The acetone was removed by rotary evaporation and the remaining aqueous residue was neutralized with sat. aq. NaHCO₃, as determined by pH paper. This aqueous solution was then extracted with Et₂O (3 x 10 mL). The pooled organic layers were dried over Na₂SO₃, filtered, and concentrated. The crude product was purified by flash chromatography (silica gel, 19:1 to 3:2 hexanes/EtOAc) to afford **34b** as an orange oil (0.312 g, 42%).

Spectroscopic results agree with previously reported data.^{43,44}



Scheme 5.22. Synthesis of substrate **34c**.

1-methoxy-4-(1-methoxyprop-1-en-2-yl)benzene (70):

Reaction of 4'-methoxyacetophenone (2.007 g, 13.36 mmol), (methoxymethyl)triphenylphosphonium chloride (6.851 g, 19.99 mmol, 1.5 equiv), and *n*BuLi (10.4 mL of a 1.92 M solution in hexanes, 19.97 mmol, 1.5 equiv) in anhydrous THF (159 mL, 0.084 M) according to **69** above afforded **70** as a colorless oil after column chromatography (silica gel, 19:1 to 2:1 hexanes/EtOAc) in a 1.29:1 ratio of *E/Z*-enol ether isomers (2.098 g, 88%).

Spectroscopic results agree with previously reported data.^{44,45}

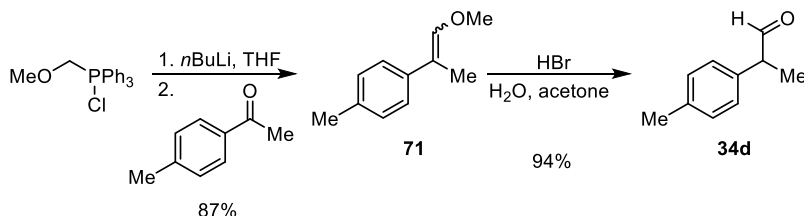
2-(4-methoxyphenyl)propanal (34c):

Reaction of enol ether **70** (2.098 g, 11.77 mmol) and conc. HBr (48%, 1.3 mL) in 4:1 acetone/H₂O (13.7

⁴⁵ Hoffmann, S.; Nicoletti, M.; List, B. *J. Am. Chem. Soc.* **2006**, *128*, 13074–13075.

mL, 0.86 M) according to **34b** above afforded **34c** as a colorless oil after column chromatography (silica gel, 19:1 to 3:2 hexanes/EtOAc) (1.731 g, 90%).

Spectroscopic results agree with previously reported data.^{43–46}



Scheme 5.23. Synthesis of substrate **34d**.

1-(1-methoxyprop-1-en-2-yl)-4-methylbenzene (**71**):

Reaction of 4'-methylacetophenone (0.70 mL, 0.704 g, 5.24 mmol), (methoxymethyl)triphenylphosphonium chloride (2.690 g, 7.85 mmol, 1.5 equiv), and *n*BuLi (4.5 mL of a 1.72 M solution in hexanes, 7.74 mmol, 1.5 equiv) in anhydrous THF (61 mL, 0.086 M) according to **69** above afforded **71** as a colorless oil after column chromatography (silica gel, 19:1 to 2:1 hexanes/EtOAc) in a 1:1 ratio of *E/Z*-enol ether isomers (0.738 g, 87%).

R_f = 0.81 (silica gel, 4:1 hexanes/Et₂O); **IR** (film) ν_{max} 2931, 1652, 1514, 1454, 1258, 1221, 1204, 1131, 1115, 1009, 812 cm⁻¹; **¹H NMR** (400 MHz, CDCl₃) δ 7.63 – 7.58 (m, 1H), 7.33 – 7.27 (m, 1H), 7.26 – 7.17 (m, 2H), 6.47 (diast., s, 0.5H), 6.16 (diast., s, 0.5H), 3.79 – 3.77 (diast., m, 1.5H), 3.74 – 3.72 (diast., m, 1.5H), 2.44 – 2.41 (m, 3H), 2.10 – 2.08 (diast., m, 1.5H), 2.02 – 1.99 (diast., m, 1.5H); **¹³C NMR** (100 MHz, CDCl₃) δ 144.5, 144.0, 137.6, 135.5, 135.4, 129.0, 128.5, 127.3, 124.8, 114.3, 110.7, 59.9, 59.7, 34.6, 34.5, 25.2, 22.6, 21.0, 20.9, 18.2, 14.1, 12.5; **MS** (ESI-TOF) calcd. for C₁₁H₁₄O [M + H⁺] 163.1117, found 163.1093.

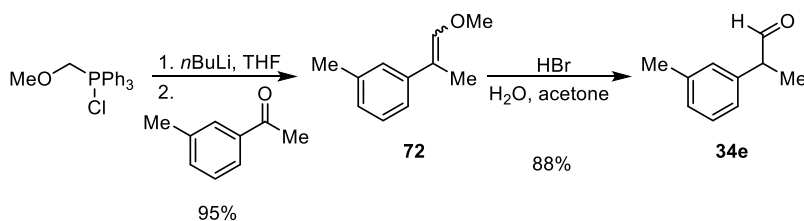
2-(*p*-tolyl)propanal (**34d**):

Reaction of enol ether **71** (1.650 g, 10.17 mmol) and conc. HBr (48%, 1.1 mL) in 4:1 acetone/H₂O (11.9 mL, 0.86 M) according to **34b** above afforded **34d** as a pale yellow oil after column chromatography (silica

⁴⁶ Vyas, D. J.; Larionov, E.; Besnard, C.; Guénée, L.; Mazet, C. *J. Am. Chem. Soc.* **2013**, *135*, 6177–6183.

gel, 19:1 to 3:2 hexanes/EtOAc) (1.412 g, 94%).

Spectroscopic results agree with previously reported data.^{43,45,47}



Scheme 5.24. Synthesis of substrate **34e**.

1-(1-methoxyprop-1-en-2-yl)-3-methylbenzene (**72**):

Reaction of 3'-methylacetophenone (0.60 mL, 0.592 g, 4.41 mmol), (methoxymethyl)triphenylphosphonium chloride (2.268 g, 6.62 mmol, 1.5 equiv), and *n*BuLi (3.2 mL of a 2.05 M solution in hexanes, 6.56 mmol, 1.5 equiv) in anhydrous THF (52 mL, 0.085 M) according to **69** above afforded **72** as a colorless oil after column chromatography (silica gel, 19:1 to 2:1 hexanes/EtOAc) in a 1.5:1 ratio of *E/Z*-enol ether isomers (0.682 g, 95%).

R_f = 0.75 (silica gel, 4:1 hexanes/Et₂O); **IR** (film) ν_{\max} 2931, 1652, 1603, 1489, 1222, 1134, 782, 699 cm^{-1} ; **¹H NMR** (400 MHz, CDCl₃) δ 7.48 (major diast., s, 0.6H), 7.40 (minor diast., dd, J = 1.8, 3.3 Hz, 0.4H), 7.31 – 7.22 (m, 1H), 7.19 – 7.15 (m, 1H), 7.07 (d, J = 5.9 Hz, 1H), 6.47 (major diast., td, J = 2.9, 1.4 Hz, 0.6H), 6.18 – 6.14 (minor diast., m, 0.4H), 3.78 – 3.75 (major diast., m, 1.8H), 3.73 – 3.70 (minor diast., m, 1.2H), 2.44 – 2.39 (m, 3H), 2.06 (major diast., dt, J = 4.5, 1.3 Hz, 1.8H), 1.98 (minor diast., dt, J = 4.2, 1.2 Hz, 1.2H); **¹³C NMR** (100 MHz, CDCl₃) δ 145.0, 144.4, 140.5, 138.3, 137.8, 137.2, 128.2, 128.1, 127.8, 126.8, 126.6, 125.7, 124.6, 122.1, 114.4, 110.9, 60.0, 59.8, 21.6, 21.5, 18.4, 12.6; **MS** (ESI-TOF) calcd. for C₁₁H₁₄O [M + H⁺] 163.1117, found 163.1085.

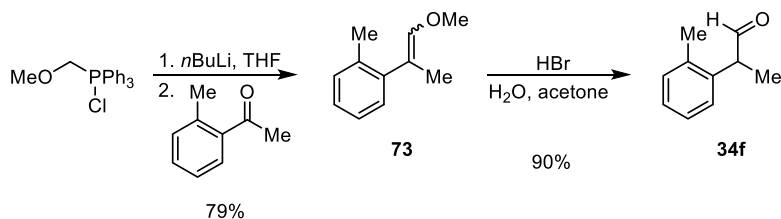
2-(*m*-tolyl)propanal (**34e**):

Reaction of enol ether **72** (1.499 g, 9.24 mmol) and conc. HBr (48%, 0.99 mL) in 4:1 acetone/H₂O (10.7 mL, 0.86 M) according to **34b** above afforded **34e** as a pale yellow oil after column chromatography (silica

⁴⁷ List, B.; Čorić, I.; Grygorenko, O. O.; Kaib, P. S. J.; Komarov, I.; Lee, A.; Leutzsch, M.; Pan, S. C.; Tymtsunik, A. V.; van Gemmeren, M. *Angew. Chem. Int. Ed.* **2014**, *53*, 282–285.

gel, 19:1 to 3:2 hexanes/EtOAc) (1.206 g, 88%).

Spectroscopic results agree with previously reported data.⁴⁷



Scheme 5.25. Synthesis of substrate **34f**.

1-(1-methoxyprop-1-en-2-yl)-2-methylbenzene (**73**):

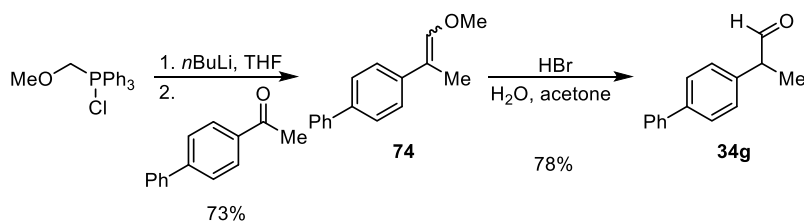
Reaction of 2'-methylacetophenone (1.7 mL, 1.744 g, 13.00 mmol), (methoxymethyl)triphenylphosphonium chloride (6.679 g, 19.48 mmol, 1.5 equiv), and *n*BuLi (10.0 mL of a 1.92 M solution in hexanes, 19.20 mmol, 1.5 equiv) in anhydrous THF (155 mL, 0.084 M) according to **69** above afforded **73** as a colorless oil after column chromatography (silica gel, 19:1 to 2:1 hexanes/EtOAc) in a 4.5:1 ratio of *E/Z*-enol ether isomers (1.661 g, 79%).

$R_f = 0.80$ (silica gel, 4:1 hexanes/Et₂O); **IR** (film) ν_{\max} 2930, 1664, 1486, 1455, 1220, 1130, 1069, 758, 727 cm^{-1} ; **¹H NMR** (400 MHz, CDCl₃) δ 7.76 (minor diast., d, $J = 2.3$ Hz, 0.18H), 7.44 – 7.38 (major diast., m, 0.82H), 7.28 – 7.16 (m, 3H), 6.10 – 6.05 (minor diast., m, 0.18H), 6.04 – 5.98 (major diast., m, 0.82H), 3.76 – 3.71 (major diast., m, 2.46H), 3.63 – 3.58 (minor diast., m, 0.54H), 2.67 – 2.60 (minor diast., m, 0.54H), 2.42 – 2.33 (major diast., m, 2.46H), 2.03 – 1.97 (major diast., m, 2.46H), 1.95 – 1.89 (minor diast., m, 0.54H); **¹³C NMR** (100 MHz, CDCl₃) δ 145.2, 142.3, 140.9, 136.3, 133.7, 133.5, 131.9, 131.4, 130.0, 129.4, 128.7, 126.6, 125.4, 115.0, 113.1, 59.4, 59.3, 29.4, 21.5, 20.0, 19.5, 14.9; **MS** (ESI-TOF) calcd. for C₁₁H₁₄O₃ [M + Na⁺] 185.0937, found 185.0535.

2-(*o*-tolyl)propanal (**34f**):

Reaction of enol ether **73** (1.661 g, 10.24 mmol) and conc. HBr (48%, 1.1 mL) in 4:1 acetone/H₂O (11.9 mL, 0.86 M) according to **34b** above afforded **34f** as a pale yellow oil after column chromatography (silica gel, 19:1 to 3:2 hexanes/EtOAc) (1.365 g, 90%).

Spectroscopic results agree with previously reported data.^{43,46}



Scheme 5.26. Synthesis of substrate **34g**.

4-(1-methoxyprop-1-en-2-yl)-1,1'-biphenyl (74):

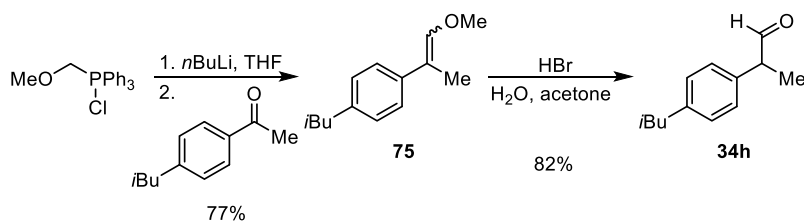
Reaction of 4-acetylphenyl (2.299 g, 11.71 mmol), (methoxymethyl)triphenylphosphonium chloride (6.030 g, 17.59 mmol, 1.5 equiv), and *n*BuLi (9.0 mL of a 1.92 M solution in hexanes, 17.28 mmol, 1.5 equiv) in anhydrous THF (140 mL, 0.084 M) according to **69** above afforded **74** as a white powder after column chromatography (silica gel, 19:1 to 2:1 hexanes/EtOAc) in a 1.2:1 ratio of *E/Z*-enol ether isomers (1.910 g, 73%).

R_f = 0.73 (silica gel, 4:1 hexanes/Et₂O); **IR** (film) ν_{max} 2931, 1648, 1486, 1223, 1133, 1078, 1007, 907, 848, 831, 764, 728, 696 cm^{-1} ; **¹H NMR** (400 MHz, CDCl₃) δ 7.82 – 7.77 (m, 1H), 7.72 – 7.64 (m, 3H), 7.64 – 7.60 (m, 1H), 7.54 – 7.45 (m, 3H), 7.44 – 7.38 (m, 1H), 6.58 (major diast., d, J = 1.2 Hz, 0.55H), 6.23 (minor diast., d, J = 1.6 Hz, 0.45H), 3.80 (major diast., s, 1.65H) 3.77 (minor diast., s, 1.35H), 2.13 (major diast., d, J = 1.2 Hz, 1.65H), 2.04 (minor diast., d, J = 1.6 Hz, 1.35H); **¹³C NMR** (100 MHz, CDCl₃) δ 145.3, 144.9, 141.1, 140.8, 139.6, 138.6, 137.4, 128.7, 128.6, 127.8, 127.0, 126.9, 126.8, 126.5, 125.2, 113.9, 110.2, 60.1, 59.9, 31.6, 22.6, 18.2, 14.1, 12.4; **MS** (ESI-TOF) calcd. for C₁₆H₁₆O [M + H⁺] 225.1274, found 225.1325.

2-([1,1'-biphenyl]-4-yl)propanal (34g):

Reaction of enol ether **74** (1.910 g, 8.52 mmol) and conc. HBr (48%, 0.92 mL) in 4:1 acetone/H₂O (9.9 mL, 0.86 M) according to **34b** above afforded **34g** as a white powder after column chromatography (silica gel, 19:1 to 3:2 hexanes/EtOAc) (1.405 g, 78%).

Spectroscopic results agree with previously reported data.⁴⁷



Scheme 5.27. Synthesis of substrate **34h**.

1-isobutyl-4-(1-methoxyprop-1-en-2-yl)benzene (75):

Reaction of 4ⁱ-isobutylacetophenone (2.2 mL, 2.094 g, 11.88 mmol), (methoxymethyl)triphenylphosphonium chloride (6.112 g, 17.83 mmol, 1.5 equiv), and *n*BuLi (10.0 mL of a 1.78 M solution in hexanes, 17.80 mmol, 1.5 equiv) in anhydrous THF (141 mL, 0.084 M) according to **69** above afforded **75** as a colorless oil after column chromatography (silica gel, 19:1 to 2:1 hexanes/EtOAc) in a 2:1 ratio of *E/Z*-enol ether isomers (1.874 g, 77%).

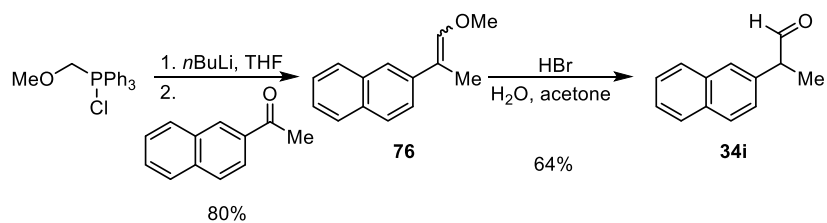
R_f = 0.60, 0.72 (both diast., silica gel, 4:1 hexanes/Et₂O); **IR** (film) ν_{\max} 2952, 1652, 1513, 1465, 1223, 1133, 1074, 838, 798 cm⁻¹; **¹H NMR** (400 MHz, CDCl₃) δ 7.55 (minor diast., d, *J* = 8.2 Hz, 0.67H), 7.24 (major diast., d, *J* = 8.2 Hz, 1.33H), 7.13 (minor diast., *J* = 8.2 Hz, 0.67H), 7.09 (major diast., d, *J* = 7.8 Hz, 1.33H), 6.42 (major diast., s, 0.67H), 6.11 (minor diast., s, 0.33H), 3.73 (major diast., s, 2H), 3.69 (minor diast., s, 1H), 2.47 (d, *J* = 7.0 Hz, 2H), 2.01 (major diast., s, 2H), 1.93 (minor diast., s, 1H), 1.87 (dt, *J* = 13.3, 6.6 Hz, 1H), 0.93 (d, *J* = 6.6 Hz, 3H); **¹³C NMR** (100 MHz, CDCl₃) δ 144.6, 144.2, 139.4, 139.3, 137.9, 135.6, 129.1, 128.7, 127.1, 124.6, 114.3, 110.7, 60.0, 59.8, 45.2, 45.0, 30.2, 22.4, 18.3, 15.5; **MS** (ESI-TOF) calcd. for C₁₄H₂₀O [M + H⁺] 205.1587, found 205.1607.

2-(4-isobutylphenyl)propanal (34h):

Reaction of enol ether **75** (1.874 g, 9.17 mmol) and conc. HBr (48%, 1.0 mL) in 4:1 acetone/H₂O (10.6 mL, 0.86 M) according to **34b** above afforded **34h** as a pale yellow oil after column chromatography (silica gel, 19:1 to 3:2 hexanes/EtOAc) (1.427 g, 82%).

Spectroscopic results agree with previously reported data.⁴⁸

⁴⁸ Friest, J. A.; Maezato, Y.; Broussy, S.; Blum, P.; Berkowitz, D. B. *J. Am. Chem. Soc.* **2010**, *132*, 5930–5931.



Scheme 5.28. Synthesis of substrate **34i**.

2-(1-methoxyprop-1-en-2-yl)naphthalene (76):

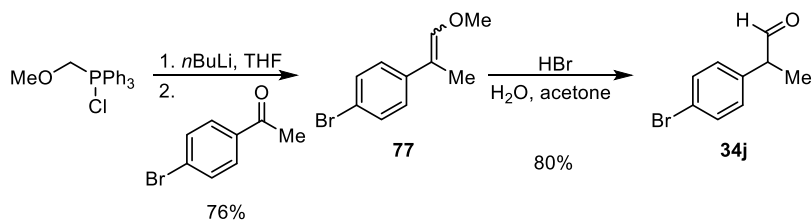
Reaction of 2-acetonaphthone (2.006 g, 11.78 mmol), (methoxymethyl)triphenylphosphonium chloride (6.041 g, 17.62 mmol, 1.5 equiv), and *n*BuLi (11.0 mL of a 1.60 M solution in hexanes, 17.60 mmol, 1.5 equiv) in anhydrous THF (140 mL, 0.084 M) according to **69** above afforded **76** as a white solid after column chromatography (silica gel, 19:1 to 2:1 hexanes/EtOAc) in a 1.3:1 ratio of *E/Z*-enol ether isomers (1.860 g, 80%).

Spectroscopic results agree with previously reported data.⁴⁴

2-(naphthalen-2-yl)propanal (34i):

Reaction of enol ether **76** (1.860 g, 9.38 mmol) and conc. HBr (48%, 1.0 mL) in 4:1 acetone/H₂O (10.9 mL, 0.86 M) according to **34b** above afforded **34i** as a white powder after column chromatography (silica gel, 19:1 to 3:2 hexanes/EtOAc) (1.106 g, 64%).

Spectroscopic results agree with previously reported data.^{43,44,46}



Scheme 5.29. Synthesis of substrate **34j**.

1-bromo-4-(1-methoxyprop-1-en-2-yl)benzene (77):

Reaction of 4'-bromoacetophenone (2.002 g, 10.06 mmol), (methoxymethyl)triphenylphosphonium chloride (5.173 g, 15.09 mmol, 1.5 equiv), and *n*BuLi (7.7 mL of a 1.96 M solution in hexanes, 15.09 mmol, 1.5 equiv) in anhydrous THF (120 mL, 0.084 M) according to **69** above afforded **77** as a colorless oil after

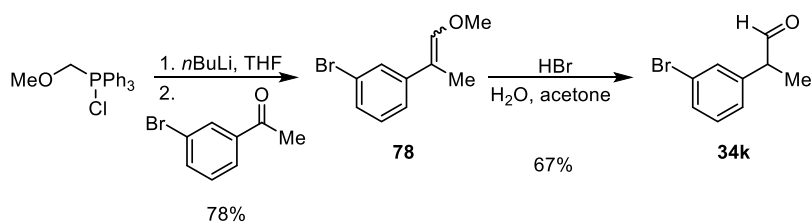
column chromatography (silica gel, 19:1 to 2:1 hexanes/EtOAc) in a 1.3:1 ratio of *E/Z*-enol ether isomers (1.732 g, 76%).

Spectroscopic results agree with previously reported data.⁴⁴

2-(4-bromophenyl)propanal (**34j**):

Reaction of enol ether **77** (1.732 g, 7.63 mmol) and conc. HBr (48%, 0.83 mL) in 4:1 acetone/H₂O (8.9 mL, 0.86 M) according to **34b** above afforded **34j** as a pale yellow oil after column chromatography (silica gel, 19:1 to 3:2 hexanes/EtOAc) (1.295 g, 80%).

Spectroscopic results agree with previously reported data.^{43–47}



Scheme 5.30. Synthesis of substrate **34k**.

1-bromo-3-(1-methoxyprop-1-en-2-yl)benzene (**78**):

Reaction of 3'-bromoacetophenone (1.5 mL, 2.258 g, 11.34 mmol), (methoxymethyl)triphenylphosphonium chloride (5.831 g, 17.01 mmol, 1.5 equiv), and *n*BuLi (8.7 mL of a 1.96 M solution in hexanes, 17.05 mmol, 1.5 equiv) in anhydrous THF (135 mL, 0.084 M) according to **69** above afforded **78** as a colorless oil after column chromatography (silica gel, 19:1 to 2:1 hexanes/EtOAc) in a 1.5:1 ratio of *E/Z*-enol ether isomers (1.997 g, 78%).

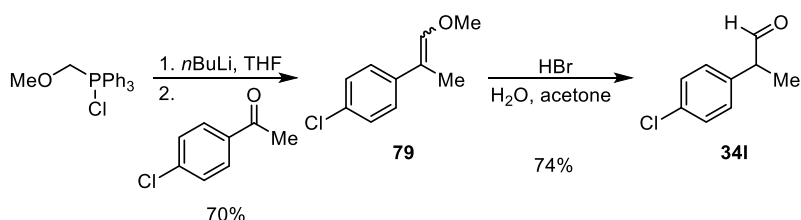
$R_f = 0.72$ (silica gel, 4:1 hexanes/Et₂O); **IR** (film) ν_{\max} 2931, 1651, 1590, 1555, 1476, 1261, 1224, 1136, 1068, 993, 779, 689 cm⁻¹; **¹H NMR** (400 MHz, CDCl₃) δ 7.80 (minor diast., dt, $J = 3.7, 2$ Hz, 0.4H), 7.55 (minor diast., ddd, $J = 4.7, 3.1, 1.2$ Hz, 0.4H), 7.49 – 7.44 (major diast., m, 0.6H), 7.37 – 7.29 (m, 1H), 7.26 – 7.22 (major diast., m, 0.6H), 7.21 – 7.14 (m, 1H), 6.45 (major diast., d, $J = 1.6$ Hz, 0.6H), 6.17 (minor diast., d, $J = 1.2$ Hz, 0.4H), 3.77 – 3.74 (major diast., m, 1.8H), 3.73 – 3.70 (minor diast., m, 1.2H), 1.98 (major diast., dd, $J = 3.1, 1.6$ Hz, 1.8H), 1.91 (minor diast., d, $J = 1.2$ Hz, 1.2H); **¹³C NMR** (100 MHz, CDCl₃) δ 146.0, 145.7, 142.9, 140.4, 130.4, 129.8, 129.3, 128.8, 128.6, 127.8, 125.9, 123.4, 122.6, 122.2,

113.2, 109.3, 60.3, 60.0, 18.1, 12.4; **MS** (ESI-TOF) calcd. for C₁₀H₁₁BrO [M + H⁺] 227.0066 and 229.0046, found 227.0064 and 229.0033.

2-(3-bromophenyl)propanal (**34k**):

Reaction of enol ether **78** (1.997 g, 8.79 mmol) and conc. HBr (48%, 0.96 mL) in 4:1 acetone/H₂O (10.2 mL, 0.86 M) according to **34b** above afforded **34k** as a yellow oil after column chromatography (silica gel, 19:1 to 3:2 hexanes/EtOAc) (1.252 g, 67%).

Spectroscopic results agree with previously reported data.⁴⁶



Scheme 5.31. Synthesis of substrate **34l**.

1-chloro-4-(1-methoxyprop-1-en-2-yl)benzene (**79**):

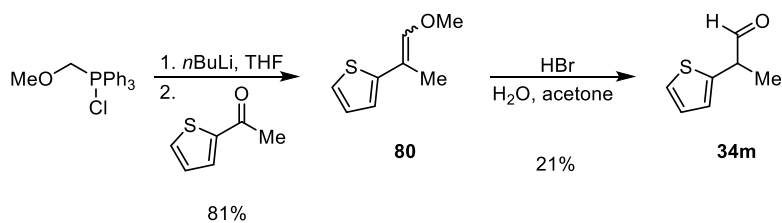
Reaction of 4'-chloroacetophenone (1.6 mL, 1.907 g, 12.34 mmol), (methoxymethyl)triphenylphosphonium chloride (6.344 g, 18.51 mmol, 1.5 equiv), and *n*BuLi (10.4 mL of a 1.78 M solution in hexanes, 18.51 mmol, 1.5 equiv) in anhydrous THF (147 mL, 0.084 M) according to **69** above afforded **79** as a colorless oil after column chromatography (silica gel, 19:1 to 2:1 hexanes/EtOAc) in a 1.1:1 ratio of *E/Z*-enol ether isomers (1.580 g, 70%).

Spectroscopic results agree with previously reported data.⁴⁴

2-(4-chlorophenyl)propanal (**34l**):

Reaction of enol ether **79** (1.580 g, 8.65 mmol) and conc. HBr (48%, 0.97 mL) in 4:1 acetone/H₂O (10.0 mL, 0.87 M) according to **34b** above afforded **34l** as a yellow oil after column chromatography (silica gel, 19:1 to 3:2 hexanes/EtOAc) (1.072 g, 74%).

Spectroscopic results agree with previously reported data.^{44,46,47}



Scheme 5.32. Synthesis of substrate **34m**.

2-(1-methoxyprop-1-en-2-yl)thiophene (80):

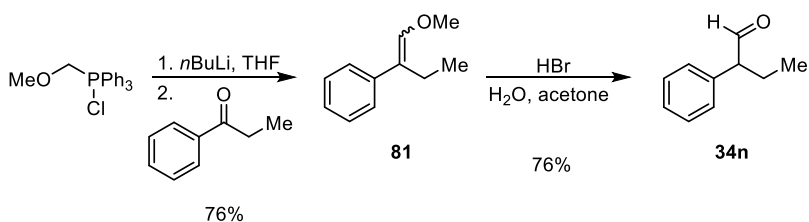
Reaction of 2-acetylthiophene (0.50 mL, 0.584 g, 4.63 mmol), (methoxymethyl)triphenylphosphonium chloride (2.381 g, 6.95 mmol, 1.5 equiv), and *n*BuLi (3.0 mL of a 2.30 M solution in hexanes, 6.90 mmol, 1.5 equiv) in anhydrous THF (55 mL, 0.084 M) according to **69** above afforded **80** as a colorless oil after column chromatography (silica gel, 19:1 to 2:1 hexanes/EtOAc) in a 1.1:1 ratio of *E/Z*-enol ether isomers (0.5803 g, 81%).

Spectroscopic results agree with previously reported data.^{44,45}

2-(thiophen-2-yl)propanal (34m):

Reaction of enol ether **80** (1.126 g, 7.30 mmol) and conc. HBr (48%, 0.82 mL) in 4:1 acetone/H₂O (8.5 mL, 0.86 M) according to **34b** above afforded **34m** as a volatile, pale yellow oil after column chromatography (silica gel, 19:1 to 3:2 hexanes/EtOAc) (0.215 g, 21%).

Spectroscopic results agree with previously reported data.^{44,45}



Scheme 5.33. Synthesis of substrate **34n**.

(1-methoxybut-1-en-2-yl)benzene (81):

Reaction of propiophenone (1.6 mL, 1.614 g, 12.03 mmol), (methoxymethyl)triphenylphosphonium chloride (6.189 g, 18.05 mmol, 1.5 equiv), and *n*BuLi (10.1 mL of a 1.78 M solution in hexanes, 17.98 mmol, 1.5 equiv) in anhydrous THF (143 mL, 0.084 M) according to **69** above afforded **81** as a pale yellow

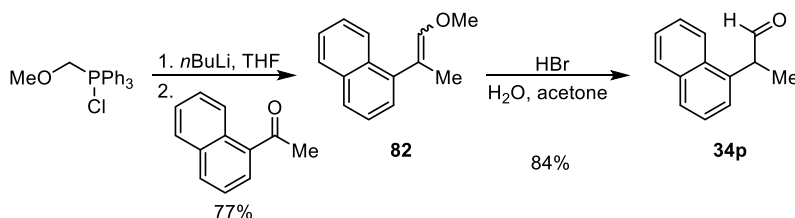
oil after column chromatography (silica gel, 19:1 to 2:1 hexanes/EtOAc) in a 1.3:1 ratio of *E/Z*-enol ether isomers (1.480 g, 76%).

Spectroscopic results agree with previously reported data.⁴⁴

2-phenylbutanal (**34n**):

Reaction of enol ether **81** (1.480 g, 9.12 mmol) and conc. HBr (48%, 1.0 mL) in 4:1 acetone/H₂O (10.6 mL, 0.86 M) according to **34b** above afforded **34n** as a pale yellow oil after column chromatography (silica gel, 19:1 to 3:2 hexanes/EtOAc) (1.030 g, 76%).

Spectroscopic results agree with previously reported data.^{44–46}



Scheme 5.34. Synthesis of substrate **34p**.

1-(1-methoxyprop-1-en-2-yl)naphthalene (**82**):

Reaction of 1-acetonaphthone (1.8 mL, 2.016 g, 11.84 mmol), (methoxymethyl)triphenylphosphonium chloride (6.091 g, 17.77 mmol, 1.5 equiv), and *n*BuLi (11.1 mL of a 1.60 M solution in hexanes, 17.76 mmol, 1.5 equiv) in anhydrous THF (141 mL, 0.084 M) according to **69** above afforded **82** as a colorless oil after column chromatography (silica gel, 19:1 to 2:1 hexanes/EtOAc) in a 1:1 ratio of *E/Z*-enol ether isomers (1.812 g, 77%).

R_f = 0.63 (silica gel, 4:1 hexanes/Et₂O); **IR** (film) ν_{\max} 2931, 1666, 1220, 1126, 801, 777 cm⁻¹; **¹H NMR** (400 MHz, CDCl₃) δ 8.16 – 8.10 (diast., m, 0.5H), 8.05 – 7.98 (diast., m, 0.5H), 7.95 – 7.88 (m, 1H), 7.85 – 7.79 (m, 1H), 7.57 – 7.45 (m, 3H), 7.43 – 7.34 (m, 1H), 6.32 – 6.27 (diast., m, 0.5H), 6.21 – 6.17 (diast., m, 0.5H), 3.79 – 3.76 (diast., m, 1.5H), 3.58 – 3.55 (diast., m, 1.5H), 2.20 – 2.15 (diast., m, 1.5H), 2.09 – 2.03 (diast., m, 1.5H); **¹³C NMR** (100 MHz, CDCl₃) δ 146.1, 143.4, 139.5, 138.0, 133.8, 133.6, 132.4, 130.9, 128.7, 128.5, 128.4, 128.3, 127.03, 126.96, 126.3, 125.93, 125.86, 125.7, 125.62, 125.55, 125.4, 113.9, 112.3, 59.7, 59.6, 20.4, 16.1; **MS** (ESI-TOF) calcd. for C₁₄H₁₄O [M + H⁺] 199.1117, found 199.1161.

2-(naphthalen-1-yl)propanal (**34p**):

Reaction of enol ether **82** (1.812 g, 9.14 mmol) and conc. HBr (48%, 1.0 mL) in 4:1 acetone/H₂O (10.6 mL, 0.86 M) according to **34b** above afforded **34p** as a colorless oil after column chromatography (silica gel, 19:1 to 3:2 hexanes/EtOAc) (1.409 g, 84%).

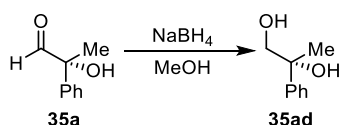
Spectroscopic results agree with previously reported data.⁴⁵

5.7.4 Procedures for α -Functionalizations and Characterization of Products

General Procedure for Primary Amine-Catalyzed α -Hydroxylations (Optimization Studies):

A 1.0-dram vial was charged with primary amine catalyst (**21** or **36–38**, 20 mol% as indicated). No precautions were taken to ensure dryness of vial or to exclude air or moisture. THF (1.0 mL, 0.15 M in aldehyde substrate as indicated) was added to the catalyst. Next, dodecane (3.4 μ L, 2.55 mg, 0.015 mmol, 10 mol%) was added by syringe as an internal standard for GC conversion analysis. Then, aldehyde **34a** (20 μ L, 20.0 mg, 0.15 mmol) was added by syringe, followed by the indicated additives (e.g., TFA, 2.4 μ L, 3.5 mg, 0.031 mmol, 20 mol%; NaHCO₃, 18.8 mg, 0.224 mmol, 1.5 equiv). Last, oxaziridine **33** was added as a solid (46.3 mg, 0.179 mmol, 1.2 equiv). The mixture was stirred at 23 °C and conversion was monitored by GC of small aliquots every 30 min for the first 4 h, then every 2 h for the next 6 h, then every 16 h.

General Procedure for Reduction of α -Hydroxyaldehydes to Diols (Optimization Studies):



Scheme 5.35. Reduction of **35a** to diol **35ad**.

α -Hydroxyaldehydes **35a** were directly reduced to diols **35ad** for HPLC analysis of *ee*. The crude reaction mixture was transferred to a 20-mL vial with MeOH (2 mL, 0.075M in aldehyde), then NaBH₄ (56 mg, 1.49 mmol, 10 equiv) was added. The reaction mixture was stirred, open to air, for 90 min at 23 °C, then quenched with sat. aq. NH₄Cl (4 mL) and EtOAc (4 mL). After an additional 30 min of stirring open to air at 23 °C, the layers were separated and the aqueous phase was extracted with EtOAc (3 x 6 mL). The pooled

organic layers were dried over Na₂SO₄, filtered, and concentrated by rotary evaporation. Enantiomeric excess was determined by chiral HPLC after chromatographic purification on silica gel.

General Procedure for Primary Amine-Catalyzed α -Fluorinations (Optimization Studies):

A 1.0-dram vial was charged with primary amine catalyst (**21** or **36–38**, 20 mol% as indicated). No precautions were taken to ensure dryness of vial or to exclude air or moisture. THF (1.0 mL, 0.15 M in aldehyde substrate as indicated) was added to the catalyst. Next, dodecane (3.4 μ L, 2.55 mg, 0.015 mmol, 10 mol%) was added by syringe as an internal standard for GC conversion analysis. Then, aldehyde **34a** (20 μ L, 20.0 mg, 0.15 mmol) was added by syringe, followed by the indicated additives (e.g., TFA, 2.4 μ L, 3.5 mg, 0.031 mmol, 20 mol%; NaHCO₃, 18.8 mg, 0.224 mmol, 1.5 equiv). Last, NFSI **12** was added as a solid (56.5 mg, 0.179 mmol, 1.2 equiv). The mixture was stirred at 23 °C and conversion was monitored by GC of small aliquots every 30 min for the first 4 h, then every 2 h for the next 6 h, then every 16 h.

General Procedure for Reduction of α -Fluoroaldehydes to Fluorohydrins (Optimization Studies):

α -Fluoroaldehydes **39a** were directly reduced to fluorohydrins **40a** for HPLC analysis of *ee*. The crude reaction mixture was transferred to a 20-mL vial with MeOH (2 mL, 0.075M in aldehyde), then NaBH₄ (56 mg, 1.49 mmol, 10 equiv) was added. The reaction mixture was stirred, open to air, for 90 min at 23 °C, then quenched with sat. aq. NH₄Cl (4 mL) and EtOAc (4 mL). After an additional 30 min of stirring open to air at 23 °C, the layers were separated and the aqueous phase was extracted with EtOAc (3 x 6 mL). The pooled organic layers were dried over Na₂SO₄, filtered, and concentrated by rotary evaporation. Enantiomeric excess was determined by chiral HPLC after chromatographic purification on silica gel (19:1 to 3:2 hexanes/EtOAc).

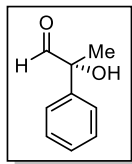
General Procedure for Primary Amine-Catalyzed α -Hydroxylations (Substrate Scope):

A 2.0-dram vial was charged with aldehyde substrate **34a–o** (1.00 mmol as indicated). No precautions were taken to ensure dryness of vial or to exclude air or moisture. The aldehyde was then dissolved in THF (0.3 M in aldehyde as indicated). Solid catalyst **38** (20 mol% as indicated) was added, followed by TFA (20 mol% as indicated) by syringe. Last, dry reagents NaHCO₃ (1.0 equiv as indicated) and oxaziridine **33** (1.0 equiv as indicated) were added to the vial sequentially. The vial was sealed and the mixture was allowed to

stir for the designated amount of time (4 or 20 h) at 23 °C. The reactions started out heterogeneous, but eventually became homogeneous. The mixture was concentrated by rotary evaporation, and the resultant residue was purified directly by silica gel flash chromatography. Racemic standards were synthesized as described, with racemic catalyst (\pm)-**38**.

General Procedure for Reduction of α -Hydroxyaldehydes to Diols (Substrate Scope):

A 20-mL vial was charged with α -hydroxyaldehyde **35a–o** (~0.1 mmol as indicated), then dissolved in MeOH (0.075 M as indicated). Solid NaBH₄ (10 equiv as indicated) was added and the reaction mixture was stirred, open to air, for 90 min at 23 °C, then quenched with sat. aq. NH₄Cl (4 mL) and EtOAc (4 mL). After an additional 30 min of stirring open to air at 23 °C, the layers were separated and the aqueous phase was extracted with EtOAc (3 x 6 mL). The pooled organic layers were dried over Na₂SO₄, filtered, and concentrated by rotary evaporation. The crude product was purified by silica gel flash chromatography.

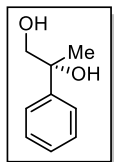


(*R*)-2-hydroxy-2-phenylpropanal (**35a**):

According to the general procedure, **34a** (134 μ L, 134 mg, 1.00 mmol), **33** (258 mg, 1.00 mmol, 1.0 equiv), **38** (74 mg, 0.20 mmol, 20 mol%), TFA (15.4 μ L, 22.8 mg, 0.20 mmol, 20 mol%), and NaHCO₃ (84 mg, 1.00 mmol, 1.0 equiv) were allowed to react in a THF solution (3.3 mL, 0.3 M) for 4 h to afford **35a** (142 mg, 95%) as a colorless oil after column chromatography (silica gel, 19:1 to 3:2 hexanes/Et₂O).

R_f = 0.59 (silica gel, 2:1 hexanes/Et₂O); **IR** (film) ν_{\max} 3448 (br), 1732, 1492, 1448, 1336, 1071, 859, 758, 699 cm⁻¹; **¹H NMR** (500 MHz, CDCl₃) δ 9.57 (s, 1H), 7.48 (d, J = 7.8 Hz, 2H), 7.42 (td, J = 7.3, 1.0 Hz, 2H), 7.37 – 7.33 (m, 1H), 3.89 (d, J = 6.4 Hz, 1H), 1.72 (s, 3H); **¹³C NMR** (126 MHz, CDCl₃) δ 199.8, 139.2, 128.9, 128.2, 125.8, 79.1, 23.6; **MS** (ESI-TOF) calcd. for C₉H₁₀O₃ [M + H⁺ – H₂O] 149.0597, found 149.0561; $[\alpha]_D^{23} = -257.6^\circ$ (c = 1.3, CHCl₃).⁴⁹

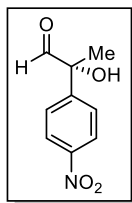
⁴⁹ For comparison: Du, Z.; Kawatani, T.; Kataoka, K.; Omatsu, R.; Nokami, J. *Tetrahedron* **2012**, *68*, 2471–2480.



(R)-2-phenylpropane-1,2-diol (35ad):

According to the general procedure, **35a** (22 mg, 0.15 mmol) and NaBH₄ (55 mg, 1.47 mmol, 10 equiv) were allowed to react in a MeOH solution (2.0 mL, 0.075 M) for 90 min to afford **35ad** (14 mg, 66%) as a colorless oil after column chromatography (silica gel, 9:1 to 2:3 hexanes/Et₂O). This material was determined to be of 90% *ee* by chiral HPLC analysis (ChiralPak AS-H, 5% *i*PrOH in hexanes, 1 mL/min, 210 nm, *t*_R(major) = 29.4 min, *t*_R(minor) = 23.3 min).

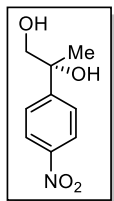
*R*_f = 0.21 (silica gel, 2:1 hexanes/Et₂O); **IR** (film) ν_{\max} 3385 (br), 1446, 1044, 1027, 763, 700 cm⁻¹; **¹H NMR** (400 MHz, CDCl₃) δ 7.47 (d, *J* = 7.5 Hz, 2H), 7.38 (t, *J* = 7.5 Hz, 2H), 7.30 (dt, *J* = 7.3, 1.6 Hz, 1H), 3.81 (d, *J* = 11.3 Hz, 1H), 3.65 (d, *J* = 10.9 Hz, 1H), 2.63 (br s, 1H), 1.89 (br s, 1H), 1.55 (s, 3H); **¹³C NMR** (100 MHz, CDCl₃) δ 144.9, 128.4, 127.2, 125.1, 74.8, 71.7, 26.0; **MS** (ESI-TOF) calcd. for C₉H₁₂O₂ [M + Na⁺] 175.0730, found 175.0686; [α]_D²⁴ = -8.1 (*c* = 1.1, CHCl₃).⁵⁰



(R)-2-hydroxy-2-(4-nitrophenyl)propanal (35b):

According to the general procedure, **34b** (179 mg, 1.00 mmol), **33** (258 mg, 1.00 mmol, 1.0 equiv), **38** (74 mg, 0.20 mmol, 20 mol%), TFA (15.4 μ L, 22.8 mg, 0.20 mmol, 20 mol%), and NaHCO₃ (84 mg, 1.00 mmol, 1.0 equiv) were allowed to react in a THF solution (3.3 mL, 0.3 M) for 4 h to afford **35b** (114 mg, 58%) as a yellow oil after column chromatography (silica gel, 19:1 to 3:2 hexanes/Et₂O).

*R*_f = 0.24 (silica gel, 2:1 hexanes/Et₂O); **IR** (film) ν_{\max} 3485 (br), 1733, 1606, 1521, 1348, 855, 702 cm⁻¹; **¹H NMR** (500 MHz, CDCl₃) δ 9.63 (s, 1H), 8.28 (d, *J* = 8.8 Hz, 2H), 7.70 (d, *J* = 8.8 Hz, 2H), 3.93 (s, 1H), 1.76 (s, 3H); **¹³C NMR** (126 MHz, CDCl₃) δ 198.5, 146.4, 126.8, 124.0, 79.2, 24.3; **MS** (ESI-TOF) calcd. for C₉H₉NO₄ [M + H⁺ - H₂O] 178.0499, found 178.0512; [α]_D²³ = -146.0 (*c* = 0.8, CHCl₃).



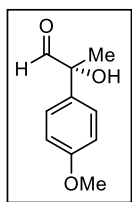
(R)-2-(4-nitrophenyl)propane-1,2-diol (35bd):

According to the general procedure, **35b** (12.8 mg, 0.07 mmol) and NaBH₄ (25 mg, 0.66 mmol, 10 equiv) were allowed to react in a MeOH solution (0.87 mL, 0.075 M) for 90 min to afford

⁵⁰ For comparison: DeBergh, J. R.; Spivey, K. M.; Ready, J. M. *J. Am. Chem. Soc.* **2008**, *130*, 7828–7829.

35bd (8.3 mg, 64%) as a yellow oil after column chromatography (silica gel, 9:1 to 2:3 hexanes/Et₂O). This material was determined to be of 84% *ee* by chiral HPLC analysis (ChiralPak AS-H, 10% *i*PrOH in hexanes, 1 mL/min, 210 nm, *t*_R(major) = 34.8 min, *t*_R(minor) = 24.5 min).

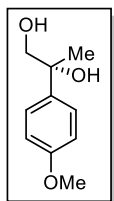
R_f = 0.07 (silica gel, 2:1 hexanes/Et₂O); **IR** (film) ν_{\max} 3373 (br), 1604, 1514, 1347, 1042, 854, 701 cm⁻¹; **¹H NMR** (500 MHz, CDCl₃) δ 8.22 (d, *J* = 8.8 Hz, 2H), 7.66 (d, *J* = 8.8 Hz, 2H), 3.83 (dd, *J* = 11.0, 4.6 Hz, 1H), 3.72 (dd, *J* = 11.0, 6.0 Hz, 1H), 2.75 (s, 1H), 1.90 (t, *J* = 5.6 Hz, 1H), 1.58 (s, 3H); **¹³C NMR** (100 MHz, CDCl₃) δ 152.5, 126.2, 123.6, 74.8, 70.6, 26.1; **MS** (ESI-TOF) calcd. for C₉H₁₁NO₄ [M + Na⁺] 220.0580, found 220.0593; [α]_D²⁴ = -14.6 (*c* = 0.5, CHCl₃).



(R)-2-hydroxy-2-(4-methoxyphenyl)propanal (35c):

According to the general procedure, **34c** (164 mg, 1.00 mmol), **33** (258 mg, 1.00 mmol, 1.0 equiv), **38** (74 mg, 0.20 mmol, 20 mol%), TFA (15.4 μ L, 22.8 mg, 0.20 mmol, 20 mol%), and NaHCO₃ (84 mg, 1.00 mmol, 1.0 equiv) were allowed to react in a THF solution (3.3 mL, 0.3 M) for 4 h to afford **35c** (140 mg, 78%) as a white solid after column chromatography (silica gel, 19:1 to 3:2 hexanes/Et₂O).

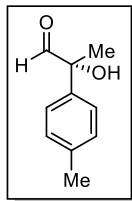
R_f = 0.22 (silica gel, 4:1 hexanes/Et₂O); **IR** (film) ν_{\max} 3444 (br), 1729, 1609, 1511, 1302, 1252, 1030, 864, 832 cm⁻¹; **¹H NMR** (500 MHz, CDCl₃) δ 9.51 (s, 1H), 7.37 (d, *J* = 9.0, 1.7 Hz, 2H), 6.96 – 6.92 (m, 2H), 3.82 (s, 3H), 3.81 (s, 1H), 1.96 (s, 3H); **¹³C NMR** (126 MHz, CDCl₃) δ 199.6, 159.5, 131.0, 127.2, 114.3, 78.7, 55.3, 23.3; **MS** (ESI-TOF) calcd. for C₁₀H₁₂O₃ [M + H⁺ – H₂O] 163.0754, found 163.0749; [α]_D²⁴ = -62.8 (*c* = 0.9, CHCl₃).



(R)-2-(4-methoxyphenyl)propane-1,2-diol (35cd):

According to the general procedure, **35c** (10.8 mg, 0.06 mmol) and NaBH₄ (23 mg, 0.60 mmol, 10 equiv) were allowed to react in a MeOH solution (0.80 mL, 0.075 M) for 90 min to afford **35cd** (2.8 mg, 26%) as a white solid after column chromatography (silica gel, 9:1 to 2:3 hexanes/Et₂O). This material was determined to be of 92% *ee* by chiral HPLC analysis (ChiralCel OD-H, 5% *i*PrOH in hexanes, 1 mL/min, 224 nm, *t*_R(major) = 27.5 min, *t*_R(minor) = 36.8 min).

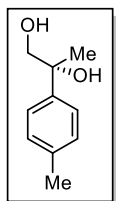
R_f = 0.14 (silica gel, 2:1 hexanes/Et₂O); **IR** (film) ν_{\max} 3388 (br), 2929, 1612, 1513, 1463, 1301, 1248, 1180, 1032, 869 cm⁻¹; **¹H NMR** (500 MHz, CDCl₃) δ 7.39 (d, J = 8.8 Hz, 2H), 6.29 (d, J = 8.8 Hz, 2H), 3.82 (s, 3H), 3.78 (dd, J = 10.7, 4.4 Hz, 1H), 3.62 (d, J = 11.2, 7.8 Hz, 1H), 2.46 (s, 1H), 1.73 (dd, J = 8.3, 4.9 Hz, 1H), 1.54 (s, 3H); **¹³C NMR** (100 MHz, CDCl₃) δ 137.0, 126.3, 113.8, 74.5, 71.2, 55.3, 26.1; **MS** (ESI-TOF) calcd. for C₁₀H₁₄O₃ [M + Na⁺] 205.0835, found 205.0835; $[\alpha]_D^{23}$ = -4.0 (c = 0.1, CHCl₃).



(R)-2-hydroxy-2-(p-tolyl)propanal (35d):

According to the general procedure, **34d** (148 mg, 1.00 mmol), **33** (258 mg, 1.00 mmol, 1.0 equiv), **38** (74 mg, 0.20 mmol, 20 mol%), TFA (15.4 μ L, 22.8 mg, 0.20 mmol, 20 mol%), and NaHCO₃ (84 mg, 1.00 mmol, 1.0 equiv) were allowed to react in a THF solution (3.3 mL, 0.3 M) for 4 h to afford **35d** (113 mg, 69%) as a white solid after column chromatography (silica gel, 19:1 to 3:2 hexanes/Et₂O).

R_f = 0.63 (silica gel, 2:1 hexanes/Et₂O); **IR** (film) ν_{\max} 3442 (br), 2929, 1730, 1511, 1350, 1093, 863, 816, 537 cm⁻¹; **¹H NMR** (400 MHz, CDCl₃) δ 9.54 (s, 1H), 7.36 (d, J = 8.2 Hz, 2H), 7.23 (d, J = 8.2 Hz, 2H), 3.83 (s, 1H), 2.36 (s, 3H), 1.70 (s, 3H); **¹³C NMR** (100 MHz, CDCl₃) δ 199.8, 138.0, 136.1, 129.6, 125.7, 78.9, 23.4, 21.0; **MS** (ESI-TOF) calcd. for C₁₀H₁₂O₂ [M + Na⁺] 187.0730, found 187.0726; $[\alpha]_D^{24}$ = -150.5 (c = 1.7, CHCl₃).

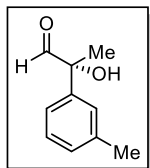


(R)-2-(p-tolyl)propane-1,2-diol (35dd):

According to the general procedure, **35d** (10.6 mg, 0.07 mmol) and NaBH₄ (24 mg, 0.65 mmol, 10 equiv) were allowed to react in a MeOH solution (0.86 mL, 0.075 M) for 90 min to afford **35dd** (9.1 mg, 85%) as a white solid after column chromatography (silica gel, 9:1 to 2:3 hexanes/Et₂O). This material was determined to be of 90% *ee* by chiral HPLC analysis (ChiralPak AD-H, 5% *i*PrOH in hexanes, 1 mL/min, 212 nm, t_R (major) = 24.2 min, t_R (minor) = 19.3 min).

R_f = 0.23 (silica gel, 2:1 hexanes/Et₂O); **IR** (film) ν_{\max} 3377 (br), 2925, 1514, 1041, 866, 527 cm⁻¹; **¹H NMR** (400 MHz, CDCl₃) δ 7.35 (d, J = 8.2 Hz, 2H), 7.19 (d, J = 7.8 Hz, 2H), 3.76 (d, J = 10.1 Hz, 1H), 3.63 (dd, J = 10.5, 7.0 Hz, 1H), 2.54 (s, 1H), 2.36 (s, 3H), 1.80 (br s, 1H), 1.53 (s, 3H); **¹³C NMR** (100

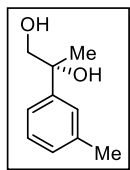
MHz, CDCl₃) δ 141.9, 136.9, 129.2, 125.0, 74.7, 71.2, 26.0, 21.0; **MS** (ESI-TOF) calcd. for C₁₀H₁₄O₂ [M + Na⁺] 189.0886, found 189.0883; $[\alpha]_D^{24} = -8.1$ ($c = 0.4$, CHCl₃).⁵¹



(R)-2-hydroxy-2-(*m*-tolyl)propanal (35e):

According to the general procedure, **34e** (148 mg, 1.00 mmol), **33** (258 mg, 1.00 mmol, 1.0 equiv), **38** (74 mg, 0.20 mmol, 20 mol%), TFA (15.4 μ L, 22.8 mg, 0.20 mmol, 20 mol%), and NaHCO₃ (84 mg, 1.00 mmol, 1.0 equiv) were allowed to react in a THF solution (3.3 mL, 0.3 M) for 4 h to afford **35e** (157 mg, 95%) as a pale yellow oil after column chromatography (silica gel, 19:1 to 3:2 hexanes/Et₂O).

$R_f = 0.72$ (silica gel, 2:1 hexanes/Et₂O); **IR** (film) ν_{\max} 3451 (br), 2980, 2928, 1732, 1077, 830, 787, 703 cm⁻¹; **¹H NMR** (500 MHz, CDCl₃) δ 9.56 (s, 1H), 7.33 – 7.26 (m, 3H), 7.16 (d, $J = 7.3$ Hz, 1H), 3.82 (d, $J = 1.0$ Hz, 1H), 2.43 – 2.37 (m, 3H), 1.71 (s, 3H); **¹³C NMR** (126 MHz, CDCl₃) δ 199.8, 139.0, 138.7, 128.9, 128.8, 126.4, 122.8, 79.0, 23.5, 21.6; **MS** (ESI-TOF) calcd. for C₁₀H₁₂O₂ [M + Na⁺] 187.0730, found 187.0730; $[\alpha]_D^{24} = -53.5$ ($c = 0.3$, CHCl₃).



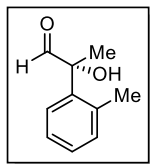
(R)-2-(*m*-tolyl)propane-1,2-diol (35ed):

According to the general procedure, **35e** (11.4 mg, 0.07 mmol) and NaBH₄ (26 mg, 0.69 mmol, 10 equiv) were allowed to react in a MeOH solution (0.93 mL, 0.075 M) for 90 min to afford **35ed** (5.8 mg, 50%) as a pale yellow oil after column chromatography (silica gel, 9:1 to 2:3 hexanes/Et₂O). This material was determined to be of 89% *ee* by chiral HPLC analysis (ChiralPak AD-H, 5% *i*PrOH in hexanes, 1 mL/min, 220 nm, t_R (major) = 25.6 min, t_R (minor) = 18.0 min).

$R_f = 0.19$ (silica gel, 2:1 hexanes/Et₂O); **IR** (film) ν_{\max} 3383 (br), 2976, 2928, 1459, 1375, 1167, 1042, 786, 705 cm⁻¹; **¹H NMR** (400 MHz, CDCl₃) δ 7.30 – 7.23 (m, 3H), 7.11 (d, $J = 6.6$ Hz, 1H), 3.81 (dd, $J = 11.1$, 4.5 Hz, 1H), 3.64 (dd, $J = 10.9$, 8.2 Hz, 1H), 2.56 (s, 1H), 2.38 (s, 3H), 1.77 (dd, $J = 8.4$, 4.5 Hz, 1H), 1.53 (s, 3H); **¹³C NMR** (126 MHz, CDCl₃) δ 144.9, 138.1, 128.4, 128.0, 125.8, 122.1, 74.8, 71.2, 26.1, 21.6;

⁵¹ For comparison: Chavan, S. P.; Khatod, H. S. *Tetrahedron: Asymmetry* **2012**, *23*, 1410–1415.

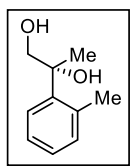
MS (ESI-TOF) calcd. for C₁₀H₁₄O₂ [M + Na⁺] 189.0886, found 189.0885; [α]_D²⁴ = -7.1 (*c* = 0.3, CHCl₃).



(R)-2-hydroxy-2-(*o*-tolyl)propanal (35f):

According to the general procedure, **34f** (148 mg, 1.00 mmol), **33** (258 mg, 1.00 mmol, 1.0 equiv), **38** (74 mg, 0.20 mmol, 20 mol%), TFA (15.4 μL, 22.8 mg, 0.20 mmol, 20 mol%), and NaHCO₃ (84 mg, 1.00 mmol, 1.0 equiv) were allowed to react in a THF solution (3.3 mL, 0.3 M) for 20 h to afford **35f** (132 mg, 80%) as a yellow oil after column chromatography (silica gel, 19:1 to 3:2 hexanes/Et₂O).

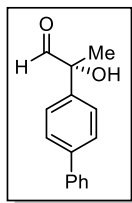
R_f = 0.71 (silica gel, 2:1 hexanes/Et₂O); **IR** (film) ν_{\max} 3440 (br), 2979, 1731, 1487, 1459, 1092, 1050, 805, 758, 726 cm⁻¹; **¹H NMR** (500 MHz, CDCl₃) δ 9.58 (s, 1H), 7.51 – 7.48 (m, 1H), 7.31 – 7.28 (m, 2H), 7.22 – 7.20 (m, 1H), 3.59 (s, 1H), 2.32 (s, 3H), 1.75 (s, 3H); **¹³C NMR** (126 MHz, CDCl₃) δ 200.4, 137.8, 136.0, 132.4, 128.9, 126.9, 126.2, 79.9, 23.2, 21.0; **MS** (ESI-TOF) calcd. for C₁₀H₁₂O₂ [M + H⁺] 187.0730, found 187.0706; [α]_D²³ = -100.5 (*c* = 0.4, CHCl₃).



(R)-2-(*o*-tolyl)propane-1,2-diol (35fd):

According to the general procedure, **35f** (11.3 mg, 0.07 mmol) and NaBH₄ (26 mg, 0.69 mmol, 10 equiv) were allowed to react in a MeOH solution (0.92 mL, 0.075 M) for 90 min to afford **35fd** (8.9 mg, 78%) as a yellow oil after column chromatography (silica gel, 9:1 to 2:3 hexanes/Et₂O). This material was determined to be of 55% *ee* by chiral HPLC analysis (ChiralPak AS-H, 5% *i*PrOH in hexanes, 1 mL/min, 210 nm, *t_R*(major) = 22.3 min, *t_R*(minor) = 16.3 min).

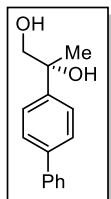
R_f = 0.21 (silica gel, 2:1 hexanes/Et₂O); **IR** (film) ν_{\max} 3380 (br), 2974, 2934, 1459, 1165, 1035, 759, 727 cm⁻¹; **¹H NMR** (400 MHz, CDCl₃) δ 7.47 – 7.43 (m, 1H), 7.21 – 7.18 (m, 3H), 4.04 (dd, *J* = 11.1, 3.7 Hz, 1H), 3.70 (dd, *J* = 11.1, 8.0 Hz, 1H), 2.58 (s, 1H), 2.57 (s, 3H), 1.91 (dd, *J* = 7.4, 4.3 Hz, 1H), 1.61 (s, 3H); **¹³C NMR** (126 MHz, CDCl₃) δ 141.9, 136.0, 132.9, 127.5, 126.2, 125.9, 75.9, 69.5, 25.4, 22.3; **MS** (ESI-TOF) calcd. for C₁₀H₁₄O₂ [M + Na⁺] 189.0886, found 189.0880; [α]_D²⁴ = -0.3 (*c* = 0.6, CHCl₃).



(R)-2-([1,1'-biphenyl]-4-yl)-2-hydroxypropanal (35g):

According to the general procedure, **34g** (210 mg, 1.00 mmol), **33** (258 mg, 1.00 mmol, 1.0 equiv), **38** (74 mg, 0.20 mmol, 20 mol%), TFA (15.4 μ L, 22.8 mg, 0.20 mmol, 20 mol%), and NaHCO₃ (84 mg, 1.00 mmol, 1.0 equiv) were allowed to react in a THF solution (3.3 mL, 0.3 M) for 4 h to afford **35g** (222 mg, 98%) as a white solid after column chromatography (silica gel, 19:1 to 3:2 hexanes/Et₂O).

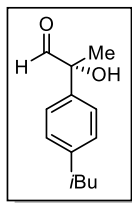
R_f = 0.54 (silica gel, 2:1 hexanes/Et₂O); **IR** (film) ν_{\max} 3493 (br), 2917, 2849, 1723, 1486, 1318, 1094, 865, 767, 736, 695 cm⁻¹; **¹H NMR** (500 MHz, CDCl₃) δ 9.61 (s, 1H), 7.65 (d, J = 7.7 Hz, 2H), 7.60 (d, J = 7.3 Hz, 2H), 7.55 (d, J = 8.3 Hz, 2H), 7.46 (t, J = 7.5 Hz, 2H), 7.38 (t, J = 7.3 Hz, 1H), 3.88 (s, 1H), 1.76 (s, 3H); **¹³C NMR** (126 MHz, CDCl₃) δ 199.6, 141.2, 140.4, 138.1, 128.8, 127.61, 127.57, 127.1, 126.3, 79.0, 23.6; **MS** (ESI-TOF) calcd. for C₁₅H₁₄O₂ [M + Na⁺] 249.0886, found 249.0871; $[\alpha]_D^{24}$ = -223.3 (c = 0.2, CHCl₃).



(R)-2-([1,1'-biphenyl]-4-yl)propane-1,2-diol (35gd):

According to the general procedure, **35g** (11.7 mg, 0.05 mmol) and NaBH₄ (20 mg, 0.52 mmol, 10 equiv) were allowed to react in a MeOH solution (0.69 mL, 0.075 M) for 90 min to afford **35gd** (6.1 mg, 52%) as a white solid after column chromatography (silica gel, 9:1 to 2:3 hexanes/Et₂O). This material was determined to be of 90% *ee* by chiral HPLC analysis (ChiralPak AS-H, 5% *i*PrOH in hexanes, 1 mL/min, 210 nm, t_R (major) = 36.0 min, t_R (minor) = 27.5 min).

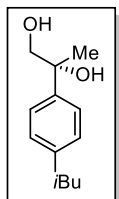
R_f = 0.19 (silica gel, 2:1 hexanes/Et₂O); **IR** (film) ν_{\max} 3383 (br), 1487, 1401, 1021, 839, 766, 733, 697 cm⁻¹; **¹H NMR** (400 MHz, CDCl₃) δ 7.61 (td, J = 6.6, 2.0 Hz, 4H), 7.54 (d, J = 8.6 Hz, 2H), 7.48 – 7.43 (m, 2H), 7.38 – 7.34 (m, 1H), 3.87 (dd, J = 10.9, 4.7 Hz, 1H), 3.70 (dd, J = 11.1, 8.0 Hz, 1H), 2.60 (s, 1H), 1.81 (dd, J = 7.8, 4.7 Hz, 1H), 1.59 (s, 3H); **¹³C NMR** (100 MHz, CDCl₃) δ 144.0, 140.7, 140.2, 128.8, 127.3, 127.2, 127.1, 125.6, 74.8, 74.1, 26.1; **MS** (ESI-TOF) calcd. for C₁₅H₁₆O₂ [M + Na⁺] 251.1043, found 251.1026; $[\alpha]_D^{24}$ = -8.2 (c = 0.5, CHCl₃).



(R)-2-hydroxy-2-(4-isobutylphenyl)propanal (35h):

According to the general procedure, **34h** (190 mg, 1.00 mmol), **33** (258 mg, 1.00 mmol, 1.0 equiv), **38** (74 mg, 0.20 mmol, 20 mol%), TFA (15.4 μ L, 22.8 mg, 0.20 mmol, 20 mol%), and NaHCO₃ (84 mg, 1.00 mmol, 1.0 equiv) were allowed to react in a THF solution (3.3 mL, 0.3 M) for 4 h to afford **35h** (202 mg, 98%) as a colorless oil after column chromatography (silica gel, 19:1 to 3:2 hexanes/Et₂O).

R_f = 0.58 (silica gel, 2:1 hexanes/Et₂O); **IR** (film) ν_{\max} 3485 (br), 2955, 2926, 2869, 1733, 1536, 1466, 1383, 1170, 1097, 865, 796, 740, 672 cm⁻¹; **¹H NMR** (500 MHz, CDCl₃) δ 9.54 (s, 1H), 7.36 (d, J = 8.3 Hz, 2H), 7.19 (d, J = 7.8 Hz, 2H), 3.82 (s, 1H), 2.48 (d, J = 7.3 Hz, 2H), 1.86 (dt, J = 13.7, 6.8 Hz, 1H), 1.71 (s, 3H), 0.91 (d, J = 6.8 Hz, 6H); **¹³C NMR** (126 MHz, CDCl₃) δ 199.8, 141.8, 136.3, 129.6, 125.6, 79.0, 45.0, 30.2, 23.4, 22.3; **MS** (ESI-TOF) calcd. for C₁₃H₁₈O₂ [M + Na⁺] 229.1199, found 229.1209; $[\alpha]_D^{24}$ = -141.9 (c = 0.5, CHCl₃).

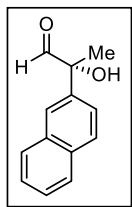


(R)-2-(4-isobutylphenyl)propane-1,2-diol (35hd):

According to the general procedure, **35h** (15.8 mg, 0.08 mmol) and NaBH₄ (29 mg, 0.77 mmol, 10 equiv) were allowed to react in a MeOH solution (1.0 mL, 0.075 M) for 90 min to afford **35hd** (16.0 mg, 99%) as a colorless oil after column chromatography (silica gel, 9:1 to 2:3 hexanes/Et₂O). This material was determined to be of 86% *ee* by chiral HPLC analysis (ChiralPak AS-H, 5% *i*PrOH in hexanes, 1 mL/min, 218 nm, t_R (major) = 14.8 min, t_R (minor) = 11.6 min).

R_f = 0.24 (silica gel, 2:1 hexanes/Et₂O); **IR** (film) ν_{\max} 3363 (br), 2954, 2925, 2868, 1531, 1465, 1348, 1167, 1042, 797, 616, 560 cm⁻¹; **¹H NMR** (500 MHz, CDCl₃) δ 7.36 (d, J = 8.3 Hz, 2H), 7.16 (d, J = 8.3 Hz, 2H), 3.80 (dd, J = 11.0, 2.7 Hz, 1H), 3.64 (dd, J = 11.0, 7.6 Hz, 1H), 2.51 (s, 1H), 2.47 (d, J = 7.3 Hz, 2H), 1.87 (dt, J = 13.7, 6.8 Hz, 1H), 1.77 (br s, 1H), 1.54 (s, 3H), 0.91 (d, J = 10.7 Hz, 6H); **¹³C NMR** (126 MHz, CDCl₃) δ 142.1, 140.7, 129.2, 124.8, 74.7, 71.2, 45.0, 30.2, 26.0, 22.4; **MS** (ESI-TOF) calcd. for C₁₃H₂₀O₂ [M + Na⁺] 231.1356, found 231.1352; $[\alpha]_D^{25}$ = -1.8 (c = 0.6, CHCl₃).⁵²

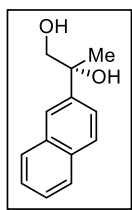
⁵² For comparison: Ishibashi, H.; Maeki, M.; Yagi, J.; Ohba, M.; Kanai, T. *Tetrahedron* **1999**, *55*, 6075–6080.



(R)-2-hydroxy-2-(naphthalen-2-yl)propanal (35i):

According to the general procedure, **34i** (184 mg, 1.00 mmol), **33** (258 mg, 1.00 mmol, 1.0 equiv), **38** (74 mg, 0.20 mmol, 20 mol%), TFA (15.4 μ L, 22.8 mg, 0.20 mmol, 20 mol%), and NaHCO₃ (84 mg, 1.00 mmol, 1.0 equiv) were allowed to react in a THF solution (3.3 mL, 0.3 M) for 4 h to afford **35i** (194 mg, 97%) as a white solid after column chromatography (silica gel, 19:1 to 3:2 hexanes/Et₂O).

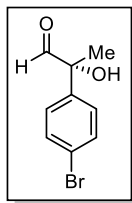
R_f = 0.56 (silica gel, 2:1 hexanes/Et₂O); **IR** (film) ν_{\max} 3461 (br), 1730, 1130, 826, 751, 478 cm⁻¹; **¹H NMR** (500 MHz, CDCl₃) δ 9.66 (s, 1H), 7.99 (s, 1H), 7.90 – 7.95 (m, 3H), 7.56 (dd, J = 8.8, 2.0 Hz, 1H), 7.54 – 7.51 (m, 2H), 3.95 (s, 1H), 1.83 (s, 3H); **¹³C NMR** (126 MHz, CDCl₃) δ 199.7, 136.5, 133.3, 132.9, 128.7, 128.2, 127.6, 126.6, 126.5, 125.2, 123.3, 79.3, 23.6; **MS** (ESI-TOF) calcd. for C₁₃H₁₂O₂ [M + K⁺] 239.0469, found 239.1281; $[\alpha]_D^{24}$ = -249.2 (c = 0.4, CHCl₃).



(R)-2-(naphthalen-2-yl)propane-1,2-diol (35id):

According to the general procedure, **35i** (22 mg, 0.11 mmol) and NaBH₄ (41 mg, 1.07 mmol, 10 equiv) were allowed to react in a MeOH solution (1.4 mL, 0.075 M) for 90 min to afford **35id** (10.5 mg, 48%) as a white solid after column chromatography (silica gel, 9:1 to 2:3 hexanes/Et₂O). This material was determined to be of 91% *ee* by chiral HPLC analysis (ChiralPak AD-H, 5% *i*PrOH in hexanes, 1 mL/min, 210 nm, t_R (major) = 36.7 min, t_R (minor) = 35.0 min).

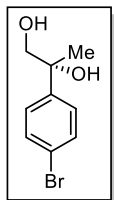
R_f = 0.16 (silica gel, 2:1 hexanes/Et₂O); **IR** (film) ν_{\max} 3371 (br), 2974, 1128, 858, 820, 747, 480 cm⁻¹; **¹H NMR** (500 MHz, CDCl₃) δ 7.97 (s, 1H), 7.85 (td, J = 8.3, 1.0 Hz, 3H), 7.54 (dt, J = 8.5, 1.6 Hz, 1H), 7.52 – 7.47 (m, 2H), 3.93 (dt, J = 11.2, 2.2 Hz, 1H), 3.74 (td, J = 8.3, 1.5 Hz, 1H), 2.71 (s, 1H), 1.79 (dd, J = 7.3, 4.9 Hz, 1H), 1.64 (s, 3H); **¹³C NMR** (126 MHz, CDCl₃) δ 142.3, 133.2, 132.5, 128.2, 128.1, 127.5, 126.3, 126.0, 124.0, 123.3, 75.0, 71.0, 26.1; **MS** (ESI-TOF) calcd. for C₁₃H₁₄O₂ [M + Na⁺] 225.0886, found 225.0910; $[\alpha]_D^{24}$ = -6.2 (c = 0.7, CHCl₃).



(R)-2-(4-bromophenyl)-2-hydroxypropanal (35j):

According to the general procedure, **34j** (213 mg, 1.00 mmol), **33** (258 mg, 1.00 mmol, 1.0 equiv), **38** (74 mg, 0.20 mmol, 20 mol%), TFA (15.4 μ L, 22.8 mg, 0.20 mmol, 20 mol%), and NaHCO₃ (84 mg, 1.00 mmol, 1.0 equiv) were allowed to react in a THF solution (3.3 mL, 0.3 M) for 4 h to afford **35j** (209 mg, 91%) as a white solid after column chromatography (silica gel, 19:1 to 3:2 hexanes/Et₂O).

R_f = 0.56 (silica gel, 2:1 hexanes/Et₂O); **IR** (film) ν_{\max} 3459 (br), 1731, 1488, 1397, 1081, 1009, 863, 821, 788, 545, 493 cm⁻¹; **¹H NMR** (500 MHz, CDCl₃) δ 9.54 (s, 1H), 7.55 (d, J = 7.8 Hz, 2H), 7.36 (d, J = 8.3 Hz, 2H), 3.82 (s, 1H), 1.70 (s, 3H); **¹³C NMR** (126 MHz, CDCl₃) δ 199.2, 138.3, 132.0, 127.6, 122.5, 78.9, 23.7; **MS** (ESI-TOF) calcd. for C₉H₉BrO₂ [M + H⁺ - H₂O] 210.9753 and 212.9733, found 210.9782 and 212.9763; $[\alpha]_D^{23}$ = -184.8 (c = 0.3, CHCl₃).

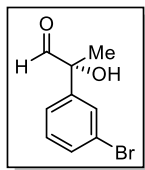


(R)-2-(4-bromophenyl)propane-1,2-diol (35jd):

According to the general procedure, **35j** (13.6 mg, 0.06 mmol) and NaBH₄ (22 mg, 0.59 mmol, 10 equiv) were allowed to react in a MeOH solution (0.79 mL, 0.075 M) for 90 min to afford **35jd** (3.3 mg, 24%) as a colorless oil after column chromatography (silica gel, 9:1 to 2:3 hexanes/Et₂O). This material was determined to be of 88% *ee* by chiral HPLC analysis (ChiralPak AS-H, 5% *i*PrOH in hexanes, 1 mL/min, 220 nm, t_R (major) = 27.2 min, t_R (minor) = 22.0 min).

R_f = 0.10 (silica gel, 2:1 hexanes/Et₂O); **IR** (film) ν_{\max} 3369 (br), 1489, 1396, 1040, 1009, 867, 822, 526 cm⁻¹; **¹H NMR** (400 MHz, CDCl₃) δ 7.50 (d, J = 8.2 Hz, 2H), 7.35 (d, J = 8.2 Hz, 2H), 3.78 (dd, J = 10.9, 4.7 Hz, 1H), 3.64 (dd, J = 10.9, 7.4 Hz, 1H), 2.54 (s, 1H), 1.73 (dd, J = 7.2, 5.3, 1H), 1.53 (s, 3H); **¹³C NMR** (100 MHz, CDCl₃) δ 131.5, 127.0, 74.6, 70.9, 26.0; **MS** (ESI-TOF) calcd. for C₉H₁₁BrO₂ [M + Na⁺] 252.9835 and 254.9814, found 252.9880 and 954.9854; $[\alpha]_D^{25}$ = -40.0 (c = 0.1, CHCl₃).⁵³

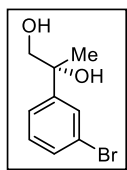
⁵³ For comparison: Cleji, M.; Archelas, A.; Furstoss, R. *Tetrahedron: Asymmetry* **1998**, *9*, 1839–1842.



(R)-2-(3-bromophenyl)-2-hydroxypropanal (35k):

According to the general procedure, **34k** (213 mg, 1.00 mmol), **33** (258 mg, 1.00 mmol, 1.0 equiv), **38** (74 mg, 0.20 mmol, 20 mol%), TFA (15.4 μ L, 22.8 mg, 0.20 mmol, 20 mol%), and NaHCO₃ (84 mg, 1.00 mmol, 1.0 equiv) were allowed to react in a THF solution (3.3 mL, 0.3 M) for 4 h to afford **35k** (188 mg, 82%) as a pale yellow oil after column chromatography (silica gel, 19:1 to 3:2 hexanes/Et₂O).

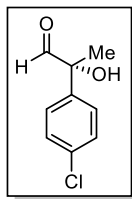
R_f = 0.52 (silica gel, 2:1 hexanes/Et₂O); **IR** (film) ν_{\max} 3461 (br), 1734, 1568, 1475, 1418, 1069, 902, 785, 719, 650 cm⁻¹; **¹H NMR** (500 MHz, CDCl₃) δ 9.56 (s, 1H), 7.66 – 7.64 (m, 1H), 7.49 – 7.46 (m, 1H), 7.40 (dd, J = 7.8, 1.0 Hz, 1H), 7.30 (d, J = 11.7 Hz, 1H), 3.85 (s, 1H), 1.70 (s, 3H); **¹³C NMR** (126 MHz, CDCl₃) δ 199.1, 141.6, 131.3, 130.4, 129.0, 124.4, 123.2, 78.8, 23.8; **MS** (ESI-TOF) calcd. for C₉H₉BrO₂ [M + H⁺ – H₂O] 210.9753 and 212.9733, found 210.9781 and 212.9764; $[\alpha]_D^{24}$ = –118.5 (c = 0.4, CHCl₃).



(R)-2-(3-bromophenyl)propane-1,2-diol (35kd):

According to the general procedure, **35k** (14.6 mg, 0.06 mmol) and NaBH₄ (24 mg, 0.64 mmol, 10 equiv) were allowed to react in a MeOH solution (0.85 mL, 0.075 M) for 90 min to afford **35kd** (3.6 mg, 56%) as a pale yellow oil after column chromatography (silica gel, 9:1 to 2:3 hexanes/Et₂O). This material was determined to be of 87% *ee* by chiral HPLC analysis (ChiralPak AD-H, 5% *i*PrOH in hexanes, 1 mL/min, 210 nm, t_R (major) = 23.1 min, t_R (minor) = 16.9 min).

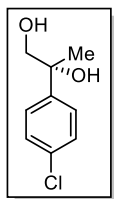
R_f = 0.20 (silica gel, 2:1 hexanes/Et₂O); **IR** (film) ν_{\max} 3356 (br), 2977, 2931, 1594, 1566, 1474, 1417, 1041, 878, 784, 762, 697 cm⁻¹; **¹H NMR** (400 MHz, CDCl₃) δ 7.65 (t, J = 1.8 Hz, 1H), 7.42 (ddd, J = 7.8, 2.0, 1.2 Hz, 1H), 7.39 (ddd, J = 7.8, 1.8, 1 Hz, 1H), 7.25 (t, J = 7.8 Hz, 1H), 3.79 (dd, J = 11.3, 4.3 Hz, 1H), 3.64 (dd, J = 10.9, 7.4 Hz, 1H), 2.62 (s, 1H), 1.80 (dd, J = 7.4, 5.1 Hz, 1H), 1.53 (s, 3H); **¹³C NMR** (100 MHz, CDCl₃) δ 147.4, 130.3, 130.0, 128.5, 123.7, 122.8, 74.5, 70.9, 26.0; **MS** (ESI-TOF) calcd. for C₉H₁₁BrO₂ [M + Na⁺] 252.9835 and 254.9814, found 252.9880 and 254.9854; $[\alpha]_D^{25}$ = –10.0 (c = 0.4, CHCl₃).



(R)-2-(4-chlorophenyl)-2-hydroxypropanal (35l):

According to the general procedure, **34l** (169 mg, 1.00 mmol), **33** (258 mg, 1.00 mmol, 1.0 equiv), **38** (74 mg, 0.20 mmol, 20 mol%), TFA (15.4 μ L, 22.8 mg, 0.20 mmol, 20 mol%), and NaHCO₃ (84 mg, 1.00 mmol, 1.0 equiv) were allowed to react in a THF solution (3.3 mL, 0.3 M) for 4 h to afford **35l** (177 mg, 96%) as a white solid after column chromatography (silica gel, 19:1 to 3:2 hexanes/Et₂O).

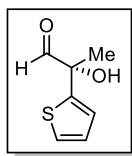
R_f = 0.63 (silica gel, 2:1 hexanes/Et₂O); IR (film) ν_{\max} 3445 (br), 2982, 1733, 1491, 1401, 1094, 1013, 863, 826, 788, 753 cm⁻¹; ¹H NMR (500 MHz, CDCl₃) δ 9.54 (s, 1H), 7.44 – 7.38 (m, 4H), 3.84 (s, 1H), 1.70 (s, 3H); ¹³C NMR (126 MHz, CDCl₃) δ 199.2, 137.7, 134.3, 129.0, 127.2, 78.8, 23.7; MS (ESI-TOF) calcd. for C₉H₉ClO₂ [M + H⁺ – H₂O] 167.0258, found 167.0244; $[\alpha]_D^{23}$ = –196.2 (*c* = 0.4, CHCl₃).



(R)-2-(4-chlorophenyl)propane-1,2-diol (35ld):

According to the general procedure, **35l** (19.0 mg, 0.10 mmol) and NaBH₄ (39 mg, 1.03 mmol, 10 equiv) were allowed to react in a MeOH solution (1.4 mL, 0.075 M) for 90 min to afford **35ld** (8.6 mg, 45%) as a colorless oil after column chromatography (silica gel, 9:1 to 2:3 hexanes/Et₂O). This material was determined to be of 90% *ee* by chiral HPLC analysis (ChiralPak AS-H, 5% *i*PrOH in hexanes, 1 mL/min, 210 nm, *t*_R(major) = 25.3 min, *t*_R(minor) = 21.3 min).

R_f = 0.18 (silica gel, 2:1 hexanes/Et₂O); IR (film) ν_{\max} 3374 (br), 2977, 2932, 1492, 1400, 1375, 1096, 1041, 1013, 828, 545 cm⁻¹; ¹H NMR (500 MHz, CDCl₃) δ 7.42 – 7.39 (m, 2H), 7.36 – 7.33 (m, 2H), 3.77 (dd, *J* = 11.0, 3.2 Hz, 1H), 3.64 (dd, *J* = 11.2, 6.8 Hz, 1H), 2.58 (s, 1H), 1.81 (br s, 1H), 1.53 (s, 3H); ¹³C NMR (126 MHz, CDCl₃) δ 143.5, 133.1, 128.5, 126.6, 74.5, 70.9, 26.0; MS (ESI-TOF) calcd. for C₉H₁₁ClO₂ [M + Na⁺] 209.0340, found 209.0324; $[\alpha]_D^{25}$ = –10.4 (*c* = 0.5, CHCl₃).

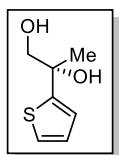


(S)-2-hydroxy-2-(thiophen-2-yl)propanal (35m):

According to the general procedure, **34m** (100 mg, 0.71 mmol), **33** (184 mg, 0.71 mmol, 1.0 equiv), **38** (53 mg, 0.14 mmol, 20 mol%), TFA (11.0 μ L, 16 mg, 0.14 mmol 20 mol%), and NaHCO₃ (60 mg, 0.71 mmol, 1.0 equiv) were allowed to react in a THF solution (3.3 mL, 0.3 M) for 4 h to

afford **35m** (80 mg, 72%) as a yellow oil after column chromatography (silica gel, 19:1 to 3:2 hexanes/Et₂O).

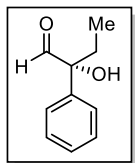
R_f = 0.71 (silica gel, 2:1 hexanes/Et₂O); **IR** (film) ν_{\max} 3435 (br), 2980, 1731, 1450, 1350, 1240, 1097, 858, 704 cm⁻¹; **¹H NMR** (500 MHz, CDCl₃) δ 9.49 (s, 1H), 7.34 (d, J = 4.9 Hz, 1H), 7.08 – 7.05 (m, 1H), 7.03 (dd, J = 2.7, 1.7 Hz, 1H), 4.06 (s, 1H), 1.76 (s, 3H); **¹³C NMR** (126 MHz, CDCl₃) δ 197.4, 143.7, 127.7, 126.4, 124.7, 78.0, 24.1; **MS** (ESI-TOF) calcd. for C₇H₈O₂S [M + H⁺ – H₂O] 139.0212, found 139.0185; **[α]_D²³** = –158.8 (c = 0.5, CHCl₃).



(S)-2-(thiophen-2-yl)propane-1,2-diol (35md):

According to the general procedure, **35m** (12.3 mg, 0.08 mmol) and NaBH₄ (30 mg, 0.79 mmol, 10 equiv) were allowed to react in a MeOH solution (1.1 mL, 0.075 M) for 90 min to afford **35md** (7.5 mg, 60%) as a yellow oil after column chromatography (silica gel, 9:1 to 2:3 hexanes/Et₂O). This material was determined to be of 77% *ee* by chiral HPLC analysis (ChiralPak AD-H, 5% *i*PrOH in hexanes, 1 mL/min, 234 nm, t_R (major) = 27.8 min, t_R (minor) = 22.2 min).

R_f = 0.16 (silica gel, 2:1 hexanes/Et₂O); **IR** (film) ν_{\max} 3371 (br), 2977, 2929, 2875, 1458, 1374, 1237, 1123, 1043, 702 cm⁻¹; **¹H NMR** (500 MHz, CDCl₃) δ 7.26 (dd, J = 5.1, 1.5 Hz, 1H), 7.01 – 6.97 (m, 2H), 3.82 (d, J = 11.2 Hz, 1H), 3.66 (d, J = 11.2 Hz, 1H), 2.81 (br s, 1H), 1.94 (br s, 1H), 1.63 (s, 3H); **¹³C NMR** (126 MHz, CDCl₃) δ 149.9, 127.0, 124.6, 123.1, 74.0, 71.5, 26.6; **MS** (ESI-TOF) calcd. for C₇H₁₀O₂S [M + Na⁺] 181.0294, found 181.0292; **[α]_D²⁵** = –1.4 (c = 0.7, CHCl₃).

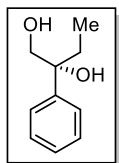


(R)-2-hydroxy-2-phenylbutanal (35n):

According to the general procedure, **34n** (148 mg, 1.00 mmol), **33** (258 mg, 1.00 mmol, 1.0 equiv), **38** (74 mg, 0.20 mmol, 20 mol%), TFA (15.4 μ L, 22.8 mg, 0.20 mmol, 20 mol%), and NaHCO₃ (84 mg, 1.00 mmol, 1.0 equiv) were allowed to react in a THF solution (3.3 mL, 0.3 M) for 4 h to afford **35n** (161 mg, 98%) as a white solid after column chromatography (silica gel, 19:1 to 3:2 hexanes/Et₂O).

R_f = 0.68 (silica gel, 2:1 hexanes/Et₂O); **IR** (film) ν_{\max} 3494 (br), 2974, 2938, 1725, 1448, 1351, 1315,

1203, 1171, 1023, 987, 740, 700 cm^{-1} ; $^1\text{H NMR}$ (500 MHz, CDCl_3) δ 9.60 (s, 1H), 7.52 – 7.49 (m, 2H), 7.44 – 7.40 (m, 2H), 7.33 (tt, $J = 7.3, 1.2$ Hz, 1H), 3.79 (s, 1H), 2.16 – 2.03 (m, 2H), 0.92 (t, $J = 7.6$ Hz, 3H); $^{13}\text{C NMR}$ (126 MHz, CDCl_3) δ 200.5, 138.3, 128.8, 127.9, 125.8, 82.1, 29.7, 7.0; **MS** (ESI-TOF) calcd. for $\text{C}_{10}\text{H}_{12}\text{O}_2$ [$\text{M} + \text{H}^+ - \text{H}_2\text{O}$] 147.0804, found 147.0759; $[\alpha]_D^{24} = -123.0$ ($c = 0.5$, CHCl_3).

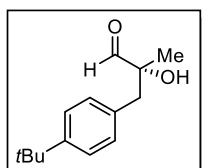


(R)-2-phenylbutane-1,2-diol (35nd):

According to the general procedure, **35n** (13.8 mg, 0.08 mmol) and NaBH_4 (32 mg, 0.84 mmol, 10 equiv) were allowed to react in a MeOH solution (1.1 mL, 0.075 M) for 90 min to afford **35nd** (5.6 mg, 40%) as a white solid after column chromatography (silica gel, 9:1 to 2:3 hexanes/ Et_2O).

This material was determined to be of 68% *ee* by chiral HPLC analysis (ChiralPak AD-H, 5% *i*PrOH in hexanes, 1 mL/min, 208 nm, t_R (major) = 18.7 min, t_R (minor) = 16.3 min).

$R_f = 0.26$ (silica gel, 2:1 hexanes/ Et_2O); **IR** (film) ν_{max} 3388 (br), 2969, 2936, 2880, 1531, 1447, 1348, 1166, 1050, 760, 701 cm^{-1} ; $^1\text{H NMR}$ (500 MHz, CDCl_3) δ 7.44 – 7.36 (m, 4H), 7.29 (dt, $J = 7.3, 1.7$ Hz, 1H), 3.87 (dd, $J = 11.2, 4.4$ Hz, 1H), 3.72 (dd, $J = 11.0, 8.1$ Hz, 1H), 2.56 (s, 1H), 1.92 – 1.80 (m, 2H), 1.61 (dd, $J = 8.1, 4.6$ Hz, 1H), 0.79 (t, $J = 7.3$ Hz, 3H); $^{13}\text{C NMR}$ (126 MHz, CDCl_3) δ 143.1, 128.4, 127.0, 125.6, 70.5, 31.1, 17.4; **MS** (ESI-TOF) calcd. for $\text{C}_{10}\text{H}_{14}\text{O}_2$ [$\text{M} + \text{Na}^+$] 189.0886, found 189.0885; $[\alpha]_D^{25} = +2.2$ ($c = 0.4$, CHCl_3).⁵⁴



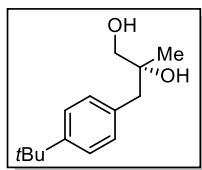
(R)-3-(4-(tert-butyl)phenyl)-2-hydroxy-2-methylpropanal (35o):

According to the general procedure, **34o** (216 μL , 204 mg, 1.00 mmol), **33** (258 mg, 1.00 mmol, 1.0 equiv), **38** (74 mg, 0.20 mmol, 20 mol%), TFA (15.4 μL , 22.8 mg, 0.20 mmol, 20 mol%), and NaHCO_3 (84 mg, 1.00 mmol, 1.0 equiv) were allowed to react in a THF solution (3.3 mL, 0.3 M) for 20 h to afford **35o** (214 mg, 97%) as a pale yellow oil after column chromatography (silica gel, 19:1 to 3:2 hexanes/ Et_2O).

$R_f = 0.63$ (silica gel, 2:1 hexanes/ Et_2O); **IR** (film) ν_{max} 3457 (br), 2965, 2868, 1734, 1364, 1269, 1126, 1109, 838, 816 cm^{-1} ; $^1\text{H NMR}$ (500 MHz, CDCl_3) δ 9.63 (s, 1H), 7.32 (d, $J = 8.3$ Hz, 2H), 7.11 (d, $J = 8.3$

⁵⁴ For comparison: Agami, C.; Couty, F.; Lequesne, C. *Tetrahedron* **1995**, *51*, 4043–4056.

Hz, 2H), 3.04 – 2.98 (m, 2H), 2.87 (d, $J = 14.2$ Hz, 1H), 1.36 (s, 3H), 1.31 (s, 9H); ^{13}C NMR (126 MHz, CDCl_3) δ 203.7, 150.0, 131.7, 129.9, 125.4, 78.1, 43.2, 34.4, 31.3, 22.4; MS (ESI-TOF) calcd. for $\text{C}_{14}\text{H}_{20}\text{O}_2$ [$\text{M} + \text{H}^+ - \text{H}_2\text{O}$] 203.1340, found 203.1421; $[\alpha]_D^{23} = -10.6$ ($c = 0.3$, CHCl_3).



(R)-3-(4-(tert-butyl)phenyl)-2-methylpropane-1,2-diol (35od):

According to the general procedure, **35o** (36 mg, 0.16 mmol) and NaBH_4 (62 mg, 1.63 mmol, 10 equiv) were allowed to react in a MeOH solution (2.2 mL, 0.075 M) for 90 min to afford **35od** (11.2 mg, 31%) as a pale yellow oil after column chromatography (silica gel, 9:1 to 2:3 hexanes/ Et_2O). This material was determined to be of 60% *ee* by chiral HPLC analysis (ChiralCel OD-H, 4% *i*PrOH in hexanes, 1 mL/min, 210 nm, t_R (major) = 17.1 min, t_R (minor) = 15.3 min).

$R_f = 0.20$ (silica gel, 2:1 hexanes/ Et_2O); IR (film) ν_{max} 3385 (br), 2963, 2869, 1514, 1462, 1364, 1269, 1124, 1049, 838 cm^{-1} ; ^1H NMR (500 MHz, CDCl_3) δ 7.34 (d, $J = 8.3$ Hz, 2H), 7.17 (d, $J = 8.3$ Hz, 2H), 3.48 (ddd, $J = 31.2, 10.7, 5.9$, 2H), 2.80 (dd, $J = 40.5, 13.2$, 2H), 1.92 (t, $J = 5.9$ Hz, 1H), 1.86 (s, 1H), 1.33 (s, 9H), 1.17 (s, 3H); ^{13}C NMR (126 MHz, CDCl_3) δ 149.5, 133.7, 130.1, 125.3, 72.9, 69.4, 44.1, 34.4, 31.4, 23.7; MS (ESI-TOF) calcd. for $\text{C}_{14}\text{H}_{22}\text{O}_2$ [$\text{M} + \text{Na}^+$] 245.1512, found 245.1521; $[\alpha]_D^{25} = +0.6$ ($c = 1.1$, CHCl_3).

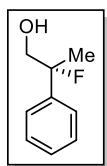
General Procedure for Primary Amine-Catalyzed α -Fluorinations (Substrate Scope):

A 2.0-dram vial was charged with aldehyde substrate **34a–p** (1.00 mmol as indicated). No precautions were taken to ensure dryness of vial or to exclude air or moisture. The aldehyde was then dissolved in THF (0.3 M in aldehyde as indicated). Solid catalyst **38** (20 mol% as indicated) was added, followed by TFA (20 mol% as indicated) by syringe. Last, dry reagents NaHCO_3 (1.0 equiv as indicated) and NFSI **12** (1.0 equiv as indicated) were added to the vial sequentially. The vial was sealed and the mixture was allowed to stir for the designated amount of time (4 or 20 h) at 23 °C. A white precipitate formed as the reactions progressed. Racemic standards were synthesized as described, with racemic catalyst (\pm)-**38**.

General Procedure for Reduction of α -Fluoroaldehydes to Fluorohydrins (Substrate Scope):

α -Fluoroaldehydes **39a–p** were directly reduced to fluorohydrins **40a–p** as follows. The crude reaction

mixture was transferred to a 200-mL round-bottom flask with MeOH (7 mL), and the vial was rinsed with 2 additional aliquots of MeOH (2 x 3 mL, 13 mL total, 0.075 M overall) to ensure complete transfer. Solid NaBH₄ (10 equiv as indicated) was added in 3 portions over the course of 10 min, then the reaction mixture was stirred, open to air, at 23 °C. After 90 min, the reaction was quenched with sat. aq. NH₄Cl (30 mL) and EtOAc (30 mL). After an additional 30 min of stirring open to air at 23 °C, the layers were separated and the aqueous phase was extracted with EtOAc (4 x 25 mL). The pooled organic layers were dried over Na₂SO₄, filtered, and concentrated by rotary evaporation. The crude product was purified by silica gel flash chromatography. Several fluorohydrins could be recrystallized to increased *ee*. Recrystallization procedures are described below where appropriate.

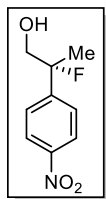


(R)-2-fluoro-2-phenylpropan-1-ol (40a):

According to the general procedures, **34a** (134 μ L, 134 mg, 1.00 mmol), **12** (316 mg, 1.00 mmol, 1.0 equiv), **38** (74 mg, 0.20 mmol, 20 mol%), TFA (15.4 μ L, 22.8 mg, 0.20 mmol, 20 mol%), and NaHCO₃ (84 mg, 1.00 mmol, 1.0 equiv) were allowed to react in a THF solution (3.3 mL, 0.3 M) for 4 h to afford crude **39a**. The mixture was then reacted with NaBH₄ (380 mg, 10.0 mmol, 10 equiv) in MeOH (13 mL, 0.075 M) for 90 min to afford **40a** (153 mg, 99%) as a colorless oil after column chromatography (silica gel, 19:1 to 3:2 hexanes/Et₂O). This material was determined to be of 80% *ee* by chiral HPLC analysis (ChiralPak AS-H, 5% *i*PrOH in hexanes, 1 mL/min, 210 nm, t_R (major) = 13.2 min, t_R (minor) = 12.3 min).

R_f = 0.46 (silica gel, 2:1 hexanes/Et₂O); **IR** (film) ν_{\max} 3359 (br), 2986, 2931, 1496, 1447, 1381, 1053, 1029, 856, 762, 669, 546 cm⁻¹; **¹H NMR** (500 MHz, CDCl₃) δ 7.44 – 7.37 (m, 4H), 7.36 – 7.32 (m, 1H), 3.89 – 3.71 (m, 2H), 2.23 – 2.13 (m, 1H), 1.72 (d, J = 22.5, 3H); **¹³C NMR** (126 MHz, CDCl₃) δ 141.5 (d, J = 21.0 Hz), 127.1, (d, J = 75.3), 124.4, (d, J = 9.5 Hz), 97.8, (d, J = 172.6 Hz), 69.4 (d, J = 24.8 Hz), 23.1 (d, J = 24.8 Hz); **¹⁹F NMR** (282 MHz, CDCl₃) δ -157.0; **MS** (ESI-TOF) calcd. for C₉H₁₁FO [M + Na⁺]

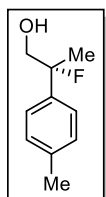
177.0686, found 177.0662; $[\alpha]_D^{23} = -9.4$ ($c = 1.1$, CHCl_3).⁵⁵



(R)-2-fluoro-2-(4-nitrophenyl)propan-1-ol (40b):

According to the general procedures, **34b** (179 mg, 1.00 mmol), **12** (315 mg, 1.00 mmol, 1.0 equiv), **38** (74 mg, 0.20 mmol, 20 mol%), TFA (15.4 μL , 22.8 mg, 0.20 mmol, 20 mol%), and NaHCO_3 (84 mg, 1.00 mmol, 1.0 equiv) were allowed to react in a THF solution (3.3 mL, 0.3 M) for 4 h to afford crude **39b**. The mixture was then reacted with NaBH_4 (378 mg, 10.0 mmol, 10 equiv) in MeOH (13 mL, 0.075 M) for 90 min to afford **40b** (179 mg, 90%) as a pale green oil after column chromatography (silica gel, 19:1 to 3:2 hexanes/ Et_2O). This material was determined to be of 74% *ee* by chiral HPLC analysis (ChiralCel OD-H, 5% *i*PrOH in hexanes, 1 mL/min, 210 nm, 1 mL/min, 210 nm, $t_R(\text{major}) = 26.5$ min, $t_R(\text{minor}) = 31.1$ min).

$R_f = 0.14$ (silica gel, 4:1 hexanes/ Et_2O); **IR** (film) ν_{max} 3372 (br), 1606, 1519, 1348, 1053, 854, 700 cm^{-1} ; **¹H NMR** (500 MHz, CDCl_3) δ 8.26 (d, $J = 10.3$ Hz, 2H), 7.56 (d, $J = 8.8$ Hz, 2H), 3.91 – 3.84 (m, 2H), 1.90 (t, $J = 6.6$ Hz, 1H), 1.73 (d, $J = 22.9$ Hz, 3H); **¹³C NMR** (126 MHz, CDCl_3) δ 148.7 (d, $J = 23.0$ Hz), 125.6 (d, $J = 10.5$ Hz), 123.5 (d, $J = 1.9$ Hz), 97.5 (d, $J = 174.5$ Hz), 69.1 (d, $J = 24.9$ Hz), 23.3 (d, $J = 24.0$ Hz); **¹⁹F NMR** (376 MHz, CDCl_3) δ -157.7; **MS** (ESI-TOF) calcd. for $\text{C}_9\text{H}_{10}\text{FNO}_3$ [$\text{M} + \text{Na}^+$] 222.1706, found 222.0562; $[\alpha]_D^{23} = -9.9$ ($c = 1.0$, CHCl_3).



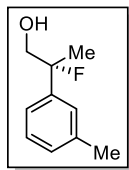
(R)-2-fluoro-2-(p-tolyl)propan-1-ol (40d):

According to the general procedures, **34d** (148 mg, 1.00 mmol), **12** (315 mg, 1.00 mmol, 1.0 equiv), **38** (74 mg, 0.20 mmol, 20 mol%), TFA (15.4 μL , 22.8 mg, 0.20 mmol, 20 mol%), and NaHCO_3 (84 mg, 1.00 mmol, 1.0 equiv) were allowed to react in a THF solution (3.3 mL, 0.3 M) for 4 h to afford crude **39d**. The mixture was then reacted with NaBH_4 (378 mg, 10.0 mmol, 10 equiv) in MeOH (13 mL, 0.075 M) for 90 min to afford **40d** (142 mg, 85%) as a colorless oil after column chromatography (silica gel, 19:1 to 3:2 hexanes/ Et_2O). This material was determined to be of 79% *ee* by chiral HPLC

⁵⁵ For comparison: Brandes, S.; Niess, B.; Bella, M.; Prieto, A.; Overgaard, J.; Jørgensen, K. A. *Chem.–Eur. J.* **2006**, *12*, 6039–6052.

analysis (ChiralPak AD-H, 5% *i*PrOH in hexanes, 1 mL/min, 212 nm, $t_R(\text{major}) = 16.2$ min, $t_R(\text{minor}) = 14.0$ min).

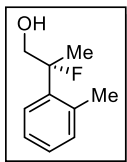
$R_f = 0.46$ (silica gel, 2:1 hexanes/Et₂O); **IR** (film) ν_{max} 3390 (br), 2987, 2925, 1516, 1450, 1379, 1189, 1050, 859, 816, 546 cm⁻¹; **¹H NMR** (500 MHz, CDCl₃) δ 7.27 (d, $J = 8.3$ Hz, 2H), 7.21 (d, $J = 8.3$ Hz, 2H), 3.90 – 3.70 (m, 2H), 2.37 (s, 1H), 1.80 (t, $J = 6.6$ Hz, 1H), 1.70 (d, $J = 22.5$ Hz, 3H); **¹³C NMR** (126 MHz, CDCl₃) δ 138.5 (d, $J = 22.1$ Hz), 137.6, 129.1, 124.4 (d, $J = 8.6$ Hz), 97.8 (d, $J = 171.7$ Hz), 69.6 (d, $J = 24.9$ Hz), 23.2 (d, $J = 24.9$ Hz), 21.0; **¹⁹F NMR** (376 MHz, CDCl₃) δ -156.7; **MS** (ESI-TOF) calcd. for C₁₀H₁₃FO₂ [M + Na⁺] 191.0843, found 191.0844; $[\alpha]_D^{23} = -11.7$ ($c = 0.8$, CHCl₃).



(R)-2-fluoro-2-(*m*-tolyl)propan-1-ol (40e):

According to the general procedures, **34e** (148 mg, 1.00 mmol), **12** (315 mg, 1.00 mmol, 1.0 equiv), **38** (74 mg, 0.20 mmol, 20 mol%), TFA (15.4 μ L, 22.8 mg, 0.20 mmol, 20 mol%), and NaHCO₃ (84 mg, 1.00 mmol, 1.0 equiv) were allowed to react in a THF solution (3.3 mL, 0.3 M) for 4 h to afford crude **39e**. The mixture was then reacted with NaBH₄ (378 mg, 10.0 mmol, 10 equiv) in MeOH (13 mL, 0.075 M) for 90 min to afford **40e** (147 mg, 88%) as a colorless oil after column chromatography (silica gel, 19:1 to 3:2 hexanes/Et₂O). This material was determined to be of 78% *ee* by chiral HPLC analysis (ChiralPak AS-H, 5% *i*PrOH in hexanes, 1 mL/min, 210 nm, $t_R(\text{major}) = 9.9$ min, $t_R(\text{minor}) = 9.0$ min).

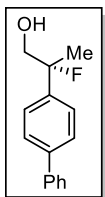
$R_f = 0.68$ (silica gel, 2:1 hexanes/Et₂O); **IR** (film) ν_{max} 3382 (br), 2989, 2923, 1449, 1378, 1189, 1051, 889, 787, 704 cm⁻¹; **¹H NMR** (500 MHz, CDCl₃) δ 7.29 (t, $J = 7.8$ Hz, 1H), 7.20 – 7.13 (m, 3H), 3.90 – 3.71 (m, 2H), 2.39 (s, 1H), 1.81 (t, $J = 6.6$ Hz, 1H), 1.70 (d, $J = 22.5$ Hz, 3H); **¹³C NMR** (126 MHz, CDCl₃) δ 141.4 (d, $J = 21.1$ Hz), 138.1, 133.8, 128.5 (d, $J = 29.7$ Hz), 125.1 (d, $J = 8.6$ Hz), 121.5 (d, $J = 9.6$ Hz), 97.9 (d, $J = 171.7$ Hz), 69.6 (d, $J = 24.9$ Hz), 23.2 (d, $J = 24.9$ Hz), 21.6; **¹⁹F NMR** (376 MHz, CDCl₃) δ -157.1; **MS** (ESI-TOF) calcd. for C₁₀H₁₃FO₂ [M + Na⁺] 191.0843, found 191.0842; $[\alpha]_D^{24} = -7.7$ ($c = 1.1$, CHCl₃).



(R)-2-fluoro-2-(*o*-tolyl)propan-1-ol (40f):

According to the general procedures, **34f** (148 mg, 1.00 mmol), **12** (315 mg, 1.00 mmol, 1.0 equiv), **38** (74 mg, 0.20 mmol, 20 mol%), TFA (15.4 μ L, 22.8 mg, 0.20 mmol, 20 mol%), and NaHCO₃ (84 mg, 1.00 mmol, 1.0 equiv) were allowed to react in a THF solution (3.3 mL, 0.3 M) for 20 h to afford crude **39f**. The mixture was then reacted with NaBH₄ (378 mg, 10.0 mmol, 10 equiv) in MeOH (13 mL, 0.075 M) for 90 min to afford **40f** (138 mg, 82%) as a colorless oil after column chromatography (silica gel, 19:1 to 3:2 hexanes/Et₂O). This material was determined to be of 73% *ee* by chiral HPLC analysis (ChiralPak AS-H, 5% *i*PrOH in hexanes, 1 mL/min, 210 nm, $t_{R(\text{major})}$ = 9.7 min, $t_{R(\text{minor})}$ = 8.8 min). Purified fluorohydrin **40f** (104 mg) was dissolved in 3:1 hexanes/Et₂O (0.3 mL) and gently heated in a 40 °C water bath for 2 min to ensure complete dissolution. The solution was cooled to 23 °C on the benchtop for 1 h, during which time white needles crystallized. The crystals were isolated by filtration and washed with cold hexanes to afford **40f** (33 mg, 32% recovery), which was determined to be of 99% *ee* by chiral HPLC analysis as above.

R_f = 0.55 (silica gel, 2:1 hexanes/Et₂O); IR (film) ν_{max} 3338 (br), 2981, 2938, 1457, 1382, 1061, 1042, 857, 759, 726 cm⁻¹; ¹H NMR (500 MHz, CDCl₃) δ 7.33 – 7.31 (m, 1H), 7.23 – 7.18 (m, 3H), 4.08 – 4.00 (m, 1H), 3.90 – 3.81 (m, 1H), 2.49 (d, J = 3.4 Hz, 3H), 1.88 (t, J = 6.3 Hz, 1H), 1.76 (d, J = 22.9 Hz, 3H); ¹³C NMR (126 MHz, CDCl₃) δ 138.8 (d, J = 20.1 Hz), 135.2, 132.6, 128.0, 125.9 (d, J = 1.9 Hz), 125.7 (d, J = 11.5 Hz), 99.3 (d, J = 171.7 Hz), 68.3 (d, J = 24.9 Hz), 23.0 (d, J = 25.9 Hz), 21.7 (d, J = 7.7 Hz); ¹⁹F NMR (282 MHz, CDCl₃) δ -150.7; MS (ESI-TOF) calcd. for C₁₀H₁₃FO₂ [M + Na⁺] 191.0843, found 191.0852; $[\alpha]_D^{23}$ = -1.1 (c = 0.9, CHCl₃).

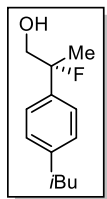


(R)-2-([1,1'-biphenyl]-4-yl)-2-fluoropropan-1-ol (40g):

According to the general procedures, **34g** (210 mg, 1.00 mmol), **12** (315 mg, 1.00 mmol, 1.0 equiv), **38** (74 mg, 0.20 mmol, 20 mol%), TFA (15.4 μ L, 22.8 mg, 0.20 mmol, 20 mol%), and NaHCO₃ (84 mg, 1.00 mmol, 1.0 equiv) were allowed to react in a THF solution (3.3 mL, 0.3 M) for 4 h to afford crude **39g**. The mixture was then reacted with NaBH₄ (378 mg, 10.0 mmol, 10 equiv) in MeOH (13

mL, 0.075 M) for 90 min to afford **40g** (204 mg, 89%) as a colorless oil after column chromatography (silica gel, 19:1 to 3:2 hexanes/Et₂O). This material was determined to be of 81% *ee* by chiral HPLC analysis (ChiralPak AD-H, 5% *i*PrOH in hexanes, 1 mL/min, 210 nm, *t*_R(major) = 18.4 min, *t*_R(minor) = 21.7 min). Purified fluorohydrin **40g** (204 mg) was dissolved in 3:1 hexanes/Et₂O (7.0 mL) and gently heated in a 50 °C water bath for 5 min to ensure complete dissolution. The solution was cooled to –10 °C in a freezer for 1 h, during which time white crystals formed. The crystals were isolated by filtration and washed with cold hexanes to afford **40g** (105 mg, 52% recovery), which was determined to be of 93% *ee* by chiral HPLC analysis as above.

R_f = 0.46 (silica gel, 2:1 hexanes/Et₂O); **IR** (film) ν_{max} 3370 (br), 1488, 1449, 1404, 1051, 763, 727, 692 cm⁻¹; **¹H NMR** (500 MHz, CDCl₃) δ 7.65 – 7.58 (m, 4H), 7.48 – 7.44 (m, 4H), 7.39 – 7.33 (m, 1H), 3.96 – 3.76 (m, 2H), 1.88 (t, *J* = 6.6 Hz, 1H), 1.75 (d, *J* = 22.5 Hz, 3H); **¹³C NMR** (126 MHz, CDCl₃) δ 140.8, 140.53, 140.49 (d, *J* = 21.0 Hz), 128.8, 127.5, 127.2, 127.1, 124.9 (d, *J* = 8.6 Hz), 97.8 (d, *J* = 172.6), 69.6 (d, *J* = 24.9 Hz), 23.2 (d, *J* = 24.9 Hz); **¹⁹F NMR** (282 MHz, CDCl₃) δ –156.9; **MS** (ESI-TOF) calcd. for C₁₅H₁₅FO [M + Na⁺] 253.0999, found 253.1021; [α]_D²³ = –17.1 (*c* = 0.8, CHCl₃).

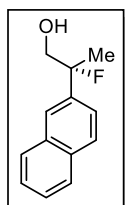


(R)-2-fluoro-2-(4-isobutylphenyl)propan-1-ol (40h):

According to the general procedures, **34h** (190 mg, 1.00 mmol), **12** (315 mg, 1.00 mmol, 1.0 equiv), **38** (74 mg, 0.20 mmol, 20 mol%), TFA (15.4 μ L, 22.8 mg, 0.20 mmol, 20 mol%), and NaHCO₃ (84 mg, 1.00 mmol, 1.0 equiv) were allowed to react in a THF solution (3.3 mL, 0.3 M) for 4 h to afford crude **39h**. The mixture was then reacted with NaBH₄ (378 mg, 10.0 mmol, 10 equiv) in MeOH (13 mL, 0.075 M) for 90 min to afford **40h** (176 mg, 84%) as a colorless oil after column chromatography (silica gel, 19:1 to 3:2 hexanes/Et₂O). This material was determined to be of 76% *ee* by chiral HPLC analysis (ChiralPak AS-H, 3% *i*PrOH in hexanes, 1 mL/min, 210 nm, *t*_R(major) = 12.3 min, *t*_R(minor) = 10.0 min). Purified fluorohydrin **40h** (151 mg) was dissolved in 3:1 hexanes/Et₂O (0.3 mL). The solution was cooled to –10 °C in a freezer for 2 h, during which time white crystals formed. The crystals were isolated by filtration and washed with cold hexanes to afford **40h** (115 mg, 75% recovery), which was

determined to be of 97% *ee* by chiral HPLC analysis as above.

R_f = 0.66 (silica gel, 2:1 hexanes/Et₂O); **IR** (film) ν_{\max} 3370 (br), 2954, 2925, 2969, 1466, 1367, 1189, 1051, 846, 796, 588, 561 cm⁻¹; **¹H NMR** (500 MHz, CDCl₃) δ 7.31 – 7.26 (m, 2H), 7.19 – 7.12 (m, 2H), 3.90 – 3.69 (m, 2H), 2.50 – 2.47 (m, 2H), 1.92 – 1.83 (m, 2H), 1.71 (d, J = 22.5 Hz, 3H), 0.92 (d, J = 6.4 Hz, 6H); **¹³C NMR** (126 MHz, CDCl₃) δ 141.4, 138.7 (d, J = 22.1 Hz), 129.1, 124.2 (d, J = 9.6 Hz), 97.9 (d, J = 170.7 Hz), 69.6 (d, J = 24.9 Hz), 45.0, 30.2, 23.1 (d, J = 24.9 Hz), 22.4; **¹⁹F NMR** (376 MHz, CDCl₃) δ -156.3; **MS** (ESI-TOF) calcd. for C₁₃H₁₉FO [M + Na⁺] 233.1312, found 233.1337; $[\alpha]_D^{24}$ = -7.0 (c = 1.4, CHCl₃).⁵⁶



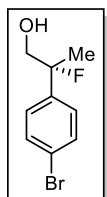
(R)-2-fluoro-2-(naphthalen-2-yl)propan-1-ol (40i):

According to the general procedures, **34i** (184 mg, 1.00 mmol), **12** (315 mg, 1.00 mmol, 1.0 equiv), **38** (74 mg, 0.20 mmol, 20 mol%), TFA (15.4 μ L, 22.8 mg, 0.20 mmol, 20 mol%), and NaHCO₃ (84 mg, 1.00 mmol, 1.0 equiv) were allowed to react in a THF solution (3.3 mL, 0.3 M) for 4 h to afford crude **39i**. The mixture was then reacted with NaBH₄ (378 mg, 10.0 mmol, 10 equiv) in MeOH (13 mL, 0.075 M) for 90 min to afford **40i** (179 mg, 88%) as a white solid after column chromatography (silica gel, 19:1 to 3:2 hexanes/Et₂O). This material was determined to be of 82% *ee* by chiral HPLC analysis (ChiralCel OD-H, 5% *i*PrOH in hexanes, 1 mL/min, 210 nm, t_R (major) = 17.4 min, t_R (minor) = 15.2 min). Purified fluorohydrin **40i** (142 mg) was dissolved in 3:1 hexanes/Et₂O (2.0 mL) and gently heated in a 50 °C water bath for 3 min to ensure complete dissolution. The solution was cooled to -10 °C in a freezer for 1 h, during which time white needles crystallized. The crystals were isolated by filtration and washed with cold hexanes to afford **40i** (74 mg, 52% recovery), which was determined to be of 91% *ee* by chiral HPLC analysis as above.

R_f = 0.46 (silica gel, 2:1 hexanes/Et₂O); **IR** (film) ν_{\max} 3368 (br), 1382, 1195, 1113, 1050, 858, 819, 748, 478 cm⁻¹; **¹H NMR** (500 MHz, CDCl₃) δ 7.90 – 7.84 (m, 4H), 7.54 – 7.50 (m, 2H), 7.46 (dd, J = 8.8, 2.0 Hz, 1H), 4.01 – 3.80 (m, 2H), 1.88 (t, J = 6.6 Hz, 1H), 1.81 (d, J = 22.9 Hz, 3H); **¹³C NMR** (126 MHz,

⁵⁶ For comparison: Goj, O.; Burchardt, A.; Haufe, G. *Tetrahedron: Asymmetry* **1997**, *8*, 399–408.

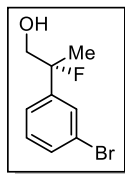
CDCl₃) δ 138.8 (d, J = 21.1 Hz), 132.9 (d, J = 28.8 Hz), 128.2 (d, J = 15.3 Hz), 127.6, 126.4, 126.3, 123.6 (d, J = 10.5 Hz), 122.4 (d, J = 8.6 Hz), 98.0 (d, J = 172.6 Hz), 69.5 (d, J = 24.9 Hz), 23.3 (d, J = 24.9 Hz); ¹⁹F NMR (282 MHz, CDCl₃) δ -156.7; MS (ESI-TOF) calcd. for C₁₃H₁₃FO [M + Na⁺] 227.0843, found 227.0872; $[\alpha]_D^{24}$ = -13.4 (c = 1.0, CHCl₃).



(R)-2-(4-bromophenyl)-2-fluoropropan-1-ol (40j):

According to the general procedures, **34j** (213 mg, 1.00 mmol), **12** (315 mg, 1.00 mmol, 1.0 equiv), **38** (74 mg, 0.20 mmol, 20 mol%), TFA (15.4 μ L, 22.8 mg, 0.20 mmol, 20 mol%), and NaHCO₃ (84 mg, 1.00 mmol, 1.0 equiv) were allowed to react in a THF solution (3.3 mL, 0.3 M) for 4 h to afford crude **39j**. The mixture was then reacted with NaBH₄ (378 mg, 10.0 mmol, 10 equiv) in MeOH (13 mL, 0.075 M) for 90 min to afford **40j** (186 mg, 79%) as a white solid after column chromatography (silica gel, 19:1 to 3:2 hexanes/Et₂O). This material was determined to be of 82% *ee* by chiral HPLC analysis (ChiralPak AD-H, 5% *i*PrOH in hexanes, 1 mL/min, 220 nm, t_R (major) = 14.1 min, t_R (minor) = 19.7 min). Purified fluorohydrin **40j** (158 mg) was dissolved in 3:1 hexanes/Et₂O (3.5 mL) and gently heated in a 50 °C water bath for 3 min to ensure complete dissolution. The solution was cooled to -10 °C in a freezer for 1 h, during which time white needles crystallized. The crystals were isolated by filtration and washed with cold hexanes to afford **40j** (64 mg, 40% recovery), which was determined to be of 99% *ee* by chiral HPLC analysis as above.

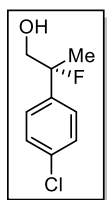
R_f = 0.49 (silica gel, 2:1 hexanes/Et₂O); IR (film) ν_{max} 3390 (br), 2998, 2926, 1399, 1052, 851, 820, 745, 539 cm⁻¹; ¹H NMR (500 MHz, CDCl₃) δ 7.54 (d, J = 7.8 Hz, 2H), 7.26 (d, J = 14.2 Hz, 2H), 3.89 – 3.72 (m, 2H), 1.86 (t, J = 5.9 Hz, 1H), 1.70 (d, J = 22.5 Hz, 3H); ¹³C NMR (126 MHz, CDCl₃) δ 140.6 (d, J = 22.1 Hz), 131.6, 126.3 (d, J = 8.6 Hz), 122.0, 97.5 (d, J = 173.6 Hz), 69.3 (d, J = 24.9 Hz), 23.1 (d, J = 24.9 Hz); ¹⁹F NMR (376 MHz, CDCl₃) δ -157.2; MS (ESI-TOF) calcd. for C₉H₁₀BrFO [M + Na⁺] 254.9791 and 256.9771, found 254.9849 and 256.9831; $[\alpha]_D^{24}$ = -13.8 (c = 0.7, CHCl₃).



(R)-2-(3-bromophenyl)-2-fluoropropan-1-ol (40k):

According to the general procedures, **34k** (213 mg, 1.00 mmol), **12** (315 mg, 1.00 mmol, 1.0 equiv), **38** (74 mg, 0.20 mmol, 20 mol%), TFA (15.4 μ L, 22.8 mg, 0.20 mmol, 20 mol%), and NaHCO₃ (84 mg, 1.00 mmol, 1.0 equiv) were allowed to react in a THF solution (3.3 mL, 0.3 M) for 4 h to afford crude **39k**. The mixture was then reacted with NaBH₄ (378 mg, 10.0 mmol, 10 equiv) in MeOH (13 mL, 0.075 M) for 90 min to afford **40k** (205 mg, 88%) as a colorless oil after column chromatography (silica gel, 19:1 to 3:2 hexanes/Et₂O). This material was determined to be of 80% *ee* by chiral HPLC analysis (ChiralPak AS-H, 5% *i*PrOH in hexanes, 1 mL/min, 210 nm, $t_R(\text{major}) = 12.7$ min, $t_R(\text{minor}) = 11.1$ min).

$R_f = 0.51$ (silica gel, 2:1 hexanes/Et₂O); **IR** (film) ν_{max} 3353 (br), 2986, 2937, 1568, 1477, 1418, 1247, 1053, 865, 786, 759, 695 cm⁻¹; **¹H NMR** (500 MHz, CDCl₃) δ 7.56 – 7.55 (m, 1H), 7.49 (dt, $J = 7.0, 1.9$ Hz, 1H), 7.32 – 7.28 (m, 2H), 3.90 – 3.74 (m, 2H), 1.88 (t, $J = 6.6$ Hz, 1H), 1.71 (d, $J = 23.2$ Hz, 3H); **¹³C NMR** (126 MHz, CDCl₃) δ 143.9 (d, $J = 22.1$ Hz), 131.0, 130.0, 127.8 (d, $J = 9.6$ Hz), 123.1 (d, $J = 8.6$ Hz), 122.7 (d, $J = 1.9$ Hz), 97.3 (d, $J = 174.5$ Hz), 69.3 (d, $J = 24.9$ Hz), 23.2 (d, $J = 24.9$ Hz); **¹⁹F NMR** (376 MHz, CDCl₃) δ -157.2; **MS** (ESI-TOF) calcd. for C₉H₁₀BrFO [M + Na⁺] 254.9791 and 256.9771, found 254.9854 and 256.9834; $[\alpha]_D^{24} = -9.7$ ($c = 1.2$, CHCl₃).

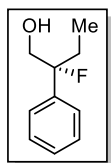


(R)-2-(4-chlorophenyl)-2-fluoropropan-1-ol (40l):

According to the general procedures, **34l** (169 mg, 1.00 mmol), **12** (315 mg, 1.00 mmol, 1.0 equiv), **38** (74 mg, 0.20 mmol, 20 mol%), TFA (15.4 μ L, 22.8 mg, 0.20 mmol, 20 mol%), and NaHCO₃ (84 mg, 1.00 mmol, 1.0 equiv) were allowed to react in a THF solution (3.3 mL, 0.3 M) for 4 h to afford crude **39l**. The mixture was then reacted with NaBH₄ (378 mg, 10.0 mmol, 10 equiv) in MeOH (13 mL, 0.075 M) for 90 min to afford **40l** (139 mg, 74%) as a white solid after column chromatography (silica gel, 19:1 to 3:2 hexanes/Et₂O). This material was determined to be of 86% *ee* by chiral HPLC analysis (ChiralPak AD-H, 5% *i*PrOH in hexanes, 1 mL/min, 220 nm, $t_R(\text{major}) = 13.4$ min, $t_R(\text{minor}) = 17.5$ min). Purified fluorohydrin **40l** (122 mg) was dissolved in 3:1 hexanes/Et₂O (2.5 mL) and gently heated in a 50

°C water bath for 3 min to ensure complete dissolution. The solution was cooled to -10 °C in a freezer for 1 h, during which time white needles crystallized. The crystals were isolated by filtration and washed with cold hexanes to afford **40l** (40 mg, 33% recovery), which was determined to be of 99% *ee* by chiral HPLC analysis as above.

R_f = 0.67 (silica gel, 2:1 hexanes/Et₂O); **IR** (film) ν_{\max} 3410 (br), 2924, 1404, 1079, 1056, 1013, 853, 824, 543 cm⁻¹; **¹H NMR** (500 MHz, CDCl₃) δ 7.37 (d, J = 8.8 Hz, 2H), 7.32 (d, J = 8.8 Hz, 2H), 3.88 – 3.71 (m, 2H), 1.82 (ddd, J = 7.7, 6.0, 1.5 Hz, 1H), 1.69 (d, J = 22.9 Hz, 3H); **¹³C NMR** (126 MHz, CDCl₃) δ 140.1 (d, J = 22.1 Hz), 133.8, 128.6, 126.0 (d, J = 8.6 Hz), 97.5 (d, J = 172.6 Hz), 69.4 (d, J = 24.9 Hz), 23.2 (d, J = 24.9 Hz); **¹⁹F NMR** (282 MHz, CDCl₃) δ -158.9; **MS** (ESI-TOF) calcd. for C₉H₁₀ClFO [M + Na⁺] 211.0296, found 211.0281; $[\alpha]_D^{25}$ = -14.1 (c = 1.1, CHCl₃).

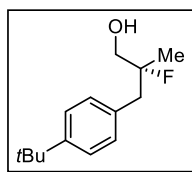


(R)-2-fluoro-2-phenylbutan-1-ol (40n):

According to the general procedures, **34n** (166 mg, 1.00 mmol), **12** (315 mg, 1.00 mmol, 1.0 equiv), **38** (74 mg, 0.20 mmol, 20 mol%), TFA (15.4 μ L, 22.8 mg, 0.20 mmol, 20 mol%), and NaHCO₃ (84 mg, 1.00 mmol, 1.0 equiv) were allowed to react in a THF solution (3.3 mL, 0.3 M) for 4 h to afford crude **39n**. The mixture was then reacted with NaBH₄ (378 mg, 10.0 mmol, 10 equiv) in MeOH (13 mL, 0.075 M) for 90 min to afford **40n** (149 mg, 88%) as a colorless oil after column chromatography (silica gel, 19:1 to 3:2 hexanes/Et₂O). This material was determined to be of 48% *ee* by chiral HPLC analysis (ChiralPak AD-H, 2% *i*PrOH in hexanes, 1 mL/min, 210 nm, t_R (major) = 49.4 min, t_R (minor) = 45.4 min).

R_f = 0.53 (silica gel, 2:1 hexanes/Et₂O); **IR** (film) ν_{\max} 3359 (br), 2974, 2937, 1448, 1058, 913, 876, 759, 700 cm⁻¹; **¹H NMR** (500 MHz, CDCl₃) δ 7.42 – 7.38 (m, 2H), 7.35 – 7.32 (m, 3H), 3.93 – 3.74 (m, 2H), 2.23 – 2.12 (m, 1H), 1.99 – 1.84 (m, 2H), 1.72 (t, J = 6.6 Hz, 1H), 0.83 (t, J = 7.3 Hz, 3H); **¹³C NMR** (126 MHz, CDCl₃) δ 139.8 (d, J = 22.1 Hz), 128.40 (d, J = 1.9 Hz), 128.38 (d, J = 67.2 Hz), 127.6, 124.8 (d, J = 9.6 Hz), 100.3 (d, J = 175.5 Hz), 68.8 (d, J = 24.0 Hz), 28.9 (d, J = 23.0 Hz), 7.2 (d, J = 5.8 Hz); **¹⁹F**

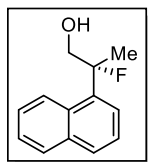
NMR (282 MHz, CDCl₃) δ -170.5; **MS** (ESI-TOF) calcd. for C₁₀H₁₃FO [M + Na⁺] 191.0843, found 191.0860; $[\alpha]_D^{24} = -2.0$ ($c = 0.7$, CHCl₃).⁵⁷



(R)-3-(4-(tert-butyl)phenyl)-2-fluoro-2-methylpropan-1-ol (40o):

According to the general procedures, **34o** (216 μ L, 204 mg, 1.00 mmol), **12** (315 mg, 1.00 mmol, 1.0 equiv), **38** (74 mg, 0.20 mmol, 20 mol%), TFA (15.4 μ L, 22.8 mg, 0.20 mmol, 20 mol%), and NaHCO₃ (84 mg, 1.00 mmol, 1.0 equiv) were allowed to react in a THF solution (3.3 mL, 0.3 M) for 20 h to afford crude **39o**. The mixture was then reacted with NaBH₄ (378 mg, 10.0 mmol, 10 equiv) in MeOH (13 mL, 0.075 M) for 90 min to afford **40o** (214 mg, 95%) as a colorless oil after column chromatography (silica gel, 19:1 to 3:2 hexanes/Et₂O). This material was determined to be of 69% *ee* by chiral HPLC analysis (ChiralPak AS-H, 3% *i*PrOH in hexanes, 1 mL/min, 218 nm, t_R (major) = 10.3 min, t_R (minor) = 11.1 min).

R_f = 0.75 (silica gel, 2:1 hexanes/Et₂O); **IR** (film) ν_{\max} 3342 (br), 2960, 2869, 1510, 1460, 1363, 1269, 1034, 841, 572 cm⁻¹; **¹H NMR** (500 MHz, CDCl₃) δ 7.31 (d, $J = 7.8$ Hz, 2H), 7.12 (d, $J = 8.3$ Hz, 2H), 3.56 (dd, $J = 10.5, 6.1$ Hz, 1H), 3.50 (dd, $J = 9.8, 5.9$ Hz, 1H), 2.72 (dd, $J = 13.7, 6.4$ Hz, 1H), 2.42 (dd, $J = 13.5, 8.1$ Hz, 1H), 2.00 – 1.92 (m, 1H), 1.33 (s, 9H), 0.94 (d, $J = 6.8$ Hz, 3H); **¹³C NMR** (126 MHz, CDCl₃) δ 148.7, 137.5, 128.8, 125.1, 67.8, 39.2, 37.8, 34.3, 31.4, 16.6; **¹⁹F NMR** (376 MHz, CDCl₃) δ -154.3; **MS** (ESI-TOF) calcd. for C₁₄H₂₁FO [M + Na⁺] 247.1469, found 247.1474; $[\alpha]_D^{24} = -1.7$ ($c = 0.7$, CHCl₃).



(R)-2-fluoro-2-(naphthalen-1-yl)propan-1-ol (40p):

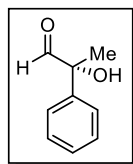
According to the general procedures, **34p** (184 mg, 1.00 mmol), **12** (315 mg, 1.00 mmol, 1.0 equiv), **38** (74 mg, 0.20 mmol, 20 mol%), TFA (15.4 μ L, 22.8 mg, 0.20 mmol, 20 mol%), and NaHCO₃ (84 mg, 1.00 mmol, 1.0 equiv) were allowed to react in a THF solution (3.3 mL, 0.3 M) for 20 h to afford crude **39p**. The mixture was then reacted with NaBH₄ (378 mg, 10.0 mmol, 10 equiv) in MeOH (13 mL, 0.075 M) for 90 min to afford **40p** (191 mg, 94%) as a colorless oil after column chromatography (silica gel, 19:1 to 3:2 hexanes/Et₂O). This material was determined to be of 69% *ee* by

⁵⁷ For comparison: Lee, S. Y.; Neufeind, S.; Fu, G. C. *J. Am. Chem. Soc.* **2014**, *136*, 8899–8902.

chiral HPLC analysis (ChiralPak AS-H, 5% *i*PrOH in hexanes, 1 mL/min, 210 nm, $t_{\text{R}}(\text{major}) = 16.1$ min, $t_{\text{R}}(\text{minor}) = 19.0$ min). Purified fluorohydrin **40p** (158 mg) was dissolved in 3:1 hexanes/Et₂O (1.5 mL) and gently heated in a 40 °C water bath for 3 min to ensure complete dissolution. The solution was cooled to –10 °C in a freezer for 24 h, during which time white crystals formed. The crystals were isolated by filtration and washed with cold hexanes to afford **40p** (61 mg, 39% recovery), which was determined to be of 90% *ee* by chiral HPLC analysis as above.

$R_f = 0.50$ (silica gel, 2:1 hexanes/Et₂O); **IR** (film) ν_{max} 3354 (br), 1511, 1242, 1111, 865, 804, 776 cm⁻¹; **¹H NMR** (500 MHz, CDCl₃) δ 8.33 (d, $J = 8.3$ Hz, 1H), 7.90 (d, $J = 7.8$ Hz, 1H), 7.85 (d, $J = 7.8$ Hz, 1H), 7.60 (dd, $J = 7.3, 1.0$ Hz), 7.55 – 7.45 (m, 3H), 4.30 (ddd, $J = 18.4, 13.1, 4.6$, 1H), 4.15 – 4.06 (m, 1H), 2.02 (d, $J = 1.0$ Hz, 1H), 1.97 (d, $J = 1.79$ Hz, 3H); **¹³C NMR** (126 MHz, CDCl₃) δ 136.4 (d, $J = 20.2$ Hz), 134.6, 129.5, 129.3, 126.1, 125.5, 125.4, 124.9, 123.9 (d, $J = 12.5$ Hz), 99.5 (d, $J = 171.7$ Hz), 68.7 (d, $J = 24.9$ Hz), 23.7 (d, $J = 25.9$ Hz); **¹⁹F NMR** (376 MHz, CDCl₃) δ –146.5; **MS** (ESI-TOF) calcd. for C₁₃H₁₃FO [M + Na⁺] 227.0843, found 227.0911; $[\alpha]_D^{24} = +0.9$ ($c = 1.4$, CHCl₃).

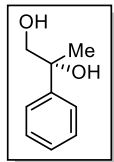
Gram-Scale Reactions:



(*R*)-2-hydroxy-2-phenylpropanal (**35a**):

A 200-mL round-bottom flask was charged with aldehyde substrate **34a** (1.50 mL, 1.50 g, 11.2 mmol). No precautions were taken to ensure dryness of flask or to exclude air or moisture. The aldehyde was then dissolved in THF (37 mL, 0.3 M). Solid catalyst **38** (0.831 g, 2.24 mmol, 20 mol%) was added, followed by TFA (170 μ L, 0.252 g, 2.21 mmol, 20 mol%) by syringe. Last, dry reagents NaHCO₃ (0.941 g, 11.2 mmol, 1.0 equiv) and oxaziridine **33** (2.892 g, 11.2 mmol, 1.0 equiv) were added to the flask sequentially. The flask was capped and the mixture was allowed to stir for 4 h at 23 °C. The reaction started out heterogeneous, but eventually became homogeneous. The mixture was concentrated by rotary evaporation, and the resultant residue was purified directly by flash chromatography (silica gel, 19:1 to 3:2 hexanes/EtOAc) to afford **35a** as a colorless oil which solidifies when stored at –78 °C (1.102 g, 66%).

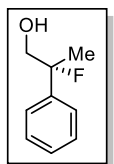
Spectroscopic results agree with those reported above.



(R)-2-phenylpropane-1,2-diol (35ad):

According to the general procedure, **35a** (27.3 mg, 0.18 mmol) and NaBH₄ (69 mg, 1.81 mmol, 10 equiv) were allowed to react in a MeOH solution (2.4 mL, 0.075 M) for 90 min to afford **35ad** (20.5 mg, 74%) as a colorless oil after column chromatography (silica gel, 9:1 to 2:3 hexanes/Et₂O). This material was determined to be of 89% *ee* by chiral HPLC analysis (ChiralPak AS-H, 5% *i*PrOH in hexanes, 1 mL/min, 210 nm, *t*_R(major) = 29.4 min, *t*_R(minor) = 23.3 min).

Spectroscopic results agree with those reported above.



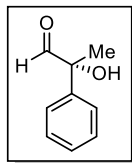
(R)-2-fluoro-2-phenylpropan-1-ol (40a):

A 200-mL round-bottom flask was charged with aldehyde substrate **34a** (1.00 mL, 1.00 g, 7.5 mmol). No precautions were taken to ensure dryness of flask or to exclude air or moisture. The aldehyde was then dissolved in THF (25 mL, 0.3 M). Solid catalyst **38** (0.138 g, 0.37 mmol, 5 mol%) was added, followed by TFA (115 μL, 0.170 g, 1.49 mmol, 20 mol%) by syringe. Last, dry reagents NaHCO₃ (0.628 g, 7.5 mmol, 1.0 equiv) and NFSI **12** (2.356 g, 7.5 mmol, 1.0 equiv) were added to the flask sequentially. The flask was capped and the mixture was allowed to stir for 4 h at 23 °C. A white precipitate formed as the reaction proceeded. After 4 h, the crude reaction mixture was transferred to a 1-L round-bottom flask with MeOH (70 mL), and the 200-mL flask was rinsed with 2 additional aliquots of MeOH (2 x 15 mL, 100 mL total, 0.075 M overall) to ensure complete transfer. The flask was cooled to 0 °C in an ice bath, then solid NaBH₄ (2.830 g, 74.8 mmol, 10 equiv) was added in 3 portions over the course of 10 min. The reaction mixture was stirred, open to air, at 23 °C. After 90 min, the reaction was quenched with sat. aq. NH₄Cl (200 mL) and EtOAc (200 mL). After an additional 30 min of stirring open to air at 23 °C, the layers were separated and the aqueous phase was extracted with EtOAc (4 x 150 mL). The pooled organic layers were dried over Na₂SO₄, filtered, and concentrated by rotary evaporation. The crude product was purified by flash chromatography (silica gel, 19:1 to 3:2 hexanes/EtOAc) to afford **40a** as a colorless oil which solidifies when stored at -10 °C (1.152 g, 100%). This material was determined to be of 80% *ee* by chiral HPLC analysis (ChiralPak AS-H, 5% *i*PrOH in hexanes, 1 mL/min, 210 nm, *t*_R(major) = 13.2 min,

$t_{R(\text{minor})} = 12.3$ min). Purified fluorohydrin **40a** (1.151 g) was dissolved in hexanes (1.0 mL) and gently heated in a 40 °C water bath for 5 min to ensure complete dissolution. The solution was cooled to -10 °C in a freezer for 1 h, during which time white crystals formed. The crystals were isolated by filtration and washed with cold hexanes to afford **40a** (0.706 g, 61% recovery), which was determined to be of 89% *ee* by chiral HPLC analysis as above.

Spectroscopic results agree with those reported above.

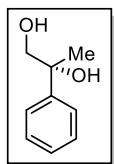
Low Temperature α -Hydroxylation:



(*R*)-2-hydroxy-2-phenylpropanal (**35a**):

A 2-dram vial was charged with aldehyde substrate **34a** (134 μ L, 134 mg, 1.00 mmol). No precautions were taken to ensure dryness of vial or to exclude air or moisture. The aldehyde was then dissolved in THF (3.3 mL, 0.3 M). Solid catalyst **38** (74 mg, 0.20 mmol, 20 mol%) was added, followed by TFA (15.4 μ L, 22.8 mg, 0.20 mmol, 20 mol%) by syringe. NaHCO_3 (84 mg, 1.00 mmol, 1.0 equiv) was added to the vial, which was then sealed and placed in a -78 °C dry ice/acetone bath. After 30 minutes, oxaziridine **33** (258 mg, 1.00 mmol, 1.0 equiv) was added to the vial, which was then resealed and placed in a bath at -25 °C. After stirring for 24 h at -25 °C, the mixture was concentrated by rotary evaporation at 23 °C, and the resultant residue was purified directly by flash chromatography (silica gel, 19:1 to 3:2 hexanes/EtOAc) to afford **35a** as a colorless oil (98 mg, 65%).

Spectroscopic results agree with those reported above.

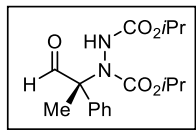


(*R*)-2-phenylpropane-1,2-diol (**35ad**):

According to the general procedure, **35a** (15.3 mg, 0.10 mmol) and NaBH_4 (39 mg, 1.02 mmol, 10 equiv) were allowed to react in a MeOH solution (1.36 mL, 0.075 M) for 90 min to afford **35ad** (10.2 mg, 66%) as a colorless oil after column chromatography (silica gel, 9:1 to 2:3 hexanes/Et₂O). This material was determined to be of 93% *ee* by chiral HPLC analysis (ChiralPak AS-H, 5% *i*PrOH in hexanes, 1 mL/min, 210 nm, $t_{R(\text{major})} = 29.4$ min, $t_{R(\text{minor})} = 23.3$ min).

Spectroscopic results agree with those reported above.

Reactions with Alternative Electrophiles:

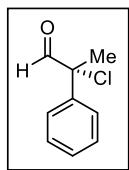


Diisopropyl (*R*)-1-(1-oxo-2-phenylpropan-2-yl)hydrazine-1,2-dicarboxylate (**56**):

A 2-dram vial was charged with aldehyde substrate **34a** (134 μ L, 134 mg, 1.00 mmol).

No precautions were taken to ensure dryness of vial or to exclude air or moisture. The aldehyde was then dissolved in THF (3.3 mL, 0.3 M). Solid catalyst **38** (74 mg, 0.20 mmol, 20 mol%) was added, followed by TFA (15.4 μ L, 22.8 mg, 0.20 mmol, 20 mol%) by syringe. Last, DIAD **55** (195 μ L, 202 mg, 1.00 mmol, 1.0 equiv) was added to the vial, which was then sealed. The mixture was allowed to stir for 4 h at 23 °C, after which the solution was concentrated by rotary evaporation. The resultant residue was purified directly by flash chromatography (silica gel, 9:1 to 2:3 hexanes/EtOAc) to afford **56** as a thick, colorless oil (319 mg, 95%). This material was determined to be of 85% *ee* by chiral HPLC analysis (ChiralPak AD-H, 5% *i*PrOH in hexanes, 0.5 mL/min, 210 nm, t_R (major) = 49.0 min, t_R (minor) = 53.3 min). A racemic standard was synthesized as described, with racemic catalyst (\pm)-**38**.

R_f = 0.60 (silica gel, 2:1 hexanes/Et₂O); **IR** (film) ν_{\max} 3304 (br), 2982, 1733, 1703, 1376, 1321, 1245, 1107 cm^{-1} ; **¹H NMR** (400 MHz, CDCl₃) δ 9.77 (minor rotamor, s, 0.24H), 9.61 (major rotamer, s, 0.76H), 7.61 – 7.30 (m, 5H), 6.32 (br s, 1H), 5.04 – 4.82 (m, 2H), 1.84 – 1.70 (m, 3H), 1.34 – 1.11 (m, 12H); **¹³C NMR** (100 MHz, CDCl₃) δ 194.2, 192.8, 156.0, 155.6, 137.1, 128.9, 128.1, 127.3, 73.0, 71.4, 21.7, 18.1; **MS** (ESI-TOF) calcd. for C₁₇H₂₄N₂O₅ [M + H⁺] 337.1758, found 337.1769; $[\alpha]_D^{24} = +42.3$ ($c = 1.1$, CHCl₃).⁵⁸



(*R*)-2-chloro-2-phenylpropanal (**64**):

A 2-dram vial was charged with aldehyde substrate **34a** (134 μ L, 134 mg, 1.00 mmol). No precautions were taken to ensure dryness of vial or to exclude air or moisture. The aldehyde

was then dissolved in THF (3.3 mL, 0.3 M). Solid catalyst **38** (74 mg, 0.20 mmol, 20 mol%) was added, followed by TFA (15.4 μ L, 22.8 mg, 0.20 mmol, 20 mol%) by syringe. Last, NaHCO₃ (84 mg, 1.00 mmol, 1.0 equiv) and 2,3,4,5,6-hexachlorocyclohexa-2,4-dienone **63** (301 mg, 1.00 mmol, 1.0 equiv) were sequentially added to the vial, which was then sealed. The mixture was allowed to stir for 4 h at 23 °C, after

⁵⁸ For comparison: Theodorou, A.; Papadopoulos, G. N.; Kokotos, C. G. *Tetrahedron* **2013**, *69*, 5438–5443.

which the solution was concentrated by rotary evaporation. The resultant residue was purified directly by flash chromatography (silica gel, 19:1 to 3:2 hexanes/EtOAc) to afford **64** as a yellow oil (120 mg, 71%). This material was determined to be of 66% *ee* by chiral HPLC analysis (ChiralPak AD-H, 2% *i*PrOH in hexanes, 0.5 mL/min, 210 nm, $t_{R(\text{major})}$ = 13.2 min, $t_{R(\text{minor})}$ = 9.8 min). A racemic standard was synthesized as described, with racemic catalyst (\pm)-**38**.

R_f = 0.80 (silica gel, 2:1 hexanes/Et₂O); **IR** (film) ν_{max} 1729, 1492, 1445, 1383, 1165, 1112, 1055, 890, 759, 695, 531 cm⁻¹; **¹H NMR** (400 MHz, CDCl₃) δ 9.47 (s), 7.51 – 7.47 (m, 2H), 7.46 – 7.37 (m, 3H), 2.00 (s, 3H); **¹³C NMR** (100 MHz, CDCl₃) δ 191.7, 137.1, 128.9, 128.8, 126.7, 73.6, 25.5; **MS** (ESI-TOF) calcd. for C₉H₉ClO [M + H⁺ – H₂O] 151.0309, found 151.0288; $[\alpha]_D^{24}$ = +33.7 (*c* = 1.0, CHCl₃).⁵⁹

5.7.5 Computational Procedures and Results

Calculations were performed at Harvard University using Gaussian 09⁶⁰ at the B3LYP⁶¹ level of density functional theory with the 6-31G(d)⁶² basis set. Relative energies are for uncorrected electronic energy differences.

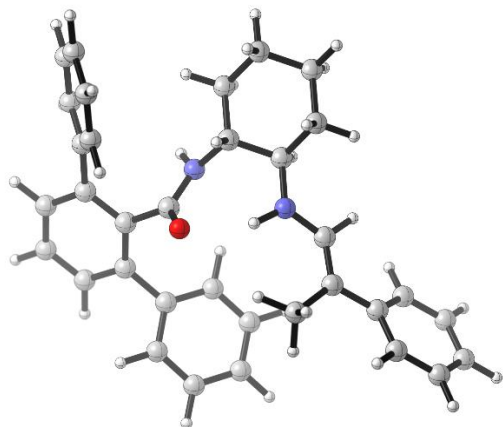
⁵⁹ For comparison: Paulmier, C.; Outurquin, F.; Plaquevant, J.-C. *Tetrahedron Lett.* **1988**, *29*, 5889–5891.

⁶⁰ Gaussian 09, Revision A.1, Frisch, M. J.; Trucks, G. W.; Schlegel, H. B.; Scuseria, G. E.; Robb, M. A.; Cheeseman, J. R.; Scalmani, G.; Barone, V.; Mennucci, B.; Petersson, G. A.; Nakatsuji, H.; Caricato, M.; Li, X.; Hratchian, H. P.; Izmaylov, A. F.; Bloino, J.; Zheng, G.; Sonnenberg, J. L.; Hada, M.; Ehara, M.; Toyota, K.; Fukuda, R.; Hasegawa, J.; Ishida, M.; Nakajima, T.; Honda, Y.; Kitao, O.; Nakai, H.; Vreven, T.; Montgomery, Jr., J. A.; Peralta, J. E.; Ogliaro, F.; Bearpark, M.; Heyd, J. J.; Brothers, E.; Kudin, K. N.; Staroverov, V. N.; Kobayashi, R.; Normand, J.; Raghavachari, K.; Rendell, A.; Burant, J. C.; Iyengar, S. S.; Tomasi, J.; Cossi, M.; Rega, N.; Millam, N. J.; Klene, M.; Knox, J. E.; Cross, J. B.; Bakken, V.; Adamo, C.; Jaramillo, J.; Gomperts, R.; Stratmann, R. E.; Yazyev, O.; Austin, A. J.; Cammi, R.; Pomelli, C.; Ochterski, J. W.; Martin, R. L.; Morokuma, K.; Zakrzewski, V. G.; Voth, G. A.; Salvador, P.; Dannenberg, J. J.; Dapprich, S.; Daniels, A. D.; Farkas, Ö.; Foresman, J. B.; Ortiz, J. V.; Cioslowski, J.; Fox, D. J. Gaussian, Inc., Wallingford CT, 2009.

⁶¹ B3LYP = Becke-3-Lee-Yang-Parr density functional theory: (a) Becke, A. D. *J. Chem. Phys.* **1993**, *98*, 1372–1377. (b) Lee, C.; Yang, W.; Parr, R. G. *Phys. Rev. B* **1988**, *37*, 785–789.

⁶² (a) Ditchfield, R.; Hehre, W. J.; Pople, J. A. *J. Chem. Phys.* **1971**, *54*, 724–728. (b) Hehre, W. J.; Ditchfield, R.; Pople, J. A. *J. Chem. Phys.* **1972**, *56*, 2257–2261. (c) Hariharan, P. C.; Pople, J. A. *Theor. Chim. Acta.* **1973**, *28*, 213–222.

E-62a:



E(RB3LYP): -1500.85238008

Zero-point correction: 0.601051 (Hartree/Particle)

Thermal correction to Energy: 0.633405

Thermal correction to Enthalpy: 0.634349

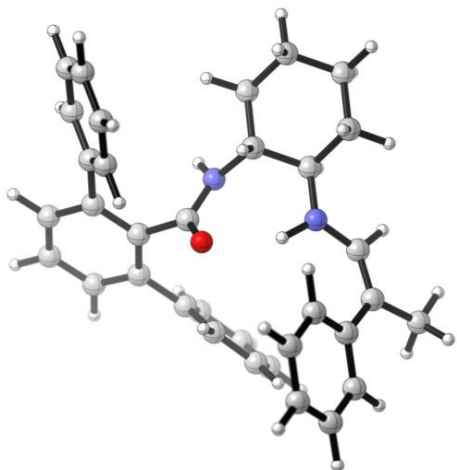
Thermal correction to Gibbs Free Energy: 0.534510

Cartesian coordinates:

C	2.1945300	3.5984000	-0.7508400	H	0.0505100	5.2709400	-0.0027100
C	1.3775400	2.4094200	-1.2978300	H	1.9050200	4.9419300	-2.4263600
C	-0.1272400	2.6163000	-0.9977500	H	2.2985900	5.7547400	-0.9173900
C	-0.6114000	3.9541900	-1.5853600	H	-0.2594100	2.6284500	0.0892400
C	0.2186400	5.1430900	-1.0807200	N	-0.9572100	1.5247500	-1.5054000
C	1.7149700	4.9312700	-1.3433900	C	-1.5066100	0.5243800	-0.7541700
H	1.4922800	2.3588300	-2.3904400	C	-2.5570600	-0.1648500	-1.3250500
H	2.0875200	3.6147400	0.3423200	C	-3.8216600	0.4533600	-1.3200000
H	3.2606300	3.4473000	-0.9596600	C	-2.3462700	-1.4096600	-1.9495000
H	-0.5517100	3.9081200	-2.6841200	C	-4.898500	-0.2146500	-1.9149600
H	-1.6683900	4.0847600	-1.3282700	C	-3.4549300	-2.0485000	-2.5254200
H	-0.1282000	6.0639100	-1.5621500	C	-4.7181000	-1.4636300	-2.5043300

H	-5.8758700	0.2585000	-1.9163300	H	-1.7303400	-3.9610400	-1.3080400
H	-3.3084400	-3.0026300	-3.0224600	C	1.4645200	-3.3806800	-2.3281500
H	-5.5586200	-1.9728800	-2.9666700	H	2.1894800	-1.4921500	-3.0774300
H	-1.3207300	1.6502800	-2.4441100	H	0.4366900	-5.1255200	-1.5840700
N	1.8187800	1.1290000	-0.7234900	H	2.4153600	-3.8910800	-2.4557700
C	2.9500700	0.4815100	-1.0397600	O	-1.0303800	0.1861700	0.5511000
H	1.1528800	0.6927200	-0.0701700	H	3.6178300	0.8949000	-1.7664700
C	-4.0268400	1.7942600	-0.6939800	C	3.2505900	-0.7091400	-0.4323500
C	-3.4894100	2.9494700	-1.2851600	C	2.2876500	-1.3017400	0.6132000
C	-4.7816000	1.9260900	0.4800400	H	2.2889600	-0.6863600	1.4885300
C	-3.6959800	4.2055300	-0.7125800	H	1.2989400	-1.3405200	0.2059600
H	-2.9423200	2.8666700	-2.2228500	H	2.6060000	-2.2900700	0.8715600
C	-4.9883800	3.1825700	1.0521800	C	4.5491100	-1.4536500	-0.7944900
H	-5.1989500	1.0381400	0.9461400	C	4.8535800	-2.6660600	-0.1749400
C	-4.4449900	4.3240200	0.4599400	C	5.4197100	-0.9169000	-1.7427400
H	-3.2871900	5.0914800	-1.1910500	C	6.0291100	-3.3411900	-0.5033800
H	-5.5776400	3.2689900	1.9609600	H	4.1668300	-3.0892900	0.5723200
H	-4.6128300	5.3015000	0.9033400	C	6.5960000	-1.5920400	-2.0709600
C	-1.0116300	-2.0652000	-2.0358700	H	5.1794800	0.0384100	-2.2315700
C	0.1125300	-1.3832400	-2.5297800	C	6.9005700	-2.8039200	-1.4511800
C	-0.8709000	-3.4200700	-1.6939100	H	6.2693200	-4.2966700	-0.0150400
C	1.3377500	-2.0333500	-2.6735700	H	7.2823200	-1.1686100	-2.8186100
H	0.0168700	-0.3452300	-2.8334600	H	7.8275500	-3.3362500	-1.7096300
C	0.3542700	-4.0721900	-1.8399800				

Z-62a:



E(RB3LYP): -1500.85033821

Zero-point correction: 0.601824 (Hartree/Particle)

Thermal correction to Energy: 0.633869

Thermal correction to Enthalpy: 0.634813

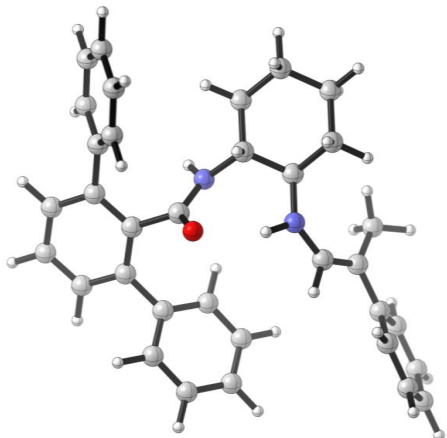
Thermal correction to Gibbs Free Energy: 0.535909

Cartesian coordinates:

C	2.1945300	3.5984000	-0.7508400	H	-0.1282000	6.0639100	-1.5621500
C	1.3775400	2.4094200	-1.2978300	H	0.0505100	5.2709400	-0.0027100
C	-0.1272400	2.6163000	-0.9977500	H	1.9050200	4.9419300	-2.4263600
C	-0.6114000	3.9541900	-1.5853600	H	2.2985900	5.7547400	-0.9173900
C	0.2186400	5.1430900	-1.0807200	H	-0.2594100	2.6284500	0.0892400
C	1.7149700	4.9312700	-1.3433900	N	-0.9572100	1.5247500	-1.5054000
H	1.4922800	2.3588300	-2.3904400	C	-1.5066100	0.5243800	-0.7541700
H	2.0875200	3.6147400	0.3423200	C	-2.5570600	-0.1648500	-1.3250500
H	3.2606300	3.4473000	-0.9596600	C	-3.8216600	0.4533600	-1.3200000
H	-0.5517100	3.9081200	-2.6841200	C	-2.3462700	-1.4096600	-1.9495000
H	-1.6683900	4.0847600	-1.3282700	C	-4.8985000	-0.2146500	-1.9149600

C	-3.4549300	-2.0485000	-2.5254200	C	0.3542700	-4.0721900	-1.8399800
C	-4.7181000	-1.4636300	-2.5043300	H	-1.7303400	-3.9610400	-1.3080400
H	-5.8758700	0.2585000	-1.9163300	C	1.4645200	-3.3806800	-2.3281500
H	-3.3084400	-3.0026300	-3.0224600	H	2.1894800	-1.4921500	-3.0774300
H	-5.5586200	-1.9728800	-2.9666700	H	0.4366900	-5.1255200	-1.5840700
H	-1.3207300	1.6502800	-2.4441100	H	2.4153600	-3.8910800	-2.4557700
N	1.8187800	1.1290000	-0.7234900	O	-1.0303800	0.1861700	0.5511000
C	2.9500700	0.4815100	-1.0397600	H	3.6178300	0.8949000	-1.7664700
H	1.1528800	0.6927200	-0.0701700	C	3.2505900	-0.7091400	-0.4323500
C	-4.0268400	1.7942600	-0.6939800	C	4.5501800	-1.4503300	-0.7974500
C	-3.4894100	2.9494700	-1.2851600	H	4.4846200	-1.8111900	-1.8026300
C	-4.7816000	1.9260900	0.4800400	H	5.3793200	-0.7793300	-0.7127400
C	-3.6959800	4.2055300	-0.7125800	H	4.6895500	-2.2754800	-0.1306600
H	-2.9423200	2.8666700	-2.2228500	C	2.2904600	-1.3053100	0.6137500
C	-4.9883800	3.1825700	1.0521800	C	2.5980600	-2.5179200	1.2313400
H	-5.1989500	1.0381400	0.9461400	C	1.1145400	-0.6324000	0.9448900
C	-4.4449900	4.3240200	0.4599400	C	1.7291700	-3.0577500	2.1795900
H	-3.2871900	5.0914800	-1.1910500	H	3.5254300	-3.0480700	0.9704500
H	-5.5776400	3.2689900	1.9609600	C	0.2450200	-1.1726900	1.8931700
H	-4.6128300	5.3015000	0.9033400	H	0.8723300	0.3237100	0.4586000
C	-1.0116300	-2.065200	-2.0358700	C	0.5523800	-2.3852500	2.5102200
C	0.1125300	-1.3832400	-2.5297800	H	1.9713700	-4.0135500	2.6663200
C	-0.8709000	-3.4200700	-1.6939100	H	-0.6821200	-0.6419800	2.1540500
C	1.3377500	-2.0333500	-2.6735700	H	-0.1327100	-2.8113200	3.2576100
H	0.0168700	-0.3452300	-2.8334600				

ZE-62a:



E(RB3LYP): -1500.84591639

Zero-point correction: 0.602142 (Hartree/Particle)

Thermal correction to Energy: 0.634163

Thermal correction to Enthalpy: 0.635107

Thermal correction to Gibbs Free Energy: 0.536151

Cartesian coordinates:

C	6.1517100	0.4026200	-1.4101900	H	8.1880900	1.4337200	-3.0666700
C	5.0124100	0.3563100	-2.4495200	H	7.2511800	-1.3284900	-2.1106800
C	5.4603300	1.0491700	-3.7596800	H	8.2245300	-0.1852200	-1.1952300
C	6.7455600	0.3955100	-4.2987200	H	5.6550800	2.1037400	-3.5380900
C	7.8766100	0.3982900	-3.2605400	N	4.4241600	1.0254400	-4.7911100
C	7.4306600	-0.2561000	-1.9468500	C	3.6315200	2.0789100	-5.1500900
H	4.7814600	-0.6911600	-2.6923900	C	3.0090300	1.9872300	-6.3783000
H	6.3481700	1.4546600	-1.1625400	C	3.7830800	2.2556200	-7.5229500
H	5.8305100	-0.0838700	-0.4811300	C	1.6669000	1.5711100	-6.4755100
H	6.5254100	-0.6420800	-4.5952100	C	3.1812000	2.1453600	-8.7820700
H	7.0527800	0.9282600	-5.2054500	C	1.1007100	1.4827800	-7.7563500
H	8.7512800	-0.1195900	-3.6688700	C	1.8443500	1.7719500	-8.8971800

H	3.7740900	2.3487200	-9.6687800	H	-0.8161400	2.4612900	-5.8902900
H	0.0711900	1.1511200	-7.8509700	C	-0.8267700	0.4423000	-3.1501900
H	1.3867900	1.6855500	-9.8783700	H	0.8127400	-0.8269800	-2.5548500
H	4.4525700	0.2324400	-5.4230900	H	-2.2861600	1.7706900	-4.0220500
N	3.7871400	0.9997200	-1.9507300	H	-1.4722400	0.1331000	-2.3324700
C	2.9500700	0.4815100	-1.0397600	O	3.4356100	3.2207500	-4.3118100
H	3.5516600	1.8953300	-2.4013300	H	2.0476100	0.9980300	-0.7874600
C	5.2188200	2.6536700	-7.4123700	C	3.2505900	-0.7091400	-0.4323500
C	6.1890300	1.7247900	-7.0016400	C	4.5501800	-1.4503300	-0.7974500
C	5.6266300	3.9538300	-7.7419700	H	4.4846200	-1.8111900	-1.8026300
C	7.5337300	2.0890100	-6.9160400	H	5.3793200	-0.7793300	-0.7127400
H	5.8927300	0.6988500	-6.7892900	H	4.6895500	-2.2754800	-0.1306600
C	6.9717000	4.3176100	-7.6566700	C	2.2904600	-1.3053100	0.6137500
H	4.8832200	4.6800200	-8.0579800	C	2.5980600	-2.5179200	1.2313400
C	7.9275000	3.3885200	-7.2417300	C	1.1145400	-0.6324000	0.9448900
H	8.2744400	1.3541600	-6.6122100	C	1.7291700	-3.0577500	2.1795900
H	7.2727500	5.3284400	-7.9177800	H	3.5254300	-3.0480700	0.9704500
H	8.9745700	3.6720300	-7.1825100	C	0.2450200	-1.1726900	1.8931700
C	0.8346300	1.2125900	-5.2934600	H	0.8723300	0.3237100	0.4586000
C	1.2782800	0.2870700	-4.3346400	C	0.5523800	-2.3852500	2.5102200
C	-0.4590200	1.7423300	-5.1583400	H	1.9713700	-4.0135500	2.6663200
C	0.4571100	-0.0934500	-3.2738100	H	-0.6821200	-0.6419800	2.1540500
H	2.2614300	-0.1614500	-4.4399300	H	-0.1327100	-2.8113200	3.2576100
C	-1.2825000	1.3600700	-4.0984300				

5.7.6 Additional Optimization Studies

Table 5.9. α -Hydroxylation catalyst screen.^a

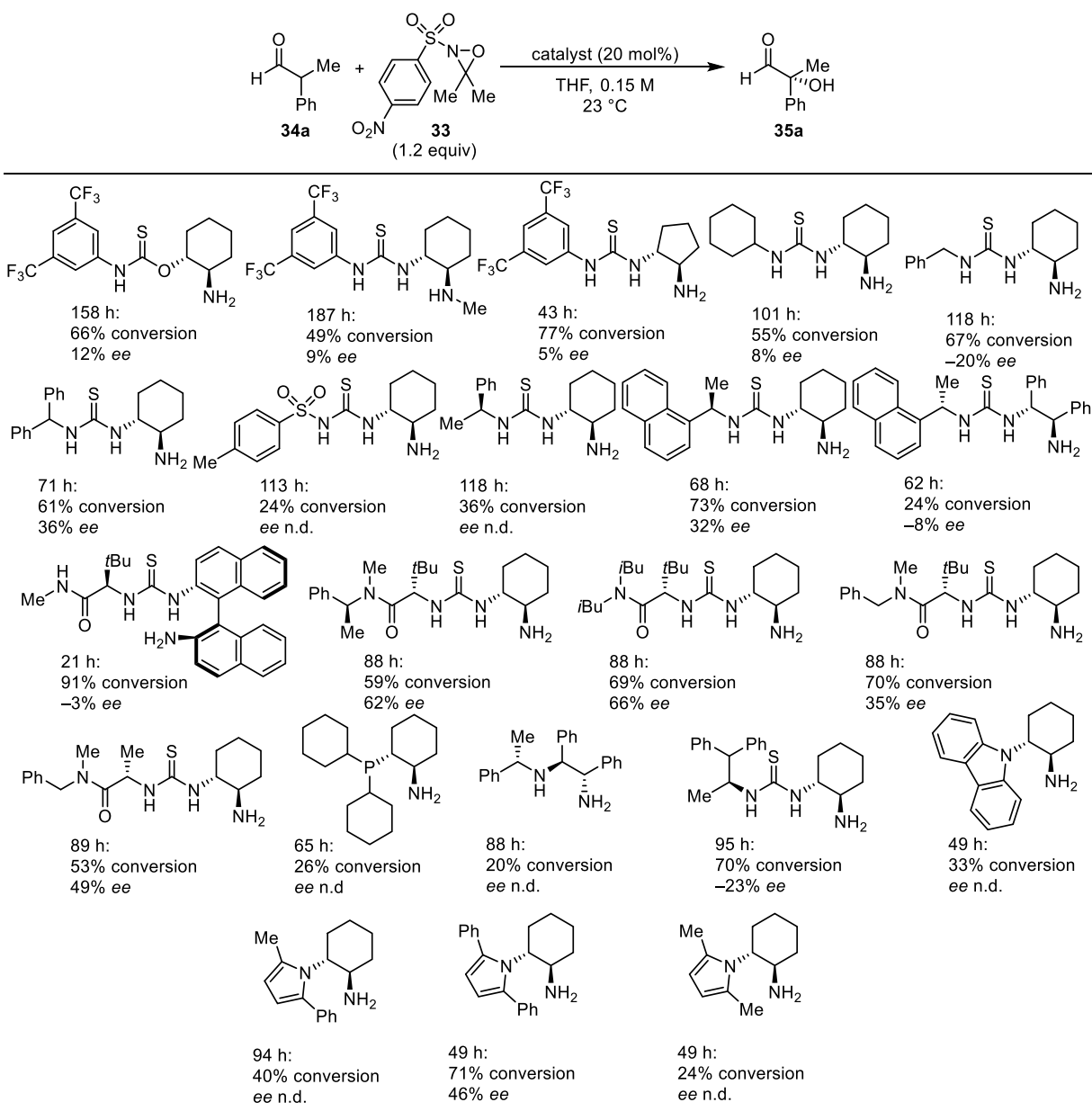
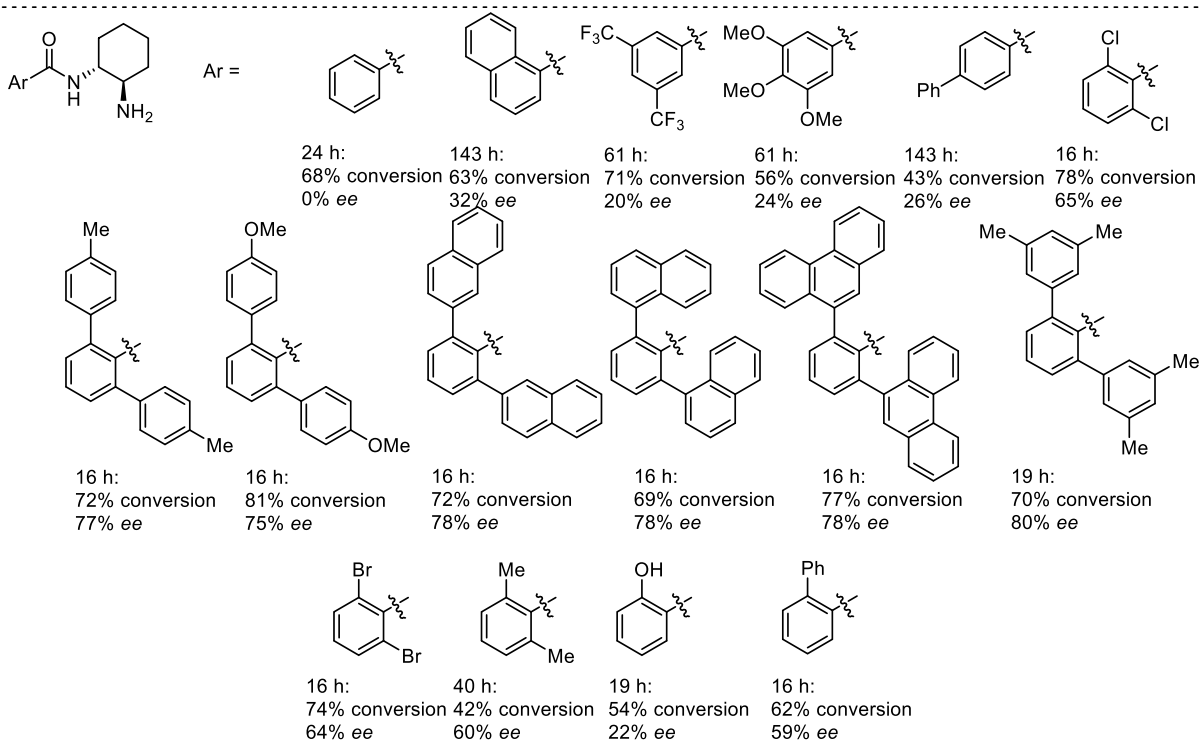
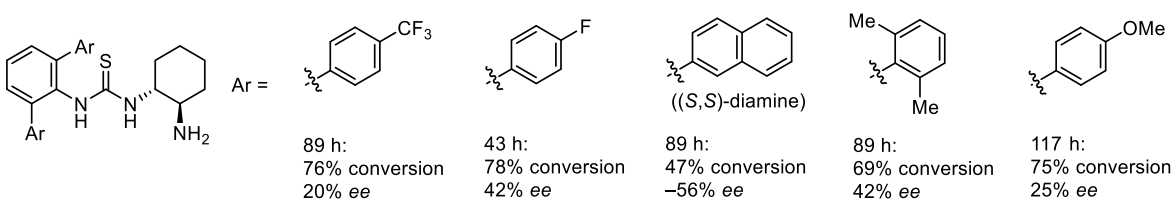
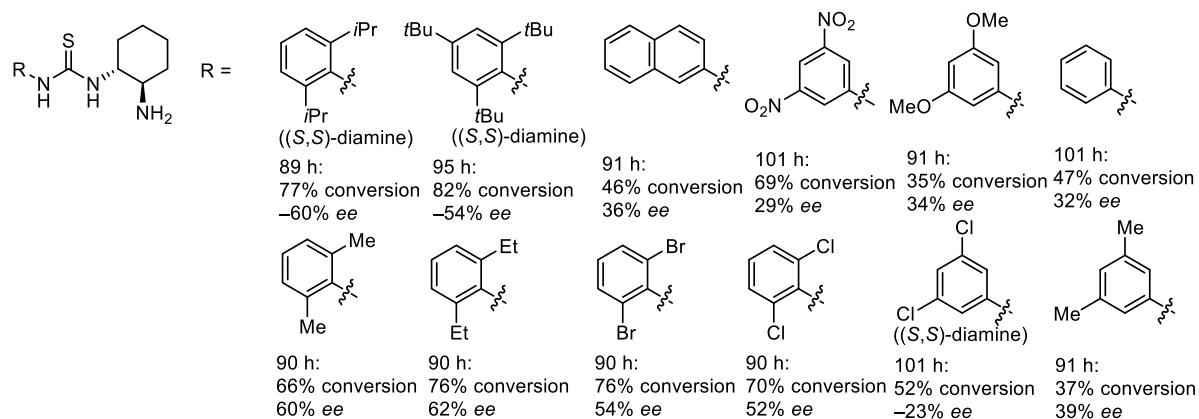
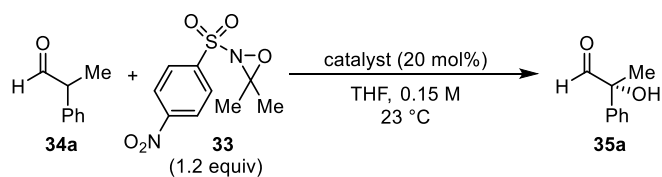


Table 5.9 (continued).



^a Reactions performed on 0.15 mmol scale. Conversions determined by GC analysis. Enantioselectivities determined by HPLC analysis of reduced diol using commercial columns with chiral stationary phases.

Table 5.10. α -Fluorination catalyst screen.^a

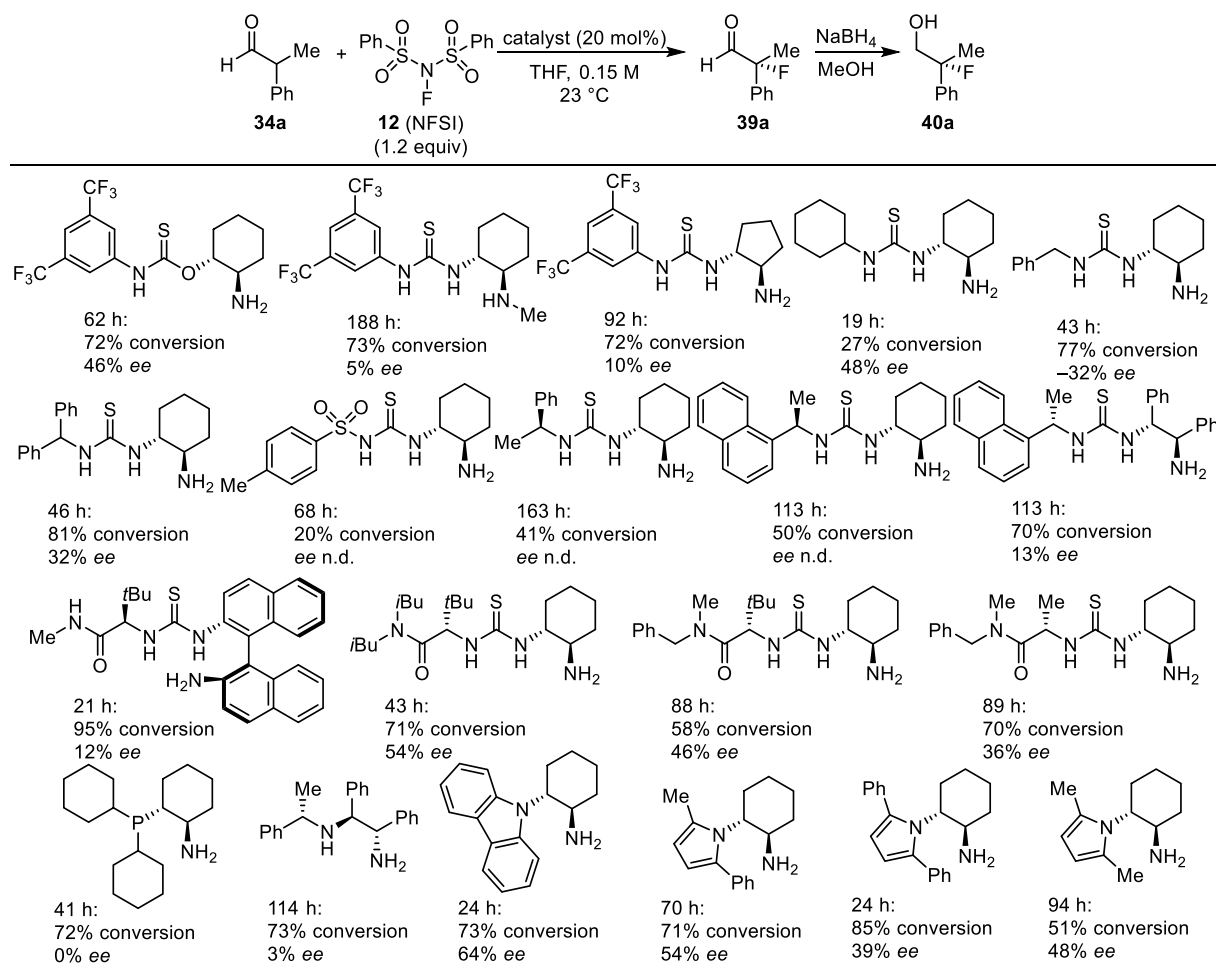
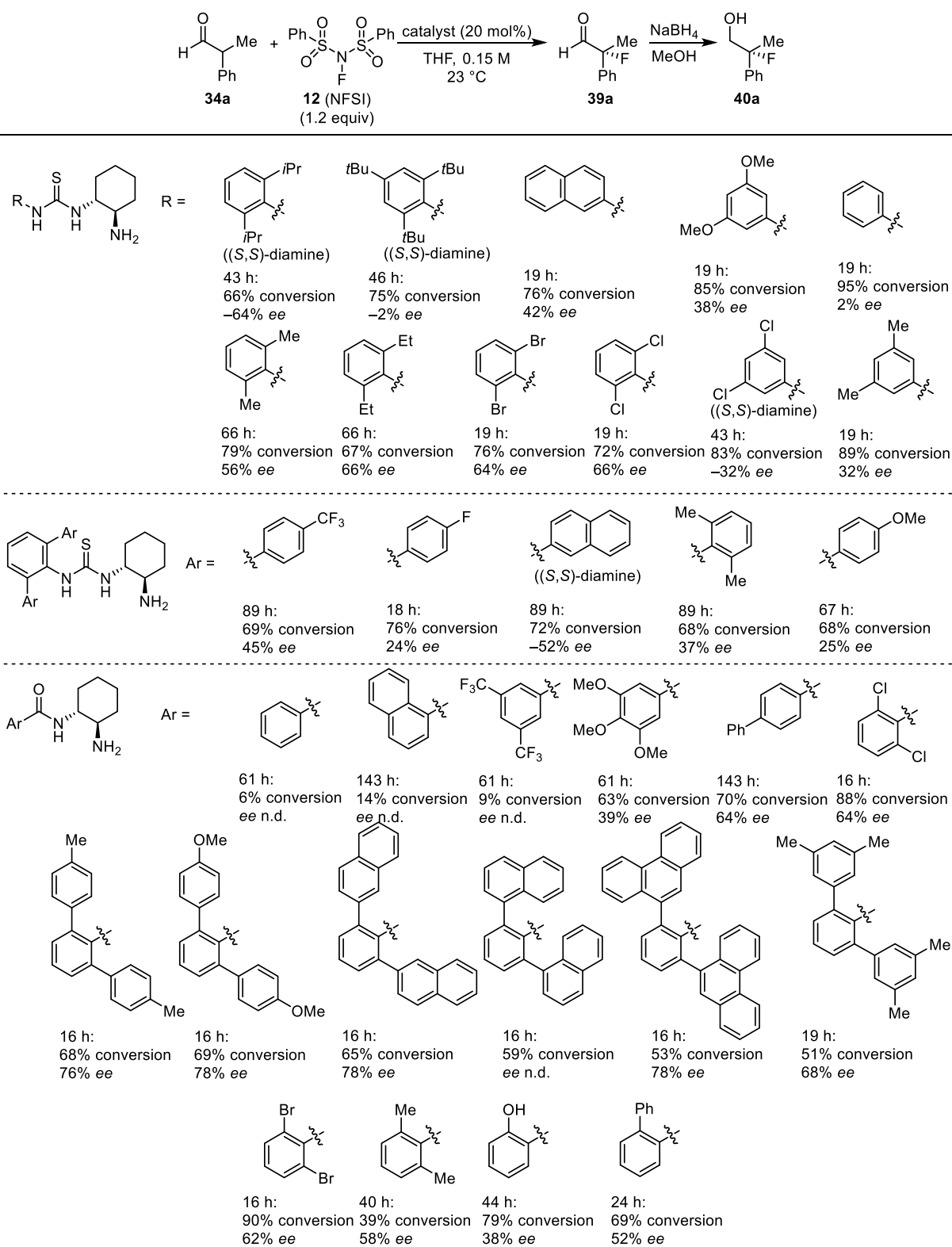
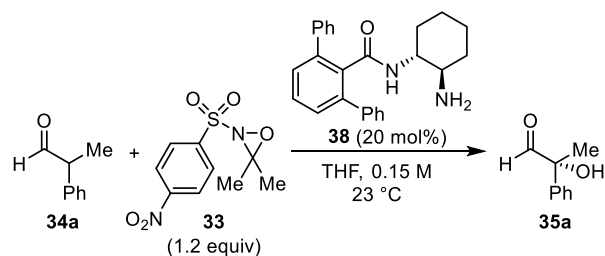


Table 5.10 (continued).

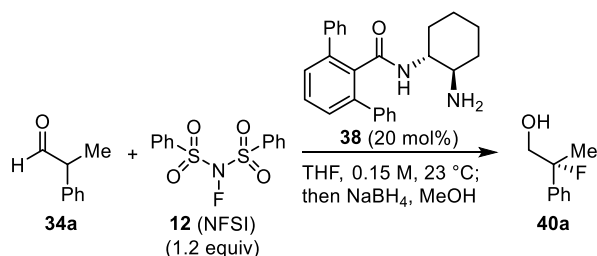


^a Reactions performed on 0.15 mmol scale. Conversions determined by GC analysis. Enantioselectivities determined by HPLC analysis of fluorhydrin using commercial columns with chiral stationary phases.

Table 5.11. α -Hydroxylation additive screen.^a


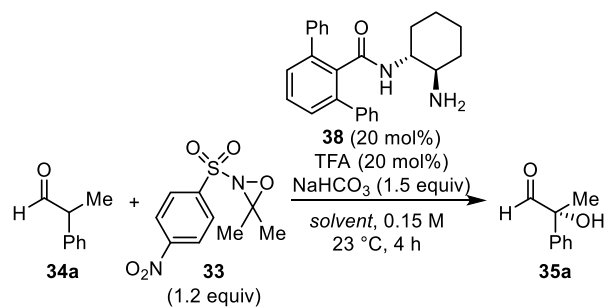
Entry	Additive(s)	Time (h)	Conversion (%) ^b	ee (%) ^c
1	None	16	73	75
2	1 equiv H ₂ O	19	77	72
3	20 mol% AcOH	19	72	79
4	20 mol% BzOH	17	61	81
5	20 mol% DCA	2	91	80
6	20 mol% TCA	2	64	70
7	20 mol% TFA	2	87	73
8	0.5 equiv NaOAc	160	54	42
9	0.5 equiv NaOBz	160	66	42
10	1.5 equiv Na ₂ CO ₃	92	52	57
11	1.5 equiv NaHCO ₃	48	72	71
12	20 mol% TFA + 1.5 equiv NaHCO ₃	4	85	87
13	20 mol% TCA + 1.5 equiv NaHCO ₃	4	66	87
14	20 mol% DCA + 1.5 equiv NaHCO ₃	4	85	84
15	20 mol% TFA + 1.5 equiv Na ₂ CO ₃	4	87	88
16	20 mol% TCA + 1.5 equiv Na ₂ CO ₃	4	67	86
17	20 mol% DCA + 1.5 equiv Na ₂ CO ₃	4	75	85
18	20 mol% TFA + 1.0 equiv NEt ₃	19	56	16
19	20 mol% TCA + 1.0 equiv NEt ₃	19	56	18

^a Reactions performed on 0.15 mmol scale. ^b Conversions determined by GC analysis. ^c Enantioselectivities determined by HPLC analysis of reduced diol using commercial columns with chiral stationary phases.

Table 5.12. α -Fluorination additive screen.^a


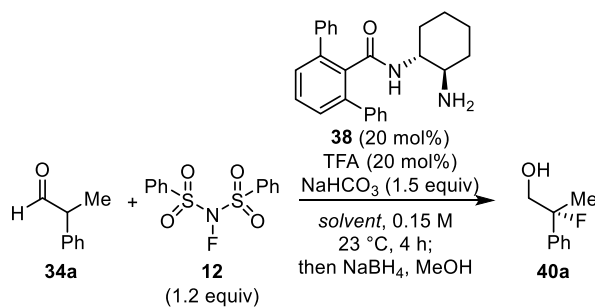
Entry	Additive(s)	Time (h)	Conversion (%) ^b	ee (%) ^c
1	None	16	74	78
2	1 equiv H ₂ O	19	71	77
3	20 mol% AcOH	19	80	77
4	20 mol% BzOH	17	79	81
5	20 mol% DCA	2	63	80
6	20 mol% TCA	2	68	80
7	20 mol% TFA	2	64	80
8	0.5 equiv NaOAc	16	89	78
9	0.5 equiv NaOBz	16	95	78
10	1.5 equiv Na ₂ CO ₃	19	87	79
11	1.5 equiv NaHCO ₃	4	82	79
12	20 mol% TFA + 1.5 equiv NaHCO ₃	4	83	83
13	20 mol% TCA + 1.5 equiv NaHCO ₃	4	73	82
14	20 mol% DCA + 1.5 equiv NaHCO ₃	4	67	79
15	20 mol% TFA + 1.5 equiv Na ₂ CO ₃	4	79	81
16	20 mol% TCA + 1.5 equiv Na ₂ CO ₃	4	73	82
17	20 mol% DCA + 1.5 equiv Na ₂ CO ₃	4	81	81
18	20 mol% TFA + 1.0 equiv NEt ₃	19	78	70
19	20 mol% TCA + 1.0 equiv NEt ₃	19	81	70

^a Reactions performed on 0.15 mmol scale. ^b Conversions determined by GC analysis. ^c Enantioselectivities determined by HPLC analysis of fluorohydrin using commercial columns with chiral stationary phases.

Table 5.13. α -Hydroxylation solvent screen.^a

Entry	Solvent	Conversion (%) ^b	ee (%) ^c
1	THF	88	87
2	2-MeTHF	87	87
3	THP	83	87
4	Dioxane	88	81
5	CPME	34	84
6	tBME	20	84
7	Et ₂ O	14	83
8	toluene	62	71
9	benzene	61	70
10	EtOAc	62	84
11	MeCN	38	79
12	MeOH	9	33
13	DMF	8	n.d.
14	CH ₂ Cl ₂	6	72
15	hexanes	7	59

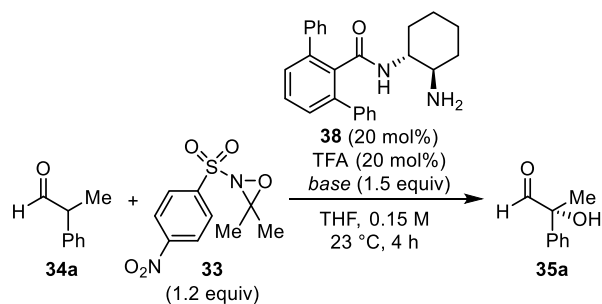
^a Reactions performed on 0.15 mmol scale. ^b Conversions determined by GC analysis. ^c Enantioselectivities determined by HPLC analysis of reduced diol using commercial columns with chiral stationary phases.

Table 5.14. α -Fluorination solvent screen.^a

Entry	Solvent	Conversion (%) ^b	ee (%) ^c
1	THF	71	83
2	2-MeTHF	59	76
3	THP	66	76
4	Dioxane	69	75
5	CPME	47	63
6	tBME	27	58
7	Et ₂ O	31	58
8	toluene	30	40
9	benzene	31	40
10	EtOAc	69	74
11	MeCN	48	71
12	MeOH	24	54
13	DMF	58	58
14	CH ₂ Cl ₂	22	45
15	hexanes	8	34

^a Reactions performed on 0.15 mmol scale. ^b Conversions determined by GC analysis. ^c Enantioselectivities determined by HPLC analysis of fluorohydrin using commercial columns with chiral stationary phases.

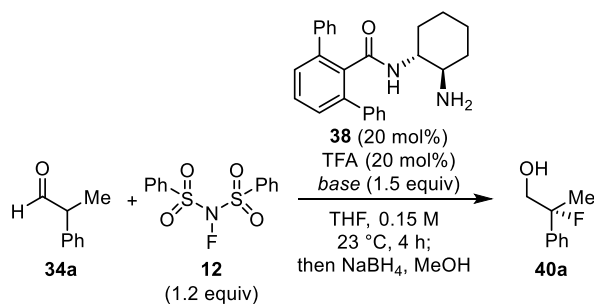
Table 5.15. α -Hydroxylation base screen.^a



Entry	Base	Conversion (%) ^b	ee (%) ^c
1	NaHCO ₃	88	87
2	Na ₂ CO ₃	87	88
3	K ₂ CO ₃	29	60
4	Li ₂ CO ₃	82	80
5	Cs ₂ CO ₃	31	47
6	BaCO ₃	87	83
7	CaCO ₃	86	79
8	NaH ₂ PO ₄	86	83
9	Na ₂ HPO ₄	86	86
10	NaOAc	71	79
11	NaOBz	82	76
12	NaClO ₄	35	84
13	LiCO ₄	11	80
14	NEt ₃	33	16

^a Reactions performed on 0.15 mmol scale. ^b Conversions determined by GC analysis. ^c Enantioselectivities determined by HPLC analysis of reduced diol using commercial columns with chiral stationary phases.

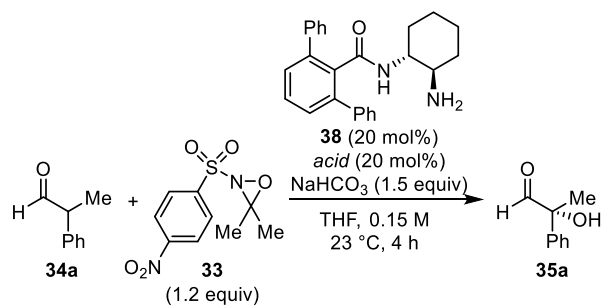
Table 5.16. α -Fluorination base screen.^a



Entry	Base	Conversion (%) ^b	ee (%) ^c
1	NaHCO ₃	83	83
2	Na ₂ CO ₃	79	81
3	K ₂ CO ₃	74	73
4	Li ₂ CO ₃	78	73
5	Cs ₂ CO ₃	56	74
6	BaCO ₃	80	82
7	CaCO ₃	80	82
8	NaH ₂ PO ₄	82	82
9	Na ₂ HPO ₄	82	80
10	NaOAc	86	75
11	NaOBz	88	75
12	NaClO ₄	26	76
13	LiCO ₄	9	72
14	NEt ₃	56	70

^a Reactions performed on 0.15 mmol scale. ^b Conversions determined by GC analysis. ^c Enantioselectivities determined by HPLC analysis of fluorohydrin using commercial columns with chiral stationary phases.

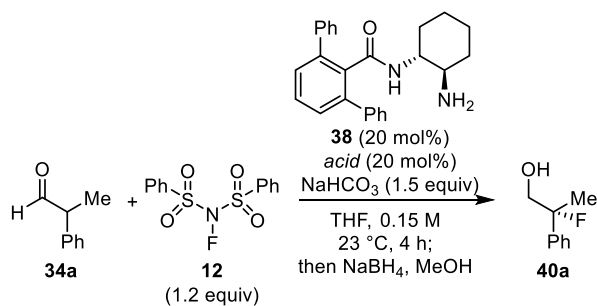
Table 5.17. α -Hydroxylation acid screen.^a



Entry	Acid	Conversion (%) ^b	ee (%) ^c
1	TFA	88	87
2	TCA	73	83
3	DCA	83	83
4	AcOH	73	75
5	BzOH	58	75
6	2-NO ₂ -BzOH	84	81
7	3-NO ₂ -BzOH	81	81
8	4-NO ₂ -BzOH	83	84
9	MeSO ₂ OH	15	78
10	PhSO ₂ OH	41	70
11	2-NBSA	28	69
12	4-NBSA	29	73
13	2,4-diNBSA	33	72
14	(PhO) ₂ PO ₂ H	71	81
15	(BnO) ₂ PO ₂ H	80	78
16	H ₂ SO ₄	23	80
17	HCl	33	70
18	HFIP	34	73
19	phenol	30	73
20	4-NO ₂ -phenol	35	72
21	L-tartaric acid	94	84
22	D-tartaric acid	90	83

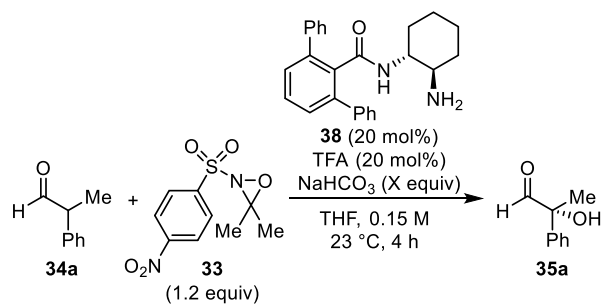
^a Reactions performed on 0.15 mmol scale. ^b Conversions determined by GC analysis. ^c Enantioselectivities determined by HPLC analysis of reduced diol using commercial columns with chiral stationary phases.

Table 5.18. α -Fluorination acid screen.^a



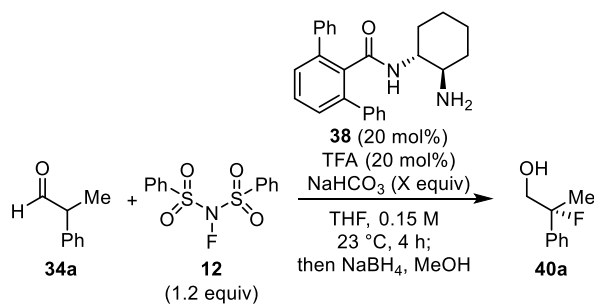
Entry	Acid	Conversion (%) ^b	ee (%) ^c
1	TFA	83	83
2	TCA	74	78
3	DCA	83	82
4	AcOH	59	80
5	BzOH	61	79
6	2-NO ₂ -BzOH	73	82
7	3-NO ₂ -BzOH	73	82
8	4-NO ₂ -BzOH	77	80
9	MeSO ₂ OH	15	78
10	PhSO ₂ OH	33	75
11	2-NBSA	41	76
12	4-NBSA	27	78
13	2,4-diNBSA	26	75
14	(PhO) ₂ PO ₂ H	61	82
15	(BnO) ₂ PO ₂ H	76	80
16	H ₂ SO ₄	22	76
17	HCl	29	74
18	HFIP	50	78
19	phenol	54	78
20	4-NO ₂ -phenol	58	78
21	L-tartaric acid	75	82
22	D-tartaric acid	74	79

^a Reactions performed on 0.15 mmol scale. ^b Conversions determined by GC analysis. ^c Enantioselectivities determined by HPLC analysis of fluorohydrin using commercial columns with chiral stationary phases.

Table 5.19. α -Hydroxylation NaHCO_3 loading.^a

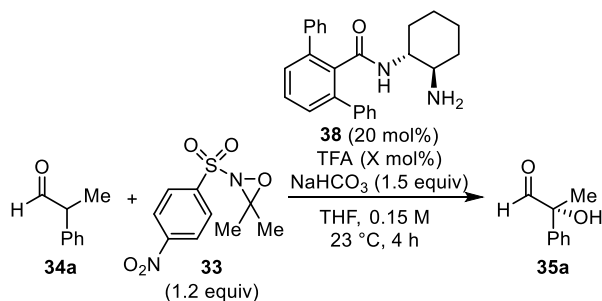
Entry	X	Conversion (%) ^b	ee (%) ^c
1	0.0	87	73
2	0.5	85	84
3	1.0	85	84
4	1.5	85	84
5	2.0	85	84
6	5.0	85	84

^a Reactions performed on 0.15 mmol scale. ^b Conversions determined by GC analysis. ^c Enantioselectivities determined by HPLC analysis of reduced diol using commercial columns with chiral stationary phases.

Table 5.20. α -Fluorination NaHCO_3 loading.^a

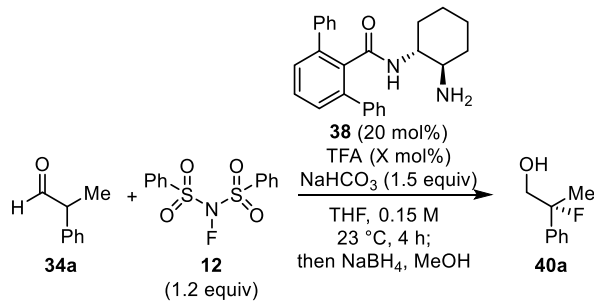
Entry	X	Conversion (%) ^b	ee (%) ^c
1	0.0	64	80
2	0.5	83	83
3	1.0	83	82
4	1.5	83	83
5	2.0	83	82
6	5.0	83	81

^a Reactions performed on 0.15 mmol scale. ^b Conversions determined by GC analysis. ^c Enantioselectivities determined by HPLC analysis of fluorohydrin using commercial columns with chiral stationary phases.

Table 5.21. α -Hydroxylation TFA loading.^a

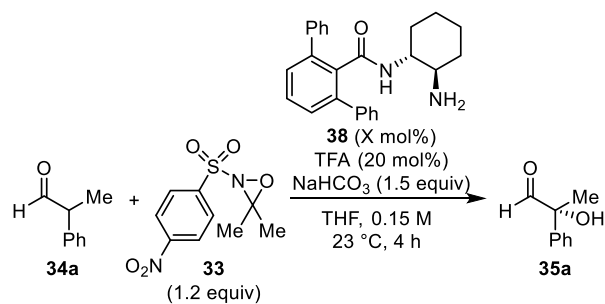
Entry	X	Conversion (%) ^b	ee (%) ^c
1	10	84	83
2	20	85	84
3	50	82	85

^a Reactions performed on 0.15 mmol scale. ^b Conversions determined by GC analysis. ^c Enantioselectivities determined by HPLC analysis of reduced diol using commercial columns with chiral stationary phases.

Table 5.22. α -Fluorination TFA loading.^a

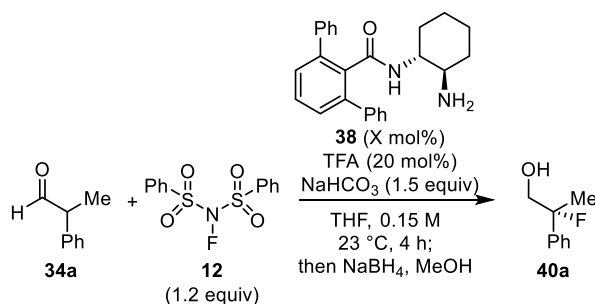
Entry	X	Conversion (%) ^b	ee (%) ^c
1	10	84	83
2	20	83	83
3	50	85	84

^a Reactions performed on 0.15 mmol scale. ^b Conversions determined by GC analysis. ^c Enantioselectivities determined by HPLC analysis of fluorohydrin using commercial columns with chiral stationary phases.

Table 5.23. α -Hydroxylation catalyst loading.^a

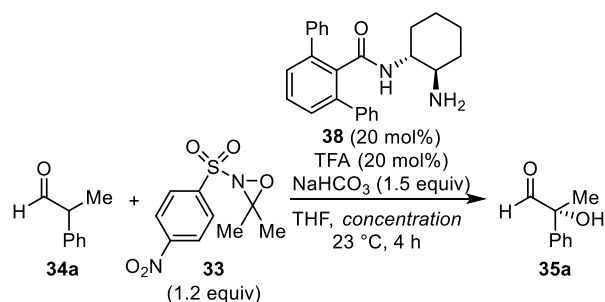
Entry	X	Conversion (%) ^b	ee (%) ^c
1	5	37	77
2	10	63	83
3	20	85	84

^a Reactions performed on 0.15 mmol scale. ^b Conversions determined by GC analysis. ^c Enantioselectivities determined by HPLC analysis of reduced diol using commercial columns with chiral stationary phases.

Table 5.24. α -Fluorination catalyst loading.^a

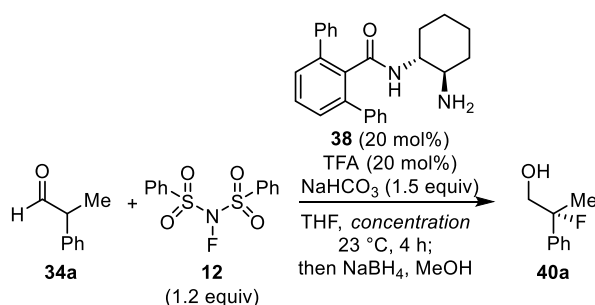
Entry	X	Conversion (%) ^b	ee (%) ^c
1	5	60	78
2	10	65	81
3	20	83	83

^a Reactions performed on 0.15 mmol scale. ^b Conversions determined by GC analysis. ^c Enantioselectivities determined by HPLC analysis of fluorohydrin using commercial columns with chiral stationary phases.

Table 5.25. α -Hydroxylation concentration.^a

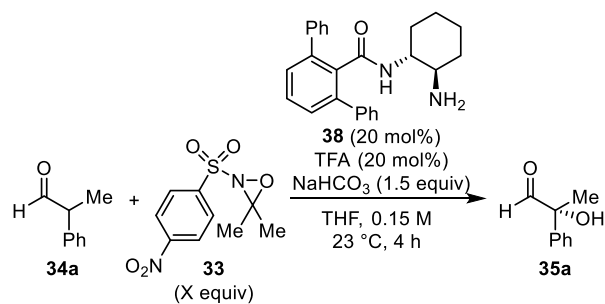
Entry	Concentration (M)	Conversion (%) ^b	ee (%) ^c
1	0.075	82	85
2	0.15	85	84
3	0.3	78	85

^a Reactions performed on 0.15 mmol scale. ^b Conversions determined by GC analysis. ^c Enantioselectivities determined by HPLC analysis of reduced diol using commercial columns with chiral stationary phases.

Table 5.26. α -Fluorination concentration.^a

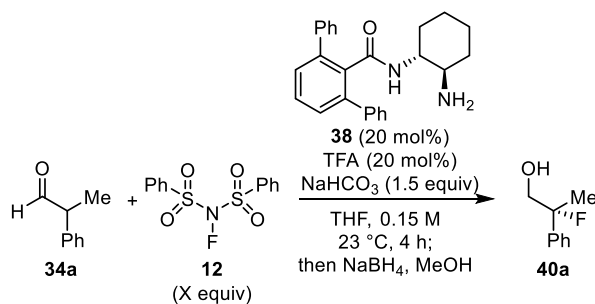
Entry	Concentration (M)	Conversion (%) ^b	ee (%) ^c
1	0.075	72	81
2	0.15	83	83
3	0.3	85	82

^a Reactions performed on 0.15 mmol scale. ^b Conversions determined by GC analysis. ^c Enantioselectivities determined by HPLC analysis of fluorohydrin using commercial columns with chiral stationary phases.

Table 5.27. α -Hydroxylation electrophile loading.^a


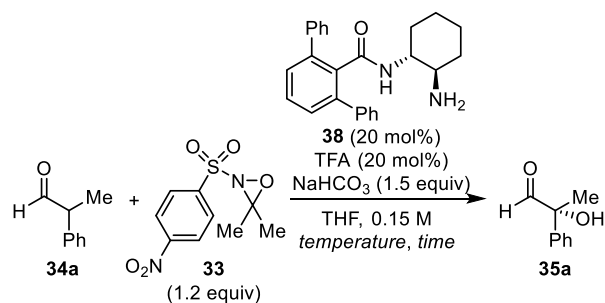
Entry	X	Conversion (%) ^b	ee (%) ^c
1	0.8	84	84
2	1.0	84	84
3	1.2	85	84
4	2.0	84	84

^a Reactions performed on 0.15 mmol scale. ^b Conversions determined by GC analysis. ^c Enantioselectivities determined by HPLC analysis of reduced diol using commercial columns with chiral stationary phases.

Table 5.28. α -Fluorination electrophile loading.^a


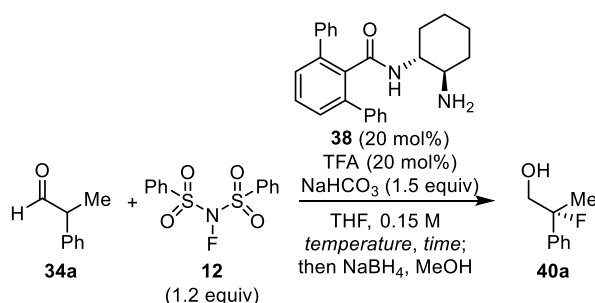
Entry	X	Conversion (%) ^b	ee (%) ^c
1	0.8	78	83
2	1.0	78	80
3	1.2	83	83
4	2.0	77	80

^a Reactions performed on 0.15 mmol scale. ^b Conversions determined by GC analysis. ^c Enantioselectivities determined by HPLC analysis of fluorohydrin using commercial columns with chiral stationary phases.

Table 5.29. α -Hydroxylation temperature screen.^a


Entry	Time (h)	Temperature (°C)	Conversion (%) ^b	ee (%) ^c
1	4	23	88	87
2	4	3	73	86
3	21	-10	61	88
4	46	-25	>65	93

^a Reactions performed on 0.15 mmol scale. ^b Conversions determined by GC analysis. ^c Enantioselectivities determined by HPLC analysis of reduced diol using commercial columns with chiral stationary phases.

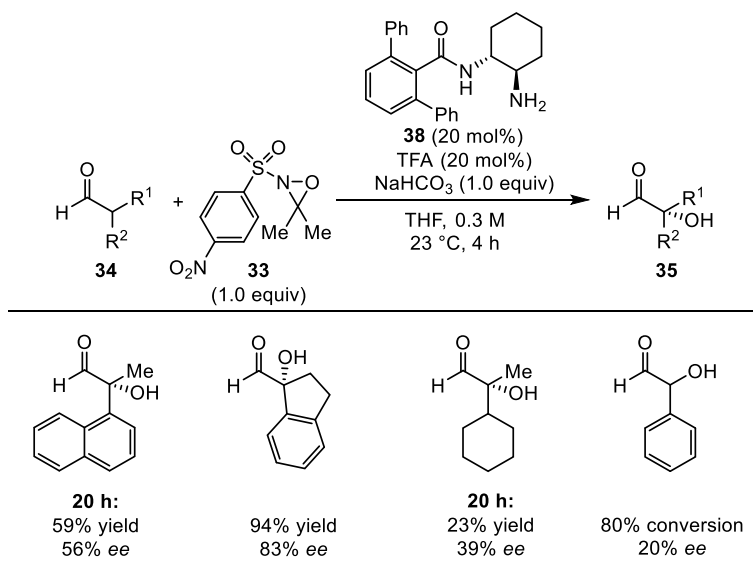
Table 5.30. α -Fluorination temperature screen.^a


Entry	Time (h)	Temperature (°C)	Conversion (%) ^b	ee (%) ^c
1	4	23	83	83
2	4	3	71	80

^a Reactions performed on 0.15 mmol scale. ^b Conversions determined by GC analysis. ^c Enantioselectivities determined by HPLC analysis of fluorohydrin using commercial columns with chiral stationary phases.

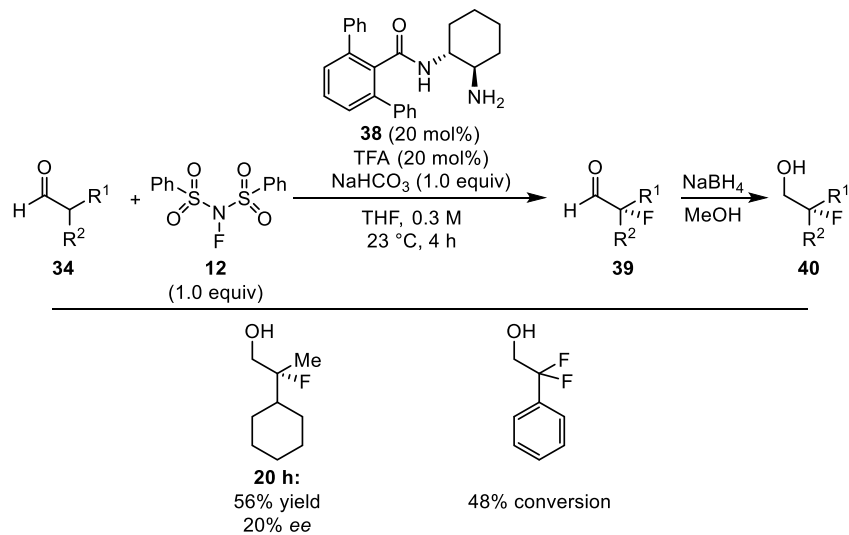
5.7.7 Results with Additional Substrates

Table 5.31. Additional α -hydroxylation reactions.^a



^a Reactions performed on 1.00 mmol scale. Yields of isolated products after column chromatography. Enantioselectivities determined by HPLC analysis of reduced diol using commercial columns with chiral stationary phases.

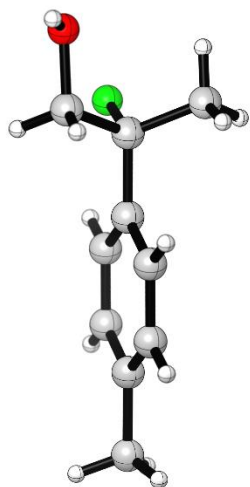
Table 5.32. Additional α -fluorination reactions.^a



^a Reactions performed on 1.00 mmol scale. Yields of isolated products after column chromatography. Enantioselectivities determined by HPLC analysis of fluorohydrin using commercial columns with chiral stationary phases.

5.7.8 Crystallographic Information⁶³

Fluorohydrin **40d**:



Fluorohydrin **40d** was crystallized from hexanes/Et₂O. A crystal was mounted on a diffractometer and data was collected at 100 K. The intensities of the reflections were collected by means of a Bruker APEX II DUO CCD diffractometer (Cu_Kα radiation, λ=1.54178 Å), equipped with an Oxford Cryosystems nitrogen flow apparatus. The collection method involved 1.0° scans in ω at 30°, 55°, 80° and 115° in 2θ . Data integration down to 0.84 Å resolution was carried out using SAINT V8.34 C⁶⁴ with reflection spot size optimization. Absorption corrections were made with the program SADABS.⁶⁴ The structure was solved by the Intrinsic Phasing methods and refined by least-squares methods against F^2 using SHELXT-2014 and SHELXL-2014⁶⁵ with OLEX 2 interface.⁶⁶ Non-hydrogen atoms were refined anisotropically, and hydrogen atoms were allowed to ride on the respective atoms.

Crystal data	
Chemical formula	C ₁₀ H ₁₃ FO
M_r	168.20

⁶³ Crystal structures solved by Dr. Shao-Liang Zheng.

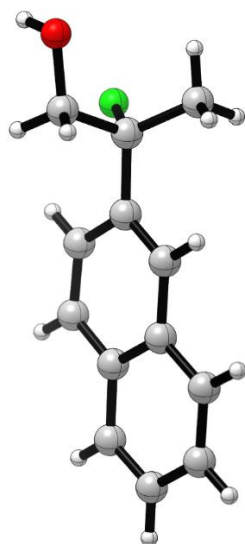
⁶⁴ Bruker AXS APEX II, Bruker AXS, Madison, Wisconsin, 2014.

⁶⁵ Sheldrick, G. M. *Acta Cryst.* **2008**, *A64*, 112–122.

⁶⁶ Dolomanov, O. V.; Bourhis, L. J.; Gildea, R. J.; Howard, J. A. K.; Puschmann, H. *J. Appl. Cryst.* **2009**, *42*, 339–341.

Crystal system, space group	Orthorhombic, $P2_12_12_1$
Temperature (K)	100
a, b, c (Å)	5.5342 (2), 11.1421 (4), 14.6505 (6)
V (Å ³)	903.39 (6)
Z	4
Radiation type	Cu $K\alpha$
μ (mm ⁻¹)	0.76
Crystal size (mm)	0.18 × 0.14 × 0.10
Data collection	
Diffractometer	Bruker D8 goniometer with CCD area detector diffractometer
Absorption correction	Multi-scan <i>SADABS</i>
T_{\min}, T_{\max}	0.687, 0.753
No. of measured, independent and observed [I $> 2\sigma(I)$] reflections	22169, 1597, 1534
R_{int}	0.036
$(\sin \theta/\lambda)_{\text{max}}$ (Å ⁻¹)	0.596
Refinement	
$R[F^2 > 2\sigma(F^2)], wR(F^2), S$	0.026, 0.068, 1.06
No. of reflections	1597
No. of parameters	115
H-atom treatment	H atoms treated by a mixture of independent and constrained refinement
$\Delta\rho_{\text{max}}, \Delta\rho_{\text{min}}$ (e Å ⁻³)	0.13, -0.13
Absolute structure	Flack x determined using 596 quotients [(I+)-(I-)]/[(I+)+(I-)] (Parsons, S.; Flack, H. D.; Wagner, T. <i>Acta Cryst.</i> , 2013 , <i>B69</i> , 249–259.)
Absolute structure parameter	0.05 (5)

Fluorohydrin **40i**:

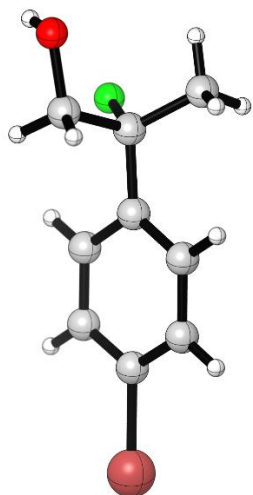


Fluorohydrin **40i** was crystallized from hexanes/Et₂O. A crystal was mounted on a diffractometer and data was collected at 100 K. The intensities of the reflections were collected by means of a Bruker APEX II DUO CCD diffractometer (Cu_{Kα} radiation, $\lambda=1.54178$ Å), equipped with an Oxford Cryosystems nitrogen flow apparatus. The collection method involved 1.0° scans in ω at 30°, 55°, 80° and 115° in 2θ . Data integration down to 0.84 Å resolution was carried out using SAINT V8.34 C⁶⁴ with reflection spot size optimization. Absorption corrections were made with the program SADABS.⁶⁴ The structure was solved by the Intrinsic Phasing methods and refined by least-squares methods again F^2 using SHELXT-2014 and SHELXL-2014⁶⁵ with OLEX 2 interface.⁶⁶ Non-hydrogen atoms were refined anisotropically, and hydrogen atoms were allowed to ride on the respective atoms.

Crystal data	
Chemical formula	C ₃₉ H ₃₉ F ₃ O ₃
M_r	612.70
Crystal system, space group	Orthorhombic, $P2_12_12_1$
Temperature (K)	100
a, b, c (Å)	6.1061 (2), 18.8064 (5), 27.8827 (7)
V (Å ³)	3201.88 (16)
Z	4

Radiation type	Cu $K\alpha$
μ (mm ⁻¹)	0.74
Crystal size (mm)	0.16 × 0.08 × 0.06
Data collection	
Diffractometer	Bruker D8 goniometer with CCD area detector diffractometer
Absorption correction	Multi-scan <i>SADABS</i>
T_{\min}, T_{\max}	0.773, 0.864
No. of measured, independent and observed [$I > 2\sigma(I)$] reflections	56690, 5672, 5034
R_{int}	0.069
$(\sin \theta/\lambda)_{\text{max}}$ (Å ⁻¹)	0.596
Refinement	
$R[F^2 > 2\sigma(F^2)], wR(F^2), S$	0.042, 0.111, 1.07
No. of reflections	5672
No. of parameters	416
No. of restraints	37
H-atom treatment	H atoms treated by a mixture of independent and constrained refinement
$\Delta\rho_{\text{max}}, \Delta\rho_{\text{min}}$ (e Å ⁻³)	0.34, -0.25
Absolute structure	Flack x determined using 1993 quotients [(I+)-(I-)]/[(I+)+(I-)] (Parsons, S.; Flack, H. D.; Wagner, T. <i>Acta Cryst.</i> , 2013 , B69, 249–259.)
Absolute structure parameter	0.05 (7)

Fluorohydrin **40j**:



Fluorohydrin **40j** was crystallized from hexanes/Et₂O. A crystal was mounted on a diffractometer and data was collected at 100 K. The intensities of the reflections were collected by means of a Bruker APEX II DUO CCD diffractometer (MoK α radiation, $\lambda=0.71073$ Å), equipped with an Oxford Cryosystems nitrogen flow apparatus. The collection method involved 0.5° scans in ω at 28° in 2θ . Data integration down to 0.78 Å resolution was carried out using SAINT V8.34 C⁶⁴ with reflection spot size optimization. Absorption corrections were made with the program SADABS.⁶⁴ The structure was solved by the direct methods procedure and refined by least-squares methods again F^2 using SHELXT-2014 and SHELXL-2014⁶⁵ with OLEX 2 interface.⁶⁶ Non-hydrogen atoms were refined anisotropically, and hydrogen atoms were allowed to ride on the respective atoms.

Crystal data	
Chemical formula	C ₉ H ₁₀ BrFO
M_r	233.08
Crystal system, space group	Monoclinic, $P2_1$
Temperature (K)	100
a, b, c (Å)	8.013 (3), 5.1662 (18), 10.972 (4)
β (°)	93.376 (5)
V (Å ³)	453.4 (3)
Z	2

Radiation type	Mo $K\alpha$
μ (mm ⁻¹)	4.50
Crystal size (mm)	0.14 × 0.12 × 0.10
Data collection	
Diffractometer	Bruker D8 goniometer with CCD area detector diffractometer
Absorption correction	Multi-scan <i>SADABS</i>
T_{\min}, T_{\max}	0.508, 0.746
No. of measured, independent and observed [$I > 2\sigma(I)$] reflections	10136, 2018, 1898
R_{int}	0.037
$(\sin \theta/\lambda)_{\text{max}}$ (Å ⁻¹)	0.646
Refinement	
$R[F^2 > 2\sigma(F^2)], wR(F^2), S$	0.019, 0.047, 1.04
No. of reflections	2018
No. of parameters	114
No. of restraints	1
H-atom treatment	H atoms treated by a mixture of independent and constrained refinement
$\Delta\rho_{\text{max}}, \Delta\rho_{\text{min}}$ (e Å ⁻³)	0.32, -0.20
Absolute structure	Flack x determined using 805 quotients [(I+)-(I-)]/[(I+)+(I-)] (Parsons, S.; Flack, H. D.; Wagner, T. <i>Acta Cryst.</i> , 2013 , B69, 249–259.)
Absolute structure parameter	-0.008 (9)